NEW TRENDS IN FRACTIONAL DIFFERENTIAL EQUATIONS WITH REAL-WORLD APPLICATIONS IN PHYSICS

EDITED BY: Jagdev Singh, Jordan Yankov Hristov and Zakia Hammouch
PUBLISHED IN: Frontiers in Physics

frontiers Research Topics

frontiers

Frontiers eBook Copyright Statement

The copyright in the text of individual articles in this eBook is the property of their respective authors or their respective institutions or funders. The copyright in graphics and images within each article may be subject to copyright of other parties. In both cases this is subject to a license granted to Frontiers.

The compilation of articles constituting this eBook is the property of Frontiers.

Each article within this eBook, and the eBook itself, are published under the most recent version of the Creative Commons CC-BY licence. The version current at the date of publication of this eBook is CC-BY 4.0. If the CC-BY licence is updated, the licence granted by Frontiers is automatically updated to the new version.

When exercising any right under the CC-BY licence, Frontiers must be attributed as the original publisher of the article or eBook, as applicable.

Authors have the responsibility of ensuring that any graphics or other materials which are the property of others may be included in the CC-BY licence, but this should be checked before relying on the CC-BY licence to reproduce those materials. Any copyright notices relating to those materials must be complied with.

Copyright and source acknowledgement notices may not be removed and must be displayed in any copy, derivative work or partial copy which includes the elements in question.

All copyright, and all rights therein, are protected by national and international copyright laws. The above represents a summary only. For further information please read Frontiers' Conditions for Website Use and Copyright Statement, and the applicable CC-BY licence.

ISSN 1664-8714
ISBN 978-2-88966-304-0
DOI 10.3389/978-2-88966-304-0

About Frontiers

Frontiers is more than just an open-access publisher of scholarly articles: it is a pioneering approach to the world of academia, radically improving the way scholarly research is managed. The grand vision of Frontiers is a world where all people have an equal opportunity to seek, share and generate knowledge. Frontiers provides immediate and permanent online open access to all its publications, but this alone is not enough to realize our grand goals.

Frontiers Journal Series

The Frontiers Journal Series is a multi-tier and interdisciplinary set of open-access, online journals, promising a paradigm shift from the current review, selection and dissemination processes in academic publishing. All Frontiers journals are driven by researchers for researchers; therefore, they constitute a service to the scholarly community. At the same time, the Frontiers Journal Series operates on a revolutionary invention, the tiered publishing system, initially addressing specific communities of scholars, and gradually climbing up to broader public understanding, thus serving the interests of the lay society, too.

Dedication to Quality

Each Frontiers article is a landmark of the highest quality, thanks to genuinely collaborative interactions between authors and review editors, who include some of the world's best academicians. Research must be certified by peers before entering a stream of knowledge that may eventually reach the public - and shape society; therefore, Frontiers only applies the most rigorous and unbiased reviews.
Frontiers revolutionizes research publishing by freely delivering the most outstanding research, evaluated with no bias from both the academic and social point of view. By applying the most advanced information technologies, Frontiers is catapulting scholarly publishing into a new generation.

What are Frontiers Research Topics?

Frontiers Research Topics are very popular trademarks of the Frontiers Journals Series: they are collections of at least ten articles, all centered on a particular subject. With their unique mix of varied contributions from Original Research to Review Articles, Frontiers Research Topics unify the most influential researchers, the latest key findings and historical advances in a hot research area! Find out more on how to host your own Frontiers Research Topic or contribute to one as an author by contacting the Frontiers Editorial Office: researchtopics@frontiersin.org

NEW TRENDS IN FRACTIONAL DIFFERENTIAL EQUATIONS WITH REAL-WORLD APPLICATIONS IN PHYSICS

Topic Editors:
Jagdev Singh, JECRC University, India
Jordan Yankov Hristov, University of Chemical Technology and Metallurgy, Bulgaria
Zakia Hammouch, Moulay Ismail University, Morocco

Citation: Singh, J., Hristov, J. Y., Hammouch, Z., eds. (2020). New Trends in Fractional Differential Equations With Real-World Applications in Physics. Lausanne: Frontiers Media SA. doi: 10.3389/978-2-88966-304-0

Table of Contents

frontiers in Physics

ORIGINAL RESEARCH
published: 20 March 2020
doi: 10.3389/fphy.2020.00064

Generalization of Caputo-Fabrizio Fractional Derivative and Applications to Electrical Circuits

Amal Alshabanat[1], *Mohamed Jleli*[1], *Sunil Kumar*[2]* *and Bessem Samet*[1]

[1] Department of Mathematics, College of Science, King Saud University, Riyadh, Saudi Arabia, [2] Department of Mathematics, National Institute of Technology, Jamshedpur, India

A new fractional derivative with a non-singular kernel involving exponential and trigonometric functions is proposed in this paper. The suggested fractional operator includes as a special case Caputo-Fabrizio fractional derivative. Theoretical and numerical studies of fractional differential equations involving this new concept are presented. Next, some applications to RC-electrical circuits are provided.

Keywords: fractional derivative, non-singular kernel, Picard iteration, RC-electrical circuit, convergence

OPEN ACCESS

Edited by:
Jagdev Singh,
JECRC University, India

Reviewed by:
Haci Mehmet Baskonus,
Harran University, Turkey
Devendra Kumar,
University of Rajasthan, India

***Correspondence:**
Sunil Kumar
skumar.math@nitjsr.ac.in

Specialty section:
This article was submitted to Mathematical Physics, a section of the journal Frontiers in Physics

Received: *25 December 2019*
Accepted: *28 February 2020*
Published: *20 March 2020*

Citation:
Alshabanat A, Jleli M, Kumar S and Samet B (2020) Generalization of Caputo-Fabrizio Fractional Derivative and Applications to Electrical Circuits. Front. Phys. 8:64. doi: 10.3389/fphy.2020.00064

1. INTRODUCTION

In the recent decades, the theory of fractional calculus has brought the attention of a great number of researchers in various disciplines. Indeed, it was observed that the use of fractional derivatives is very useful for modeling many problems in engineering sciences (see e.g., [1–10]). Various notions of fractional derivatives exist in the literature. The basic notions are those introduced by Riemann-Liouville and Caputo (see e.g., [11]), which involve the singular kernel $k(t,s) = \frac{(t-s)^{-\alpha}}{\Gamma(1-\alpha)}$, $0 < \alpha < 1$. These fractional derivatives play an important role for modeling many phenomena in physics. However, as it was mentioned in Caputo and Fabrizio [12], certain phenomena related to material heterogeneities cannot be well-modeled using Riemann-Liouville or Caputo fractional derivatives. Due to this fact, Caputo and Fabrizio [12] suggested a new fractional derivative involving the non-singular kernel $k(t,s) = e^{\frac{-\alpha(t-s)}{1-\alpha}}$, $0 < \alpha < 1$. Later, Caputo-Fabrizio fractional derivative was used by many authors for modeling various problems in engineering sciences (see e.g., [13–24]). Furthermore, other fractional derivatives with non-singular kernels were introduced by some authors (see e.g., [10, 25–29]).

In this paper, a new fractional derivative with a non-singular kernel involving exponential and trigonometric functions is proposed. The introduced fractional derivative includes as a special case Caputo-Fabrizio fractional derivative. Theoretical and numerical investigations of fractional differential equations involving this new fractional operator are presented. Next, some applications to electrical circuits are provided.

In section 2, some preliminaries on harmonic analysis are presented. In section 3, we develop a general theory of fractional calculus using an arbitrary non-singular kernel. In section 4, we introduce a generalized Caputo-Fabrizio fractional derivative and study its properties. Some applications to fractional differential equations are given in section 5. A numerical method based on Picard iterations is presented in section 6 with some numerical examples. In section 7, some applications to RC-electrical circuits are provided.

2. SOME PRELIMINARIES ON HARMONIC ANALYSIS

We recall briefly some results on harmonic analysis that will be used later.

Lemma 2.1. Folland [30]. *Let $\psi \in L^1(\mathbb{R})$ be such that*

$$\int_{\mathbb{R}} \psi(t)\, dt = 1.$$

Consider the sequence of functions $\{\psi_\varepsilon\}_{\varepsilon>0}$ defined by

$$\psi_\varepsilon(t) = \frac{1}{\varepsilon}\psi\left(\frac{t}{\varepsilon}\right), \quad t \in \mathbb{R}.$$

If $\mu \in L^1(\mathbb{R})$, then

$$\psi_\varepsilon * \mu \in L^1(\mathbb{R}), \quad \varepsilon > 0$$

and

$$\lim_{\varepsilon\to 0^+} \|\psi_\varepsilon * \mu - \mu\|_{L^1(\mathbb{R})} = 0,$$

where $*$ denotes the convolution product.

Lemma 2.2. *Let $\psi \in L^1(0,\infty)$ be such that*

$$\int_0^\infty \psi(t)\, dt = 1. \tag{2.1}$$

Consider the sequence of functions $\{\psi_\varepsilon\}_{\varepsilon>0}$ defined by

$$\psi_\varepsilon(t) = \frac{1}{\varepsilon}\psi\left(\frac{t}{\varepsilon}\right), \quad t > 0.$$

If $\mu \in L^1(0,\infty)$, then the sequence of functions $\{I_\varepsilon^\mu\}_{\varepsilon>0}$ defined by

$$I_\varepsilon^\mu(t) = \int_0^t \psi_\varepsilon(t-s)\mu(s)\, ds, \quad t > 0$$

satisfies the following properties:

$$I_\varepsilon^\mu \in L^1(0,\infty), \quad \varepsilon > 0$$

and

$$\lim_{\varepsilon\to 0^+} \|I_\varepsilon^\mu - \mu\|_{L^1(0,\infty)} = 0.$$

Proof: For any function f defined almost every where in $(0,\infty)$, let

$$\widetilde{f}(t) = \begin{cases} f(t) & \text{a.e. } t > 0, \\ 0 & \text{if } \quad t \le 0. \end{cases}$$

From (2.1), one has $\widetilde{\psi} \in L^1(\mathbb{R})$ and

$$\int_{\mathbb{R}} \widetilde{\psi}(t)\, dt = 1.$$

Hence, by Lemma 2.1, for all $f \in L^1(\mathbb{R})$, we have

$$\widetilde{\psi_\varepsilon} * f \in L^1(\mathbb{R}), \quad \varepsilon > 0$$

and

$$\lim_{\varepsilon\to 0^+} \|\widetilde{\psi_\varepsilon} * f - f\|_{L^1(\mathbb{R})} = 0,$$

where

$$\widetilde{\psi_\varepsilon}(t) = \frac{1}{\varepsilon}\widetilde{\psi}\left(\frac{t}{\varepsilon}\right), \quad t \in \mathbb{R}.$$

In particular, for $\mu \in L^1(0,\infty)$, we have

$$\widetilde{\psi_\varepsilon} * \widetilde{\mu} \in L^1(\mathbb{R}), \quad \varepsilon > 0 \tag{2.2}$$

and

$$\lim_{\varepsilon\to 0^+} \|\widetilde{\psi_\varepsilon} * \widetilde{\mu} - \widetilde{\mu}\|_{L^1(\mathbb{R})} = 0. \tag{2.3}$$

For all $t > 0$, we have

$$\begin{aligned} \widetilde{\psi_\varepsilon} * \widetilde{\mu}(t) &= \int_{\mathbb{R}} \widetilde{\psi_\varepsilon}(t-s)\widetilde{\mu}(s)\, ds \\ &= \int_0^t \psi_\varepsilon(t-s)\mu(s)\, ds \\ &= I_\varepsilon^\mu(t). \end{aligned}$$

Hence, using (2.2) and (2.3), one obtains

$$\int_0^\infty |I_\varepsilon^\mu(t)|\, dt = \int_0^\infty |\widetilde{\psi_\varepsilon} * \widetilde{\mu}(t)|\, dt \le \|\widetilde{\psi_\varepsilon} * \widetilde{\mu}\|_{L^1(\mathbb{R})} < \infty$$

and

$$\begin{aligned} \|I_\varepsilon^\mu - \mu\|_{L^1(0,\infty)} &= \int_0^\infty |\widetilde{\psi_\varepsilon} * \widetilde{\mu}(t) - \widetilde{\mu}(t)|\, dt \\ &\le \|\widetilde{\psi_\varepsilon} * \widetilde{\mu} - \widetilde{\mu}\|_{L^1(\mathbb{R})} \longrightarrow 0 \text{ as } \varepsilon \longrightarrow 0^+. \end{aligned}$$

This completes the proof of Lemma 2.2. □

Definition 2.1. *We say that f is of exponential order θ, if for t large enough, one has*

$$|f(t)| \le Ce^{\theta t},$$

where $C > 0$ and θ are constants.

We denote by $\mathcal{L}\{f(t)\}$ the Laplace transform of the function f, i.e.,

$$\mathcal{L}\{f(t)\}(s) = \int_0^\infty e^{-st} f(t)\, dt.$$

Recall that, if $f \in C[0,\infty)$ and f is of exponential order θ, then $\mathcal{L}\{f(t)\}(s)$ exists for $s > \theta$.

We denote by $\mathbb{N}$ the set of positive integers.

Lemma 2.3. Schiff [31]. *Let $n \in \mathbb{N}$. If $f \in C^n[0,\infty)$ and for all $i = 0, 1, \cdots, n-1$, the function $f^{(i)}$ is of exponential order, then*

$$\mathcal{L}\{f^{(n)}(t)\}(s) = s^n\mathcal{L}\{f(t)\}(s) - \sum_{i=1}^{n} s^{i-1} f^{(n-i)}(0).$$

3. FRACTIONAL DERIVATIVE WITH AN ARBITRARY NON-SINGULAR KERNEL

We consider the set of non-singular kernel functions

$$\mathcal{K} = \left\{ k \in C[0,\infty) \cap L^1(0,\infty) : \int_0^\infty k(\sigma)\, d\sigma = 1 \right\}. \quad (3.1)$$

Definition 3.1. *Given $k \in \mathcal{K}$, $0 < \alpha < 1$ and $f \in C^1[0,\infty)$, the fractional derivative of order α of f with respect to the non-singular kernel function k is defined by*

$$\left(D^{\alpha}_{0,k} f\right)(t) = \frac{1}{1-\alpha} \int_0^t k\left(\frac{\alpha(t-s)}{1-\alpha}\right) f'(s)\, ds, \quad t > 0.$$

Remark 3.1. *We can also define $D^{\alpha}_{0,k} f$ for functions $f \in AC[0,\infty)$ (f is an absolutely continuous function in $[0,\infty)$). In this case, $f'(t)$ exists for almost every where $t > 0$ and $f' \in L^1(0,\infty)$.*

The following properties hold.

Theorem 3.1. *Let $k \in \mathcal{K}$ and $f \in C^1[0,\infty)$. Then*

(i) *For all $0 < \alpha < 1$,*

$$\lim_{t \to 0^+} \left(D^{\alpha}_{0,k} f\right)(t) = 0.$$

(ii) *If $f' \in L^1(0,\infty)$, one has*

$$D^{\alpha}_{0,k} f \in L^1(0,\infty), \quad 0 < \alpha < 1$$

and

$$\lim_{\alpha \to 1^-} \left\| D^{\alpha}_{0,k} f - f' \right\|_{L^1(0,\infty)} = 0.$$

Proof: (i) Let $0 < \alpha < 1$. For $0 < t < T < \infty$, one has

$$\left| \left(D^{\alpha}_{0,k} f\right)(t) \right| \le \frac{\|k\|_{L^\infty(0,T_\alpha)} \|f'\|_{L^\infty(0,T)}}{1-\alpha} t,$$

where $T_\alpha = \frac{\alpha}{1-\alpha} T$. Passing to the limit as $t \to 0^+$ in the above inequality, (i) follows.
(ii) Suppose that $f' \in L^1(0,\infty)$. For $0 < \alpha < 1$, let $\varepsilon = \frac{1-\alpha}{\alpha}$. One has

$$\begin{aligned} \left(D^{\alpha}_{0,k} f\right)(t) &= \frac{\varepsilon+1}{\varepsilon} \int_0^t k\left(\frac{1}{\varepsilon}(t-s)\right) f'(s)\, ds \\ &= (\varepsilon+1) \int_0^t \frac{1}{\varepsilon} k\left(\frac{1}{\varepsilon}(t-s)\right) f'(s)\, ds \\ &= (\varepsilon+1) \int_0^t k_\varepsilon(t-s) f'(s)\, ds, \quad t > 0, \end{aligned}$$

where

$$k_\varepsilon(x) = \frac{1}{\varepsilon} k\left(\frac{x}{\varepsilon}\right), \quad x > 0.$$

Hence, using Lemma 2.2, (ii) follows. □

Definition 3.2. *Given $k \in \mathcal{K}$, $0 < \alpha < 1$, $n \in \mathbb{N} \cup \{0\}$ and $f \in C^{n+1}[0,\infty)$, the fractional derivative of order $\alpha + n$ of f with respect to the non-singular kernel k is defined by*

$$\left(D^{\alpha+n}_{0,k} f\right)(t) = \frac{1}{1-\alpha} \int_0^t k\left(\frac{\alpha(t-s)}{1-\alpha}\right) f^{(n+1)}(s)\, ds, \quad t > 0.$$

Remark 3.2. *We can also define $D^{\alpha+n}_{0,k} f$ for functions $f \in AC^{n+1}[0,\infty)$. In this case, $f^{n+1}(t)$ exists for almost every where $t > 0$ and $f^{(n+1)} \in L^1(0,\infty)$.*

Similarly to the case $n = 0$, one has

Theorem 3.2. *Let $k \in \mathcal{K}$, $n \in \mathbb{N} \cup \{0\}$ and $f \in C^{n+1}[0,\infty)$. Then*

(i) *For all $0 < \alpha < 1$,*

$$\lim_{t \to 0^+} \left(D^{\alpha+n}_{0,k} f\right)(t) = 0.$$

(ii) *If $f^{(n+1)} \in L^1(0,\infty)$, then*

$$D^{\alpha+n}_{0,k} f \in L^1(0,\infty), \quad 0 < \alpha < 1$$

and

$$\lim_{\alpha \to 1^-} \left\| D^{\alpha+n}_{0,k} f - f^{(n+1)} \right\|_{L^1(0,\infty)} = 0.$$

Remark 3.3. *From the assertion (ii) of Theorem 3.2, if $f^{(n+1)} \in L^1(0,\infty)$, one has*

$$\lim_{\alpha \to 1^-} \left(D^{\alpha+n}_{0,k} f\right)(t) = f^{(n+1)}(t), \quad a.e.\ t > 0.$$

Theorem 3.3. *Given $k \in \mathcal{K}$, $0 < \alpha < 1$, $n \in \mathbb{N} \cup \{0\}$ and $f \in C^{n+1}[0,\infty)$ with $f^{(i)}$, $i = 0, 1, \cdots, n$, are of exponential order, one has*

$$\begin{aligned} &\mathcal{L}\left\{ \left(D^{\alpha+n}_{0,k} f\right)(t) \right\}(s) \\ &= \frac{1}{1-\alpha} \left(s^{n+1} \mathcal{L}\{f(t)\}(s) - \sum_{i=1}^{n+1} s^{i-1} f^{(n+1-i)}(0) \right) \mathcal{L}\left\{ k_\alpha(t) \right\}(s), \end{aligned}$$

where

$$k_\alpha(t) = k\left(\frac{\alpha t}{1-\alpha}\right), \quad t > 0.$$

Proof: One has

$$\begin{aligned} &\mathcal{L}\left\{ \left(D^{\alpha+n}_{0,k} f\right)(t) \right\}(s) \\ &= \int_0^\infty e^{-ts} \left(D^{\alpha+n}_{0,k} f\right)(t)\, dt \\ &= \int_0^\infty e^{-ts} \left(\frac{1}{1-\alpha} \int_0^t k\left(\frac{\alpha(t-\sigma)}{1-\alpha}\right) f^{(n+1)}(\sigma)\, d\sigma \right) dt. \end{aligned}$$

Using Fubini's theorem, one obtains

$$\mathcal{L}\left\{\left(D_{0,k}^{\alpha+n}f\right)(t)\right\}(s) = \frac{1}{1-\alpha}\int_0^\infty f^{(n+1)}(\sigma)\left(\int_\sigma^\infty e^{-ts}k\left(\frac{\alpha(t-\sigma)}{1-\alpha}\right)dt\right)d\sigma. \tag{3.2}$$

Using the change of variable $\tau = t-\sigma$, it holds

$$\begin{aligned}&\int_\sigma^\infty e^{-ts}k\left(\frac{\alpha(t-\sigma)}{1-\alpha}\right)dt\\ &= e^{-\sigma s}\int_0^\infty e^{-\tau s}k\left(\frac{\alpha\tau}{1-\alpha}\right)d\tau\\ &= e^{-\sigma s}\mathcal{L}\left\{k_\alpha(t)\right\}(s).\end{aligned}$$

Hence, by (3.2), one deduces that

$$\mathcal{L}\left\{\left(D_{0,k}^{\alpha+n}f\right)(t)\right\}(s) = \frac{1}{1-\alpha}\mathcal{L}\left\{f^{(n+1)}(t)\right\}(s)\mathcal{L}\left\{k_\alpha(t)\right\}(s).$$

Next, using Lemma 2.3, we obtain

$$\mathcal{L}\left\{\left(D_{0,k}^{\alpha+n}f\right)(t)\right\}(s) = \frac{1}{1-\alpha}\left(s^{n+1}\mathcal{L}\{f(t)\}(s) - \sum_{i=1}^{n+1}s^{i-1}f^{(n+1-i)}(0)\right)\mathcal{L}\left\{k_\alpha(t)\right\}(s),$$

which yields the desired result. □

4. A GENERALIZED CAPUTO-FABRIZIO FRACTIONAL DERIVATIVE

Consider the kernel function

$$k_{a,b}(t) = \left(\frac{a^2+b^2}{a}\right)e^{-at}\cos(bt), \quad t \geq 0,$$

where $a > 0$ and $b \geq 0$ are constants. It can be easily seen that

$$k_{a,b} \in \mathcal{K}, \tag{4.1}$$

where $\mathcal{K}$ is the set of kernel functions defined by (3.1). Hence, using Definition 3.2, we define the fractional derivative with respect to the kernel function $k_{a,b}$ as follows.

Definition 4.1. *Given $a > 0$, $b \geq 0$, $0 < \alpha < 1$, $n \in \mathbb{N}\cup\{0\}$ and $f \in C^{n+1}[0,\infty)$, the fractional derivative of order $\alpha+n$ of f with respect to the kernel function $k_{a,b}$ is defined by*

$$\left(D_{0,a,b}^{\alpha+n}f\right)(t) = \left(\frac{1}{1-\alpha}\right)\left(\frac{a^2+b^2}{a}\right)\int_0^t e^{-\frac{a\alpha(t-s)}{1-\alpha}}\cos\left(\frac{b\alpha(t-s)}{1-\alpha}\right)f^{(n+1)}(s)\,ds, \quad t > 0.$$

Remark 4.1. *Taking $a = 1$ and $b = 0$ in the above definition, one obtains*

$$\left(D_{0,1,0}^{\alpha+n}f\right)(t) = \left({}^{CF}D_0^{\alpha+n}f\right)(t), \quad t > 0,$$

where ${}^{CF}D_0^{\alpha+n}$ is the Caputo–Fabrizio fractional derivative operator of order $\alpha+n$ (see [12]).

Remark 4.2. *Definition 4.1 can be extended to the case of functions $f \in C^{n+1}[0,T]$, where $0 < T < \infty$.*

From (4.1) and Theorem 3.2, one deduces that

Corollary 4.1. *Let $a > 0$, $b \geq 0$, $n \in \mathbb{N}\cup\{0\}$ and $f \in C^{n+1}[0,\infty)$. Then*

(i) *For all $0 < \alpha < 1$,*

$$\lim_{t\to 0^+}\left(D_{0,a,b}^{\alpha+n}f\right)(t) = 0.$$

(ii) *If $f^{(n+1)} \in L^1(0,\infty)$, then*

$$D_{0,a,b}^{\alpha+n}f \in L^1(0,\infty), \quad 0 < \alpha < 1$$

and

$$\lim_{\alpha\to 1^-}\left\|D_{0,a,b}^{\alpha+n}f - f^{(n+1)}\right\|_{L^1(0,\infty)} = 0.$$

Let

$$k_{a,b,\alpha}(t) = k_{a,b}\left(\frac{\alpha t}{1-\alpha}\right), \quad t > 0,$$

that is,

$$k_{a,b,\alpha}(t) = \left(\frac{a^2+b^2}{a}\right)e^{-\frac{a\alpha t}{1-\alpha}}\cos\left(\frac{b\alpha t}{1-\alpha}\right), \quad t > 0.$$

Lemma 4.1. Abramowitz and Stegun [32]. *Let $a > 0$, $b \geq 0$ and $0 < \alpha < 1$. Then*

$$\mathcal{L}\left\{k_{a,b,\alpha}(t)\right\}(s) = \frac{(1-\alpha)(a^2+b^2)}{a}\left[\frac{(1-\alpha)s+\alpha a}{((1-\alpha)s+\alpha a)^2+b^2\alpha^2}\right], \quad s > 0.$$

Using Theorem 3.3 and Lemma 4.1, one deduces that

Corollary 4.2. *Let $a > 0$, $b \geq 0$, $0 < \alpha < 1$, $n \in \mathbb{N}\cup\{0\}$ and $f \in C^{n+1}[0,\infty)$ with $f^{(i)}$, $i = 0,1,\cdots,n$, are of exponential order. Then*

$$\mathcal{L}\left\{\left(D_{0,a,b}^{\alpha+n}f\right)(t)\right\}(s) = \frac{(a^2+b^2)}{a}\left(s^{n+1}\mathcal{L}\{f(t)\}(s) - \sum_{i=1}^{n+1}s^{i-1}f^{(n+1-i)}(0)\right)\left[\frac{(1-\alpha)s+\alpha a}{((1-\alpha)s+\alpha a)^2+b^2\alpha^2}\right], \quad s > 0.$$

For $n = 0$, one obtains

Corollary 4.3. *Let $a > 0$, $b \geq 0$, $0 < \alpha < 1$ and $f \in C^1[0,\infty)$ with f is of exponential order. Then*

$$\mathcal{L}\left\{\left(D_{0,a,b}^{\alpha}f\right)(t)\right\}(s) = \frac{(a^2+b^2)}{a}\left(s\mathcal{L}\{f(t)\}(s) - f(0)\right)\left[\frac{(1-\alpha)s+\alpha a}{((1-\alpha)s+\alpha a)^2+b^2\alpha^2}\right].$$

5. APPLICATIONS TO FRACTIONAL DIFFERENTIAL EQUATIONS

Let $a > 0, b \geq 0, 0 < T < \infty$ and $0 < \alpha < 1$.

Definition 5.1. *Let $g \in C[0,T]$. The fractional integral of order α of g is defined by*

$$\left(I^{\alpha}_{0,a,b}g\right)(t) = \frac{a(1-\alpha)}{a^2+b^2}g(t) + \alpha\left(\int_0^t g(\sigma)\,d\sigma - \frac{b^2}{a^2+b^2}\int_0^t e^{\frac{-a\alpha(t-\sigma)}{1-\alpha}}g(\sigma)\,d\sigma\right), \quad 0 \leq t \leq T,$$

with $\left(I^{\alpha}_{0,a,b}g\right)(0) = 0$.

Given $f_0 \in \mathbb{R}$ and $g \in C^1[0,T]$ with $g(0) = 0$, we consider the initial value problem

$$\begin{cases} \left(D^{\alpha}_{0,a,b}f\right)(t) = g(t), & 0 < t < T, \\ f(0) = f_0. \end{cases} \tag{5.1}$$

Theorem 5.1. *Problem (5.1) admits a unique solution $f \in C^1[0,T]$, which is given by*

$$f(t) = f_0 + \left(I^{\alpha}_{0,a,b}g\right)(t), \quad 0 \leq t \leq T. \tag{5.2}$$

Proof: Let $f \in C^1[0,T]$ be a solution of (5.1). One has

$$\left(D^{\alpha}_{0,a,b}f\right)'(t) = g'(t), \quad 0 < t < T. \tag{5.3}$$

By Definition 4.1, one has

$$\begin{aligned}\left(D^{\alpha}_{0,a,b}f\right)'(t) &= \left(\frac{1}{1-\alpha}\right)\left(\frac{a^2+b^2}{a}\right)\left\{f'(t) + \int_0^t \frac{d}{dt}\left(e^{-\frac{a\alpha(t-s)}{1-\alpha}}\cos\left(\frac{b\alpha(t-s)}{1-\alpha}\right)\right)f'(s)\,ds\right\} \\ &= \left(\frac{1}{1-\alpha}\right)\left(\frac{a^2+b^2}{a}\right)f'(t) \\ &- \left(\frac{a\alpha}{1-\alpha}\right)\left(\frac{1}{1-\alpha}\right)\left(\frac{a^2+b^2}{a}\right)\int_0^t e^{-\frac{a\alpha(t-s)}{1-\alpha}}\cos\left(\frac{b\alpha(t-s)}{1-\alpha}\right)f'(s)\,ds \\ &- \left(\frac{b\alpha}{1-\alpha}\right)\left(\frac{1}{1-\alpha}\right)\left(\frac{a^2+b^2}{a}\right)\int_0^t e^{-\frac{a\alpha(t-s)}{1-\alpha}}\sin\left(\frac{b\alpha(t-s)}{1-\alpha}\right)f'(s)\,ds \\ &= \left(\frac{1}{1-\alpha}\right)\left(\frac{a^2+b^2}{a}\right)f'(t) - \left(\frac{a\alpha}{1-\alpha}\right)g(t) \\ &- \left(\frac{b\alpha}{1-\alpha}\right)\left(\frac{1}{1-\alpha}\right)\left(\frac{a^2+b^2}{a}\right)\gamma(t),\end{aligned} \tag{5.4}$$

where

$$\gamma(t) = \int_0^t e^{-\frac{a\alpha(t-s)}{1-\alpha}}\sin\left(\frac{b\alpha(t-s)}{1-\alpha}\right)f'(s)\,ds.$$

On the other hand,

$$\begin{aligned}\gamma'(t) &= \int_0^t \frac{d}{dt}\left(e^{-\frac{a\alpha(t-s)}{1-\alpha}}\sin\left(\frac{b\alpha(t-s)}{1-\alpha}\right)\right)f'(s)\,ds \\ &= -\left(\frac{a\alpha}{1-\alpha}\right)\gamma(t) + \left(\frac{b\alpha}{1-\alpha}\right) \\ &\int_0^t e^{-\frac{a\alpha(t-s)}{1-\alpha}}\cos\left(\frac{b\alpha(t-s)}{1-\alpha}\right)f'(s)\,ds \\ &= -\left(\frac{a\alpha}{1-\alpha}\right)\gamma(t) + \left(\frac{ab\alpha}{a^2+b^2}\right)g(t).\end{aligned}$$

Integrating the above equality and using that $\gamma(0) = 0$, one obtains

$$\gamma(t) = \frac{ab\alpha}{a^2+b^2}\int_0^t e^{-\frac{a\alpha(t-s)}{1-\alpha}}g(s)\,ds.$$

Hence by (5.4), one deduces that

$$\left(D^{\alpha}_{0,a,b}f\right)'(t) = \left(\frac{1}{1-\alpha}\right)\left(\frac{a^2+b^2}{a}\right)f'(t) - \left(\frac{a\alpha}{1-\alpha}\right)g(t) - \left(\frac{b\alpha}{1-\alpha}\right)^2\int_0^t e^{-\frac{a\alpha(t-s)}{1-\alpha}}g(s)\,ds.$$

Next, using (5.3), one obtains

$$f'(t) = \frac{a^2\alpha}{a^2+b^2}g(t) + \left(\frac{ab^2\alpha^2}{(1-\alpha)(a^2+b^2)}\right)\int_0^t e^{-\frac{a\alpha(t-s)}{1-\alpha}}g(s)\,ds + \frac{a(1-\alpha)}{a^2+b^2}g'(t).$$

Integrating the above equality, using that $f(0) = f_0$ and $g(0) = 0$, it holds

$$f(t) - f_0 = \left(\frac{a^2\alpha}{a^2+b^2}\right)\int_0^t g(\sigma)\,d\sigma + \frac{a(1-\alpha)}{a^2+b^2}g(t) + \left(\frac{ab^2\alpha^2}{(1-\alpha)(a^2+b^2)}\right)\int_0^t\int_0^{\sigma} e^{-\frac{a\alpha(\sigma-s)}{1-\alpha}}g(s)\,ds\,d\sigma \tag{5.5}$$

On the other hand, using Fubini's theorem, one gets

$$\begin{aligned}&\int_0^t\int_0^{\sigma} e^{-\frac{a\alpha(\sigma-s)}{1-\alpha}}g(s)\,ds\,d\sigma \\ &= \int_0^t g(s)e^{\frac{a\alpha s}{1-\alpha}}\left(\int_s^t e^{-\frac{a\alpha\sigma}{1-\alpha}}\,d\sigma\right)ds \\ &= \left(\frac{1-\alpha}{a\alpha}\right)\int_0^t g(s)\,ds - \left(\frac{1-\alpha}{a\alpha}\right)\int_0^t e^{-\frac{a\alpha(t-s)}{1-\alpha}}g(s)\,ds.\end{aligned} \tag{5.6}$$

It follows from (5.5) and (5.6) that

$$f(t) = f_0 + \left(I^{\alpha}_{0,a,b}g\right)(t),$$

i.e., f is a solution of (5.2).

Suppose now that f satisfies (5.2). Clearly, one has $f \in C^1[0,T]$. Since $g(0)=0$, one has $f(0)=f_0$. On the other hand, an elementary calculation shows that $\left(D^{\alpha}_{0,a,b}f\right)(t)=g(t)$ for all $0<t<T$. Therefore, f is a solution of (5.1). □

Consider now the non-linear initial value problem

$$\begin{cases} \left(D^{\alpha}_{0,a,b}u\right)(t) &= F(t,u(t)), \quad 0<t<T, \\ u(0) &= u_0, \end{cases} \tag{5.7}$$

where the function $F:[0,T]\times\mathbb{R}\to\mathbb{R}$ is continuous and satisfies $F(0,u_0)=0$.

Definition 5.2. *We say that $u\in C[0,T]$ is a weak solution of* (5.7), *if u solves the integral equation*

$$u(t)=u_0+\left(I^{\alpha}_{0,a,b}F(\cdot,u(\cdot))\right)(t), \quad 0\le t\le T,$$

i.e.,

$$u(t)=u_0+\frac{a(1-\alpha)}{a^2+b^2}F(t,u(t)) +\alpha\left(\int_0^t F(\sigma,u(\sigma))\,d\sigma-\frac{b^2}{a^2+b^2}\int_0^t e^{\frac{-a\alpha(t-\sigma)}{1-\alpha}}F(\sigma,u(\sigma))\,d\sigma\right),$$

for all $0\le t\le T$.

Remark 5.1. *Observe that, if $F\in C^1([0,T]\times\mathbb{R})$, and $u\in C^1[0,T]$ is a solution of* (5.7), *then $u\in C[0,T]$ is a weak solution of* (5.7).

Theorem 5.2. *Suppose that*

$$|F(t,\eta)-F(t,\xi)|\le\ell|\eta-\xi|, \quad (\eta,\xi)\in\mathbb{R}^2, \tag{5.8}$$

where $\ell>0$ is a constant. If

$$\ell\left(A_{\alpha}+(\alpha+B_{\alpha})T\right)<1, \tag{5.9}$$

where $A_{\alpha}=\frac{a(1-\alpha)}{a^2+b^2}$ and $B_{\alpha}=\frac{\alpha b^2}{a^2+b^2}$, then (5.7) *admits a unique weak solution $u^*\in C[0,T]$. Moreover, for any $z_0\in C[0,T]$, the Picard sequence $\{z_n\}$ defined by*

$$z_{n+1}(t)=u_0+\frac{a(1-\alpha)}{a^2+b^2}F(t,z_n(t)) +\alpha\left(\int_0^t F(\sigma,z_n(\sigma))\,d\sigma-\frac{b^2}{a^2+b^2}\int_0^t e^{\frac{-a\alpha(t-\sigma)}{1-\alpha}}F(\sigma,z_n(\sigma))\,d\sigma\right),$$

for all $0\le t\le T$, converges uniformly to u^*.

Proof: Consider the self-mapping $H:C[0,T]\to C[0,T]$ defined by

$$(Hu)(t)=u_0+\frac{a(1-\alpha)}{a^2+b^2}F(t,u(t)) +\alpha\left(\int_0^t F(\sigma,u(\sigma))\,d\sigma-\frac{b^2}{a^2+b^2}\int_0^t e^{\frac{-a\alpha(t-\sigma)}{1-\alpha}}F(\sigma,u(\sigma))\,d\sigma\right),$$

for all $0\le t\le T$. We endow $C[0,T]$ with the norm

$$\|u\|_{\infty}=\max\left\{|u(t)|:0\le t\le T\right\}.$$

Then $(C[0,T],\|\cdot\|_{\infty})$ is a Banach space. For all $u,v\in C[0,T]$ and $0\le t\le T$, using (5.8), one has

$$\begin{aligned} &|(Hu)(t)-(Hv)(t)| \\ &\le A_{\alpha}|F(t,u(t))-F(t,v(t)|+\alpha\int_0^t|F(\sigma,u(\sigma))-F(\sigma,v(\sigma))|\,d\sigma \\ &+B_{\alpha}\int_0^t e^{\frac{-a\alpha(t-\sigma)}{1-\alpha}}|F(\sigma,u(\sigma))-F(\sigma,v(\sigma))|\,d\sigma \\ &\le \ell A_{\alpha}\|u-v\|_{\infty}+\alpha\ell T\|u-v\|_{\infty}+B_{\alpha}\ell T\|u-v\|_{\infty} \\ &=\ell\left(A_{\alpha}+(\alpha+B_{\alpha})T\right)\|u-v\|_{\infty}, \end{aligned}$$

which yields

$$\|Hu-Hv\|_{\infty}\le\ell\left(A_{\alpha}+(\alpha+B_{\alpha})T\right)\|u-v\|_{\infty}.$$

Hence by (5.9), one deduces that H is a contraction. Therefore, the result follows from Banach fixed point theorem. □

6. NUMERICAL SOLUTION VIA PICARD ITERATION

Consider the initial value problem

$$\begin{cases} \left(D^{\alpha}_{0,1,1}u\right)(t) &= \frac{u(t)}{3}+e^t, \quad 0<t<1, \\ u(0) &= -3, \end{cases} \tag{6.1}$$

where $0<\alpha<1$. For $\alpha=1$, (6.1) reduces to

$$\begin{cases} u'(t) &= \frac{u(t)}{3}+e^t, \quad 0<t<1, \\ u(0) &= -3. \end{cases} \tag{6.2}$$

The exact solution of (6.2) is given by

$$u_1(t)=\frac{3}{2}e^t-\frac{9}{2}e^{\frac{t}{3}}, \quad 0\le t\le 1.$$

(6.1) is a special case of (5.7) with $T=1$, $a=b=1$, $u_0=-3$ and $F(t,x)=\frac{x}{3}+e^t$. One can check easily that F satisfies (5.8) with $\ell=\frac{1}{3}$. Moreover, one has

$$\ell\left(A_{\alpha}+(\alpha+B_{\alpha})T\right)=\frac{1}{3}\left(\frac{1}{2}+\alpha\right)<1.$$

Hence by Theorem 5.2, (6.1) has a unique weak solution $u^*\in C[0,1]$. Consider now the Picard sequence $\{z_n\}\subset C[0,1]$ given by $z_0(t)=-3$ and

$$z_{n+1}(t)=-3+\frac{(1-\alpha)}{2}F(t,z_n(t)) +\alpha\left(\int_0^t F(\sigma,z_n(\sigma))\,d\sigma-\frac{1}{2}\int_0^t e^{\frac{-\alpha(t-\sigma)}{1-\alpha}}F(\sigma,z_n(\sigma))\,d\sigma\right), \tag{6.3}$$

for all $n=0,1,,2,\cdots$ By Theorem 5.2, the sequence $\{z_n\}$ converges uniformly to u^*. In **Figure 1A**, for $\alpha=0.95$, we plot $u_1(t)$ [the exact solution of (6.2)], $z_1(t)$, $z_3(t)$, and $z_{10}(t)$. In **Figure 1B**, for $\alpha=0.7$, we plot $z_1(t)$, $z_3(t)$, and $z_{10}(t)$.

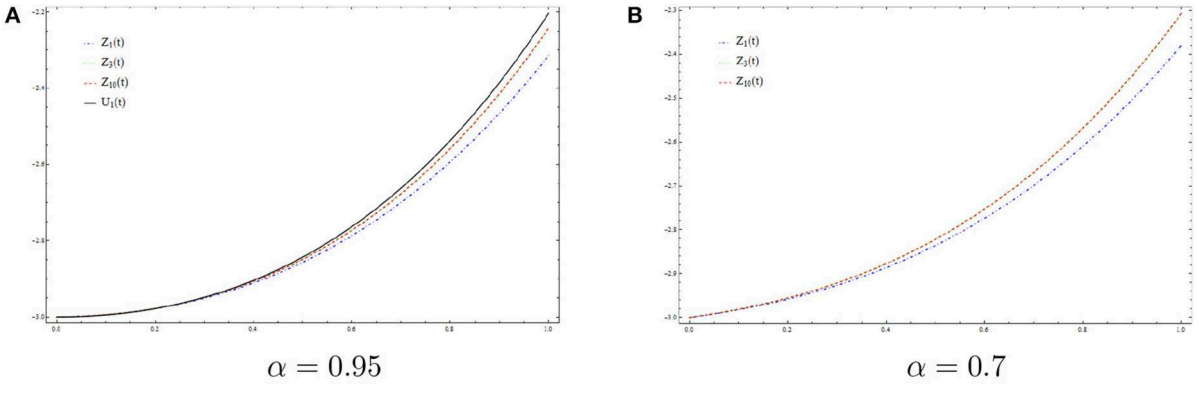

FIGURE 1 | Picard iterations for different values of α. **(A)** $\alpha = 0.95$. **(B)** $\alpha = 0.7$.

7. APPLICATIONS TO RC ELECTRICAL CIRCUITS

In this section, we give some applications to RC electrical circuits using the generalized Caputo-Fabrizio fractional derivative introduced in section 4.

The governing ODE of an RC electrical circuit (see **Figure 2**) is given by

$$\frac{dV(t)}{dt} + \frac{V(t)}{RC} = \frac{\mu(t)}{RC}, \tag{7.1}$$

where V is the voltage, R is the resistance, C is the capacitance and $\mu(t)$ is the source of volt. In this part, we consider a fractional version of (7.1) using the generalized Caputo-Fabrizio fractional derivative introduced in section 4. Namely, using the following transformation suggested in [33]:

$$\frac{d}{dt} \longrightarrow \frac{1}{\sigma^{1-\alpha}} D^{\alpha}_{0,a,b}, \quad a > 0, b \geq 0, \, 0 < \alpha < 1, \tag{7.2}$$

where σ is a positive parameter having dimensions of seconds, we obtain the fractional differential equation

$$\left(D^{\alpha}_{0,a,b} V\right)(t) + \frac{1}{\kappa_{\alpha}} V(t) = \frac{1}{\kappa_{\alpha}} \mu(t), \tag{7.3}$$

where

$$\kappa_{\alpha} = \frac{RC}{\sigma^{1-\alpha}}.$$

We consider (7.3) with the source term

$$\mu(t) = \sin(\phi t)$$

and the initial condition

$$V(0) = 0. \tag{7.4}$$

In this case, (7.3) reduces to

$$\left(D^{\alpha}_{0,a,b} V\right)(t) = AV(t) + B\sin(\phi t),$$

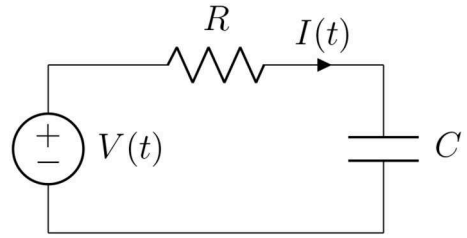

FIGURE 2 | RC circuit.

where $A = -\frac{1}{\kappa_{\alpha}}$ and $B = -A$. Applying the Laplace transform and using Corollary 4.3, one obtains

$$\frac{(a^2+b^2)}{a}\left(s\mathcal{L}\{V(t)\}(s) - V(0)\right)\left[\frac{(1-\alpha)s + \alpha a}{((1-\alpha)s+\alpha a)^2 + b^2\alpha^2}\right] = A\mathcal{L}\{V(t)\}(s) + \frac{B\phi}{s^2+\phi^2}.$$

Using (7.4), it holds

$$\mathcal{L}\{V(t)\}(s) = \frac{B\phi}{s^2+\phi^2}\left(sF_{\alpha,a,b}(s) - A\right)^{-1},$$

where

$$F_{\alpha,a,b}(s) = \frac{(a^2+b^2)}{a}\left[\frac{(1-\alpha)s+\alpha a}{((1-\alpha)s+\alpha a)^2 + b^2\alpha^2}\right]. \tag{7.5}$$

By Laplace transform inverse, one gets

$$V(t) = \mathcal{L}^{-1}\left\{\frac{B\phi}{s^2+\phi^2}\left(sF_{\alpha,a,b}(s) - A\right)^{-1}\right\}(t).$$

Examples. All simulations are obtained using MATLAB 7.5. Consider an RC circuit with $R = 10\Omega$, $C = 0.1F$, $\phi = 15$ and $\sigma = RC\alpha$. In this case, we have $\kappa_{\alpha} = \alpha^{\alpha-1}(RC)^{\alpha}$,

$A = -\alpha^{1-\alpha}(RC)^{-\alpha}$ and $B = \alpha^{1-\alpha}(RC)^{-\alpha}$. **Figure 3** shows the voltage $V(t)$ for different values of α in the case $(a, b) = (1, 0)$ (Caputo-Fabrizio case). **Figure 4** shows the voltage $V(t)$ for different values of α in the case $(a, b) = (2, \sqrt{2})$. **Figure 5** shows the voltage $V(t)$ for different values of α in the case $(a, b) = (10, 3)$.

8. CONCLUSION

In this contribution, we suggested a fractional derivative involving the kernel function

$$k_{a,b}(t,s) = \left(\frac{1}{1-\alpha}\right)\left(\frac{a^2+b^2}{a}\right) e^{-\frac{a\alpha(t-s)}{1-\alpha}} \cos\left(\frac{b\alpha(t-s)}{1-\alpha}\right), \quad a > 0,\ b \geq 0,\ 0 < \alpha < 1.$$

In the particular case $(a, b) = (1, 0)$, the above function reduces to Caputo-Fabrizio kernel. We studied fractional differential equations via this new concept in both theoretical and numerical aspects. In the theoretical point of view, we investigated the existence and uniqueness of solutions to nonlinear fractional boundary value problems involving the new introduced fractional derivative. Namely, using Banach fixed

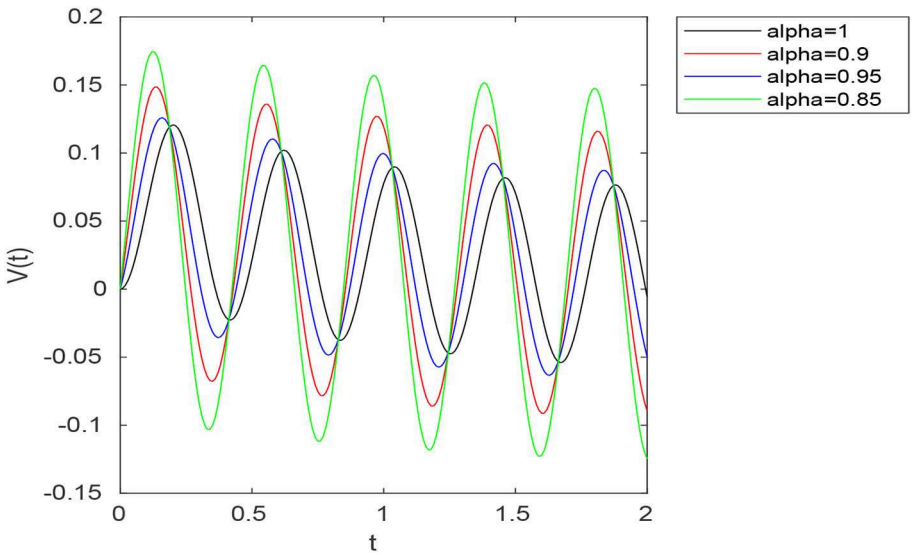

FIGURE 3 | Graph of the voltage in the RC circuit for different values of α with $\mu(t) = \sin(15t)$ and $(a, b) = (1, 0)$.

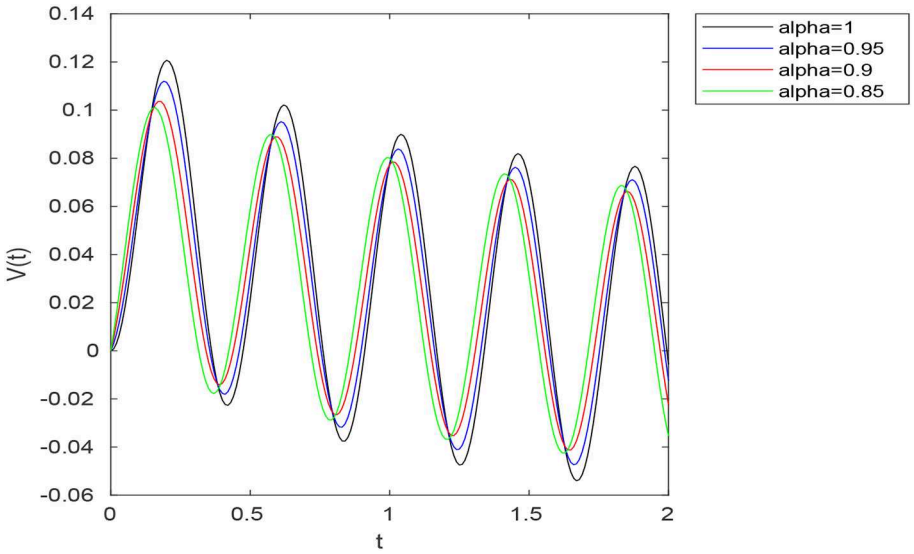

FIGURE 4 | Graph of the voltage in the RC circuit for different values of α with $\mu(t) = \sin(15t)$ and $(a, b) = (2, \sqrt{2})$.

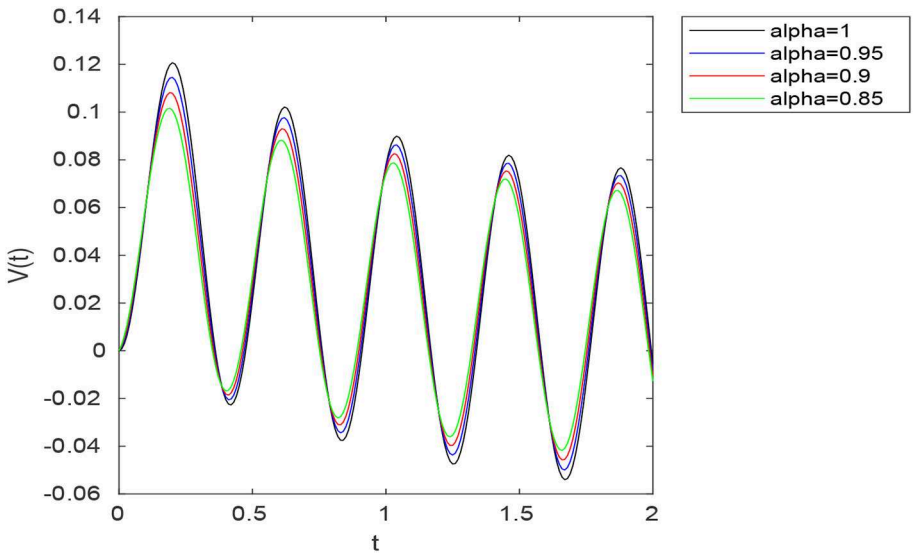

FIGURE 5 | Graph of the voltage in the RC circuit for different values of α with $\mu(t) = \sin(15t)$ and $(a, b) = (10, 3)$.

point theorem, the existence and uniqueness of weak solutions to (5.7) was established under certain conditions imposed on the non-linear term F and the parameters a, b and α. In the numerical point of view, a numerical algorithm based on Picard iterations was proposed for solving the considered problem. Numerical experiments were provided using as a model example the fractional boundary value problem (6.1). In **Figure 1**, we presented the exact solution $(u_1(t))$ for $\alpha = 1$ and numerical solutions $z_1(t), z_3(t)$, and $z_{10}(t)$ to (6.1) for $\alpha \in \{0.95, 0.7\}$. One observes that for $n = 10$, $z_n(t)$ is close enough to $u_1(t)$, which confirms the convergence of the proposed algorithm. Finally, as application, we proposed a fractional model of an RC electrical circuit using the new introduced fractional derivative. One can compare the voltage $V(t)$ obtained for different values of α in the Caputo-Fabrizio case $(a, b) = (1, 0)$ (see **Figure 3**) with that obtained using different values of (a, b) (see **Figures 4**, **5**). Namely, one can show that the voltage $V(t)$ obtained with the use of the generalized fractional Caputo-Fabrizio derivative is more stable with respect to α than that obtained with the use of Caputo-Fabrizio fractional derivative.

DATA AVAILABILITY STATEMENT

All datasets generated for this study are included in the article/supplementary material.

AUTHOR CONTRIBUTIONS

All authors listed have made a substantial, direct and intellectual contribution to the work, and approved it for publication.

FUNDING

BS was supported by Researchers Supporting Project RSP-2019/4, King Saud University, Riyadh, Saudi Arabia.

REFERENCES

1. Frunzo L, Garra R, Giusti A, Luongo V. Modeling biological systems with an improved fractional Gompertz law. *Commun Nonlinear Sci Num.* (2019) **74**:260–7. doi: 10.1016/j.cnsns.2019.03.024
2. Gao W, Veeresha P, Prakasha D, Baskonus HM, Yel G. A powerful approach for fractional Drinfeld-Sokolov-Wilson equation with Mittag-Leffler law. *Alex Eng J.* (2019) **58**:1301–11. doi: 10.1016/j.aej.2019.11.002
3. Gao W, Yel G, Baskonus HM, Cattani C. Complex solitons in the conformable (2+1)-dimensional Ablowitz-Kaup-Newell-Segur equation. *AIMS Math.* (2020) **5**:507–21. doi: 10.3934/math.2020034
4. Jleli M, Kirane M, Samet B. A numerical approach based on ln-shifted Legendre polynomials for solving a fractional model of pollution. *Math Methods Appl Sci.* (2017) **40**:7356–67. doi: 10.1002/mma.4534
5. Qin S, Liu F, Turner I, Yang Q, Yu Q. Modelling anomalous diffusion using fractional Bloch-Torrey equations on approximate irregular domains. *Comput Math Appl.* (2018) **75**:7–21. doi: 10.1016/j.camwa.2017.08.032
6. Song F, Yang H. Modeling and analysis of fractional neutral disturbance waves in arterial vessels. *Math Model Nat Phenom.* (2019) **14**:301. doi: 10.1051/mmnp/2018072
7. Srivastava H, Gunerhan H. Analytical and approximate solutions of fractional-order susceptible-infected-recovered epidemic model of childhood disease. *Math Methods Appl Sci.* (2019) **42**:935–41. doi: 10.1002/mma.5396
8. Srivastava H, Saad K. Some new models of the time-fractional gas dynamics equation. *Adv Math Model Appl.* (2018) **3**:5–17.
9. Yang X, Machado J, Baleanu D. Exact traveling-wave solution for local fractional Boussinesq equation in fractal domain. *Fractals.* (2018) **25**:1740006. doi: 10.1142/S0218348X17400060
10. Yang X, Mahmoud A, Cattani C. A new general fractional-order derivative with Rabotnov fractional-exponential kernel applied to model the anomalous heat transfer. *Therm Sci.* (2019) **23**:1677–81. doi: 10.2298/TSCI180825254Y
11. Machado J, Kiryakova V, Mainardi F. Recent history of fractional calculus. *Commun Nonlinear Sci Numer Simul.* (2011) **16**:1140–53. doi: 10.1016/j.cnsns.2010.05.027

12. Caputo M, Fabrizio M. A new definition of fractional derivative without singular kernel. *Progr Fract Differ Appl.* (2015) **1**:1–13. doi: 10.12785/pfda/010201
13. Ali F, Saqib M, Khan I, Sheikh N. Application of Caputo-Fabrizio derivatives to MHD free convection flow of generalized Walters'-B fluid model. *Eur Phys J Plus.* (2016) **131**:377. doi: 10.1140/epjp/i2016-16377-x
14. Atangana A. On the new fractional derivative and application to nonlinear Fisher's reaction-diffusion equation. *Appl Math Comput.* (2016) **273**:948–56. doi: 10.1016/j.amc.2015.10.021
15. Bhatter S, Mathur A, Kumar D, Singh J. A new analysis of fractional Drinfeld–Sokolov–Wilson model with exponential memory. *Phys A.* (2020) **573**:122578. doi: 10.1016/j.physa.2019.122578
16. Caputo M, Fabrizio M. Applications of new time and spatial fractional derivatives with exponential kernels. *Progr Fract Differ Appl.* (2016) **2**:1–11. doi: 10.18576/pfda/020101
17. Gao F, Yang XJ. Fractional Maxwell fluid with fractional derivative without singular kernel. *Therm Sci.* (2016) **20**:871–7. doi: 10.2298/TSCI16S3871G
18. Gómez-Aguilar J, Yépez-Martinez H, Calderón-Ramón C, Cruz-Orduna I, Escobar-Jiménez R, Olivares-Peregrinoictor V. Modeling of a mass-spring-damper system by fractional derivatives with and without a singular kernel. *Entropy.* (2015) **17**:6289–303. doi: 10.3390/e17096289
19. Hristov J. Transient heat diffusion with a non-singular fading memory: from the Cattaneo constitutive equation with Jeffrey's kernel to the Caputo-Fabrizio time-fractional derivative. *Therm Sci.* (2016) **20**:765–70. doi: 10.2298/TSCI160112019H
20. Kumar D, Singh J, Al Qurashi ADB. A new fractional SIRS-SI malaria disease model with application of vaccines, antimalarial drugs, and spraying. *Adv Differ Equat.* (2019) **2019**:278. doi: 10.1186/s13662-019-2199-9
21. Kumar D, Singh J, Baleanu D, Sushila D. Analysis of regularized long-wave equation associated with a new fractional operator with Mittag-Leffler type kernel. *Phys A.* (2018) **492**:155–67. doi: 10.1016/j.physa.2017.10.002
22. Kumar D, Singh J, Tanwar K, Baleanu D. A new fractional exothermic reactions model having constant heat source in porous media with power, exponential and Mittag-Leffler laws. *Int J Heat Mass Transf.* (2019) **138**:1222–7. doi: 10.1016/j.ijheatmasstransfer.2019.04.094
23. Losada J, Nieto J. Properties of a new fractional derivative without singular kernel. *Progr Fract Differ Appl.* (2015) **1**:87–92. doi: 10.12785/pfda/010202
24. Singh J, Kumar D, Baleanu D. New aspects of fractional Biswas-Milovic model with Mittag-Leffler law. *Math Model Nat Phenom.* (2019) **14**:303. doi: 10.1051/mmnp/2018068
25. Atangana A, Baleanu D. New fractional derivative with non-local and non-singular kernel. *Therm Sci.* (2016) **20**:757–63. doi: 10.2298/TSCI160111018A
26. Gao W, Ghanbari B, Baskonus HM. New numerical simulations for some real world problems with Atangana-Baleanu fractional derivative. *Chaos Solit Fract.* (2019) **128**:34–43. doi: 10.1016/j.chaos.2019.07.037
27. Jarad F, Abdeljawad T, Hammouch Z. On a class of ordinary differential equations in the frame of Atangana-Baleanu fractional derivative. *Chaos Solit Fract.* (2019) **117**:16–20. doi: 10.1016/j.chaos.2018.10.006
28. Kumar D, Singh J, Baleanu D. On the analysis of vibration equation involving a fractional derivative with Mittag-Leffler law. *Math Methods Appl Sci.* (2019) **43**:443–57. doi: 10.1002/mma.5903
29. Singh J, Kumar D, Hammouch Z, Atangana A. A fractional epidemiological model for computer viruses pertaining to a new fractional derivative. *Appl Math Comput.* (2018) **316**:504–15. doi: 10.1016/j.amc.2017.08.048
30. Folland GB. *Fourier Analysis and Its Applications*. Providence, RI: American Mathematical Society (1992).
31. Schiff J. *The Laplace Transform: Theory and Applications*. New York, NY: Springer (2013).
32. Abramowitz M, Stegun I. *Handbook of Mathematical Functions With Formulas, Graphs, and Mathematical Tables*. New York, NY: Dover (1972).
33. Gómez-Aguilar J, Razo-Hernández R, Granados-Lieberman D. A physical interpretation of fractional calculus in observables terms: analysis of the fractional time constant and the transitory response. *Rev Mex Fis.* (2014) **60**:32–8.

Conflict of Interest: The authors declare that the research was conducted in the absence of any commercial or financial relationships that could be construed as a potential conflict of interest.

Copyright © 2020 Alshabanat, Jleli, Kumar and Samet. This is an open-access article distributed under the terms of the Creative Commons Attribution License (CC BY). The use, distribution or reproduction in other forums is permitted, provided the original author(s) and the copyright owner(s) are credited and that the original publication in this journal is cited, in accordance with accepted academic practice. No use, distribution or reproduction is permitted which does not comply with these terms.

frontiers in Physics

ORIGINAL RESEARCH
published: 30 April 2020
doi: 10.3389/fphy.2020.00120

Numerical Investigation of the Fractional-Order Liénard and Duffing Equations Arising in Oscillating Circuit Theory

Harendra Singh[1]* *and H. M. Srivastava*[2,3,4]*

[1] Department of Mathematics, Post Graduate College, Ghazipur, Ghazipur, India, [2] Department of Mathematics and Statistics, University of Victoria, Victoria, BC, Canada, [3] Department of Medical Research, China Medical University Hospital, China Medical University, Taichung, China, [4] Department of Mathematics and Informatics, Azerbaijan University, Baku, Azerbaijan

In this article, we present the Jacobi spectral colocation method to solve the fractional model of Liénard and Duffing equations with the Liouville–Caputo fractional derivative. These equations are the generalization of the spring–mass system equation and describe the oscillating circuit. The main reason for using this technique is high accuracy and low computational cost compared to some other methods. The main solution behaviors of these equations are due to fractional orders, which are explained graphically. The convergence analysis of the proposed method is also provided. A comparison is made between the exact and approximate solutions.

Keywords: fractional Liénard equation, fractional Duffing equation, spectral colocation method, Jacobi polynomials, convergence analysis

OPEN ACCESS

Edited by:
Jordan Yankov Hristov, University of Chemical Technology and Metallurgy, Bulgaria

Reviewed by:
Devendra Kumar, University of Rajasthan, India
Yasir Khan, Zhejiang University, China

***Correspondence:**
Harendra Singh
harendra059@gmail.com
H. M. Srivastava
harimsri@math.uvic.ca

Specialty section:
This article was submitted to Mathematical Physics, a section of the journal Frontiers in Physics

Received: *11 January 2020*
Accepted: *25 March 2020*
Published: *30 April 2020*

Citation:
Singh H and Srivastava HM (2020) Numerical Investigation of the Fractional-Order Liénard and Duffing Equations Arising in Oscillating Circuit Theory. Front. Phys. 8:120. doi: 10.3389/fphy.2020.00120

INTRODUCTION

The standard Liénard equation (LE) is a generalization of the damped pendulum equation or spring–mass system. Because this equation can be applied to describe the oscillating circuits, therefore, it is used in the development of radio and vacuum-tube technology. The LE was given by Liénard [1], and it is written as follows:

$$D''v + \tau_1(v)\,D'v + \tau_2(v) = \tau_3(t), \tag{1}$$

where $\tau_1(v)\,D'v$ is the damping force, $\tau_2(v)$ is the restoring force, and $\tau_3(t)$ is the external force. For different choices of the variable coefficients $\tau_1(v)$, $\tau_2(v)$, and $\tau_3(t)$, the LE is used in many phenomena. The Liénard Equation (1) becomes the van der Pol equation for $\tau_1(v) = \varepsilon\left(v^2 - 1\right)$, $\tau_2(v) = v$, and $\tau_3(t) = 0$, which has many applications [2, 3].

By usual way, we cannot find the exact solution for these equations [4]. Kong [5] studied the LE given as follows:

$$D''v + aD'v + bv^3 + cv^5 = 0, \tag{2}$$

where a, b, and c are real constants.

In particular, if we take $c = 0$ in the LE, then it reduces to the Duffing equation (DE). This special case of the LE is known as the DE and is given as follows;

$$D''v + aD'v + dv + bv^3 = 0, \tag{3}$$

where a, d, and b are real constants.

In recent years, fractional calculus has become an interesting and useful part of mathematical analysis and applied mathematics. The importance of fractional calculus arises because of its non-local nature. The real-life applications of fractional calculus are in fluid dynamics [6], signal processing [7], chemistry [8], viscoelasticity [9], and bioengineering [10]. For some other applications, see Srivastava et al. [11], Kilbas et al. [12], and Robinson [13]. Many physical problems are modeled by fractional-order LE (FLE) and DE. In addition, we are familiar with the fact that non-integer-order derivatives handle models accurately. So, for the accurate modeling of these equations, it is fundamentally needed to change integer-order equations to fractional-order equations.

Fractional-Order Liénard Equation

The FLE is given by

$$D^{\alpha}v(t) + aD'v + bv^3 + cv^5 = 0, 1 < \alpha \leq 2, \ \ t \in [0,1], \quad (4)$$

with the conditions:

$$v(0) = \xi, \quad v'(0) = \eta, \quad (5)$$

where ξ and η are real constants.

Fractional-Order DE

The fractional-order DE (FDE) is given by

$$D^{\beta}v(t) + aD'v + dv + bv^3 = 0, 1 < \beta \leq 2, \ \ t \in [0,1], \quad (6)$$

with the following conditions:

$$v(0) = \mu, \quad v'(0) = \sigma, \quad (7)$$

where μ and σ are real constants.

The innovator approach to solve the LE originates in the work by Kong [5], who provided an exact solution of these equations in some particular cases. For some particular choices of the involved real constants, Feng [14] obtained an exact solution of these equations, which were the generalization of Kong's [5] results. In 2008, Matinfar et al. [15] suggested a variational iteration method in order to obtain the approximate solutions of the LE. Subsequently, in 2011, a variational homotopy perturbation method was applied in order to solve LE (see Matinfar et al. [16]). Recently in 2017, a numerical method using homotopy analysis transform method (HATM) in order to solve fractional LE was proposed, and the uniqueness and existence of solutions were also given (see Kumar et al. [17]). Further, Singh [18, 19] used Legendre polynomials and Chebyshev polynomials, respectively, to solve fractional models of these equations.

In this article, we propose an effective method for the FLE and DE. The proposed method is a spectral colocation method based on the applications of operational matrix of differentiation for the Jacobi polynomials. Spectral colocation method is used to solve many problems in differential calculus (see [20–29]). By using the spectral colocation method, these equations are converted into a system of non-linear algebraic equations whose solution gives approximate solution to these equations. The derived solution is discussed for different fractional orders. The obtained results are compared with the exact solution and presented in the form of numerical tables. Because fractional order derivatives are non-local in nature, and integer-order derivatives are a special case of fractional order derivative, it is important to study fractional order models. The proposed method is easy to implement because it is computer oriented. It is also a time-saving method. The integer as well as fractional order behavior of solution is shown in numerical section. The main solution behaviors of these equations are due to fractional orders, and using the proposed method, these behaviors of solution are explained clearly.

PRELIMINARIES

In this article, we have considered the non-integer-order differentiations in Liouville–Caputo (LC) sense, which are defined as follows:

Definition 2.1 The LC non-integer derivative of order β is defined as follows [30, 31]:

$$D^{\beta}f(x) = I^{l-\beta}D^{l}f(x) = \frac{1}{(l-\beta)}\int_0^x (x-t)^{l-\beta-1}\frac{d^l}{dt^l}f(t)dt,$$
$$l-1 < \beta < l, x > 0. \quad (8)$$

In this article, we have used Jacobi polynomials as a basis for the approximation of unknown functions. The shifted Jacobi polynomial is given as follows [32–34]:

$$\lambda_i^{(e,f)}(t) = \sum_{k=0}^{i}(-1)^{i-k}\frac{\Gamma(\mathrm{i}+\mathrm{f}+1)\,\Gamma(\mathrm{i}+\mathrm{k}+\mathrm{e}+\mathrm{f}+1)}{\Gamma(\mathrm{k}+\mathrm{f}+1)\,\Gamma(\mathrm{i}+\mathrm{e}+\mathrm{f}+1)(\mathrm{i}-\mathrm{k})!\mathrm{k}!}t^k, \quad (9)$$

where e and f are parameters in Jacobi polynomials as given in Doha et al. [32].

The orthogonal property of Jacobi polynomials is as follows:

$$\int_0^1 \lambda_n^{(e,f)}(t)\,\lambda_m^{(e,f)}(t)\,g^{(e,f)}(t)\,dt = v_n^{e,f}\delta_{mn}, \quad (10)$$

where $g^{(e,f)}(t)$ is weight function, and δ_{mn} is kronecker delta function and given as

$$g^{(e,f)}(t) = (1-t)^e t^f \text{ and } v_n^{e,f} = \frac{\Gamma(n+e+1)\,\Gamma(n+f+1)}{(2n+e+f+1)\,n!\Gamma(n+e+f+1)}. \quad (11)$$

A function $f \in L_g^2[0,1]$, with $|f''(t)| \leq A$, can be expanded as follows:

$$f(t) = \lim_{n\to\infty}\sum_{i=0}^{n} c_i\lambda_i^{(e,f)}(t), \quad (12)$$

where $f(t) = \langle c_i, \lambda_i^{(e,f)}(t)\rangle$, and $\langle .,. \rangle$ denotes the usual inner product space.

Equation (12), for finite dimensional approximation, is written as follows:

$$f \cong \sum_{i=0}^{m} c_i \lambda_i^{(e,f)}(t) = C^T p_m(t), \tag{13}$$

where C and $p_m(t)$ are $(m+1)\times 1$ matrices given by

$$C = [c_0, c_1, \ldots, c_m]^T \text{and } p_m(t) = [\lambda_0^{(e,f)}, \lambda_1^{(e,f)}, \ldots, \lambda_m^{(e,f)}]^T. \tag{14}$$

Theorem 1. *If* $p_n(t) = [\lambda_0^{(e,f)}, \lambda_1^{(e,f)}, \ldots, \lambda_n^{(e,f)}]^T$ be the shifted Jacobi vector and *if* $\nu > 0$, then

$$D^{\nu}\lambda_i^{(e,f)}(t) = D^{(\nu)} p_n(t), \tag{15}$$

where $D^{(\nu)} = \left(q(i,j)\right)$ is an $(n+1)\times(n+1)$ operational matrix of non-integer derivative of order ν, and its entries are given by

$$q(i,j,e,f) = \sum_{k=[\nu]}^{i} (-1)^{i-k} \frac{\Gamma(i+f+1)\,\Gamma(i+k+e+f+1)}{(i-k)!\;\Gamma(k+f+1)\,\Gamma(i+e+f+1)\,\Gamma(k-\nu+1)}$$
$$\times \sum_{l=0}^{j} (-1)^{j-l} \frac{\Gamma(e+1)\,\Gamma(j+l+e+f+1)\,\Gamma(k+l-\nu+f+1)\,(2j+e+f+1)\,j!}{(j-l)!(l)!\;\Gamma(j+e+1)\,\Gamma(l+f+1)\,\Gamma(k+l-\nu+e+f+2)}.$$

Proof. See Doha et al. [32], Ahmadian et al. [33], and Bhrawy et al. [34].

OUTLINE OF THE METHOD

Here, we will describe the algorithm for the construction of the solution for the fractional LE and DE using operational matrix and colocation method [27–29]. Let us take the following approximation:

$$\nu(t) = \sum_{i=0}^{n} c_i \lambda_i^{(e,f)}(t) = C^T p_n(t). \tag{16}$$

Then, by taking the derivative of order one on both sides of Equation (16), we get

$$D'\nu(t) = C^T D' p_n(t) \cong C^T D^{(1)} p_n(t), \tag{17}$$

where $D^{(1)}$ is the operational matrix of differentiations for the Jacobi polynomials of order 1.

Next, by taking the derivatives of orders α and β on both sides of Equation (16), we find that

$$D^{\alpha}\nu(t) = C^T D^{\alpha} p_n(t) \cong C^T D^{(\alpha)} p_n(t) \tag{18}$$
$$D^{\beta}\nu(t) = C^T D^{\beta} p_n(t) \cong C^T D^{(\beta)} p_n(t), \tag{19}$$

where $D^{(\alpha)}$ and $D^{(\beta)}$ are the operational matrices of differentiations for the Jacobi polynomials of orders α and β, respectively.

From Equations (16) and (17), we can write,

$$\nu(0) = C^T p_n(0), \tag{20}$$
$$\nu'(0) = C^T D^{(1)} p_n(0), \tag{21}$$

Fractional-Order LE

Grouping Equations (4) and (16)–(18), we get

$$C^T D^{(\alpha)} p_n(t) + a C^T D^{(1)} p_n(t) + b(C^T p_n(t))^3 + c(C^T p_n(t))^5 = 0. \tag{22}$$

The residual for Equation (22) is given as follows:

$$R_n(t) = C^T D^{(\alpha)} p_n(t) + a C^T D^{(1)} p_n(t) + b(C^T p_n(t))^3 + c(C^T p_n(t))^5. \tag{23}$$

Now, colocating Equation (23) at $n-1$ points given by $t_i = \frac{i}{n}$, $i = 1, 2, \ldots, n-1$, we find that

$$R_n(t_i) = C^T D^{(\alpha)} p_n(t_i) + a C^T D^{(1)} p_n(t_i) + b(C^T p_n(t_i))^3 + c(C^T p_n(t_i))^5. \tag{24}$$

Further, from Equations (5), (20), and (21), we can write

$$C^T p_n(0) = \xi, \quad C^T D^{(1)} p_n(0) = \eta, \tag{25}$$

where ξ and η are real constants.

Using the colocation points in Equation (24), together with Equation (25), we get a system of non-linear algebraic equations with the same number of unknowns. The solution of this system leads the solution for FLE.

Fractional-Order DE

Grouping Equations (6), (16), (17), and (19), we get

$$C^T D^{(\beta)} p_n(t) + a C^T D^{(1)} p_n(t) + d C^T p_n(t) + b(C^T p_n(t))^3 = 0. \tag{26}$$

The residual for Equation (26) is given as follows:

$$R_n(t) = C^T D^{(\beta)} p_n(t) + a C^T D^{(1)} p_n(t) + d C^T p_n(t) + b(C^T p_n(t))^3. \tag{27}$$

Now, colocating Equation (27) at the $n-1$ points given by $t_i = \frac{i}{n}$, $i = 1, 2, \ldots, n-1$, we get

$$R_n(t_i) = C^T D^{(\beta)} p_n(t_i) + a C^T D^{(1)} p_n(t_i) + d C^T p_n(t_i) + b(C^T p_n(t_i))^3. \tag{28}$$

Further, from Equations (7), (20), and (21), we can write

$$C^T p_n(0) = \mu, \quad C^T D^{(1)} p_n(0) = \sigma, \tag{29}$$

where μ and σ are real constants.

By using the colocation points in Equation (28), together with the Equation (29), we get a system of equations with the same number of unknowns. The solution of this system leads the approximate solution for the FDE.

CONVERGENCE ANALYSIS

Theorem 4.1. Let the function $v:[0,1] \to R$, and $v \in C^{(n+1)}[0,1]$ and $v_n(t)$ be the n^{th} approximation obtained by using Jacobi polynomials, then

$$E^g_{v,\,n} = ||v - v_n||_{L^2_g[0,1]}, \tag{30}$$

and the error vector in Equation (30) tends to zero as $n \to \infty$.

Proof: See Rivlin [35], Kreyszig [36], and Behroozifar and Sazmand [37].

Theorem 4.2. If $E^{\alpha,\,g}_{D,\,n}$ be the error vector for α order operational matrix integration, which is obtained using $(n+1)$ Jacobi polynomials. Then

$$E^{\alpha,\,g}_{D,\,n} = D^{(\alpha)} p_n(t) - D^{\alpha} p_n(t), \tag{31}$$

and the error vector in Equation (31) tends to zero as $n \to \infty$.

Proof: See Kazem [38].

Let V_n be the n-dimensional subspace generated by $\left(\lambda_i^{(e,f)}\right)_{0 \le i \le n}$ for $L^2_g[0,1]$. Let δ_n is the minimum value of the functional on the space V_n. We can write

$$V_n \subset V_{n+1} \text{ and } \delta_{n+1} \ge \delta_n.$$

Theorem 4.3. Consider the functional L, then

$$\lim_{n\to\infty} \delta_n(t) = \delta(t) = \inf_{t\in[0,1]} L(t).$$

Proof: See Ezz-Eldien [39].

Functional for FLE is given as follows:

$$L(t) = D^{\alpha} v(t) + aD'v + bv^3 + cv^5 = 0. \tag{32}$$

Using Equations (16)–(18), we get

$$L^{(E)}(t) = C^T D^{(\alpha)} p_n(t) + E^{\alpha,\,g}_{D,\,n} + aC^T D^{(1)} p_n(t) + aE^{1,\,g}_{D,\,n} + b(C^T p_n(t) + E^g_{v,\,n})^3 + c(C^T p_n(t) + E^g_{v,\,n})^5. \tag{33}$$

where

$$E^g_{v,\,n} = C^T p(t) - C^T p_n(t), \tag{34}$$

$$E^{\alpha,\,g}_{D,\,n} = D^{(\alpha)} p_n(t) - D^{\alpha} p_n(t), \tag{35}$$

$$E^{1,\,g}_{D,\,n} = D^{(1)} p_n(t) - D^{1} p_n(t). \tag{36}$$

Residual for Equation (33), is given as

$$R^{(E)}_n(t) = C^T D^{(\alpha)} p_n(t) + E^{\alpha,\,g}_{D,\,n} + aC^T D^{(1)} p_n(t) + aE^{1,\,g}_{D,\,n} + b(C^T p_n(t) + E^g_{v,\,n})^3 + c(C^T p_n(t) + E^g_{v,\,n})^5. \tag{37}$$

Now, similar as in Equation (23), colocating Equation (37), at $n-1$ points given by $t_i = \frac{i}{n}, \quad i = 1, 2, \ldots, n-1$, we get

$$R^{(E)}_n(t_i) = 0. \tag{38}$$

Using the colocation points in Equation (37), together with Equation (25), we get a system of non-linear algebraic equations. The solution of this system leads the solution for FLE. Let this solution be denoted by $\delta^*_n(t)$.

Using Theorems 4.1 and 4.2 and taking $n \to \infty$,

$$\delta^*_n(t) \to \delta_n(t). \tag{39}$$

From Theorem 4.3 and Equation (39), we achieve that

$$\lim_{n\to\infty} \delta^*_n(t) = \delta(t).$$

Proof completed. Similar proof can be written for convergence of DE.

NUMERICAL SIMULATION OF RESULTS

In this section, we implement our proposed algorithm by testing it on some special cases of the LE and DE. We study the applicability and accuracy of our proposed computational method by applying it on the FLE and DE. The parameters in the LE and DE are chosen in such a way for which the exact solution is known.

Case 1. For the particular choices of the parameters $a = -1$, $b = 4$ and $c = 3$ in Equation (4), the FLE is given as follows (see Singh [18] and Tohidi et al. [20]):

$$D^{\alpha} v(t) - D'v + 4v^3 + 3v^5 = 0, 1 < \alpha \le 2, \tag{40}$$

$$v(0) = \xi = \sqrt{\frac{\tau}{2+\delta}} \text{ and } v'(0) = \eta = 0, \tag{41}$$

where

$$\tau = 4\sqrt{\frac{3a^2}{3b^2 - 16ac}} \text{and } \delta = -1 + \frac{\sqrt{3}b}{\sqrt{(3b^2 - 16ac)}}. \tag{42}$$

The exact solution for the FLE given by Equation (40), with conditions in Equation (41), is given by

$$v(t) = \sqrt{\frac{\tau\ sech^2\sqrt{-a}t}{2 + \delta\ sech^2\sqrt{-a}t}}, \text{at } \alpha = 2, \tag{43}$$

where τ and δ are as given in Equation (42).

In **Figures 1**, **2**, we have shown the approximate solution for different values of α for the FLE choosing different parameters in the Jacobi polynomials. In **Figure 3**, we have compared

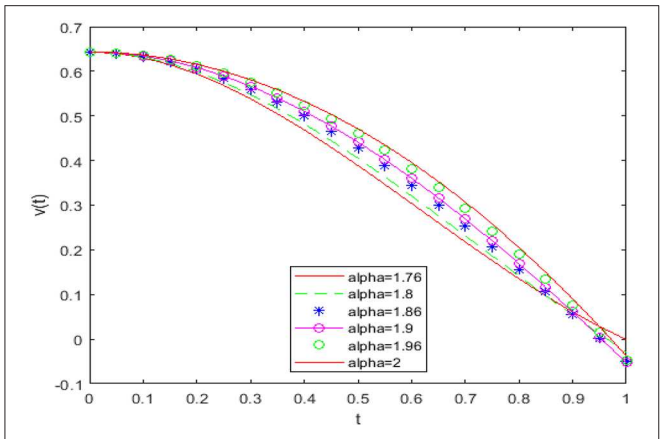

FIGURE 1 | Numerical solutions at $\alpha = 1.76,\ 1.8,\ 1.86,\ 1.9,\ 1.96$, and 2 for case 1 at $e = 1$ and $f = 1$.

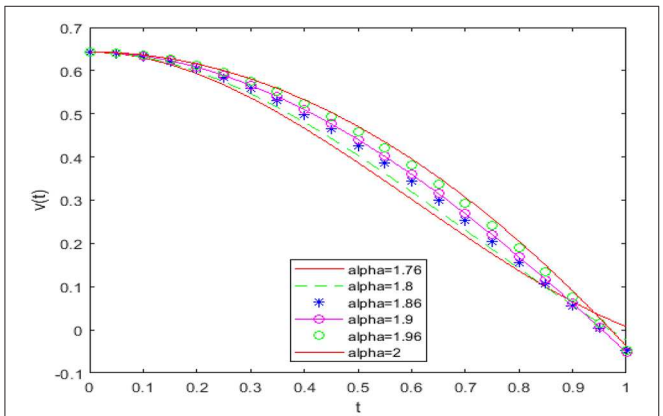

FIGURE 2 | Numerical solutions at $\alpha = 1.76,\ 1.8,\ 1.86,\ 1.9,\ 1.96$, and 2 for case 1 at $e = 0.8$ and $f = 0.8$.

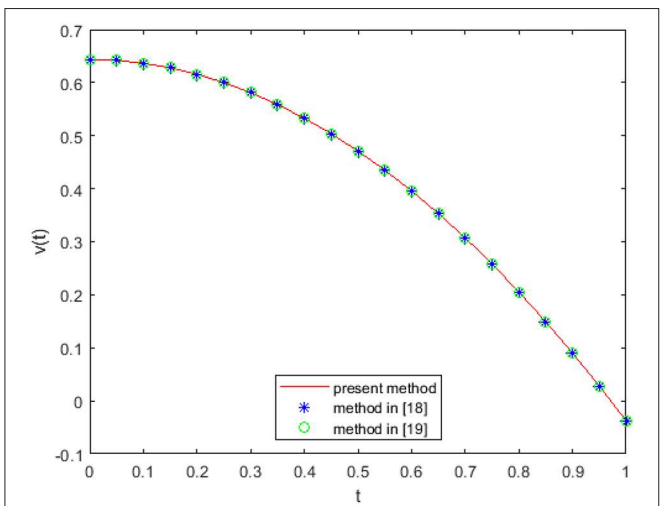

FIGURE 3 | Comparison of solutions at $e = f = 1$ and $\alpha = 2$.

TABLE 1 | Comparison with the exact solution at $\alpha = 2$ and $n = 3$ for Liénard equation.

t	Exact solution	Present method	Absolute error
0.00	0.643594	0.643594	0
0.01	0.643556	0.643524	3.2164e-5
0.02	0.643443	0.643314	1.2861e-4
0.03	0.643255	0.642965	2.8931e-4
0.04	0.642991	0.642477	5.1429e-4
0.05	0.642653	0.641894	8.0360e-4
0.06	0.642239	0.641082	1.1573e-3
0.07	0.641751	0.640176	1.5757e-3
0.08	0.641189	0.639130	2.0589e-3
0.09	0.640553	0.637946	2.6073e-3
0.1	0.639844	0.636623	3.2210e-3

TABLE 2 | Comparison with the methods of Singh [18, 19] at $\alpha = 2$ and $n = 3$ for Liénard equation.

t	Present method	Method Singh [18]	Method in Singh [19]
0.1	0.6366235	0.6366235	0.6366235
0.2	0.6157811	0.6157811	0.6157811
0.3	0.5811714	0.5811714	0.5811714
0.4	0.5328986	0.5328986	0.5328986
0.5	0.4710672	0.4710672	0.4710672
0.6	0.3957817	0.3957817	0.3957817
0.7	0.3071462	0.3071462	0.3071462
0.8	0.2052653	0.2052653	0.2052653
0.9	0.0902432	0.0902432	0.0902432
1	−0.0378154	−0.0378154	−0.0378154

approximate solution by our proposed method and solution obtained by the methods of Singh [18, 19] for integer-order LE.

Figures 1, **2** show that the period will be really affected by the non-integer-order values, and the solution varies continually from non-integer-order solution to integer-order solution and coincides with the integer-order solution at $\alpha = 2$. The solution has some different behavior when the value of fractional order is 1.76, and this is because the main solution behavior of LE takes place when α is very close to 2. **Figure 3** shows that solution has exact the behavior as the methods of Singh [18, 19]. In **Table 1**, we have listed approximate and exact solutions for the integer-order equation. **Table 1** shows a good accuracy of the achieved solution. In **Table 2**, we have listed approximate solution by our method and the methods of Singh [18, 19]. **Table 2** shows good agreement with these methods.

Case 2. For the particular choices of the parameters $a = 0.5$, $b = 25$, and $c = 25$ in Equation (6), the fractional DE is given as follows [see Singh [18, 19] and Nourazar and Mirzabeigy [40]]:

$$D^{\beta}v(t) + 0.5D'v + 25v + 25v^3 = 0, 1 < \beta \leq 2, \tag{44}$$

$$v(0) = \mu = 0.1 \text{ and } v'(0) = \sigma = 0, \tag{45}$$

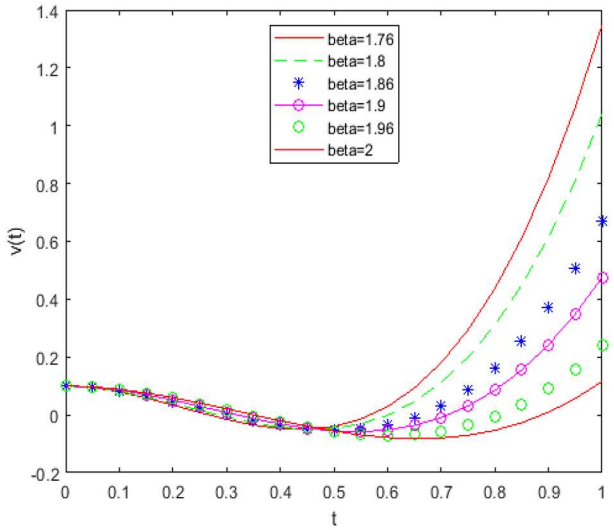

FIGURE 4 | Numerical solutions at $\beta = 1.76,\ 1.8,\ 1.86,\ 1.9,\ 1.96$, and 2 for case 2 at $e = 1$ and $f = 1$.

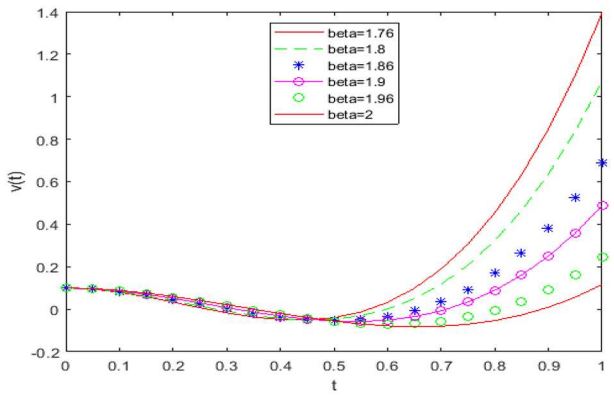

FIGURE 5 | Numerical solutions at $\beta = 1.76,\ 1.8,\ 1.86,\ 1.9,\ 1.96$, and 2 for case 2 at $e = 0.8$ and $f = 0.8$.

The analytical solution using the differential transform method (DTM) for fractional DE given by Equation (44), with the initial conditions in Equation (45), is given by

$$v(t) = 0.1 - 1.2625t^2 + 0.2104t^3 + 2.6828t^4 - 0.5392t^5 - 2.6563t^6 + 0.6152t^7 \text{at } \alpha = 2. \quad (46)$$

In **Figures 4**, **5**, we have shown the behavior of the approximate solution for different values of β for fractional DE for different choices of the parameters in the Jacobi polynomials. In **Figure 6**, we have compared approximate solution by our proposed method and solution obtained by the methods of Singh [18, 19] for integer-order DE.

Figures 4, **5** reveal that the solution varies continually from the fractional-order solution to the integer-order solution and coincides with the integer-order solution at $\beta = 2$. The solution has some different behavior when the value of fractional order is 1.76, and this is because the main solution behavior of DE takes place when β is very close to 2. **Figure 6** shows that solution has the exact behavior as the methods of Singh [18, 19]. In **Table 3**, we have listed the approximate and exact solutions by the DTM method for the integer-order equation. **Table 3** shows a good accuracy of the achieved solution.

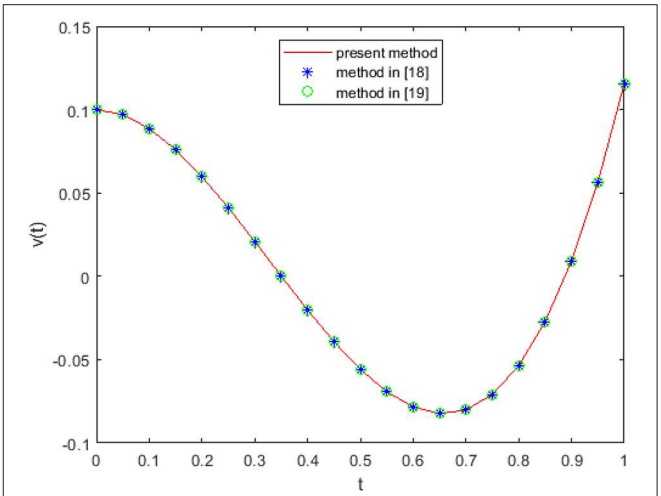

FIGURE 6 | Comparison of solutions at $e = f = 1$ and $\beta = 2$.

TABLE 3 | Comparison between results by our proposed method and DTM [40] for fractional Duffing equation at $\beta = 2$ and $n = 3$ for case 2.

t	Method in Nourazar and Mirzabeigy [40]	Present method	Absolute error
0.00	0.100000	0.100000	0.00000
0.01	0.099874	0.099874	7.0821e-7
0.02	0.099497	0.099502	5.4931e-6
0.03	0.098871	0.098889	1.7960e-5
0.04	0.098002	0.098041	4.1211e-5
0.05	0.096886	0.096964	7.7852e-5
0.06	0.095534	0.095664	1.3001e-4
0.07	0.093949	0.094148	1.9934e-4
0.08	0.092135	0.092422	2.8706e-4
0.09	0.090098	0.090492	3.9394e-4
0.1	0.087845	0.088366	5.2036e-4

CONCLUSIONS

In this article, we have presented numerical solution and simulation for fractional-order and integer-order LE and DE. The proposed algorithm is easy to implement because the construction of the operational matrix is sufficiently easy, which makes our method remarkably attractive for practical applications. In the numerical section, it is presented how the approximate solution varies continuously for different values of the fractional time derivatives and for the integer-order

approximate solution is the same as the exact solution for the fractional LE and DE. Recently, many equations in science and engineering appear in the form of non-linear fractional differential equations, which makes it necessary to investigate the method of solution for such equations. The main advantage of the proposed method is that it works for such type of equations arising in science and engineering. In the future, we can use operational matrices of different orthogonal polynomials to achieve better accuracy.

DATA AVAILABILITY STATEMENT

All datasets generated for this study are included in the article/supplementary material.

AUTHOR CONTRIBUTIONS

All authors listed have made a substantial, direct and intellectual contribution to the work, and approved it for publication.

REFERENCES

1. Liénard A. Etude des oscillations entretenues. *Rev Gen Electr.* (1928) **23**:901–12.
2. Guckenheimer J. Dynamics of the van der pol equation. *IEEE Trans Circ Syst.* (1980) **27**:938–89. doi: 10.1109/TCS.1980.1084738
3. Zhang ZF, Ding T, Huang HW. *Qualitative Theory of Differential Equations*. Peking: Science Press (1985).
4. Hale JK. *Ordinary Differential Equations*. New York, NY: Wiley (1980).
5. Kong D. Explicit exact solutions for the Liénard equation and its applications. *Phys Lett A.* (1995) **196**:301–6 doi: 10.1016/0375-9601(94)00866-N
6. Singh H. A new stable algorithm for fractional Navier-Stokes equation in polar coordinate. *Int J Appl Comput Math.* (2017) **3**:3705–22. doi: 10.1007/s40819-017-0323-7
7. Panda R, Dash M. Fractional generalized splines and signal processing. *Signal Process.* (2006) **86**:2340–50. doi: 10.1016/j.sigpro.2005.10.017
8. Singh H. Operational matrix approach for approximate solution of fractional model of Bloch equation. *J King Saud University Sci.* (2017) **29**:235–40. doi: 10.1016/j.jksus.2016.11.001
9. Bagley RL, Torvik PJ. Fractional calculus in the transient analysis of viscoelasticity damped structures. *AIAA J.* (1985) **23**:918–25. doi: 10.2514/3.9007
10. Magin RL. Fractional calculus in bioengineering. *Critical Rev Biomed Engrg.* (2004) **32**:1–104. doi: 10.1615/CritRevBiomedEng.v32.10
11. Srivastava HM, Shah FA, Abass R. An application of the Gegenbauer wavelet method for the numerical solution of the fractional Bagley-Torvik equation. Russian *J Math Phys.* (2019) **26**:77–93. doi: 10.1134/S1061920819010096
12. Kilbas AA, Srivastava HM, Trujillo JJ. *Theory and Applications of Fractional Differential Equations, North-Holland Mathematical Studies, Vol. 204.* Amsterdam; London; New York, NY: Elsevier (North-Holland) Science Publishers (2006).
13. Robinson AD. The use of control systems analysis in neurophysiology of eye movements. *Ann Rev Neurosci.* (1981) **4**:462–503. doi: 10.1146/annurev.ne.04.030181.002335
14. Feng Z. On explicit exact solutions for the Liénard equation and its applications. *Phys Lett A.* (2002) **239**:50–6. doi: 10.1016/S0375-9601(01)00823-4
15. Matinfar M, Hosseinzadeh H, Ghanbari M. A numerical implementation of the variational iteration method for the Liénard equation. *World J Model Simul.* (2008) **4**:205–10.
16. Matinfar M, Mahdavi M, Raeisy Z. Exact numerical solution of Liénard's equation by the variational homotopy perturbation method. *J Inform Comput Sci.* (2011) **6**:73–80.
17. Kumar D, Agarwal RP, Singh JA. Modified numerical scheme convergence analysis for fractional model of Liénard's equation. *J Comput Appl Math.* **339**:405–13. doi: 10.1016/j.cam.2017.03.011
18. Singh H. An efficient computational method for non-linear fractional Lienard equation arising in oscillating circuits. In: Singh H, Kumar D, Baleanu D, editors. *Methods of Mathematical Modelling: Fractional Differential Equations.* London; New York, NY: CRC Press Taylor and Francis Group (2019).
19. Singh H. Solution of fractional Lienard equation using Chebyshev operational matrix method, nonlinear. *Sci Lett A.* (2017) **8**:397–404.8
20. Tohidi E, Bhrawy AH, Erfani K. A collocation method based on Bernoulli operational matrix for numerical solution of generalized pantograph equation. *Appl Math Model.* (2013) **37**:4283–94. doi: 10.1016/j.apm.2012.09.032
21. Singh H, Srivastava HM, Kumar D. A reliable numerical algorithm for the fractional vibration equation. *Chaos Solitons Fractals.* (2017) **103**:131–8. doi: 10.1016/j.chaos.2017.05.042
22. Kazem S, Abbasbandy S, Kumar S. Fractional order Legendre functions for solving fractional-order differential equations. *Appl Math Model.* **37**:5498–510. doi: 10.1016/j.apm.2012.10.026
23. Singh H. An efficient computational method for the approximate solution of nonlinear Lane-Emden type equations arising in astrophysics. *Astrophys Space Sci.* (2018) **363**:363–71. doi: 10.1007/s10509-018-3286-1
24. Lakestani M, Dehghan M, Pakchin SI. The construction of operational matrix of fractional derivatives using B-spline functions. *Commun Nonlinear Sci Numer Simulat.* (2012) **17**:1149–62. doi: 10.1016/j.cnsns.2011.07.018
25. Wu JL. A wavelet operational method for solving fractional partial differential equations numerically. *Appl Math Comput.* (2009) **214**:31–40. doi: 10.1016/j.amc.2009.03.066
26. Yousefi SA, Behroozifar M, Dehghan M. The operational matrices of Bernstein polynomials for solving the parabolic equation subject to the specification of the mass. *J Comput Appl Math.* (2011) **235**:5272–83. doi: 10.1016/j.cam.2011.05.038
27. Singh H. Approximate solution of fractional vibration equation using Jacobi polynomials. *Appl Math Comput.* (2018) **317**:85–100. doi: 10.1016/j.amc.2017.08.057
28. Singh CS, Singh H, Singh VK, Singh, Om P. Fractional order operational matrix methods for fractional singular integro-differential equation. *Appl Math Model.* (2016) **40**:10705–18. doi: 10.1016/j.apm.2016.08.011
29. Singh H. A new numerical algorithm for fractional model of Bloch equation in nuclear magnetic resonance. *Alexandria Engrg J.* (2016) **55**:2863–9. doi: 10.1016/j.aej.2016.06.032
30. Miller K, Ross B. *An Introduction to Fractional Calculus and Fractional Differential Equations*. New York, NY: John Wiley & Sons Inc (1993).
31. Diethelm K, Ford NJ, Freed AD, Luchko Y. Algorithms for fractional calculus: a selection of numerical methods. *Comput Meth Appl Mech Eng.* (2005) **194**:743–73. doi: 10.1016/j.cma.2004.06.006
32. Doha EH, Bhrawy AH, Baleanu D, Ezz-Eldien SS. The operational matrix formulation of the Jacobi tau approximation for space fractional diffusion equation. *Adv Differ Equ.* (2014) **2014**:231. doi: 10.1186/1687-1847-2014-231
33. Ahmadian A, Suleiman M, Salahshour S, Baleanu D. A Jacobi operational matrix for solving a fuzzy linear fractional differential equation. *Adv Differ Equ.* (2013) **2013**:104. doi: 10.1186/1687-1847-2013-104
34. Bhrawy AH, Tharwat MM, Alghamdi MA. A new operational matrix of fractional integration for shifted Jacobi polynomials. *Bull Malays Math Sci Soc.* (2014) **37:**983.
35. Rivlin TJ. *An Introduction to the Approximation of Functions.* New York, NY: Dover Publications (1981).
36. Kreyszig E. *Introductory Functional Analysis with Applications*. New York, NY: John Wiley and Sons, Inc. (1978).
37. Behroozifar M, Sazmand A. An approximate solution based on Jacobi polynomials for time-fractional convection-diffusion equation. *Appl Math Comp.* (2017) **296:**1–17. doi: 10.1016/j.amc.2016.09.028

38. Kazem S. An integral operational matrix based on Jacobi polynomials for solving fractional-order differential equations. *Appl Math Model.* (2013) **37:**1126–36. doi: 10.1016/j.apm.2012.03.033
39. Ezz-Eldien SS. New quadrature approach based on operational matrix for solving a class of fractional variational problems. *J Comp Phys.* (2016) **317:**362–81. doi: 10.1016/j.jcp.2016.04.045
40. Nourazar S, Mirzabeigy A. Approximate solution for nonlinear Duffing oscillator with damping effect using the modified differential transform method. *Sci Iranica B.* (2013) **20**:364–68.

Conflict of Interest: The authors declare that the research was conducted in the absence of any commercial or financial relationships that could be construed as a potential conflict of interest.

Copyright © 2020 Singh and Srivastava. This is an open-access article distributed under the terms of the Creative Commons Attribution License (CC BY). The use, distribution or reproduction in other forums is permitted, provided the original author(s) and the copyright owner(s) are credited and that the original publication in this journal is cited, in accordance with accepted academic practice. No use, distribution or reproduction is permitted which does not comply with these terms.

frontiers in Physics

ORIGINAL RESEARCH
published: 12 May 2020
doi: 10.3389/fphy.2020.00136

A New Numerical Method for Time Fractional Non-linear Sharma-Tasso-Oliver Equation and Klein-Gordon Equation With Exponential Kernel Law

Sachin Kumar[1]* *and Dumitru Baleanu*[2,3,4]

[1] Department of Mathematics, Govt. M.G.M. College, Itarsi, India, [2] Department of Mathematics, Cankaya University, Ankara, Turkey, [3] Institute of Space Sciences, Magurele-Bucharest, Romania, [4] Department of Medical Research, China Medical University Hospital, China Medical University, Taichung, Taiwan

In this work, we derived a novel numerical scheme to find out the numerical solution of fractional PDEs having Caputo-Fabrizio (C-F) fractional derivatives. We first find out the formula of approximation for the C-F derivative of the function $f(t) = t^K$. We approximate the C-F derivative in time direction with the help of Legendre spectral method and approximation formula of t^K. The unknown function and their derivatives in spatial direction are approximated with the help of the method which is based on a quasi wavelet. We implement this newly derived method to solve the non-linear Sharma-Tasso-Oliver equation and non-linear Klein-Gordon equation in which time-fractional derivative is of C-F type. The accuracy and validity of this new method are depicted by giving the numerical solution of some numerical examples. The numerical results for the particular cases of Klein-Gordon equation are compared with the existing exact solutions and from the obtained error we can conclude that our proposed numerical method achieves accurate results. The effect of time-fractional exponent α on the solution profile is characterized by figures. The comparison of solution profile $u(x, t)$ for different type time-fractional derivative (C-F vs. Caputo) is depicted by figures.

Keywords: fractional PDE, Sharma-Tasso-Oliver equation, Klein-Gordon equation, Caputo-Fabrizio fractional derivative, quasi wavelet, Legendre polynomial

OPEN ACCESS

Edited by:
Horacio Sergio Wio, Institute of Interdisciplinary Physics and Complex Systems (IFISC), Spain

Reviewed by:
Ilyas Khan, Ton Duc Thang University, Vietnam
Devendra Kumar, University of Rajasthan, India

***Correspondence:**
Sachin Kumar
sachinraghav522@gmail.com

Specialty section:
This article was submitted to Mathematical Physics, a section of the journal Frontiers in Physics

Received: *22 November 2019*
Accepted: *07 April 2020*
Published: *12 May 2020*

Citation:
Kumar S and Baleanu D (2020) A New Numerical Method for Time Fractional Non-linear Sharma-Tasso-Oliver Equation and Klein-Gordon Equation With Exponential Kernel Law. Front. Phys. 8:136. doi: 10.3389/fphy.2020.00136

1. INTRODUCTION

In the recent years fractional differential equations have received more attention of the researchers due to its exact description of the physical phenomenon. Many physical phenomenons have been described through fractional diffusion equation viz., transport in porous medium, ground water contamination problem through porous medium etc. As we know as far as fractional calculus is a classical branch of mathematics whose have history like as integer calculus [1]. Its progress is still increasing with day to day. N. H. Abel and J. Liouville have developed the theory of this fractional calculus. We can find wide details of fractional calculus in Kilbas et al. [2] and Podlubny [3]. We are allowed to generalize integer integrals and derivatives to arbitrary and real order with the help of fractional calculus. It is that branch of mathematical analysis that permit us to study operators and equations having integral are singular and convolution type. Many application of this calculus are found in special functions, control theory, computational complexity [4] and stochastic process.

Fractional calculus was assumed to esoteric theory having no applications but a lot of applications to finance, control system and economics have been discovered in last few years.

In literature many types of differential operators have discovered like as Grunwald-Letnikov, Hadamard, Caputo, Riesz, Riemann-Liouville, Caputo-Fabrizio [5, 6] and Atangana-Baleanu derivatives [7–9]. The variable form of above operators have also been introduced. The application of fractional differential equation is go on increasing so researchers started to develop new methods to solve these differential equation numerically as they have to face many problems solve these equations analytically. The methods which are available in literature are as predictor-corrector method [10], Adomain decomposition method [11], homotopy perturbation method [12], generalized block pulse operational matrix method [13], eigen-vector expansion, Adams-Bashforth scheme [14], and fractional differential transform method [15], etc. The operational matrix method is easy and efficient method which is so widely used now a days. This method based on some polynomials and wavelets are available in literature. Haar wavelets [16], Chebyshev wavelets [17], sine wavelets, Legendre wavelets [18] is used to develop for the numerical solutions of integral equations, integro-differential equations and FPDEs. Some polynomials which can be utilized derive the operational matrix are Laguerre polynomial [19], Chebyshev polynomial, Legendre polynomial [20], and Genocchi polynomial [21] which is semi-orthogonal.

The process of diffusion and reaction has been studied from last some years. In the diffusion process the molecules or any other quantity is transferred from the higher concentration region to low concentration region. When the reaction process is happened together with the process of diffusion then combined process is called reaction-diffusion process. In the reaction process more molecules is consumed or created and this term mathematically denoted by adding a reaction term in classical diffusion equation

$$\frac{\partial \varrho}{\partial t} = D\nabla^2 \varrho + R(\varrho, t), \tag{1}$$

where first term on the right hand side presents diffusion process with D diffusion coefficient while $R(\varrho, t)$ characterize the reaction term at space point ϱ and time t. We can extend this reaction -diffusion equation to advection-reaction-diffusion equation where advection term denotes the movement of particle or molecules due to the bulk flow of fluid. Many beautiful an curious phenomena in nature as chemistry, physics, biology, and medical sciences could be depicted by reaction diffusion equation.

A heat transfer analysis in sodium alginate based nanofluid using MoS2 nanoparticles is studied in article [22]. The behavior of normal and tumor cells with the effect of radiotherapy in fractional derivative environment is investigated in Farayola et al. [23]. The De-Levie's model is studied by researchers in Abro et al. [24]. The investigation of heat dissipation in transmission line of electrical circuit is given in Abro et al. [25]. A analysis of generalized Jeffery nanofluid in a rotating frame with non-singular fractional derivative is given in Ali et al. [26]. The behavior of heat transfer in different model with singular and non-singular is given in articles [27–31]. The study of electro-osmotic flow of viscoelastic fluids with non-singular Mittag-Leffler fractional derivative is given in Ali et al. [32]. The Drinfeld-Sokolov-Wilson model with exponential fractional derivative is investigated in article [33]. An analysis of fractional vibration equation with ABC fractional derivative is studied in Kumar et al. [34]. The study of FDEs equations occurring in ion acoustic waves in plasma is done in Goswami et al. [35]. The FDEs is very useful in biological model as SIRS-SI malaria disease model with application of vaccines [36] and fractional equal width equations describing hydro-magnetic waves in cold plasma [37].

We organized our article as follows. The definition of R-L, Caputo, and Caputo-Fabrizio is given in section 2. We also discussed about quasi wavelet and quasi wavelet-based numerical method. In section 3, we derived the general formula of C-F derivative of the function x^k. Some properties of Legendre polynomial is also included in this section. In section 4, we described the proposed method for solving FPDEs with C-F derivative. In section 5, some numerical examples and results are presents including the variation of different parameters. The conclusion of all over the article is given in the last section.

2. PRELIMINARY DEFINITIONS

In the last few years, many definitions of fractional integration and differentiation have come into the light. All of them have own special properties and applications. Caputo's definition is more reliable as compare to Riemann-Liouville's definition as an application point of view. These definitions are with power or singular kernel law. Nowadays many generalized definitions of the fractional derivative with exponential and Mittag-Leffler kernel law have been introduced. We discussed brief definitions and properties of R-L, Caputo and recently developed Caputo-Fabrizio derivative.

2.1. Riemann-Liouville Order Derivative and Integration

The R-L integration of order $\varrho > 0$ of a function $h(t)$ is given by

$$I^{\vartheta} h(z) = \frac{1}{\Gamma(\varrho)} \int_0^z (z-\varpi)^{\varrho-1} h(\varpi)\, d\varpi, \quad z > 0, \quad \vartheta \in R^+. \tag{2}$$

Now Riemann-Liouville fractional order differentiation of a function $h(t)$ with order $\vartheta > 0$ is defined as

$$D_l^{\vartheta} h(t) = (\frac{d}{dt})^m (I^{m-\vartheta} h)(t), \quad (m-1 < \vartheta < m, \quad \vartheta > 0). \tag{3}$$

2.2. Definition of Caputo Derivative

The Caputo derivative of a function $h(t)$ having order $\vartheta > 0$ is given as follows

$$D_c^{\vartheta} h(t) = \begin{cases} \frac{1}{\Gamma(\vartheta)} \int_0^t (-\eta + t)^{-\vartheta-1+l} h^l(\eta)\, d\eta & l-1 < \vartheta < l, \\ \frac{d^l}{dt^l} h(t) & \vartheta = l \in N. \end{cases} \tag{4}$$

with l an integer and time interval $t > 0$.

Some important properties of Caputo differentiation are given as follows

$$D_c^{\vartheta} C = 0, \tag{5}$$

where C is a constant. The fractional differentiation operator D_c^{ϑ} follow the linear property so we have

$$D_c^{\vartheta}(c_1 h(t) + c_2 g(t)) = c_1 D_c^{\vartheta} h(t) + c_2 D_c^{\vartheta} g(t), \tag{6}$$

where c_1 *and* c_2 denotes constants. We can relate the Caputo differential operator and R-L operator as

$$(I^{\vartheta} D_c^{\vartheta} g)(t) = g(t) - \sum_{k=0}^{l-1} g^k(0^+)\frac{t^k}{k!}, \qquad l-1 < \vartheta \leq l. \tag{7}$$

2.3. Definition of Caputo-Fabrizio Derivative [38, 39]

Consider a function $g(t)$ which is a element of Sobolev space $H^1(a,b), b > a$ then C-F derivative of order $n < \vartheta < n+1$ is given as [40]

$$\begin{aligned} {}_0^{CF}D_t^{\vartheta} g(t) &= \frac{B(\vartheta)}{\lceil \vartheta \rceil - \vartheta}\int_0^t \exp\left[\frac{-\vartheta(x,t)}{\lceil \vartheta \rceil - \vartheta}(t-s)\right] \\ &\times \frac{\partial^{n+1} g(s)}{\partial t^{n+1}} ds, \quad n < \vartheta \leq n+1. \end{aligned} \tag{8}$$

Here $B(\vartheta)$ denotes the normalization function. In all our calculations we have taken $B(\vartheta) = 1$.

2.4. Definition of Caputo-Fabrizio Integral

The C-F integral of order $n < \vartheta < n+1$ associated with the function $g(t)$ is defined as follows

$$\begin{aligned} {}_0^{CF}I_t^{\vartheta} g(t) &= \sum_{i=0}^{n} \frac{t^i}{i!} g^{(i)}(0) + \frac{(1-\eta)}{B(\eta)(n-1)!}\int_0^t (t-s)^{n-1} g(s) ds \\ &+ \frac{\eta}{M(\eta) n!}\int_0^t (t-s)^n g(u) du, \end{aligned} \tag{9}$$

where η denotes the fractional part of the order ϑ. If the fractional part $\eta = 0$ then CF integral is given by

$${}_0^{CF}I_x^{\vartheta} g(x) = \frac{(1-\eta)}{B(\eta)} g(x) + \frac{\eta}{M(\eta)}\int_0^t g(u) du. \tag{10}$$

2.5. Why We Are Using C-F Derivative?

The operators play an important role in science and the interchange of these operators is an important property. Let us consider two operators A and B we say these two commutes if they follow the property $AB = BA$. Many operators arising in physics, biology, statistics, and mathematics do not follow the property of commutativity and are called non-commutative operators. We give some examples of non-commutative operators:

- Product of two matrices.
- Division operator on real numbers as $\frac{3}{4} \neq \frac{4}{3}$.
- Linear operators like z and $\frac{d}{dz}$ do not follow the commutative property on wave function $\Psi(y)$ in the case when we formulate the Schrodinger equation in quantum mechanics.
- Lie bracket of Lie ring.
- Lie bracket of a Lie algebra.

The general form of fractional type derivatives in Caputo and Riemann-Liouville form are defined as

$${}_0^{RL}D_z^{\vartheta} g(z) = \frac{d}{dz}\int_0^z \kappa(z-x) g(z) dz \frac{d}{dz}\kappa * g,$$

$${}_0^{C}D_z^{\vartheta} g(z) = \int_0^z \kappa(z-x)\frac{d}{dz} g(z) dz = \kappa * \frac{d}{dz} g.$$

In fractional calculus, many form of kernel is discovered as $\kappa(z-x) = \frac{1}{\Gamma(1-\vartheta)}(z-x)^{-\vartheta}$ and $\kappa(z-x) = \frac{M(\vartheta)}{(1-\vartheta)}\exp\left(\frac{-\vartheta}{1-\vartheta}(z-x)^{-\vartheta}\right)$. The kernel $\kappa(z-x) = \frac{1}{\Gamma(1-\vartheta)}(z-x)^{-\vartheta}$ is known as power kernel law which has been used in classical fractional calculus and the kernel $\kappa(z-x) = \frac{M(\vartheta)}{(1-\vartheta)}\exp\left(\frac{-\vartheta}{1-\vartheta}(z-x)^{-\vartheta}\right)$ is exponential kernel law which is newly discovered. The general derivatives having exponential kernel known as Caputo-Fabrizio derivative. In statistics, Pareto distribution which describes the fitting of the shape of a large portion of wealth for a small portion of the population and the wealth in our society has corresponded to the power-law kernel. The negative exponential distribution is mainly used in statistics as a probability distribution. This type of distribution is used to characterize the time between events between Poisson point distribution. The important property of this distribution is that it depicts infinite divisibility and infinite divisible distribution shows an important role in the context of limit theorem and Levy process. This type of derivatives is beneficial when the distribution of waiting time is not dependent upon elapsed time [41]. Here we give some properties of C-F derivative:

1. The mean square displacement associated with Caputo-Fabrizio fraction derivative is a usual to sub-diffusion crossover.
2. The Caputo-Fabrizio distribution follow the rule from Gaussian to non-Gaussian crossover.
3. The asymptotic behavior of Caputo-Fabrizio satisfies the power law behavior and connect the theory of fading memory concept with kernels which are non-singular [42].

Nowadays the derivative with exponential kernel law has become so popular and capture the attention of researchers. This derivative has many applications which can be found in elasticity, Keller Segel equation, flow of complex rheological medium and flow of ground water in mass-spring damped system [43].

2.6. Approximation of Function by Quasi-Wavelets

In literature there are many polynomial and wavelets which are used to approximate an arbitrary function. But the procedure based upon the quasi-wavelets is growing rapidly as spectral collocation method which is local. It is very useful to solve different type of space-time fractional FPDEs and partial integro-differential equation of different order. We define a mathematical

transformation known as the singular discrete convolution in distribution theory

$$\Phi(v) = (F * s)(z) = \int_{-\infty}^{\infty} F(-t+z)s(t)dt, \tag{11}$$

where $s(t)$ is called a test function and F is recognized as singular kernel. We can find a family of wavelet by a function which is known as mother wavelet ς using operations of dilation and translation.

$$\varsigma_{\beta,\delta}(z) = \beta^{\frac{-1}{2}}\varsigma\Big(\frac{z-\delta}{\beta}\Big). \tag{12}$$

The parameter δ represents the translation process while β represents the process of dilation. An orthonormal wavelet base generates any arbitrary subspace by using orthogonal scaling functions. A Shannon's delta sequence kernel is used in our work which is defined as

$$\delta_\alpha(z) = \frac{1}{\pi}\int_0^\pi \cos(zy)dy = \frac{\sin(\alpha z)}{\pi z}, \tag{13}$$

where $\lim_{\alpha\to\alpha_0}\delta_\alpha(z) = \delta(z)$. δ is discussed by Dirac and so known as Dirac delta function. For a $\alpha > 0$, Shannon's delta sequence kernel generates a basis for the Paley-Wiener reproducing kernel Hilbert space $\mathbf{B}_\alpha^2$[44] which is a subspace of $\mathbf{L}^2(R)$. We can reproduce the function $g(z) \in \mathbf{B}_\alpha^2$ as follows

$$g(z) = \int_{-\infty}^{\infty} g(z)\delta_\alpha(z-t)dt = \int_{-\infty}^{\infty} g(z)\frac{\sin((z-t)\alpha)}{(z-t)\pi}dt,\ \forall g(z) \in \mathbf{B}_\alpha^2. \tag{14}$$

This sampling scaling function can be put in another form in reproducing kernel of Paley-Wiener

$$\delta_{\alpha,k} = \delta_\alpha(z-z_k) = \frac{\sin((z-z_k)\alpha)}{(z-z_k)\pi}, \tag{15}$$

the points $\{x_k\}$ is known as collection of sampling points which is placed around x. We can put all functions $\forall g \in \mathbf{B}_\alpha^2$ in discrete form using Equations (11) and (12)

$$g(z) = \sum_{k=-\infty}^{\infty} g(z_k)\delta_\alpha(z-z_k). \tag{16}$$

According to Shannnon sampling theorem the uniformly spatial discrete samples for a given band-limited signal in B_γ^2 can depicted the sampling at the Nyquist frequency γ. We represent Δ by grid size in spatial direction and $\gamma = \frac{\pi}{\Delta}$. So

$$g(z) = \sum_{k=-\infty}^{\infty} g(z_k)\delta_\alpha(z-z_k) = \sum_{k=-\infty}^{\infty} g(z_k)\frac{\sin(\frac{\pi(z-z_k)}{\Delta})}{\frac{\pi(z-z_k)}{\Delta}} \tag{17}$$

A method for the improvement of Dirichlet's delta kernel is given by Wan. If we introduce a regularizer $R_\sigma(y)$ then we can increases its regularity

$$\delta_\alpha(z) \to \delta_{\alpha,\sigma} = \delta_\alpha(z)R_\sigma(z). \tag{18}$$

here R_σ satisfies

$$\lim_{\sigma\to\infty} R_\sigma(z) = 1$$

and

$$\int_{-\infty}^{\infty}\lim_{\sigma\to\infty} R_\sigma(y)\delta_\alpha(y)dy = R_\sigma(0) = 1.$$

Many regularizers satisfies the two conditions which is given as above. But Gaussian type regularizer is so commonly used

$$R_\sigma(z) = e\Big(\frac{-z^2}{2\sigma^2}\Big), \quad \sigma > 0, \tag{19}$$

where σ represents the width parameter. The relation between Δ and σ is $\sigma = r\times\Delta$, where r is a computation parameter. We can define regularized orthogonal sampling scaling function which are Gaussian type as

$$\delta_{\Delta,\sigma}(z) = \frac{\sin(\frac{\pi z}{\Delta})}{\frac{\pi z}{\Delta}}\exp\Big(\frac{-z^2}{2\sigma^2}\Big). \tag{20}$$

Here

$$\lim_{\sigma\to\infty}\delta_{\Delta,\sigma}(x) = \frac{\sin(\frac{\pi x}{\Delta})}{\frac{\pi x}{\Delta}},$$

Gaussian regularized sampling scaling function has no property of orthonormal wavelet scaling function so it is called a quasi scaling function.

By using quasi scaling function, we can approximate a function $\theta \in \mathbf{B}_\alpha^2$

$$\theta(z) = \sum_{k=-\infty}^{\infty}\theta(z_k)\delta_\alpha(z-z_k) = \sum_{k=-\infty}^{\infty}\theta(z_k)\delta_\alpha(z-z_k)R_\alpha(z-z_k). \tag{21}$$

For computation purpose we have to take finite sampling points as infinite sampling points is not possible in computer computation. We choose $2W+1$ sampling points in our work. All sampling points are chosen close to x. We can rewrite Equation (18) as

$$\theta(z) = \sum_{k=-W}^{W}\theta(z_k)\delta_{\Delta,\sigma}(z-z_k), \tag{22}$$

The n^{th} order derivatives of a function $\theta(z)$

$$\theta^n(z) = \sum_{k=-W}^{W}\theta(z_k)\delta_{\Delta,\sigma}^n(z-z_k), \quad n = 1,2,\cdots. \tag{23}$$

We have chosen the computational width equal to $2W+1$. We present the description of formulas of $\delta_{\Delta,\sigma}, \delta_{\Delta,\sigma}^1$ and $\delta_{\Delta,\sigma}^2$[45] which are helpful in calculation as follows

$$\delta_{\Delta,\sigma}(y) = \begin{cases} \frac{\exp\{-\frac{y^2}{2\sigma^2}\}\sin(\frac{\pi y}{\Delta})}{\frac{\pi y}{\Delta}}, & y \neq 0 \\ 1 & y = 0. \end{cases} \tag{24}$$

$$\delta^1_{\Delta,\sigma}(y) = \begin{cases} \Big(-\frac{\sin(\frac{\pi y}{\Delta})}{\frac{\pi y^2}{\Delta}} - \frac{\Delta \sin(\frac{\pi y}{\Delta})}{\frac{\pi \sigma^2}{\Delta}} + \frac{\cos(\frac{\pi y}{\Delta})}{y} \Big) & \\ \exp\big(-\frac{y^2}{2\sigma^2}\big) & y \neq 0, \\ 0 & y = 0. \end{cases} \tag{25}$$

$$\delta^2_{\Delta,\sigma}(y) = \begin{cases} \Big(\frac{2\Delta \sin\left(\frac{y\pi}{\Delta}\right)}{\pi y^3} - \frac{2\cos\left(\frac{\pi y}{\Delta}\right)}{y^2} + \frac{\Delta y \sin\left(\frac{y\pi}{\Delta}\right)}{\pi \sigma^4} & \\ + \frac{\Delta \sin\left(\frac{\pi y}{\Delta}\right)}{\pi \sigma^2 y} - \frac{2\cos\left(\frac{\pi y}{\Delta}\right)}{\sigma^2} - \frac{\pi \sin\left(\frac{y\pi}{\Delta}\right)}{y\Delta} \Big) & y \neq 0, \\ \exp\big(-\frac{y^2}{2\sigma^2}\big) & \\ 0 & y = 0. \end{cases} \tag{26}$$

3. APPROXIMATION OF CAPUTO-FABRIZIO DERIVATIVE

In the following theorem, we will find out an approximate expression of Caputo-Fabrizio derivative of the function $f(t) = t^k$

Theorem 1: The C-F derivative of function $f(t) = t^k$ having order $n < \alpha < n+1$ with $k \geq \lceil \alpha \rceil$ is given by

$${}^{CF}_{0}D^{\alpha}_{t}t^k = \frac{B(\alpha)\Gamma(1+k)}{\lceil\alpha\rceil - \alpha}\Big(\sum_{r=0}^{k-n-1} \frac{(-1)^r t^{k-n-1-r}}{\Gamma(k-n-r)(\frac{-\alpha}{\lceil\alpha\rceil-\alpha})^{r+1}} + \frac{(-1)^{k-n}}{(\frac{-\alpha}{\lceil\alpha\rceil-\alpha})^{k-n}} \exp\big(\frac{-\alpha}{\lceil\alpha\rceil-\alpha}t\big)\Big). \tag{27}$$

Proof: By the definition of CF derivative $D^n t^k = 0$, $k = 0, 1, \cdots, \lceil\alpha\rceil - 1$. Now for $k \geq \lceil\alpha\rceil$ we have

$$\begin{aligned} {}^{CF}_{0}D^{\alpha}_{t}t^k &= \frac{B(\alpha)}{\lceil\alpha\rceil-\alpha}\int_0^t D^{n+1}s^k \exp\Big(\frac{-\alpha}{\lceil\alpha\rceil-\alpha}(t-s)\Big)ds \\ &= \frac{B(\alpha)}{\lceil\alpha\rceil-\alpha}\int_0^t \frac{\Gamma(k+1)}{\Gamma(k-n)}s^{k-n-1}\exp\Big(\frac{-\alpha}{\lceil\alpha\rceil-\alpha}(t-s)\Big)ds \\ &= \frac{B(\alpha)}{\lceil\alpha\rceil-\alpha}\frac{\Gamma(k+1)}{\Gamma(k-n)}\exp\Big(\frac{-\alpha}{\lceil\alpha\rceil-\alpha}t\Big) \\ &\int_0^t s^{k-n-1}\exp\Big(\frac{\alpha}{\lceil\alpha\rceil-\alpha}s\Big)ds \\ &= \frac{B(\alpha)}{\lceil\alpha\rceil-\alpha} \times \frac{\Gamma(k+1)}{\Gamma(k-n)}\exp\Big(\frac{-\alpha}{\lceil\alpha\rceil-\alpha}t\Big)\times \\ &\Big[\exp\Big(\frac{\alpha}{\lceil\alpha\rceil-\alpha}t\Big)\sum_{r=0}^{k-n-1}(-1)^r\frac{\Gamma(k-n)t^{k-n-1-r}}{\Gamma(k-n-r)(\frac{\alpha}{1-\alpha})^{r+1}} \\ &- \frac{(-1)^{k-n-1}\Gamma(k-n)}{(\frac{\alpha}{1-\alpha})^{k-n}}\Big] \\ &= \frac{B(\alpha)\Gamma(k+1)}{\lceil\alpha\rceil-\alpha}\Big[\sum_{r=0}^{k-n-1}\frac{(-1)^r t^{k-n-1-r}}{\Gamma(k-n-r)(\frac{\alpha}{1-\alpha})^{r+1}} \\ &- \frac{(-1)^{k-n-1}}{(\frac{\alpha}{1-\alpha})^{k-n}}\exp\Big(\frac{-\alpha}{\lceil\alpha\rceil-\alpha}t\Big)\Big]. \end{aligned}$$

3.1. Legendre Polynomials

Now we discussed here about Legendre polynomials and their some properties. We shifted Legendre polynomials on the $[0,1]$ from the interval $[-1,1]$ by the transformation $z = 2x - 1$. The analytical form of these polynomials of degree i are given as follows

$$\psi_i(x) = \sum_{k=0}^{i}\frac{(-1)^{i+k}(i+k)!}{(k!)^2(l-k)!}x^k \tag{28}$$

where $i = 0, 1, \cdots$.

The Legendre polynomials follows the orthogonality property with weight function 1 and orthogonality condition can be described as

$$\int_0^1 \psi_j(x)\psi_i(x) = \begin{cases} \frac{1}{2i+1}, & j = i, \\ 0 & j \neq i. \end{cases} \tag{29}$$

A function $u(x)$ which belongs to the $L^2[0,1]$ can be approximated by a linear sum of shifted Legendre polynomials as

$$u(x) = u_m(x) = \sum_{j=0}^{m} a_j\psi_i(x), \tag{30}$$

where the linear coefficients are given by

$$a_j = (2j+1)\int_0^1 u(x)\psi_j(x). \tag{31}$$

Similarly, a function $u(x,t)$ of two variable can be approximated as

$$u(x,t) = \sum_{i=0}^{m-1}\sum_{l=0}^{m-1} a_{il}\psi_i(x)\psi_l(t), \tag{32}$$

where a_{il} are unknown coefficient.

4. PROPOSED NEW METHOD

In this section, we develop a new algorithm with the combination of Legendre spectral method and quasi wavelet method and then apply it to derive the numerical solution of C-F time fractional non-linear Sharma-Tasso-Oliver equation and C-F time-fractional non-linear Klein-Gordon equation. We approximate the C-F time fractional derivative by using Legendre spectral method. On the other hand spatial derivatives and unknown functions are approximated with the help of quasi wavelet based numerical method. We have used fractional derivative in our model as they are better than the integer ones. The fractional differential equations are more comprehensive and depict the memory effect of physical process as compare to ordinary differential equation. Recent study shows that the fractional model perfectly describe the test data of various

memory phenomena at different fields. Sharma-Tasso-Oliver C-F fractional model is as follows

$$
\begin{aligned}
{}_0^{CF}D_t^{\alpha}u(t,x) + 3\mu\Big(\frac{\partial u(x,t)}{\partial x}\Big)^2 + 3\mu(u(x,t))^2\frac{\partial u(x,t)}{\partial x} \\
+ 3\mu(u(x,t))\frac{\partial^2 u(x,t)}{\partial x^2} + \mu\frac{\partial^2 u(x,t)}{\partial x^2} = f(x,t).
\end{aligned} \tag{33}
$$

The prescribed initial and boundary conditions for this model are taken as follows

$$
\begin{aligned}
u(0,x) &= f_1(x), \\
u(t,0) &= f_2(t), \\
u(t,1) &= f_3(t).
\end{aligned} \tag{34}
$$

where $0 < \alpha \leq 1, 0 \leq x \leq 1$, and $0 \leq t \leq 1$.
The model of Klein-Gordon equation is

$$
\begin{aligned}
{}_0^{CF}D_t^{\alpha}u(t,x) + a\frac{\partial u(x,t)}{\partial t} + bu(x,t) = \frac{\partial^2 u(x,t)}{\partial x^2} \\
+ c(u)^2 + d(u)^3 + f(x,t),
\end{aligned} \tag{35}
$$

where $1 < \alpha \leq 2, 0 \leq x \leq 1$, and $0 \leq t \leq 1$.
The initial and boundary conditions for above model are

$$
\begin{aligned}
u(0,x) &= g_1(x), \\
u(t,0) &= g_2(t), \\
u(1,t) &= g_3(t), \\
\frac{\partial u(x,0)}{\partial t} &= g_4(x).
\end{aligned} \tag{36}
$$

Now we develop the method with the help of Legendre spectral and a method which is based on quasi wavelet to investigate the models (34) and (36).
Approximating the unknown function in terms of shifted Legendre polynomial

$$
u(x,t) = \sum_{i=0}^{m-1}\sum_{l=0}^{m-1} c_{il}\psi_i(x)\psi_l(t), \tag{37}
$$

where c_{il} are unknown coefficients for $i = 0, 2, \cdots$; and $l = 0, 1, 2, \cdots$.
Now operating the C-F time fractional operator and using Equation (38) we get

$$
\begin{aligned}
{}_0^{CF}D_t^{\alpha}u(t,x) &= \sum_{i=0}^{m-1}\sum_{l=0}^{m-1} c_{il}\psi_i(x)\Big({}_0^{CF}D_t^{\alpha}\psi_l(t)\Big), \\
&= \sum_{i=0}^{m-1}\sum_{l=0}^{m-1}\sum_{k=0}^{l}\frac{c_{il}(-1)^{l+k}(l+k)!}{(k!)^2(l-k)!}\psi_i(x)\Big({}_0^{CF}D_t^{\alpha}t^k\Big), \\
&= \sum_{i=0}^{m-1}\sum_{l=0}^{m-1}\sum_{k=0}^{l}\frac{c_{il}(-1)^{l+k}(l+k)!}{(k!)^2(l-k)!}\psi_i(x), \Pi_{k,t,\alpha},
\end{aligned} \tag{38}
$$

where

$$
\begin{aligned}
\Pi_{k,t,\alpha} = \frac{B(\alpha)\Gamma(1+k)}{\lceil\alpha\rceil-\alpha}\Big(\sum_{r=0}^{k-n-1}\frac{(-1)^r t^{k-n-1-r}}{\Gamma(k-n-r)(\gamma)^{r+1}} \\
+ \frac{(-1)^{k-n}}{(\gamma)^{k-n}}e^{-\gamma t}\Big)
\end{aligned} \tag{39}
$$

with $\gamma = \frac{\alpha}{\lceil\alpha\rceil-\alpha}$. Similarly, we can find the value of time fractional derivative ${}_0^{C}D_t^{\alpha}u(t,x)$ when its type is Caputo.
Differentiating Equation (38) with respect to t we get the following

$$
\begin{aligned}
\frac{\partial u(x,t)}{\partial t} &= \sum_{i=0}^{m-1}\sum_{l=0}^{m-1} c_{il}\psi_i(x)\Big(\frac{\partial\psi_l(t)}{\partial t}\Big), \\
&= \sum_{i=0}^{m-1}\sum_{l=0}^{m-1}\sum_{k=0}^{l}\frac{c_{il}kt^{k-1}(-1)^{l+k}(l+k)!}{(k!)^2(l-k)!}\psi_i(x).
\end{aligned} \tag{40}
$$

We have approximated derivative in the time direction with the help of Legendre spectral method. To approximate the unknown function $u(x,t)$ and derivative in time direction we take the help of quasi wavelet based numerical method. We know a function and its all derivatives can be approximated by

$$
u^{(n)}(x) = \sum_{k=-W}^{W}\delta_{\Delta,\sigma}^{n}(x-x_k)u(x_k), \quad n = 0, 1, \cdots \tag{41}
$$

where the superscript (n) denotes the n^{th} order derivative with respect to x. At spatial point $x = x_j$ we can rewrite above equation as

$$
u^{(n)}(x_j,t) = \sum_{s=-W}^{W}\delta_{\Delta,\sigma}^{n}(-s\Delta x)u(x_{j+s}), \quad n = 0, 1, \cdots \tag{42}
$$

where Δx is the spatial step. Putting the value of $u(x,t)$ and their space and time derivatives in model (34) we get the following

residual

$$\begin{aligned}\xi_1(x,t) &= \sum_{i=0}^{m-1}\sum_{l=0}^{m-1}\sum_{k=0}^{l}\frac{c_{il}(-1)^{l+k}(l+k)!}{(k!)^2(l-k)!}\psi_i(x),\Pi_{k,t,\alpha}\\ &+3\mu\Big(\sum_{i=0}^{m-1}\sum_{l=0}^{m-1}\sum_{k=-W}^{W}\delta^1_{\Delta,\sigma}(x-x_k)\psi_i(x_k)a_{il}\psi_l(t)\Big)^2\\ &+3\mu\Big(\sum_{i=0}^{m-1}\sum_{l=0}^{m-1}\sum_{k=-W}^{W}\delta^0_{\Delta,\sigma}(x-x_k)\psi_i(x_k)a_{il}\psi_l(t)\Big)^2\\ &\times\Big(\sum_{i=0}^{m-1}\sum_{l=0}^{m-1}\sum_{k=-W}^{W}\delta^1_{\Delta,\sigma}(x-x_k)\psi_i(x_k)a_{il}\psi_l(t)\Big)\\ &+3\mu\Big(\sum_{i=0}^{m-1}\sum_{l=0}^{m-1}\sum_{k=-W}^{W}\delta^0_{\Delta,\sigma}(x-x_k)\psi_i(x_k)a_{il}\psi_l(t)\Big)\\ &\times\Big(\sum_{i=0}^{m-1}\sum_{l=0}^{m-1}\sum_{k=-W}^{W}\delta^2_{\Delta,\sigma}(x-x_k)\psi_i(x_k)a_{il}\psi_l(t)\Big)\\ &+\mu\Big(\sum_{i=0}^{m-1}\sum_{l=0}^{m-1}\sum_{k=-W}^{W}\delta^2_{\Delta,\sigma}(x-x_k)\psi_i(x_k)a_{il}\psi_l(t)\Big)-f(x,t)\end{aligned} \tag{43}$$

The initial and boundary conditions takes the following form in view of Equation (33)

$$\begin{aligned}&\sum_{i=0}^{m-1}\sum_{l=0}^{m-1}a_{il}\psi_i(x)\psi_l(0)=f_1(x),\\ &\sum_{i=0}^{m-1}\sum_{l=0}^{m-1}a_{il}\psi_i(0)\psi_l(t)=f_2(t),\\ &\sum_{i=0}^{m-1}\sum_{l=0}^{m-1}a_{il}\psi_i(1)\psi_l(t)=f_3(t).\end{aligned} \tag{44}$$

Similarly the residual of model (36) with initial and boundary conditions (37) is given by

$$\begin{aligned}\xi_2(x,t) &= \sum_{i=0}^{m-1}\sum_{l=0}^{m-1}\sum_{k=0}^{l}\frac{c_{il}(-1)^{l+k}(l+k)!}{(k!)^2(l-k)!}\psi_i(x),\Pi_{k,t,\alpha}\\ &+a\sum_{i=0}^{m-1}\sum_{l=0}^{m-1}\sum_{k=0}^{l}\frac{c_{il}kt^{k-1}(-1)^{l+k}(l+k)!}{(k!)^2(l-k)!}\psi_i(x)\\ &+b\sum_{i=0}^{m-1}\sum_{l=0}^{m-1}\sum_{k=-W}^{W}\delta^0_{\Delta,\sigma}(x-x_k)\psi_i(x_k)a_{il}\psi_l(t)\\ &-\sum_{i=0}^{m-1}\sum_{l=0}^{m-1}\sum_{k=-W}^{W}\delta^2_{\Delta,\sigma}(x-x_k)\psi_i(x_k)a_{il}\psi_l(t)\\ &-c\Big(\sum_{i=0}^{m-1}\sum_{l=0}^{m-1}\sum_{k=-W}^{W}\delta^0_{\Delta,\sigma}(x-x_k)\psi_i(x_k)a_{il}\psi_l(t)\Big)^2\\ &-d\Big(\sum_{i=0}^{m-1}\sum_{l=0}^{m-1}\sum_{k=-W}^{W}\delta^0_{\Delta,\sigma}(x-x_k)\psi_i(x_k)a_{il}\psi_l(t)\Big)^3-f(x,t).\end{aligned} \tag{45}$$

$$\begin{aligned}&\sum_{i=0}^{m-1}\sum_{l=0}^{m-1}a_{il}\psi_i(x)\psi_l(0)=g_1(x)\\ &\sum_{i=0}^{m-1}\sum_{l=0}^{m-1}a_{il}\psi_i(0)\psi_l(t)=g_2(t),\\ &\sum_{i=0}^{m-1}\sum_{l=0}^{m-1}a_{il}\psi_i(1)\psi_l(t)=g_3(t),\\ &\sum_{i=0}^{m-1}\sum_{l=0}^{m-1}a_{il}\psi_i(x)\frac{\partial\psi_l(0)}{\partial t}=g_4(x).\end{aligned} \tag{46}$$

Now collocating Equations (44) and (45) at suitable collocation points (x_j,t_j) and in Equation (44) considering the discrete sampling points $x_k = x_j$ equal to the collocation points and using Equation (43) an non-linear system of algebraic equations is obtained.

$$\begin{aligned}\xi_1(x_j,t_j) &= \sum_{i=0}^{m-1}\sum_{l=0}^{m-1}\sum_{k=0}^{l}\frac{c_{il}(-1)^{l+k}(l+k)!}{(k!)^2(l-k)!}\psi_i(x_j),\Pi_{k,t_j,\alpha}\\ &+3\mu\Big(\sum_{i=0}^{m-1}\sum_{l=0}^{m-1}\sum_{s=-W}^{W}\delta^1_{\Delta,\sigma}(-s\Delta x)\psi_i(x_{j+s})a_{il}\psi_l(t_j)\Big)^2\\ &+3\mu\Big(\sum_{i=0}^{m-1}\sum_{l=0}^{m-1}\sum_{s=-W}^{W}\delta^0_{\Delta,\sigma}(-s\Delta x)\psi_i(x_{j+s})a_{il}\psi_l(t_j)\Big)^2\\ &\times\Big(\sum_{i=0}^{m-1}\sum_{l=0}^{m-1}\sum_{s=-W}^{W}\delta^1_{\Delta,\sigma}(-s\Delta x)\psi_i(x_{j+s})a_{il}\psi_l(t_j)\Big)\\ &+3\mu\Big(\sum_{i=0}^{m-1}\sum_{l=0}^{m-1}\sum_{s=-W}^{W}\delta^0_{\Delta,\sigma}(-s\Delta x)\psi_i(x_{j+s})a_{il}\psi_l(t_j)\Big)\\ &\times\Big(\sum_{i=0}^{m-1}\sum_{l=0}^{m-1}\sum_{s=-W}^{W}\delta^2_{\Delta,\sigma}(-s\Delta x)\psi_i(x_{j+s})a_{il}\psi_l(t_j)\Big)\\ &+\mu\Big(\sum_{i=0}^{m-1}\sum_{l=0}^{m-1}\sum_{s=-W}^{W}\delta^2_{\Delta,\sigma}(-s\Delta x)\psi_i(x_{j+s})a_{il}\psi_l(t_j)\Big)-f(x,t).\end{aligned} \tag{47}$$

Similarly collocating Equations (46) and (47) we get the following system of non-linear algebraic equation

$$\begin{aligned}\xi_2(x_j,t_j) &= \sum_{i=0}^{m-1}\sum_{l=0}^{m-1}\sum_{k=0}^{l}\frac{c_{il}(-1)^{l+k}(l+k)!}{(k!)^2(l-k)!}\psi_i(x_j),\Pi_{k,t_j,\alpha}\\ &+a\sum_{i=0}^{m-1}\sum_{l=0}^{m-1}\sum_{k=0}^{l}\frac{c_{il}kt^{k-1}(-1)^{l+k}(l+k)!}{(k!)^2(l-k)!}\psi_i(x)\\ &+b\sum_{i=0}^{m-1}\sum_{l=0}^{m-1}\sum_{s=-W}^{W}\delta^0_{\Delta,\sigma}(-s\Delta x)\psi_i(x_{j+s})a_{il}\psi_l(t_j)\\ &-\sum_{i=0}^{m-1}\sum_{l=0}^{m-1}\sum_{s=-W}^{W}\delta^2_{\Delta,\sigma}(-s\Delta x)\psi_i(x_{j+s})a_{il}\psi_l(t_j)\\ &-c\Big(\sum_{i=0}^{m-1}\sum_{l=0}^{m-1}\sum_{s=-W}^{W}\delta^0_{\Delta,\sigma}(-s\Delta x)\psi_i(x_{j+s})a_{il}\psi_l(t_j)\Big)^2\\ &-d\Big(\sum_{i=0}^{m-1}\sum_{l=0}^{m-1}\sum_{s=-W}^{W}\delta^0_{\Delta,\sigma}(-s\Delta x)\psi_i(x_{j+s})a_{il}\psi_l(t_j)\Big)^3-f(x,t).\end{aligned} \tag{48}$$

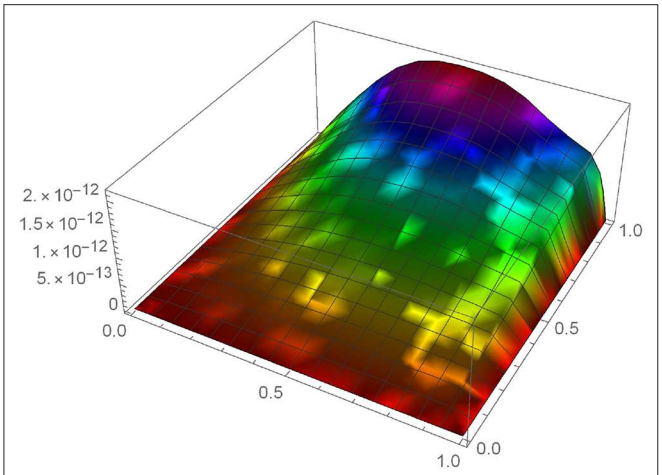

FIGURE 1 | 3D-plot of absolute error for $m = 10$.

By Solving that system of non-linear algebraic Equations (48) and (49) in the addition of Equations (35) and (37), respectively and finding a_{ij} we obtained numerical solution of our proposed models.

5. NUMERICAL RESULTS

Our motive in this section is to depict accuracy and the validity of our new derived method by solving some examples which have $C - F$ time fractional derivative. We perform all our numerical simulations with the help of Wolfram Mathematica version-11.3.

Example 1: If we consider the following Sharma-Tasso-Oliver equation with $\mu = 1$ and $\alpha = 0.9$

$$ {}_0^{CF}D_t^{\alpha}u(t,x) + 3\Big(\frac{\partial u(x,t)}{\partial x}\Big)^2 + 3(u(x,t))^2\frac{\partial u(x,t)}{\partial x} + 3(u(x,t))\frac{\partial^2 u(x,t)}{\partial x^2} + \frac{\partial^2 u(x,t)}{\partial x^2} = f(x,t). \tag{49} $$

The initial and boundary conditions are considered as

$$ u(t,0) = 0, u(t,1) = t, u(0,x) = 0. \tag{50} $$

We take exact solution as $u(x,t) = x^2t$ with suitable force function $f(x,t)$. the exact analytical solution of above problem is $u(x,t) = x^2t$.

To show the accuracy and validity of our proposed method we draw the 3D graph of absolute error between exact and numerical solution for $m = 10$ represented by **Figure 1**. The representation of absolute error for various m at time $t = 0.1$ is shown by **Table 1**.

Figures 2, **3** shows the variation of $u(x,t)$ at different value of α in t and x direction, respectively. We can conclude that at a fixed space point value of $u(x,t)$ increases with in increment in α. Same nature can be found at a fixed time but this time rate of growth of $u(x,t)$ is very slow. We compare the values of $u(x,t)$ in **Figures 4**, **5** when time fractional derivative is Caputo-Fabrizio and Caputo type in space and time direction, respectively.

TABLE 1 | Deviation of absolute error at time $t = 0.1$.

x ↓	$m = 4$	$m = 10$
$\frac{1}{9}$	8.1×10^{-4}	2.7×10^{-13}
$\frac{2}{9}$	1.4×10^{-3}	4.8×10^{-13}
$\frac{3}{9}$	1.9×10^{-3}	6.4×10^{-13}
$\frac{4}{9}$	2.2×10^{-3}	7.1×10^{-13}
$\frac{5}{9}$	2.3×10^{-3}	7.3×10^{-13}
$\frac{6}{9}$	2.1×10^{-3}	7.2×10^{-13}
$\frac{7}{9}$	1.7×10^{-3}	6.4×10^{-13}
$\frac{8}{9}$	1×10^{-3}	5.6×10^{-13}

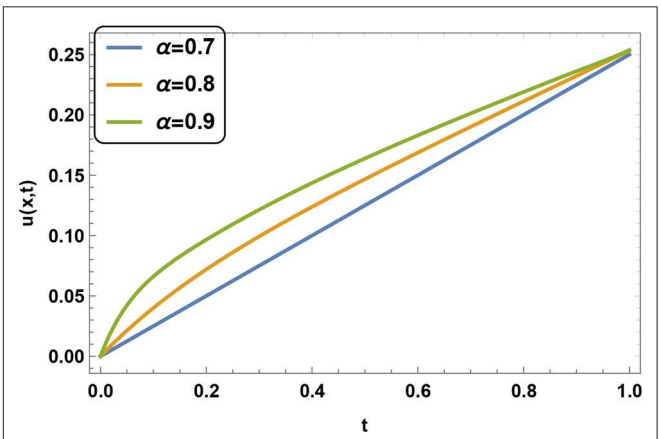

FIGURE 2 | Plots of u at space position $x = 0.1$ for $m = 4$ at different value of α.

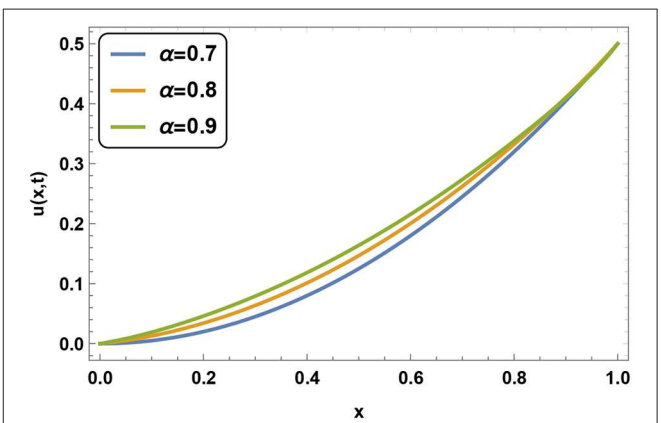

FIGURE 3 | Plots of u at time $t = 0.1$ for $m = 4$ at different value of α.

Example 2: Considering C-F time fractional reaction-diffusion equation

$$ {}_0^{CF}D_t^{0.9}u(x,t) = \frac{\partial^2 u(x,t)}{\partial x^2} + cu^2(x,t) + f(x,t). \tag{51} $$

We take the following equations as initial-boundary conditions

$$ u(0,x) = x^2, u(t,0) = 0, u(t,1) = e^t. \tag{52} $$

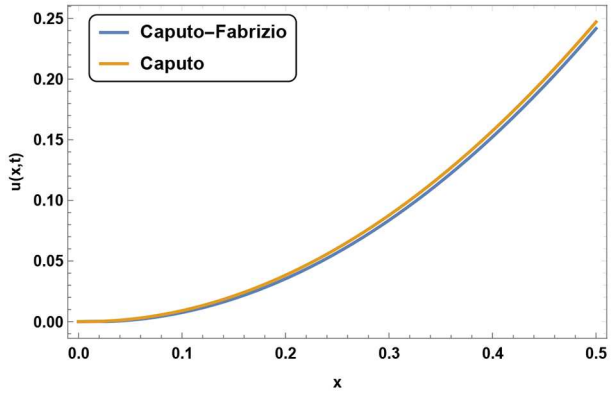

FIGURE 4 | Variation of u for $\alpha = 0.9$, $m = 4$, and $t = 0.1$ in case when time-fractional derivative is of Caputo Fabrizio and Caputo type.

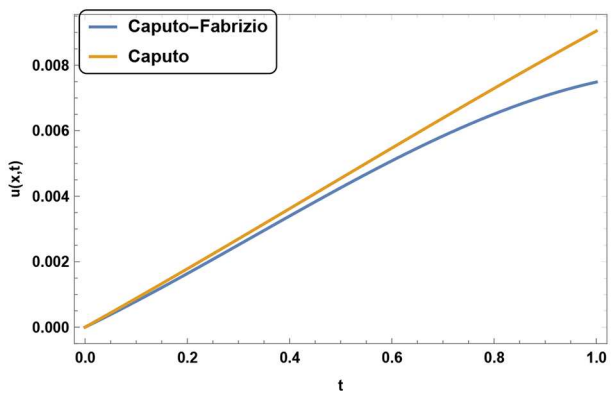

FIGURE 5 | Variation of u for $\alpha = 0.9$, $m = 4$, and $t = 0.1$ in case when time-fractional derivative is of Caputo Fabrizio and Caputo type.

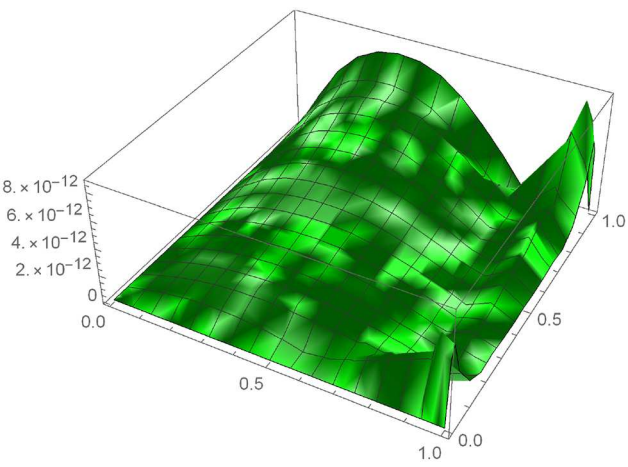

FIGURE 6 | 3D-plot of absolute error for $m = 10$.

We take $u(x,t) = x^2e^t$ as the exact solution where $f(x,t)$ is suitable force function.

To show the accuracy and validity of our proposed method we draw the 3D graph of absolute error between exact and numerical solution for $m = 10$ which is depict by **Figure 6**. **Table 2** present the variations of absolute error for different value of m.

TABLE 2 | Deviation of absolute error at time $t = 0.1$.

x ↓	$m = 4$	$m = 10$
$\frac{1}{9}$	6.9×10^{-4}	1.5×10^{-12}
$\frac{2}{9}$	1.1×10^{-3}	2.5×10^{-12}
$\frac{3}{9}$	1.4×10^{-3}	2.9×10^{-12}
$\frac{4}{9}$	1.5×10^{-3}	2.0×10^{-12}
$\frac{5}{9}$	1.5×10^{-3}	2.5×10^{-12}
$\frac{6}{9}$	1.4×10^{-3}	1.7×10^{-13}
$\frac{7}{9}$	1.1×10^{-3}	7.2×10^{-13}
$\frac{8}{9}$	4.8×10^{-3}	7.0×10^{-13}

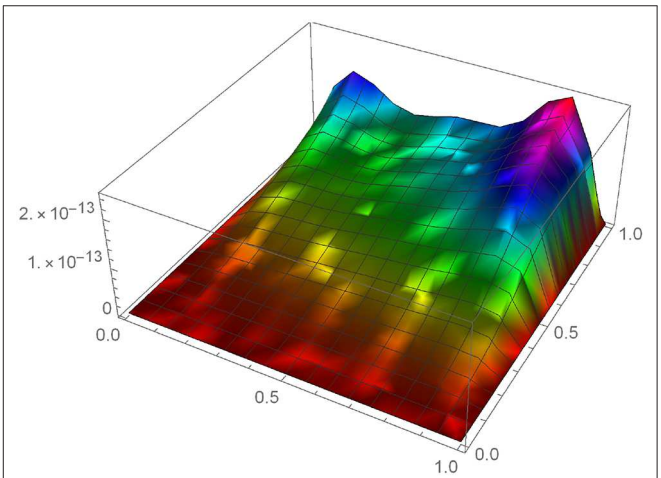

FIGURE 7 | 3D-plot of absolute error for $m = 10$.

Example 3: Considering $d = 0$, $a = 1$, $b = 1$, $c = 1$, and $\alpha = 1.5$ we get the following C-F time fractional Klein-Gordon equation

$$ {}_0^{CF}D_t^{\alpha}u(t,x) + \frac{\partial u(x,t)}{\partial t} + u(t,x) = \frac{\partial^2 u(t,x)}{\partial x^2} + (u)^2 + f(t,x). \tag{53} $$

The initial and boundary conditions are taken as follows

$$ \begin{aligned} u(x,0) &= 0, \\ u(0,t) &= 0, \\ u(1,t) &= t^2, \\ \frac{\partial u(x,0)}{\partial t} &= 0. \end{aligned} \tag{54} $$

The exact solution is taken as $u(x,t) = t^2x^2$ with force function $f(x,t)$.

To show the accuracy and validity of our proposed method we draw the 3D graph of absolute error between exact and numerical solution for $m = 10$ which is depict by **Figure 7**. The representation of absolute error at $t = 0.1$ is shown by

TABLE 3 | Deviation of absolute error for different m at time $t = 0.1$.

x ↓	$m = 4$	$m = 10$
$\frac{1}{9}$	1.0×10^{-4}	3.6×10^{-14}
$\frac{2}{9}$	1.7×10^{-4}	4.4×10^{-14}
$\frac{3}{9}$	2.2×10^{-4}	4.9×10^{-14}
$\frac{4}{9}$	2.5×10^{-4}	6.0×10^{-14}
$\frac{5}{9}$	2.5×10^{-4}	7.1×10^{-14}
$\frac{6}{9}$	2.2×10^{-4}	8.1×10^{-14}
$\frac{7}{9}$	1.7×10^{-4}	9.6×10^{-13}
$\frac{8}{9}$	1.0×10^{-4}	1.0×10^{-13}

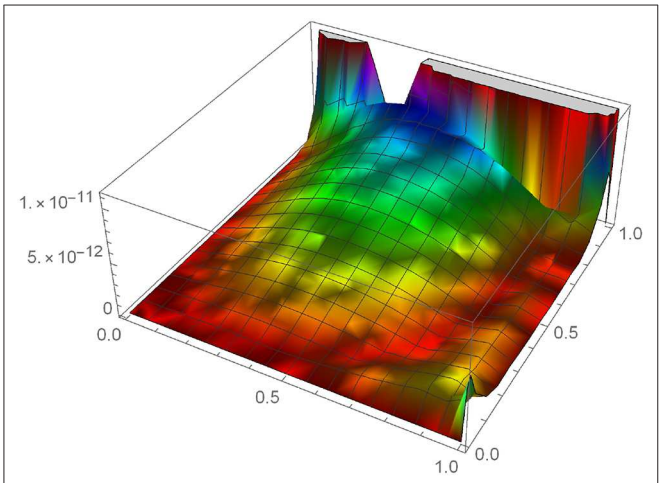

FIGURE 8 | 3D-plot of absolute error for $m = 10$.

Table 3. Our results clearly shown the complete agreement of obtained results.

Example 4: Considering $a = 1$, $b = 1$ and $c = 1$, $d = 1$ $\alpha = 1.5$ we get the following non-linear C-F time fractional Klein-Gordon equation

$$ {}_0^{CF}D_t^{\alpha} u(t,x) + \frac{\partial u(x,t)}{\partial t} + u(x,t) = \frac{\partial^2 u(x,t)}{\partial x^2} + (u)^2 + u^3 + f(x,t), \tag{55} $$

The Equation (55) with the initial-boundary conditions

$$ \begin{aligned} u(0,t) &= 0, \\ u(1,t) &= e^t + t, \\ \frac{\partial u(x,0)}{\partial t} &= x^2 + x, \\ u(x,0) &= x^2. \end{aligned} \tag{56} $$

We chose forced function $f(x,t)$ such that the exact solution of above problem is $u(x,t) = e^t x^2 + xt$.

Figure 8 represents the absolute error for this problem between exact and numerical solution. We have taken $m = 10$ at the time of plotting the absolute error graph. The variation of absolute error for various m at time $t = 0.1$ is depicted by **Table 4**. We

TABLE 4 | Deviation of absolute error at time $t = 0.1$.

x ↓	$m = 4$	$m = 10$
$\frac{1}{9}$	1.5×10^{-3}	1.2×10^{-12}
$\frac{2}{9}$	2.7×10^{-3}	2.5×10^{-12}
$\frac{3}{9}$	3.6×10^{-3}	3.4×10^{-12}
$\frac{4}{9}$	4.0×10^{-3}	3.5×10^{-12}
$\frac{5}{9}$	4.1×10^{-3}	3.1×10^{-12}
$\frac{6}{9}$	3.8×10^{-3}	2.4×10^{-12}
$\frac{7}{9}$	3.1×10^{-3}	1.1×10^{-12}
$\frac{8}{9}$	2.0×10^{-3}	1.0×10^{-13}

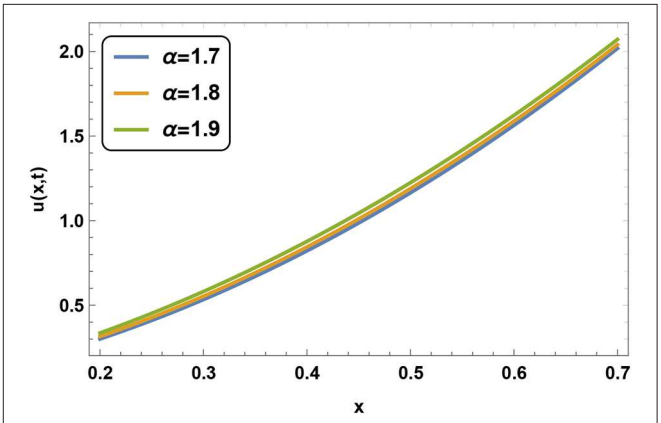

FIGURE 9 | Variation of u with $m = 10$ and $t = 0.1$ at different value of α.

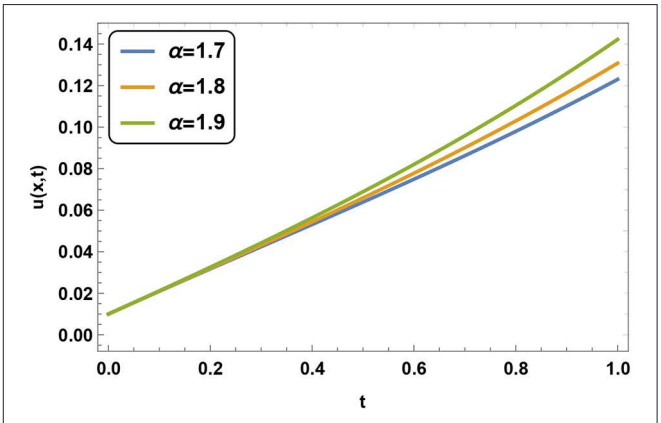

FIGURE 10 | Variation of u with$m = 10$ and $x = 0.1$ at different value of α.

have plotted the **Figures 9**, **10** of $u(x,t)$ for $\alpha = 1.7$, $\alpha = 1.8$ and $\alpha = 1.9$ at fixed t and x, respectively. We can conclude that at a fixed space point value of $u(x,t)$ increases with in increment in α. Same nature can be found at a fixed time but this time, rate of growth of $u(x,t)$ is slow and increases as time increases to $t = 1$.

6. CONCLUSION

In this work, first, we find out the approximate expression of C-F fractional derivative of the function t^k. We developed a

new numerical algorithm with the combination of the Legendre spectral method and quasi wavelet-based numerical method to solve fractional PDEs having a C-F fractional derivative. We implement this new algorithm to solve the C-F time-fractional Sharma-Tasso-Oliver equation and Klein-Gordon equation. We have shown the successful implementation of this method to solve the C-F time-fractional FPDEs. This implies that our proposed method has reasonable accuracy and valid different type of FPDEs. The 3D graphs of absolute error depicted the validity and effectiveness of our proposed method. The behavior of $u(x,t)$ in the diffusion equation with the variation in α at space and time direction is also shown by figures. We see the comparative behavior of the solution profile for C-F and Caputo derivatives. In future work, our new algorithm can be applied to another type of non-singular fractional models as Mittag-Leffler kernel derivative. It can also be applied to the system of a fractional differential equations and to investigate a different types of models.

DATA AVAILABILITY STATEMENT

All datasets generated for this study are included in the article/supplementary material.

AUTHOR CONTRIBUTIONS

All authors listed have made a substantial, direct and intellectual contribution to the work, and approved it for publication.

REFERENCES

1. Baleanu D, Machado JAT, Luo AC. *Fractional Dynamics and Control*. Berlin: Springer Science & Business Media (2011).
2. Kilbas AA, Srivastava HM, Trujillo JJ. *Theory and Applications of the Fractional Differential Equations*. Vol. 204. Amsterdam: Elsevier (North-Holland) (2006).
3. Podlubny I. Fractional Differential Equations, to Methods of Their Solution and Some of Their Applications. Fractional Differential Equations: An Introduction to Fractional Derivatives. San Diego, CA: Academic Press (1998).
4. Xiao-Jun Y, Zhang ZZ, Machado J, Baleanu D. On local fractional operators view of computational complexity. *Thermal Sci*. (2016) **20**:S755–67. doi: 10.2298/TSCI16S3755Y
5. Aydoğan SM, Baleanu D, Mousalou A, Rezapour S. On approximate solutions for two higher-order Caputo-Fabrizio fractional integro-differential equations. *Adv Differ Equat*. (2017) **2017**:221. doi: 10.1186/s13662-017-1088-3
6. Baleanu D, Mousalou A, Rezapour S. On the existence of solutions for some infinite coefficient-symmetric Caputo-Fabrizio fractional integro-differential equations. *Bound Value Probl*. (2017) **2017**:145. doi: 10.1186/s13661-017-0867-9
7. Atangana A, Baleanu D. New fractional derivatives with nonlocal and non-singular kernel: theory and application to heat transfer model. *arXiv*. (2016) 160203408. doi: 10.2298/TSCI160111018A
8. Atangana A, Koca I. Chaos in a simple nonlinear system with Atangana-Baleanu derivatives with fractional order. *Chaos Solit Fract*. (2016) **89**:447–54. doi: 10.1016/j.chaos.2016.02.012
9. Korpinar Z, Inc M, Baleanu D, Bayram M. Theory and application for the time fractional Gardner equation with Mittag-Leffler kernel. *J Taibah Univ Sci*. (2019) **13**:813–9. doi: 10.1080/16583655.2019.1640446
10. Diethelm K, Ford NJ, Freed AD. A predictor-corrector approach for the numerical solution of fractional differential equations. *Nonlin Dyn*. (2002) **29**:3–22. doi: 10.1023/A:1016592219341
11. Suarez L, Shokooh A. An eigenvector expansion method for the solution of motion containing fractional derivatives. *J Appl Mech*. (1997) **64**:629–35. doi: 10.1115/1.2788939
12. Hashim I, Abdulaziz O, Momani S. Homotopy analysis method for fractional IVPs. *Commun Nonlin Sci Numer Simul*. (2009) **14**:674–84. doi: 10.1016/j.cnsns.2007.09.014
13. Li Y, Sun N. Numerical solution of fractional differential equations using the generalized block pulse operational matrix. *Comput Math Appl*. (2011) **62**:1046–54. doi: 10.1016/j.camwa.2011.03.032
14. Owolabi KM, Atangana A. Analysis and application of new fractional Adams-Bashforth scheme with Caputo-Fabrizio derivative. *Chaos Solit Fract*. (2017) **105**:111–9. doi: 10.1016/j.chaos.2017.10.020
15. Darania P, Ebadian A. A method for the numerical solution of the integro-differential equations. *Appl Math Comput*. (2007) **188**:657–68. doi: 10.1016/j.amc.2006.10.046
16. Li Y, Zhao W. Haar wavelet operational matrix of fractional order integration and its applications in solving the fractional order differential equations. *Appl Math Comput*. (2010) **216**:2276–85. doi: 10.1016/j.amc.2010.03.063
17. Yuanlu L. Solving a nonlinear fractional differential equation using Chebyshev wavelets. *Commun Nonlin Sci Numer Simul*. (2010) **15**:2284–92. doi: 10.1016/j.cnsns.2009.09.020
18. Jafari H, Yousefi S, Firoozjaee M, Momani S, Khalique CM. Application of Legendre wavelets for solving fractional differential equations. *Comput Math Appl*. (2011) **62**:1038–45. doi: 10.1016/j.camwa.2011.04.024
19. Gürbüz B, Sezer M. Laguerre polynomial solutions of a class of initial and boundary value problems arising in science and engineering fields. *Acta Phys Pol A*. (2016) **130**:194–7. doi: 10.12693/APhysPolA.130.194
20. Odibat Z. On Legendre polynomial approximation with the VIM or HAM for numerical treatment of nonlinear fractional differential equations. *J Comput Appl Math*. (2011) **235**:2956–68. doi: 10.1016/j.cam.2010.12.013
21. Araci S. Novel identities for q-Genocchi numbers and polynomials. *J Funct Spaces Appl*. (2012) **2012**:214961. doi: 10.1155/2012/214961
22. Tassaddiq A, Khan I, Nisar K. Heat transfer analysis in sodium alginate based nanofluid using MoS2 nanoparticles: Atangana-Baleanu fractional model. *Chaos Solit Fract*. (2020) **130**:109445. doi: 10.1016/j.chaos.2019.109445
23. Farayola MF, Shafie S, Siam FM, Khan I. Numerical simulation of normal and cancer cells' populations with fractional derivative under radiotherapy. *Comput Methods Prog Biomed*. (2020) **187**:105202. doi: 10.1016/j.cmpb.2019.105202
24. Abro KA, Shaikh PH, Gómez-Aguilar J, Khan I. Analysis of De-Levie's model via modern fractional differentiations: an application to supercapacitor. *Alexandr Eng J*. (2019) **58**:1375–84. doi: 10.1016/j.aej.2019.11.009
25. Abro KA, Khan I, Nisar KS. Novel technique of Atangana and Baleanu for heat dissipation in transmission line of electrical circuit. *Chaos Solit Fract*. (2019) **129**:40–5. doi: 10.1016/j.chaos.2019.08.001
26. Ali F, Murtaza S, Sheikh NA, Khan I. Heat transfer analysis of generalized Jeffery nanofluid in a rotating frame: Atangana-Balaenu and Caputo-Fabrizio fractional models. *Chaos Solit Fract*. (2019) **129**:1–15. doi: 10.1016/j.chaos.2019.08.013
27. Saqib M, Khan I, Shafie S. Application of fractional differential equations to heat transfer in hybrid nanofluid: modeling and solution via integral transforms. *Adv Differ Equat*. (2019) **2019**:52. doi: 10.1186/s13662-019-1988-5
28. Abro KA, Memon AA, Abro SH, Khan I, Tlili I. Enhancement of heat transfer rate of solar energy via rotating Jeffrey nanofluids using Caputo-Fabrizio fractional operator: an application to solar energy. *Energy Rep*. (2019) **5**:41–9. doi: 10.1016/j.egyr.2018.09.009
29. Khan A, Khan D, Khan I, Taj M, Ullah I, Aldawsari AM, et al. MHD flow and heat transfer in sodium alginate fluid with thermal radiation and porosity effects: fractional model of Atangana-Baleanu derivative of non-local and non-singular kernel. *Symmetry*. (2019) **11**:1295. doi: 10.3390/sym11101295
30. Ali F, Khan N, Imtiaz A, Khan I, Sheikh NA. The impact of magnetohydrodynamics and heat transfer on the unsteady flow of Casson

fluid in an oscillating cylinder via integral transform: a Caputo-Fabrizio fractional model. *Pramana*. (2019) **93**:47. doi: 10.1007/s12043-019-1805-4
31. Arif M, Ali F, Sheikh NA, Khan I, Nisar KS. Fractional model of couple stress fluid for generalized couette flow: a comparative analysis of Atangana-Baleanu and Caputo-Fabrizio fractional derivatives. *IEEE Access*. (2019) **7**:88643–55. doi: 10.1109/ACCESS.2019.2925699
32. Ali F, Iftikhar M, Khan I, Sheikh NA. Atangana-Baleanu fractional model for electro-osmotic flow of viscoelastic fluids. *Chaos Solit Fract*. (2019) **124**:125–33. doi: 10.1016/j.chaos.2019.05.001
33. Bhatter S, Mathur A, Kumar D, Singh J. A new analysis of fractional Drinfeld-Sokolov-Wilson model with exponential memory. *Phys A Stat Mech Appl*. (2020) **537**:122578. doi: 10.1016/j.physa.2019.122578
34. Kumar D, Singh J, Baleanu D. On the analysis of vibration equation involving a fractional derivative with Mittag-Leffler law. *Math Methods Appl Sci*. (2019) **43**:443–57. doi: 10.1002/mma.5903
35. Goswami A, Singh J, Kumar D, Gupta S, Sushila. An efficient analytical technique for fractional partial differential equations occurring in ion acoustic waves in plasma. *J Ocean Eng Sci*. (2019) **4**:85–99. doi: 10.1016/j.joes.2019.01.003
36. Kumar D, Singh J, Al Qurashi M, Baleanu D. A new fractional SIRS-SI malaria disease model with application of vaccines, antimalarial drugs, and spraying. *Adv Differ Equat*. (2019) **2019**:278. doi: 10.1186/s13662-019-2199-9
37. Goswami A, Singh J, Kumar D, Sushila. An efficient analytical approach for fractional equal width equations describing hydro-magnetic waves in cold plasma. *Phys A Stat Mech Appl*. (2019) **524**:563–75. doi: 10.1016/j.physa.2019.04.058
38. Qureshi S, Rangaig NA, Baleanu D. New numerical aspects of Caputo-Fabrizio fractional derivative operator. *Mathematics*. (2019) **7**:374. doi: 10.3390/math7040374
39. Caputo M, Fabrizio M. A new definition of fractional derivative without singular kernel. *Progr Fract Differ Appl*. (2015) **1**:1–13. doi: 10.18576/pfda/020101
40. Loh JR, Isah A, Phang C, Toh YT. On the new properties of Caputo-Fabrizio operator and its application in deriving shifted Legendre operational matrix. *Appl Numer Math*. (2018) **132**:138–53. doi: 10.1016/j.apnum.2018.05.016
41. Atangana A, Gómez-Aguilar J. Fractional derivatives with no-index law property: application to chaos and statistics. *Chaos Solit Fract*. (2018) **114**:516–35. doi: 10.1016/j.chaos.2018.07.033
42. Hristov J. On the Atangana-Baleanu derivative and its relation to the fading memory concept: the diffusion equation formulation. In: J. F. Gómez, L. Torres, R. F. Escobar eds *Fractional Derivatives with Mittag-Leffler Kernel*. New York, NY: Springer (2019). p. 175–93. doi: 10.1007/978-3-030-11662-0_11
43. Hristov J. Derivatives with non-singular kernels from the Caputo-Fabrizio definition and beyond: appraising analysis with emphasis on diffusion models. *Front Fract Calc*. (2017) **1**:270–342. doi: 10.2174/9781681085999118010013
44. Wei G. Discrete singular convolution for the solution of the Fokker-Planck equation. *J Chem Phys*. (1999) **110**:8930–42. doi: 10.1063/1.478812
45. Yang X, Xu D, Zhang H. Quasi-wavelet based numerical method for fourth-order partial integro-differential equations with a weakly singular kernel. *Int J Comput Math*. (2011) **88**:3236–54. doi: 10.1080/00207160.2011.587003

Conflict of Interest: The authors declare that the research was conducted in the absence of any commercial or financial relationships that could be construed as a potential conflict of interest.

Copyright © 2020 Kumar and Baleanu. This is an open-access article distributed under the terms of the Creative Commons Attribution License (CC BY). The use, distribution or reproduction in other forums is permitted, provided the original author(s) and the copyright owner(s) are credited and that the original publication in this journal is cited, in accordance with accepted academic practice. No use, distribution or reproduction is permitted which does not comply with these terms.

frontiers in Physics

ORIGINAL RESEARCH
published: 15 May 2020
doi: 10.3389/fphy.2020.00167

New Optical Solutions of the Fractional Gerdjikov-Ivanov Equation With Conformable Derivative

Behzad Ghanbari[1,2]* *and Dumitru Baleanu*[3,4,5]

[1] Department of Engineering Science, Kermanshah University of Technology, Kermanshah, Iran, [2] Department of Mathematics, Faculty of Engineering and Natural Sciences, Bahçeşehir University, Istanbul, Turkey, [3] Department of Mathematics, Faculty of Arts and Sciences, Cankaya University, Ankara, Turkey, [4] Institute of Space Sciences, Magurele-Bucharest, Romania, [5] Department of Medical Research, China Medical University Hospital, China Medical University, Taichung, Taiwan

Finding exact analytic solutions to the partial equations is one of the most challenging problems in mathematical physics. Generally speaking, the exact solution to many categories of such equations can not be found. In these cases, the use of numerical and approximate methods is inevitable. Nevertheless, the exact PDE solver methods are always preferred because they present the solution directly without any restrictions to use. This article aims to examine the perturbed Gerdjikov-Ivanov equation in an exact approach point of view. This equation plays a significant role in non-linear fiber optics. It also has many important applications in photonic crystal fibers. To this end, firstly, we obtain some novel optical solutions of the equation via a newly proposed analytical method called generalized exponential rational function method. In order to understand the dynamic behavior of these solutions, several graphs are plotted. To the best of our knowledge, these two techniques have never been tested for the equation in the literature. The findings of this article may have a high significance application while handling the other non-linear PDEs.

Keywords: PDEs, generalized exponential rational function method, non-linear Schrödinger equation, exact solutions, the perturbed Gerdjikov-Ivanov equation

OPEN ACCESS

Edited by:
Jordan Yankov Hristov, University of Chemical Technology and Metallurgy, Bulgaria

Reviewed by:
Hernando Quevedo, National Autonomous University of Mexico, Mexico
Asim Zafar, COMSATS University Islamabad, Pakistan
Necati Özdemir, Balıkesir University, Turkey

***Correspondence:**
Behzad Ghanbari
b.ghanbary@yahoo.com

Specialty section:
This article was submitted to Mathematical Physics, a section of the journal Frontiers in Physics

Received: *22 February 2020*
Accepted: *22 April 2020*
Published: *15 May 2020*

Citation:
Ghanbari B and Baleanu D (2020) New Optical Solutions of the Fractional Gerdjikov-Ivanov Equation With Conformable Derivative. Front. Phys. 8:167. doi: 10.3389/fphy.2020.00167

1. INTRODUCTION

Non-linear Schrödinger equations (NLSE) are often studied from different points of view. In recent years a great variety of analytical and numerical methods have been proposed for solving these equations [1–4]. The most studied NLSE equation is that which has a cubic non-linearity. In the present paper, we will explore an NLSE that has a quintic non-linearity, namely the perturbed Gerdjikov-Ivanov (**pGI**) equation.

The main achievement of this research is to utilize a new method to derive some novel solutions to a variant form of NLSE. In particular, we consider the **pGI** equation is given by [5–11]

$$i\frac{\partial q}{\partial t}+a\frac{\partial^2 q}{\partial x^2}+b|q|^4q=i\left[cq^2\frac{\partial \overline{q}}{\partial x}+\lambda_1\frac{\partial q}{\partial x}+\lambda_2\frac{\partial\left(|q|^2q\right)}{\partial x}+\theta\frac{\partial|q|^2}{\partial x}q\right], \tag{1}$$

provided that $q(x,t)$ indicates the macroscopic complex-valued wave profile of temporal and spatial independent variables of t and x, respectively. In this equation, $\partial q/\partial t$ is linear temporal evolution, $\partial^2 q/\partial x^2$ stands for the group velocity dispersion (**GVD**), and $|q|^4q$ is the present quintic non-linearity of the model. The parameters a, b are the coefficients of these quantities,

respectively. Moreover c is the non-linear dispersion coefficient. Finally, the constants λ_1, λ_2, and θ are known parameters related to perturbative effects. More information on this model can be found in the references as mentioned earlier.

In recent years, because of its high importance, the model has attracted the attention of many researchers. For instance, Biswas and Alqahtani [6] have presented two varieties of bright soliton solutions by the use of the semi-inverse variational principle. The sine-Gordon equation approach has been used to extract the dark, bright, dark-bright, singular, and combined singular optical solitons of the equation in Yaşar et al. [7]. Biswas et al. [8] have retrieved some bright and singular optical soliton solutions to the **pGI** equation by the implementation of the extended trial equation method. The $exp(\phi(\xi))$-Expansion and the Kudryashov methods are two reliable techniques that have been used in Arshed [9] to investigate some solitary wave solutions of the equation. In Kaur and Wazwaz [10], several hyperbolic, trigonometric or rational function solutions have been proposed using two efficient techniques, namely $exp(\phi(\xi))$-Expansion and $\frac{G'}{G^2}$-expansion methods. Very recently, Hosseini et al. [11] have listed several Kink, bright, and dark optical solitons of the model by the aid of the exp_a-function method and a new version of the Kudryashov method.

In light of previous work, we will apply the generalized exponential rational function method (**GERFM**) to retrieve some new analytical optical solutions of the fractional **pGI** equation with the conformable derivative [12]. This new definition of derivative is based on the basic limit definition of the derivative that has been successfully tackled in solving many different problems [13–22]. The main structure of the present article is as outlined. In the second section of this paper, some mathematical preliminaries have been reviewed. This section includes the necessary steps of applying **GERFM**, and the definition and basic properties of the conformable derivative will be presented. The main results of this article are achieved by following these steps in section 3 of this contribution. In section 4, we have performed some numerical simulations of the obtained results. These graphs can help us in better understanding of their dynamic properties. Finally, the article concludes with some conclusions.

2. MATHEMATICAL PRELIMINARIES AND BACKGROUNDS

This section first deals with the structure of the **GERFM**. Then in the next subsection, the basic concepts of the conformable derivative are expressed.

2.1. Analysis of GERFM

GERFM is a newly developed method introduced by Ghanbari and Inc [23] to solve the resonance non-linear Schrödinger equation [23]. Other successful applications of the technique in solving different types of PDEs have also been reported in references [24–27].

We will review how to use the method below.

1. Let us consider a typical non-linear PDE for $q = q(x,t)$, giving by
$$\mathcal{N}(q, q_x, q_t, q_{xx}, \ldots) = 0. \tag{2}$$
Under the wave transformations of $q(x,t) = Q(\xi)$ and $\xi = \sigma x - lt$, Equation (2) becomes an ordinary differential equation given by:
$$\mathcal{N}(Q, \sigma Q', -lQ', \sigma^2 Q'', \ldots) = 0. \tag{3}$$
2. Now, we assume that Equation (3) admits the exact solution giving by
$$Q(\xi) = \mathcal{A}_0 + \sum_{k=1}^{N} \mathcal{A}_k \Phi(\xi)^k + \sum_{k=1}^{N} \mathcal{B}_k \Phi(\xi)^{-k}, \tag{4}$$
where
$$\Phi(\xi) = \frac{m_1 e^{n_1 \xi} + m_2 e^{n_2 \xi}}{m_3 e^{n_3 \xi} + m_4 e^{n_4 \xi}}. \tag{5}$$
and m_i, n_i's and $\mathcal{A}_0, \mathcal{A}_k$, and $\mathcal{B}_k$'s are disposal parameters. Finally, N is a constant, which is evaluated by applying the homogeneous balance to Equation (3).
3. Inserting Equation (4) into (3) with Equation (5), and then gathering all possible powers of $\mathcal{E}_i = e^{n_i \xi}$ for $i = 1, \ldots, 4$, forms a polynomial equation as $P(\mathcal{E}_1, \mathcal{E}_2, \mathcal{E}_3, \mathcal{E}_4) = 0$. Equating coefficients of P to zero, one derives a simultaneous system of equations regarding $m_i, n_i (1 \leq i \leq 4)$, and $\sigma, l, \mathcal{A}_0, \mathcal{A}_k$ and $\mathcal{B}_k (1 \leq k \leq N)$.
4. Finally, solving the non-linear system and substituting the obtained solutions in Equations (4) and (5), the explicit form of the solutions of (2) will be extracted.

2.2. The Conformable Derivative

Definition: Let $q : \mathbb{R}^+ \to \mathbb{R}$, then the conformable derivative of q of order α, is giving by [12]
$$\mathcal{D}_t^\alpha(q)(t) = \lim_{\eta \to 0} \frac{q(t + \eta t^{1-\alpha}) - q(t)}{\eta}, \quad \alpha \in (0, 1]. \tag{6}$$

Theorem: For any $\alpha \in (0, 1]$, and two α-differentiable functions p, q, the following propositions hold

- $\mathcal{D}_t^\alpha(c_1 p + c_2 q) = c_1 \mathcal{D}_t^\alpha(p) + c_2 \mathcal{D}_t^\alpha(q)$, for $c_1, c_2 \in \mathbb{R}$.
- $\mathcal{D}_t^\alpha(t^c) = c t^{c-\alpha}$, for $c \in \mathbb{R}$.
- $\mathcal{D}_t^\alpha(pq) = p\mathcal{D}_t^\alpha(q) + q\mathcal{D}_t^\alpha(p)$.
- $\mathcal{D}_t^\alpha(\frac{p}{q}) = \frac{q\mathcal{D}_t^\alpha(p) - p\mathcal{D}_t^\alpha(q)}{q^2}$.
- If q is a differentiable function (in standard sense), thereupon $\mathcal{D}_t^\alpha(q)(t) = t^{1-\alpha} \frac{dq}{dt}$ holds.

Theorem [14]: Let $p : (0, 1] \to \mathbb{R}$ be a function such that p is classical, and α-conformable differentiable. Moreover, consider q as a differentiable function defined in the range of p. Thus, we have
$$D_t^\alpha(poq)(t) = t^{1-\alpha} q'(t) p'(q(t)),$$
where prime stands for standard derivatives respect to t.

Some of the benefits of the conformable derivative compared to other new definitions for the derivative are as follows:

- According to this definition of the operator, the derivative of a constant function is zero. This feature is not available in many other definitions.
- Unlike many existing definitions, this definition satisfies the known formula of the derivative of the product of two functions.
- The conformable derivative does satisfy the known formula of the derivative of the quotient of two functions.
- The conformable derivative does satisfy the well-known chain rule.
- The conformable derivative satisfies the well-known semi group property.

The mentioned properties are very important and valuable features for any derivative definition that the conformable derivative has all of them.

3. MATHEMATICAL ANALYSIS

The main contribution in this paper is to consider the derivatives in the Equation (1) with the conformable derivative defined by (6), as follows

$$iD_t^\alpha q + aD_x^{2\alpha} q + b|q|^4 q = i\left[cq^2 D_x^\alpha \overline{q} + \lambda_1 D_x^\alpha q + \lambda_2 D_x^\alpha \left(|q|^2 q\right) + \theta D_x^\alpha |q|^2 q\right]. \quad (7)$$

The main assumption is to taking the stationary soliton solution form of

$$q(x,t) = Q(\xi)e^{i\phi(x,t)}, \quad \xi = \left(\frac{1}{\alpha}\right)x^\alpha - \left(\frac{\nu}{\alpha}\right)t^\alpha,$$
$$\phi = \left(\frac{-k}{\alpha}\right)x^\alpha + \left(\frac{\omega}{\alpha}\right)t^\alpha, \quad (8)$$

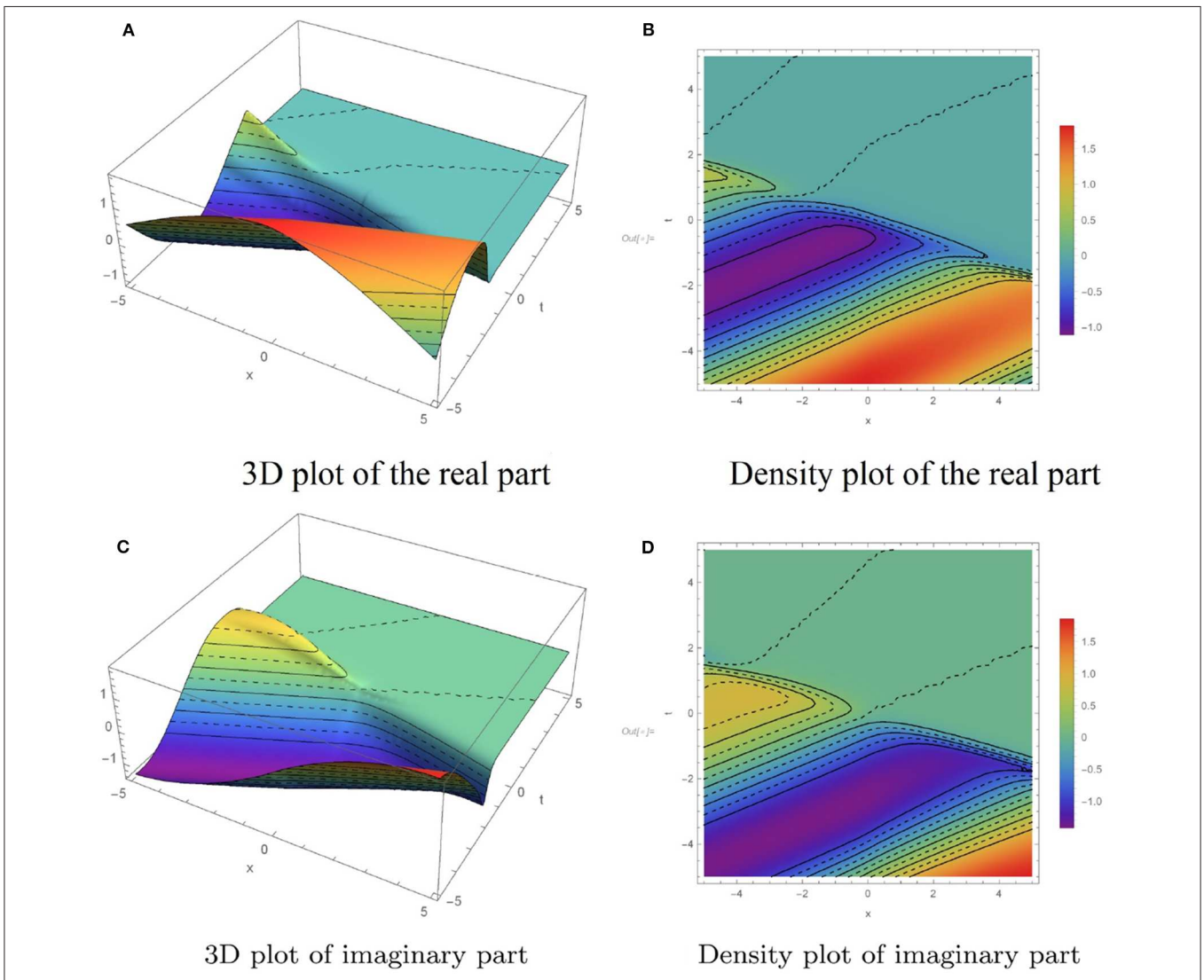

FIGURE 1 | Dynamic behaviors of $q_1(x,t)$ for $a = 0.2, b = -0.5, c = 0.5, \lambda_1 = 3, \lambda_2 = 3, \alpha = 0.97$. **(A)** 3D plot of the real part. **(B)** Density plot of the real part. **(C)** 3D plot of imaginary part. **(D)** Density plot of imaginary part.

where v, k, and ω are the phase component, the frequency of solitons, and the wavenumber, respectively.

Substituting the stationary soliton solution form (8) into Equation (7), we arrive at a complex equation whose real part is as follows

$$\left(v + \lambda_1 + 2ak\right) + \left(c + 3\lambda_2 + 2\theta\right) Q^2 = 0. \tag{9}$$

So, we will have

$$v = -\lambda_1 - 2ak, \quad \theta = -\frac{1}{2}\left(c + 3\lambda_2\right). \tag{10}$$

From the real part, the following formula is also extracted

$$aQ'' - \left(\omega + ak^2 + \lambda_1 k\right) Q + \left(c - \lambda_2\right) kQ^3 + bQ^5 = 0. \tag{11}$$

Thus, in the following, we focus our attention on deriving solutions of Equation (11). Now balancing between two terms of Q^5 and Q'' in Equation (11) suggests $N = \frac{1}{2}$. If we want to get a closed-form solution, we need to define a new variable of $Q(\xi) = \mathcal{R}^2(\xi)$. This substitution leads us to

$$\begin{aligned} a\left(2\mathcal{R}\mathcal{R}'' - (\mathcal{R}')^2\right) - 4\left(\omega + ak^2 + \lambda_1 k\right)\mathcal{R}^2 \\ +4\left(c - \lambda_2\right) k\mathcal{R}^3 + 4b\mathcal{R}^4 = 0. \end{aligned} \tag{12}$$

Now, the homogeneous balance in Equation (12) suggests $N = 1$. Setting $N = 1$ along with Equation (4), one gets

$$\mathcal{R}(\xi) = \mathcal{A}_0 + \mathcal{A}_1 \Phi(\xi) + \frac{\mathcal{B}_1}{\Phi(\xi)}. \tag{13}$$

Inserting (13) into (12) and pursuing the steps outlined for the method, the analytical solutions for the Equation (7) will be determined consequently.

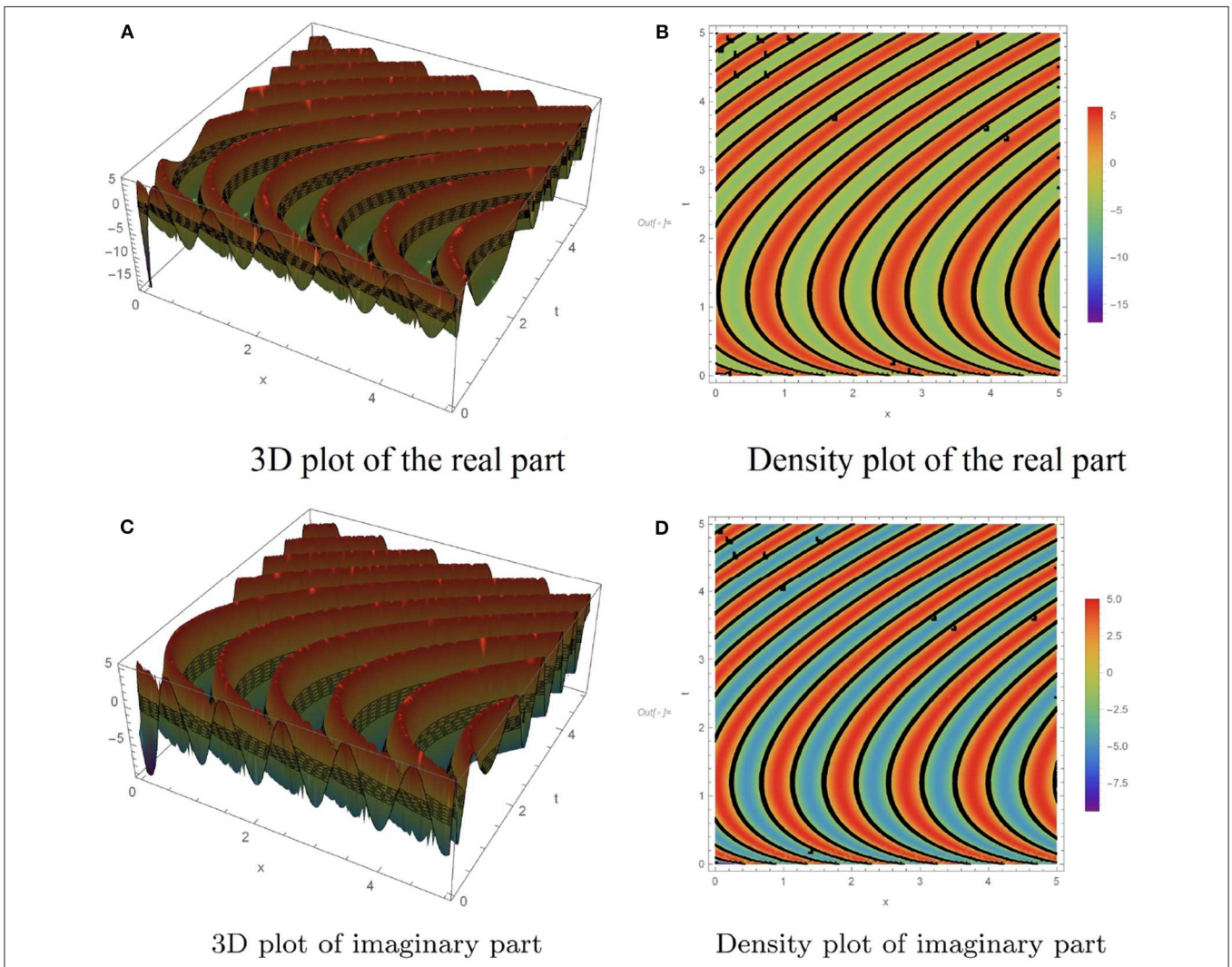

FIGURE 2 | Dynamic behaviors of $q_2(x, t)$ for $a = -4, b = 2, c = 2, \lambda_1 = 0.1, \lambda_2 = 0.1, \alpha = 0.95$. **(A)** 3D plot of the real part. **(B)** Density plot of the real part. **(C)** 3D plot of imaginary part. **(D)** Density plot of imaginary part.

Category 1: It is attained $m = [1, 1, -1, 1]$ and $n = [1, -1, 1, -1]$, which offers

$$\Phi(\xi) = -\frac{\cosh(\xi)}{\sinh(\xi)}. \tag{14}$$

Case 1:

$$k = \frac{-4\sqrt{-3ab}}{3(c-\lambda_1)},$$
$$w = \sqrt{\frac{-3a}{b}}\frac{-16ab\sqrt{-3ab} - 3\left(\sqrt{-3ab}(\lambda_2 - c) + 4\lambda_1 b\right)(\lambda_2 - c)}{9(\lambda_2 - c)^2},$$
$$\mathcal{A}_0 = \frac{1}{2}\sqrt{\frac{-3a}{b}}, \mathcal{A}_1 = 0, \mathcal{B}_1 = \frac{-1}{2}\sqrt{\frac{-3a}{b}}.$$

Inserting these values in Equation (13), yields

$$\mathcal{R}(\xi) = \sqrt{\frac{-3a}{b}}\frac{1 - \coth(\xi)}{2\coth(\xi)}.$$

Accordingly, we derive a soliton solution of given PDE in (7) as

$$q_1(x,t) = \left(\sqrt{\frac{-3a}{b}}\frac{1 - \coth(\xi)}{2\coth(\xi)}\right)^{1/2} \times e^{i\left(\left(\frac{-k}{\alpha}\right)x^\alpha + \left(\frac{\omega}{\alpha}\right)t^\alpha\right)}, \tag{15}$$

provided that $ab < 0$, and

$$\xi = \frac{8a\sqrt{3ab}t^\alpha + 3(\lambda_1 t^\alpha + x^\alpha)(\lambda_2 - c)}{\alpha(3\lambda_2 - 3c)}.$$

Case 2:

$$k = \frac{8\sqrt{-3ab}}{3(c-\lambda_1)},$$
$$w = \frac{-64}{3}\sqrt{\frac{-a}{b}}\frac{ab\sqrt{-ab} + 3/16\left(\sqrt{-ab}(\lambda_2 - c) - 2/3\lambda_1 b\sqrt{3}\right)(\lambda_2 - c)}{(\lambda_2 - c)^2},$$
$$\mathcal{A}_0 = -\sqrt{\frac{-3a}{b}}, \mathcal{A}_1 = -\sqrt{\frac{-3a}{b}}, \mathcal{B}_1 = \frac{-1}{2}\sqrt{\frac{-3a}{b}}.$$

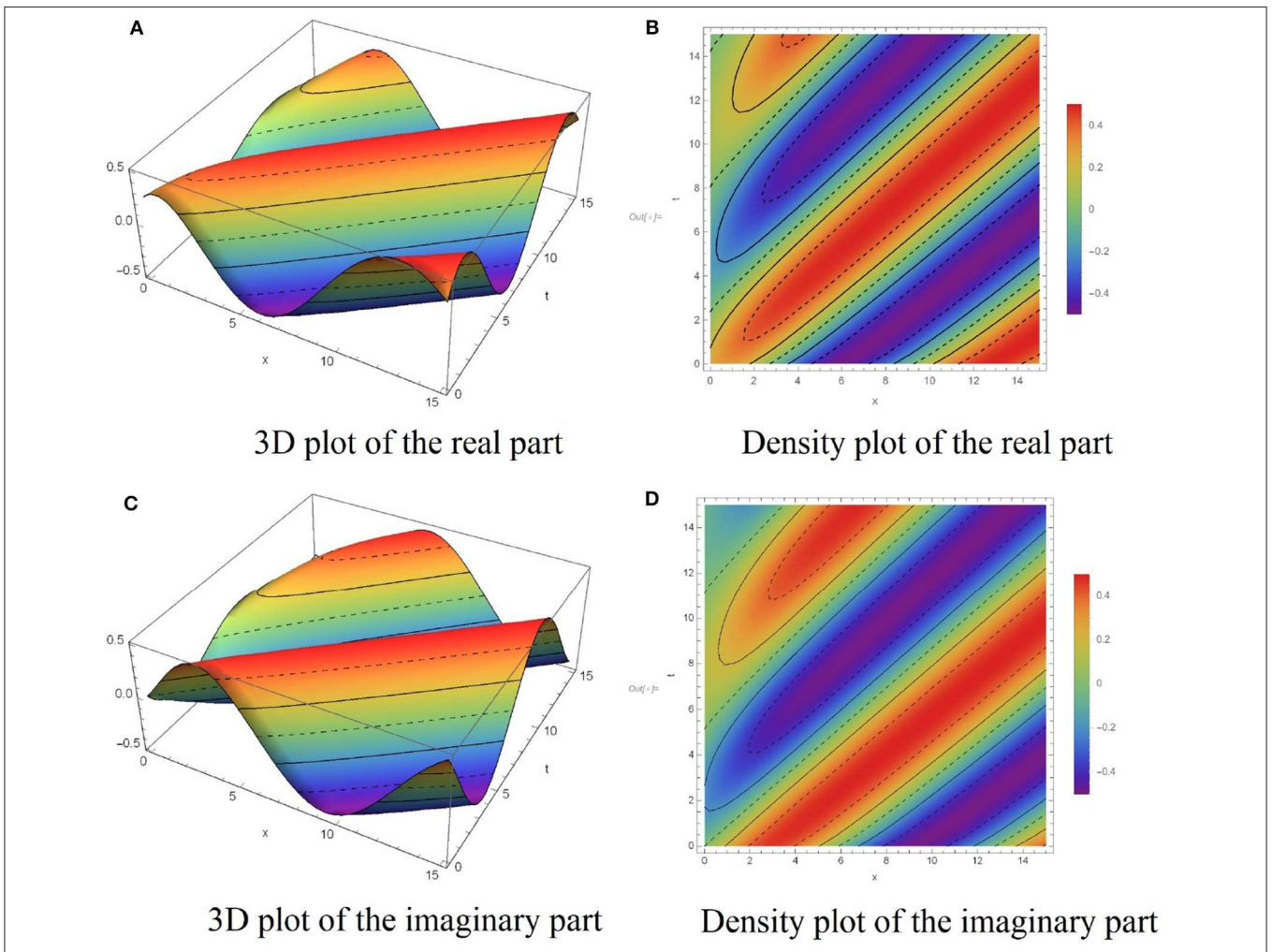

FIGURE 3 | Dynamic behaviors of $q_3(x,t)$ for $a = 1, b = -3, c = 0.5, \lambda_1 = 1, \lambda_2 = 4, \alpha = 0.9$. **(A)** 3D plot of the real part. **(B)** Density plot of the real part. **(C)** 3D plot of the imaginary part. **(D)** Density plot of the imaginary part.

Inserting these values in Equation (13), yields

$$\mathcal{R}(\xi) = \sqrt{\frac{-3a}{b}}\frac{(\coth(\xi)+1)^2}{2\coth(\xi)}.$$

Accordingly, we derive a soliton solution of given PDE in (7) as

$$q_2(x,t) = \left(\sqrt{\frac{-3a}{b}}\frac{(\coth(\xi)+1)^2}{2\coth(\xi)}\right)^{1/2} \times e^{i\left(\left(\frac{-k}{\alpha}\right)x^\alpha + \left(\frac{\omega}{\alpha}\right)t^\alpha\right)}, \tag{16}$$

provided that $ab < 0$, and

$$\xi = \frac{-16a\sqrt{-3ab}t^\alpha + 3(\lambda_1 t^\alpha + x^\alpha)(\lambda_2 - c)}{\alpha(3\lambda_2 - 3c)}.$$

Category 2: It is attained $m = [2, 0, 1, -1]$ and $n = [1, 0, 1, -1]$, which offers

$$\Phi(\xi) = \frac{\cosh(\xi) + \sinh(\xi)}{\sinh(\xi)}. \tag{17}$$

Case 1:

$$k = \frac{-2\sqrt{-3ab}}{3(c-\lambda_1)},$$

$$w = \frac{-8\lambda_1\sqrt{-3ab}(\lambda_2 - c) + 3\left(\lambda_2^2 - 2\lambda_2 c + 16/3ab + c^2\right)a}{12(\lambda_2 - c)^2},$$

$$\mathcal{A}_0 = \frac{1}{2}\sqrt{\frac{-3a}{b}}, \mathcal{A}_1 = \frac{1}{2}\sqrt{\frac{-3a}{b}}, \mathcal{B}_1 = 0.$$

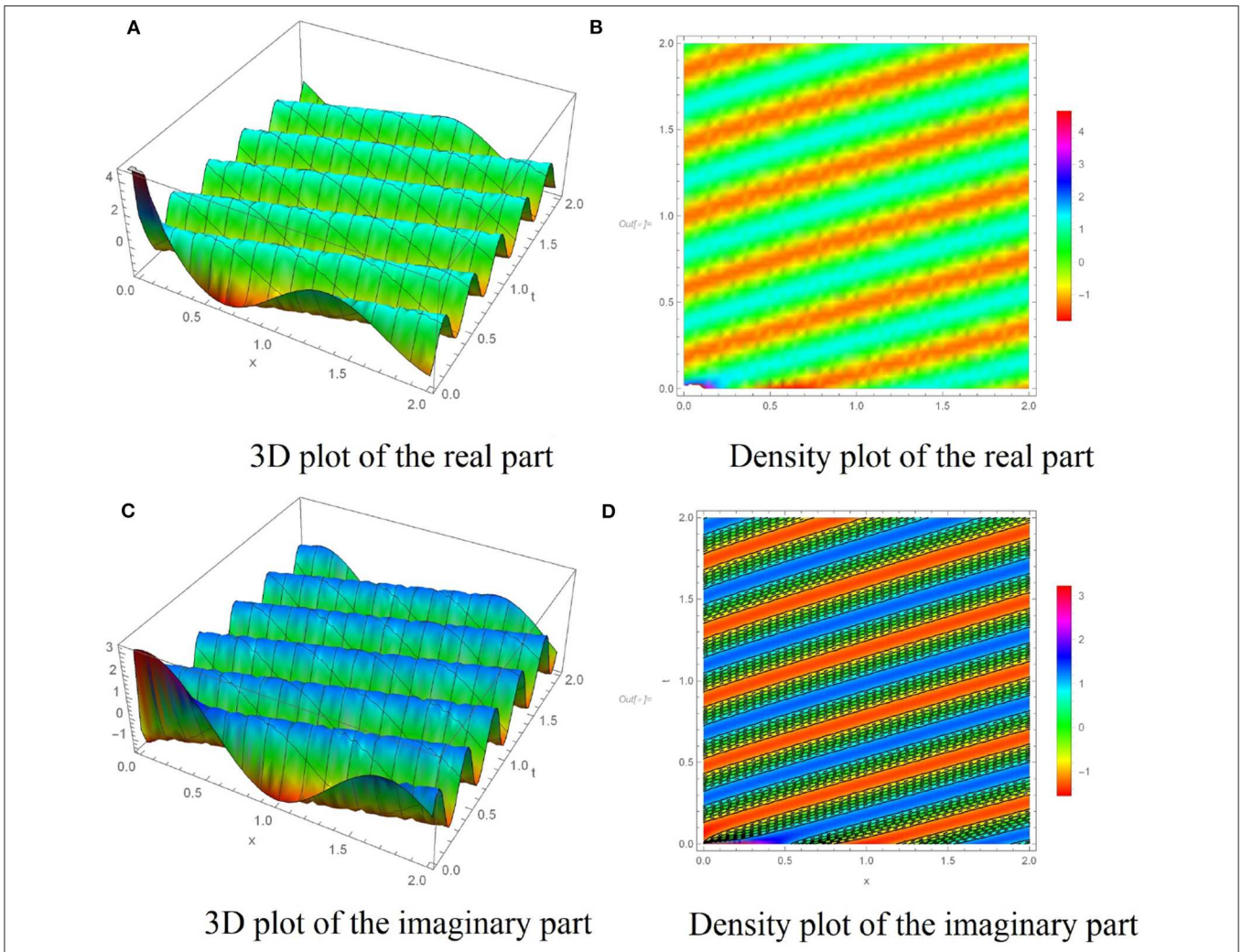

FIGURE 4 | Dynamic behaviors of $q_4(x,t)$ for $a = 1.5, b = -2.5, c = 1, \lambda_1 = 7, \lambda_2 = 2, \alpha = 0.9$. **(A)** 3D plot of the real part. **(B)** Density plot of the real part. **(C)** 3D plot of the imaginary part. **(D)** Density plot of the imaginary part.

Inserting these values in Equation (13), yields

$$\mathcal{R}(\xi) = \sqrt{\frac{-3a}{b}}\frac{e^{\xi}}{2\left(1+e^{\xi}\right)}.$$

Accordingly, we derive a soliton solution of given PDE in (7) as

$$q_3(x,t) = \left(\sqrt{\frac{-3a}{b}}\frac{e^{\xi}}{2\left(1+e^{\xi}\right)}\right)^{1/2} \times e^{i\left(\left(\frac{-k}{\alpha}\right)x^{\alpha}+\left(\frac{\omega}{\alpha}\right)t^{\alpha}\right)}, \tag{18}$$

provided that $ab < 0$, and

$$\xi = \frac{-8a\sqrt{-3ab}t^{\alpha} + 3\left(\lambda_1 t^{\alpha} + x^{\alpha}\right)(\lambda_2 - c)}{\alpha\left(3\lambda_2 - 3c\right)}.$$

Case 2:

$$k = \frac{-2\sqrt{-3ab}}{3(c-\lambda_1)},$$

$$w = \sqrt{\frac{-3a}{b}}\frac{-16ab\sqrt{-3ab} - 3\left(\sqrt{-3ab}\left(\lambda_2 - c\right) + 4\lambda_1 b\right)(\lambda_2 - c)}{9(\lambda_2 - c)^2},$$

$$\mathcal{A}_0 = 0, \mathcal{A}_1 = \frac{1}{2}\sqrt{\frac{-3a}{b}}, \mathcal{B}_1 = 0.$$

Inserting these values in Equation (13), yields

$$\mathcal{R}(\xi) = \sqrt{\frac{-3a}{b}}\frac{\cosh(\xi) + \sinh(\xi)}{2\sinh(\xi)}$$

Accordingly, we derive a soliton solution of given PDE in (7) as

$$q_4(x,t) = \left(\sqrt{\frac{-3a}{b}}\frac{\cosh(\xi) + \sinh(\xi)}{2\sinh(\xi)}\right)^{1/2} \times e^{i\left(\left(\frac{-k}{\alpha}\right)x^{\alpha}+\left(\frac{\omega}{\alpha}\right)t^{\alpha}\right)}, \tag{19}$$

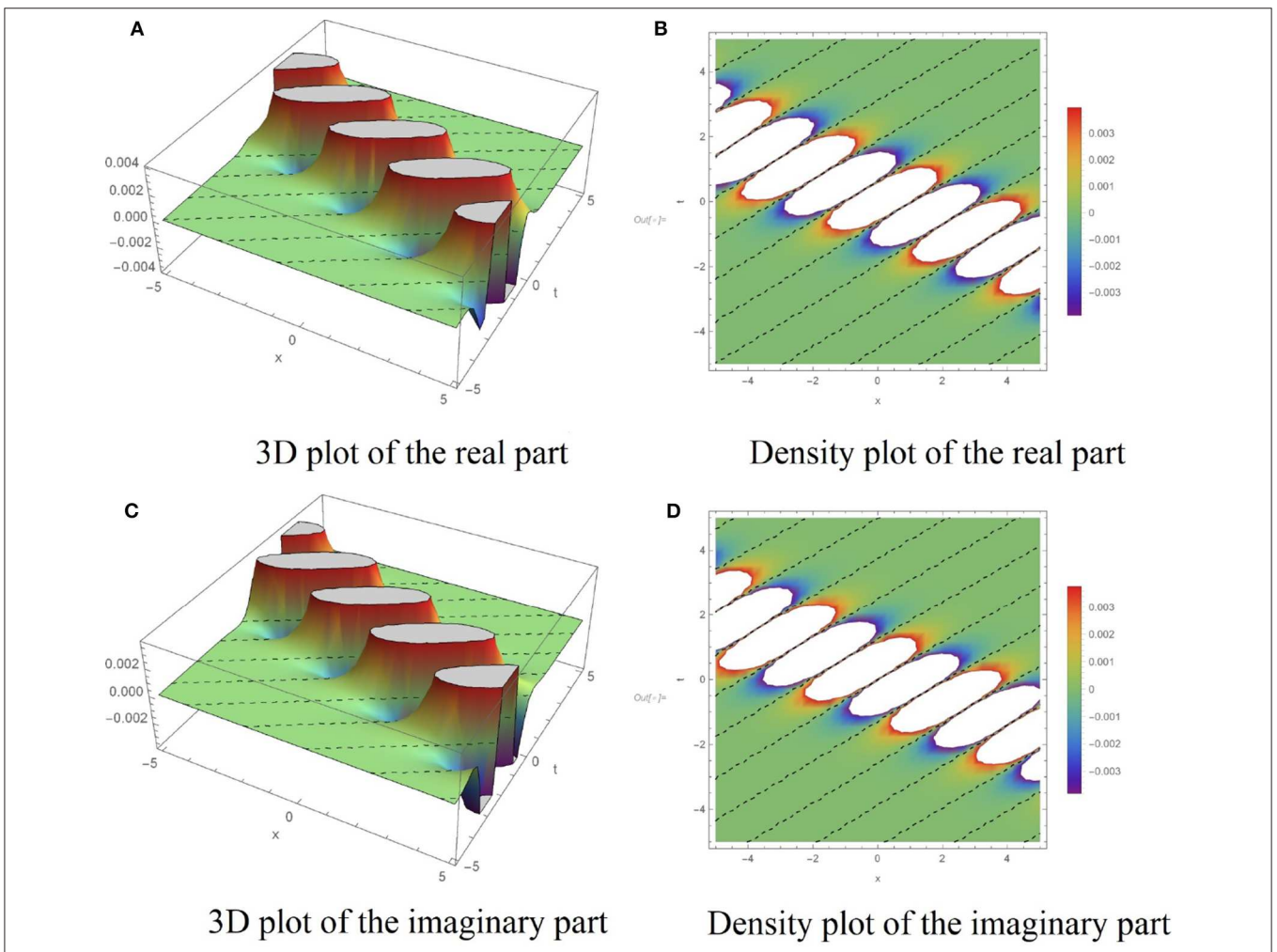

FIGURE 5 | Dynamic behaviors of $q_5(x,t)$ for $a = 0.2, b = -2, c = 0.5, \lambda_1 = 2, \lambda_2 = 2, \alpha = 0.99$. **(A)** 3D plot of the real part. **(B)** Density plot of the real part. **(C)** 3D plot of the imaginary part. **(D)** Density plot of the imaginary part.

provided that $ab < 0$, and

$$\xi = \frac{8a\sqrt{-3ab}t^{\alpha} + 3\left(\lambda_1 t^{\alpha} + x^{\alpha}\right)\left(\lambda_2 - c\right)}{\alpha\left(3\lambda_2 - 3c\right)}.$$

Category 3: It is attained $m = [3, 2, 1, 1]$ and $n = [1, 0, 1, 0]$, which offers

$$\Phi(\xi) = \frac{3e^{\xi} + 2}{e^{\xi} + 1}. \tag{20}$$

Case 1:

$$k = \frac{-2\sqrt{-3ab}}{3\left(c - \lambda_1\right)},$$
$$w = \sqrt{\frac{-a}{b}}\frac{-4ab\sqrt{-ab} - 3/4\left(\sqrt{-ab}\left(\lambda_2 - c\right) + 8\sqrt{3}/3\lambda_1 b\right)\left(\lambda_2 - c\right)}{3\left(\lambda_2 - c\right)^2},$$
$$\mathcal{A}_0 = \frac{3}{2}\sqrt{\frac{-3a}{b}}, \mathcal{A}_1 = 0, \mathcal{B}_1 = -3\sqrt{\frac{-3a}{b}}.$$

Accordingly, we derive a soliton solution of given PDE in (7) as

$$\mathcal{R}(\xi) = \frac{3}{2}\sqrt{\frac{-3a}{b}}\frac{e^{\xi}}{3e^{\xi} + 2}.$$

Accordingly, we derive a soliton solution of given PDE in (7) as

$$q_5(x,t) = \left(\frac{3}{2}\sqrt{\frac{-3a}{b}}\frac{e^{\xi}}{3e^{\xi} + 2}\right)^{1/2} \times e^{i\left(\left(\frac{-k}{\alpha}\right)x^{\alpha} + \left(\frac{\omega}{\alpha}\right)t^{\alpha}\right)}, \tag{21}$$

provided that $ab < 0$, and

$$\xi = \frac{4a\sqrt{-3ab}t^{\alpha} + 3\left(\lambda_1 t^{\alpha} + x^{\alpha}\right)\left(\lambda_2 - c\right)}{\alpha\left(3\lambda_2 - 3c\right)}.$$

Case 2:

$$k = \frac{-10\sqrt{-3ab}}{3\left(c - \lambda_1\right)},$$
$$w = -\frac{100}{3\left(\lambda_2 - c\right)^2}\sqrt{\frac{-a}{b}}\left(ab\sqrt{-ab} + \frac{3\lambda_2 - 3c}{400}\left(\sqrt{-ab}\left(\lambda_2 - c\right) + \frac{40\lambda_1 b\sqrt{3}}{3}\right)\right),$$
$$\mathcal{A}_0 = \frac{5}{2}\sqrt{\frac{-3a}{b}}, \mathcal{A}_1 = -\frac{1}{2}\sqrt{\frac{-3a}{b}}, \mathcal{B}_1 = -3\sqrt{\frac{-3a}{b}}.$$

Accordingly, we derive a soliton solution of given PDE in (7) as

$$\mathcal{R}(\xi) = \sqrt{\frac{-3a}{b}}\frac{e^{\xi}}{6e^{2\xi} + 10e^{\xi} + 4}.$$

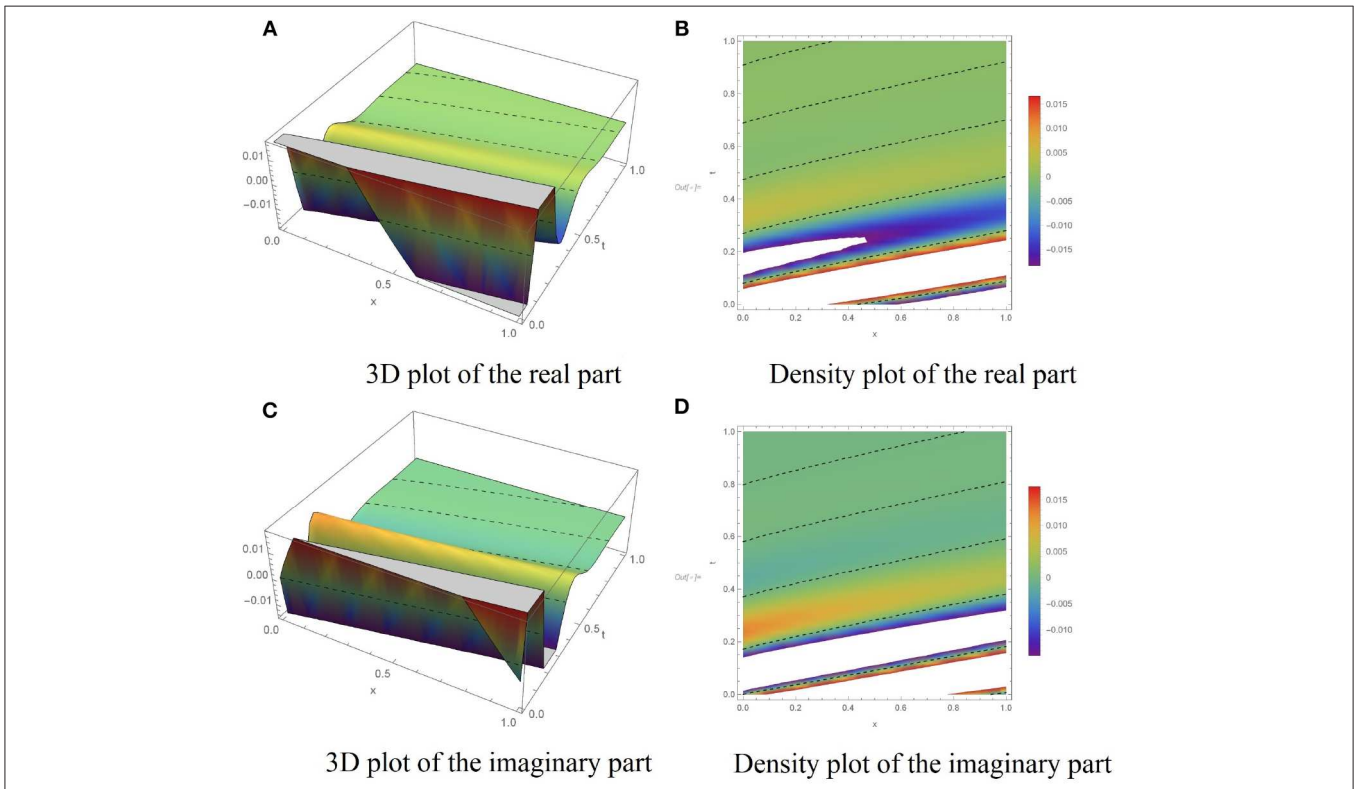

FIGURE 6 | Dynamic behaviors of $q_6(x, t)$ for $a = 1.5, b = -5, c = 65, \lambda_1 = 0.3, \lambda_2 = 0.7, \alpha = 0.9$. **(A)** 3D plot of the real part. **(B)** Density plot of the real part. **(C)** 3D plot of the imaginary part. **(D)** Density plot of the imaginary part.

Accordingly, we derive a soliton solution of given PDE in (7) as

$$q_6(x,t) = \left(\sqrt{\frac{-3a}{b}}\frac{e^{\xi}}{6e^{2\xi}+10e^{\xi}+4}\right)^{1/2} \times e^{i\left(\left(\frac{-k}{\alpha}\right)x^{\alpha}+\left(\frac{\omega}{\alpha}\right)t^{\alpha}\right)}, \tag{22}$$

provided that $ab < 0$, and

$$\xi = \frac{20a\sqrt{-3ab}t^{\alpha} + 3\left(\lambda_1 t^{\alpha} + x^{\alpha}\right)(\lambda_2 - c)}{\alpha(3\lambda_2 - 3c)}.$$

Category 4: It is attained $m = [-1, 0, 1, 0]$ and $n = [0, 1, 0, 1]$, which offers

$$\Phi(\xi) = -\frac{1}{e^{\xi}+1}. \tag{23}$$

Case 1:

$$k = \frac{2\sqrt{-3ab}}{3(c-\lambda_1)},$$

$$w = \frac{-8\sqrt{-3ab}(c-\lambda_2)\lambda_1 + 16a^2b + 3ac^2 - 6ac\lambda_2 + 3a{\lambda_2}^2}{12(c-\lambda_2)^2},$$

$$\mathcal{A}_0 = 0, \mathcal{A}_1 = \frac{1}{2}\sqrt{\frac{-3a}{b}}, \mathcal{B}_1 = 0.$$

Inserting these values in Equation (13), yields

$$\mathcal{R}(\xi) = -\sqrt{\frac{-3a}{b}}\frac{1}{\left(2+e^{\xi}\right)}.$$

Accordingly, we derive a soliton solution of given PDE in (7) as

$$q_7(x,t) = \left(-\sqrt{\frac{-3a}{b}}\frac{1}{\left(2+e^{\xi}\right)}\right)^{1/2} \times e^{i\left(\left(\frac{-k}{\alpha}\right)x^{\alpha}+\left(\frac{\omega}{\alpha}\right)t^{\alpha}\right)}, \tag{24}$$

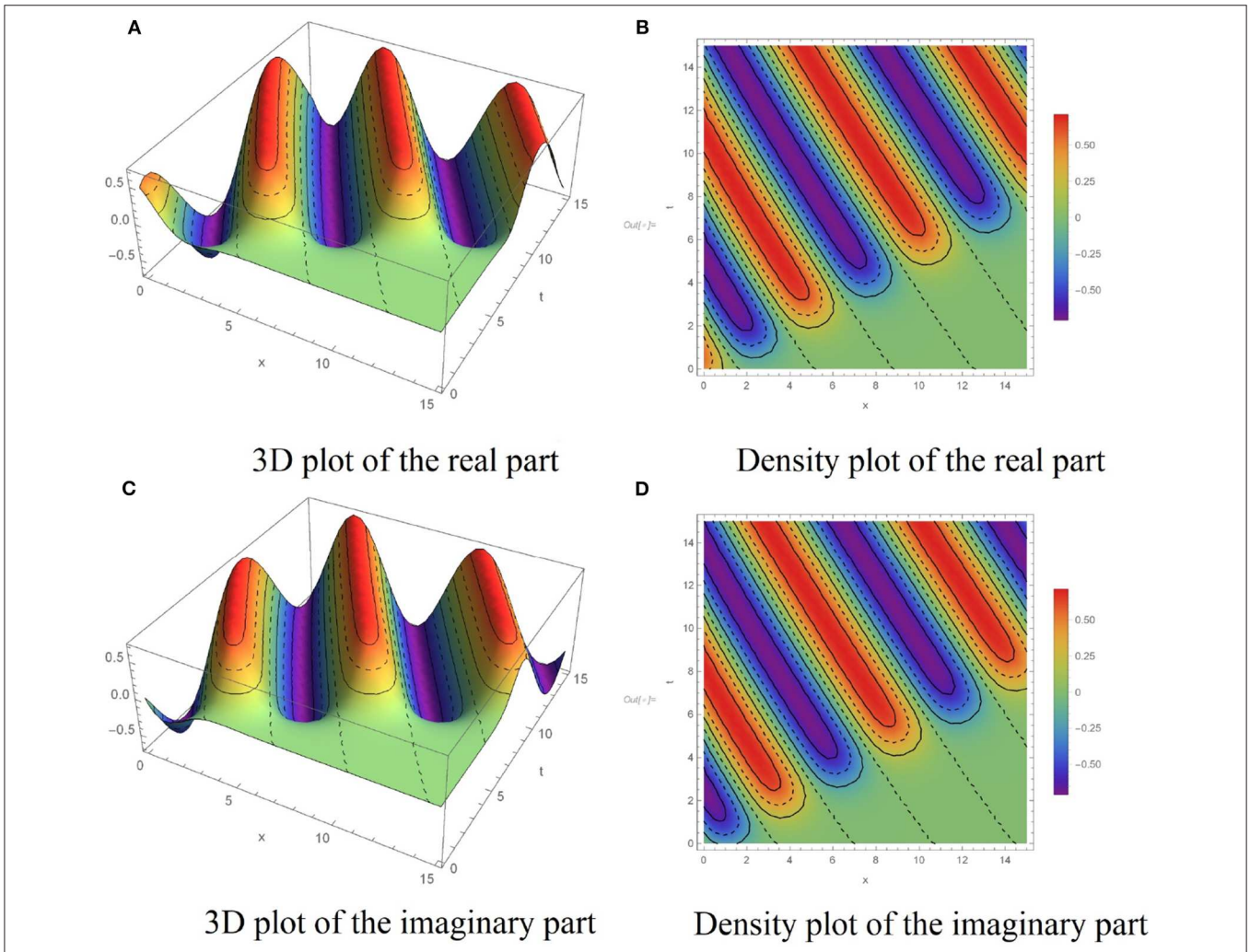

FIGURE 7 | Dynamic behaviors of $q_7(x,t)$ for $a = -2, b = 3, c = 3.5, \lambda_1 = 2, \lambda_2 = 0.5, \alpha = 0.95$. **(A)** 3D plot of the real part. **(B)** Density plot of the real part. **(C)** 3D plot of the imaginary part. **(D)** Density plot of the imaginary part.

provided that $ab < 0$, and

$$\xi = \frac{-4a\sqrt{-3ab}t^{\alpha} + 3\left(\lambda_1 t^{\alpha} + x^{\alpha}\right)\left(\lambda_2 - c\right)}{\alpha\left(3\lambda_2 - 3c\right)}.$$

Comparing our acquired solutions with other existing reported in the literature shows that ours are different and new. All the acquired solutions are new and have not been reported in the previous papers. Particularly, since the form of the equation and derivative considered in this article are the same as those given in reference [7], we can check that the results and the requirements for their existence in the two papers are quite different. Furthermore, we have checked the correctness of all obtained solutions, and found they satisfy the original equation.

4. NUMERICAL SIMULATIONS

In this section, we have presented several numerical simulations using the algorithm proposed in subsection 2.1. To illustrate the dynamic behaviors of the analytical results obtained in section 3, **Figures 1**–**7** have been depicted. **Figure 1** shows the dynamic behavior of the solution $q_1(x,t)$ defined in (15) for $a = 0.2, b = -0.5, c = 0.5, \lambda_1 = 3, \lambda_2 = 3, \alpha = 0.97$. The solution attributes of $q_2(x,t)$ presented in (16), are displayed in the **Figure 2**, where the parameters $a = -4, b = 2, c = 2, \lambda_1 = 0.1, \lambda_2 = 0.1, \alpha = 0.95$ are used. The graph of the solution $q_3(x,t)$ as explained in (18), for the given values $a = 1, b = -3, c = 0.5, \lambda_1 = 1, \lambda_2 = 4, \alpha = 0.9$ is plotted in **Figure 3**. Moreover, the diagram of $q_4(x,t)$ is displayed in **Figure 4** corresponding to the choices of $a = 1.5, b = -2.5, c = 1, \lambda_1 = 7, \lambda_2 = 2, \alpha = 0.9$. Taking the parameters $a = 0.2, b = -2, c = 0.5, \lambda_1 = 2, \lambda_2 = 2, \alpha = 0.99$ into consideration, the graph of the solution $q_5(x,t)$ presented in the Equation (21) is plotted in **Figure 5**. Moreover, **Figure 6** illustrate the dynamic behaviors of the analytical solution $q_6(x,t)$ obtained in Equation (22) by taking $a = 1.5, b = -5, c = 65, \lambda_1 = 0.3, \lambda_2 = 0.7, \alpha = 0.9$. And finally, the profiles of the exact solution $q_7(x,t)$ presented in Equation (24) is displayed in **Figure 7**, when $a = -2, b = 3, c = 3.5, \lambda_1 = 2, \lambda_2 = 0.5, \alpha = 0.95$ are chosen as parameters in the main PDE of (7). The performed numerical simulations admit that the solutions are of kinky and anti-kinky, and the trigonometric classifications. Also, by carefully looking at the structure of the obtained solutions, it can be seen that the corresponding conformable derivative parameter of α appears in the formula of all the solutions.

5. CONCLUSIONS

Partial differential equation is a powerful and effective tool for modeling non-linear systems. Finding the exact solution to such equations is one of the most challenging problems in mathematics. There is also no specific way of solving many of these equations. In these cases, we must resort to the approximate analytical methods due to the limitations of exact solver methods. According to what stated above, new approaches to solving PDE equations are of great importance and application. The main objective of this paper is to employ a well-known technique called GERFM to solve the perturbed Gerdjikov-Ivanov equation with the comfortable derivative. One of the outstanding features of the model considered in this article is the use of the definition of the comfortable derivative in the structure of the model. This definition is one of the most interesting definitions for a derivative that has many ideal features for a derivative. Applying this definition to the model will provide us with many advantages compared to the standard derivative. One of the advantages of the method used in this article is the determination of various categories of solutions during the method. Several numerical simulations are presented to gain a better understanding of the properties of the acquired solutions. By comparing the obtained results with the results of the present papers, it can be seen that the obtained results are not reported in any of the previous literature. It is worth mentioning that GERFM is capable of reducing the volume of needed computational compared to some other analytical method. The straightforward application is another advantage of the technique compared to other known techniques. This method can also be utilized to solve many other similar problems.

DATA AVAILABILITY STATEMENT

The raw data supporting the conclusions of this article will be made available by the authors, without undue reservation, to any qualified researcher.

AUTHOR CONTRIBUTIONS

All authors listed have made a substantial, direct and intellectual contribution to the work, and approved it for publication.

REFERENCES

1. Wazwaz AM. *Partial Differential Equations and Solitary Waves Theory*. Berlin; Heidelberg: Springer Berlin Heidelberg (2009).
2. Arshad M, Seadawy AR, Lu D. Modulation stability and dispersive optical soliton solutions of higher order nonlinear Schrödinger equation and its applications in mono-mode optical fibers. *Superlatt. Microstruct.* (2018) **113**:419–29. doi: 10.1016/j.spmi.2017.11.022
3. Hosseini K, Samadani F, Kumar D, Faridi M. New optical solitons of cubic-quartic nonlinear Schrödinger equation. *Optik.* (2018) **157**:1101–5. doi: 10.1016/j.ijleo.2017.11.124
4. González-Gaxiola O, Franco P, Bernal-Jaquez R. Solution of the nonlinear Schrödinger equation with defocusing strength nonlinearities through the Laplace-Adomian decomposition method. *Int J Appl Comput Math.* (2017) **3**:3723–43. doi: 10.1007/s40819-017-0325-5
5. Arshed S, Biswas A, Abdelaty M, Zhou Q, Moshokoa SP, Belic M. Optical soliton perturbation for Gerdjikov-Ivanov equation via two analytical techniques. *Chin J Phys.* (2018) **56**:2879–86. doi: 10.1016/j.cjph.2018.09.023
6. Biswas A, Alqahtani RT. Chirp-free bright optical solitons for perturbed Gerdjikov-Ivanov equation by semi-inverse variational principle. *Optik.* (2017) **147**:72–6. doi: 10.1016/j.ijleo.2017.08.019

7. Yaşar E, Yıldırım Y, Yaşar E. New optical solitons of space-time conformable fractional perturbed Gerdjikov-Ivanov equation by sine-Gordon equation method. *Results Phys.* (2018) **9**:1666–72. doi: 10.1016/j.rinp.2018.04.058
8. Biswas A, Ekici M, Sonmezoglu A, Majid FB, Triki H, Zhou Q, et al. Optical soliton perturbation for Gerdjikov-Ivanov equation by extended trial equation method. *Optik.* (2018) **158**:747–52. doi: 10.1016/j.ijleo.2017.12.191
9. Arshed S. Two reliable techniques for the soliton solutions of perturbed Gerdjikov-Ivanov equation. *Optik.* (2018) **164**:93–9. doi: 10.1016/j.ijleo.2018.02.119
10. Kaur L, Wazwaz AM. Optical solitons for perturbed Gerdjikov-Ivanov equation. *Optik.* (2018) **174**:447–51. doi: 10.1016/j.ijleo.2018.08.072
11. Hosseini K, Mirzazadeh M, Ilie M, Radmehr S. Dynamics of optical solitons in the perturbed Gerdjikov-Ivanov equation. *Optik.* (2020) **206**:164350. doi: 10.1016/j.ijleo.2020.164350
12. Khalil R, Horani MA, Yousef A, Sababheh M. A new definition of fractional derivative. *J Comput Appl Math.* (2014) **264**:65–70. doi: 10.1016/j.cam.2014.01.002
13. Eslami M, Rezazadeh H. The first integral method for Wu-Zhang system with conformable time-fractional derivative. *Calcolo.* (2015) **53**:475–85. doi: 10.1007/s10092-015-0158-8
14. Atangana A, Baleanu D, Alsaedi A. New properties of conformable derivative. *Open Math.* (2015) **13**:81. doi: 10.1515/math-2015-0081
15. Çenesiz Y, Baleanu D, Kurt A, Tasbozan O. New exact solutions of Burgers' type equations with conformable derivative. *Waves Random Complex Med.* (2016) **27**:103–16. doi: 10.1080/17455030.2016.1205237
16. Anastassiou, G. A., editor. "Fractional conformable approximation of Csiszar's f-divergence," in *Intelligent Analysis: Fractional Inequalities and Approximations Expanded*. Cham: Springer International Publishing (2020). p. 463–480. doi: 10.1007/978-3-030-38636-8_25
17. Harir A, Melliani S, Chadli LS. Fuzzy generalized conformable fractional derivative. *Adv Fuzzy Syst.* (2020) **2020**:1–7. doi: 10.1155/2020/1954975
18. Zafar A, Seadawy AR. The conformable space-time fractional mKdV equations and their exact solutions. *J King Saud Univ Sci.* (2019) **31**:1478–84. doi: 10.1016/j.jksus.2019.09.003
19. Zafar A, Raheel M, Bekir A. Exploring the dark and singular soliton solutions of Biswas-Arshed model with full nonlinear form. *Optik.* (2020) **204**:164133. doi: 10.1016/j.ijleo.2019.164133
20. Zafar A, Rezazadeh H, Bekir A, Malik A. Exact solutions of (3+1)-dimensional fractional mKdV equations in conformable form via $exp(-\phi(\tau))$ expansion method. *SN Appl Sci.* (2019) **1**:11. doi: 10.1007/s42452-019-1424-1
21. Rezazadeh H, Vahidi J, Zafar A, Bekir A. The functional variable method to find new exact solutions of the nonlinear evolution equations with dual-power-law nonlinearity. *Int J Nonlin Sci Numer Simul.* (2019). doi: 10.1515/ijnsns-2019-0064. [Epub ahead of print].
22. Zafar A. Rational exponential solutions of conformable space-time fractional equal-width equations. *Nonlin Eng.* (2019) **8**:350–5. doi: 10.1515/nleng-2018-0076
23. Ghanbari B, Inc M. A new generalized exponential rational function method to find exact special solutions for the resonance nonlinear Schrödinger equation. *Eur Phys J Plus.* (2018) **133**:1. doi: 10.1140/epjp/i2018-11984-1
24. Osman MS, Ghanbari B. New optical solitary wave solutions of Fokas-Lenells equation in presence of perturbation terms by a novel approach. *Optik.* (2018) **175**:328–33. doi: 10.1016/j.ijleo.2018.08.007
25. Ghanbari B, Baleanu D. A novel technique to construct exact solutions for nonlinear partial differential equations. *Eur Phys J Plus.* (2019) **134**:506. doi: 10.1140/epjp/i2019-13037-9
26. Ghanbari B, Baleanu D. New solutions of Gardner's equation using two analytical methods. *Front Phys.* (2019) **7**:202. doi: 10.3389/fphy.2019.00202
27. Srivastava HM, Günerhan H, Ghanbari B. Exact traveling wave solutions for resonance nonlinear Schrödinger equation with intermodal dispersions and the Kerr law nonlinearity. *Math Methods Appl Sci.* (2019) **42**:7210–21. doi: 10.1002/mma.5827

Conflict of Interest: The authors declare that the research was conducted in the absence of any commercial or financial relationships that could be construed as a potential conflict of interest.

Copyright © 2020 Ghanbari and Baleanu. This is an open-access article distributed under the terms of the Creative Commons Attribution License (CC BY). The use, distribution or reproduction in other forums is permitted, provided the original author(s) and the copyright owner(s) are credited and that the original publication in this journal is cited, in accordance with accepted academic practice. No use, distribution or reproduction is permitted which does not comply with these terms.

frontiers in Physics

ORIGINAL RESEARCH
published: 03 June 2020
doi: 10.3389/fphy.2020.00165

A New Dynamic Scheme via Fractional Operators on Time Scale

Saima Rashid[1], *Muhammad Aslam Noor*[2], *Kottakkaran Sooppy Nisar*[3]*, *Dumitru Baleanu*[4,5,6] *and Gauhar Rahman*[7]

[1] Department of Mathematics, Government College University, Faisalabad, Pakistan, [2] Department of Mathematics, COMSATS University Islamabad, Islamabad, Pakistan, [3] Department of Mathematics, College of Arts and Sciences, Prince Sattam Bin Abdulaziz University, Wadi Aldawaser, Saudi Arabia, [4] Department of Mathematics, Faculty of Arts and Sciences, Cankaya University, Ankara, Turkey, [5] Institute of Space Sciences, Magurele, Romania, [6] Department of Medical Research, China Medical University Hospital, China Medical University, Taichung, Taiwan, [7] Department of Mathematics, Shaheed Benazir Bhutto University, Sheringal, Pakistan

The present work investigates the applicability and effectiveness of the generalized Riemann-Liouville fractional integral operator integral method to obtain new Minkowski, Grüss type and several other associated dynamic variants on an arbitrary time scale, which are communicated as a combination of delta and fractional integrals. These inequalities extend some dynamic variants on time scales, and tie together and expand some integral inequalities. The present method is efficient, reliable, and it can be used as an alternative to establishing new solutions for different types of fractional differential equations applied in mathematical physics.

Keywords: Minkowski' inequlity, gruss inequality, fractional calculus, rimenn-liouville fractional integral operator, generalized riemann-liouville fractional integral operator, time sccale, holder inequality

OPEN ACCESS

Edited by:
Cosmas K. Zachos,
Argonne National Laboratory (DOE),
United States

Reviewed by:
Yudhveer Singh,
Amity University Jaipur, India
Sushila Rathore,
Vivekananda Global University, India

***Correspondence:**
Kottakkaran Sooppy Nisar
n.sooppy@psau.edu.sa

Specialty section:
This article was submitted to Mathematical Physics, a section of the journal Frontiers in Physics

Received: *03 December 2019*
Accepted: *21 April 2020*
Published: *03 June 2020*

Citation:
Rashid S, Aslam Noor M, Nisar KS, Baleanu D and Rahman G (2020) A New Dynamic Scheme via Fractional Operators on Time Scale. Front. Phys. 8:165. doi: 10.3389/fphy.2020.00165

1. INTRODUCTION

Fractional calculus has also been comprehensively utilized in several instances, but the concept has been popularized and implemented in numerous disciplines of science, technology and engineering as a mathematical model (see [1, 2]). Numerous distinguished generalized fractional integral operators consist of the Hadamard operator, Erdlelyi-Kober operators, the Saigo operator, the Gaussian hypergeometric operator, the Marichev-Saigo-Maeda fractional integral operator, and so on.; out of the ones, the Riemann-Liouville fractional integral operator has been extensively utilized by researchers in theory as well as applications (see [1, 3–8]).

Stefan Hilger began the theories of time scales in his doctoral dissertation [9] and combined discrete and continuous analysis (see [10, 11]). From this moment, this hypothesis has received a lot of attention. In the book written by Bohner and Peterson [12] on the issues of time scale, a brief summary is given and several time calculations are performed. Over the past decade, many analysts working in specific applications have proved a reasonable number of dynamic inequalities on a time scale (see [13–15]). Several researchers have created various results relating to fractional calculus on time scales to obtain the corresponding dynamic inequalities (see [16–20]).

Recently, the idea of the fractional-order derivative has been expounded by Bastos et al. [16] via Riemann-Liouville fractional operators on scale versions by considering linear dynamic equations. Another approach on time scales shifts to the inverse Laplace transform [18]. Following such innovator work, the investigation of fractional calculus on time scales created in a mainstream look into research studies on time scales (see [18, 21–29] and references therein). Since the publications in 2015, several researchers made significant contributions to the history of time scales. Sun and Hou [30] employed the fractional q-symmetric systems on time scales. Yaslan and Liceli [29] obtained the three-point boundary value problem with delta Riemann-Liouville fractional

derivative on time scales. Yan et al. [31] adopted the Caputo fractional techniques on differential equations on time scales. Zhu and Wu [32] employed Caputo nabla fractional derivatives in order to find the existence of solutions for Cauchy problems. As certifiable utilities, we refer to the study of calcium ion channels that are impeded with an infusion of calcium-chelator ethylene glycol tetraacetic acid [33]. Actually, physical utilization of initial value-fractional problems in diverse time scales proliferates [10, 34, 35]. For instance, the continuous time scale $\mathbb{T} = \mathbb{R}$, the fractional differential equations that oversee the practices of viscoelastic materials with memory and creep tendencies have been investigated in Chidouh et al. [36].

Integral Inequalities are an excellent way to investigate many scientific fields of research, including engineering, flow dynamics, biology, chaos, meteorology, vibration analysis, biochemistry, aerodynamics and many more. Since the productions of the above outcome in 1883, several works have been published in the literature of time calculus, with varied evidence, various speculations and improvements [37–51]. Recently, numerous analysts examined various inequalities, such as Hermite-Hadamard inequalities, Ostrowski inequalities and the expanded version of Hardy-type inequalities (see [13–15, 24, 52] and the references therein).

Here, we broaden accessible outcomes in the literature [53] by presenting increasingly broad ideas of fractional integral inequalities on time scales in the frame of generalized Riemann-Liouville fractional integral. At that point, we study the dynamic variants of corresponding generalized fractional-order on time scales. We obtain the inequalities Grüss, Minkowski and several others using the delta integrals in arbitrary time scales. For $\delta = 1$, the integral will become delta integral and for $\delta = 0$, it advances toward turning out to be nabla integral. An astounding audit about the time scale calculus can be found in the paper [54]. The proposed dynamical integral method is reliable and effective to obtain new solutions. This method has more advantages: it is direct and concise. Thus, the proposed method can be extended to solve many systems of nonlinear fractional partial differential equations in mathematical and physical sciences. Also, the new exact analytical solutions can be obtained for the generalized ordinary differential equations to obtain new theorems related to stability and continuous dependence on parameters for dynamic equations on time scales.

The present work investigates the applicability and effectiveness of the several dynamic variants that are presented, which are based primarily on the generalized Riemann-Liouville fractional integral operators. We will show that the Gr*ü*ss and Minkowski type, that we participated in are very specific to the current work. From an application point of view, the results ultimately relate to the study of Young's inequality, arithmetic, and geometry inequality. Our computed outcomes can be very useful as a starting point of comparison when some approximate methods are applied to this nonlinear space-time fractional equation. Furthermore, there are likewise some occurrences that can be derived from our outcomes.

2. PRELIMINARIES

A non-empty closed subsets $\mathbb{R}$ of $\mathbb{T}$ is known as the time scale. The well-known examples of time scales theory are the set of real numbers $\mathbb{R}$ and the integers $\mathcal{Z}$. Throughout the paper, we refer $\mathbb{T}$ as time scale and a time-scaled interval is $\Upsilon_{\mathbb{T}} = [\upsilon_1, \upsilon_2]_{\mathbb{T}}$. We need the concept of jump operators. The forward jump operator is denoted by the symbol $\diamond$ and the backward jump operator is denoted by ϑ, are said through the formulas:

$$\diamond(t) = \inf\{\lambda \in \mathbb{T} : \rho > t\} \in \mathbb{T}, \quad \vartheta(\omega) = \sup\{\rho \in \mathbb{T} : \rho < \omega\} \in \mathbb{T}.$$

We accumulate as:

$$\inf \emptyset := \sup \mathbb{T}, \quad \sup \emptyset := \inf \mathbb{T}.$$

If $\diamond(t) > t$, then the term t is allude to be right-scattered and ω is allude to be left-scattered $\varrho(\omega) < \omega$. The elements that are most likely all the while appropriate-scattered and scattered are known as isolated. The term t is said to be right dense, if $\diamond(t) = t$, and ω is said to be left dense, if $\varrho(\omega) = \omega$. In addition, the focuses t, ω are known to be dense if they are most likely right-dense and left-dense.
The mappings $\mu, \nu : \mathbb{T} \to [0, +\infty)$ defined by

$$\mu(t) := \diamond(t) - t,$$

$$\nu(t) := t - \vartheta(t)$$

are called the forward and backward graininess functions, respectively.

Definition 2.1. [12, 55] "Let $\hbar : \mathbb{T} \to \mathbb{R}$ be a real-valued function. Then $\hbar$ is said to be $\mathcal{RD}$-continuous on $\mathbb{R}$ if its left limit at any left dense point of $\mathbb{T}$ is finite and it is continuous on every right dense point of $\mathbb{T}$. All $\mathcal{RD}$-continuous functions are denoted by $\mathbb{C}_{\mathcal{RD}}$."

Definition 2.2. "A function $\mathcal{F} : \mathbb{T} \to \mathbb{R}$ is called a delta antiderivative of $\hbar : \mathbb{T} \to \mathbb{R}$ if $\mathcal{F}^{\Delta}(t) = \hbar(t)$, for all $t \in \mathbb{T}^k$. Then, one defines the delta integral by $\int_{\upsilon_1}^{t} \hbar(s)\Delta s = \mathcal{F}(t) - \mathcal{F}(\upsilon_1)$."

Theorem 2.1. *[55]. If $\hbar \in \mathbb{C}_{RD}$ and $t \in \mathbb{T}^k$, then*

$$\int_{t}^{\diamond(t)} \hbar(s)\Delta s = \mu(t)\hbar(t).$$

Theorem 2.2. *[55]. Let $\upsilon_1, \upsilon_2, \upsilon_3 \in \mathbb{T}$, $\beta \in \mathbb{R}$ and $\hbar, \omega \in \mathbb{C}_{RD}$, then*

(*i*). $\int_{\upsilon_1}^{\upsilon_2} \big(\hbar_1(\rho) + \hbar_2(\rho)\big)\Delta\rho = \int_{\upsilon_1}^{\upsilon_2} \hbar_1(\rho)\Delta\rho + \int_{\upsilon_1}^{\upsilon_2} \hbar_2(\rho)\Delta\rho;$

(*ii*). $\int_{\upsilon_1}^{\upsilon_2} \beta\hbar(\rho)\Delta\rho = \beta \int_{\upsilon_1}^{\upsilon_2} \hbar(\rho)\Delta\rho;$

(*iii*). $\int_{\upsilon_1}^{\upsilon_2} \hbar(\rho)\Delta\rho = -\int_{\upsilon_2}^{\upsilon_1} \hbar(\rho)\Delta\rho;$

(*iv*). $\int_{\upsilon_1}^{\upsilon_2} \hbar(\rho)\Delta\rho = \int_{\upsilon_1}^{\varsigma_3} \hbar(\rho)\Delta\rho + \int_{\varsigma_3}^{\upsilon_2} \hbar(\rho)\Delta\rho;$

(*v*). $\int_{\upsilon_1}^{\upsilon_2} \hbar_1^{\diamond}(\rho)\hbar_2^{\Delta}\Delta\rho = (\hbar_1\hbar_2)(\upsilon_2) - (\hbar_1\hbar_2)(\upsilon_1) - \int_{\upsilon_1}^{\upsilon_2} \hbar_1^{\Delta}(\rho)\hbar_2(\rho)\Delta(\rho);$

(*vi*). $\int_{\upsilon_1}^{\upsilon_2} \hbar_1(\rho)\hbar_2^{\Delta}\Delta\rho = (\hbar_1\hbar_2)(\upsilon_2) - (\hbar_1\hbar_2)(\upsilon_1) - \int_{\upsilon_1}^{\upsilon_2} \hbar_1^{\Delta}(\rho)\hbar_2^{\diamond}(\rho)\Delta(\rho);$

(*vii*). $\int_{\upsilon_1}^{\upsilon_2} \hbar(\rho)\Delta(\rho) = 0;$

(*viii*). *If* $\hbar(\rho) \geq 0$ *for all* ρ, *then* $\int_{\upsilon_1}^{\upsilon_2} \hbar(\rho)\Delta(\rho) \geq 0;$

(*ix*). *If* $|\hbar_1(\rho)| \leq \hbar_2(\rho)$ *on* $[\upsilon_1, \upsilon_2]$, *then* $\left|\int_{\upsilon_1}^{\upsilon_2} \hbar_1(\rho)\Delta\rho\right| \leq \int_{\upsilon_1}^{\upsilon_2} \hbar_2(\rho)\Delta(\rho).$

From Theorem 2.2 (ix), for $\hbar_2(\rho) = |\hbar_1(\rho)|$ on $[\upsilon_1, \upsilon_2]$, we have

$$\left|\int_{\upsilon_1}^{\upsilon_2} \hbar(\rho)\Delta\rho\right| \leq \int_{\upsilon_1}^{\upsilon_2} |\hbar(\rho)|\Delta(\rho).$$

Proposition 2.1. *[56] Consider a time scale* $\mathbb{T}$ *and* $\hbar$ *is an increasing continuous function on* $\Upsilon_{\mathbb{T}}$. *An extension of* $\hbar$ *on* $\Upsilon_{\mathbb{T}}$ *is* $\mathcal{F}$ *given as*

$$\mathcal{F}(\theta) := \begin{cases} \hbar(\theta), & \text{if} \quad \theta \in \mathbb{T} \\ \hbar(\eta), & \text{if } \theta \in (\eta, \sigma(\eta)) \not\subset \mathbb{T}, \end{cases}$$

then

$$\int_{\upsilon_1}^{\upsilon_2} \hbar(\eta)\Delta\hbar \leq \int_{\upsilon_1}^{\upsilon_2} \mathcal{F}(\hbar)d\hbar.$$

Next we demonstrate the idea of fractional integral on time scale, which is mainly due to [16].

Definition 2.3. [16] "For $0 < \delta < 1$, let $\Upsilon_{\mathbb{T}} \subset \mathbb{T}$ is a time scale and $\mathcal{F}$ be an integrable function on $\Upsilon_{\mathbb{T}}$. Then the (left) fractional integral of order δ of $\mathcal{F}$ is defined by

$${}_{\upsilon_1}^{\mathbb{T}}\mathcal{J}_{\eta}^{\delta}(\eta) = \frac{1}{\Gamma(\delta)} \int_{\upsilon_1}^{\eta} (\eta - \theta)^{\delta-1}\mathcal{F}(\theta)\Delta\theta, \tag{1}$$

where Γ is the gamma function."

Again, we demonstrate the concept of generalized Riemann-Liouville fractional integral operator which is proposed by [24].

Definition 2.4. [24] "For $0 < \delta < 1$, let $\mathbb{T}$ is a time scale and $[\upsilon_1, \upsilon_2]$ is an interval of $\mathbb{T}$. Suppose $\mathcal{F}$ be an integrable function on $[\upsilon_1, \upsilon_2]$ and Φ is monotone having a delta derivative Φ^{Δ} with $\Phi^{\Delta} \neq 0$ for any $\eta \in [\upsilon_1, \upsilon_2]$. Let $0 < \delta < 1$, then the (left) generalized fractional integral of order δ of $\mathcal{F}$ with respect to Φ is defined by

$${}_{\upsilon_1;\Phi}^{\mathbb{T}}\mathcal{J}_{\eta}^{\delta}(\eta) = \frac{1}{\Gamma(\delta)} \int_{\upsilon_1}^{\eta} (\Phi(\eta) - \Phi(\theta))^{\delta-1}\Phi^{\Delta}(\theta)\mathcal{F}(\theta)\Delta\theta."\ (2)$$

Remark 2.1. *If* $\mathbb{T} = \mathbb{R}$, *then Definitions 2.3 and 2.4 reduces to the well-known Riemann-Liouville and generalized Riemann-Liouville fractional integral, respectively (see [7]).*

3. MINKOWSKI TYPE INEQUALITIES FOR GENERALIZED RIEMANN-LIOUVILLE FRACTIONAL INTEGRAL ON TIME SCALE

This section is inaugurated to establishing generalizations of some reverse Minkowski inequality by introducing the generalized Riemann-Liouville fractional integral on time scale.

Theorem 3.1. *Let* $\delta, \gamma > 1$, *and* $\mathbb{T}$ *is a time scale. Suppose* $\mathcal{F}, \mathcal{G}$ *be two positive functions on* $[0, \infty)_{\mathbb{T}}$, *and* Φ *is monotone, delta differentiable* Φ^{Δ} *with* $\Phi^{\Delta} \neq 0$ *such that for all* $\eta > 0$, ${}_{0^+;\Phi}^{\mathbb{T}}\mathcal{J}_{\eta}^{\delta}\mathcal{F}(\eta) < \infty$, ${}_{0^+;\Phi}^{\mathbb{T}}\mathcal{J}_{\eta}^{\delta}\mathcal{G}(\eta) < \infty$. *If* $0 < \mathfrak{m} \leq \frac{\mathcal{F}(\theta)}{\mathcal{G}(\theta)} \leq \mathcal{M}, \theta \in [0, \eta]$, *then*

$$\left[{}_{0^+;\Phi}^{\mathbb{T}}\mathcal{J}_{\eta}^{\delta}\mathcal{F}(\eta)\right]^{\frac{1}{\alpha}} \left[{}_{0^+;\Phi}^{\mathbb{T}}\mathcal{J}_{\eta}^{\delta}\mathcal{G}(\eta)\right]^{\frac{1}{\beta}} \leq \left(\frac{\mathcal{M}}{\mathfrak{m}}\right)^{\frac{1}{\alpha\beta}} \left[{}_{0^+;\Phi}^{\mathbb{T}}\mathcal{J}_{\eta}^{\delta}\big(\mathcal{F}(\theta)\big)^{\frac{1}{\alpha}}\big(\mathcal{G}(\eta)\big)^{\frac{1}{\beta}}\right]. \tag{3}$$

Proof: Since $\frac{\mathcal{F}(\theta)}{\mathcal{G}(\theta)} \leq \mathcal{M}, \theta \in [0, \eta]$, $\eta > 0$, we find that

$$\big(\mathcal{G}(\theta)\big)^{\frac{1}{\alpha}} \geq \mathcal{M}^{-\frac{1}{\beta}}\big(\mathcal{F}(\theta)\big)^{\frac{1}{\beta}} \tag{4}$$

and

$$\big(\mathcal{F}(\theta)\big)^{\frac{1}{\alpha}}\big(\mathcal{G}(\theta)\big)^{\frac{1}{\beta}} \geq \mathcal{M}^{-\frac{1}{\beta}}\mathcal{F}(\theta). \tag{5}$$

Taking product on both sides of (5) $\frac{\big(\Phi(\eta)-\Phi(\theta)\big)^{\delta-1}\Phi^{\Delta}(\theta)}{\Gamma(\delta)}$, which is positive because $\theta \in (0, \eta)$, $\eta > 0$, we integrate the resulting identity with respect to θ from 0 to η we have

$$\frac{1}{\Gamma(\delta)} \int_0^{\eta} \big(\Phi(\eta) - \Phi(\theta)\big)^{\delta-1}\Phi^{\Delta}(\theta)\big(\mathcal{F}(\theta)\big)^{\frac{1}{\alpha}}\big(\mathcal{G}(\theta)\big)^{\frac{1}{\beta}}\Delta\theta \geq \frac{\mathcal{M}^{-\frac{1}{\beta}}}{\Gamma(\delta)} \int_0^{\eta} \big(\Phi(\eta) - \Phi(\theta)\big)^{\delta-1}\Phi^{\Delta}(\theta)\mathcal{F}(\theta)\Delta\theta, \tag{6}$$

which implies that

$$ {}^{\mathbb{T}}_{0^+;\Phi}\mathcal{J}^{\delta}_{\eta}\big(\mathcal{F}(\theta)\big)^{\frac{1}{\alpha}}\big(\mathcal{G}(\eta)\big)^{\frac{1}{\beta}} \geq \mathcal{M}^{-\frac{1}{\beta}}\,{}^{\mathbb{T}}_{0^+;\Phi}\mathcal{J}^{\delta}_{\eta}\mathcal{F}(\eta). \tag{7} $$

It follows that

$$ \left({}^{\mathbb{T}}_{0^+;\Phi}\mathcal{J}^{\delta}_{\eta}\big(\mathcal{F}(\theta)\big)^{\frac{1}{\alpha}}\big(\mathcal{G}(\eta)\big)^{\frac{1}{\beta}}\right)^{\frac{1}{\alpha}} \geq \mathcal{M}^{-\frac{1}{\alpha\beta}}\left({}^{\mathbb{T}}_{0^+;\Phi}\mathcal{J}^{\delta}_{\eta}\mathcal{F}(\eta)\right)^{\frac{1}{\alpha}}. \tag{8} $$

Accordingly, $\mathfrak{m}\mathcal{G}(\theta) \leq \mathcal{F}(\theta), \theta \in (0,\eta)$, $\eta > 0$, therefore we have

$$ \big(\mathcal{F}(\theta)\big)^{\frac{1}{\alpha}} \geq \mathfrak{m}^{\frac{1}{\alpha}}\big(\mathcal{G}(\theta)\big)^{\frac{1}{\alpha}}. \tag{9} $$

Taking product (9) by $(\mathcal{G}(\theta))^{\frac{1}{\beta}}$, we arrive at

$$ \big(\mathcal{G}(\theta)\big)^{\frac{1}{\beta}}\big(\mathcal{F}(\theta)\big)^{\frac{1}{\alpha}} \geq \mathfrak{m}^{\frac{1}{\alpha}}\mathcal{G}(\theta). \tag{10} $$

Taking product on both sides of (11) $\frac{\big(\Phi(\eta)-\Phi(\theta)\big)^{\delta-1}\Phi^{\Delta}(\theta)}{\Gamma(\delta)}$, which is positive because $\theta \in (0,\eta)$, $\eta > 0$, we integrate the resulting identity with respect to θ from 0 to η we have

$$ \begin{aligned} &\frac{1}{\Gamma(\delta)}\int_0^{\eta}\big(\Phi(\eta)-\Phi(\theta)\big)^{\delta-1}\Phi^{\Delta}(\theta)\big(\mathcal{G}(\theta)\big)^{\frac{1}{\beta}}\big(\mathcal{F}(\theta)\big)^{\frac{1}{\alpha}}\Delta\theta \\ &\geq \mathfrak{m}^{\frac{1}{\alpha}}\frac{1}{\Gamma(\delta)}\int_0^{\eta}\big(\Phi(\eta)-\Phi(\theta)\big)^{\delta-1}\Phi^{\Delta}(\theta)\mathcal{G}(\theta)\Delta\theta. \end{aligned} \tag{11} $$

Hence, we can write

$$ \left({}^{\mathbb{T}}_{0^+;\Phi}\mathcal{J}^{\delta}_{\eta}\big(\mathcal{F}(\theta)\big)^{\frac{1}{\alpha}}\big(\mathcal{G}(\eta)\big)^{\frac{1}{\beta}}\right)^{\frac{1}{\beta}} \geq \mathfrak{m}^{\frac{1}{\alpha\beta}}\left({}^{\mathbb{T}}_{0^+;\Phi}\mathcal{J}^{\delta}_{\eta}\mathcal{G}(\eta)\right)^{\frac{1}{\beta}}. \tag{12} $$

Conducting product between (8) and (12), we can draw the desired conclusion easily. □

Corollary 3.1. *Letting $\mathbb{T} = \mathbb{R}$, then under the assumption of Theorem 3.1, we have the following inequality in generalized Riemann-Liouville fractional integral:*

$$ \Big[\Phi\mathcal{J}^{\delta}_{\eta}\mathcal{F}(\eta)\Big]^{\frac{1}{\alpha}}\Big[\Phi\mathcal{J}^{\delta}_{\eta}\mathcal{G}(\eta)\Big]^{\frac{1}{\beta}} \leq \Big(\frac{\mathcal{M}}{\mathfrak{m}}\Big)^{\frac{1}{\alpha\beta}}\Big[\Phi\mathcal{J}^{\delta}_{\eta}\big(\mathcal{F}(\theta)\big)^{\frac{1}{\alpha}}\big(\mathcal{G}(\eta)\big)^{\frac{1}{\beta}}\Big]. $$

Theorem 3.2. *Let $\delta,\gamma > 1$, and $\mathbb{T}$ is a time scale. Suppose $\mathcal{F},\mathcal{G}$ be two positive functions on $[0,\infty)_{\mathbb{T}}$, and Φ is monotone, delta differentiable Φ^{Δ} with $\Phi^{\Delta} \neq 0$ such that for all $\eta > 0$, ${}^{\mathbb{T}}_{0^+;\Phi}\mathcal{J}^{\delta}_{\eta}\mathcal{F}^{\alpha}(\eta) < \infty$, ${}^{\mathbb{T}}_{0^+;\Phi}\mathcal{J}^{\delta}_{\eta}\mathcal{G}^{\beta}(\eta) < \infty$. If $0 < \mathfrak{m} \leq \frac{\mathcal{F}^{\alpha}(\theta)}{\mathcal{G}^{\beta}(\theta)} \leq \mathcal{M}, \theta \in [0,\eta]$, then*

$$ \begin{aligned} &\Big[{}^{\mathbb{T}}_{0^+;\Phi}\mathcal{J}^{\delta}_{\eta}\mathcal{F}^{\alpha}(\eta)\Big]^{\frac{1}{\alpha}}\Big[{}^{\mathbb{T}}_{0^+;\Phi}\mathcal{J}^{\delta}_{\eta}\mathcal{G}^{\beta}(\eta)\Big]^{\frac{1}{\beta}} \\ &\leq \Big(\frac{\mathcal{M}}{\mathfrak{m}}\Big)^{\frac{1}{\alpha\beta}}\Big[{}^{\mathbb{T}}_{0^+;\Phi}\mathcal{J}^{\delta}_{\eta}\big(\mathcal{F}(\theta)\mathcal{G}(\eta)\big)\Big], \end{aligned} \tag{13} $$

where $\alpha > 1$, $\frac{1}{\alpha}+\frac{1}{\beta} = 1$.

Proof: Replacing $\mathcal{F}(\theta)$ and $\mathcal{G}(\theta)$ by $\mathcal{F}^{\alpha}(\theta)$ and $\mathcal{G}^{\beta}(\theta)$, $\theta \in [0,\eta]$, $\eta > 0$ in Theorem 3.1, we acquire the desired result. This completes the proof. □

4. GRÜSS TYPE INEQUALITIES VIA GENERALIZED RIEMANN-LIOUVILLE FRACTIONAL INTEGRAL ON TIME SCALE

Our coming result is the generalization of Grüss type inequality via generalized Reimann-Liouville fractional integral operator on time scale.

Theorem 4.1. *Let $\delta,\gamma > 1$, and $\mathbb{T}$ is a time scale. Suppose there is a positive function $\mathcal{F}$ on $[0,\infty)_{\mathbb{T}}$, and Φ is monotone, delta differentiable Φ^{Δ} with $\Phi^{\Delta} \neq 0$ such that for all $\eta > 0$. Assume that the subsequent.*
(I) There exist two integrable functions φ_1,φ_2 on $[0,\infty)_{\mathbb{T}}$ such that

$$ \varphi_1(\eta) \leq \mathcal{F}(\eta) \leq \varphi_2(\eta), \quad \forall \eta \in [0,\infty)_{\mathbb{T}}. \tag{14} $$

Then, for $\eta > 0, \delta,\gamma > 1$, one has

$$ \begin{aligned} &{}^{\mathbb{T}}_{0^+;\Phi}\mathcal{J}^{\delta}_{\eta}\varphi_2(\eta)\,{}^{\mathbb{T}}_{0^+;\Phi}\mathcal{J}^{\gamma}_{\eta}\mathcal{F}(\eta) + {}^{\mathbb{T}}_{0^+;\Phi}\mathcal{J}^{\delta}_{\eta}\mathcal{F}(\eta)\,{}^{\mathbb{T}}_{0^+;\Phi}\mathcal{J}^{\lambda}_{\eta}\varphi_1(\eta) \\ &\geq {}^{\mathbb{T}}_{0^+;\Phi}\mathcal{J}^{\delta}_{\eta}\varphi_2(\eta)\,{}^{\mathbb{T}}_{0^+;\Phi}\mathcal{J}^{\lambda}_{\eta}\varphi_1(\eta) + {}^{\mathbb{T}}_{0^+;\Phi}\mathcal{J}^{\delta}_{\eta}\mathcal{F}(\eta)\,{}^{\mathbb{T}}_{0^+;\Phi}\mathcal{J}^{\lambda}_{\eta}\mathcal{F}(\eta), \end{aligned} \tag{15} $$

Proof: From (I), for all $\theta \geq 0, \lambda \geq 0$, we have

$$ \big(\varphi_2(\theta)-\mathcal{F}(\theta)\big)\big(\mathcal{F}(\lambda)-\varphi_1(\lambda)\big) \geq 0. \tag{16} $$

Therefore,

$$ \varphi_2(\theta)\mathcal{F}(\lambda)+\varphi_1(\lambda)\mathcal{F}(\theta) \geq \varphi_1(\lambda)\varphi_2(\theta)+\mathcal{F}(\theta)\mathcal{F}(\lambda). \tag{17} $$

Taking product on both sides of (17) $\frac{\big(\Phi(\eta)-\Phi(\theta)\big)^{\delta-1}\Phi^{\Delta}(\theta)}{\Gamma(\delta)}$, which is positive because $\theta \in (0,\eta)$, $\eta > 0$, we integrate the resulting identity with respect to θ from 0 to η we have

$$ \begin{aligned} &\mathcal{F}(\lambda)\frac{1}{\Gamma(\delta)}\int_0^{\eta}\big(\Phi(\eta)-\Phi(\theta)\big)^{\delta-1}\Phi^{\Delta}(\theta)\varphi_2(\theta)\Delta\theta \\ &\quad+\varphi_1(\lambda)\frac{1}{\Gamma(\delta)}\int_0^{\eta}\big(\Phi(\eta)-\Phi(\theta)\big)^{\delta-1}\Phi^{\Delta}(\theta)\mathcal{F}(\theta)\Delta\theta \\ &\geq \varphi_1(\lambda)\frac{1}{\Gamma(\delta)}\int_0^{\eta}\big(\Phi(\eta)-\Phi(\theta)\big)^{\delta-1}\Phi^{\Delta}(\theta)\varphi_2(\theta)\Delta\theta \\ &\quad+\mathcal{F}(\lambda)\frac{1}{\Gamma(\delta)}\int_0^{\eta}\big(\Phi(\eta)-\Phi(\theta)\big)^{\delta-1}\Phi^{\Delta}(\theta)\mathcal{F}(\theta)\Delta\theta, \end{aligned} \tag{18} $$

arrives at

$$ \begin{aligned} \mathcal{F}(\lambda)\,{}^{\mathbb{T}}_{0^+;\Phi}\mathcal{J}^{\delta}_{\eta}\varphi_2(\eta)+\varphi_1(\lambda)\,{}^{\mathbb{T}}_{0^+;\Phi}\mathcal{J}^{\delta}_{\eta}\mathcal{F}(\eta) &\geq \varphi_1(\lambda)\,{}^{\mathbb{T}}_{0^+;\Phi}\mathcal{J}^{\delta}_{\eta}\varphi_2(\eta) \\ &\quad+\mathcal{F}(\lambda)\,{}^{\mathbb{T}}_{0^+;\Phi}\mathcal{J}^{\delta}_{\eta}\mathcal{F}(\eta). \end{aligned} \tag{19} $$

Taking product on both sides of (19) $\frac{\big(\Phi(\eta)-\Phi(\lambda)\big)^{\gamma-1}\Phi^{\Delta}(\lambda)}{\Gamma(\gamma)}$, which is positive because $\lambda \in (0,\eta)$, $\eta > 0$, we integrate the resulting identity with respect to λ from 0 to η we have

$$
\begin{aligned}
&{}^{\mathbb{T}}_{0^+;\Phi}\mathcal{J}^{\delta}_{\eta}\varphi_2(\eta)\frac{1}{\Gamma(\gamma)}\int_0^{\eta}\big(\Phi(\eta)-\Phi(\lambda)\big)^{\gamma-1}\Phi^{\Delta}(\lambda)\mathcal{F}(\lambda)\Delta\lambda\\
&\quad+{}^{\mathbb{T}}_{0^+;\Phi}\mathcal{J}^{\delta}_{\eta}\mathcal{F}(\eta)\frac{1}{\Gamma(\gamma)}\int_0^{\eta}\big(\Phi(\eta)-\Phi(\lambda)\big)^{\gamma-1}\Phi^{\Delta}(\lambda)\varphi_1(\lambda)\Delta\lambda\\
&\geq {}^{\mathbb{T}}_{0^+;\Phi}\mathcal{J}^{\delta}_{\eta}\varphi_2(\eta)\frac{1}{\Gamma(\gamma)}\int_0^{\eta}\big(\Phi(\eta)-\Phi(\lambda)\big)^{\gamma-1}\Phi^{\Delta}(\lambda)\varphi_1(\lambda)\Delta\lambda\\
&\quad+{}^{\mathbb{T}}_{0^+;\Phi}\mathcal{J}^{\delta}_{\eta}\mathcal{F}(\eta)\frac{1}{\Gamma(\gamma)}\int_0^{\eta}\big(\Phi(\eta)-\Phi(\lambda)\big)^{\gamma-1}\Phi^{\Delta}(\lambda)\mathcal{F}(\lambda)\Delta\lambda.
\end{aligned}
\tag{20}
$$

Hence, we conclude the desired inequality. This completes the proof. □

Special cases of Theorem 4.1, we attain the subsequent results.

Corollary 4.1. *Letting $\Phi(\eta)=\eta$, then Theorem 4.1 will lead to the Riemann-Liouville fractional integral on time scales:*

$$
\begin{aligned}
&{}^{\mathbb{T}}_{0^+}\mathcal{J}^{\delta}_{\eta}\varphi_2(\eta)\,{}^{\mathbb{T}}_{0^+}\mathcal{J}^{\gamma}_{\eta}\mathcal{F}(\eta)+{}^{\mathbb{T}}_{0^+}\mathcal{J}^{\delta}_{\eta}\mathcal{F}(\eta)\,{}^{\mathbb{T}}_{0^+}\mathcal{J}^{\lambda}_{\eta}\varphi_1(\eta)\\
&\geq {}^{\mathbb{T}}_{0^+}\mathcal{J}^{\delta}_{\eta}\varphi_2(\eta)\,{}^{\mathbb{T}}_{0^+}\mathcal{J}^{\lambda}_{\eta}\varphi_1(\eta)+{}^{\mathbb{T}}_{0^+}\mathcal{J}^{\delta}_{\eta}\mathcal{F}(\eta)\,{}^{\mathbb{T}}_{0^+}\mathcal{J}^{\lambda}_{\eta}\mathcal{F}(\eta).
\end{aligned}
$$

Remark 4.1. *If $\mathbb{T}=\mathbb{R}$, then Theorem 4.1 will lead to Theorem 2.11 in [57] and corollary 4.1 will lead to Corollary 3 in [57]. Also, if we choose $\mathbb{T}=\mathbb{R}$ along with $\Phi(\eta)=\eta$, then Theorem 4.1 will lead to Theorem 2 in [58].*

Theorem 4.2. *Let $\delta,\gamma>1$, and $\mathbb{T}$ is a time scale. Suppose there are two positive functions $\mathcal{F},\mathcal{G}$ on $[0,\infty)_{\mathbb{T}}$, and Φ is monotone, delta differentiable Φ^{Δ} with $\Phi^{\Delta}\neq 0$ such that for all $\eta>0$. Suppose that (I) holds and moreover one assumes the following.*
(II) There exist ω_1 and ω_2 integrable functions on $[0,\infty)_{\mathbb{T}}$ such that

$$
\omega_1(\eta)\leq\mathcal{G}(\eta)\leq\omega_2(\eta)\quad\forall\eta\in[0,\infty)_{\mathbb{T}}. \tag{21}
$$

Then, for $\eta>0,\delta,\gamma>1$,the following inequalities hold:

$$
\begin{aligned}
(A_1)\quad &{}^{\mathbb{T}}_{0^+;\Phi}\mathcal{J}^{\delta}_{\eta}\varphi_2(\eta)\,{}^{\mathbb{T}}_{0^+;\Phi}\mathcal{J}^{\gamma}_{\eta}\mathcal{G}(\eta)+{}^{\mathbb{T}}_{0^+;\Phi}\mathcal{J}^{\delta}_{\eta}\mathcal{F}(\eta)\,{}^{\mathbb{T}}_{0^+;\Phi}\mathcal{J}^{\gamma}_{\eta}\omega_1(\eta)\\
&\geq {}^{\mathbb{T}}_{0^+;\Phi}\mathcal{J}^{\delta}_{\eta}\varphi_2(\eta)\,{}^{\mathbb{T}}_{0^+;\Phi}\mathcal{J}^{\gamma}_{\eta}\omega_1(\eta)\\
&\quad+{}^{\mathbb{T}}_{0^+;\Phi}\mathcal{J}^{\delta}_{\eta}\mathcal{F}(\eta)\,{}^{\mathbb{T}}_{0^+;\Phi}\mathcal{J}^{\gamma}_{\eta}\mathcal{G}(\eta),\\
(B_1)\quad &{}^{\mathbb{T}}_{0^+;\Phi}\mathcal{J}^{\gamma}_{\eta}\varphi_1(\eta)\,{}^{\mathbb{T}}_{0^+;\Phi}\mathcal{J}^{\delta}_{\eta}\mathcal{G}(\eta)+{}^{\mathbb{T}}_{0^+;\Phi}\mathcal{J}^{\gamma}_{\eta}\omega_2(\eta)\,{}^{\mathbb{T}}_{0^+;\Phi}\mathcal{J}^{\gamma}_{\eta}\mathcal{F}(\eta)\\
&\geq {}^{\mathbb{T}}_{0^+;\Phi}\mathcal{J}^{\gamma}_{\eta}\varphi_1(\eta)\,{}^{\mathbb{T}}_{0^+;\Phi}\mathcal{J}^{\delta}_{\eta}\omega_2(\eta)\\
&\quad+{}^{\mathbb{T}}_{0^+;\Phi}\mathcal{J}^{\gamma}_{\eta}\mathcal{F}(\eta)\,{}^{\mathbb{T}}_{0^+;\Phi}\mathcal{J}^{\delta}_{\eta}\mathcal{G}(\eta),\\
(C_1)\quad &{}^{\mathbb{T}}_{0^+;\Phi}\mathcal{J}^{\gamma}_{\eta}\omega_2(\eta)\,{}^{\mathbb{T}}_{0^+;\Phi}\mathcal{J}^{\delta}_{\eta}\varphi_2(\eta)+{}^{\mathbb{T}}_{0^+;\Phi}\mathcal{J}^{\delta}_{\eta}\mathcal{F}(\eta)\,{}^{\mathbb{T}}_{0^+;\Phi}\mathcal{J}^{\gamma}_{\eta}\mathcal{G}(\eta)\\
&\geq {}^{\mathbb{T}}_{0^+;\Phi}\mathcal{J}^{\delta}_{\eta}\varphi_2(\eta)\,{}^{\mathbb{T}}_{0^+;\Phi}\mathcal{J}^{\gamma}_{\eta}\mathcal{G}(\eta)\\
&\quad+{}^{\mathbb{T}}_{0^+;\Phi}\mathcal{J}^{\delta}_{\eta}\mathcal{F}(\eta)\,{}^{\mathbb{T}}_{0^+;\Phi}\mathcal{J}^{\gamma}_{\eta}\omega_2(\eta),\\
(D_1)\quad &{}^{\mathbb{T}}_{0^+;\Phi}\mathcal{J}^{\delta}_{\eta}\varphi_1(\eta)\,{}^{\mathbb{T}}_{0^+;\Phi}\mathcal{J}^{\gamma}_{\eta}\omega_1(\eta)\\
&\quad+{}^{\mathbb{T}}_{0^+;\Phi}\mathcal{J}^{\delta}_{\eta}\mathcal{F}(\eta)\,{}^{\mathbb{T}}_{0^+;\Phi}\mathcal{J}^{\delta}_{\eta}\,{}^{\mathbb{T}}_{0^+;\Phi}\mathcal{J}^{\gamma}_{\eta}\mathcal{G}(\eta)\\
&\geq {}^{\mathbb{T}}_{0^+;\Phi}\mathcal{J}^{\delta}_{\eta}\varphi_1(\eta)\,{}^{\mathbb{T}}_{0^+;\Phi}\mathcal{J}^{\gamma}_{\eta}\mathcal{G}(\eta)\\
&\quad+{}^{\mathbb{T}}_{0^+;\Phi}\mathcal{J}^{\gamma}_{\eta}\omega_1(\eta)\,{}^{\mathbb{T}}_{0^+;\Phi}\mathcal{J}^{\delta}_{\eta}\mathcal{F}(\eta).
\end{aligned}
\tag{22}
$$

Proof: To prove (A_1), from (I) and (II), we have for $x\in[0,\infty)_{\mathbb{T}}$ that

$$
\big(\varphi_2(\theta)-\mathcal{F}(\theta)\big)\big(\mathcal{G}(\lambda)-\omega_1(\lambda)\big)\geq 0. \tag{23}
$$

Therefore,

$$
\varphi_2(\theta)\mathcal{G}(\lambda)+\omega_1(\lambda)\mathcal{F}(\theta)\geq\omega_1(\lambda)\varphi_2(\theta)+\mathcal{G}(\lambda)\mathcal{F}(\theta). \tag{24}
$$

Taking product on both sides of (24) $\frac{\big(\Phi(\eta)-\Phi(\theta)\big)^{\delta-1}\Phi^{\Delta}(\theta)}{\Gamma(\delta)}$, which is positive because $\theta\in(0,\eta)$, $\eta>0$, we integrate the resulting identity with respect to θ from 0 to η we have

$$
\begin{aligned}
&\mathcal{G}(\lambda)\frac{1}{\Gamma(\delta)}\int_0^{\eta}\big(\Phi(\eta)-\Phi(\theta)\big)^{\delta-1}\Phi^{\Delta}(\theta)\varphi_2(\theta)\Delta\theta\\
&\quad+\omega_1(\lambda)\frac{1}{\Gamma(\delta)}\int_0^{\eta}\big(\Phi(\eta)-\Phi(\theta)\big)^{\delta-1}\Phi^{\Delta}(\theta)\mathcal{F}(\theta)\Delta\theta\\
&\geq\omega_1(\lambda)\frac{1}{\Gamma(\delta)}\int_0^{\eta}\big(\Phi(\eta)-\Phi(\theta)\big)^{\delta-1}\Phi^{\Delta}(\theta)\varphi_2(\theta)\Delta\theta\\
&\quad+\mathcal{G}(\lambda)\frac{1}{\Gamma(\delta)}\int_0^{\eta}\big(\Phi(\eta)-\Phi(\theta)\big)^{\delta-1}\Phi^{\Delta}(\theta)\mathcal{F}(\theta)\Delta\theta.
\end{aligned}
\tag{25}
$$

Then we have

$$
\begin{aligned}
&\mathcal{G}(\lambda)\,{}^{\mathbb{T}}_{0^+;\Phi}\mathcal{J}^{\delta}_{\eta}\varphi_2(\eta)+\omega_1(\lambda)\,{}^{\mathbb{T}}_{0^+;\Phi}\mathcal{J}^{\delta}_{\eta}\mathcal{F}(\eta)\\
&\geq\omega_1(\lambda)\,{}^{\mathbb{T}}_{0^+;\Phi}\mathcal{J}^{\delta}_{\eta}\varphi_2(\eta)+\mathcal{G}(\lambda)\,{}^{\mathbb{T}}_{0^+;\Phi}\mathcal{J}^{\delta}_{\eta}\mathcal{F}(\eta).
\end{aligned}
\tag{26}
$$

Again, multiplying both sides of (26) by $\frac{\big(\Phi(\eta)-\Phi(\lambda)\big)^{\gamma-1}\Phi^{\Delta}(\lambda)}{\Gamma(\gamma)}$, which is positive because $\lambda\in(0,\eta)$, $\eta>0$, we integrate the resulting identity with respect to λ from 0 to η we have

$$
\begin{aligned}
&{}^{\mathbb{T}}_{0^+;\Phi}\mathcal{J}^{\delta}_{\eta}\varphi_2(\eta)\frac{1}{\Gamma(\gamma)}\int_0^{\eta}\big(\Phi(\eta)-\Phi(\lambda)\big)^{\gamma-1}\Phi^{\Delta}(\lambda)\mathcal{G}(\lambda)\Delta\lambda\\
&\quad+{}^{\mathbb{T}}_{0^+;\Phi}\mathcal{J}^{\delta}_{\eta}\mathcal{F}(\eta)\frac{1}{\Gamma(\gamma)}\int_0^{\eta}\big(\Phi(\eta)-\Phi(\lambda)\big)^{\gamma-1}\Phi^{\Delta}(\lambda)\omega_1(\lambda)\Delta\lambda\\
&\geq {}^{\mathbb{T}}_{0^+;\Phi}\mathcal{J}^{\delta}_{\eta}\varphi_2(\eta)\frac{1}{\Gamma(\gamma)}\int_0^{\eta}\big(\Phi(\eta)-\Phi(\lambda)\big)^{\gamma-1}\Phi^{\Delta}(\lambda)\omega_1(\lambda)\Delta\lambda\\
&\quad+{}^{\mathbb{T}}_{0^+;\Phi}\mathcal{J}^{\delta}_{\eta}\mathcal{F}(\eta)\frac{1}{\Gamma(\gamma)}\int_0^{\eta}\big(\Phi(\eta)-\Phi(\lambda)\big)^{\gamma-1}\Phi^{\Delta}(\lambda)\mathcal{G}(\lambda)\Delta\lambda.
\end{aligned}
$$

This follows that

$$
\begin{aligned}
&{}^{\mathbb{T}}_{0^+;\Phi}\mathcal{J}^{\delta}_{\eta}\varphi_2(\eta)\,{}^{\mathbb{T}}_{0^+;\Phi}\mathcal{J}^{\gamma}_{\eta}\mathcal{G}(\eta)+{}^{\mathbb{T}}_{0^+;\Phi}\mathcal{J}^{\delta}_{\eta}\mathcal{F}(\eta)\,{}^{\mathbb{T}}_{0^+;\Phi}\mathcal{J}^{\delta}_{\eta}\,{}^{\mathbb{T}}_{0^+;\Phi}\mathcal{J}^{\gamma}_{\eta}\omega_1(\eta)\\
&\geq {}^{\mathbb{T}}_{0^+;\Phi}\mathcal{J}^{\delta}_{\eta}\varphi_2(\eta)\,{}^{\mathbb{T}}_{0^+;\Phi}\mathcal{J}^{\gamma}_{\eta}\omega_1(\eta)+{}^{\mathbb{T}}_{0^+;\Phi}\mathcal{J}^{\delta}_{\eta}\mathcal{F}(\eta)\,{}^{\mathbb{T}}_{0^+;\Phi}\mathcal{J}^{\gamma}_{\eta}\mathcal{G}(\eta),
\end{aligned}
$$

we acquire the desired inequality (A_1).
To prove $(B_1)-(D_1)$, we utilizes the subsequent variants:

$$
\begin{aligned}
&(B_1)\quad \big(\omega_2(\theta)-\mathcal{G}(\theta)\big)\big(\mathcal{F}(\lambda)-\varphi_1(\lambda)\big)\geq 0,\\
&(C_1)\quad \big(\varphi_2(\theta)-\mathcal{F}(\theta)\big)\big(\mathcal{G}(\lambda)-\omega_2(\lambda)\big)\leq 0,\\
&(D_1)\quad \big(\varphi_1(\theta)-\mathcal{F}(\theta)\big)\big(\mathcal{G}(\lambda)-\omega_1(\lambda)\big)\leq 0.
\end{aligned}
$$

□

Special case of Theorem 4.2, we have the subsequent corollaries.

Corollary 4.2. *Letting $\Phi(\eta)=\eta$, then Theorem 4.2 will lead to a new result for Riemann-Liouville fractional integral on time scales:*

$$
\begin{aligned}
(A_2)\quad &{}^{\mathbb{T}}_{0^+;\Phi}\mathcal{J}^{\delta}_{\eta}\varphi_2(\eta)\,{}^{\mathbb{T}}_{0^+}\mathcal{J}^{\gamma}_{\eta}\mathcal{G}(\eta)+{}^{\mathbb{T}}_{0^+}\mathcal{J}^{\delta}_{\eta}\mathcal{F}(\eta)\,{}^{\mathbb{T}}_{0^+}\mathcal{J}^{\gamma}_{\eta}\omega_1(\eta)\\
&\geq {}^{\mathbb{T}}_{0^+}\mathcal{J}^{\delta}_{\eta}\varphi_2(\eta)\,{}^{\mathbb{T}}_{0^+}\mathcal{J}^{\gamma}_{\eta}\omega_1(\eta)+{}^{\mathbb{T}}_{0^+}\mathcal{J}^{\delta}_{\eta}\mathcal{F}(\eta)\,{}^{\mathbb{T}}_{0^+}\mathcal{J}^{\gamma}_{\eta}\mathcal{G}(\eta),\\
(B_2)\quad &{}^{\mathbb{T}}_{0^+;\Phi}\mathcal{J}^{\gamma}_{\eta}\varphi_1(\eta)\,{}^{\mathbb{T}}_{0^+}\mathcal{J}^{\delta}_{\eta}\mathcal{G}(\eta)+{}^{\mathbb{T}}_{0^+}\mathcal{J}^{\gamma}_{\eta}\omega_2(\eta)\,{}^{\mathbb{T}}_{0^+}\mathcal{J}^{\gamma}_{\eta}\mathcal{F}(\eta)\\
&\geq {}^{\mathbb{T}}_{0^+}\mathcal{J}^{\gamma}_{\eta}\varphi_1(\eta)\,{}^{\mathbb{T}}_{0^+}\mathcal{J}^{\delta}_{\eta}\omega_2(\eta)+{}^{\mathbb{T}}_{0^+}\mathcal{J}^{\gamma}_{\eta}\mathcal{F}(\eta)\,{}^{\mathbb{T}}_{0^+}\mathcal{J}^{\delta}_{\eta}\mathcal{G}(\eta),\\
(C_2)\quad &{}^{\mathbb{T}}_{0^+;\Phi}\mathcal{J}^{\gamma}_{\eta}\omega_2(\eta)\,{}^{\mathbb{T}}_{0^+}\mathcal{J}^{\delta}_{\eta}\varphi_2(\eta)+{}^{\mathbb{T}}_{0^+}\mathcal{J}^{\delta}_{\eta}\mathcal{F}(\eta)\,{}^{\mathbb{T}}_{0^+}\mathcal{J}^{\gamma}_{\eta}\mathcal{G}(\eta)\\
&\geq {}^{\mathbb{T}}_{0^+}\mathcal{J}^{\delta}_{\eta}\varphi_2(\eta)\,{}^{\mathbb{T}}_{0^+}\mathcal{J}^{\gamma}_{\eta}\mathcal{G}(\eta)+{}^{\mathbb{T}}_{0^+}\mathcal{J}^{\delta}_{\eta}\mathcal{F}(\eta)\,{}^{\mathbb{T}}_{0^+}\mathcal{J}^{\gamma}_{\eta}\omega_2(\eta),\\
(D_2)\quad &{}^{\mathbb{T}}_{0^+;\Phi}\mathcal{J}^{\delta}_{\eta}\varphi_1(\eta)\,{}^{\mathbb{T}}_{0^+}\mathcal{J}^{\gamma}_{\eta}\omega_1(\eta)+{}^{\mathbb{T}}_{0^+}\mathcal{J}^{\delta}_{\eta}\mathcal{F}(\eta)\,{}^{\mathbb{T}}_{0^+}\mathcal{J}^{\delta}_{\eta}\,{}^{\mathbb{T}}_{0^+}\mathcal{J}^{\gamma}_{\eta}\mathcal{G}(\eta)\\
&\geq {}^{\mathbb{T}}_{0^+}\mathcal{J}^{\delta}_{\eta}\varphi_1(\eta)\,{}^{\mathbb{T}}_{0^+}\mathcal{J}^{\gamma}_{\eta}\mathcal{G}(\eta)+{}^{\mathbb{T}}_{0^+}\mathcal{J}^{\gamma}_{\eta}\omega_1(\eta)\,{}^{\mathbb{T}}_{0^+}\mathcal{J}^{\delta}_{\eta}\mathcal{F}(\eta).
\end{aligned}
$$

Remark 4.2. *If $\mathbb{T}=\mathbb{R}$, then Theorem 4.2 will lead to Theorem 2.15 in [57] and corollary 4.2 will lead to Corollary 2.16 in [57]. Also, If we choose $\mathbb{T}=\mathbb{R}$ along with $\Phi(\eta)=\eta$, then Theorem 4.2 will lead to Theorem 5 in [58].*

5. SOME OTHER BOUNDS VIA GENERALIZED RIEMANN-LIOUVILLE FRACTIONAL INTEGRAL ON TIME SCALE

Theorem 5.1. *Let $\delta,\gamma>1$, and $\mathbb{T}$ is a time scale. Suppose there are two positive functions $\mathcal{F},\mathcal{G}$ on $[0,\infty)_{\mathbb{T}}$, and Φ is monotone, delta differentiable Φ^{Δ} with $\Phi^{\Delta}\neq 0$ such that for all $\eta>0$, $\alpha,\beta>1$ satisfying $\frac{1}{\alpha}+\frac{1}{\beta}=1$. Then, for $\eta>0$, one has*

$$
\begin{aligned}
(A_3)\quad &\frac{1}{\alpha}\,{}^{\mathbb{T}}_{0^+;\Phi}\mathcal{J}^{\delta}_{\eta}\mathcal{F}^{\alpha}(\eta)\,{}^{\mathbb{T}}_{0^+;\Phi}\mathcal{J}^{\gamma}_{\eta}\mathcal{G}^{\alpha}(\eta)\\
&+\frac{1}{\beta}\,{}^{\mathbb{T}}_{0^+;\Phi}\mathcal{J}^{\delta}_{\eta}\mathcal{G}^{\beta}(\eta)\,{}^{\mathbb{T}}_{0^+;\Phi}\mathcal{J}^{\gamma}_{\eta}\mathcal{F}^{\beta}(\eta)\\
&\geq {}^{\mathbb{T}}_{0^+;\Phi}\mathcal{J}^{\delta}_{\eta}\mathcal{F}(\eta)\mathcal{G}(\eta)\,{}^{\mathbb{T}}_{0^+;\Phi}\mathcal{J}^{\gamma}_{\eta}\mathcal{G}(\eta)\mathcal{F}(\eta),\\
(B_3)\quad &\frac{1}{\alpha}\,{}^{\mathbb{T}}_{0^+;\Phi}\mathcal{J}^{\gamma}_{\eta}\mathcal{G}^{\beta}(\eta)\,{}^{\mathbb{T}}_{0^+;\Phi}\mathcal{J}^{\delta}_{\eta}\mathcal{F}^{\alpha}(\eta)\\
&+\frac{1}{\beta}\,{}^{\mathbb{T}}_{0^+;\Phi}\mathcal{J}^{\gamma}_{\eta}\mathcal{F}^{\alpha}(\eta)\,{}^{\mathbb{T}}_{0^+;\Phi}\mathcal{J}^{\delta}_{\eta}\mathcal{G}^{\beta}(\eta)\\
&\geq {}^{\mathbb{T}}_{0^+;\Phi}\mathcal{J}^{\gamma}_{\eta}\mathcal{G}^{\beta-1}(\eta)\mathcal{F}^{\alpha-1}(\eta)\,{}^{\mathbb{T}}_{0^+;\Phi}\mathcal{J}^{\delta}_{\eta}\mathcal{F}(\eta)\mathcal{G}(\eta),\\
(C_3)\quad &\frac{1}{\alpha}\,{}^{\mathbb{T}}_{0^+;\Phi}\mathcal{J}^{\gamma}_{\eta}\mathcal{G}^{2}(\eta)\,{}^{\mathbb{T}}_{0^+;\Phi}\mathcal{J}^{\delta}_{\eta}\mathcal{F}^{\alpha}(\eta)\\
&+\frac{1}{\beta}\,{}^{\mathbb{T}}_{0^+;\Phi}\mathcal{J}^{\gamma}_{\eta}\mathcal{F}^{2}(\eta)\,{}^{\mathbb{T}}_{0^+;\Phi}\mathcal{J}^{\delta}_{\eta}\mathcal{G}^{\beta}(\eta)\\
&\geq {}^{\mathbb{T}}_{0^+;\Phi}\mathcal{J}^{\gamma}_{\eta}\mathcal{F}^{\frac{2}{\beta}}(\eta)\mathcal{G}^{\frac{2}{\alpha}}(\eta)\,{}^{\mathbb{T}}_{0^+;\Phi}\mathcal{J}^{\delta}_{\eta}\mathcal{F}(\eta)\mathcal{G}(\eta),\\
(D_3)\quad &\frac{1}{\alpha}\,{}^{\mathbb{T}}_{0^+;\Phi}\mathcal{J}^{\gamma}_{\eta}\mathcal{G}^{\beta}(\eta)\,{}^{\mathbb{T}}_{0^+;\Phi}\mathcal{J}^{\delta}_{\eta}\mathcal{F}^{2}(\eta)\\
&+\frac{1}{\beta}\,{}^{\mathbb{T}}_{0^+;\Phi}\mathcal{J}^{\gamma}_{\eta}\mathcal{F}^{\alpha}(\eta)\,{}^{\mathbb{T}}_{0^+;\Phi}\mathcal{J}^{\delta}_{\eta}\mathcal{G}^{2}(\eta)\\
&\geq {}^{\mathbb{T}}_{0^+;\Phi}\mathcal{J}^{\gamma}_{\eta}\mathcal{F}^{\alpha-1}(\eta)\mathcal{G}^{\beta-1}(\eta)\,{}^{\mathbb{T}}_{0^+;\Phi}\mathcal{J}^{\delta}_{\eta}\mathcal{F}^{\frac{2}{\alpha}}(\eta)\mathcal{G}^{\frac{2}{\beta}}(\eta).
\end{aligned}
\tag{27}
$$

Proof: Taking into account the Young's inequality [59]:

$$
\frac{1}{\alpha}a^{\alpha}+\frac{1}{\beta}b^{\beta}\geq ab,\quad \forall a,b\geq 0,\ \alpha,\beta>0,\ \frac{1}{\alpha}+\frac{1}{\beta}=1,
\tag{28}
$$

setting $a=\mathcal{F}(\theta)\mathcal{G}(\lambda)$ and $b=\mathcal{F}(\lambda)\mathcal{G}(\theta)$, $\theta,\lambda>0$, we have

$$
\frac{1}{\alpha}\big(\mathcal{F}(\theta)\mathcal{G}(\lambda)\big)^{\alpha}+\frac{1}{\beta}\big(\mathcal{F}(\lambda)\mathcal{G}(\theta)\big)^{\beta}\geq\big(\mathcal{F}(\theta)\mathcal{G}(\lambda)\big)\big(\mathcal{F}(\lambda)\mathcal{G}(\theta)\big).
\tag{29}
$$

Taking product on both sides of (29) $\frac{\left(\Phi(\eta)-\Phi(\theta)\right)^{\delta-1}\Phi^{\Delta}(\theta)}{\Gamma(\delta)}$, which is positive because $\theta\in(0,\eta)$, $\eta>0$, we integrate the resulting identity with respect to θ from 0 to η we have

$$
\begin{aligned}
&\frac{\mathcal{G}^{\alpha}(\lambda)}{\alpha\Gamma(\delta)}\int_0^{\eta}\big(\Phi(\eta)-\Phi(\theta)\big)^{\delta-1}\Phi^{\Delta}(\theta)\Gamma(\delta)\mathcal{F}^{\alpha}(\theta)\Delta\theta\\
&+\frac{\mathcal{F}^{\beta}(\lambda)}{\beta\Gamma(\delta)}\int_0^{\eta}\big(\Phi(\eta)-\Phi(\theta)\big)^{\delta-1}\Phi^{\Delta}(\theta)\Gamma(\delta)\mathcal{G}^{\beta}(\theta)\Delta\theta\\
&\geq\frac{\mathcal{G}(\lambda)\mathcal{F}(\lambda)}{\Gamma(\delta)}\int_0^{\eta}\big(\Phi(\eta)-\Phi(\theta)\big)^{\delta-1}\Phi^{\Delta}(\theta)\Gamma(\delta)\mathcal{F}(\theta)\mathcal{G}(\theta)\Delta\theta,
\end{aligned}
\tag{30}
$$

we get

$$
\begin{aligned}
&\frac{\mathcal{G}^{\alpha}(\lambda)}{\alpha}\,{}^{\mathbb{T}}_{0^+;\Phi}\mathcal{J}^{\delta}_{\eta}\mathcal{F}^{\alpha}(\eta)+\frac{\mathcal{F}^{\beta}(\lambda)}{\beta}\,{}^{\mathbb{T}}_{0^+;\Phi}\mathcal{J}^{\delta}_{\eta}\mathcal{G}^{\beta}(\eta)\\
&\geq\mathcal{G}(\lambda)\mathcal{F}(\lambda)\,{}^{\mathbb{T}}_{0^+;\Phi}\mathcal{J}^{\delta}_{\eta}\mathcal{F}(\eta)\mathcal{G}(\eta).
\end{aligned}
\tag{31}
$$

Again, multiplying both sides of (31) by $\frac{\left(\Phi(\eta)-\Phi(\lambda)\right)^{\gamma-1}\Phi^{\Delta}(\lambda)}{\Gamma(\gamma)}$, which is positive because $\lambda\in(0,\eta)$, $\eta>0$, we integrate the resulting identity with respect to λ from 0 to η we have

$$
\begin{aligned}
&\frac{1}{\alpha}\,{}^{\mathbb{T}}_{0^+;\Phi}\mathcal{J}^{\delta}_{\eta}\mathcal{F}^{\alpha}(\eta)\frac{1}{\Gamma(\gamma)}\int_0^{\eta}\big(\Phi(\eta)-\Phi(\lambda)\big)^{\gamma-1}\Phi^{\Delta}(\lambda)\mathcal{G}^{\alpha}(\lambda)\Delta\lambda\\
&+\frac{1}{\beta}\,{}^{\mathbb{T}}_{0^+;\Phi}\mathcal{J}^{\delta}_{\eta}\mathcal{G}^{\beta}(\eta)\frac{1}{\Gamma(\gamma)}\int_0^{\eta}\big(\Phi(\eta)-\Phi(\lambda)\big)^{\gamma-1}\Phi^{\Delta}(\lambda)\mathcal{F}^{\beta}(\lambda)\Delta\lambda
\end{aligned}
$$

$$\geq \frac{{}^{\mathbb{T}}_{0^+;\Phi}\mathcal{J}^{\delta}_{\eta}\mathcal{F}(\eta)\mathcal{G}(\eta)}{\Gamma(\gamma)}\int_0^{\eta}\big(\Phi(\eta)-\Phi(\lambda)\big)^{\gamma-1}\Phi^{\Delta}(\lambda)\mathcal{G}(\lambda)\mathcal{F}(\lambda)\Delta\lambda, \tag{32}$$

consequently, we get

$$\begin{aligned}&\frac{1}{\alpha}\,{}^{\mathbb{T}}_{0^+;\Phi}\mathcal{J}^{\delta}_{\eta}\mathcal{F}^{\alpha}(\eta)\,{}^{\mathbb{T}}_{0^+;\Phi}\mathcal{J}^{\gamma}_{\eta}\mathcal{G}^{\alpha}(\eta)+\frac{1}{\beta}\,{}^{\mathbb{T}}_{0^+;\Phi}\mathcal{J}^{\delta}_{\eta}\mathcal{G}^{\beta}(\eta)\,{}^{\mathbb{T}}_{0^+;\Phi}\mathcal{J}^{\gamma}_{\eta}\mathcal{F}^{\beta}(\eta)\\&\geq {}^{\mathbb{T}}_{0^+;\Phi}\mathcal{J}^{\delta}_{\eta}\mathcal{F}(\eta)\mathcal{G}(\eta)\,{}^{\mathbb{T}}_{0^+;\Phi}\mathcal{J}^{\gamma}_{\eta}\mathcal{G}(\eta)\mathcal{F}(\eta),\end{aligned} \tag{33}$$

which implies (A_3). The remaining variants can be proved by adopting the same technique as we did in (A_3).

$$\begin{aligned}&(B_3)\quad a=\frac{\mathcal{F}(\theta)}{\mathcal{F}(\lambda)},\qquad b=\frac{\mathcal{G}(\theta)}{\mathcal{G}(\lambda)},\ \ \mathcal{F}(\lambda),\mathcal{G}(\lambda)\neq 0,\\&(C_3)\quad a=\mathcal{F}(\theta)\mathcal{G}^{\frac{2}{\alpha}}(\lambda),\quad b=\mathcal{F}^{\frac{2}{\beta}}(\lambda)\mathcal{G}(\theta),\\&(D_3)\quad a=\mathcal{F}^{\frac{2}{\alpha}}(\theta)\mathcal{F}(\lambda),\quad b=\mathcal{G}^{\frac{2}{\beta}}(\theta)\mathcal{G}(\lambda),\ \ \mathcal{F}(\lambda),\mathcal{G}(\lambda)\neq 0.\end{aligned}$$

Repeating the foregoing argument, we obtain $(B_3)-(D_3)$. □

Theorem 5.2. *Let $\delta,\gamma>1$, and $\mathbb{T}$ is a time scale. Suppose $\mathcal{F},\mathcal{G}$ be two positive functions on $[0,\infty)_{\mathbb{T}}$, and Φ is monotone, delta differentiable Φ^{Δ} with $\Phi^{\Delta}\neq 0$ such that for all $\eta>0$, and $\alpha,\beta>0$ satisfying $\alpha+\beta=1$. Then, for $\eta>0$, one has*

$$\begin{aligned}&(A_4)\quad p\,{}^{\mathbb{T}}_{0^+;\Phi}\mathcal{J}^{\delta}_{\eta}\mathcal{F}(\eta)\,{}^{\mathbb{T}}_{0^+;\Phi}\mathcal{J}^{\gamma}_{\eta}\mathcal{G}(\eta)\\&\quad+q\,{}^{\mathbb{T}}_{0^+;\Phi}\mathcal{J}^{\gamma}_{\eta}\mathcal{F}(\eta)\,{}^{\mathbb{T}}_{0^+;\Phi}\mathcal{J}^{\delta}_{\eta}\mathcal{G}(\beta)\\&\quad\geq {}^{\mathbb{T}}_{0^+;\Phi}\mathcal{J}^{\delta}_{\eta}\big(\mathcal{F}^{\alpha}(\eta)\mathcal{G}^{\beta}(\eta)\big)\,{}^{\mathbb{T}}_{0^+;\Phi}\mathcal{J}^{\gamma}_{\eta}\big(\mathcal{F}^{\beta}(\eta)\mathcal{G}^{\alpha}(\eta)\big),\\&(B_4)\quad p\,{}^{\mathbb{T}}_{0^+;\Phi}\mathcal{J}^{\delta}_{\eta}\mathcal{F}^{\alpha-1}(\eta)\,{}^{\mathbb{T}}_{0^+;\Phi}\mathcal{J}^{\gamma}_{\eta}\big(\mathcal{F}(\eta)\mathcal{G}^{\beta}(\eta)\big)\\&\quad+q\,{}^{\mathbb{T}}_{0^+;\Phi}\mathcal{J}^{\gamma}_{\eta}\mathcal{G}^{\beta-1}(\eta)\,{}^{\mathbb{T}}_{0^+;\Phi}\mathcal{J}^{\delta}_{\eta}\big(\mathcal{F}^{\beta}(\eta)\mathcal{G}(\eta)\big)\\&\quad\geq {}^{\mathbb{T}}_{0^+;\Phi}\mathcal{J}^{\delta}_{\eta}\mathcal{G}^{\beta}(\eta)\,{}^{\mathbb{T}}_{0^+;\Phi}\mathcal{J}^{\gamma}_{\eta}\mathcal{F}^{\alpha}(\eta),\\&(C_4)\quad p\,{}^{\mathbb{T}}_{0^+;\Phi}\mathcal{J}^{\delta}_{\eta}\mathcal{F}(\eta)\,{}^{\mathbb{T}}_{0^+;\Phi}\mathcal{J}^{\gamma}_{\eta}\mathcal{G}^{\frac{2}{\alpha}}(\eta)\\&\quad+q\,{}^{\mathbb{T}}_{0^+;\Phi}\mathcal{J}^{\delta}_{\eta}\mathcal{G}(\eta)\,{}^{\mathbb{T}}_{0^+;\Phi}\mathcal{J}^{\gamma}_{\eta}\mathcal{F}^{\frac{2}{\beta}}(\eta)\\&\quad\geq {}^{\mathbb{T}}_{0^+;\Phi}\mathcal{J}^{\delta}_{\eta}\mathcal{F}^{\alpha}(\eta)\mathcal{G}(\eta)\,{}^{\mathbb{T}}_{0^+;\Phi}\mathcal{J}^{\gamma}_{\eta}\mathcal{G}^{\beta}(\eta)\mathcal{F}^{2}(\eta),\\&(D_4)\quad p\,{}^{\mathbb{T}}_{0^+;\Phi}\mathcal{J}^{\delta}_{\eta}\mathcal{F}^{\frac{2}{\alpha}}(\eta)\mathcal{G}^{\beta}(\eta)\,{}^{\mathbb{T}}_{0^+;\Phi}\mathcal{J}^{\gamma}_{\eta}\mathcal{G}^{\alpha-1}(\eta)\\&\quad+q\,{}^{\mathbb{T}}_{0^+;\Phi}\mathcal{J}^{\delta}_{\eta}\mathcal{G}^{\beta-1}(\eta)\,{}^{\mathbb{T}}_{0^+;\Phi}\mathcal{J}^{\gamma}_{\eta}\mathcal{F}^{\frac{2}{\beta}}(\eta)\mathcal{G}^{\alpha}(\eta)\\&\quad\geq {}^{\mathbb{T}}_{0^+;\Phi}\mathcal{J}^{\delta}_{\eta}\mathcal{F}^{2}(\eta)\,{}^{\mathbb{T}}_{0^+;\Phi}\mathcal{J}^{\gamma}_{\eta}\mathcal{G}^{2}(\eta).\end{aligned} \tag{34}$$

Proof: Taking into account the weighted $AM-GM$ inequality

$$\alpha a+\beta b\geq a^{\alpha}b^{\beta},\quad \forall a,b\geq 0,\ \alpha,\beta>0,\ \alpha+\beta=1, \tag{35}$$

by setting $a=\mathcal{F}(\theta)\mathcal{G}(\lambda)$ and $b=\mathcal{F}(\lambda)\mathcal{G}(\theta),\ \lambda,\theta>0$, we have

$$\alpha\mathcal{F}(\theta)\mathcal{G}(\lambda)+\beta\mathcal{F}(\lambda)\mathcal{G}(\theta)\geq\big(\mathcal{F}(\theta)\mathcal{G}(\lambda)\big)^{\alpha}\big(\mathcal{F}(\lambda)\mathcal{G}(\theta)\big)^{\beta}. \tag{36}$$

Multiplying both sides of (36) by $\frac{1}{\Gamma(\delta)\Gamma(\gamma)}(\Phi(\eta)-\Phi(\theta))^{\delta-1}\Phi^{\Delta}(\theta)(\Phi(\eta)-\Phi(\lambda))^{\gamma-1}\Phi^{\Delta}(\lambda)$, which is positive because $\theta,\lambda\in(0,\eta)$, $\eta>0$ and integrating the resulting identity from 0 to η we have

$$\begin{aligned}&\frac{\alpha}{\Gamma(\delta)\Gamma(\gamma)}\int_0^{\eta}\int_0^{\eta}(\Phi(\eta)-\Phi(\theta))^{\delta-1}(\Phi(\eta)\\&\quad-\Phi(\lambda))^{\gamma-1}\Phi^{\Delta}(\theta)\Phi^{\Delta}(\lambda)\mathcal{F}(\theta)\mathcal{G}(\lambda)\Delta\theta\Delta\lambda\\&\quad+\frac{\beta}{\Gamma(\delta)\Gamma(\gamma)}\int_0^{\eta}\int_0^{\eta}(\Phi(\eta)-\Phi(\theta))^{\delta-1}(\Phi(\eta)\\&\quad-\Phi(\lambda))^{\gamma-1}\Phi^{\Delta}(\theta)\Phi^{\Delta}(\lambda)\mathcal{F}(\lambda)\mathcal{G}(\theta)\Delta\theta\Delta\lambda\\&\geq\frac{1}{\Gamma(\delta)\Gamma(\gamma)}\int_0^{\eta}\int_0^{\eta}(\Phi(\eta)-\Phi(\theta))^{\delta-1}(\Phi(\eta)\\&\quad-\Phi(\lambda))^{\gamma-1}\Phi^{\Delta}(\theta)\Phi^{\Delta}(\lambda)\\&\quad\times\big(\mathcal{F}(\theta)\mathcal{G}(\lambda)\big)^{\alpha}\big(\mathcal{F}(\lambda)\mathcal{G}(\theta)\big)^{\beta}\Delta\lambda\Delta\theta,\end{aligned} \tag{37}$$

we conclude that

$$\begin{aligned}&p\,{}^{\mathbb{T}}_{0^+;\Phi}\mathcal{J}^{\delta}_{\eta}\mathcal{F}(\eta)\,{}^{\mathbb{T}}_{0^+;\Phi}\mathcal{J}^{\gamma}_{\eta}\mathcal{G}(\eta)+q\,{}^{\mathbb{T}}_{0^+;\Phi}\mathcal{J}^{\gamma}_{\eta}\mathcal{F}(\eta)\,{}^{\mathbb{T}}_{0^+;\Phi}\mathcal{J}^{\delta}_{\eta}\mathcal{G}(\eta)\\&\geq {}^{\mathbb{T}}_{0^+;\Phi}\mathcal{J}^{\delta}_{\eta}\big(\mathcal{F}^{\alpha}(\eta)\mathcal{G}^{\beta}(\eta)\big)\,{}^{\mathbb{T}}_{0^+;\Phi}\mathcal{J}^{\gamma}_{\eta}\big(\mathcal{F}^{\beta}(\eta)\mathcal{G}^{\alpha}(\eta)\big),\end{aligned} \tag{38}$$

which implies (A_4). The rest of inequalities can be shown in similar way by the following choice of parameters in $AM-GM$ inequality.

$$\begin{aligned}&(B_4)\quad a=\frac{\mathcal{F}(\lambda)}{\mathcal{F}(\theta)},\qquad b=\frac{\mathcal{G}(\theta)}{\mathcal{G}(\lambda)},\ \ \mathcal{F}(\theta),\mathcal{G}(\lambda)\neq 0.\\&(C_4)\quad a=\mathcal{F}(\theta)\mathcal{G}^{\frac{2}{\alpha}}(\lambda),\qquad b=\mathcal{F}^{\frac{2}{\beta}}(\lambda)\mathcal{G}(\theta),\\&(D_4)\quad a=\frac{\mathcal{F}^{\frac{2}{\alpha}}(\theta)}{\mathcal{G}(\lambda)},\qquad b=\frac{\mathcal{F}^{\frac{2}{\beta}}(\lambda)}{\mathcal{G}(\theta)},\ \ \mathcal{G}(\theta),\mathcal{G}(\theta)\neq 0.\end{aligned}$$

□

Example 5.1. Let $\delta,\gamma>1$, and $\mathbb{T}$ is a time scale. Suppose $\mathcal{F},\mathcal{G}$ be two positive functions on $[0,\infty)_{\mathbb{T}}$, and Φ is monotone, delta differentiable Φ^{Δ} with $\Phi^{\Delta}\neq 0$ such that for all $\eta>0$, and $\alpha,\beta>0$ satisfying $\frac{1}{\alpha}+\frac{1}{\beta}=1$. Let

$$\mathfrak{m}=\min_{0\leq\theta\leq\eta}\frac{\mathcal{F}(\theta)}{\mathcal{G}(\theta)}\qquad\text{and}\qquad\mathcal{M}=\max_{0\leq\theta\leq\eta}\frac{\mathcal{F}(\theta)}{\mathcal{G}(\theta)}. \tag{39}$$

Then, for $\eta>0$, $\delta,\gamma>1$, one has the following inequalities:

$$\begin{aligned}&(1)\quad 0\leq {}^{\mathbb{T}}_{0^+;\Phi}\mathcal{J}^{\delta}_{\eta}\mathcal{F}^{2}(\eta)\,{}^{\mathbb{T}}_{0^+;\Phi}\mathcal{J}^{\delta}_{\eta}\mathcal{G}^{2}(\eta)\\&\qquad\leq\frac{\mathfrak{m}+\mathcal{M}}{4\mathfrak{m}\mathcal{M}}\big({}^{\mathbb{T}}_{0^+;\Phi}\mathcal{J}^{\delta}_{\eta}\mathcal{F}(\eta)\mathcal{G}(\eta)\big)^{2},\\&(2)\quad 0\leq\sqrt{{}^{\mathbb{T}}_{0^+;\Phi}\mathcal{J}^{\delta}_{\eta}\mathcal{F}^{2}(\eta)\,{}^{\mathbb{T}}_{0^+;\Phi}\mathcal{J}^{\delta}_{\eta}\mathcal{G}^{2}(\eta)}-\big({}^{\mathbb{T}}_{0^+;\Phi}\mathcal{J}^{\delta}_{\eta}\mathcal{F}(\eta)\mathcal{G}(\eta)\big)\\&\qquad\leq\frac{\sqrt{\mathcal{M}}-\sqrt{\mathfrak{m}}}{2\sqrt{\mathfrak{m}\mathcal{M}}}\big({}^{\mathbb{T}}_{0^+;\Phi}\mathcal{J}^{\delta}_{\eta}\mathcal{F}(\eta)\mathcal{G}(\eta)\big),\\&(3)\quad 0\leq {}^{\mathbb{T}}_{0^+;\Phi}\mathcal{J}^{\delta}_{\eta}\mathcal{F}^{2}(\eta)\,{}^{\mathbb{T}}_{0^+;\Phi}\mathcal{J}^{\delta}_{\eta}\mathcal{G}^{2}(\eta)-\big({}^{\mathbb{T}}_{0^+;\Phi}\mathcal{J}^{\delta}_{\eta}\mathcal{F}(\eta)\mathcal{G}(\eta)\big)^{2}\\&\qquad\leq\frac{\mathcal{M}-\mathfrak{m}}{4\mathfrak{m}\mathcal{M}}\big({}^{\mathbb{T}}_{0^+;\Phi}\mathcal{J}^{\delta}_{\eta}\mathcal{F}(\eta)\mathcal{G}(\eta)\big)^{2}.\end{aligned}$$

Proof: From Equation (39) and the inequality

$$\Big(\frac{\mathcal{F}(\theta)}{\mathcal{G}(\theta)}-\mathfrak{m}\Big)\Big(\mathcal{M}-\frac{\mathcal{F}(\theta)}{\mathcal{G}(\theta)}\Big)\mathcal{G}^{2}(\theta)\geq 0,\ \ 0\leq\theta\leq\eta, \tag{40}$$

then we can write as,

$$\mathcal{F}^2(\theta) + \mathfrak{m}\mathcal{M}\mathcal{G}^2(\theta) \leq (\mathfrak{m} + \mathcal{M})\mathcal{F}(\theta)\mathcal{G}(\theta). \tag{41}$$

Multiplying both sides of (41) by $\frac{1}{\Gamma(\delta)}(\Phi(\eta)-\Phi(\theta))\Phi^{\Delta}(\theta)$, which is positive because $\theta \in (0,\eta)$, $\eta > 0$ and integrating the resulting identity from 0 to η, we have

$$\begin{aligned}
&\frac{1}{\Gamma(\delta)}\int_0^{\eta}(\Phi(\eta)-\Phi(\theta))\Phi^{\Delta}(\theta)\mathcal{F}^2(\theta)\Delta\theta \\
&\quad + \mathfrak{m}\mathcal{M}\frac{1}{\Gamma(\delta)}\int_0^{\eta}(\Phi(\eta)-\Phi(\theta))\Phi^{\Delta}(\theta)\mathcal{G}^2(\theta)\Delta\theta \\
&\leq (\mathfrak{m}+\mathcal{M})\frac{1}{\Gamma(\delta)}\int_0^{\eta}(\Phi(\eta)-\Phi(\theta))\Phi^{\Delta}(\theta)\mathcal{F}(\theta)\mathcal{G}(\theta)\Delta\theta,
\end{aligned} \tag{42}$$

implies that

$${}^{\mathbb{T}}_{0^+;\Phi}\mathcal{J}^{\delta}_{\eta}\mathcal{F}^2(\eta) + \mathfrak{m}\mathcal{M}\,{}^{\mathbb{T}}_{0^+;\Phi}\mathcal{J}^{\delta}_{\eta}\mathcal{G}^2(\eta) \leq (\mathfrak{m}+\mathcal{M})\,{}^{\mathbb{T}}_{0^+;\Phi}\mathcal{J}^{\delta}_{\eta}\mathcal{F}(\eta)\mathcal{G}(\eta), \tag{43}$$

on the other hand, it follows from $\mathfrak{m}\mathcal{M} > 0$ and

$$\left(\sqrt{{}^{\mathbb{T}}_{0^+;\Phi}\mathcal{J}^{\delta}_{\eta}\mathcal{F}^2(\eta)} - \sqrt{\mathfrak{m}\mathcal{M}\,{}^{\mathbb{T}}_{0^+;\Phi}\mathcal{J}^{\delta}_{\eta}\mathcal{G}^2(\eta)}\right)^2 \geq 0, \tag{44}$$

that

$$\begin{aligned}
2\sqrt{{}^{\mathbb{T}}_{0^+;\Phi}\mathcal{J}^{\delta}_{\eta}\mathcal{F}^2(\eta)}\sqrt{\mathfrak{m}\mathcal{M}\,{}^{\mathbb{T}}_{0^+;\Phi}\mathcal{J}^{\delta}_{\eta}\mathcal{G}^2(\eta)} &\leq \sqrt{{}^{\mathbb{T}}_{0^+;\Phi}\mathcal{J}^{\delta}_{\eta}\mathcal{F}^2(\eta)} \\
&\quad + \sqrt{\mathfrak{m}\mathcal{M}\,{}^{\mathbb{T}}_{0^+;\Phi}\mathcal{J}^{\delta}_{\eta}\mathcal{G}^2(\eta)}
\end{aligned} \tag{45}$$

then from equation (43) and (45), we obtain,

$$4\mathfrak{m}\mathcal{M}\,{}^{\mathbb{T}}_{0^+;\Phi}\mathcal{J}^{\delta}_{\eta}\mathcal{F}^2(\eta)\,{}^{\mathbb{T}}_{0^+;\Phi}\mathcal{J}^{\delta}_{\eta}\mathcal{G}^2(\eta) \leq (\mathfrak{m}+\mathcal{M})^2({}^{\mathbb{T}}_{0^+;\Phi}\mathcal{J}^{\delta}_{\eta}\mathcal{F}(\eta)\mathcal{G}(\eta)). \tag{46}$$

Which implies (1). By some transformation of (1), similarly, we obtain (2) and (3). □

6. CONCLUSION

The succinct view of this paper to establish numerous inequalities on an arbitrary time scale for generalized Riemann-Liouville fractional integrals. For the suitable selection of Φ on time scale, one can discover numerous novel and existing outcomes as specific cases. This shows the idea of generalized Riemann-Liouville fractional integral is wide and unifying one, yet additionally, improve few consequences in the study on the time scale hypothesis. Numerous variants are explored, when $\mathbb{T} = \mathbb{R}$. Finally, we introduced various dynamic variants by employing generalized Riemann-Liouville fractional integral as an example. Our consequences have potential applications in calcium ion channels, fractional calculus of variations on time scales, involving fractional fundamentalism in mechanics and physics, quantization, control theory, and description of conservative, nonconservative, and constrained systems. The performance of the fractional dynamical integral method is reliable and effective to obtain new solutions. This method has more advantages: it is direct and concise. Thus, the proposed method can be extended to solve many systems of nonlinear fractional partial differential equations in mathematical and physical sciences. Also, the new exact analytical solutions, can be obtained for the generalized ordinary differential equations to obtain new theorems related to stability and continuous dependence on parameters for dynamic equations on time scales. Our computed outcomes can be very useful as a starting point of comparison when some approximate methods are applied to this nonlinear space-time fractional equation.

AUTHOR CONTRIBUTIONS

SR and MA: Conceptualization; SR, MA, and KN: Writing original draft preparation; DB and GR: Formal Analysis; SR and DB: Methodology; KN, DB, and GR: Writing review and Editing.

ACKNOWLEDGMENTS

Authors were grateful to the referees for their valuable suggestions and comments.

REFERENCES

1. Almeida R. A Caputo fractional derivative of a function with respect to another function. *Commun Nonlin Sci Numer Simulat.* (2017) **44**:460–81. doi: 10.1016/j.cnsns.2016.09.006
2. Khalil R, Horani MA, Yousef A, Sababheh M. A new definition of fractional derivative. *J Comp Appl Math.* (2014) **264**:65–70. doi: 10.1016/j.cam.2014.01.002
3. Atangana A, Gomez-Aguilar JF. Numerical approximation of Riemann-Liouville definition of fractional derivative: from Riemann-Liouville to Atangana-Baleanu. *Numer Methods Partial Differ Equat.* (2018) **34**:1502–23. doi: 10.1002/num.22195
4. Cheng JF, Chu YM. Solution to the linear fractional differential equation using Adomian decomposition method. *Math Prob Eng.* (2011) **2011**:587068. doi: 10.1155/2011/587068
5. Cheng JF, Chu YM. On the fractional difference equations of order (2,q). *Abst Appl Anal.* (2011) **2011**:497259. doi: 10.1155/2011/497259
6. Cheng JF, Chu YM. Fractional difference equations with real variable. *Abst Appl Anal.* (2012) **2012**:918529. doi: 10.1155/2012/918529
7. Kilbas AA, Srivastava HM, Trujillo JJ. Theory and applications of fractional differential equations. *North-Holland Math Stud.* (2006) **204**:540.
8. Kumar D, Singh J, Baleanu D. On the analysis of vibration equation involving a fractional derivative with Mittag-Leffler law. *Math Methods Appl Sci.* (2019) **43**:443–57. doi: 10.1002/mma.5903

9. Hilger S. *Ein Mabkettenkalkul mit Anwendung auf Zentrumsmannigfaltigkeiten* (Ph.D. thesis), Universitot Wurzburg (1988).
10. Hilger S. Analysis on measure chains a unified approach to continuous and discrete calculus. *Results Math.* (1990) **18**:18–56. doi: 10.1007/BF03323153
11. Hilger S. Differential and difference calculus unified. *Nonlin Anal.* (1997) **30**:2683–94.
12. Bohner M, Peterson A. *Dynamic Equations on Time Scales*. Boston, MA: Birkhauser Boston, Inc. (2001).
13. Bohner EA, Bohner M, Akin F. Pachpatte inequalities on time scales. *J Inequal Pure Appl Math.* (2005) **6**:1–23.
14. Dinu C. Hermite-Hadamard inequality on time scale. *J Inequal Appl.* (2008) **2008**:24. doi: 10.1155/2008/287947
15. Dinu C. Ostrowski type inequalities on time scales. *An Univ Craiova Math Comput Sci Ser.* (2007) **34**:43–58.
16. Bastos NRO. *Fractional calculus on time scales* (Ph.D. thesis), University of Aveiro (2012).
17. Bastos NRO, Mozyrska D, Torres DFM. Fractional derivatives and integrals on time scales via the inverse generalized Laplace transform. *Int J Math Comput.* (2011) **11**:1–9.
18. Benkhettou N, Hassani S, Torres DFM. A conformable fractional calculus on arbitrary time scales. *J King Saud Univ Sci.* (2016) **28**:93–8. doi: 10.1016/j.jksus.2015.05.003
19. Gomez-Aguilar JF, Yepez-Martinez H, Escobar-Jimenez RF, Olivares-Peregrino VH, Reyes JM, Sosa IO. Series solution for the time-fractional coupled mKdV equation using the homotopy analysis method. *Math Prob Eng.* (2016) **2016**:7047126. doi: 10.1155/2016/7047126
20. Yepez-Martinez H, Gomez-Aguilar JF, Sosa IO, Reyes JM, Torres-Jimenez J. The Feng's first integral method applied to the nonlinear mKdV space-time fractional partial differential equation. *Rev Mex Fis.* (2016) **62**:310–6.
21. Gomez-Aguilar JF, Yepez-Martinez H, Torres-Jimenez J, Cordova-Fraga T, Escobar-Jimenez RF, Olivares-Peregrino VH. Homotopy perturbation transform method for nonlinear differential equations involving to fractional operator with exponential kernel. *Adv Differ Equat.* (2017) **2017**:1–18. doi: 10.1186/s13662-017-1120-7
22. Goswami A, Singh J, Kumar D, Sushila. An efficient analytical approach for fractional equal width equations describing hydro-magnetic waves in cold plasma. *Phys A Stat Mech Appl.* (2019) **524**:563–75. doi: 10.1016/j.physa.2019.04.058
23. Kumar D, Singh J, Al Qurashi M, Baleanu D. A new fractional SIRS-SI malaria disease model with application of vaccines, anti-malarial drugs, and spraying. *Adv Differ Equat.* (2019) **2019**:278. doi: 10.1186/s13662-019-2199-9
24. Mekhalfi K, Torres DFM. Generalized fractional operators on time scales with applications to dynamic equations. *Eur Phy J Spec Top.* (2019) **226**:3489–99. doi: 10.1140/epjst/e2018-00036-0
25. Morales-Delgado VF, Gomez-Aguilar JF, Yepez-Martinez M, Baleanu D, Escobar-Jimenez RF, Olivares-Peregrino VH. Laplace homotopy analysis method for solving linear partial differential equations using a fractional derivative with and without kernel singular. *Adv Differ Equat.* (2016) **2016**:1–16. doi: 10.1186/s13662-016-0891-6
26. Saad KM, Khader MM, Gomez-Aguilar JF, Baleanu D. Numerical solutions of the fractional Fisher's type equations with Atangana-Baleanu fractional derivative by using spectral collocation methods. *Chaos Interdiscipl J Nonlin Sci.* (2019) **29**:1–13. doi: 10.1063/1.5086771
27. Singh J, Kumar D, Baleanu D. New aspects of fractional Biswas-Milovic model with Mittag-Leffler law. *Math Model Nat Phenom.* (2019) **14**:303. doi: 10.1051/mmnp/2018068
28. Singh J, Kumar D, Baleanu D, Rathore S. On the local fractional wave equation in fractal strings. *Math Method Appl Sci.* (2019) **42**:1588–95. doi: 10.1002/mma.5458
29. Yaslan I, Liceli O. Three-point boundary value problems with delta Riemann-Liouville fractional derivative on time scales. *Fract. Differ. Calc.* (2016) **6**:1–16. doi: 10.7153/fdc-06-01
30. Sun M, Hou C. Fractional q-symmetric calculus on a time scale. *Adv Differ Equat.* (2017) **2017**:166. doi: 10.1186/s13662-017-1219-x
31. Yan RA, Sun R, Han ZL. Existence of solutions of boundary value problems for Caputo fractional differential equations on time scales. *Bull Iranian Math Soc.* (2016) **42**:247–62.
32. Zhu J, Wu L. Fractional Cauchy problem with Caputo nabla derivative on time scales. *Abstr Appl Anal.* (2015) **2015**:486054. doi: 10.1155/2015/486054
33. Gao SL. Fractional time scale in calcium ion channels model. *Int J Biomath.* (2013) **6**:1350023. doi: 10.1142/S179352451350023X
34. Hilfer R. *Applications of Fractional Calculus in Physics*. River Edge, NJ: World Scientific Publishing Co., Inc. (2000).
35. Mohan JS. Variation of parameters for nabla fractional difference equations. *Novi Sad J Math.* (2014) **44**:149–59.
36. Chidouh A, Guezane-Lakoud A, Bebbouchi R, Bouaricha A, Torres DFM. Linear and nonlinear fractional Voigt models. In: Babiarz A, Czornik A, Klamka J, Niezabitowski M, editors. *Theory and Applications of Non-integer Order Systems, Lecture Notes in Electrical Engineering*, Vol. 407. Cham: Springer (2017). p. 157–67.
37. Grüss G. Uber das Maximum des absoluten Betrages von $\frac{1}{b-a}\int_a^b \mathcal{P}(t)\mathcal{U}(t)dt - \left(\frac{1}{b-a}\right)^2 \int_a^b \mathcal{P}(t)dt \int_a^b \mathcal{U}(t)dt$. *Math Zeitschr.* (1935) **39**:215–26. doi: 10.1007/BF01201355
38. Adil Khan M, Begum S, Khurshid Y, Chu YM. Ostrowski type inequalities involving conformable fractional integrals. *J Inequal Appl.* (2018) **2018**:70. doi: 10.1186/s13660-018-1664-4
39. Adil Khan M, Chu YM, Kashuri A, Liko R, Ali G. Conformable fractional integrals versions of Hermite-Hadamard inequalities and their generalizations. *J Fun Spaces.* (2018) **2018**:6928130. doi: 10.1155/2018/6928130
40. Adil Khan M, Iqbal A, Suleman M, Chu YM. Hermite-Hadamard type inequalities for fractional integrals via Green's function. *J Inequal Appl.* (2018) **2018**:161. doi: 10.1186/s13660-018-1751-6
41. Adil Khan M, Khurshid Y, Du TS, Chu YM. Generalization of Hermite-Hadamard type inequalities via conformable fractional integrals. *J Fun Spaces.* (2018) **2018**:5357463. doi: 10.1155/2018/5357463
42. Dahmani Z. New inequalities in fractional integrals. *Int J Nonlin Sci.* (2010) **9**:493–7.
43. Dahmani Z, Tabharit L, Taf S. New generalisations of Grüss inequality using Riemann-Liouville fractional integrals. *Bull Math Anal Appl.* (2010) **2**:93–9.
44. Rashid S, Abdeljawad T, Jarad F, Noor MA. Some estimates for generalized Riemann-Liouville fractional integrals of exponentially convex functions and their applications. *Mathematics.* (2019) **7**:807. doi: 10.3390/math7090807
45. Rashid S, Jarad F, Noor MA, Kalsoom H, Chu YM. Inequalities by means of generalized proportional fractional integral operators with respect to another function. *Mathematics.* (2020) **7**:1225. doi: 10.3390/math7121225
46. Rashid S, Latif MA, Hammouch Z, Chu YM. Fractional integral inequalities for strongly h-preinvex functions for a kth order differentiable functions. *Symmetry.* (2019) **11**:1448. doi: 10.3390/sym11121448
47. Rashid S, Noor MA, Noor KI. Some generalize Riemann-Liouville fractional estimates involving functions having exponentially convexity property. *Punjab Univ J Math.* (2019) **51**:1–15.
48. Rashid S, Noor MA, Noor KI, Akdemir AO. Some new generalizations for exponentially s-convex functions and inequalities via fractional operators. *Fractal Fract.* (2019) **3**:24. doi: 10.3390/fractalfract3020024
49. Rashid S, Noor MA, Noor KI, Safdar F. Integral inequalities for generalized preinvex functions. *Punjab Univ J Math.* (2019) **51**:77–91. doi: 10.1186/s13660-019-2248-7
50. Rashid S, Noor MA, Noor KI, Safdar F, Chu YM. Hermite-Hadamard inequalities for the class of convex functions on time scale. *Mathematics.* (2019) **7**:956. doi: 10.3390/math7100956
51. Rashid S, Safdar F, Akdemir AO, Noor MA, Noor KI. Some new fractional integral inequalities for exponentially m-convex functions via extended generalized Mittag-Leffler function. *J Inequal Appl.* (2019) **2019**:299. doi: 10.1109/ICAEM.2019.8853807
52. Li JF, Rashid S, Liu JB, Akdemir AO, Safdar F. Inequalities involving conformable approach for exponentially convex functions and their applications. *J Fun Spaces.* (2020) **2020**:6517068. doi: 10.1155/2020/6517068

53. Nwaeze ER, Torres DFM. Chain rules and inequalities for the BHT fractional calculus on arbitrary timescales. *Arab J Math.* (2017) **6**:13–20. doi: 10.1007/s40065-016-0160-2
54. Sheng Q, Fadag M, Henderson J, Davis JM. An exploration of combined dynamic derivatives on time scales and their applications. *Nonlin Anal Real World Appl.* (2006) **7**:395–413. doi: 10.1016/j.nonrwa.2005.03.008
55. Agarwal R, Bohner M, Regan D, Peterson A. Dynamic equations on time scales: a survey, *J Comput Appl Math.* (2002) **141**:1–26. doi: 10.1016/S0377-0427(01)00432-0
56. Ahmadkhanlu A, Jahanshahi M. On the existence and uniqueness of solution of initial value problem for fractional order differential equations on time scales. *Bull Iranian Math Soc.* (2012) **38**:241–52.
57. Kacar E, Kacar Z, Yildirim H. Integral inequalities for Riemann-Liouville fractional integrals of a function with respect to another function. *Iranian J Math Sci Inform.* (2018) **13**: 1–13. doi: 10.7508/ijmsi.2018.1.001
58. Tariboon J, Ntouyas SK, Sudsutad W. Some new Riemann-Liouville fractional integral inequalities. *Int J Math Sci.* (2014) **2014**:869434. doi: 10.1186/s13661-014-0253-9
59. Kreyszig E. *Introductory Functional Analysis with Applications.* New York, NY: Wiley (1989).

Conflict of Interest: The authors declare that the research was conducted in the absence of any commercial or financial relationships that could be construed as a potential conflict of interest.

Copyright © 2020 Rashid, Aslam Noor, Nisar, Baleanu and Rahman. This is an open-access article distributed under the terms of the Creative Commons Attribution License (CC BY). The use, distribution or reproduction in other forums is permitted, provided the original author(s) and the copyright owner(s) are credited and that the original publication in this journal is cited, in accordance with accepted academic practice. No use, distribution or reproduction is permitted which does not comply with these terms.

frontiers in Physics

ORIGINAL RESEARCH
published: 10 June 2020
doi: 10.3389/fphy.2020.00192

Some Effective Numerical Techniques for Chaotic Systems Involving Fractal-Fractional Derivatives With Different Laws

Behzad Ghanbari[1,2] *and Kottakkaran Sooppy Nisar*[3]*

[1] Department of Engineering Science, Kermanshah University of Technology, Kermanshah, Iran, [2] Department of Mathematics, Faculty of Engineering and Natural Sciences, Bahçeşehir University, Istanbul, Turkey, [3] Department of Mathematics, College of Arts and Sciences, Prince Sattam Bin Abdulaziz University, Wadi Aldawaser, Saudi Arabia

Chaotic systems are dynamical systems that are highly sensitive to initial conditions. Such systems are used to model many real-world phenomena in science and engineering. The main purpose of this paper is to present several efficient numerical treatments for chaotic systems involving fractal-fractional operators. Several numerical examples test the performance of the proposed methods. Simulations with different values of the fractional and fractal parameters are also conducted. It is demonstrated that the fractal-fractional derivative enables one to capture all the useful information from the history of the phenomena under consideration. The numerical schemes can also be implemented for other chaotic systems with fractal-fractional operators.

Keywords: chaotic attractors, computational efficiency, fractal-fractional operators, thomas attractor, Newton's method, product integration rule

OPEN ACCESS

Edited by:
Jordan Yankov Hristov, University of Chemical Technology and Metallurgy, Bulgaria

Reviewed by:
Sania Qureshi, Mehran University of Engineering and Technology, Pakistan
Hossein Jaferi, University of South Africa, South Africa

***Correspondence:**
Kottakkaran Sooppy Nisar
n.sooppy@psau.edu.sa; ksnisar1@gmail.com

Specialty section:
This article was submitted to Mathematical Physics, a section of the journal Frontiers in Physics

Received: *19 March 2020*
Accepted: *30 April 2020*
Published: *10 June 2020*

Citation:
Ghanbari B and Nisar KS (2020) Some Effective Numerical Techniques for Chaotic Systems Involving Fractal-Fractional Derivatives With Different Laws. Front. Phys. 8:192. doi: 10.3389/fphy.2020.00192

1. INTRODUCTION

In recent decades numerical methods have been recognized as powerful mathematical techniques for solving nonlinear equations that model real-world problems [1–5]. Numerical techniques have been used to solve different classes of differential equations, including those of arbitrary order. Due to the outstanding contribution of nonlinear models to human understanding of many phenomena and the prediction of the future behavior of systems, many researchers are devoting their attention to developing new and reliable numerical techniques that could be applied to more complex cases. Chaotic behaviors are among the natural phenomena that have attracted the attention of many researchers, who aim to replicate and predict those behaviors. To achieve this, differential operators are often used as mathematical tools to construct the underlying models. Recently a new class of differential operators was introduced, which are convolutions of fractal derivatives and fractional kernels with different forms such as power law, exponential decay and the Mittag-Leffler function [6]. These differential operators are able to represent complexities that cannot be described with classical fractional differentiation and integration. One of the strengths of these operators is their two orders, where one is considered a fractional order and the other is the fractal dimension [7–9]. With these efficient operators, a new class of nonlinear differential and integral equations can be constructed, and existing chaotic models can be extended. Nevertheless, to verify the effectiveness of such fractal-fractional operators in modeling chaotic attractors, one needs to solve the models numerically as their exact solutions cannot be easily obtained by existing analytical methods. So far, a few numerical methods have been used to discretize such models, and some numerical results

for chaotic attractors have been obtained. A different numerical scheme was suggested very recently [10–27] and was found to be efficient for solving nonlinear differential equations. Some articles have examined the analysis of errors and the determination of error bands in the context of the possible deficit differential equations [28–30]. Since the operators defined in this paper are novel in the field, the numerical methods associated with them are also very limited. One of the main motivations for this article was to introduce methods for solving fractal-fractional problems that have not been considered before. By using the proposed methods, approximate solutions to these problems can be determined more easily and with higher accuracy. In addition, the methods can be applied to real-world problems. In this work, we present applications of such numerical schemes in solving chaotic models that involve the new class of differential operators. We consider some well-known chaotic models with fractal-fractional differential operators, so that we can compare our results with those in the literature. The article is organized as follows. In section 2, we give a brief overview of some basic definitions of fractional differential calculus. Two efficient and effective numerical methods for determining approximate solutions to fractal-fractional problems are presented in section 3. The first is for the Caputo derivative and the second is for the Atangana-Baleanu-Caputo derivative. The kernels used in these two definitions are singular and non-singular, respectively. Several numerical simulations for chaotic systems are described in section 4. The results obtained are accurate, interesting, and meaningful. Finally, we present our overall conclusions.

2. PRELIMINARY DEFINITIONS

In this section, we give a brief review of some existing definitions of fractal-fractional operators. These operators result from the combination of two important concepts: fractional differentiation and fractal derivatives. Most of the definitions given here are taken from Atangana [6] and Atangana and Qureshi [31].

Definition 1. If $g(t)$ is a differentiable function on a finite open interval, then we define the fractal-fractional derivative of $g(t)$ in the Caputo sense as

$$ {}_0^{\text{FF-C}}\mathbb{D}_t^{\rho,\tau} g(t) = \frac{1}{\Gamma(k-\rho-1)} \int_0^t \frac{dg(\omega)}{dt^\tau} (t-\omega)^{k-\rho-1}\, d\omega, \quad k-1 < \rho \le k,\ 0 < k-1 < \tau \le k, \tag{1} $$

where

$$ \frac{dg(\omega)}{dt^\tau} = \lim_{t\to y} \frac{g(t)-g(\omega)}{t^\beta - \omega^\beta}. \tag{2} $$

Definition 2. If $g(t)$ is a differentiable function on a finite open interval, then we define the fractal-fractional derivative of $g(t)$ in the Caputo-Fabrizio sense as

$$ {}_0^{\text{FF-CF}}\mathbb{D}_t^{\rho,\tau} g(t) = \frac{L(\rho)}{1-\rho} \int_0^t \frac{dg(\omega)}{dt^\tau} \exp\left[-\frac{\rho}{1-\rho}(t-\omega)\right] d\omega, \quad n-1 < \rho, \tau \le n, \tag{3} $$

provided $K(0) = K(1) = 1$.

Definition 3. If $g(t)$ is a differentiable function on a finite open interval, then we define the fractal-fractional derivative of $g(t)$ in the Atangana-Baleanu sense as

$$ {}_0^{\text{FF-AB}}\mathbb{D}_t^{\rho,\tau} g(t) = \frac{\mathbf{AB}(\rho)}{1-\rho} \int_0^t \frac{dg(\omega)}{dt^\tau} E_\rho\left[-\frac{\rho}{1-\rho}(t-\omega)\right] d\omega, \quad n-1 < \rho, \tau \le n, \tag{4} $$

where $E_\rho(.)$ is the Mittag-Leffler function, defined by

$$ E_\rho(\omega) = \sum_{k=0}^{\infty} \frac{\omega^k}{\Gamma(\rho k+1)}, \quad \rho > 0. \tag{5} $$

This function is an essential function in the modeling of physical processes using fractional calculus concepts. We know that Equation (5) reduces to the exponential function e^x if one takes $\rho = 1$. Also, $\mathbf{AB}(\cdot)$ is a function used for normalization, and it satisfies the property $\mathbf{AB}(0) = \mathbf{AB}(1) = 1$. One of the most popular definitions of $\mathbf{AB}(\cdot)$ is

$$ \mathbf{AB}(\rho) = 1 - \rho + \frac{\rho}{\Gamma(\rho)}. $$

Definition 4. If $g(t)$ is a differentiable function on a finite open interval, then we define the fractal-fractional integral of $g(t)$ in the Caputo sense [31] as

$$ {}_0^{\text{FF-C}}\mathbb{I}_t^{\rho,\tau} g(t) = \frac{\tau}{\Gamma(\rho)} \int_0^t \frac{\omega^{\tau-1} g(\omega)\, d\omega}{(t-\omega)^{1-\rho}}. \tag{6} $$

Definition 5. If $g(t)$ is a differentiable function on a finite open interval, then we define the fractal-fractional integral of $g(t)$ in the Caputo-Fabrizio sense [31] as

$$ {}_0^{\text{FF-CF}}\mathbb{I}_t^{\rho,\tau} g(t) = \frac{\tau\rho}{M(\rho)} \int_0^t \frac{g(\omega)\, d\omega}{\omega^{1-\rho}} + \frac{\tau(1-\rho)t^{\tau-1} g(t)}{M(\rho)}. \tag{7} $$

Definition 6. If $g(t)$ is a differentiable function on a finite open interval, then we define the fractal-fractional integral of $g(t)$ in the Atangana-Baleanu sense [31] as

$$ {}_0^{\text{FF-AB}}\mathbb{I}_t^{\rho,\tau} g(t) = \frac{\tau\rho}{\mathbf{AB}(\rho)} \int_0^t \frac{\omega^{\tau-1} g(\omega)\, d\omega}{(t-\omega)^{1-\rho}} + \frac{\tau(1-\rho)t^{\tau-1} g(t)}{\mathbf{AB}(\rho)}. \tag{8} $$

3. THE PROPOSED NUMERICAL METHODS

In what follows, the main aim is to construct two equations involving fractal-fractional derivatives,

$$ {}_0^{\text{FF}}\mathbb{D}_t^{\rho,\tau} \xi(t) = \mathbb{N}(t, \xi(t)), \quad t \in [t_0, T], \tag{9} $$

with the initial condition $\xi(0) = \xi_0$.

3.1. The Caputo Fractal-Fractional Derivative

From the results in Atangana and Qureshi [31], Equation (9) reduces to the following Caputo fractional representation:

$$ {}_0^C\mathbb{D}_t^{\rho}\xi(t) = \tau t^{\tau-1}\mathbb{N}(t,\xi(t)). \tag{10} $$

Now, taking into account the fundamental theorem of calculus, one gets

$$ \xi(t) - \xi(t_0) = \frac{\tau}{\Gamma(\rho)}\int_0^t \frac{\omega^{\tau-1}\mathbb{N}(\omega,\xi(\omega))\,d\omega}{(t-\omega)^{1-\rho}}. \tag{11} $$

Then, inserting $t = t_n = t_0 + n\Delta t$ into (17) leads to the following expression:

$$ \begin{aligned} \xi(t_n) &= \xi(t_0) + \frac{\tau}{\Gamma(\rho)}\sum_{i=0}^{n-1}\int_{t_i}^{t_{i+1}} \frac{\omega^{\tau-1}\mathbb{N}(\omega,\xi(\omega))\,d\omega}{(t_n-\omega)^{1-\rho}}, \\ &1 \le n \le N, \end{aligned} \tag{12} $$

where $\Delta t = \frac{T-t_0}{N}$ is the time step for the discretization points.

Next, taking the linear Lagrange interpolation into account for the function of $f(\omega) = \omega^{\tau-1}\mathbb{N}(\omega,\xi(\omega))$, we obtain

$$ \begin{aligned} &\omega^{\tau-1}\mathbb{N}(\omega,\xi(\omega)) \approx t_{i+1}^{\tau-1}\mathbb{N}(t_{i+1},\xi_{i+1}) \\ &+ \frac{\omega - t_{i+1}}{\Delta t}\left(t_{i+1}^{\tau-1}\mathbb{N}(t_{i+1},\xi_{i+1}) - t_i^{\tau-1}\mathbb{N}(t_i,\xi_i)\right), \\ &\omega \in [t_i, t_{i+1}], \end{aligned} \tag{13} $$

where $\xi_i = \xi(t_i)$. At this point, the result obtained in formula (13) can be used in relation (12). This substitution results in the following relationship:

$$ \xi_n = \xi_0 + \tau\Delta t^{\rho}\left(\xi_n t_0^{\tau-1}\mathbb{N}(t_0,\xi_0) + \sum_{i=0}^{n}\eth_{n-i}t_i^{\tau-1}\mathbb{N}(t_i,\xi_i)\right), \tag{14} $$

where

$$ \begin{aligned} \xi_n &= \frac{(n-1)^{\rho+1} - n^{\rho}(n-\rho-1)}{\Gamma(\rho+2)}, \\ \eth_m &= \begin{cases} \dfrac{1}{\Gamma(\rho+2)}, & j = 0, \\ \dfrac{(m-1)^{\rho+1} - 2m^{\rho+1} + (m+1)^{\rho+1}}{\Gamma(\rho+2)}, & m = 1,2,\ldots,n-1. \end{cases} \end{aligned} \tag{15} $$

3.2. The Atangana-Baleanu Fractal-Fractional Derivative

In this case we can convert Equation (9) to the following Atangana-Baleanu fractional form [31]:

$$ {}_0^{AB}\mathbb{D}_t^{\rho}\xi(t) = \tau t^{\tau-1}\mathbb{N}(t,\xi(t)). \tag{16} $$

Upon applying the integral operator to both sides of Equation (16), the following Volterra integral equation is constructed:

$$ \begin{aligned} \xi(t) - \xi(t_0) &= \frac{\tau-\tau\rho}{\mathbf{AB}(\rho)}t^{\tau-1}\mathbb{N}(t,\xi(t)) \\ &+ \frac{\tau\rho}{\mathbf{AB}(\rho)\Gamma(\rho)}\int_0^t (t-\omega)^{\rho-1}\omega^{\tau-1}\mathbb{N}(\omega,\xi(\omega))\,d\omega. \end{aligned} \tag{17} $$

Taking $t = t_n = t_0 + n\Delta t$ in (17), we have

$$ \begin{aligned} \xi(t_n) &= \xi(t_0) + \frac{\tau-\tau\rho}{\mathbf{AB}(\rho)}t_n^{\tau-1}\mathbb{N}(t_n,\xi(t_n)) \\ &+ \frac{\tau\rho}{\mathbf{AB}(\rho)\Gamma(\rho)}\sum_{i=0}^{n-1}\int_{t_i}^{t_{i+1}}(t_n-\omega)^{\rho-1}\omega^{\tau-1}\mathbb{N}(\omega,\xi(\omega))\,d\omega. \end{aligned} \tag{18} $$

Now, substituting (13) into (18), we get the following implicit Atangana-Baleanu-Caputo scheme:

$$ \begin{aligned} \xi_n &= \xi_0 + \frac{\tau-\tau\rho}{\mathbf{AB}(\rho)}t_n^{\tau-1}\mathbb{N}(t_n,\xi_n) \\ &+ \frac{\tau\rho\Delta t^{\rho}}{\mathbf{AB}(\rho)}\left(\xi_n t_0^{\tau-1}\mathbb{N}(t_0,\xi_0) + \sum_{i=0}^{n}\eth_{n-i}t_i^{\tau-1}\mathbb{N}(t_i,\xi_i)\right), \end{aligned} \tag{19} $$

where ξ_n and $\eth_j$ are the coefficients defined in (15). A closer look at relations (14) and (19) shows that these expressions are implicit equations for determining y_n. The Newton iteration method is one of the most popular and efficient techniques for solving such problems. In this article, as in Garrappa [32], Ghanbari and Kumar [33], and Ghanbari et al. [34], we will use the Newton method to solve these equations. By solving these equations, approximate solutions to the original problem will be determined.

4. NUMERICAL SIMULATIONS FOR SOME CHAOTIC SYSTEMS

In this section, to show the validity of the proposed numerical technique, three chaotic systems involving Atangana-Baleanu-Caputo fractional derivatives are considered.

Example 1. Consider the following modified cyclically symmetric Thomas attractor given by [35]

$$ \begin{aligned} {}^{FF}_0\mathbb{D}_t^{\rho,\tau}x(t) &= \sin\big(\exp\big(y(t)\big)\big) - \mathbb{B}x(t), \\ {}^{FF}_0\mathbb{D}_t^{\rho,\tau}y(t) &= \cos\big(\sin\big(z(t)\big)\big) - \mathbb{B}y(t), \\ {}^{FF}_0\mathbb{D}_t^{\rho,\tau}z(t) &= \exp\big(\cos\big(x(t)\big)\big) - \mathbb{B}z(t). \end{aligned} \tag{20} $$

Now we take into account the iterative methods given by (14) and (19) to solve (20). Taking (14) into account, we get the iterative structure

$$
\begin{aligned}
x_n &= x_0 + \tau\Delta t^{\rho}\Bigg(\xi_n t_0^{\tau-1}\big[\sin\big(\exp(y_0)\big) - \mathbb{B}x_0\big] \\
&\quad + \sum_{i=0}^{n} \eth_{n-i} t_i^{\tau-1}\big[\sin\big(\exp(y_i)\big) - \mathbb{B}x_i\big]\Bigg), \\
y_n &= y_0 + \tau\Delta t^{\rho}\Bigg(\xi_n t_0^{\tau-1}\big[\cos\big(\sin(z_0)\big) - \mathbb{B}y_0\big] \\
&\quad + \sum_{i=0}^{n} \eth_{n-i} t_i^{\tau-1}\big[\cos\big(\sin(z_i)\big) - \mathbb{B}y_i\big]\Bigg), \\
z_n &= z_0 + \tau\Delta t^{\rho}\Bigg(\xi_n t_0^{\tau-1}\big[\exp\big(\cos(x_0)\big) - \mathbb{B}z_0\big] \\
&\quad + \sum_{i=0}^{n} \eth_{n-i} t_i^{\tau-1}\big[\exp\big(\cos(x_i)\big) - \mathbb{B}z_i\big]\Bigg).
\end{aligned} \tag{21}
$$

Moreover, from (19) we get

$$
\begin{aligned}
x_n &= x_0 + \frac{\tau-\tau\rho}{\mathbf{AB}(\rho)} t_n^{\tau-1}\big[\sin\big(\exp(y_n)\big) - \mathbb{B}x_n\big] \\
&\quad + \frac{\tau\rho\Delta t^{\rho}}{\mathbf{AB}(\rho)}\Bigg(\xi_n t_0^{\tau-1}\big[\sin\big(\exp(y_0)\big) - \mathbb{B}x_0\big] \\
&\quad + \sum_{i=0}^{n} \eth_{n-i} t_i^{\tau-1}\big[\sin\big(\exp(y_i)\big) - \mathbb{B}x_i\big]\Bigg), \\
y_n &= y_0 + \frac{\tau-\tau\rho}{\mathbf{AB}(\rho)} t_n^{\tau-1}\big[\cos\big(\sin(z_n)\big) - \mathbb{B}y_n\big] \\
&\quad + \frac{\tau\rho\Delta t^{\rho}}{\mathbf{AB}(\rho)}\Bigg(\xi_n t_0^{\tau-1}\big[\cos\big(\sin(z_0)\big) - \mathbb{B}y_0\big] \\
&\quad + \sum_{i=0}^{n} \eth_{n-i} t_i^{\tau-1}\big[\cos\big(\sin(z_i)\big) - \mathbb{B}y_i\big]\Bigg), \\
z_n &= z_0 + \frac{\tau-\tau\rho}{\mathbf{AB}(\rho)} t_n^{\tau-1}\big[\exp\big(\cos(x_n)\big) - \mathbb{B}z_n\big] \\
&\quad + \frac{\tau\rho\Delta t^{\rho}}{\mathbf{AB}(\rho)}\Bigg(\xi_n t_0^{\tau-1}\big[\exp\big(\cos(x_0)\big) - \mathbb{B}z_0\big] \\
&\quad + \sum_{i=0}^{n} \eth_{n-i} t_i^{\tau-1}\big[\exp\big(\cos(x_i)\big) - \mathbb{B}z_i\big]\Bigg).
\end{aligned} \tag{22}
$$

In **Figures 1**–**4** we plot the results of numerical simulations using the two iterative schemes (21) and (22) with $\mathbb{B} = 0.2$. For the numerical implementations we took $(x_0, y_0, z_0) = (0, 3, 11)$ as the initial condition. The results of the iterative scheme (21) are plotted in **Figures 5**–**8**. In each figure we have taken a fixed value of τ and different values of ρ. In these experiments we set $\Delta t = 10^{-3}$ and $T = 800$.

Example 2. In this example we consider the chaotic system

$$
\begin{aligned}
{}^{\mathrm{FF}}_{0}\mathbb{D}_t^{\rho,\tau} x(t) &= x(t)z(t) - \mathbb{B}x(t) - \mathbb{D}y(t), \\
{}^{\mathrm{FF}}_{0}\mathbb{D}_t^{\rho,\tau} y(t) &= \mathbb{D}x(t) + y(t)z(t) - \mathbb{B}y(t), \\
{}^{\mathrm{FF}}_{0}\mathbb{D}_t^{\rho,\tau} z(t) &= \mathbb{C} + \mathbb{A}z(t) - \tfrac{z(t)^3}{3} - x(t)^2 + \mathbb{E}z(t)x(t)^3,
\end{aligned} \tag{23}
$$

To solve this chaotic system, we use the following iterative scheme obtained from (14):

$$
\begin{aligned}
x_n &= x_0 + \tau\Delta t^{\rho}\Bigg(\xi_n t_0^{\tau-1}\big[x_0z_0 - \mathbb{B}x_0 - \mathbb{D}y_0\big] \\
&\quad + \sum_{i=0}^{n} \eth_{n-i} t_i^{\tau-1}\big[x_iz_i - \mathbb{B}x_i - \mathbb{D}y_i\big]\Bigg), \\
y_n &= y_0 + \tau\Delta t^{\rho}\Bigg(\xi_n t_0^{\tau-1}\big[\mathbb{D}x_0 + y_0z_0 - \mathbb{B}y_0\big] \\
&\quad + \sum_{i=0}^{n} \eth_{n-i} t_i^{\tau-1}\big[\mathbb{D}x_i + y_iz_i - \mathbb{B}y_i\big]\Bigg), \\
z_n &= z_0 + \tau\Delta t^{\rho}\Bigg(\xi_n t_0^{\tau-1}\big[\mathbb{C} + \mathbb{A}z_0 - \frac{z_0^3}{3} - x_0^2 + \mathbb{E}z_0x_0^3\big] \\
&\quad + \sum_{i=0}^{n} \eth_{n-i} t_i^{\tau-1}\big[\mathbb{C} + \mathbb{A}z_i - \frac{z_i^3}{3} - x_i^2 + \mathbb{E}z_ix_i^3\big]\Bigg).
\end{aligned} \tag{24}
$$

Using (19) one gets

$$
\begin{aligned}
x_n &= x_0 + \frac{\tau-\tau\rho}{\mathbf{AB}(\rho)} t_n^{\tau-1}\big[x_nz_n - \mathbb{B}x_n - \mathbb{D}y_n\big] \\
&\quad + \frac{\tau\rho\Delta t^{\rho}}{\mathbf{AB}(\rho)}\Bigg(\xi_n t_0^{\tau-1}\big[x_0z_0 - \mathbb{B}x_0 - \mathbb{D}y_0\big] \\
&\quad + \sum_{i=0}^{n} \eth_{n-i} t_i^{\tau-1}\big[x_iz_i - \mathbb{B}x_i - \mathbb{D}y_i\big]\Bigg), \\
y_n &= y_0 + \frac{\tau-\tau\rho}{\mathbf{AB}(\rho)} t_n^{\tau-1}\big[\mathbb{D}x_n + y_nz_n - \mathbb{B}y_n\big] \\
&\quad + \frac{\tau\rho\Delta t^{\rho}}{\mathbf{AB}(\rho)}\Bigg(\xi_n t_0^{\tau-1}\big[\mathbb{D}x_0 + y_0z_0 - \mathbb{B}y_0\big] \\
&\quad + \sum_{i=0}^{n} \eth_{n-i} t_i^{\tau-1}\big[\mathbb{D}x_i + y_iz_i - \mathbb{B}y_i\big]\Bigg), \\
z_n &= z_0 + \frac{\tau-\tau\rho}{\mathbf{AB}(\rho)} t_n^{\tau-1}\big[\mathbb{C} + \mathbb{A}z_n - \frac{z_n^3}{3} - x_n^2 + \mathbb{E}z_nx_n^3\big] \\
&\quad + \frac{\tau\rho\Delta t^{\rho}}{\mathbf{AB}(\rho)}\Bigg(\xi_n t_0^{\tau-1}\big[\mathbb{C} + \mathbb{A}z_0 - \frac{z_0^3}{3} - x_0^2 + \mathbb{E}z_0x_0^3\big] \\
&\quad + \sum_{i=0}^{n} \eth_{n-i} t_i^{\tau-1}\big[\mathbb{C} + \mathbb{A}z_i - \frac{z_i^3}{3} - x_i^2 + \mathbb{E}z_ix_i^3\big]\Bigg).
\end{aligned} \tag{25}
$$

The approximate solutions obtained from (24) are plotted in **Figures 5**, **6**, and those obtained from (25) are plotted in **Figures 7**, **8**. The parameter values used in the model are $\mathbb{A} = 0.95$, $\mathbb{B} = 0.7$, $\mathbb{C} = 0.6$, $\mathbb{D} = 3.5$, and $\mathbb{E} = 0.1$. We used the initial guess $(x_0, y_0, z_0) = (0.1, 0, 0)$ for different fractional orders of ρ and τ.

Example 3. Consider the chaotic system given by [31]

$$
\begin{aligned}
{}^{\mathrm{FF}}_{0}\mathbb{D}_t^{\rho,\tau} x(t) &= \mathbb{A}\big(y(t) - x(t)\big), \\
{}^{\mathrm{FF}}_{0}\mathbb{D}_t^{\rho,\tau} y(t) &= (\mathbb{C} - \mathbb{A})\,x(t) - \big[\mathbb{S}_0 z(t) - \mathbb{S}_1 \sin(z(t))\big]x(t) + \mathbb{C}y(t), \\
{}^{\mathrm{FF}}_{0}\mathbb{D}_t^{\rho,\tau} z(t) &= x(t)y(t) - \mathbb{B}z(t),
\end{aligned} \tag{26}
$$

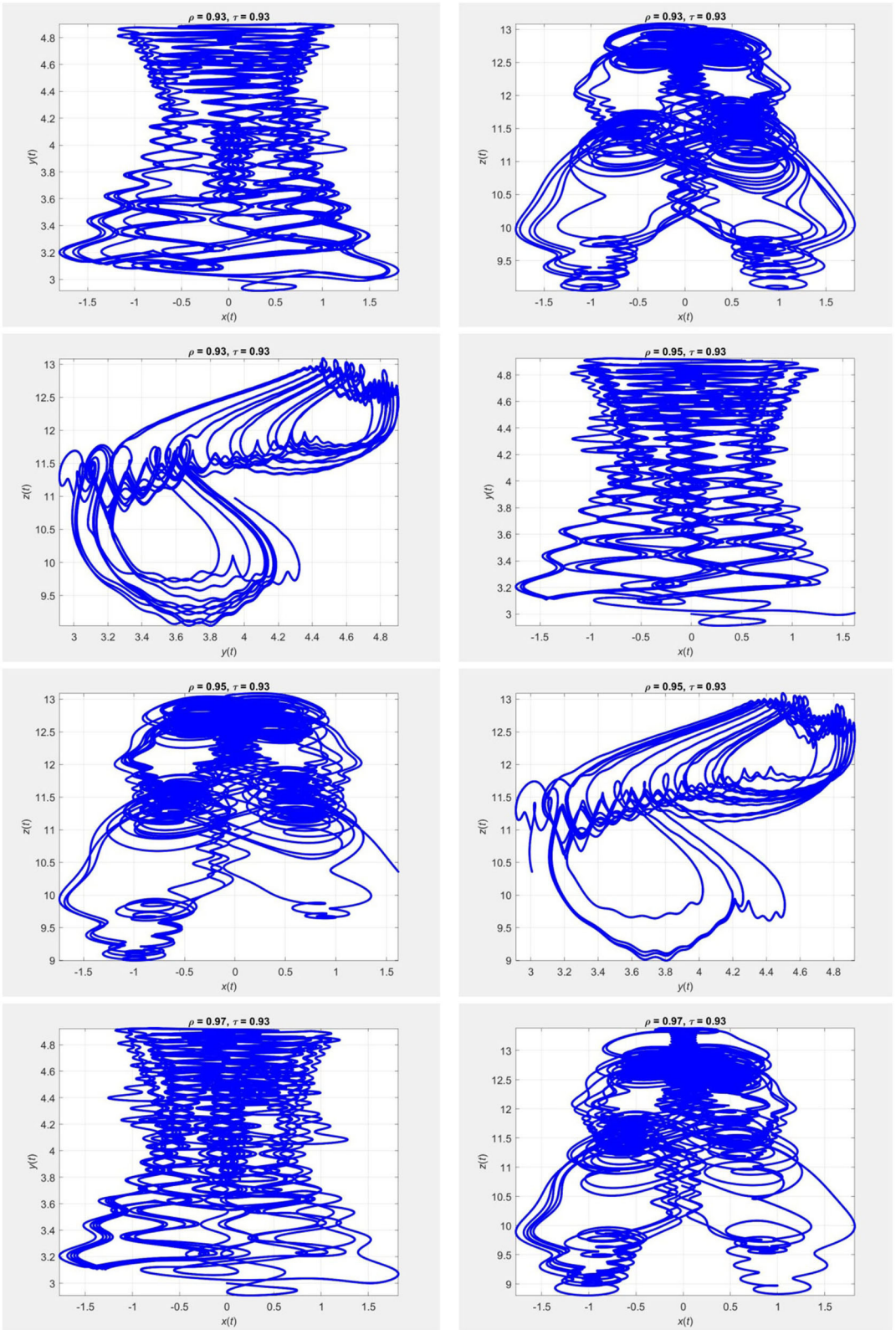

FIGURE 1 | Evolution of the chaotic system (20) for $\tau = 0.93$ and different values of ρ, using the iterative scheme (21).

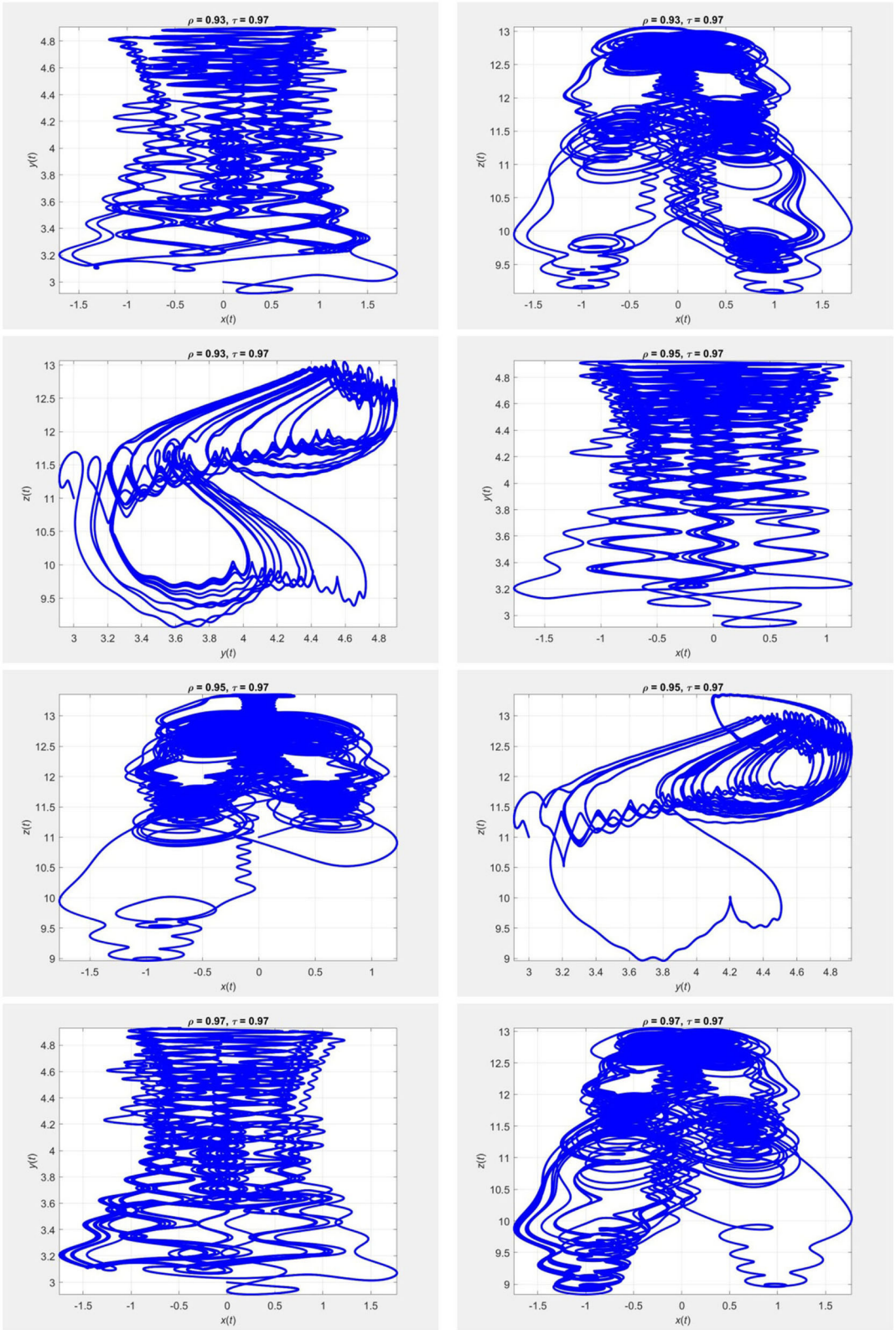

FIGURE 2 | Evolution of the chaotic system (20) for $\tau = 0.97$ and different values of ρ, using the iterative scheme (21).

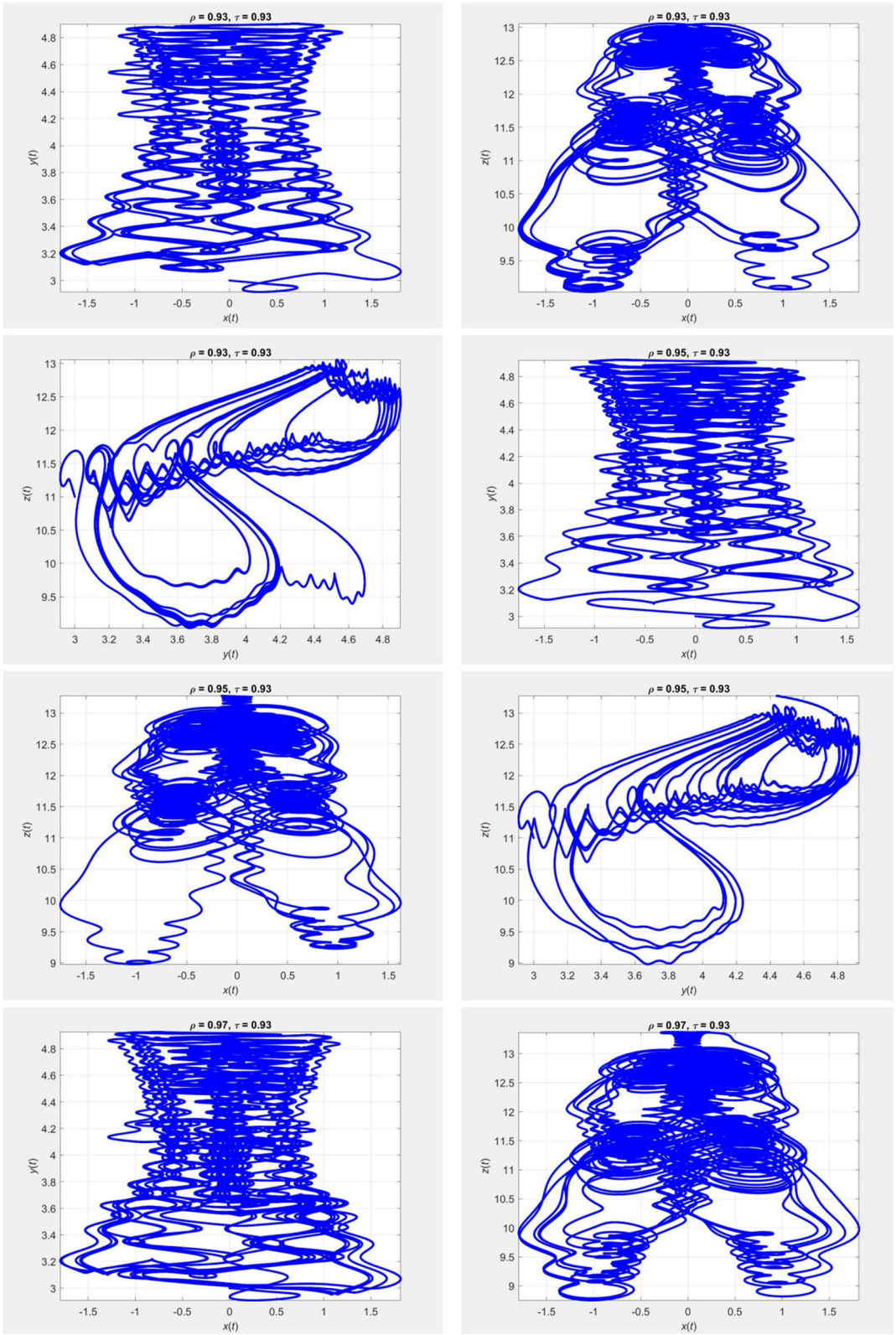

FIGURE 3 | Evolution of the chaotic system (20) for $\tau = 0.93$ and different values of ρ, using the iterative scheme (22).

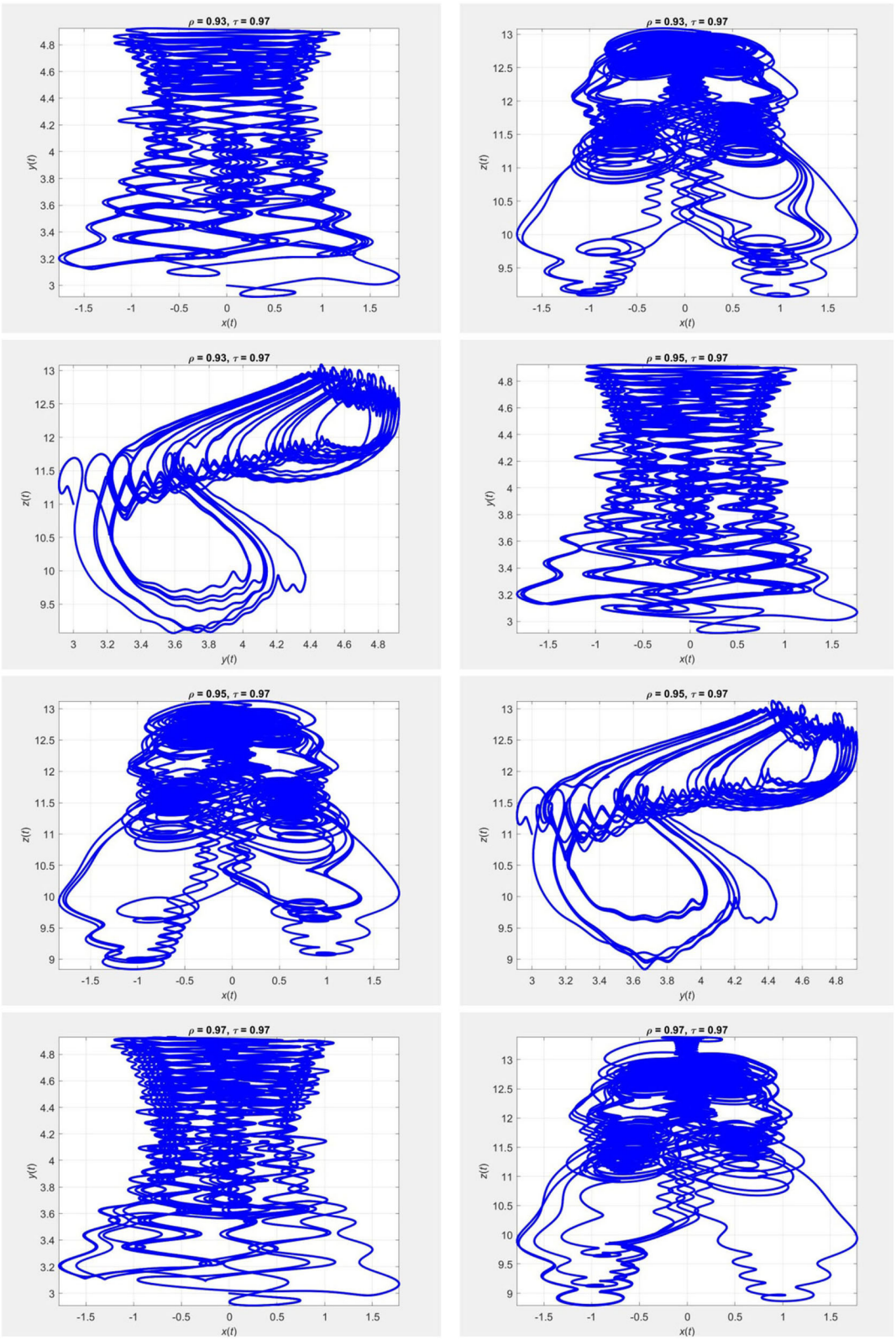

FIGURE 4 | Evolution of the chaotic system (20) for $\tau = 0.97$ and different values of ρ, using the iterative scheme (22).

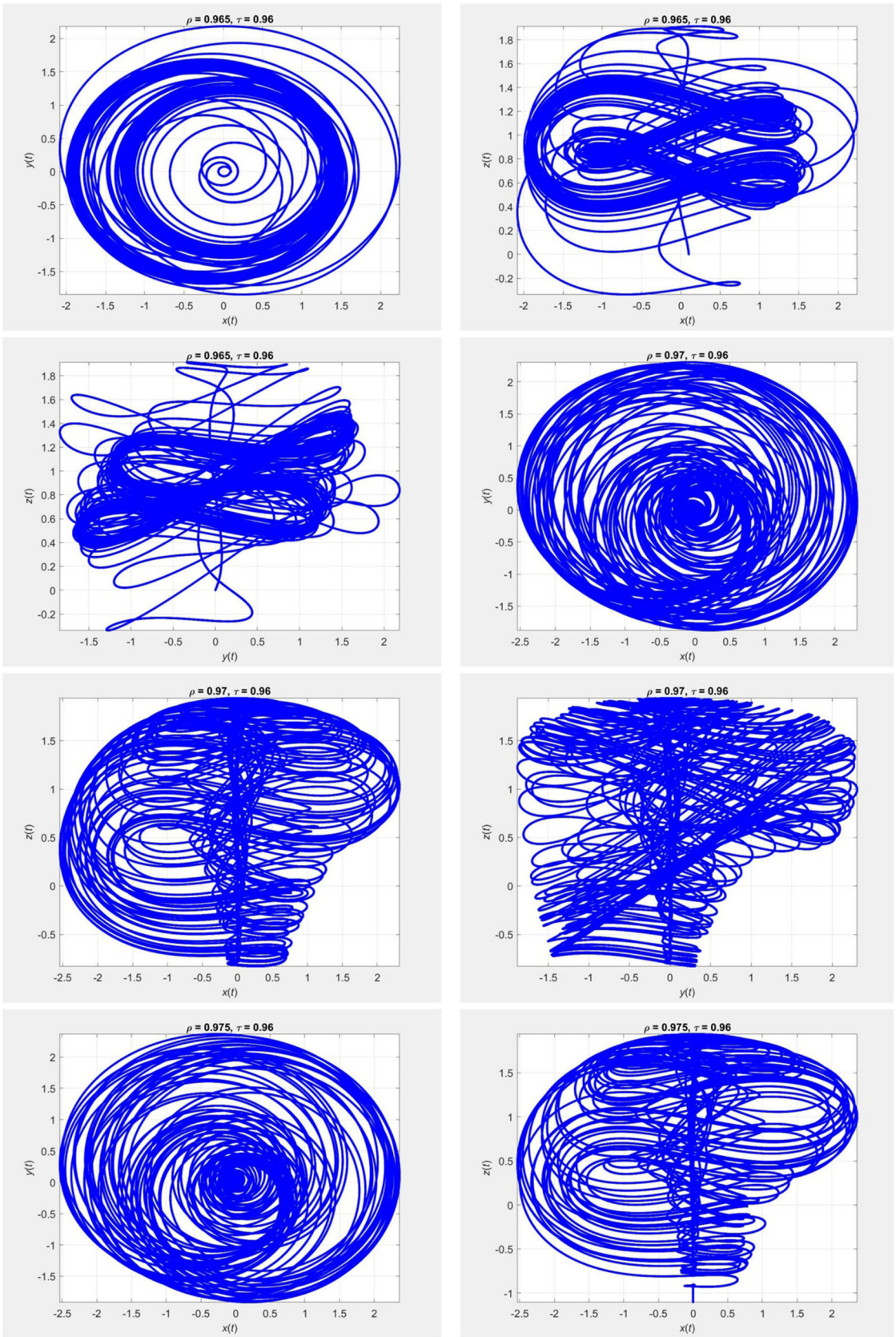

FIGURE 5 | Evolution of the chaotic system (23) for $\tau = 0.96$ and different values of ρ, using the iterative scheme (24).

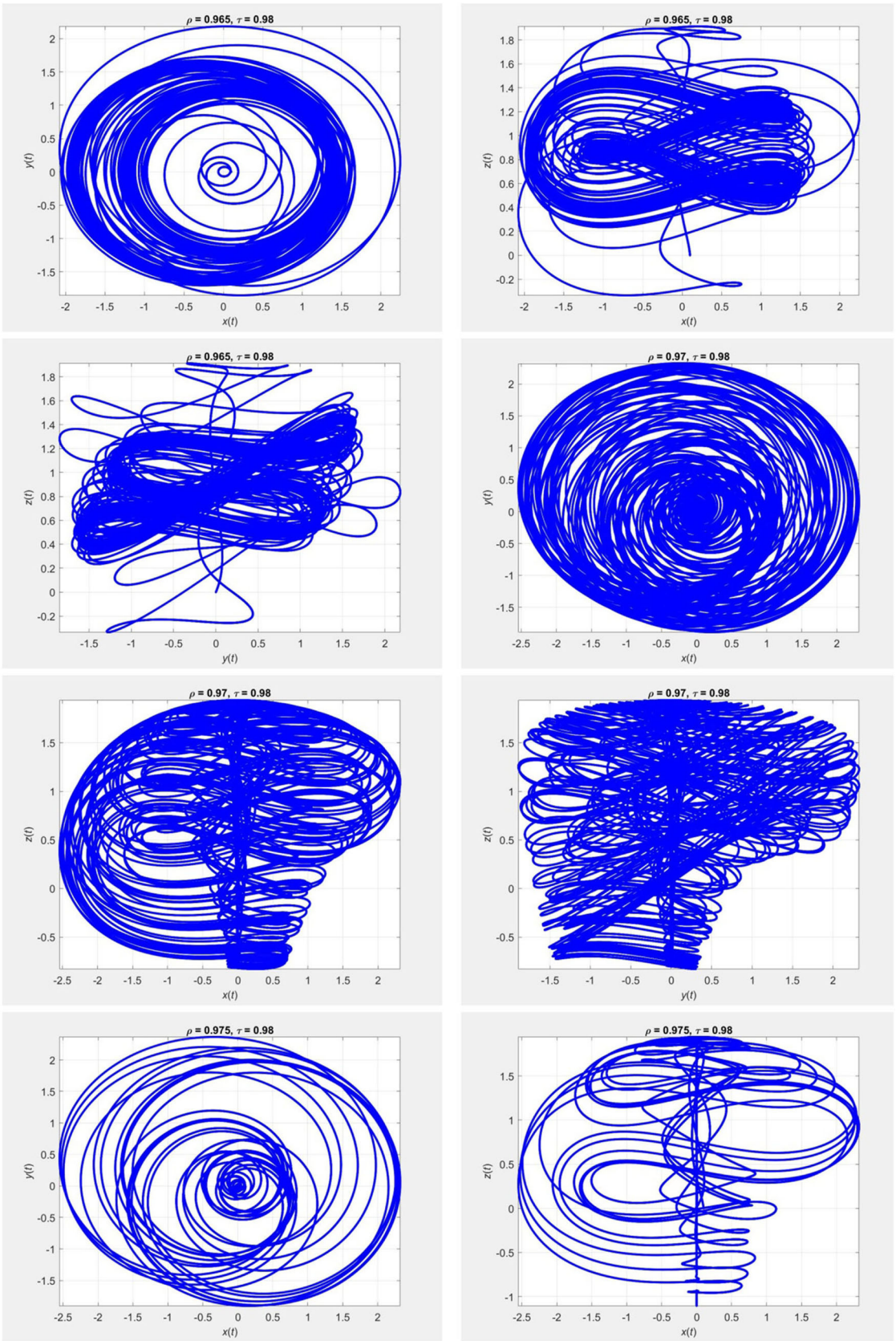

FIGURE 6 | Evolution of the chaotic system (23) for $\tau = 0.98$ and different values of ρ, using the iterative scheme (24).

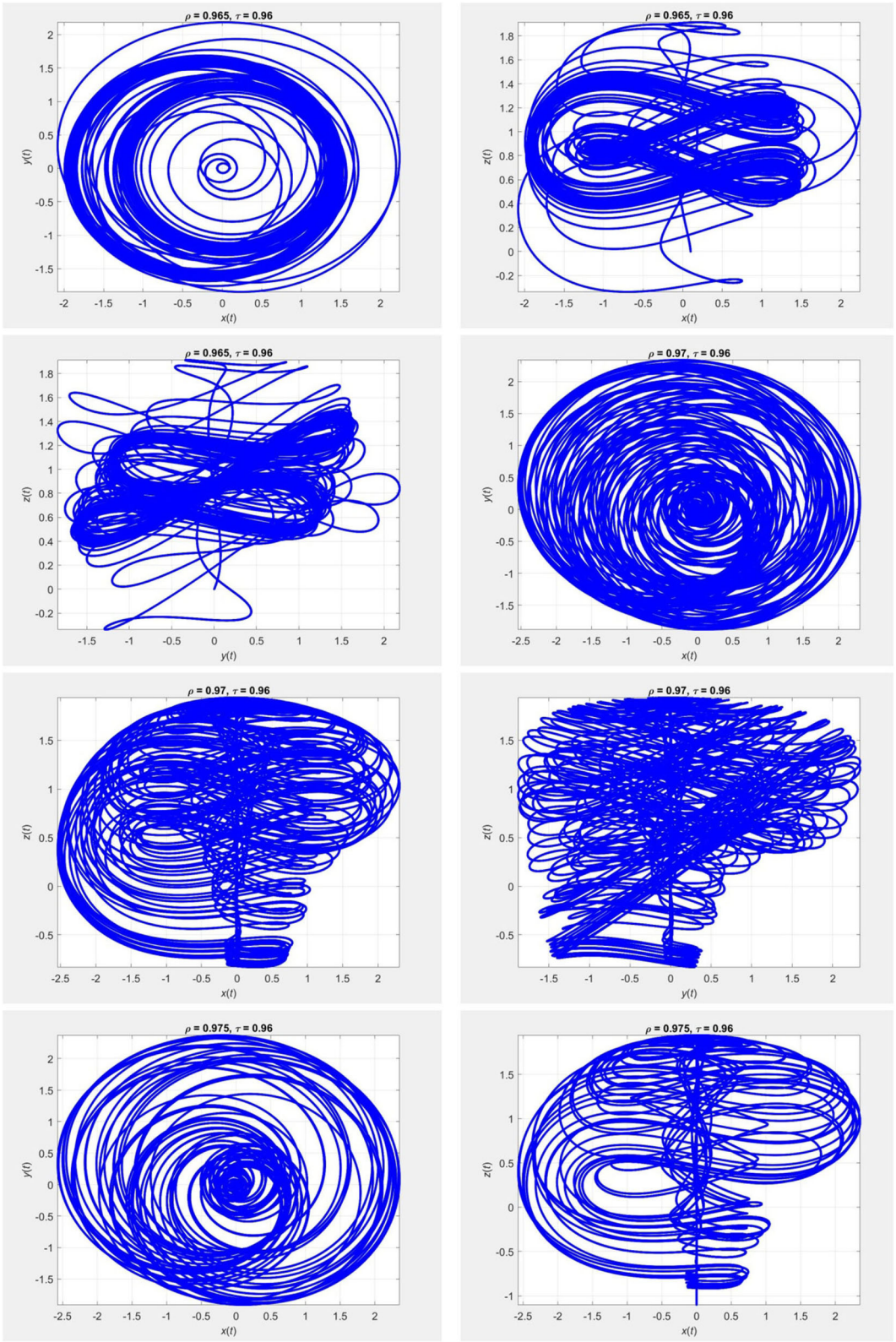

FIGURE 7 | Evolution of the chaotic system (23) for $\tau = 0.96$ and different values of ρ, using the iterative scheme (25).

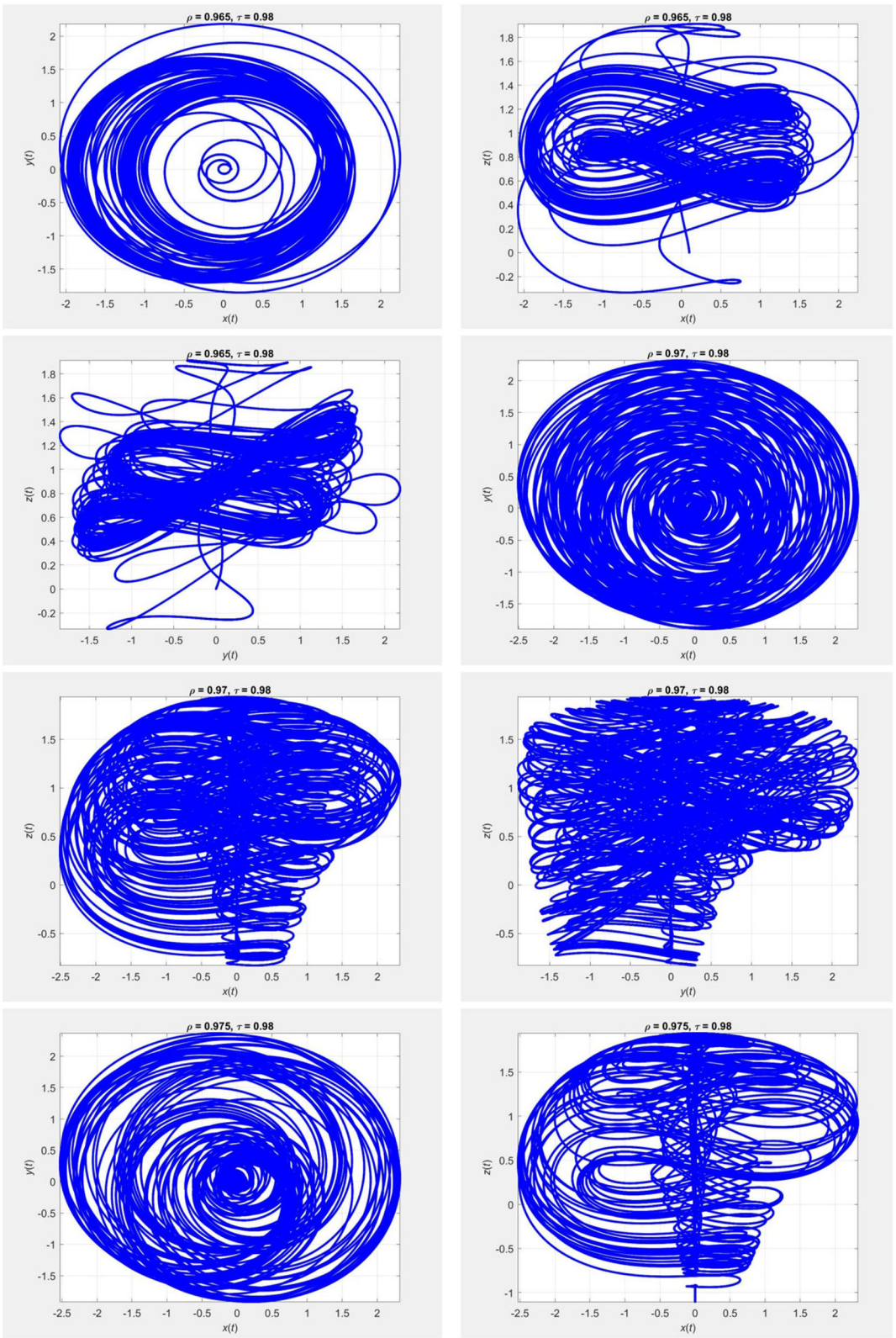

FIGURE 8 | Evolution of the chaotic system (23) for $\tau = 0.98$ and different values of ρ, using the iterative scheme (25).

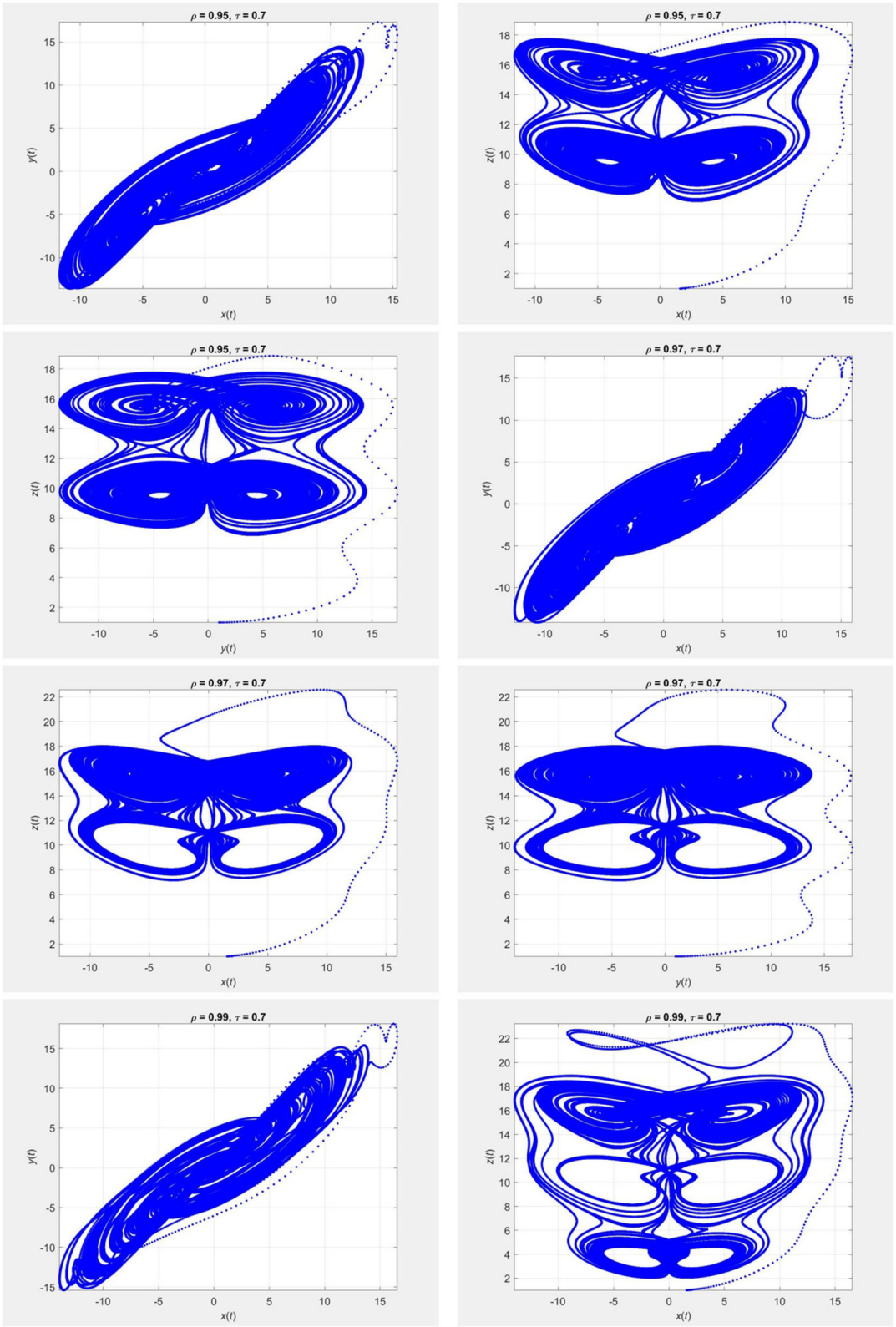

FIGURE 9 | Evolution of the chaotic system (26) for $\tau = 0.7$ and different values of ρ, using the iterative scheme (27).

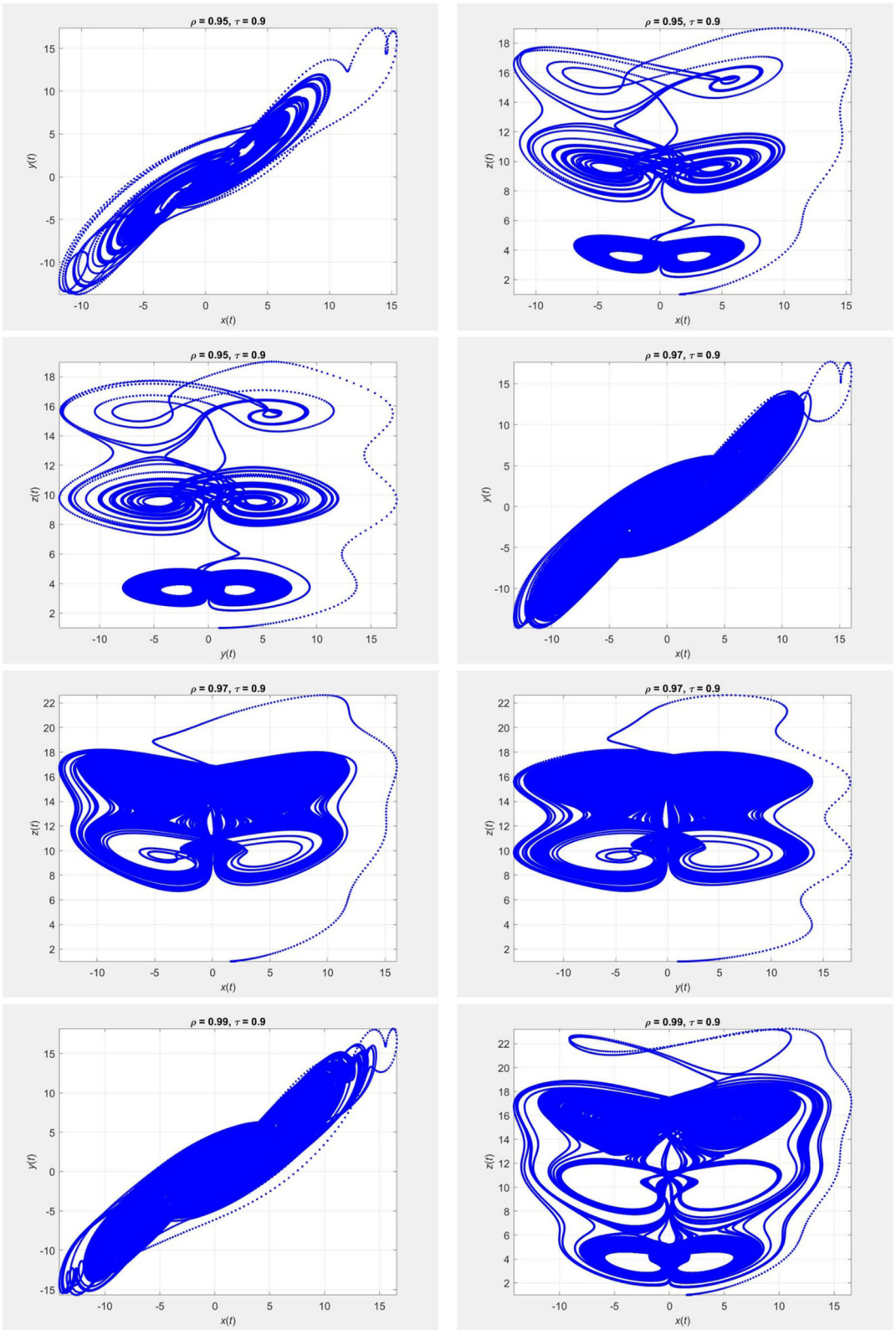

FIGURE 10 | Evolution of the chaotic system (26) for $\tau = 0.9$ and different values of ρ, using the iterative scheme (27).

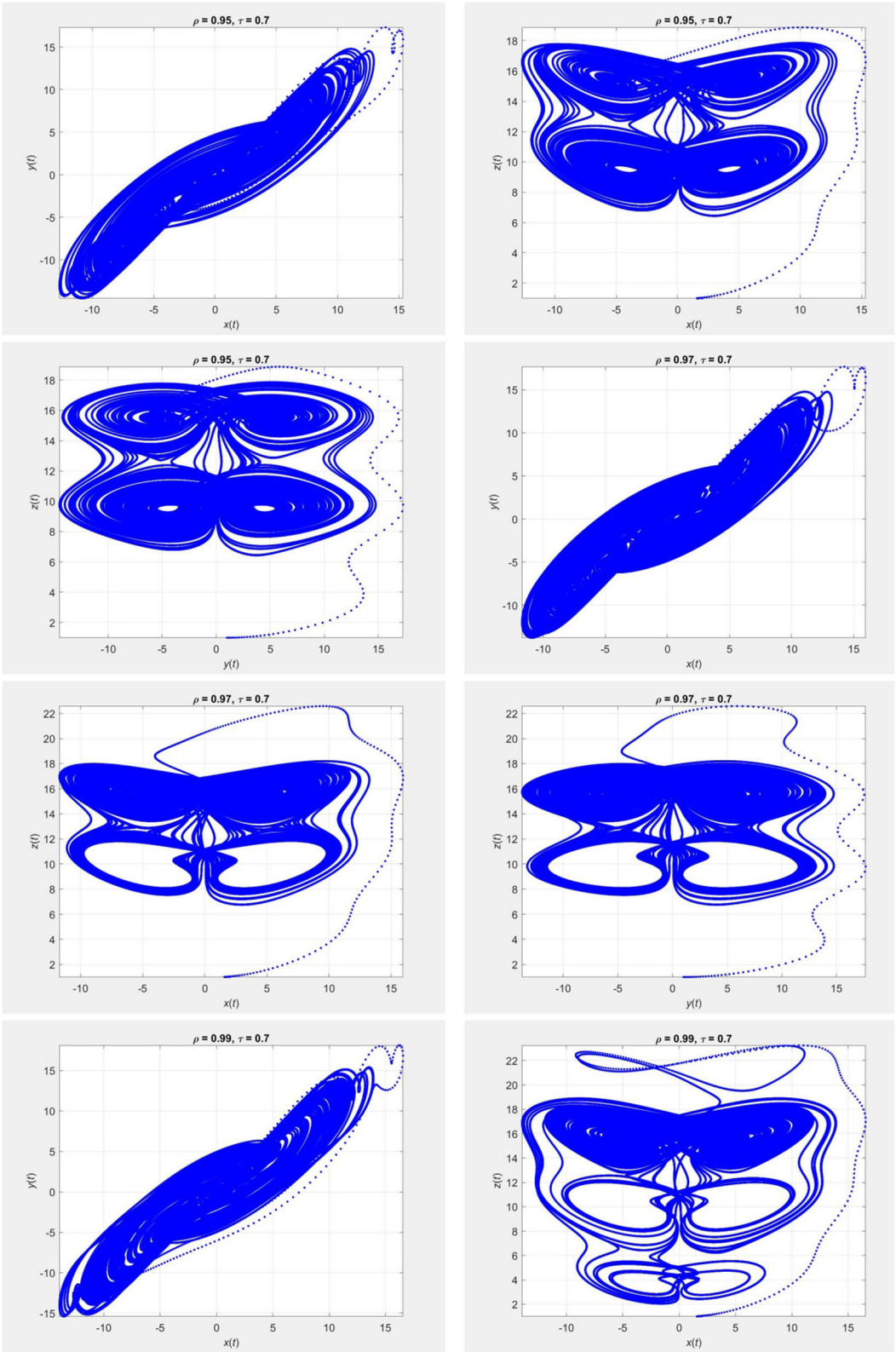

FIGURE 11 | Evolution of the chaotic system (26) for $\tau = 0.7$ and different values of ρ, using the iterative scheme (28).

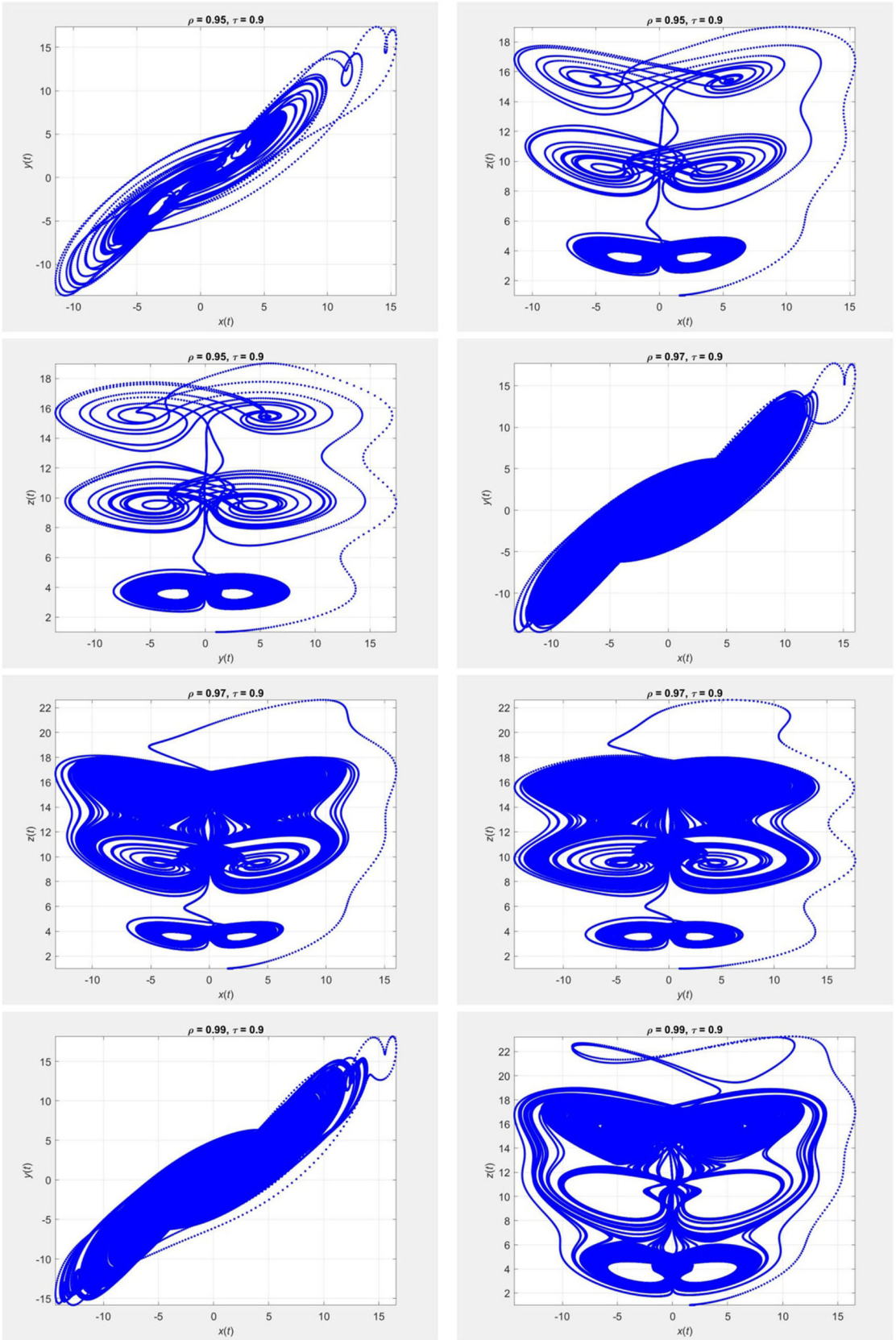

FIGURE 12 | Evolution of the chaotic system (26) for $\tau = 0.9$ and different values of ρ, using the iterative scheme (28).

For this system, from (14) we obtain the following iterative scheme:

$$\begin{aligned}
x_n &= x_0 + \tau\Delta t^{\rho}\left(\xi_n t_0^{\tau-1}\left[\mathbb{A}\left(y_0 - x_0\right)\right] + \sum_{i=0}^{n}\eth_{n-i}t_i^{\tau-1}\left[\mathbb{A}\left(y_i - x_i\right)\right]\right),\\
y_n &= y_0 + \tau\Delta t^{\rho}\left(\xi_n t_0^{\tau-1}\left[\left(\mathbb{C}-\mathbb{A}\right)x_0 - \left[\mathbb{S}_0 z_0 - \mathbb{S}_1\sin(z_0)\right]x_0 + \mathbb{C}y_0\right]\right.\\
&\quad\left. + \sum_{i=0}^{n}\eth_{n-i}t_i^{\tau-1}\left[\left(\mathbb{C}-\mathbb{A}\right)x_0 - \left[\mathbb{S}_0 z_i - \mathbb{S}_1\sin(z_i)\right]x_i + \mathbb{C}y_i\right]\right),\\
z_n &= z_0 + \tau\Delta t^{\rho}\left(\xi_n t_0^{\tau-1}\left[x_0 y_0 - \mathbb{B}z_0\right] + \sum_{i=0}^{n}\eth_{n-i}t_i^{\tau-1}\left[x_i y_i - \mathbb{B}z_i\right]\right).
\end{aligned} \tag{27}$$

Moreover, from (19), the approximate solution is obtained as

$$\begin{aligned}
x_n &= x_0 + \frac{\tau-\tau\rho}{\mathbf{AB}(\rho)}t_n^{\tau-1}\left[\mathbb{A}\left(y_n - x_n\right)\right]\\
&\quad + \frac{\tau\rho\Delta t^{\rho}}{\mathbf{AB}(\rho)}\left(\xi_n t_0^{\tau-1}\left[\mathbb{A}\left(y_0 - x_0\right)\right] + \sum_{i=0}^{n}\eth_{n-i}t_i^{\tau-1}\left[\mathbb{A}\left(y_i - x_i\right)\right]\right),\\
y_n &= y_0 + \frac{\tau-\tau\rho}{\mathbf{AB}(\rho)}t_n^{\tau-1}\left[\left(\mathbb{C}-\mathbb{A}\right)x_0 - \left[\mathbb{S}_0 z_n - \mathbb{S}_1\sin(z_n)\right]x_n + \mathbb{C}y_n\right]\\
&\quad + \frac{\tau\rho\Delta t^{\rho}}{\mathbf{AB}(\rho)}\left(\xi_n t_0^{\tau-1}\left[\left(\mathbb{C}-\mathbb{A}\right)x_0 - \left[\mathbb{S}_0 z_0 - \mathbb{S}_1\sin(z_0)\right]x_0 + \mathbb{C}y_0\right]\right.\\
&\quad\left. + \sum_{i=0}^{n}\eth_{n-i}t_i^{\tau-1}\left[\left(\mathbb{C}-\mathbb{A}\right)x_0 - \left[\mathbb{S}_0 z_i - \mathbb{S}_1\sin(z_i)\right]x_i + \mathbb{C}y_i\right]\right),\\
z_n &= z_0 + \frac{\tau-\tau\rho}{\mathbf{AB}(\rho)}t_n^{\tau-1}\left[x_n y_n - \mathbb{B}z_n\right]\\
&\quad + \frac{\tau\rho\Delta t^{\rho}}{\mathbf{AB}(\rho)}\left(\xi_n t_0^{\tau-1}\left[x_0 y_0 - \mathbb{B}z_0\right] + \sum_{i=0}^{n}\eth_{n-i}t_i^{\tau-1}\left[x_i y_i - \mathbb{B}z_i\right]\right).
\end{aligned} \tag{28}$$

Figures 9–12 show the portraits corresponding to the chaotic system in (26) obtained using (27) and (28). The parameters for the model are $\mathbb{A} = 50, \mathbb{B} = 2, \mathbb{C} = 30, \mathbb{S}_1 = 1$, and $\mathbb{S}_2 = 20$. We used the initial guess $(x_0, y_0, z_0) = (2, 1, 1)$ for different fractional orders of ρ.

5. CONCLUSION

Although many numerical methods are available, the development of new efficient numerical schemes has always been one of the most important concerns in applied mathematics and engineering. A foremost reason for the widespread interest in new numerical methods is that they may reveal new facts about real-world phenomena. This paper has presented some efficient approximate methods for solving chaotic systems that use new definitions for the derivative, called fractal-fractional derivatives. The concept of memory is one of the most important features of these types of derivatives. With this valuable feature, the evolution of the phenomena modeled by such systems can be more accurately predicted. The proposed new techniques have been tested by using them to solve several important practical problems. Application of the methods to these problems revealed very interesting behaviors of the systems that have meaningful interpretations. The numerical methods presented in this article have the potential to be used for solving similar models. Since any new numerical method should be validated in terms of convergence, stability and consistency of solutions, these are important research directions left to future work.

DATA AVAILABILITY STATEMENT

The raw data supporting the conclusions of this article will be made available by the authors, without undue reservation, to any qualified researcher.

AUTHOR CONTRIBUTIONS

All authors listed have made a substantial, direct and intellectual contribution to the work, and approved it for publication.

REFERENCES

1. Kilbas AAA, Srivastava HM, Trujillo JJ. *Theory and Applications of Fractional Differential Equations. Vol. 204*. Amsterdam; Boston, MA: Elsevier Science Limited (2006).
2. Caputo M, Fabrizio M. A new definition of fractional derivative without singular kernel. *Progr Fract Differ Appl*. (2015) **1**:1–13. doi: 10.18576/pfda/020101
3. Atangana A, Baleanu D. New fractional derivatives with nonlocal and non-singular kernel: theory and application to heat transfer model. *arXiv preprint arXiv:160203408*. (2016). doi: 10.2298/TSCI160111018A
4. Gao W, Ghanbari B, Baskonus HM. New numerical simulations for some real world problems with Atangana-Baleanu fractional derivative. *Chaos Solit Fract*. (2019) **128**:34–43. doi: 10.1016/j.chaos.2019.07.037
5. Ghanbari B, Gómez-Aguilar J. Modeling the dynamics of nutrient-phytoplankton-zooplankton system with variable-order fractional derivatives. *Chaos Solit Fract*. (2018) **116**:114–20. doi: 10.1016/j.chaos.2018.09.026
6. Atangana A. Fractal-fractional differentiation and integration: connecting fractal calculus and fractional calculus to predict complex system. *Chaos Solit Fract*. (2017) **102**:396–406. doi: 10.1016/j.chaos.2017.04.027
7. Losada J, Nieto JJ. Properties of a new fractional derivative without singular kernel. *Progr Fract Differ Appl*. (2015) **1**:87–92.
8. Chen W, Sun H, Zhang X, Korošak D. Anomalous diffusion modeling by fractal and fractional derivatives. *Comput Math Appl*. (2010) **59**:1754–8. doi: 10.1016/j.camwa.2009.08.020
9. Kanno R. Representation of random walk in fractal space-time. *Phys A*. (1998) **248**:165–75. doi: 10.1016/S0378-4371(97)00422-6
10. Singh J, Kumar D, Baleanu D, Rathore S. An efficient numerical algorithm for the fractional Drinfeld-Sokolov-Wilson equation. *Appl Math Comput*. (2018) **335**:12–24. doi: 10.1016/j.amc.2018.04.025
11. Qureshi S, Yusuf A, Shaikh AA, Inc M, Baleanu D. Fractional modeling of blood ethanol concentration system with real data application. *Chaos*. (2019) **29**:013143. doi: 10.1063/1.5082907
12. Gill V, Singh J, Singh Y. Analytical solution of generalized space-time fractional advection-dispersion equation via coupling of Sumudu and Fourier transforms. *Front Phys*. (2019) **6**:151. doi: 10.3389/fphy.2018.00151
13. Qureshi S, Atangana A, Shaikh AA. Strange chaotic attractors under fractal-fractional operators using newly proposed numerical methods. *Eur Phys J Plus*. (2019) **134**:523. doi: 10.1140/epjp/i2019-13003-7

14. Kumar S, Kumar R, Singh J, Nisar K, Kumar D. An efficient numerical scheme for fractional model of HIV-1 infection of CD4+ T-cells with the effect of antiviral drug therapy. *Alexandria Eng J*. (2020). doi: 10.1016/j.aej.2019.12.046. [Epub ahead of print].
15. Berhe HW, Qureshi S, Shaikh AA. Deterministic modeling of dysentery diarrhea epidemic under fractional Caputo differential operator via real statistical analysis. *Chaos Solit Fract*. (2020) **131**:109536. doi: 10.1016/j.chaos.2019.109536
16. Singh J. A new analysis for fractional rumor spreading dynamical model in a social network with Mittag-Leffler law. *Chaos*. (2019) **29**:013137. doi: 10.1063/1.5080691
17. Qureshi S, Rangaig NA, Baleanu D. New numerical aspects of Caputo-Fabrizio fractional derivative operator. *Mathematics*. (2019) **7**:374. doi: 10.3390/math7040374
18. Srivastava H, Kumar D, Singh J. An efficient analytical technique for fractional model of vibration equation. *Appl Math Model*. (2017) **45**:192–204. doi: 10.1016/j.apm.2016.12.008
19. Qureshi S. Effects of vaccination on measles dynamics under fractional conformable derivative with Liouville-Caputo operator. *Eur Phys J Plus*. (2020) **135**:63. doi: 10.1140/epjp/s13360-020-00133-0
20. Solís-Pérez J, Gómez-Aguilar J, Atangana A. Novel numerical method for solving variable-order fractional differential equations with power, exponential and Mittag-Leffler laws. *Chaos Solit Fract*. (2018) **114**:175–85. doi: 10.1016/j.chaos.2018.06.032
21. Owolabi KM. Computational study of noninteger order system of predation. *Chaos*. (2019) **29**:013120. doi: 10.1063/1.5079616
22. Yavuz M, Bonyah E. New approaches to the fractional dynamics of schistosomiasis disease model. *Phys A*. (2019) **525**:373–93. doi: 10.1016/j.physa.2019.03.069
23. Jajarmi A, Ghanbari B, Baleanu D. A new and efficient numerical method for the fractional modeling and optimal control of diabetes and tuberculosis co-existence. *Chaos*. (2019) **29**:093111. doi: 10.1063/1.5112177
24. Ghanbari B, Gómez-Aguilar J. Analysis of two avian influenza epidemic models involving fractal-fractional derivatives with power and Mittag-Leffler memories. *Chaos*. (2019) **29**:123113. doi: 10.1063/1.5117285
25. Ganji R, Jafari H, Baleanu D. A new approach for solving multi variable orders differential equations with Mittag-Leffler kernel. *Chaos Solit Fract*. (2020) **130**:109405. doi: 10.1016/j.chaos.2019.109405
26. Kadkhoda N, Jafari H. An analytical approach to obtain exact solutions of some space-time conformable fractional differential equations. *Adv Differ Equat*. (2019) **2019**:428. doi: 10.1186/s13662-019-2349-0
27. Jafari H, Babaei A, Banihashemi S. A novel approach for solving an inverse reaction-diffusion-convection problem. *J Optim Theory Appl*. (2019) **183**:688–704. doi: 10.1007/s10957-019-01576-x
28. Liu B, Hill DJ, Chen G. Synchronization errors and uniform synchronization with an error bound for chaotic systems. *Int J Bifur Chaos*. (2008) **18**:3341–54. doi: 10.1142/S021812740802241X
29. Sorrentino F, Barlev G, Cohen AB, Ott E. The stability of adaptive synchronization of chaotic systems. *Chaos*. (2010) **20**:013103. doi: 10.1063/1.3279646
30. Kazemi BF, Jafari H. Error estimate of the MQ-RBF collocation method for fractional differential equations with Caputo-Fabrizio derivative. *Math Sci*. (2017) **11**:297–305. doi: 10.1007/s40096-017-0232-2
31. Atangana A, Qureshi S. Modeling attractors of chaotic dynamical systems with fractal-fractional operators. *Chaos Solit Fract*. (2019) **123**:320–337. doi: 10.1016/j.chaos.2019.04.020
32. Garrappa R. Numerical solution of fractional differential equations: a survey and a software tutorial. *Mathematics*. (2018) **6**:16. doi: 10.3390/math6020016
33. Ghanbari B, Kumar D. Numerical solution of predator-prey model with Beddington-DeAngelis functional response and fractional derivatives with Mittag-Leffler kernel. *Chaos*. (2019) **29**:063103. doi: 10.1063/1.5094546
34. Ghanbari B, Kumar S, Kumar R. A study of behaviour for immune and tumor cells in immunogenetic tumour model with non-singular fractional derivative. *Chaos Solit Fract*. (2020) **133**:109619. doi: 10.1016/j.chaos.2020.109619
35. Chepyzhov VV, Vishik MI. *Attractors for Equations of Mathematical Physics*. Vol. 49. American Mathematical Society (2002). doi: 10.1090/coll/049

Conflict of Interest: The authors declare that the research was conducted in the absence of any commercial or financial relationships that could be construed as a potential conflict of interest.

Copyright © 2020 Ghanbari and Nisar. This is an open-access article distributed under the terms of the Creative Commons Attribution License (CC BY). The use, distribution or reproduction in other forums is permitted, provided the original author(s) and the copyright owner(s) are credited and that the original publication in this journal is cited, in accordance with accepted academic practice. No use, distribution or reproduction is permitted which does not comply with these terms.

frontiers in Physics

ORIGINAL RESEARCH
published: 16 June 2020
doi: 10.3389/fphy.2020.00177

A Variety of Novel Exact Solutions for Different Models With the Conformable Derivative in Shallow Water

Dipankar Kumar[1,2], *Melike Kaplan*[3]*, *Md. Rabiul Haque*[4], *M. S. Osman*[5,6]* and *Dumitru Baleanu*[7,8,9]*

[1] Graduate School of Systems and Information Engineering, University of Tsukuba, Tsukuba, Japan, [2] Department of Mathematics, Bangabandhu Sheikh Mujibur Rahman Science and Technology University, Gopalganj, Bangladesh, [3] Department of Mathematics, Art-Science Faculty, Kastamonu University, Kastamonu, Turkey, [4] Department of Mathematics, University of Rajshahi, Rajshahi, Bangladesh, [5] Department of Mathematics, Faculty of Science, Cairo University, Giza, Egypt, [6] Department of Mathematics, Faculty of Applied Science, Umm Alqura University, Makkah, Saudi Arabia, [7] Department of Mathematics, Faculty of Arts and Sciences, Çankaya University, Ankara, Turkey, [8] Institute of Space Sciences, Magurele-Bucharest, Romania, [9] Department of Medical Research, China Medical University Hospital, China Medical University, Taichung, Taiwan

OPEN ACCESS

Edited by:
Jordan Yankov Hristov, University of Chemical Technology and Metallurgy, Bulgaria

Reviewed by:
Haci Mehmet Baskonus, Harran University, Turkey
Mustafa Bayram, Gelişim Üniversitesi, Turkey

***Correspondence:**
Melike Kaplan
mkaplan@kastamonu.edu.tr
M. S. Osman
mofatzi@sci.cu.edu.eg
Dumitru Baleanu
dumitru.baleanu@gmail.com

Specialty section:
This article was submitted to Mathematical Physics, a section of the journal Frontiers in Physics

Received: 27 March 2020
Accepted: 27 April 2020
Published: 16 June 2020

Citation:
Kumar D, Kaplan M, Haque MR, Osman MS and Baleanu D (2020) A Variety of Novel Exact Solutions for Different Models With the Conformable Derivative in Shallow Water. Front. Phys. 8:177. doi: 10.3389/fphy.2020.00177

For different nonlinear time-conformable derivative models, a versatile built-in gadget, namely the generalized $\exp(-\varphi(\xi))$-expansion (GEE) method, is devoted to retrieving different categories of new explicit solutions. These models include the time-fractional approximate long-wave equations, the time-fractional variant-Boussinesq equations, and the time-fractional Wu-Zhang system of equations. The GEE technique is investigated with the help of fractional complex transform and conformable derivative. As a result, we found four types of exact solutions involving hyperbolic function, periodic function, rational functional, and exponential function solutions. The physical significance of the explored solutions depends on the choice of arbitrary parameter values. Finally, we conclude that the GEE method is more effective in establishing the explicit new exact solutions than the $\exp(-\varphi(\xi))$-expansion method.

Keywords: time-fractional approximate long-wave equations, time-fractional variant-Boussinesq equations, time-fractional Wu-Zhang system of equations, the GEE method, exact solutions

INTRODUCTION

Analytical solutions of the non-linear partial differential equation (NPDEs) are significantly more important for describing the physical meaning for any real-world problems. Due to the rapid expansion of computer technologies and computer-based symbolic tools, researchers have concentrated increasingly on the analytical and numerical solutions for the NPDEs, including integer and fractional orders. During recent decades, several analytical and semi-analytical methods, such as the improved fractional sub-equation [1], the exp function method [2, 3], the G'/G-expansion [4–7], the $\tan(\Phi(\xi)/2)$-expansion [8], the modified Kudryashov [9, 10], the new extended direct algebraic [11], the extended $exp(-\varphi(\xi))$-expansion [12], the RB sub-ODE [13], the sine-Gordon expansion [14–16], the unified [17, 18], and the generalized unified [19, 20] methods, have been investigated and also employed for acquiring the new exact solutions of the well-known NPDEs that arise in applied sciences. Presenting new exact solution of PDEs provides a better understanding of the phenomena, which are governed by three special form of time-fractional WKB equations.

The time-fractional Whitham-Broer-Kaup (WBK) equation has the following structure [21]

$$\left.\begin{array}{c} D_t^{\alpha}u + uu_x + v_x + \beta u_{xx} = 0 \\ D_t^{\alpha}v + (uv)_x - \beta v_{xx} + \gamma u_{xxx} = 0 \end{array}\right\},\ t \geq 0,\ 0 < \alpha \leq 1. \quad (1)$$

Eq. (1) describes the dispersive long wave in shallow water [22] where $u = u(x,t)$ is the velocity field in the horizontal direction, $v = v(x,t)$ is he height which deviates from the liquid balance position, and β and γ are real parameters [23]. $D_t^{\alpha}(.)$ is conformable derivative of order α. In the past, many researchers studied the WBK equation via different analytical approaches according to their field, particularly within mathematical physics and ocean engineering. For instance, Guo et al. [24] employed the improved sub-equation method to extract analytical solutions for space- and time-fractional WBK equations. El-Borai et al. [25] applied the exp-function method under the sense of the modified Riemann-Liouville derivative for solving the time-fractional coupled WBK equations.

If we choose the free parameters as $\beta = \frac{1}{2}$ and $\gamma = 0$, Eq. (1) is converted to the time-fractional approximate long-wave equations [21]:

$$\left.\begin{array}{c} D_t^{\alpha}u + uu_x + v_x + \frac{1}{2}u_{xx} = 0 \\ D_t^{\alpha}v + (uv)_x - \frac{1}{2}v_{xx} = 0 \end{array}\right\},\ t \geq 0,\ 0 < \alpha \leq 1. \quad (2)$$

In past, Eq. (2) have been solved by the fractional sub-equation method [26], the G'/G-expansion method [24], and the generalized Kudryashov method [27] for establishing different wave solutions.

Again, we substitute $\beta = 0$ and $\gamma = 1$ in Eq. (1), and Eq. (1) is converted to the following time-fractional variant Boussinesq equations [21]:

$$\left.\begin{array}{c} D_t^{\alpha}u + uu_x + v_x = 0 \\ D_t^{\alpha}v + (uv)_x + u_{xxx} = 0 \end{array}\right\},\ t \geq 0,\ 0 < \alpha \leq 1. \quad (3)$$

Equation (3) was solved by Yan [26] by using fractional sub-equation method. The improved fractional sub-equation method [24] was applied for producing the new generalized exact solutions of the space–time-fractional variant Boussinesq equations.

Finally, if we choose the free parameter values $\beta = 0$ and $\gamma = \frac{1}{3}$ in Eq. (1), Eq. (1) is the converted to the following time-fractional Wu-Zhang system of equations [27]:

$$\left.\begin{array}{c} D_t^{\alpha}u + uu_x + v_x = 0 \\ D_t^{\alpha}v + (uv)_x + \frac{1}{3}u_{xxx} = 0 \end{array}\right\},\ t \geq 0,\ 0 < \alpha \leq 1. \quad (4)$$

Eslami et al. [27] solved the time-fractional Wu-Zhang system of equations using the first integral method by considering conformable fractional sense.

If we consider $\alpha = 1$in Eq. (1), then it is converted to the classical coupled WBK equation, which was first introduced by Whitham [28], Broer [29], and Kaup [30]. When $\alpha = 1,\ \beta \neq 0$, and $\gamma = 1$, Eq. (1) is the classical long-wave equation that describes the shallow water wave with diffusion. When $\alpha = 1,\ \beta = 0$, and $\gamma = 1$, Eq. (1) reduces the classical variant Boussinesq equations [31], and when $\alpha = 1,\ \beta = 0$ and $\gamma = 1/3$, Eq. (1) reduces the classical Wu-Zhang system of equations [32]. Sometimes, the classical Wu-Zhang system of equations are introduced by the (1+1) dimensional dispersive long-wave equations [33–35].

For the simplicity of the solutions, we did not consider solving the time-fractional WKB equations by the generalized $exp(-\varphi(\xi))$-expansion method. The main aim of this work is to construct the new exact traveling wave solutions of the three-special form of time-fractional WKB equations, such as the time-fractional approximate long-wave equations, the time-fractional variant Boussinesq equations, and the time-fractional Wu-Zhang system of equations using the generalized $exp(-\varphi(\xi))$-expansion method with a conformable derivative sense. The generalized $exp(-\varphi(\xi))$-expansion method is an effectual and easily applicable technique that is used to investigate the new exact solution for different integer- and fractional-order PDEs. Very recently, Lu et al. [36] used the generalized $exp(-\varphi(\xi))$-expansion method and construct the exact solutions of space–time-fractional generalized fifth-order KdV equation with Jumarie's modified Riemann-Liouville derivatives.

The rest of the paper is arranged as follows. In section Conformable derivative and the generalized $exp(-\varphi(\xi))$-expansion method, some basic definitions of conformable derivative and the main steps of the generalized $exp(-\varphi(\xi))$-expansion method are given. In section Application of the generalized $exp(-\varphi(\xi))$-expansion method, we look for the exact solutions of Eq. (2) to Eq. (4) via the generalized $exp(-\varphi(\xi))$-expansion method. Finally, a brief conclusion is provided in the last section.

THE CONFORMABLE DERIVATIVE AND THE GENERALIZED exp(−φ(ξ))-EXPANSION METHOD

Khalil et al. [37] started to give us the first definition of the conformable derivative (CD) with a limit operator as follows.

Definition 1. If $f:(0,\infty) \to R$, then the CFD of f order α is defined as

$$D_t^{\alpha}f(t) = \lim_{\varepsilon \to 0}\frac{f\left(t + \varepsilon t^{1-\alpha}\right) - f(t)}{\varepsilon},\ \text{for all t} > 0,\ 0 < \alpha \leq 1.$$

The CD satisfies some workable features that are demonstrated in the following theorems [37–41].

Theorem 1. Let $\alpha \in (0,1]$ and $f = f(t)$, $g = g(t)$ be α-conformable differentiable at a point $t > 0$, then

$$\begin{array}{ll} (i) & D_t^{\alpha}\left(af + bg\right) = aD_t^{\alpha}f + bD_t^{\alpha}g,\ \textit{for all } a,b \in R, \\ (ii) & D_t^{\alpha}\left(t^{\mu}\right) = \mu t^{\mu-\alpha},\ \textit{for all } \mu \in R, \\ (iii) & D_t^{\alpha}\left(fg\right) = gD_t^{\alpha}\left(f\right) + fD_t^{\alpha}\left(g\right), \\ (iv) & D_t^{\alpha}\left(\frac{f}{g}\right) = \frac{gD_t^{\alpha}\left(f\right) - fD_t^{\alpha}\left(g\right)}{g^2}. \end{array}$$

Furthermore, if f is differentiable, then $D_t^{\alpha}\left(f(t)\right) = t^{1-\alpha}\frac{df}{dt}$.

Theorem 2. Let $f:(0,\infty) \rightarrow R$ be a function such that f is differentiable and α-conformable differentiable. Also, let g be a differentiable function defined in the range of f. Then

$$D_t^{\alpha}\left(fog\right)(t) = t^{1-\alpha} g(t)^{\alpha-1} g'(t) D_t^{\alpha}\left(f(t)\right)_{t=g(t)}$$

where prime denotes the classical derivatives with respect to t.

Now, we impose the generalized $exp(-\varphi(\xi))$-expansion method for solving some fractional differential equations. In this respect, we described the essential steps of the generalized $exp(-\varphi(\xi))$- expansion method [36] as follows.

Step-1: Suppose that a general form of the non-linear FDEs, say in two independent variables x and t, is given by

$$\left.\begin{array}{l} P_1\left(u, v, D_t^{\alpha}u, D_t^{\alpha}v, D_t^{2\alpha}u, D_t^{2\alpha}v, u_x, v_x, u_{xx}, v_{xx}, \ldots\ldots\right) = 0 \\ P_2\left(u, v, D_t^{\alpha}u, D_t^{\alpha}v, D_t^{2\alpha}u, D_t^{2\alpha}v, u_x, v_x, u_{xx}, v_{xx}, \ldots\ldots\right) = 0 \end{array}\right\} , 0 < \alpha \leq 1,\ t > 0, \quad (5)$$

where $D_t^{\alpha}u$ and $D_t^{\alpha}v$ are conformable derivatives of u and v, respectively, $u = u(x,t)$ and $v = v(x,t)$ are an unknown functions, and P_1 and P_2 are a polynomial in their arguments.

Step-2: To construct the exact solution of Eq. (5), we introduce the variable transformation, combine the real variables x and t by a compound variable ξ

$$u = U(\xi) \text{ and } v = V(\xi), \xi = x - \left(\frac{c}{\alpha}\right) t^{\alpha}, \quad (6)$$

where, c is a constant which is determined later. The traveling wave transformation of Eq. (6) converts Eq. (5) into an ordinary differential equation (ODE) for $u = U(\xi)$ and $v = V(\xi)$:

$$\left.\begin{array}{l} Q_1\left(U,\ V, U',\ V', U'', V'', \ldots\ldots\right) = 0 \\ Q_1\left(U,\ V, U',\ V', U'', V'', \ldots\ldots\right) = 0 \end{array}\right\}, \quad (7)$$

where $Q_1$and Q_2 are a polynomial of U, V, and its derivatives with respect to ξ.

Step 3: Suppose that the traveling wave solution of system Eq. (7) can be presented as follows

$$\left.\begin{array}{l} U(\xi) = \mathrm{a}_0 + \sum_{i=1}^{m} a_i \left(exp\left(-\varphi(\xi)\right)\right)^i \\ V(\xi) = b_0 + \sum_{i=1}^{n} \mathrm{b_i} \left(\exp\left(-\varphi(\xi)\right)\right)^{\mathrm{i}} \end{array}\right\}, \quad (8)$$

where the arbitrary constants $a_i (i = 1, 2 \ldots, m)$ and $b_i (i = 1, 2 \ldots, n)$ are determined latter, but $a_m \neq 0$ and $b_n \neq 0$ and also m and n are a positive integer, which can be determined by using homogeneous balance principle on Eq. (7), and $\varphi = \varphi(\xi)$ satisfies the following new ansatz equation

$$\varphi'(\xi) = p\, exp\left(-\varphi(\xi)\right) + q\, exp\left(\varphi(\xi)\right) + r \quad (9)$$

where p, q, and r are constant. The general solutions of the equation are the following.

Case-I: When $p = 1$ and $\Delta = r^2 - 4q$, one obtains 8.510.5

$$\left.\begin{array}{c} \varphi(\xi) = \ln\left(\frac{-\sqrt{\Delta}\tanh\left(\frac{1}{2}\sqrt{\Delta}\ (\xi+E)\right) - r}{2q}\right),\ q \neq 0, \\ \Delta = r^2 - 4q > 0 \\ \varphi(\xi) = \ln\left(\frac{-\sqrt{\Delta}\coth\left(\frac{1}{2}\sqrt{\Delta}\ (\xi+E)\right) - r}{2q}\right),\ q \neq 0, \\ \Delta = r^2 - 4q > 0 \end{array}\right\}, \quad (10)$$

$$\left.\begin{array}{c} \varphi(\xi) = \ln\left(\frac{\sqrt{-\Delta}\tan\left(\frac{1}{2}\sqrt{-\Delta}\ (\xi+E)\right) - r}{2q}\right),\ q \neq 0, \\ \Delta = r^2 - 4q < 0 \\ \varphi(\xi) = \ln\left(\frac{\sqrt{-\Delta}\cot\left(\frac{1}{2}\sqrt{-\Delta}\ (\xi+E)\right) - r}{2q}\right),\ q \neq 0, \\ \Delta = r^2 - 4q < 0 \end{array}\right\}, \quad (11)$$

$$\varphi(\xi) = -\ln\left(\frac{r}{exp\left(r\left(\xi + E\right)\right) - 1}\right), \quad q = 0,\ r \neq 0,\ = r^2 - 4q > 0, \quad (12)$$

and

$$\varphi(\xi) = \ln\left(-\frac{2\left(r\left(\xi + E\right) + 2\right)}{r^2\left(\xi + E\right)}\right), \quad q \neq 0,\ r \neq 0,\ \Delta = r^2 - 4q = 0. \quad (13)$$

Case-II: When $r = 0$, one obtains

$$\varphi(\xi) = \ln\left(\sqrt{\frac{p}{q}}\ tan\left(\sqrt{pq}\ (\xi + E)\right)\right), p > 0, q > 0. \quad (14)$$

$$\varphi(\xi) = \ln\left(-\sqrt{\frac{p}{q}}\ cot\left(\sqrt{pq}\ (\xi + E)\right)\right), p < 0, q < 0. \quad (15)$$

$$\varphi(\xi) = \ln\left(\sqrt{-\frac{p}{q}}\ tanh\left(\sqrt{-pq}\ (\xi + E)\right)\right), \quad p > 0, q < 0. \quad (16)$$

$$\varphi(\xi) = \ln\left(-\sqrt{-\frac{p}{q}}\ coth\left(\sqrt{-pq}\ (\xi + E)\right)\right), \quad p < 0, q > 0. \quad (17)$$

Case-III: When $q = 0$ and $r = 0$, one obtains

$$\varphi(\xi) = \ln\left(p\ (\xi + E)\right). \quad (18)$$

For all cases, E is the integrating constant.

Step 4: Inserting Eq. (9) in Eq. (8) and compiling the terms in the resulting equation yields a set of algebraic non-linear equations. Finally, by solving this set we reach the exact solutions of the non-linear fractional PDEs.

APPLICATION OF THE GENERALIZED exp(−φ(ξ))-EXPANSION METHOD

In this part, we will execute the generalized exp(−φ(ξ))-expansion method to solve three well-known non-linear fractional partial differential equations in shallow water, namely, the time-fractional approximate long wave (ALW) equations, the time-fractional variant-Boussinesq equations, and the time-fractional Wu-Zhang system of equations. All the above mentioned equations are the special-form WBK equations that describe the physical phenomena arising in fluid mechanics.

The Time-Fractional ALW Equations

Let us consider the time-fractional ALW equations

$$\left.\begin{array}{l} D_t^{\alpha}u + uu_x + v_x + \frac{1}{2}u_{xx} = 0 \\ D_t^{\alpha}v + (uv)_x - \frac{1}{2}v_{xx} = 0 \end{array}\right\},\ t \geq 0,\ 0 < \alpha \leq 1. \quad (19)$$

Now, applying under the traveling wave transformation of Eq. (6), Eq. (19) reduces to a non-linear ODE as

$$\left.\begin{array}{c} -cU' + UU' + V' + \frac{1}{2}U'' = 0 \\ -cV' + (UV)' - \frac{1}{2}V'' = 0 \end{array}\right\}. \tag{20}$$

This integrates with respect to ξ of Eq. (20) and considers that the integration constant is zero. Eq. (20) then yields

$$\left.\begin{array}{c} -cU + \frac{1}{2}U^2 + V + \frac{1}{2}U' = 0 \\ -cV + UV - \frac{1}{2}V' = 0 \end{array}\right\}. \tag{21}$$

The balancing rule in Eq. (21) yields $m = 1$ and $n = 2$, assuming the general solution Eq. (21) in the presence Eq. (8) is given by

$$\left.\begin{array}{c} U(\xi) = a_0 + a_1 exp(-\varphi(\xi)) \\ V(\xi) = b_0 + b_1 exp(-\varphi(\xi)) + b_2 exp(-2\varphi(\xi)) \end{array}\right\}, \tag{22}$$

where $a_1 \neq 0$ and $b_2 \neq 0$.

Plugging Eq. (22) into Eq. (21), we obtain a set of an algebraic non-linear equations that solve to

Set-1: $a_0 = -\frac{1}{2}r + \frac{1}{2}\sqrt{-4pq + r^2}$, $a_1 = -p$, $b_0 = -pq$, $b_1 = -pr$, $b_2 = -p^2$

and $c = \frac{1}{2}\sqrt{-4pq + r^2}$, $-4pq + r^2 > 0$.

By putting the values of Set-1 into Eq. (22) along with the Eq. (10) to Eq. (18), we obtain the following traveling wave solutions for the time-fractional ALW equations.

For p = 1:

$$\left.\begin{array}{c} u_1(x,t) = -\frac{1}{2}r + \frac{1}{2}\sqrt{r^2 - 4q} \\ \quad + \frac{2q}{\sqrt{\Delta}\ \tanh\left(\frac{1}{2}\sqrt{\Delta}\ (\xi+E)\right) + r} \\ v_1(x,t) = -q + \frac{2rq}{\sqrt{\Delta}\ \tanh\left(\frac{1}{2}\sqrt{\Delta}\ (\xi+E)\right) + r} \\ \quad - \frac{4q^2}{\left(\sqrt{\Delta}\ \tanh\left(\frac{1}{2}\sqrt{\Delta}\ (\xi+E)\right) + r\right)^2} \end{array}\right\}, \tag{23}$$

$$\left.\begin{array}{c} u_2(x,t) = -\frac{1}{2}r + \frac{1}{2}\sqrt{r^2 - 4q} \\ \quad + \frac{2q}{\sqrt{\Delta}\ \coth\left(\frac{1}{2}\sqrt{\Delta}\ (\xi+E)\right) + r} \\ v_2(x,t) = -q + \frac{2rq}{\sqrt{\Delta}\ \coth\left(\frac{1}{2}\sqrt{}\ (\xi+E)\right) + r} \\ \quad - \frac{4q^2}{\left(\sqrt{\Delta}\ \coth\left(\frac{1}{2}\sqrt{\Delta}\ (\xi+E)\right) + r\right)^2} \end{array}\right\}, \tag{24}$$

$$\left.\begin{array}{c} u_3(x,t) = -\frac{1}{2}r + \frac{1}{2}\sqrt{r^2 - 4q} \\ \quad - \frac{2q}{\sqrt{-\Delta}\ \tan\left(\frac{1}{2}\sqrt{-\Delta}\ (\xi+E)\right) - r} \\ v_3(x,t) = -q - \frac{2rq}{\sqrt{-\Delta}\ \tan\left(\frac{1}{2}\sqrt{-\Delta}\ (\xi+E)\right) - r} \\ \quad - \frac{4q^2}{\left(\sqrt{-\Delta}\ \tan\left(\frac{1}{2}\sqrt{-\Delta}\ (\xi+E)\right) - r\right)^2} \end{array}\right\}, \tag{25}$$

$$\left.\begin{array}{c} u_4(x,t) = -\frac{1}{2}r + \frac{1}{2}\sqrt{r^2 - 4q} \\ \quad - \frac{2q}{\sqrt{-\Delta}\ \cot\left(\frac{1}{2}\sqrt{-\Delta}\ (\xi+E)\right) - r} \\ v_4(x,t) = -q - \frac{2rq}{\sqrt{-\Delta}\ \cot\left(\frac{1}{2}\sqrt{-\Delta}\ (\xi+E)\right) - r} \\ \quad - \frac{4q^2}{\left(\sqrt{-\Delta}\ \cot\left(\frac{1}{2}\sqrt{-\Delta}\ (\xi+E)\right) - r\right)^2} \end{array}\right\}, \tag{26}$$

$$\left.\begin{array}{c} u_5(x,t) = -\frac{1}{2}r + \frac{1}{2}\sqrt{r^2 - 4q} - \frac{r}{e^{r(\xi+E)} - 1} \\ v_5(x,t) = -q - \frac{r^2}{e^{r(\xi+E)} - 1} - \frac{r^2}{\left(e^{r(\xi+E)} - 1\right)^2} \end{array}\right\}, \tag{27}$$

and

$$\left.\begin{array}{c} u_6(x,t) = -\frac{1}{2}r + \frac{1}{2}\sqrt{r^2 - 4q} + \frac{1}{2}\frac{r^2(\xi+E)}{r(\xi+E)+2} \\ v_6(x,t) = -q + \frac{1}{2}\frac{r^3(\xi+E)}{r(\xi+E)+2} - \frac{1}{4}\left(\frac{r^2(\xi+E)}{r(\xi+E)+2}\right)^2 \end{array}\right\}, \tag{28}$$

where, $\xi = x - \left(\frac{1}{2}\sqrt{r^2 - 4q}\right)\frac{t^\alpha}{\alpha}$ and $= r^2 - 4q > 0$.

For r = 0:

$$\left.\begin{array}{c} u_7(x,t) = \frac{1}{2}\sqrt{-4pq} + \frac{\sqrt{pq}}{\tan\left(\sqrt{pq}(\xi+E)\right)} \\ v_7(x,t) = -pq - \left(\frac{\sqrt{pq}}{\tan\left(\sqrt{pq}(\xi+E)\right)}\right)^2 \end{array}\right\}, \tag{29}$$

$$\left.\begin{array}{c} u_8(x,t) = \frac{1}{2}\sqrt{-4pq} + \frac{\sqrt{pq}}{\cot\left(\sqrt{pq}(\xi+E)\right)} \\ v_8(x,t) = -pq - \left(\frac{\sqrt{pq}}{\cot\left(\sqrt{pq}(\xi+E)\right)}\right)^2 \end{array}\right\}, \tag{30}$$

$$\left.\begin{array}{c} u_9(x,t) = \frac{1}{2}\sqrt{-4pq} - \frac{\sqrt{-pq}}{\tanh\left(\sqrt{-pq}(\xi+E)\right)} \\ v_9(x,t) = -pq + \left(\frac{\sqrt{pq}}{\tanh\left(\sqrt{pq}(\xi+E)\right)}\right)^2 \end{array}\right\}, \tag{31}$$

and

$$\left.\begin{array}{c} u_{10}(x,t) = \frac{1}{2}\sqrt{-4pq} + \frac{\sqrt{-pq}}{\coth\left(\sqrt{-pq}(\xi+E)\right)} \\ v_{10}(x,t) = -pq + \left(\frac{\sqrt{pq}}{\coth\left(\sqrt{-pq}(\xi+E)\right)}\right)^2 \end{array}\right\}, \tag{32}$$

where, $\xi = x - \left(\frac{1}{2}\sqrt{-4pq}\right)\frac{t^\alpha}{\alpha}$, $pq < 0$.

For q = 0 and r = 0:

$$\left.\begin{array}{c} u_{11}(x,t) = -\frac{1}{x+E} \\ v_{11}(x,t) = -\left(\frac{1}{x+E}\right)^2 \end{array}\right\}, \tag{33}$$

Set-2: $a_0 = -\frac{1}{2}r - \frac{1}{2}\sqrt{-4pq + r^2}$, $a_1 = -p$, $b_0 = -pq$, $b_1 = -pr$, $b_2 = -p^2$

and $c = -\frac{1}{2}\sqrt{-4pq + r^2}$, $-4pq + r^2 > 0$.

Consequently, by substituting the values of Set-2 into Eq. (22) along with the Eq. (10) to Eq. (18), we produce the following traveling wave solutions for the time-fractional ALW equations.

For p = 1:

$$\left.\begin{array}{c} u_{12}(x,t) = -\frac{1}{2}r - \frac{1}{2}\sqrt{r^2 - 4q} \\ \quad + \frac{2q}{\sqrt{\Delta}\ \tanh\left(\frac{1}{2}\sqrt{\Delta}\ (\xi+E)\right) + r} \\ v_{12}(x,t) = -q + \frac{2rq}{\sqrt{\Delta}\ \tanh\left(\frac{1}{2}\sqrt{\Delta}\ (\xi+E)\right) + r} \\ \quad - \frac{4q^2}{\left(\sqrt{\Delta}\ \tanh\left(\frac{1}{2}\sqrt{\Delta}\ (\xi+E)\right) + r\right)^2} \end{array}\right\}, \tag{34}$$

$$\left.\begin{array}{c} u_{13}(x,t) = -\frac{1}{2}r - \frac{1}{2}\sqrt{r^2 - 4q} \\ \quad + \frac{2q}{\sqrt{\Delta}\ \coth\left(\frac{1}{2}\sqrt{\Delta}\ (\xi+E)\right) + r} \\ v_{13}(x,t) = -q + \frac{2rq}{\sqrt{\Delta}\ \coth\left(\frac{1}{2}\sqrt{\Delta}\ (\xi+E)\right) + r} \\ \quad - \frac{4q^2}{\left(\sqrt{\Delta}\ \coth\left(\frac{1}{2}\sqrt{\Delta}\ (\xi+E)\right) + r\right)^2} \end{array}\right\}, \tag{35}$$

$$\left.\begin{array}{c} u_{14}(x,t) = -\frac{1}{2}r - \frac{1}{2}\sqrt{r^2-4q} \\ -\frac{2q}{\sqrt{-\Delta}\,\tan\left(\frac{1}{2}\sqrt{-\Delta}\,(\xi+E)\right)-r} \\ v_{14}(x,t) = -q - \frac{2rq}{\sqrt{-\Delta}\,\tan\left(\frac{1}{2}\sqrt{-}\,(\xi+E)\right)-r} \\ -\frac{4q^2}{\left(\sqrt{-\Delta}\,\tan\left(\frac{1}{2}\sqrt{-\Delta}\,(\xi+E)\right)-r\right)^2} \end{array}\right\}, \quad (36)$$

$$\left.\begin{array}{c} u_{15}(x,t) = -\frac{1}{2}r - \frac{1}{2}\sqrt{r^2-4q} \\ -\frac{2q}{\sqrt{-\Delta}\,\cot\left(\frac{1}{2}\sqrt{-\Delta}\,(\xi+E)\right)-r} \\ v_{15}(x,t) = -q - \frac{2rq}{\sqrt{-\Delta}\,\cot\left(\frac{1}{2}\sqrt{-\Delta}\,(\xi+E)\right)-r} \\ -\frac{4q^2}{\left(\sqrt{-\Delta}\,\cot\left(\frac{1}{2}\sqrt{-\Delta}\,(\xi+E)\right)-r\right)^2} \end{array}\right\}, \quad (37)$$

$$\left.\begin{array}{c} u_{16}(x,t) = -\frac{1}{2}r - \frac{1}{2}\sqrt{r^2-4q} - \frac{r}{e^{r(\xi+E)}-1} \\ v_{16}(x,t) = -q - \frac{r^2}{e^{r(\xi+E)}-1} - \frac{r^2}{\left(e^{r(\xi+E)}-1\right)^2} \end{array}\right\}, \quad (38)$$

and

$$\left.\begin{array}{c} u_{17}(x,t) = -\frac{1}{2}r - \frac{1}{2}\sqrt{r^2-4q} + \frac{1}{2}\frac{r^2(\xi+E)}{r(\xi+E)+2} \\ v_{17}(x,t) = -q + \frac{1}{2}\frac{r^3(\xi+E)}{r(\xi+E)+2} - \frac{1}{4}\left(\frac{r^2(\xi+E)}{r(\xi+E)+2}\right)^2 \end{array}\right\}, \quad (39)$$

where, $\xi = x + \left(\frac{1}{2}\sqrt{r^2-4q}\right)\frac{t^\alpha}{\alpha}$ and $= r^2 - 4q > 0$.

For r = 0:

$$\left.\begin{array}{c} u_{18}(x,t) = -\frac{1}{2}\sqrt{-4pq} - \frac{\sqrt{pq}}{\tan\left(\sqrt{pq}(\xi+E)\right)} \\ v_{18}(x,t) = -pq - \left(\frac{\sqrt{pq}}{\tan\left(\sqrt{pq}(\xi+E)\right)}\right)^2 \end{array}\right\}, \quad (40)$$

$$\left.\begin{array}{c} u_{19}(x,t) = -\frac{1}{2}\sqrt{-4pq} + \frac{\sqrt{pq}}{\cot\left(\sqrt{pq}(\xi+E)\right)} \\ v_{19}(x,t) = -pq - \left(\frac{\sqrt{pq}}{\cot\left(\sqrt{pq}(\xi+E)\right)}\right)^2 \end{array}\right\}, \quad (41)$$

$$\left.\begin{array}{c} u_{20}(x,t) = -\frac{1}{2}\sqrt{-4pq} - \frac{\sqrt{pq}}{\tanh\left(\sqrt{-pq}(\xi+E)\right)} \\ v_{20}(x,t) = -pq + \left(\frac{\sqrt{pq}}{\tanh\left(\sqrt{-pq}(\xi+E)\right)}\right)^2 \end{array}\right\}, \quad (42)$$

and

$$\left.\begin{array}{c} u_{21}(x,t) = -\frac{1}{2}\sqrt{-4pq} + \frac{\sqrt{-pq}}{\coth\left(\sqrt{-pq}(\xi+E)\right)} \\ v_{21}(x,t) = -pq + \left(\frac{\sqrt{pq}}{\coth\left(\sqrt{-pq}(\xi+E)\right)}\right)^2 \end{array}\right\}, \quad (43)$$

where, $\xi = x + \left(\frac{1}{2}\sqrt{-4pq}\right)\frac{t^\alpha}{\alpha}$, $pq < 0$.

For q = 0 and r = 0:

$$\left.\begin{array}{c} u_{22}(x,t) = -\frac{1}{x+E} \\ v_{22}(x,t) = -\left(\frac{1}{x+E}\right)^2 \end{array}\right\}, \quad (44)$$

Figures 1, **2** represent the solutions given by Eq. (23) for different values of α when $r = 3$, $q = 2$, and $E = 0$.

The Time-Fractional Variant-Boussinesq Equations

Let us consider the time-fractional variant-Boussinesq equations

$$\left.\begin{array}{c} D_t^\alpha u + uu_x + v_x = 0 \\ D_t^\alpha v + (uv)_x + u_{xxx} = 0 \end{array}\right\}, \; t \geq 0, \; 0 < \alpha \leq 1. \quad (45)$$

Now, applying under the traveling wave transformation of Eq. (6), Eq. (45) reduces to a non-linear ODE as

$$\left.\begin{array}{c} -cU' + UU' + V' = 0 \\ -cV' + (UV)' + U''' = 0 \end{array}\right\}. \quad (46)$$

This integrates with respect to ξ of Eq. (46) and considers the integration constant to be zero. Eq. (46) then yields

$$\left.\begin{array}{c} -cU + \frac{1}{2}U^2 + V = 0 \\ -cV + UV + U'' = 0 \end{array}\right\}. \quad (47)$$

From the balancing condition in Eq. (47), we have $m = 1$ and $n = 2$. Now, the formal solution of (47) in the existence of (8) will be

$$\left.\begin{array}{c} U(\xi) = a_0 + a_1 \exp\left(-\varphi(\xi)\right) \\ V(\xi) = b_0 + b_1 \exp\left(-\varphi(\xi)\right) + b_2 \exp\left(-2\varphi(\xi)\right) \end{array}\right\} \quad (48)$$

where $a_1 \neq 0$ and $b_2 \neq 0$.

By inserting Eq. (48) into Eq. (47) along with Eq. (9) and using the same techniques investigated in the previous section we get

Set-1: $a_0 = -r \pm \sqrt{-4pq + r^2}$, $a_1 = -2p$, $b_0 = -2pq$, $b_1 = -2pr$, $b_2 = -2p^2$

and $c = \pm\sqrt{-4pq + r^2}$, $-4pq + r^2 > 0$.

Therefore, by substituting the values of Set-1 into Eq. (48), along with the Eq. (10) to Eq. (18), we generate the following traveling wave solutions for the time-fractional variant-Boussinesq equations.

For p = 1:

$$\left.\begin{array}{c} u_1(x,t) = -r \pm \sqrt{r^2-4q} \\ +\frac{4q}{\sqrt{\Delta}\,\tan h\left(\frac{1}{2}\sqrt{\Delta}\,(\xi+E)\right)+r} \\ v_1(x,t) = -2q + \frac{4rq}{\sqrt{\Delta}\,\tan h\left(\frac{1}{2}\sqrt{\Delta}\,(\xi+E)\right)+r} \\ -\frac{8q^2}{\left(\sqrt{\Delta}\,\tan h\left(\frac{1}{2}\sqrt{\Delta}\,(\xi+E)\right)+r\right)^2} \end{array}\right\}, \quad (49)$$

$$\left.\begin{array}{c} u_2(x,t) = -r \pm \sqrt{r^2-4q} \\ +\frac{4q}{\sqrt{\Delta}\,\cot h\left(\frac{1}{2}\sqrt{\Delta}\,(\xi+E)\right)+r} \\ v_2(x,t) = -2q + \frac{4rq}{\sqrt{\Delta}\,\cot h\left(\frac{1}{2}\sqrt{}\,(\xi+E)\right)+r} \\ -\frac{8q^2}{\left(\sqrt{\Delta}\,\cot h\left(\frac{1}{2}\sqrt{\Delta}\,(\xi+E)\right)+r\right)^2} \end{array}\right\}, \quad (50)$$

$$\left.\begin{array}{c} u_3(x,t) = -r \pm \sqrt{r^2-4q} \\ -\frac{4q}{\sqrt{-\Delta}\,\tan\left(\frac{1}{2}\sqrt{-}\,(\xi+E)\right)-r} \\ v_3(x,t) = -2q - \frac{4rq}{\sqrt{-\Delta}\,\tan\left(\frac{1}{2}\sqrt{-\Delta}\,(\xi+E)\right)-r} \\ -\frac{8q^2}{\left(\sqrt{-\Delta}\,\tan\left(\frac{1}{2}\sqrt{-\Delta}\,(\xi+E)\right)-r\right)^2} \end{array}\right\}, \quad (51)$$

$$\left.\begin{array}{c} u_4(x,t) = -r \pm \sqrt{r^2-4q} \\ -\frac{4q}{\sqrt{-\Delta}\,\cot\left(\frac{1}{2}\sqrt{-\Delta}\,(\xi+E)\right)-r} \\ v_4(x,t) = -2q - \frac{4rq}{\sqrt{-\Delta}\,\cot\left(\frac{1}{2}\sqrt{-\Delta}\,(\xi+E)\right)-r} \\ -\frac{8q^2}{\left(\sqrt{-\Delta}\,\cot\left(\frac{1}{2}\sqrt{-}\,(\xi+E)\right)-r\right)^2} \end{array}\right\}, \quad (52)$$

$$\left.\begin{array}{c} u_5(x,t) = -r \pm \sqrt{r^2-4q} - \frac{2r}{e^{r(\xi+E)}-1} \\ v_5(x,t) = -2q - \frac{2r^2}{e^{r(\xi+E)}-1} - \frac{2r^2}{\left(e^{r(\xi+E)}-1\right)^2} \end{array}\right\}, \quad (53)$$

and

$$\left.\begin{array}{c} u_6(x,t) = -r \pm \sqrt{r^2-4q} + \frac{r^2(\xi+E)}{r(\xi+E)+2} \\ v_6(x,t) = -2q + \frac{r^3(\xi+E)}{r(\xi+E)+2} - \frac{1}{2}\left(\frac{r^2(\xi+E)}{r(\xi+E)+2}\right)^2 \end{array}\right\} \quad (54)$$

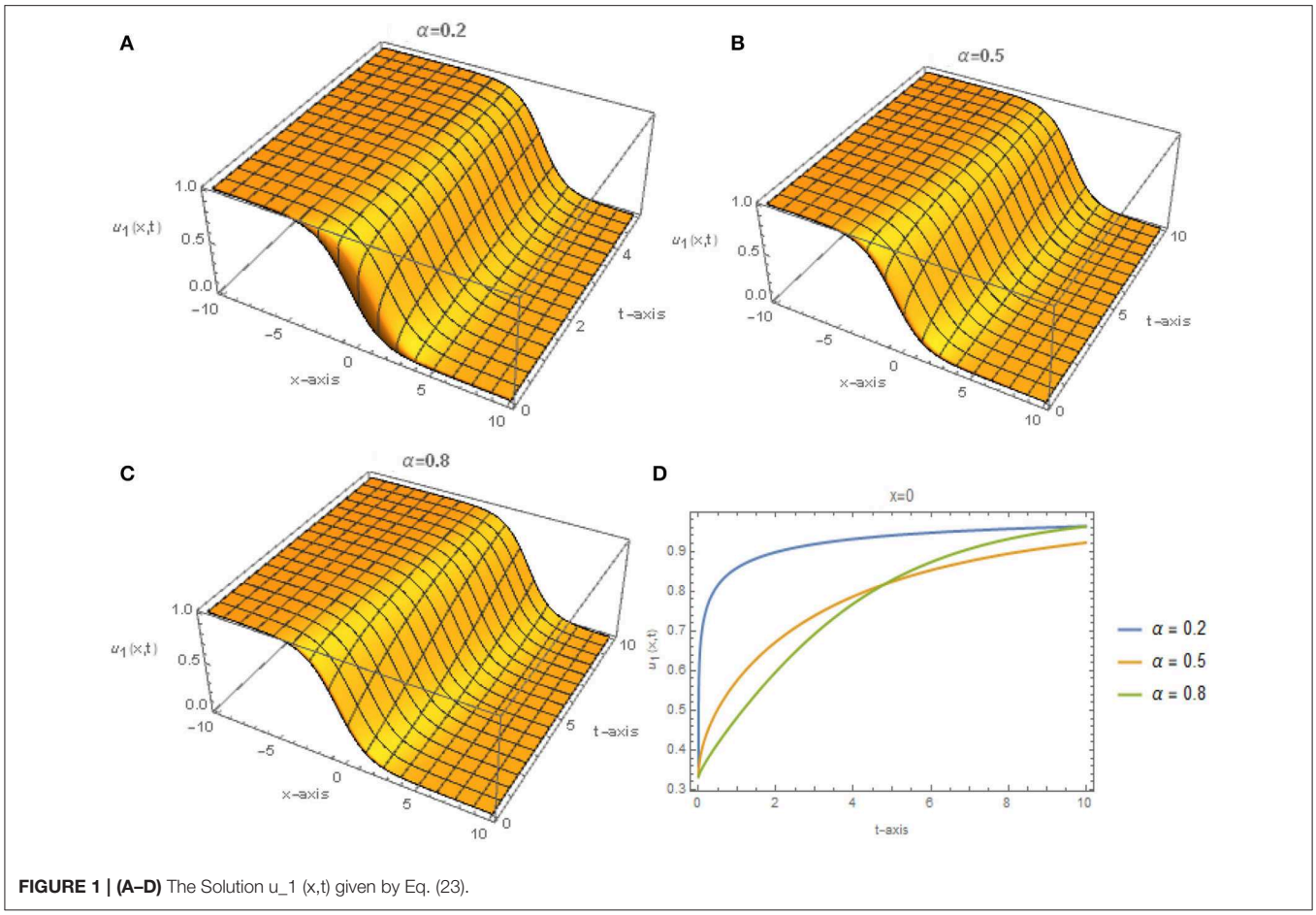

FIGURE 1 | (A–D) The Solution u_1 (x,t) given by Eq. (23).

where $\xi = x \mp \left(\sqrt{r^2 - 4q}\right) \frac{t^\alpha}{\alpha}$ and $= r^2 - 4q > 0$.

For r = 0:

$$\left.\begin{aligned} u_7(x,t) &= \pm\sqrt{-4pq} - \frac{2\sqrt{pq}}{\tan\left(\sqrt{pq}(\xi+E)\right)} \\ v_7(x,t) &= -2pq - \left(\frac{\sqrt{2pq}}{\tan\left(\sqrt{pq}(\xi+E)\right)}\right)^2 \end{aligned}\right\}, \tag{55}$$

$$\left.\begin{aligned} u_8(x,t) &= \pm\sqrt{-4pq} + \frac{2\sqrt{pq}}{\cot\left(\sqrt{pq}(\xi+E)\right)} \\ v_8(x,t) &= -2pq - \left(\frac{\sqrt{2pq}}{\cot\left(\sqrt{pq}(\xi+E)\right)}\right)^2 \end{aligned}\right\}, \tag{56}$$

$$\left.\begin{aligned} u_9(x,t) &= \pm\sqrt{-4pq} - \frac{2\sqrt{-pq}}{\tanh\left(\sqrt{-pq}(\xi+E)\right)} \\ v_9(x,t) &= -2pq + \left(\frac{\sqrt{2pq}}{\tanh\left(\sqrt{-pq}(\xi+E)\right)}\right)^2 \end{aligned}\right\}, \tag{57}$$

$$\left.\begin{aligned} u_{10}(x,t) &= \pm\sqrt{-4pq} + \frac{2\sqrt{-pq}}{\coth\left(\sqrt{-pq}(\xi+E)\right)} \\ v_{10}(x,t) &= -2pq + \left(\frac{\sqrt{2pq}}{\coth\left(\sqrt{-pq}(\xi+E)\right)}\right)^2 \end{aligned}\right\}, \tag{58}$$

where, $\xi = x \mp \left(\sqrt{-4pq}\right) \frac{t^\alpha}{\alpha}$, $pq < 0$.

For q = 0 and r = 0:

$$\left.\begin{aligned} u_{11}(x,t) &= -\frac{2}{x+E} \\ v_{11}(x,t) &= -2\left(\frac{1}{x+E}\right)^2 \end{aligned}\right\}, \tag{59}$$

Set-2: $a_0 = r \pm \sqrt{-4pq + r^2}$, $a_1 = 2p$, $b_0 = -2pq$, $b_1 = -2pr$, $b_2 = -2p^2$ and $c = \pm\sqrt{-4pq + r^2}$, $-4pq + r^2 > 0$.

Consequently, by substituting the values of Set-2 into Eq. (48) along with the Eq. (10) to Eq. (18), we generate the following traveling wave solutions for the time-fractional variant-Boussinesq equations:

For p = 1:

$$\left.\begin{aligned} u_{12}(x,t) &= r \pm \sqrt{r^2 - 4q} \\ &\quad - \frac{4q}{\sqrt{\Delta}\,\tanh\left(\frac{1}{2}\sqrt{\Delta}\,(\xi+E)\right)+r} \\ v_{12}(x,t) &= -2q + \frac{4rq}{\sqrt{\Delta}\,\tanh\left(\frac{1}{2}\sqrt{\Delta}\,(\xi+E)\right)+r} \\ &\quad - \frac{8q^2}{\left(\sqrt{\Delta}\,\tanh\left(\frac{1}{2}\sqrt{\Delta}\,(\xi+E)\right)+r\right)^2} \end{aligned}\right\}, \tag{60}$$

$$\left.\begin{aligned} u_{13}(x,t) &= r \pm \sqrt{r^2 - 4q} \\ &\quad - \frac{4q}{\sqrt{\Delta}\,\coth\left(\frac{1}{2}\sqrt{\Delta}\,(\xi+E)\right)+r} \\ v_{13}(x,t) &= -2q + \frac{4rq}{\sqrt{\Delta}\,\coth\left(\frac{1}{2}\sqrt{}\,(\xi+E)\right)+r} \\ &\quad - \frac{8q^2}{\left(\sqrt{\Delta}\,\coth\left(\frac{1}{2}\sqrt{\Delta}\,(\xi+E)\right)+r\right)^2} \end{aligned}\right\}, \tag{61}$$

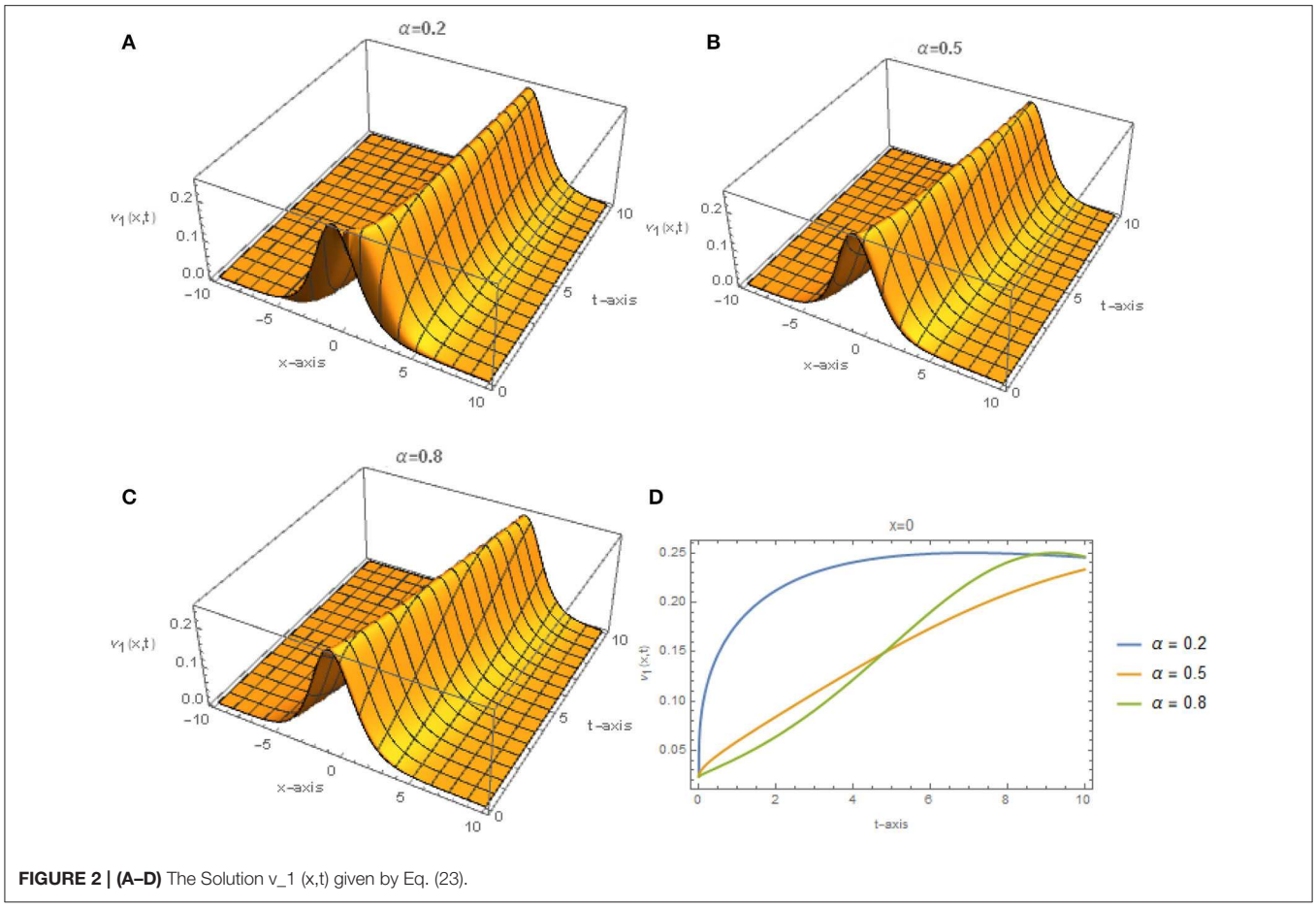

FIGURE 2 | (A–D) The Solution v_1 (x,t) given by Eq. (23).

$$\left.\begin{aligned} u_{14}(x,t) &= r \pm \sqrt{r^2-4q} \\ &+ \frac{4q}{\sqrt{-\Delta}\,\tan\left(\frac{1}{2}\sqrt{-\Delta}\,(\xi+E)\right)-r} \\ v_{14}(x,t) &= -2q - \frac{4rq}{\sqrt{-\Delta}\,\tan\left(\frac{1}{2}\sqrt{-\Delta}\,(\xi+E)\right)-r} \\ &- \frac{8q^2}{\left(\sqrt{-\Delta}\,\tan\left(\frac{1}{2}\sqrt{-\Delta}\,(\xi+E)\right)-r\right)^2} \end{aligned}\right\}, \tag{62}$$

$$\left.\begin{aligned} u_{15}(x,t) &= r \pm \sqrt{r^2-4q} \\ &+ \frac{4q}{\sqrt{-\Delta}\,\cot\left(\frac{1}{2}\sqrt{-\Delta}\,(\xi+E)\right)-r} \\ v_{15}(x,t) &= -2q - \frac{4rq}{\sqrt{-\Delta}\,\cot\left(\frac{1}{2}\sqrt{-\Delta}\,(\xi+E)\right)-r} \\ &- \frac{8q^2}{\left(\sqrt{-\Delta}\,\cot\left(\frac{1}{2}\sqrt{-\Delta}\,(\xi+E)\right)-r\right)^2} \end{aligned}\right\}, \tag{63}$$

$$\left.\begin{aligned} u_{16}(x,t) &= r \pm \sqrt{r^2-4q} + \frac{2r}{e^{r(\xi+E)}-1} \\ v_{16}(x,t) &= -2q - \frac{2r^2}{e^{r(\xi+E)}-1} - \frac{2r^2}{\left(e^{r(\xi+E)}-1\right)^2} \end{aligned}\right\}, \tag{64}$$

and

$$\left.\begin{aligned} u_{17}(x,t) &= r \pm \sqrt{r^2-4q} - \frac{r^2(\xi+E)}{r(\xi+E)+2} \\ v_{17}(x,t) &= -2q + \frac{r^3(\xi+E)}{r(\xi+E)+2} - \frac{1}{2}\left(\frac{r^2(\xi+E)}{r(\xi+E)+2}\right)^2 \end{aligned}\right\},$$

where, $\xi = x \mp \left(\sqrt{r^2-4q}\right)\frac{t^\alpha}{\alpha}$ and $= r^2 - 4q > 0$.

For r = 0:

$$\left.\begin{aligned} u_{18}(x,t) &= \pm\sqrt{-4pq} + \frac{2\sqrt{pq}}{\tan((\xi+E))} \\ v_{18}(x,t) &= -2pq - \left(\frac{\sqrt{2pq}}{\tan((\xi+E))}\right)^2 \end{aligned}\right\}, \tag{65}$$

$$\left.\begin{aligned} u_{19}(x,t) &= \pm\sqrt{-4pq} - \frac{2\sqrt{pq}}{\cot((\xi+E))} \\ v_{19}(x,t) &= -2pq - \left(\frac{\sqrt{2pq}}{\cot((\xi+E))}\right)^2 \end{aligned}\right\}, \tag{66}$$

$$\left.\begin{aligned} u_{20}(x,t) &= \pm\sqrt{-4pq} + \frac{2\sqrt{-pq}}{\tanh((\xi+E))} \\ v_{20}(x,t) &= -2pq + \left(\frac{\sqrt{2pq}}{\tanh((\xi+E))}\right)^2 \end{aligned}\right\}, \tag{67}$$

and

$$\left.\begin{aligned} u_{21}(x,t) &= \pm\sqrt{-4pq} - \frac{2\sqrt{-pq}}{\coth((\xi+E))} \\ v_{21}(x,t) &= -2pq + \left(\frac{\sqrt{2pq}}{\coth((\xi+E))}\right)^2 \end{aligned}\right\}, \tag{68}$$

where, $\xi = x \mp \left(\sqrt{-4pq}\right)\frac{t^\alpha}{\alpha}$, $pq < 0$.

For q = 0 and r = 0:

$$\left.\begin{aligned} u_{22}(x,t) &= \frac{2}{x+E} \\ v_{22}(x,t) &= -2\left(\frac{1}{x+E}\right)^2 \end{aligned}\right\}. \tag{69}$$

Figures 3, 4 represent the solutions given by Eq. (50) for different values of α when $r = 3$, $q = 2$ and $E = 0$.

The Time-Fractional Wu-Zhang System of Equations

Let us consider the time-fractional Wu-Zhang system of equations

$$\left.\begin{aligned} D_t^\alpha u + uu_x + v_x &= 0 \\ D_t^\alpha v + (uv)_x + \tfrac{1}{3}u_{xxx} &= 0 \end{aligned}\right\},\ t \geq 0,\ 0 < \alpha \leq 1. \tag{70}$$

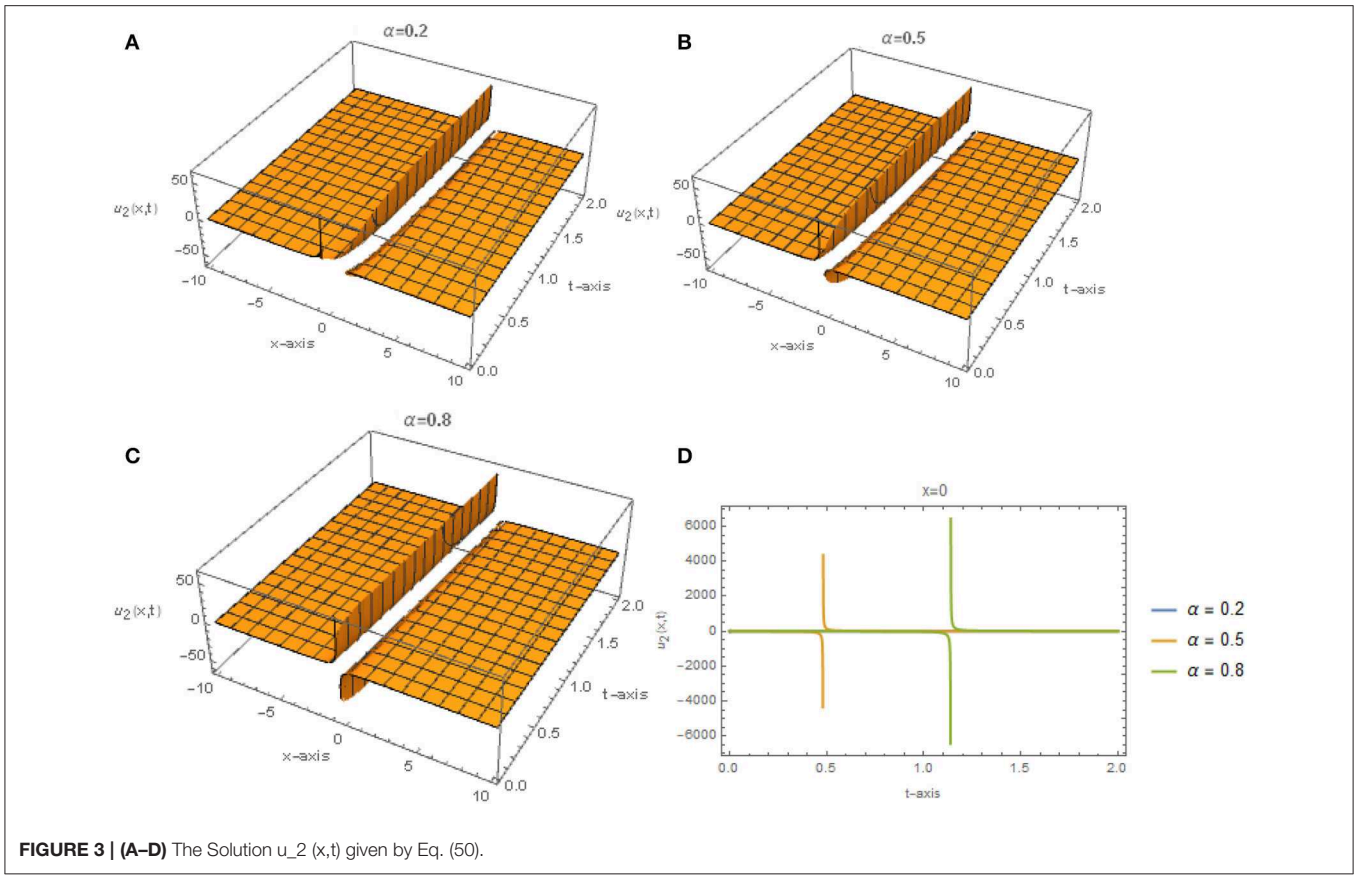

FIGURE 3 | (A–D) The Solution u_2 (x,t) given by Eq. (50).

Now, applying under the traveling wave transformation of Eq. (6), Eq. (71) reduces to a non-linear ODE as

$$\left.\begin{array}{c} -cU' + UU' + V' = 0 \\ -cV' + (UV)' + \frac{1}{3}U''' = 0 \end{array}\right\}. \tag{71}$$

Integrating with respect to ξ of Eq. (71) and considering the integration constant is zero. Then Eq. (72) yields

$$\left.\begin{array}{c} -cU + \frac{1}{2}U^2 + V = 0 \\ -cV + UV + \frac{1}{3}U'' = 0 \end{array}\right\}, \tag{72}$$

Following the steps given in the last two sections we reach to $m = 1$ and $n = 2$. Consequently, the general solution will take the form

$$\left.\begin{array}{c} U(\xi) = a_0 + a_1 \exp(-\varphi(\xi)) \\ V(\xi) = b_0 + b_1 \exp(-\varphi(\xi)) + b_2 \exp(-2\varphi(\xi)) \end{array}\right\}, \tag{73}$$

where $a_1 \neq 0$ and $b_2 \neq 0$.

Put Eq. (74) into Eq. (73) along with Eq. (9), and we get a new system of algebraic equations that solve to

Set-1: $a_0 = \frac{1}{3}\sqrt{3}\, r \pm \frac{1}{3}\sqrt{3\left(r^2 - 4pq\right)}$, $a_1 = \frac{2}{3}\sqrt{3}p$, $b_0 = -\frac{2}{3}pq$, $b_1 = -\frac{2}{3}pr$, $b_2 = -\frac{2}{3}p^2$

and $c = \pm\frac{1}{3}\sqrt{3\left(r^2 - 4pq\right)}$, $-4pq + r^2 > 0$.

Therefore, by substituting the values of Set-1 into Eq. (74) along with the Eq. (10) to Eq. (18), we generate the following traveling wave solutions for the time-fractional Wu-Zhang system of equations.

For p = 1:

$$\left.\begin{array}{c} u_1(x,t) = \frac{1}{3}\sqrt{3}\, r \pm \frac{1}{3}\sqrt{3\left(r^2 - 4q\right)} \\ -\frac{4}{3}\frac{\sqrt{3}\, q}{\sqrt{\Delta}\, \tanh\left(\frac{1}{2}\sqrt{\Delta}\,(\xi+E)\right)+r} \\ v_1(x,t) = -\frac{2}{3}q + \frac{4}{3}\frac{rq}{\sqrt{\Delta}\, \tanh\left(\frac{1}{2}\sqrt{\Delta}\,(\xi+E)\right)+r} \\ -\frac{8}{3}\frac{q^2}{\left(\sqrt{\Delta}\, \tanh\left(\frac{1}{2}\sqrt{\Delta}\,(\xi+E)\right)+r\right)^2} \end{array}\right\}, \tag{74}$$

$$\left.\begin{array}{c} u_2(x,t) = \frac{1}{3}\sqrt{3}\, r \pm \frac{1}{3}\sqrt{3\left(r^2 - 4q\right)} \\ -\frac{4}{3}\frac{\sqrt{3}\, q}{\sqrt{\Delta}\, \coth\left(\frac{1}{2}\sqrt{\Delta}\,(\xi+E)\right)+r} \\ v_2(x,t) = -\frac{2}{3}q + \frac{4}{3}\frac{rq}{\sqrt{\Delta}\, \coth\left(\frac{1}{2}\sqrt{\Delta}\,(\xi+E)\right)+r} \\ -\frac{8}{3}\frac{q^2}{\left(\sqrt{\ } \coth\left(\frac{1}{2}\sqrt{\Delta}\,(\xi+E)\right)+r\right)^2} \end{array}\right\}, \tag{75}$$

$$\left.\begin{array}{c} u_3(x,t) = \frac{1}{3}\sqrt{3}\, r \pm \frac{1}{3}\sqrt{3\left(r^2 - 4q\right)} \\ +\frac{4}{3}\frac{\sqrt{3}\, q}{\sqrt{-\Delta}\, \tan\left(\frac{1}{2}\sqrt{-\Delta}\,(\xi+E)\right)-r} \\ v_3(x,t) = -\frac{2}{3}q - \frac{4}{3}\frac{rq}{\sqrt{-\Delta}\, \tan\left(\frac{1}{2}\sqrt{-\Delta}\,(\xi+E)\right)+r} \\ -\frac{8}{3}\frac{q^2}{\left(\sqrt{-\Delta}\, \tan\left(\frac{1}{2}\sqrt{-\Delta}\,(\xi+E)\right)-r\right)^2} \end{array}\right\}, \tag{76}$$

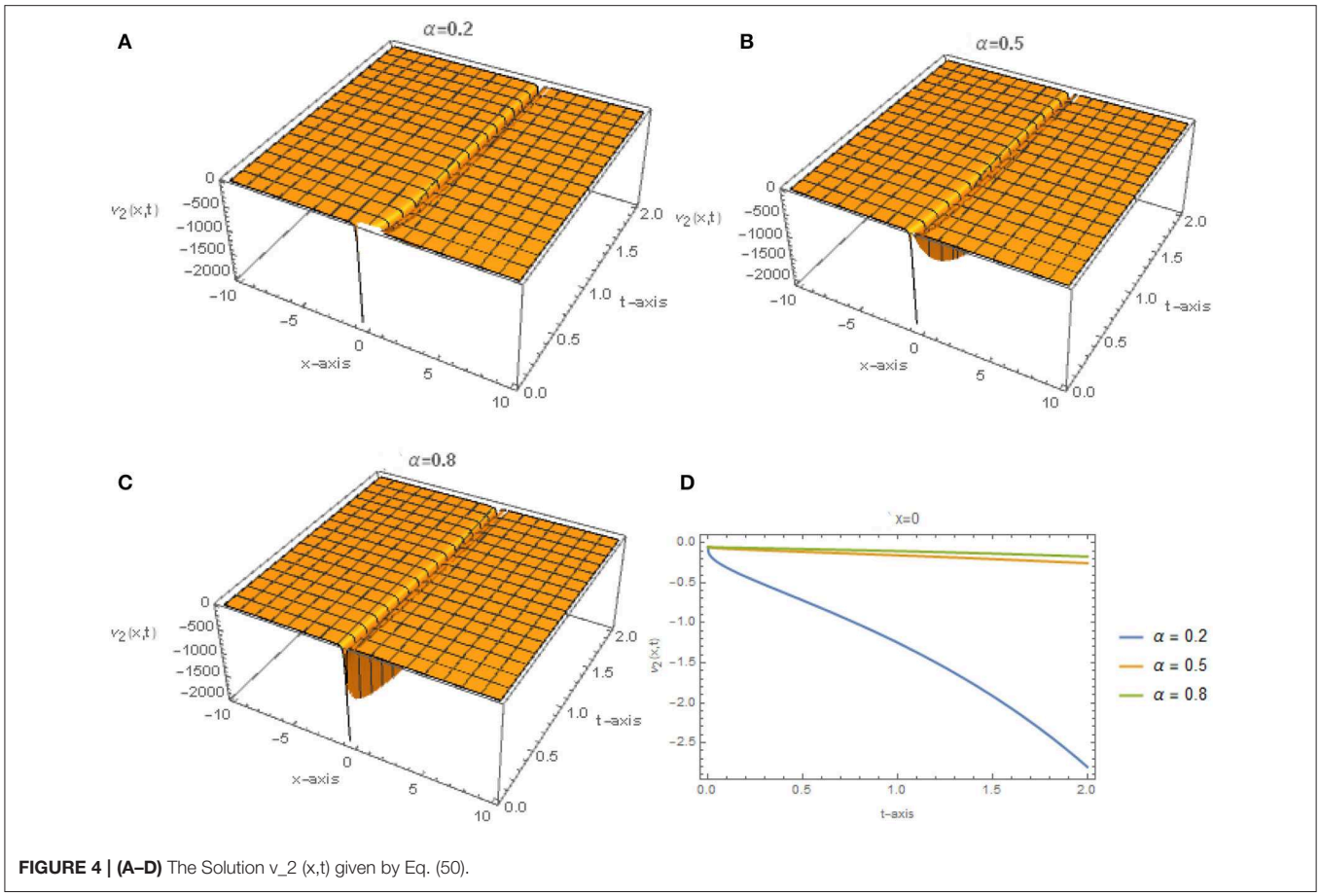

FIGURE 4 | (A–D) The Solution v_2 (x,t) given by Eq. (50).

$$\left.\begin{aligned} u_4(x,t) &= \tfrac{1}{3}\sqrt{3}\,r \pm \tfrac{1}{3}\sqrt{3\left(r^2-4q\right)} \\ &\quad + \tfrac{4}{3}\frac{\sqrt{3}\,q}{\sqrt{-\Delta}\,\cot\left(\frac{1}{2}\sqrt{-\Delta}\,(\xi+E)\right)-r} \\ v_4(x,t) &= -\tfrac{2}{3}q - \tfrac{4}{3}\frac{rq}{\sqrt{-\Delta}\,\cot\left(\frac{1}{2}\sqrt{-\Delta}\,(\xi+E)\right)+r} \\ &\quad - \tfrac{8}{3}\frac{q^2}{\left(\sqrt{-\Delta}\,\cot\left(\frac{1}{2}\sqrt{-\Delta}\,(\xi+E)\right)-r\right)^2} \end{aligned}\right\}, \quad (77)$$

$$\left.\begin{aligned} u_5(x,t) &= \tfrac{1}{3}\sqrt{3}\,r \pm \tfrac{1}{3}\sqrt{3\left(r^2-4q\right)} + \tfrac{2}{3}\frac{\sqrt{3}\,r}{e^{r(\xi+E)}-1} \\ v_5(x,t) &= -\tfrac{2}{3}q - \tfrac{2}{3}\frac{r^2}{e^{r(\xi+E)}-1} - \tfrac{2}{3}\frac{r^2}{\left(e^{r(\xi+E)}-1\right)^2} \end{aligned}\right\}, \quad (78)$$

and

$$\left.\begin{aligned} u_6(x,t) &= \tfrac{1}{3}\sqrt{3}\,r \pm \tfrac{1}{3}\sqrt{3\left(r^2-4q\right)} - \tfrac{1}{3}\frac{\sqrt{3}\,r^2(\xi+E)}{r(\xi+E)+2} \\ v_6(x,t) &= -\tfrac{2}{3}q + \tfrac{1}{3}\frac{r^3(\xi+E)}{r(\xi+E)+2} - \tfrac{1}{6}\left(\frac{r^2(\xi+E)}{r(\xi+E)+2}\right)^2 \end{aligned}\right\}, \quad (79)$$

where, $\xi = x \mp \left(\frac{1}{3}\sqrt{3\left(r^2-4q\right)}\right)\frac{t^\alpha}{\alpha}$ and $\Delta = r^2 - 4q > 0$.

For r = 0:

$$\left.\begin{aligned} u_7(x,t) &= \pm\tfrac{2}{3}\sqrt{-3pq} + \tfrac{2}{3}\frac{\sqrt{3pq}}{\tan\left(\sqrt{pq}(\xi+E)\right)} \\ v_7(x,t) &= -\tfrac{2}{3}pq - \tfrac{2}{3}\left(\frac{\sqrt{pq}}{\tan\left(\sqrt{pq}(\xi+E)\right)}\right)^2 \end{aligned}\right\}, \quad (80)$$

$$\left.\begin{aligned} u_8(x,t) &= \pm\tfrac{2}{3}\sqrt{-3pq} - \tfrac{2}{3}\frac{\sqrt{3pq}}{\cot\left(\sqrt{pq}(\xi+E)\right)} \\ v_8(x,t) &= -\tfrac{2}{3}pq - \tfrac{2}{3}\left(\frac{\sqrt{pq}}{\cot\left(\sqrt{pq}(\xi+E)\right)}\right)^2 \end{aligned}\right\}, \quad (81)$$

$$\left.\begin{aligned} u_9(x,t) &= \pm\tfrac{2}{3}\sqrt{-3pq} + \tfrac{2}{3}\frac{\sqrt{-3pq}}{\tanh\left(\sqrt{-pq}(\xi+E)\right)} \\ v_9(x,t) &= -\tfrac{2}{3}pq + \tfrac{2}{3}\left(\frac{\sqrt{pq}}{\tanh\left(\sqrt{-pq}(\xi+E)\right)}\right)^2 \end{aligned}\right\}, \quad (82)$$

and

$$\left.\begin{aligned} u_{10}(x,t) &= \pm\tfrac{2}{3}\sqrt{-3pq} - \tfrac{2}{3}\frac{\sqrt{-3pq}}{\coth\left(\sqrt{-pq}(\xi+E)\right)} \\ v_{10}(x,t) &= -\tfrac{2}{3}pq + \tfrac{2}{3}\left(\frac{\sqrt{pq}}{\coth\left(\sqrt{-pq}(\xi+E)\right)}\right)^2 \end{aligned}\right\}, \quad (83)$$

where, $\xi = x \mp \left(\frac{2}{3}\sqrt{-3pq}\right)\frac{t^\alpha}{\alpha}$, $pq < 0$.

For q = 0 and r = 0:

$$\left.\begin{aligned} u_{11}(x,t) &= \tfrac{2}{3}\frac{\sqrt{3}}{x+E} \\ v_{11}(x,t) &= -\tfrac{2}{3}\left(\frac{1}{x+E}\right)^2 \end{aligned}\right\}. \quad (84)$$

Set-2: $a_0 = -\frac{1}{3}\sqrt{3}\,r \pm \frac{1}{3}\sqrt{3\left(r^2-4pq\right)}$, $a_1 = -\frac{2}{3}\sqrt{3}p$, $b_0 = -\frac{2}{3}pq$, $b_1 = -\frac{2}{3}pr$, $b_2 = -\frac{2}{3}p^2$

and $c = \pm\frac{1}{3}\sqrt{3\left(r^2-4pq\right)}$, $-4pq + r^2 > 0$.

Consequently, by substituting the values of Set-2 into Eq. (74) along with the Eq. (10) to Eq. (18), we generate the following traveling wave solutions for the time-fractional Wu-Zhang system of equations.

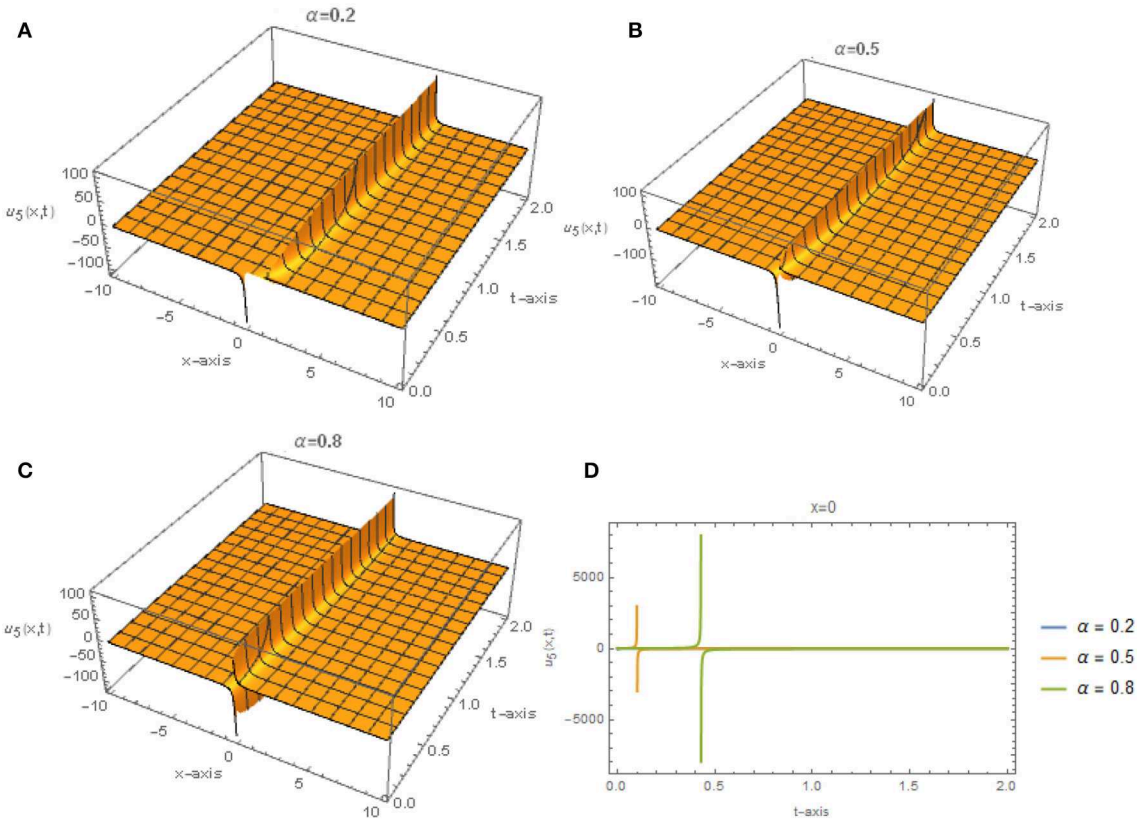

FIGURE 5 | (A–D) The Solution u_5 (x,t) given by Eq. (79).

For p = 1:

$$\left.\begin{aligned} u_{12}(x,t) &= -\tfrac{1}{3}\sqrt{3}\,r \pm \tfrac{1}{3}\sqrt{3\left(r^2-4q\right)} \\ &\quad +\tfrac{4}{3}\frac{\sqrt{3}\,q}{\sqrt{\Delta}\,\tanh\left(\frac{1}{2}\sqrt{\Delta}\,(\xi+E)\right)+r} \\ v_{12}(x,t) &= -\tfrac{2}{3}q + \tfrac{4}{3}\frac{rq}{\sqrt{\Delta}\,\tanh\left(\frac{1}{2}\sqrt{\Delta}\,(\xi+E)\right)+r} \\ &\quad -\tfrac{8}{3}\frac{q^2}{\left(\sqrt{\Delta}\,\tanh\left(\frac{1}{2}\sqrt{\Delta}\,(\xi+E)\right)+r\right)^2} \end{aligned}\right\}, \quad (85)$$

$$\left.\begin{aligned} u_{13}(x,t) &= -\tfrac{1}{3}\sqrt{3}\,r \pm \tfrac{1}{3}\sqrt{3\left(r^2-4q\right)} \\ &\quad +\tfrac{4}{3}\frac{\sqrt{3}\,q}{\sqrt{\Delta}\,\coth\left(\frac{1}{2}\sqrt{\Delta}\,(\xi+E)\right)+r} \\ v_{13}(x,t) &= -\tfrac{2}{3}q + \tfrac{4}{3}\frac{rq}{\sqrt{\Delta}\,\coth\left(\frac{1}{2}\sqrt{\Delta}\,(\xi+E)\right)+r} \\ &\quad -\tfrac{8}{3}\frac{q^2}{\left(\sqrt{\Delta}\,\coth\left(\frac{1}{2}\sqrt{\Delta}\,(\xi+E)\right)+r\right)^2} \end{aligned}\right\} \quad (86)$$

$$\left.\begin{aligned} u_{14}(x,t) &= -\tfrac{1}{3}\sqrt{3}\,r \pm \tfrac{1}{3}\sqrt{3\left(r^2-4q\right)} \\ &\quad -\tfrac{4}{3}\frac{\sqrt{3}\,q}{\sqrt{-\Delta}\,\tan\left(\frac{1}{2}\sqrt{-\Delta}\,(\xi+E)\right)-r} \\ v_{14}(x,t) &= -\tfrac{2}{3}q + \tfrac{4}{3}\frac{rq}{\sqrt{-\Delta}\,\tan\left(\frac{1}{2}\sqrt{-\Delta}\,(\xi+E)\right)+r} \\ &\quad -\tfrac{8}{3}\frac{q^2}{\left(\sqrt{-\Delta}\,\tan\left(\frac{1}{2}\sqrt{-\Delta}\,(\xi+E)\right)-r\right)^2} \end{aligned}\right\}, \quad (87)$$

$$\left.\begin{aligned} u_{15}(x,t) &= -\tfrac{1}{3}\sqrt{3}\,r \pm \tfrac{1}{3}\sqrt{3\left(r^2-4q\right)} \\ &\quad -\tfrac{4}{3}\frac{\sqrt{3}\,q}{\sqrt{-\Delta}\,\cot\left(\frac{1}{2}\sqrt{-\Delta}\,(\xi+E)\right)-r} \\ v_{15}(x,t) &= -\tfrac{2}{3}q - \tfrac{4}{3}\frac{rq}{\sqrt{-\Delta}\,\cot\left(\frac{1}{2}\sqrt{-\Delta}\,(\xi+E)\right)+r} \\ &\quad -\tfrac{8}{3}\frac{q^2}{\left(\sqrt{-\Delta}\,\cot\left(\frac{1}{2}\sqrt{-\Delta}\,(\xi+E)\right)-r\right)^2} \end{aligned}\right\}, \quad (88)$$

$$\left.\begin{aligned} u_{16}(x,t) &= -\tfrac{1}{3}\sqrt{3}\,r \pm \tfrac{1}{3}\sqrt{3\left(r^2-4q\right)} - \tfrac{2}{3}\frac{\sqrt{3}\,r}{e^{r(\xi+E)}-1} \\ v_{16}(x,t) &= -\tfrac{2}{3}q - \tfrac{2}{3}\frac{r^2}{e^{r(\xi+E)}-1} - \tfrac{2}{3}\frac{r^2}{\left(e^{r(\xi+E)}-1\right)^2} \end{aligned}\right\}, \quad (89)$$

and

$$\left.\begin{aligned} u_{17}(x,t) &= -\tfrac{1}{3}\sqrt{3}\,r \pm \tfrac{1}{3}\sqrt{3\left(r^2-4q\right)} + \tfrac{1}{3}\frac{\sqrt{3}\,r^2(\xi+E)}{r(\xi+E)+2} \\ v_{17}(x,t) &= -\tfrac{2}{3}q + \tfrac{1}{3}\frac{r^3(\xi+E)}{r(\xi+E)+2} - \tfrac{1}{6}\left(\frac{r^2(\xi+E)}{r(\xi+E)+2}\right)^2 \end{aligned}\right\}, \quad (90)$$

where, $\xi = x \mp \left(\frac{1}{3}\sqrt{3\left(r^2-4q\right)}\right)\frac{t^\alpha}{\alpha}$ and $\Delta = r^2 - 4q > 0$.

For r = 0:

$$\left.\begin{aligned} u_{18}(x,t) &= \pm\tfrac{2}{3}\sqrt{-3pq} - \tfrac{2}{3}\frac{\sqrt{3pq}}{\tan((\xi+E))} \\ v_{18}(x,t) &= -\tfrac{2}{3}pq - \tfrac{2}{3}\left(\frac{\sqrt{pq}}{\tan\left(\sqrt{pq}(\xi+E)\right)}\right)^2 \end{aligned}\right\}, \quad (91)$$

$$\left.\begin{aligned} u_{19}(x,t) &= \pm\tfrac{2}{3}\sqrt{-3pq} + \tfrac{2}{3}\frac{\sqrt{3pq}}{\cot\left(\sqrt{pq}(\xi+E)\right)} \\ v_{19}(x,t) &= -\tfrac{2}{3}pq - \tfrac{2}{3}\left(\frac{\sqrt{pq}}{\cot\left(\sqrt{pq}(\xi+E)\right)}\right)^2 \end{aligned}\right\}, \quad (92)$$

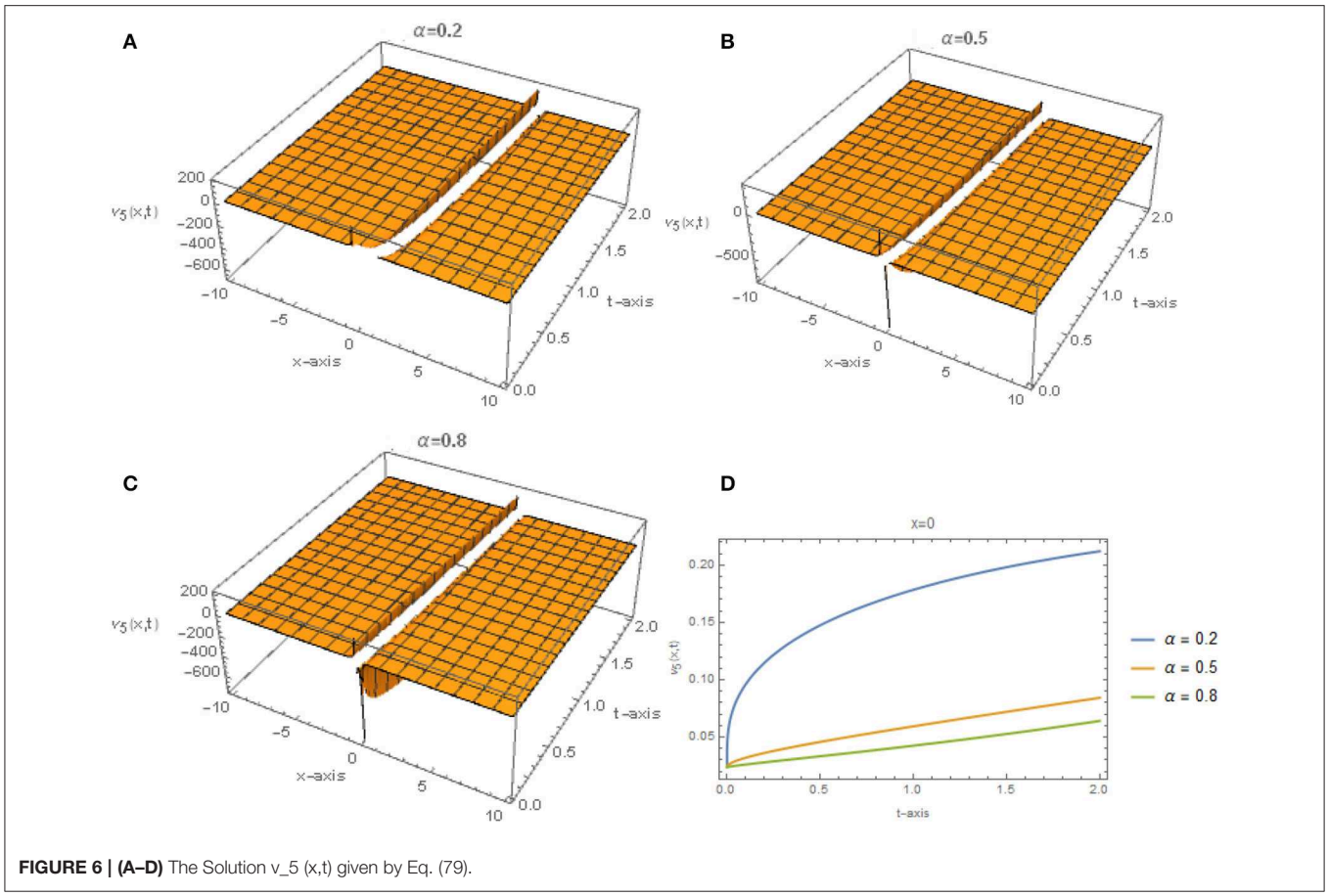

FIGURE 6 | (A–D) The Solution v_5 (x,t) given by Eq. (79).

$$\left.\begin{aligned} u_{20}(x,t) &= \pm\tfrac{2}{3}\sqrt{-3pq} - \tfrac{2}{3}\frac{\sqrt{-3pq}}{\tanh\left(\sqrt{-pq}(\xi+E)\right)} \\ v_{20}(x,t) &= -\tfrac{2}{3}pq + \tfrac{2}{3}\left(\frac{\sqrt{-pq}}{\tanh\left(\sqrt{pq}(\xi+E)\right)}\right)^2 \end{aligned}\right\}, \tag{93}$$

and

$$\left.\begin{aligned} u_{21}(x,t) &= \pm\tfrac{2}{3}\sqrt{-3pq} + \tfrac{2}{3}\frac{\sqrt{-3pq}}{\coth\left(\sqrt{-pq}(\xi+E)\right)} \\ v_{21}(x,t) &= -\tfrac{2}{3}pq + \tfrac{2}{3}\left(\frac{\sqrt{pq}}{\coth\left(\sqrt{-pq}(\xi+E)\right)}\right)^2 \end{aligned}\right\}, \tag{94}$$

where, $\xi = x \mp \left(\frac{2}{3}\sqrt{-3pq}\right)\frac{t^{\alpha}}{\alpha}$, $pq < 0$.

For q = 0 and r = 0:

$$\left.\begin{aligned} u_{22}(x,t) &= \tfrac{2}{3}\frac{\sqrt{3}}{x+E} \\ v_{22}(x,t) &= -\tfrac{2}{3}\left(\frac{1}{x+E}\right)^2 \end{aligned}\right\}. \tag{95}$$

Figures 5, **6** represent the solutions given by Eq. (79) for different values of α when $r = 3$, $q = 2$ and $E = 0$.

CONCLUSION

This research successfully applied the generalized $exp(-\varphi(\xi))$-expansion method combined with the complex fractional transformation and conformable derivative to exactly solve a special class of time-fractional WBK equations in shallow water, such as the time-fractional ALW equations, the time-fractional variant-Boussinesq equations, and the time fractional Wu-Zhang system of equations. Afterwards, a sequence of new analytical wave solutions for these models were established. Finally, some 3D and 2D plots were added for some of the gained solutions for every model to illustrate the effect of the parameter α on the behaviors of these solutions. In conclusion, we found that the method mentioned here—with the aid of symbolic computations—is aspiring and efficient, and it is a superior mathematical construction with which to deal with the NPDEs.

DATA AVAILABILITY STATEMENT

The original contributions presented in the study are included in the article/supplementary materials, further inquiries can be directed to the corresponding author/s.

AUTHOR CONTRIBUTIONS

All authors listed have made a substantial, direct and intellectual contribution to the work, and approved it for publication.

REFERENCES

1. Guo S, Mei LQ, Li Y, Sun YF. The improved fractional sub-equation method and its applications to the space–time-fractional differential equations in fluid mechanics. *Phys Lett A*. (2012) 376:407–11. doi: 10.1016/j.physleta.2011.10.056
2. El-Borai MM, El-Sayed WG, Al-Masroub RM. Exact solution for time-fractional coupled Whitham-Broer-Kaup equations via exp-function method. *Int Res J Eng Tech*. (2015) 2:307–15. doi: 10.1016/j.chaos.2004.09.017
3. Ghanbari B, Osman MS, Baleanu D. Generalized exponential rational function method for extended Zakharov–Kuzetsov equation with conformable derivative. *Modern Phys Lett A*. (2019) 34:1950155. doi: 10.1142/S0217732319501554
4. Guner O, Atik H, Kayyrzhanovich AA. New exact solution for space–time-fractional differential equations via $G^{'}/G$-expansion method. *Optik*. (2017) 130:696–701. doi: 10.1016/j.ijleo.2016.10.116
5. Liu JG, Osman MS, Zhu WH, Zhou L, Ai GP. Different complex wave structures described by the hirota equation with variable coefficients in inhomogeneous optical fibers. *Appl Phys B*. (2019) 125:175. doi: 10.1007/s00340-019-7287-8
6. Ding Y, Osman MS, Wazwaz AM. Abundant complex wave solutions for the nonautonomous Fokas–Lenells equation in presence of perturbation terms. *Optik*. (2019) 181:503–13. doi: 10.1016/j.ijleo.2018.12.064
7. Liu JG, Osman MS, Wazwaz, AM. A variety of nonautonomous complex wave solutions for the (2+ 1)-dimensional nonlinear Schrödinger equation with variable coefficients in nonlinear optical fibers. *Optik*. (2019) 180:917–23. doi: 10.1016/j.ijleo.2018.12.002
8. Manafian J, Lakestani M. Abundant soliton solutions for the Kundu–Eckhaus equation via $\tan(\Phi(\xi)/2)$-expansion method. *Optik*. (2016) 127:5543–51. doi: 10.1016/j.ijleo.2016.03.041
9. Ray SS. New analytical exact solutions of time-fractional KdV–KZK equation by Kudryashov methods. *Chinese Phys B*. (2016) 25:040204. doi: 10.1088/1674-1056/25/4/040204
10. Hosseini K, Mayeli P, Kumar D. New exact solutions of the coupled sine-Gordon equation in nonlinear optics using the modified Kudryashov method. *J Modern Optics*. (2018) 65:361–4. doi: 10.1080/09500340.2017.1380857
11. Rezazadeh H, Mirhosseini-Alizamini SM, Eslami M, Rezazadeh M, Mirzazadeh, Abbagari MS. New optical solitons of conformable fractional Schrödinger-Hirota equation. *Optik*. (2018) 172:545–53. doi: 10.1016/j.ijleo.2018.06.111
12. Kumar D, Kaplan M. New analytical solutions of (2+1)-dimensional conformable time-fractional Zoomeron equation via two distinct techniques. *Chinese J Phys*. (2018) 56:2173–85. doi: 10.1016/j.cjph.2018.09.013
13. Inc M, Yusuf A, Aliyu AI, Baleanu D. Soliton structures to some time-fractional nonlinear differential equations with conformable derivative. *Opt Quant Elect*. (2018) 50:20. doi: 10.1007/s11082-018-1459-3
14. Kumar D, Hosseini K, Samadani F. The sine-Gordon expansion method to look for the traveling wave solutions of the Tzitzeica type equations in nonlinear optics. *Optik*. (2017) 149:439–46. doi: 10.1016/j.ijleo.2017.09.066
15. Ali KK, Wazwaz AM, Osman MS. Optical soliton solutions to the generalized nonautonomous nonlinear Schrödinger equations in optical fibers via the sine-Gordon expansion method. *Optik*. (2019) 208:164132. doi: 10.1016/j.ijleo.2019.164132
16. Ali KK, Osman MS, Abdel-Aty M. New optical solitary wave solutions of Fokas-Lenells equation in optical fiber via Sine-Gordon expansion method. *Alexand Eng J*. (2020). doi: 10.1016/j.aej.2020.01.037
17. Osman MS, Lu D, Khater MM. A study of optical wave propagation in the nonautonomous Schrödinger-Hirota equation with power-law nonlinearity. *Res Phys*. (2019) 13:102157. doi: 10.1016/j.rinp.2019.102157
18. Osman MS. New analytical study of water waves described by coupled fractional variant Boussinesq equation in fluid dynamics. *Pramana*. (2019) 93:26. doi: 10.1007/s12043-019-1785-4
19. Javid A, Raza N, Osman MS. Multi-solitons of thermophoretic motion equation depicting the wrinkle propagation in substrate-supported graphene sheets. *Commun Theor Phys*. (2019) 71:362. doi: 10.1088/0253-6102/71/4/362
20. Osman MS. Nonlinear interaction of solitary waves described by multi-rational wave solutions of the (2+1)-dimensional Kadomtsev–Petviashvili equation with variable coefficients. *Nonlinear Dynamics*. (2017) 87:1209–16. doi: 10.1007/s11071-016-3110-9
21. Ray SS. A novel method for travelling wave solutions of fractional Whitham-Broer-Kaup, fractional modified Boussinesq and fractional approximate long wave equations in shallow water. *Math Methods Appl Sci*. (2015) 38:1352–68. doi: 10.1002/mma.3151
22. Ping Z. New exact solutions to breaking solution equations and Whitham–Broer–Kaup equation. *Appl. Math. Comput*. (2010) 217:1688–96. doi: 10.1016/j.amc.2009.09.062
23. Kupershmidt BA. Mathematics of dispersive water waves. *Commun Math Phys*. (1985) 99:51–73. doi: 10.1007/BF01466593
24. Guo S, Liquan M. Exact solutions of space–time-fractional variant Boussinesq equations. *Adv Sci Lett*. (2012) 10:700–2. doi: 10.1166/asl.2012.3388
25. El-Borai MM, El-Sayed WG, Al-Masroub RM. Exact solution for time-fractional coupled Whitham-Broer-Kaup equations via exp-function method. *Int. Res. J. Eng. Tech*. (2015) 2:307–15.
26. Yan L. New travelling wave solutions for coupled fractional variant Boussinesq equation and approximate long water wave equation. *Int. J. Numer. Methods Heat Fluid Flow*. (2015) 25:33–40. doi: 10.1108/HFF-04-2013-0126
27. Eslami M, Rezazadeh H. The first integral method for Wu-Zhang system with conformable time-fractional derivative. *Calcolo*. (2016) 53:475–85. doi: 10.1007/s10092-015-0158-8
28. Whitham GB. Variational methods and applications to water waves. *Proc R Soc Lond Series A*. (1967) 299:6–25. doi: 10.1098/rspa.1967.0119
29. Broer LJF. Approximate equations for long water waves. *Appl Sci Res*. (1975) 31:377–95. doi: 10.1007/BF00418048
30. Kaup DJ. A higher-order water-wave equation and the method for solving it. *Prog Theor Phys*. (1975) 54:396–408. doi: 10.1143/PTP.54.396
31. Gao H, Tianzhou X, Shaojie Y, Gangwei W. Analytical study of solitons for the variant Boussinesq equations. *Nonlinear Dyn*. (2017) 88:1139–46. doi: 10.1007/s11071-016-3300-5
32. Hosseini K, Ansari R, Gholamin P. Exact solutions of some nonlinear systems of partial differential equations by using the first integral method. *J Math Anal App*. (2012) 387:807–14. doi: 10.1016/j.jmaa.2011.09.044
33. Zheng X, Yong C, Hongqing Z. Generalized extended tanh-function method and its application to (1+1)-dimensional dispersive long wave equation. *Phys Lett A*. (2003) 311:145–57. doi: 10.1016/S0375-9601(03)00451-1
34. Chen Y, Qi W. A new general algebraic method with symbolic computation to construct new travelling wave solution for the (1+1)-dimensional dispersive long wave equation. *Appl Math Comput*. (2005) 168:1189–204. doi: 10.1016/j.amc.2004.10.012
35. Elgarayhi A. New solitons and periodic wave solutions for the dispersive long wave equations. *Phys A*. (2006) 361:416–28. doi: 10.1016/j.physa.2005.05.103
36. Lu D, Chen Y, Muhammad A. Traveling wave solutions of space–time-fractional generalized fifth-order KdV equation. *Adv Math Phys*. (2017) 12:1–6. doi: 10.1155/2017/6743276

37. Khalil R, Al Horani M, Yousef A, Sababheh M. A new definition of fractional derivative. *J Comput Appl Math*. (2014) 264:65–70. doi: 10.1016/j.cam.2014.01.002
38. Abdeljawad T. On conformable fractional calculus. *J Comput Appl Math*. (2015) 279:57–66. doi: 10.1016/j.cam.2014.10.016
39. Atangana A, Baleanu D, Alsaedi A. New properties of conformable derivative. *Open Math*. (2015) 13:889–98. doi: 10.1515/math-2015-0081
40. Çenesiz Y, Baleanu D, Kurt A, Tasbozan O. New exact solutions of Burgers' type equations with conformable derivative. *Waves Rand Compl Media*. (2017) 27:103–16. doi: 10.1080/17455030.2016.1205237
41. Zhou HW, Yang S, Zhang SQ. Conformable derivative approach to anomalous diffusion. *Physica A*. (2018) 491:1001–13. doi: 10.1016/j.physa.2017.09.101

Conflict of Interest: The authors declare that the research was conducted in the absence of any commercial or financial relationships that could be construed as a potential conflict of interest.

The reviewer MB declared a past co-authorship with one of the authors DB to the handling editor.

Copyright © 2020 Kumar, Kaplan, Haque, Osman and Baleanu. This is an open-access article distributed under the terms of the Creative Commons Attribution License (CC BY). The use, distribution or reproduction in other forums is permitted, provided the original author(s) and the copyright owner(s) are credited and that the original publication in this journal is cited, in accordance with accepted academic practice. No use, distribution or reproduction is permitted which does not comply with these terms.

frontiers in Physics

ORIGINAL RESEARCH
published: 25 June 2020
doi: 10.3389/fphy.2020.00220

A New Iterative Method for the Numerical Solution of High-Order Non-linear Fractional Boundary Value Problems

Amin Jajarmi[1]* *and Dumitru Baleanu*[2,3]

[1] Department of Electrical Engineering, University of Bojnord, Bojnord, Iran, [2] Department of Mathematics, Faculty of Arts and Sciences, Cankaya University, Ankara, Turkey, [3] Institute of Space Sciences, Măgurele, Romania

The boundary value problems (BVPs) have attracted the attention of many scientists from both practical and theoretical points of view, for these problems have remarkable applications in different branches of pure and applied sciences. Due to this important property, this research aims to develop an efficient numerical method for solving a class of non-linear fractional BVPs. The proposed method is free from perturbation, discretization, linearization, or restrictive assumptions, and provides the exact solution in the form of a uniformly convergent series. Moreover, the exact solution is determined by solving only a sequence of linear BVPs of fractional-order. Hence, from practical viewpoint, the suggested technique is efficient and easy to implement. To achieve an approximate solution with enough accuracy, we provide an iterative algorithm that is also computationally efficient. Finally, four illustrative examples are given verifying the superiority of the new technique compared to the other existing results.

Keywords: fractional calculus, boundary value problems, series expansion, uniform convergence, iterative method

OPEN ACCESS

Edited by:
Jordan Yankov Hristov, University of Chemical Technology and Metallurgy, Bulgaria

Reviewed by:
Ahmed Elwakil, University of Sharjah, United Arab Emirates
Aydin Secer, Yildiz Technical University, Turkey

***Correspondence:**
Amin Jajarmi
a.jajarmi@ub.ac.ir

Specialty section:
This article was submitted to Mathematical Physics, a section of the journal Frontiers in Physics

Received: *08 January 2020*
Accepted: *22 May 2020*
Published: *25 June 2020*

Citation:
Jajarmi A and Baleanu D (2020) A New Iterative Method for the Numerical Solution of High-Order Non-linear Fractional Boundary Value Problems. Front. Phys. 8:220. doi: 10.3389/fphy.2020.00220

1. INTRODUCTION

The application of boundary value problems (BVPs) can be found in different fields of pure and applied sciences; for instance, the narrow converting layers bounded by stable layers, which are believed to surround A-type stars, may be modeled by BVPs [1]. Also, these problems may model the dynamo action in some stars [2]. More discussions on the application of BVPs have also been provided in Chandrasekhar [3], Baldwin [4], and Khalid et al. [5]. More to the point, the approximation schemes to solve non-linear BVPs can be found in different sources of numerical analysis [6, 7]. In Agarwal [8], Agarwal discussed the existence of unique solution for these problems; however, no numerical method is contained therein. Boutayeb and Twizell [9] developed the finite difference methods to solve the above-mentioned problems effectively. They also improved a second-order method in Twizell and Boutayeb [10] to solve the general and special BVPs. Besides, Twizell [11] advanced a finite difference scheme of order two to investigate the solution of these problems. However, the existing methods suffer from enormous computational effort. To solve this difficulty, some alternative schemes have been presented including the Adomian decomposition method (ADM) with Green's function [12], homotopy perturbation method (HPM) [13], and variational iteration method (VIM) [14].

During the past decades, many scientists have frequently shown that the mathematical equations with fractional calculus architectures can describe the reality more precisely than the classic

integer models with ordinary time-derivatives [15–19]. Recently, the advantages of this approach have been extensively investigated for various practical applications [20–27]. Concerning the fractional BVPs, some noticeable efforts have been done in Ali et al. [28] and Ugurlu et al. [29]. The aforesaid problems have also noteworthy real applications in different areas of science and technology. For instance, a hybrid Caputo fractional modeling was considered in Baleanu et al. [30] for thermostat with hybrid boundary conditions. In Patnaik et al. [31], the application of a fractional-order non-local continuum model was studied for a Euler-Bernoulli beam. The authors in Salem et al. [32] analyzed the coupled system of non-linear fractional Langevin equations with multi-point and non-local integral boundary conditions. The existence of extremal solutions of fractional Langevin equation involving non-linear boundary conditions was also investigated in Fazli et al. [33]. However, the properties of fractional BVPs should be studied deeply and approximation schemes should be continuously improved solving the above-mentioned problems appropriately. To this end, some valuable studies have been carried out, and a number of noteworthy results have been achieved. For instance, an existence theorem was discussed in Zhang and Su [34] for a linear fractional differential equation (FDE) with non-linear boundary conditions by using the method of upper and lower solutions in reverse order. In Arqub et al. [35], a new kind of analytical method was proposed to predict and represent the multiplicity of solutions to non-linear fractional BVPs. In Khalil et al. [36], the authors studied a coupled system of non-linear FDEs whose approximate solution was achieved under two different types of boundary conditions. In Cui et al. [37], a monotone iterative method was investigated for non-linear fractional BVPs while the fractional order was considered between 2 and 3. In Asaduzzaman and Ali [38], the existence of positive solution was investigated to the BVPs for coupled system of non-linear FDEs.

Motivated by the aforementioned statement, this manuscript aims to design a new iterative method to generate the approximate solution of non-linear fractional BVPs in the form of uniformly convergent series. The proposed method is free from perturbation, discretization, linearization, or restrictive assumptions. Moreover, contrary to the VIM [14] or the ADM [12], the suggested technique provides the exact solution without identifying the Lagrange multipliers or calculating the Adomian's polynomials. The new scheme just requires solving a sequence of linear fractional-order BVPs. Finally, four numerical examples are solved to verify the efficiency of the new technique.

The rest of paper is structured in the following way. Hereinafter, we review the fractional calculus approach and its main definitions. Section 3 describes the problem statement. A numerical technique is extended in section 4 solving non-linear fractional BVPs. Numerical and comparative results are reported in section 5, and finally, the paper is finished in section 6 by some concluding remarks.

2. PRELIMINARIES

This part is devoted to some preliminary results concerning the fractional operators. In the following, the Caputo derivative and the Riemann-Liouville integral are introduced, and their main properties are investigated as well [15].

Definition 2.1. For $t \in (0, T)$ and $n-1 < \alpha \leq n$, the αth-order Caputo derivative of a function $x(t)$ is defined by

$$ {}_0^C\mathscr{D}_t^{\alpha}(x(t)) = \frac{1}{\Gamma(n-\alpha)} \int_0^t (t-\tau)^{n-\alpha-1} x^{(n)}(\tau) d\tau, \tag{1} $$

where $\Gamma(\cdot)$ is the gamma function. The corresponding Riemann-Liouville integral is also described as

$$ {}_0^C\mathscr{I}_t^{\alpha}(x(t)) = \frac{1}{\Gamma(\alpha)} \int_0^t (t-\tau)^{\alpha-1} x(\tau) d\tau. \tag{2} $$

With regard to the Caputo derivative (1), we can write

$$ {}_0^C\mathscr{D}_t^{\alpha}(a_1 x_1(t) + a_2 x_2(t)) = a_1 {}_0^C\mathscr{D}_t^{\alpha} x_1(t) + a_2 {}_0^C\mathscr{D}_t^{\alpha} x_2(t). \tag{3} $$

Furthermore, the Caputo derivative of a constant function is zero, i.e., if $x(t) \equiv k$, then we have ${}_0^C\mathscr{D}_t^{\alpha} k = 0$. Additionally, the derivative and integral operators (1) and (2) satisfy the following anti-derivative property

$$ {}_0^C\mathscr{I}_t^{\alpha}\left[{}_0^C\mathscr{D}_t^{\alpha} x(t)\right] = x(t) - x(0). \tag{4} $$

More to the point, the Lipschitz condition is satisfied by the Caputo derivative (1)

$$ \left\| {}_0^C\mathscr{D}_t^{\alpha} x_1(t) - {}_0^C\mathscr{D}_t^{\alpha} x_2(t) \right\| \leq L \left\| x_1(t) - x_2(t) \right\|, \tag{5} $$

where $L > 0$ is the Lipschitz constant.

For additional information, the interested readers can refer to Kilbas et al. [15].

3. THE STATEMENT OF THE PROBLEM

To formulate a fractional BVP, consider the following FDE

$$ {}_0^C\mathscr{D}_t^{\alpha}(x(t)) = f(x(t), t),\ n-1 < \alpha \leq n,\ t \in (0, T), \tag{6} $$

where the function $f(\cdot)$ is analytic with regard to its arguments and $f(0, t) = 0, \forall t \in (0, T)$. The expression ${}_0^C\mathscr{D}_t^{\alpha}$ denotes the αth-order Caputo derivative, and n is an even number. The boundary conditions for Equation (6) are given by

$$ x^{(2k)}(0) = a_{2k},\ x^{(2k)}(T) = b_{2k},\ k = 0, 1, \ldots, \frac{n}{2}, \tag{7} $$

where a_{2k}, b_{2k} $(k = 0, 1, \ldots, \frac{n}{2})$ are real finite numbers. As is well-known, the exact solution of the fractional BVP (6)-(7) can hardly be achieved except in very special cases. Hence, an efficient iterative technique will be developed hereinafter in order to derive the corresponding approximate solution.

4. THE ITERATIVE METHOD

In this section, an efficient iterative method is improved to solve the fractional BVP (6), (7). To this end, first the following lemma is presented and proved.

Lemma 4.1. *The solution of the fractional BVP (6)-(7) is analytic with respect to the boundary conditions* a_{2k}, b_{2k}, $k = 0, 1, \ldots, \frac{n}{2}$.

Proof: Let $x(\cdot)$ be the solution of the BVP (6)-(7). Define $\alpha_i = x^{(i)}(0)$ and $\beta_j = x^{(j)}(T)$, $i, j = 0, \ldots, n-1$. Then $x(\cdot)$ is the solution of the following initial value problems (IVPs)

$$\begin{cases} {}_0^C\mathscr{D}_t^\alpha(x(t)) = f(x(t), t),\ n-1 < \alpha \le n,\ t \in (0, T), \\ x^{(i)}(0) = \alpha_i,\ i = 0, \ldots, n-1, \end{cases} \tag{8}$$

$$\begin{cases} {}_0^C\mathscr{D}_t^\alpha(x(t)) = f(x(t), t),\ n-1 < \alpha \le n,\ t \in (0, T), \\ x^{(j)}(T) = \beta_j,\ j = 0, \ldots, n-1. \end{cases} \tag{9}$$

Since $f(x(t), t)$ is assumed to be analytic, $x(\cdot)$, as the solution of the IVPs (8) and (9), is analytic with respect to α_i and β_i, respectively [39]. Thus, $x(\cdot)$, as the solution of the BVP (6)-(7), is analytic with respect to a_{2k}, b_{2k}, $k = 0, 1, \ldots, \frac{n}{2}$.

Now, we state and prove the following theorem.

Theorem 4.1. *The solution of the fractional BVP (6)-(7) is expressed by the uniformly convergent series* $x(t) = \sum_{i=1}^{\infty} \hat{x}_i(t)$, *where* $\hat{x}_i(t)$ *is attained by solving the sequence of linear fractional BVPs*

$$\begin{cases} {}_0^C\mathscr{D}_t^\alpha(\hat{x}_1(t)) = \lambda_1(t)\hat{x}_1(t), \\ \hat{x}_1^{(2k)}(0) = a_{2k},\ \hat{x}_1^{(2k)}(T) = b_{2k},\ k = 0, 1, \ldots, \frac{n}{2}, \end{cases} \tag{10}$$

and for $i = 2, 3, 4, \ldots$

$$\begin{cases} {}_0^C\mathscr{D}_t^\alpha(\hat{x}_i(t)) = \lambda_1(t)\hat{x}_i(t) + F_i(t, \hat{x}_1(t), \hat{x}_2(t), \ldots, \hat{x}_{i-1}(t)), \\ \hat{x}_i^{(2k)}(0) = 0,\ \hat{x}_i^{(2k)}(T) = 0,\ k = 0, 1, \ldots, \frac{n}{2}. \end{cases} \tag{11}$$

The non-homogeneous term F_i *is determined by*

$$F_i(t, \hat{x}_1(t), \hat{x}_2(t), \ldots, \hat{x}_{i-1}(t)) = \sum_{j=2}^{i} \lambda_j(t) \sum_{k_1, \ldots, k_{i+1-j}} \frac{j!}{k_1! \cdots k_{i+1-j}!} \prod_{p=1}^{i+1-j} \hat{x}_p^{k_p}(t), \tag{12}$$

$\lambda_j(t) = \frac{1}{j!}\frac{\partial^j}{\partial x^j} f(x, t)\Big|_{x=0}$, *and the summation* $\sum_{k_1, \ldots, k_{i+1-j}}$ *is taken over all combinations of non-negative integer indices* k_1 *through* k_{i+1-j} *such that*

$$\begin{cases} \sum_{p=1}^{i+1-j} k_p = j, \\ \sum_{p=1}^{i+1-j} p k_p = i. \end{cases} \tag{13}$$

Proof: By using the Maclaurin series of $f(x(t), t)$ with respect to $x(t)$, we have

$${}_0^C\mathscr{D}_t^\alpha(x(t)) = \lambda_1(t)x(t) + \lambda_2(t)x^2(t) + \lambda_3(t)x^3(t) + \cdots, \tag{14}$$

where $\lambda_j(t) = \frac{1}{j!}\frac{\partial^j}{\partial x^j} f(x, t)\Big|_{x=0}$. Besides, the solution of the fractional BVP (6)-(7) for an arbitrary vector $x_b = (a_0, a_2, \ldots, a_n, b_0, b_2, \ldots, b_n)$ is expressed by

$$x(t) = g(x_b, t), \tag{15}$$

where the vector function $g : \mathbb{R}^n \times (0, T) \to \mathbb{R}$ is analytic based on Lemma 4.1. In addition, we have $g(0, t) = 0, \forall t \in (0, T)$, since we have assumed that $f(0, t) = 0$ for all $t \in (0, T)$. Therefore, by applying the Maclaurin series of $g(x_b, t)$ with respect to x_b, from Equation (15) we derive

$$\begin{aligned} x(t) = \underbrace{g(x_b, t)\big|_{x_b=0}}_{0} + \underbrace{\frac{\partial}{\partial x_b} g(x_b, t)\Big|_{x_b=0} x_b}_{\hat{x}_1(t)} \\ + \underbrace{x_b^T \left(\frac{1}{2!}\frac{\partial^2}{\partial x_b^2} g(x_b, t)\Big|_{x_b=0} \right) x_b}_{\hat{x}_2(t)} + \cdots. \end{aligned} \tag{16}$$

Since the function $g(x_b, t)$ is analytic with respect to x_b, the Maclaurin series (16) exists and is uniformly convergent. Now, we perturb the boundary conditions by an arbitrary parameter $\varepsilon > 0$, i.e., $x_b \to \varepsilon x_b$. Then, Equation (16) is reformulated by

$$x(t) = g(\varepsilon x_b, t) = \varepsilon\hat{x}_1(t) + \varepsilon^2\hat{x}_2(t) + \cdots. \tag{17}$$

Substituting $x(t)$ from Equation (17) into the expansion (14) yields

$$\begin{aligned} {}_0^C\mathscr{D}_t^\alpha(\varepsilon\hat{x}_1(t) + \varepsilon^2\hat{x}_2(t) + \cdots) = \lambda_1(t)\left(\varepsilon\hat{x}_1(t) + \varepsilon^2\hat{x}_2(t) + \cdots\right) \\ + \lambda_2(t)\left(\varepsilon\hat{x}_1(t) + \varepsilon^2\hat{x}_2(t) + \cdots\right)^2 + \cdots. \end{aligned} \tag{18}$$

Rearranging Equation (18) with respect to the order of ε results

$$\begin{aligned} \varepsilon\,{}_0^C\mathscr{D}_t^\alpha(\hat{x}_1(t)) + \varepsilon^2\,{}_0^C\mathscr{D}_t^\alpha(\hat{x}_2(t)) + \cdots + \varepsilon^i\,{}_0^C\mathscr{D}_t^\alpha(\hat{x}_i(t)) + \cdots = \\ \varepsilon\left(\lambda_1(t)\hat{x}_1(t)\right) + \varepsilon^2\left(\lambda_1(t)\hat{x}_2(t) + \lambda_2(t)\hat{x}_1^2(t)\right) + \cdots \\ + \varepsilon^i\left(\lambda_1(t)\hat{x}_i(t) + F_i(t, \hat{x}_1(t), \hat{x}_2(t), \ldots, \hat{x}_{i-1}(t))\right) + \cdots, \end{aligned} \tag{19}$$

where

$$F_i(t, \hat{x}_1(t), \hat{x}_2(t), \ldots, \hat{x}_{i-1}(t)) = \sum_{j=2}^{i} \lambda_j(t) \sum_{k_1, \ldots, k_{i+1-j}} \frac{j!}{k_1! \cdots k_{i+1-j}!} \prod_{p=1}^{i+1-j} \hat{x}_p^{k_p}(t), \tag{20}$$

and the summation $\sum_{k_1,\ldots,k_{i+1-j}}$ is taken over all combinations of non-negative integer indices k_1 through k_{i+1-j} such that

$$\begin{cases} \sum_{p=1}^{i+1-j} k_p = j, \\ \sum_{p=1}^{i+1-j} p k_p = i. \end{cases} \tag{21}$$

Since, Equation (19) must be satisfied for any $\varepsilon > 0$, we should equalize the coefficient of ε^i on the left-hand side of Equation (19) with its corresponding coefficient on the right-hand side. This procedure yields

$$\varepsilon^1 : {}_0^C\mathscr{D}_t^\alpha(\hat{x}_1(t)) = \lambda_1(t)\hat{x}_1(t), \tag{22}$$
$$\varepsilon^2 : {}_0^C\mathscr{D}_t^\alpha(\hat{x}_2(t)) = \lambda_1(t)\hat{x}_2(t) + \lambda_2(t)\hat{x}_1^2(t), \tag{23}$$
$$\vdots$$
$$\varepsilon^i : {}_0^C\mathscr{D}_t^\alpha(\hat{x}_i(t)) = \lambda_1(t)\hat{x}_i(t) + F_i(t, \hat{x}_1(t), \hat{x}_2(t), \ldots, \hat{x}_{i-1}(t)), \tag{24}$$
$$\vdots$$

Now, we put $t = 0$ and $t = T$ in Equation (17) and in its second- and fourth-order derivatives in order to achieve the boundary conditions for the sequence (22)-(24). Again, we should equalize the coefficients of ε^i on the both sides of the resultant equations. Thus, we obtain

$$\varepsilon^1 : \hat{x}_1^{(2k)}(0) = a_{2k},\ \hat{x}_1^{(2k)}(T) = b_{2k},\ k = 0, 1, \ldots, \frac{n}{2}, \tag{25}$$

$$\varepsilon^i : \hat{x}_i^{(2k)}(0) = 0,\ \hat{x}_i^{(2k)}(T) = 0,\ k = 0, 1, \ldots, \frac{n}{2},\ i \geq 2, \tag{26}$$

and the proof is complete.

As can be seen, Equation (10) formulates a homogeneous linear BVP of fractional-order. By solving this problem, $\hat{x}_1(t)$ is achieved in the first step. Following the proposed procedure in Theorem 4.1, we then obtain $\hat{x}_i(t)$ $(i \geq 2)$ by solving the non-homogeneous linear fractional BVP (11) in the ith step. Moreover, the non-homogeneous term in (11) is determined from Equation (12) by using the known functions provided in the previous steps. Thus, a recursive procedure should be employed here to solve the considered sequence.

4.1. Approximate Solution

Although Theorem 4.1 suggests a closed-form expression for the solution of BVP (6)-(7), it is almost impossible to compute this solution in its present form since it is an infinite series. Hence, for the purpose of practical implementation, we need to truncate the series by considering its first M components where M is a positive integer number. Thus, the Mth-order approximate solution $x_M(t)$ becomes

$$x_M(t) = \sum_{i=1}^{M} \hat{x}_i(t). \tag{27}$$

To evaluate the value of M in Equation (27), the following criterion is considered according to the required accuracy. Indeed, the Mth-order approximate solution (27) has enough accuracy if for $\delta > 0$, a given positive constant, the two consecutive solutions $y_{M-1}(t)$ and $y_M(t)$ satisfy

$$\left\| x_M(t) - x_{M-1}(t) \right\|_\infty = \left\| \hat{x}_M(t) \right\|_\infty < \delta,\ t \in (0, T). \tag{28}$$

Here, we present an iterative algorithm to design an approximate solution with enough accuracy.

Algorithm:

Step 1. Determine the first-order term $\hat{x}_1(t)$ from Equation (10) and set $i = 2$.
Step 2. Determine the ith-order term $\hat{x}_i(t)$ from Equation (11).
Step 3. Set $M = i$. By using the expression (27), compute $x_M(t)$.
Step 4. If the condition (28) holds for a given small enough constant $\delta > 0$, go to Step 5; else, replace i by $i + 1$ and go to Step 2.
Step 5. Consider $x_M(t)$ as the appropriate approximate solution.

TABLE 1 | The suggested technique at different iterations for Example 5.1.

i (iteration time)	$\|y_i(t) - y_{i-1}(t)\|_\infty$
1	-
2	2.2×10^{-3}
3	4.6574×10^{-6}
4	1.2394×10^{-8}
5	3.7049×10^{-11}
6	1.1878×10^{-13}
7	3.9916×10^{-16}
8	1.3874×10^{-18}
9	4.9470×10^{-21}
10	1.7993×10^{-23}

5. NUMERICAL SIMULATIONS

In this part, four numerical examples are employed in order to verify the effectiveness of the new suggested technique. Here, we consider the examples form [13, 14] for the purpose of comparison with the other existing results.

Example 5.1. *Consider a fractional BVP in the form below*

$$\begin{cases} {}_0^C\mathscr{D}_t^\alpha x(t) = e^{-t}x^2(t),\ 5 < \alpha \leq 6,\ t \in (0, 1), \\ x^{(2k)}(0) = 1,\ x^{(2k)}(1) = e,\ k = 0, 1, 2, \end{cases} \tag{29}$$

whose exact solution is $x(t) = e^t$ *for* $\alpha = 6$.

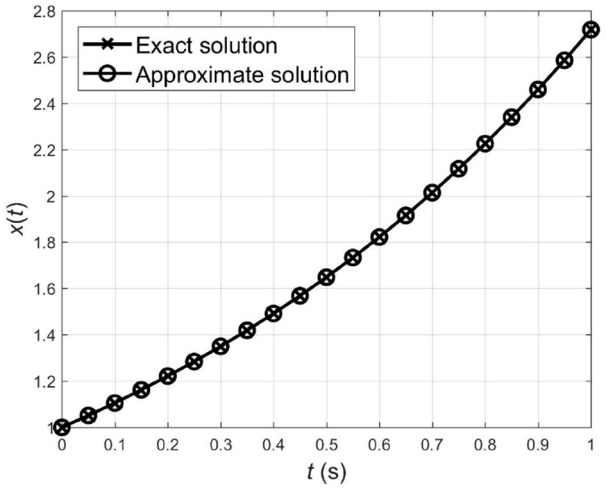

FIGURE 1 | Simulation curves of the exact solution and the second-order approximate solution for Example 5.1.

TABLE 2 | Numerical comparison between the proposed iterative method and the other approximation techniques for Example 5.1.

t	Exact solution	Absolute error*	
		HPM [13] and VIM [14]	Proposed method ($M = 2$)
0.0	1.000000000	0.000000	0.000000
0.1	1.105170918	4.56500×10^{-5}	$9.196986030 \times 10^{-5}$
0.2	1.221402758	1.1522210×10^{-3}	$2.207276648 \times 10^{-4}$
0.3	1.349858808	4.4830030×10^{-3}	$3.678794412 \times 10^{-4}$
0.4	1.491824698	1.1323624×10^{-2}	$7.357588824 \times 10^{-4}$
0.5	1.648721271	2.3094929×10^{-2}	$3.678794412 \times 10^{-4}$
0.6	1.822118800	4.1367190×10^{-2}	$7.357588824 \times 10^{-4}$
0.7	2.013752707	6.7875828×10^{-2}	$7.357588824 \times 10^{-4}$
0.8	2.225540928	$1.04538781 \times 10^{-1}$	$8.829106592 \times 10^{-4}$
0.9	2.459603111	$1.53475695 \times 10^{-1}$	$1.839397206 \times 10^{-3}$
1.0	2.718281828	$2.17029144 \times 10^{-1}$	0.000000

* |*Exact solution* − *Approximate solution*|.

Following the new technique as in section 4, we solve the presented sequence of fractional BVPs (10)-(11) in a recursive manner. Simulation results up to 10th iteration for $\alpha = 6$ are reported in **Table 1**. As is shown, the error is reduced further by considering more components of $x(t)$. To achieve an approximate solution with enough accuracy, the new algorithm is applied with $\delta = 0.01$. From **Table 1**, we observe that the convergence is achieved just in the second step, i.e., $\left\|x_2(t) - x_1(t)\right\|_\infty = 2.2 \times 10^{-3} < \delta$. Simulation curve of $x_2(t)$ and the exact solution are plotted in **Figure 1**. This figure indicates that the second-order approximate solution is in good agreement with the exact solution.

The problem (31) for $\alpha = 6$ has also been solved by using the HPM [13] and the VIM [14], respectively. Notice that the results of both methods are exactly the same as shown in Noor et al. [14]. **Table 2** depicts the exact solution and the absolute errors achieved by applying two iterations of the HPM, VIM, and the proposed technique in this paper. Comparative results in this table verify the superiority of the suggested algorithm compared to the other approximation methods available in the literature.

TABLE 3 | The suggested technique at different iterations for Example 5.2.

i (iteration time)	$\left\|y^{(i)}(t) - y^{(i-1)}(t)\right\|_\infty$
1	-
2	1.3343×10^{-5}
3	4.3500×10^{-10}
4	1.8102×10^{-14}
5	8.4664×10^{-19}
6	4.2478×10^{-23}
7	2.2340×10^{-27}
8	1.2153×10^{-31}
9	6.7823×10^{-36}
10	3.8611×10^{-40}

Example 5.2. *Consider the following non-linear BVP of fractional-order*

$$\begin{cases} {}_0^C\mathscr{D}_t^\alpha x(t) = e^t x^2(t),\ 5 < \alpha \le 6,\ t \in (0,1), \\ x(0) = 1,\ \dot{x}(0) = -1,\ \ddot{x}(0) = 1, \\ x(1) = e^{-1},\ \dot{x}(1) = -e^{-1},\ \ddot{x}(1) = e^{-1}, \end{cases} \tag{30}$$

whose exact solution is in the form $x(t) = e^{-t}$ *for* $\alpha = 6$.

Following the same procedure as in Example 5.1, we report the simulation results up to 10th iteration in **Table 3**. This table shows that considering more components of $x(t)$ provides more precise results. From this table, it is also indicated that the proposed algorithm with $\delta = 10^{-4}$ converges after only two iterations, i.e., $\left\|x_2(t) - x_1(t)\right\|_\infty = 1.3343 \times 10^{-5} < \delta$. In **Figure 2**, the simulation curve of $x_2(t)$ is compared with the exact solution. Comparative results indicate that the second-order approximate solution is very close to the exact solution. **Figure 3** shows the relation between the iteration time and the error given by the expression (28) using infinite norm for Examples 5.1 and 5.2. In this figure, the logarithmic scale is applied for the vertical axis. This figure verifies that the error decreases significantly as the iteration time increases.

The problem given by Equation (32) for $\alpha = 6$ has also been solved by using the HPM and the VIM in Noor and Mohyud-Din [13] and Noor et al. [14], respectively. As can be seen in Noor et al. [14], the results of both methods are exactly the same. **Table 4** exhibits the exact solution along with the absolute errors related to the HPM, VIM, and the proposed iterative algorithm. Comparing the results shows that the new approach is superior to the other existing methods.

Example 5.3. *Consider the following non-linear fractional BVP*

$$\begin{cases} {}_0^C\mathscr{D}_t^\alpha x(t) = E_\alpha(-t^\alpha)x^2(t),\ 5 < \alpha \le 6,\ t \in (0,1), \\ x^{(2k)}(0) = E_\alpha^{(2k)}(t^\alpha)\Big|_{t=0},\ x^{(2k)}(1) = E_\alpha^{(2k)}(t^\alpha)\Big|_{t=1},\ k = 0,1,2, \end{cases} \tag{31}$$

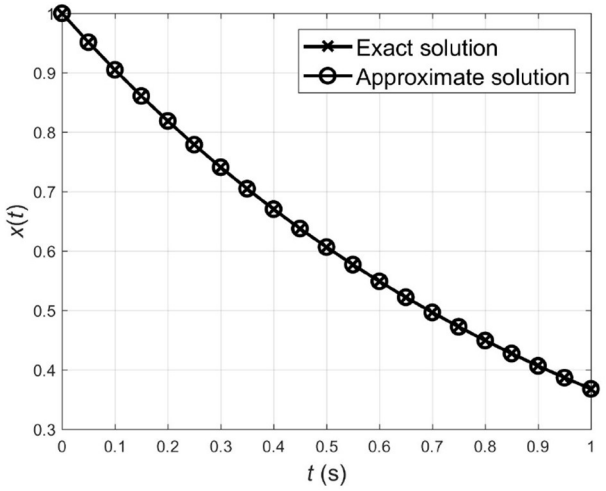

FIGURE 2 | Simulation curves of the exact solution and the second-order approximate solution for Example 5.2.

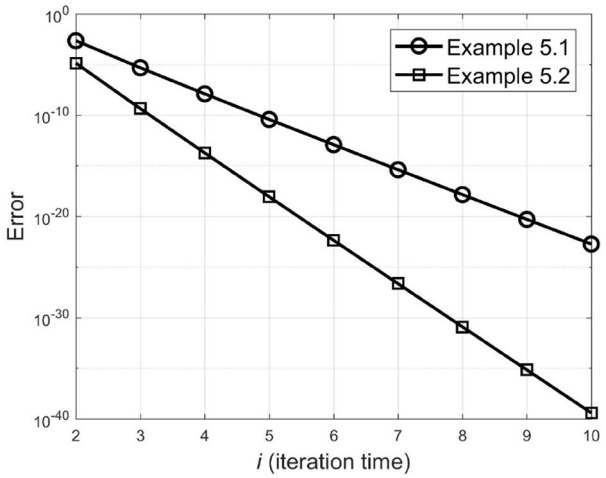

FIGURE 3 | Relation between the iteration time and the error for Examples 5.1 and 5.2.

whose exact solution is $x(t) = E_\alpha(t^\alpha)$ *where* $E_\alpha(\cdot)$ *is known as the Mittag-Leffler function.*

Simulation curve of $x_2(t)$, i.e., the second-order approximate solution, for different values of α are plotted in **Figure 4A**. This figure indicates that the approximate solution tends to the classic integer solution for $\alpha = 6$ when $\alpha \to 6$ as expected.

Example 5.4. *Consider the non-linear fractional BVP*

$$\begin{cases} {}_0^C\mathscr{D}_t^\alpha x(t) = E_\alpha(t^\alpha)x^2(t),\ 5 < \alpha \le 6,\ t \in (0,1), \\ x^{(k)}(0) = E_\alpha^{(k)}(-t^\alpha)\Big|_{t=0},\ x^{(k)}(1) = E_\alpha^{(k)}(-t^\alpha)\Big|_{t=1},\ k = 0,1,2, \end{cases} \tag{32}$$

TABLE 4 | Numerical comparison between the proposed iterative method and the other approximation techniques for Example 5.2.

		Absolute error*	
t	Exact solution	HPM [13] and VIM [14]	Proposed method ($M = 2$)
0.0	1.000000000	0.000000	0.000000
0.1	0.9048374180	1.6258200×10^{-4}	1.4715178×10^{-4}
0.2	0.8187307531	1.2692469×10^{-3}	1.2140022×10^{-3}
0.3	0.7408182207	4.1817793×10^{-3}	5.3342519×10^{-4}
0.4	0.6703200460	9.6799540×10^{-3}	8.8291066×10^{-4}
0.5	0.6065306597	1.8469340×10^{-2}	5.5181916×10^{-4}
0.6	0.5488116361	3.1188364×10^{-2}	0.000000
0.7	0.4965853038	4.8414696×10^{-2}	5.5181916×10^{-4}
0.8	0.4493289641	7.0671036×10^{-2}	5.8860711×10^{-4}
0.9	0.4065696597	9.8430340×10^{-2}	3.3109150×10^{-3}
1.0	0.3678794412	1.3212056×10^{-1}	0.000000

* |*Exact solution* − *Approximate solution*|.

whose exact solution is $x(t) = E_\alpha(-t^\alpha)$.

In the same way as in Example 5.3, **Figure 4B** depicts the second-order approximate solution tending to the classic integer solution as α goes to 6.

6. CONCLUSION

This paper studied a new iterative scheme to provide the solution of non-linear fractional BVPs in terms of a uniformly convergent series. The proposed procedure was free from perturbation, discretization, linearization, or restrictive assumptions. Furthermore, contrary to the other approximation schemes such as ADM [12] and VIM [14], the suggested technique kept away from calculating the Adomian's polynomials or identifying the Lagrange multipliers, respectively. Hence, from practical viewpoint, the suggested technique is more efficient than the above-mentioned approximation methods. Simulation results, demonstrating the efficacy, high accuracy, and simplicity of the proposed method, were also included. In the following, we summarize the main aspects of our numerical findings. **Tables 1**, **3** provided the simulation results up to 10th iteration, and **Figure 3** depicted the relation between the iteration time and the error given by the expression (28). From these results it is obvious that the error is reduced further by considering more components of $x(t)$. Simulation curves in **Figures 1**, **2** also indicated that the second-order approximate solution is in good agreement with the exact solution. **Tables 2**, **4** exhibited the exact solution and the absolute error derived by employing two iterations of the HPM [13], VIM [14], and our new iterative algorithm. These tables clearly indicated the improvements made by employing the proposed method. The simulation curves for different values of α were given in **Figures 4A,B** verifying that the numerical approximate solution for $\alpha < 6$ tends to the classic integer solution as $\alpha \to 6$. Future works can be focused on

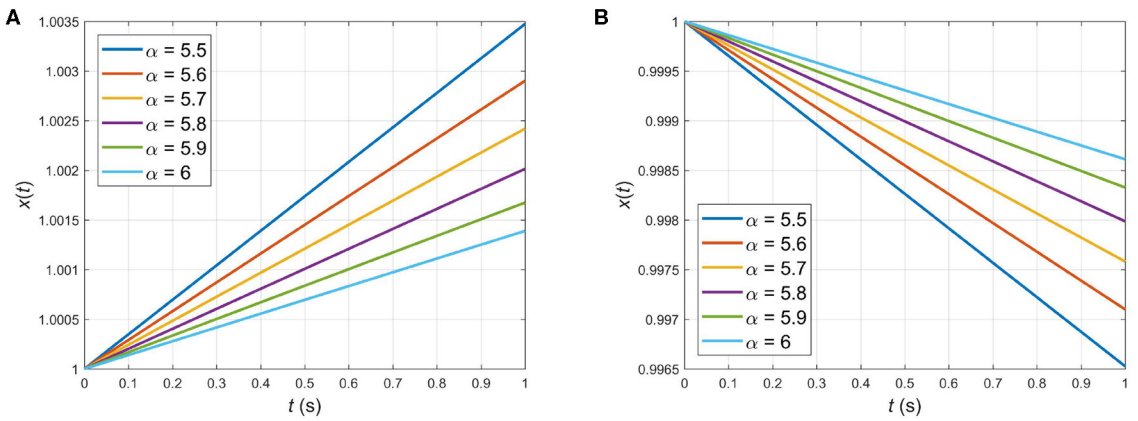

FIGURE 4 | Simulation curves of the second-order approximate solution for $\alpha = 5.5, 5.6, 5.7, 5.8, 5.9, 6$ [**(A)** Example 5.3 and **(B)** Example 5.4].

extending the suggested numerical technique to solve other types of BVPs.

DATA AVAILABILITY STATEMENT

All datasets generated for this study are included in the article/supplementary material.

AUTHOR CONTRIBUTIONS

All authors contributed equally to each part of this work. All authors read and approved the final manuscript.

FUNDING

This research was in part supported by a grant from University of Bojnord (No. 97/367/18077).

REFERENCES

1. Toomore J, Zahn JP, Latour J, Spiegel EA. Stellar convection theory II: single-mode study of the second convection zone in A-type stars. *Astrophys J*. (1976) **207**:545–63. doi: 10.1086/154522
2. Glatzmaier GA. Numerical simulations of stellar convection dynamics III: at the base of the convection zone. *Geophys Astrophys Fluid Dyn*. (1985) **31**:137–50. doi: 10.1080/03091928508219267
3. Chandrasekhar S. Hydrodynamics and Hydromagnetic Stability. New York, NY: Dover (1981).
4. Baldwin P. A localized instability in a Benard layer. *Appl Anal*. (1987) **24**:1127–56. doi: 10.1080/00036818708839658
5. Khalid A, Naeem MN, Ullah Z, Ghaffar A, Baleanu D, Nisar KS, et al. Numerical solution of the boundary value problems arising in magnetic fields and cylindrical shells. *Mathematics*. (2019) **7**:508. doi: 10.3390/math7060508
6. Akgul A, Akgul EK, Khan Y, Baleanu D. Solving the nonlinear system of third-order boundary value problems. In: Tas K, Baleanu D, Machado J, editors. *Mathematical Methods in Engineering. Nonlinear Systems and Complexity*. Cham: Springer (2019). p. 24. doi: 10.1007/978-3-319-90972-1_8
7. Akgul A, Akgul EK, Baleanu D, Inc M. New numerical method for solving tenth order boundary value problems. *Mathematics*. (2018) **6**:245. doi: 10.3390/math6110245
8. Agarwal RP. Boundary Value Problems for Higher Order Differential Equations. Singapore: World Scientific (1986).
9. Boutayeb A, Twizell EH. Numerical methods for the solution of special sixth-order boundary value problems. *Int J Comput Math*. (1992) **45**:207–233. doi: 10.1080/00207169208804130
10. Twizell EH, Boutayeb A. Numerical methods for the solution of special and general sixth-order boundary value problems, with applications to Benard layer eigen value problem. *Proc R Soc A Math Phys Eng Sci*. (1990) **431**:433–50. doi: 10.1098/rspa.1990.0142
11. Twizell EH. Numerical methods for sixth-order boundary value problems. In: Agarwal RP, Chow YM, Wilson SJ, editors. *Numerical Mathematics Singapore 1988. International Series of Numerical Mathematics*. Basel: Birkhauser (1988). p. 495–506. doi: 10.1007/978-3-0348-6303-2_40
12. Al-Hayani W. Adomian decomposition method with Green's function for sixth-order boundary value problems. *Comput Math Appl*. (2011) **61**:1567–75. doi: 10.1016/j.camwa.2011.01.025
13. Noor MA, Mohyud-Din ST. Homotopy perturbation method for solving sixth order boundary value problems. *Comput Math Appl*. (2008) **55**:2953–72. doi: 10.1016/j.camwa.2007.11.026
14. Noor MA, Noor KI, Mohyud-Din ST. Variational iteration method for solving sixth-order boundary value problems. *Commun Nonlinear Sci Num Simu*. (2009) **14**:2571–80. doi: 10.1016/j.cnsns.2008.10.013
15. Kilbas AA, Srivastava HH, Trujillo JJ. Theory and Applications of Fractional Differential Equations. New York, NY: Elsevier (2006).
16. Baleanu D, Asad JH, Jajarmi A. The fractional model of spring pendulum: new features within different kernels. *Proc Roman Acad Ser A*. (2018) **19**:447–54.
17. Baleanu D, Asad JH, Jajarmi A. New aspects of the motion of a particle in a circular cavity. *Proc Roman Acad Ser A*. (2018) **19**:361–7.
18. Baleanu D, Jajarmi A, Mohammadi H, Rezapour S. A new study on the mathematical modelling of human liver with Caputo-Fabrizio fractional derivative. *Chaos Solitons Fractals*. (2020) **134**:109705. doi: 10.1016/j.chaos.2020.109705
19. Jajarmi A, Yusuf A, Baleanu D, Inc M. A new fractional HRSV model and its optimal control: a non-singular operator approach. *Phys A Stat Mech Appl*. (2020) **547**:123860. doi: 10.1016/j.physa.2019.123860
20. Mohammadi F, Moradi L, Baleanu D, Jajarmi A. A hybrid functions numerical scheme for fractional optimal control problems: application to non-analytic dynamical systems. *J Vibrat Control*. (2018) **24**:5030–43.
21. Jajarmi A, Arshad S, Baleanu D. A new fractional modelling and control strategy for the outbreak of dengue fever. *Phys A Stat Mech Appl*. (2019) **535**:122524. doi: 10.1016/j.physa.2019.122524

22. Jajarmi A, Baleanu D, Sajjadi SS, Asad JH. A new feature of the fractional Euler-Lagrange equations for a coupled oscillator using a nonsingular operator approach. *Front Phys*. (2019) **7**:196. doi: 10.3389/fphy.2019.00196
23. Jajarmi A, Ghanbari B, Baleanu D. A new and efficient numerical method for the fractional modelling and optimal control of diabetes and tuberculosis co-existence. *Chaos*. (2019) **29**:093111. doi: 10.1063/1.5112177
24. Baleanu D, Jajarmi A, Sajjadi SS, Mozyrska D. A new fractional model and optimal control of a tumor-immune surveillance with non-singular derivative operator. *Chaos*. (2019) **29**:083127. doi: 10.1063/1.5096159
25. Baleanu D, Sajjadi SS, Jajarmi A, Asad JH. New features of the fractional Euler-Lagrange equations for a physical system within non-singular derivative operator. *Eur Phys J Plus*. (2019) **134**:181. doi: 10.1140/epjp/i2019-12561-x
26. Baleanu D, Jajarmi A, Sajjadi SS, Asad JH. The fractional features of a harmonic oscillator with position-dependent mass. *Commun Theor Phys*. (2020) **72**:055002. doi: 10.1088/1572-9494/ab7700
27. Yıldız TA, Jajarmi A, Yıldız B, Baleanu D. New aspects of time fractional optimal control problems within operators with nonsingular kernel. *Discrete Continuous Dyn Syst S*. (2020) **13**:407–28. doi: 10.3934/dcdss.2020023
28. Ali A, Shah K, Baleanu D. Ulam stability results to a class of nonlinear implicit boundary value problems of impulsive fractional differential equations. *Adv Diff Equat*. (2019) 2019:5. doi: 10.1186/s13662-018-1940-0
29. Ugurlu E, Baleanu D, Tas K. On the solutions of a fractional boundary value problem. *Turkish J Math*. (2018) **42**:1307–11. doi: 10.3906/mat-1609-64
30. Baleanu D, Etemad S, Rezapour S. A hybrid Caputo fractional modeling for thermostat with hybrid boundary value conditions. *Bound Value Probl*. (2020) **2020**:64. doi: 10.1186/s13661-020-01361-0
31. Patnaik S, Sidhardh S, Semperlotti F. A Ritz-based finite element method for a fractional-order boundary value problem of nonlocal elasticity. arXiv preprint arXiv:200106885 (2020).
32. Salem A, Alzahrani F, Alnegga M. Coupled system of nonlinear fractional Langevin equations with multipoint and nonlocal integral boundary conditions. *Math Probl Eng*. (2020) **2020**:7345658. doi: 10.1155/2020/7345658
33. Fazli H, Sun H, Aghchi S. Existence of extremal solutions of fractional Langevin equation involving nonlinear boundary conditions. *Int J Comput Math*. (2020) doi: 10.1080/00207160.2020.1720662
34. Zhang S, Su X. The existence of a solution for a fractional differential equation with nonlinear boundary conditions considered using upper and lower solutions in reverse order. *Comput Math Appl*. (2011) **62**:1269–1274. doi: 10.1016/j.camwa.2011.03.008
35. Arqub OA, El-Ajou A, Zhour ZA, Momani S. Multiple solutions of nonlinear boundary value problems of fractional order: a new analytic iterative technique. *Entropy*. (2014) **16**:471–93. doi: 10.3390/e16010471
36. Khalil H, Al-Smadi M, Moaddy K, Khan RA, Hashim I. Toward the approximate solution for fractional order nonlinear mixed derivative and nonlocal boundary value problems. *Discrete Dyn Nat Soc*. (2016) **2016**:5601821. doi: 10.1155/2016/5601821
37. Cui Y, Sun Q, Su X. Monotone iterative technique for nonlinear boundary value problems of fractional order $p \in (2, 3]$. *Adv Diff Equat*. (2017) **2017**:248. doi: 10.1186/s13662-017-1314-z
38. Asaduzzaman M, Ali MZ. Existence of positive solution to the boundary value problems for coupled system of nonlinear fractional differential equations. *AIMS Math*. (2019) **4**:880–95. doi: 10.3934/math.2019.3.880
39. Diethelm K. (2010). Multi-term caputo fractional differential equations. In: *The Analysis of Fractional Differential Equations. Lecture Notes in Mathematics*, Vol. 2004. Berlin; Heidelberg: Springer (2010). doi: 10.1007/978-3-642-14574-2_8

Conflict of Interest: The authors declare that the research was conducted in the absence of any commercial or financial relationships that could be construed as a potential conflict of interest.

Copyright © 2020 Jajarmi and Baleanu. This is an open-access article distributed under the terms of the Creative Commons Attribution License (CC BY). The use, distribution or reproduction in other forums is permitted, provided the original author(s) and the copyright owner(s) are credited and that the original publication in this journal is cited, in accordance with accepted academic practice. No use, distribution or reproduction is permitted which does not comply with these terms.

frontiers in Physics

ORIGINAL RESEARCH
published: 04 September 2020
doi: 10.3389/fphy.2020.00275

Computational Results With Non-singular and Non-local Kernel Flow of Viscous Fluid in Vertical Permeable Medium With Variant Temperature

Muhammad B. Riaz[1,2], *Syed T. Saeed*[3]*, *Dumitru Baleanu*[4,5] and *Muhammad M. Ghalib*[6]

[1] Department of Mathematics, University of Management and Technology, Lahore, Pakistan, [2] Institute for Groundwater Studies (IGS), University of the Free State, Bloemfontein, South Africa, [3] Department of Science & Humanities, National University of Computer and Emerging Sciences, Lahore, Pakistan, [4] Department of Mathematics, Çankaya University, Ankara, Turkey, [5] Department of Medical Research, China Medical University Hospital, China Medical University, Taichung City, Taiwan, [6] Department of Mathematics and Statistics, The University of Lahore, Lahore, Pakistan

This present article explores the transversal magnetized flow of a viscous fluid. The flow is confined to a vertical wall, saturated in permeable medium, along with ramped wall temperature. In this study, the conjugate impact of heat and mass transfer with slip and non-slip conditions are considered in the velocity field and energy equation. The dimensionless Atangana-Baleanu fractional governing equations are derived with Laplace transformation. Computational results are expressed graphically with the effect of various physical parameters. Comparative graphical analysis of the Atangana-Baleanu derivative for temperature, concentration and velocity field, with slip and non-slip impact, shows that the memory effects of the Atangana-Baleanu derivative are better than the results that exist in the literature.

Keywords: slip effect, heat and mass transfer, conjugate effect, magnetic effect, Stehfest's algorithm, fractional derivative

OPEN ACCESS

Edited by:
Zakia Hammouch,
Moulay Ismail University, Morocco

Reviewed by:
Marin I. Marin,
Transilvania University of Braşov, Romania
Kashif Ali Abro,
Mehran University of Engineering and Technology, Pakistan

***Correspondence:**
Syed T. Saeed
tauseefsaeed301@gmail.com

Specialty section:
This article was submitted to Mathematical and Statistical Physics, a section of the journal Frontiers in Physics

Received: *16 March 2020*
Accepted: *19 June 2020*
Published: *04 September 2020*

Citation:
Riaz MB, Saeed ST, Baleanu D and Ghalib MM (2020) Computational Results With Non-singular and Non-local Kernel Flow of Viscous Fluid in Vertical Permeable Medium With Variant Temperature. Front. Phys. 8:275. doi: 10.3389/fphy.2020.00275

1. INTRODUCTION

In nature, heat and mass transfer is a common conjugate phenomenon for chemical reaction, evaporation, and condensation caused by temperature and concentration. Consequently, the behavior of heat transfer exists in different practical applications. The heat transfer mechanism is linked with mass, to jointly produce electrically conducting fluid flow with a conjugate effect. In a preamble surface the process of thermal and mass transfer with a conjugate effect have different applications in the area of nuclear production, industry, oil production, and engineering disciplines [1, 2]. The conjugate effect with convection flow over an infinite plate in preamble medium, along time dependent velocity, electrically flow with a magnetic effect and have been studied by different researchers. Ramped wall temperatures with thermal radiation have received much interest in convection flow over boundless vertical plates [3–6]. In literature, Toki and Tokis [7] studied time dependent boundary conditions on viscous fluid over a boundless preamble plate. Senapatil et al. [8] investigated the influence of chemical parameters on viscous fluid over preamble medium with a bounded slip region. Khan et al. [9] discussed the influence of heat and mass diffusion of a viscous fluid over an oscillating plate. Das et al. [10] and Narahari and Ishaq [11] investigated the solution of unsteady Walter's fluids on convection flow over preamble medium with a magnetic effect and

constant suction heat. Recently, Kumar et al. [12] discussed the fractional model for radial fins with heat transfer. Some of the latest results, according to this research, are given in Gupta et al. [13], Khan et al. [14], and Imran et al. [15].

Moreover, the application of magnetic fields is significant, with heat transfer in different situations of flow of an incompressible fluid, for example, geothermal energy, magnetic generator, and metallurgical processes. The influence of the slip and non-slip condition with the magnetic field and chemical reaction of an electrically conducting fluid over a porous surface, have been developed by Boussinesqu's approximation [16]. Jha and Apere [17] and Seth et al. [18] analyzed the ion slip and hall effect boundary conditions on a magnetized electrically conducting flow between parallel plates. The impact of the current and rotation with heat radiation and mass transfer, on time depending heat observation over a preamble surface, were taken into account. Over the last few years, fractional calculus has played a significant role in viscoelastic models. The derivative of the fractional order can be achieved by constitutive equations of well-known models through time ordinary derivatives. Recently, many fractional time derivative problems have been studied [19, 20]. Different real life problems have been investigated through fractional time operators [21–23]. A modern fractional approach has been presented without a singular kernel. A non-singular kernel is used to find the solution for MHD convection flow with ramped temperature, was investigated by Riaz et al. [24]. Furthermore, Riaz and Saeed [25] discussed the solution of MHD Oldroyd-B fluid using integer and fractional order derivatives with slip effect and time boundary conditions. The Study of natural convection flow with in channel using non-singular kernels is discussed by Saeed et al. [26].

In this paper, we discuss the computational calculation for the magnetized flow of Newtonian fluid with slip and conjugate effect, through a preamble surface. Computational results for the velocity profile, temperature gradient, and concentration field are calculated with the Atangana-Baleanu fractional derivative, through the Laplace transform. Tzou and Stehfest's algorithm is used to find the inverse Laplace transform. Further, We show the strength of non-singular and non-kernels. Fractional order Atangana-Baleanu (*ABC*) derivatives are used to analyze fractional parameters (memory effect) on the dynamics of fluid. We conclude that the fractional order model is best for memory effect and flow behavior of the fluid with reference to classical models. *ABC* is good at highlighting the dynamics of fluid. The influence of transverse magnetic fields are studied for *ABC* and *CF*. Moreover, the impact of parameters on the velocity profile are analyzed through numerical simulation and graphs for *ABC* and *CF* models. Expression from some limited and special cases were also obtained in terms of the velocity profile with different flow parameters.

2. MATHEMATICAL MODEL WITH STATEMENT OF THE PROBLEM

In this article, we assumed the slip effect between fluid and a wall. After $t = 0^+$, the temperature on the plate is enhanced or reduced to $\theta_\infty + (\theta_\omega - \theta_\infty)\frac{t}{t_o}$ when $t \leq t_o$ and therefore, for $t > t_o$, is retained at a constant temperature θ_ω and the concentration is enhanced to C_ω. The set of governing equations are given in [27]:

$$v_t = v_{\xi\xi} + G_r\theta + G_m C - K_p v - M^2 v, \tag{1}$$

$$\left(P_{reff}\right)\theta_t = \theta_{\xi\xi}, \tag{2}$$

$$S_c C_t = C_{\xi\xi}. \tag{3}$$

With suitable conditions

$$v(\xi,0) = 0, \theta(\xi,0) = \theta_\infty, C(\xi,0) = C_\infty, \quad \forall \xi \geq 0, \tag{4}$$

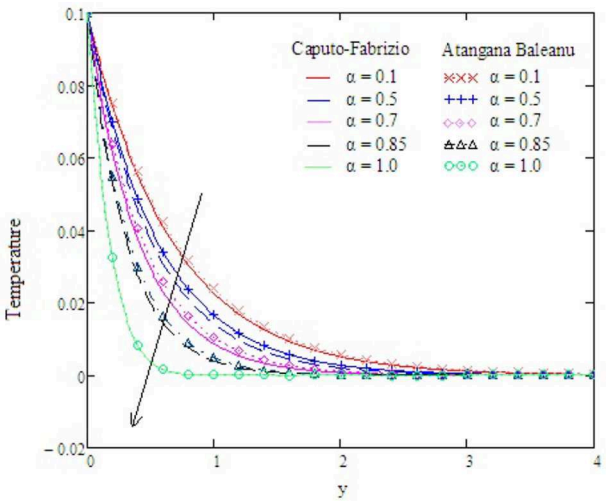

FIGURE 1 | Variations in temperature with altered values of α and other parameters are $k_p = 1.5$, $G_r = 2$, $P_{reff} = 0.1$, $G_m = 0.75$, $M = 0.9$, and $S_c = 0.5$.

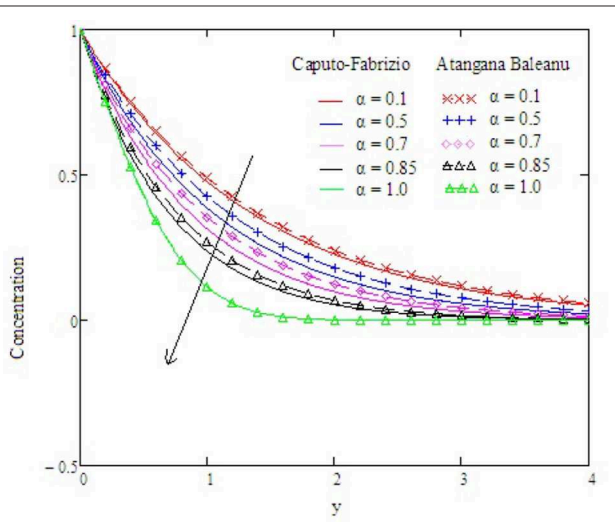

FIGURE 2 | Variations in concentration with altered values of α and other parameters are $k_p = 1.5$, $G_r = 2$, $P_{reff} = 0.1$, $G_m = 0.75$, and $M = 0.9$.

$$v(\xi,t) - L(v_\xi\ |_{\xi=0}) = \frac{f(t)}{\mu}, C(0,t) = C_\omega, \quad t > 0, \tag{5}$$

$$\theta(\xi,0) = \theta_\infty + (\theta_w - \theta_\infty)\frac{t}{t_o}, \quad 0 < t < t_o, \tag{6}$$

$$v(y,t) = \theta_\infty, C(y,t) = C_\infty, \quad t > 0,$$
$$\theta(y,t) = \theta_\omega, \quad t > t_o, y \to \infty. \tag{7}$$

We arrive at the governing equations, in terms of the Atangana-Baleanu fractional derivative, as:

$${}^{ABC}D_t^\alpha v = v_{\xi\xi} + G_r\theta + G_m C - k_p v - M^2 v, \tag{8}$$

$${}^{ABC}D_t^\alpha \theta = \left(\frac{1}{P_{reff}}\right)\theta_{\xi\xi}, \tag{9}$$

$${}^{ABC}D_t^\alpha C = \left(\frac{1}{S_c}\right)C_{\xi\xi}, \tag{10}$$

where ${}^{ABC}D_t^\alpha$ is the fractional differential operator of order $0 < \alpha < 1$ called the Atangana-Baleanu fractional operator as defined by [21, 28]:

$${}^{ABC}D_t^\alpha f(\xi,\tau) = \frac{M(\alpha)}{1-\alpha}\int_0^\tau \mathbf{E}_\alpha\left(-\frac{\alpha(t-\tau)^\alpha}{1-\alpha}\right)\frac{\partial f(\xi,\tau)}{\partial\tau}d\tau,$$

$$with \quad \sum_{m=0}^{\infty}\frac{(-t)^{\alpha m}}{\Gamma(1+\alpha m)} = \mathbf{E}_\alpha(-t)^\alpha, \tag{11}$$

where $M(\alpha)$ denotes a normalization function obeying $M(0) = M(1) = 1$.

The Laplace transform of Equation (11) is as follows [26]:

$$L\left[{}^{ABC}D_t^\alpha f(\xi,\tau)\right] = \frac{s^\alpha L[f(\xi,\tau)] - s^{\alpha-1}f(\xi,0)}{(1-\alpha)s^\alpha + \alpha}. \tag{12}$$

The appropriate initial and boundary conditions are:

$$v(\xi,0) = \theta(\xi,0) = C(\xi,0) = 0, \quad \forall\xi \geq 0, \tag{13}$$

$$v(\xi,t) - hv_\xi\ |_{\xi=0} = Z(t), \tag{14}$$

$$C(0,t) = 1,\ C(\infty,t) = 0,\ t > 0, \tag{15}$$

$$\theta(\infty,t) = 0,\ v(\infty,t) = 0,\ t > 0, \tag{16}$$

$$\theta(0,t) = t, \quad 0 < t \leq 1, \quad \theta(0,t) = 1, \quad t > 1. \tag{17}$$

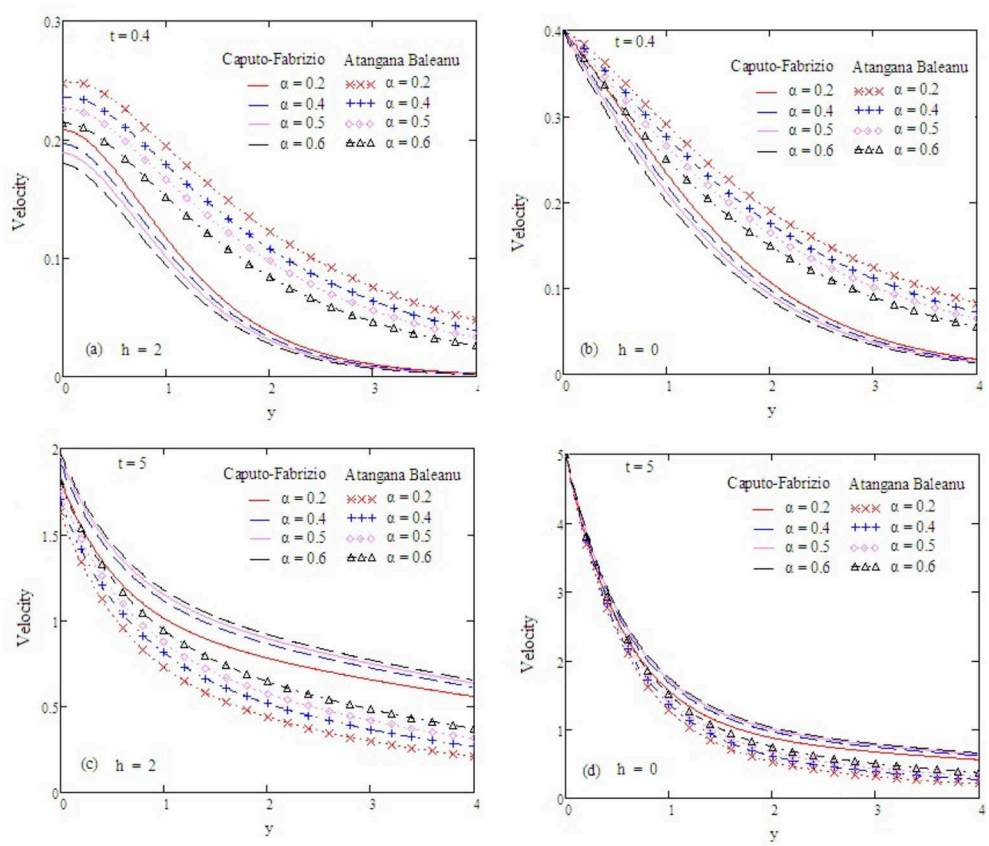

FIGURE 3 | Velocity profiles with altered values of α and other parameters are $k_p = 1.5$, $G_r = 2$, $P_{reff} = 0.1$, $G_m = 0.75$, $M = 0.9$, and $S_c = 0.5$.

3. SOLUTION OF THE PROBLEM

3.1. Distribution of Temperature Gradient With Fractional Model $0 < \alpha < 1$

In order to find the solution of fractional concentration distribution, we employ Equation (12) into Equation (9), and obtain:

$$\left(\frac{s^{\alpha}}{(1-\alpha)s^{\alpha}+\alpha}\right)\bar{\theta}(\xi,s)=\frac{1}{P_{reff}}\bar{\theta_{\xi\xi}}(\xi,s), \tag{18}$$

$$\bar{\theta}(\xi,s)=c_1 e^{-\xi\sqrt{P_{reff}\left(\frac{s^{\alpha}}{(1-\alpha)s^{\alpha}+\alpha}\right)}}+c_2 e^{\xi\sqrt{P_{reff}\left(\frac{s^{\alpha}}{(1-\alpha)s^{\alpha}+\alpha}\right)}}, \tag{19}$$

with the help of (13)–(17), we find the values of constants c_1 and c_2, and we have.

$$\bar{\theta}(\xi,s)=\left(\frac{1-e^{-s}}{s^2}\right)e^{-\xi\sqrt{P_{reff}\left(\frac{s^{\alpha}}{(1-\alpha)s^{\alpha}+\alpha}\right)}}. \tag{20}$$

3.2. Distribution of Concentration Gradient With Fractional Model $0 < \alpha < 1$

In order to find the solution of fractional concentration distribution, we employ Equation (12) into Equation (10), and obtain:

$$\left(\frac{s^{\alpha}}{(1-\alpha)s^{\alpha}+\alpha}\right)\bar{C}(\xi,s)=\frac{1}{S_c}\bar{C_{\xi\xi}}(\xi,s), \tag{21}$$

$$\bar{C}(\xi,s)=c_1 e^{-\xi\sqrt{S_c\left(\frac{s^{\alpha}}{(1-\alpha)s^{\alpha}+\alpha}\right)}}+c_2 e^{\xi\sqrt{S_c\left(\frac{s^{\alpha}}{(1-\alpha)s^{\alpha}+\alpha}\right)}}, \tag{22}$$

with the help of (13)–(17), we find the values of constants c_1 and c_2, and we have.

$$\bar{C}(\xi,s)=\left(\frac{1}{s}\right)e^{-\xi\sqrt{S_c\left(\frac{s^{\alpha}}{(1-\alpha)s^{\alpha}+\alpha}\right)}}. \tag{23}$$

3.3. Distribution of Velocity Field With Fractional Model $0 < \alpha < 1$

In order to find the solution of the fractional concentration distribution, we employ Equation (12) into Equation (8), and obtain:

$$\left(\frac{s^{\alpha}}{(1-\alpha)s^{\alpha}+\alpha}\right)\bar{v}(\xi,s)=v_{\xi\xi}+G_r\bar{\theta}(\xi,s)+G_m\bar{C}(\xi,s) - k_p\bar{v}(\xi,s)-M^2\bar{v}(\xi,s). \tag{24}$$

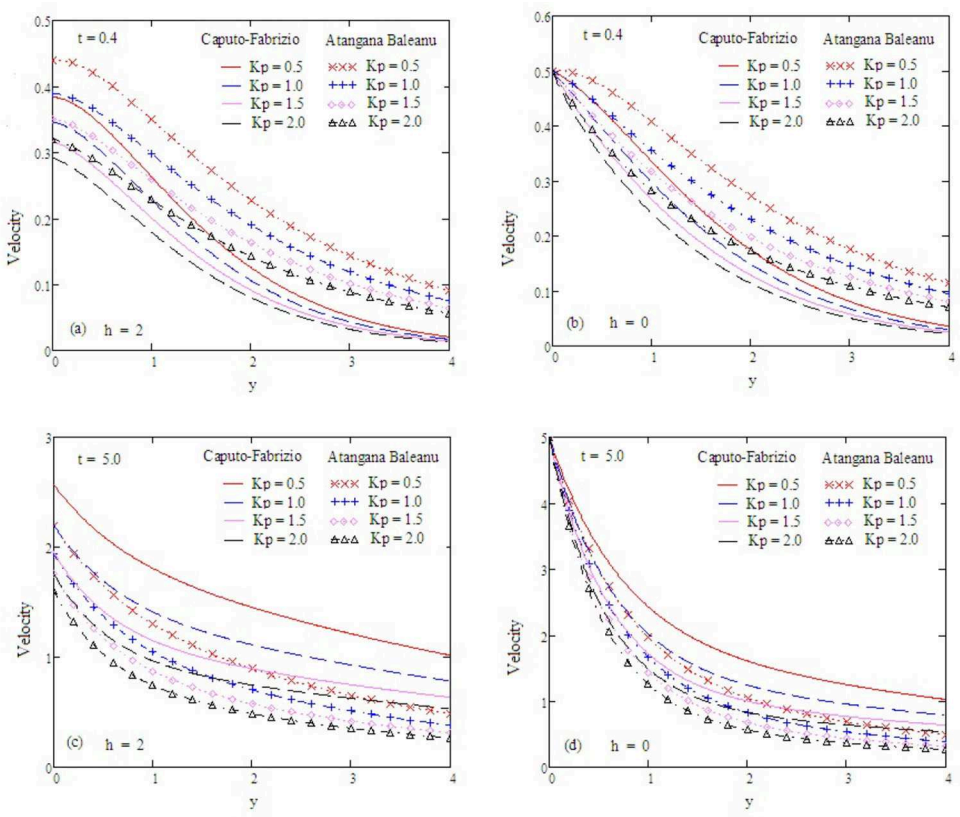

FIGURE 4 | Velocity profiles with altered values of k_p and other parameters are $G_r = 2$, $\alpha = 0.5$, $P_{reff} = 0.1$, $G_m = 0.75$, $M = 0.9$, and $S_c = 0.5$.

The solution of the homogeneous part of the second order partial differential equation say that (24) is,

$$\bar{v}(\xi,s) = c_1 e^{-\xi\sqrt{\left(\frac{s^\alpha}{(1-\alpha)s^\alpha+\alpha}\right)+k_p+M^2}} + c_2 e^{\xi\sqrt{\left(\frac{s^\alpha}{(1-\alpha)s^\alpha+\alpha}\right)+k_p+M^2}}. \tag{25}$$

The general solution can be give as follows, after making use of $\bar{\theta}(\xi,s)$ and $\bar{C}(\xi,s)$,

$$\begin{aligned}\bar{v}(\xi,s) = {} & c_1 e^{-\xi\sqrt{\left(\frac{s^\alpha}{(1-\alpha)s^\alpha+\alpha}\right)+k_p+M^2}} + c_2 e^{\xi\sqrt{\left(\frac{s^\alpha}{(1-\alpha)s^\alpha+\alpha}\right)+k_p+M^2}} \\ & - \frac{G_r(1-e^{-s})\Big((1-\alpha)s^\alpha+\alpha\Big)}{s^2\left(\frac{s^\alpha}{(1-\alpha)s^\alpha+\alpha}(P_{reff}-1)-(k_p+M^2)\right)} e^{-\xi\sqrt{P_{reff}\left(\frac{s^\alpha}{(1-\alpha)s^\alpha+\alpha}\right)}} \\ & - \frac{G_3\Big((1-\alpha)s^\alpha+\alpha\Big)}{s\left(\frac{s^\alpha}{(1-\alpha)s^\alpha+\alpha}(S_c-1)-(k_p+M^2)\right)} e^{-\xi\sqrt{S_c\left(\frac{s^\alpha}{(1-\alpha)s^\alpha+\alpha}\right)}}, \end{aligned} \tag{26}$$

with the help of Equations (13)–(17), we find the values of constants c_1 and c_2 for the velocity equation:

$$\begin{aligned}\bar{v}(\xi,s) = {} & \left[\frac{1}{1+h\sqrt{\frac{s^\alpha}{(1-\alpha)s^\alpha+\alpha}}+k_p+M^2}\right. \\ & \left\{\frac{G_r(1-e^{-s})}{s^2}\left(\frac{1+h\sqrt{s^\alpha P_{reff}}}{\frac{s^\alpha}{(1-\alpha)s^\alpha+\alpha}(P_{reff}-1)-(k_p+M^2)}\right)\right. \\ & \left.\left. + \frac{G_m}{s}\left(\frac{1+h\sqrt{s^\alpha S_c}}{\frac{s^\alpha}{(1-\alpha)s^\alpha+\alpha}(S_c-1)-(k_p+M^2)}\right)+Z(s)\right\}\right] \\ & \left(e^{-\xi\sqrt{\frac{s^\alpha}{(1-\alpha)s^\alpha+\alpha}+k_p+M^2}}\right) \\ & - \frac{G_r(1-e^{-s})}{s^2}\left(\frac{e^{-\xi\sqrt{s^\alpha P_{reff}}}}{\frac{s^\alpha}{(1-\alpha)s^\alpha+\alpha}(P_{reff}-1)-(k_p+M^2)}\right) \\ & - \frac{G_m}{s}\left(\frac{e^{-\xi\sqrt{s^\alpha S_c}}}{\frac{s^\alpha}{(1-\alpha)s^\alpha+\alpha}(S_c-1)-(k_p+M^2)}\right). \end{aligned} \tag{27}$$

The skin friction is defined as:

$$\bar{\tau}(\xi,s) = -\frac{\partial\bar{v}(\xi,s)}{\partial\xi}\,|_{\xi=0}, \tag{28}$$

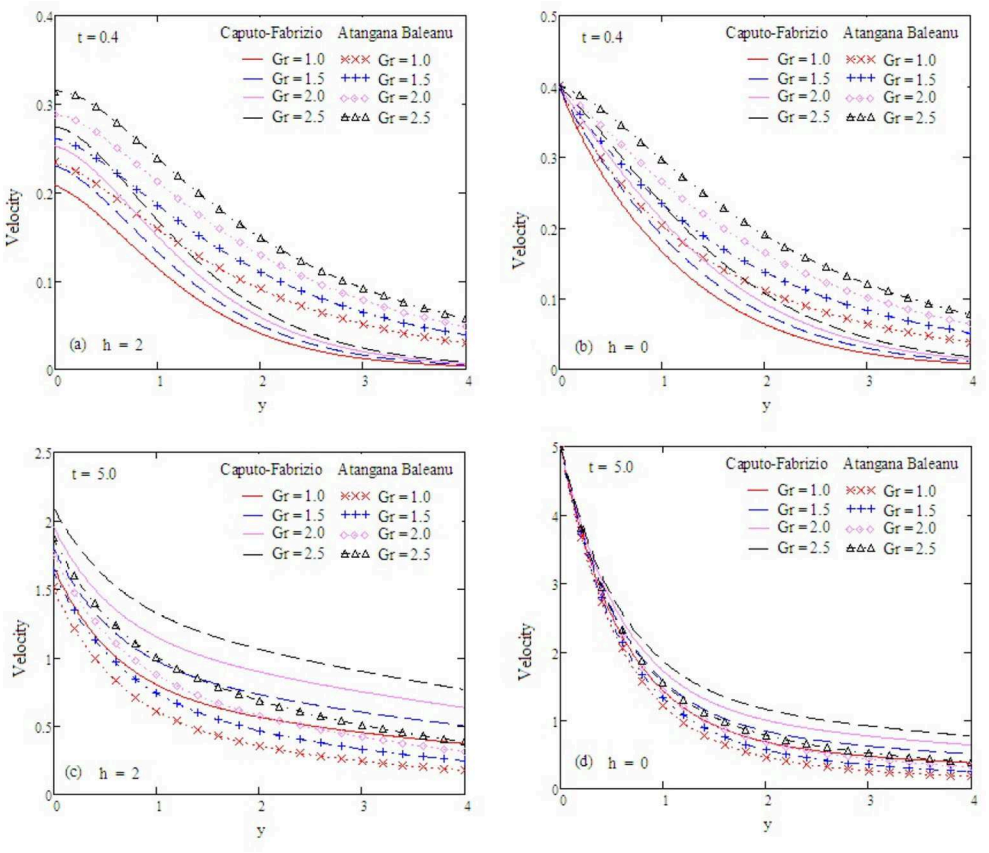

FIGURE 5 | Velocity profiles with altered values of G_r and other parameters are $k_p = 1.5$, $G_m = 0.75$, $P_{reff} = 0.1$, $\alpha = 0.5$, $M = 0.9$, and $S_c = 0.5$ $G_r = 2$.

$$\bar{\tau}(\xi,s)=\left[\frac{1}{1+h\sqrt{\frac{s^{\alpha}}{(1-\alpha)s^{\alpha}+\alpha}}+k_p+M^2}\right.$$
$$\left\{\frac{G_r(1-e^{-s})}{s^2}\left(\frac{1+h\sqrt{s^{\alpha}P_{reff}}}{\frac{s^{\alpha}}{(1-\alpha)s^{\alpha}+\alpha}(P_{reff}-1)-(k_p+M^2)}\right)\right.$$
$$\left.\left.+\frac{G_m}{s}\left(\frac{1+h\sqrt{s^{\alpha}S_c}}{\frac{s^{\alpha}}{(1-\alpha)s^{\alpha}+\alpha}(S_c-1)-(k_p+M^2)}\right)+Z(s)\right\}\right]$$
$$\left(\sqrt{\frac{s^{\alpha}}{(1-\alpha)s^{\alpha}+\alpha}+k_p+M^2}\right)$$
$$-\frac{G_r(1-e^{-s})}{s^2}\left(\frac{\sqrt{s^{\alpha}P_{reff}}}{\frac{s^{\alpha}}{(1-\alpha)s^{\alpha}+\alpha}(P_{reff}-1)-(k_p+M^2)}\right)$$
$$-\frac{G_m}{s}\left(\frac{\sqrt{s^{\alpha}S_c}}{\frac{s^{\alpha}}{(1-\alpha)s^{\alpha}+\alpha}(S_c-1)-(k_p+M^2)}\right). \quad (29)$$

4. LIMITING CASES

A comparative study of the existing literature and the Atangana-Baleanu derivative for some limiting cases are recovered from the general solution of (Equation 30, [27]) and the general solution of the given problem at Equation (27), are both discussed in this section.

4.1. Results With Ramped Wall Temperature and Without Porosity Effect ($k_p \to 0$)

The velocity profile with the Atangana-Baleanu derivative is expressed for a general solution of the given problem at Equation (27) is given as:

$$\bar{v}(\xi,s)=\left[\frac{1}{1+h\sqrt{\frac{s^{\alpha}}{(1-\alpha)s^{\alpha}+\alpha}}+M^2}\right.$$
$$\left\{\frac{G_r(1-e^{-s})}{s^2}\left(\frac{1+h\sqrt{s^{\alpha}P_{reff}}}{\frac{s^{\alpha}}{(1-\alpha)s^{\alpha}+\alpha}(P_{reff}-1)-M^2}\right)\right.$$
$$\left.\left.+\frac{G_m}{s}\left(\frac{1+h\sqrt{s^{\alpha}S_c}}{\frac{s^{\alpha}}{(1-\alpha)s^{\alpha}+\alpha}(S_c-1)-M^2}\right)+Z(s)\right\}\right]$$
$$\left(e^{-\xi\sqrt{\frac{s^{\alpha}}{(1-\alpha)s^{\alpha}+\alpha}+M^2}}\right)-\frac{G_r(1-e^{-s})}{s^2}$$
$$\left(\frac{e^{-\xi\sqrt{s^{\alpha}P_{reff}}}}{\frac{s^{\alpha}}{(1-\alpha)s^{\alpha}+\alpha}(P_{reff}-1)-M^2}\right)$$
$$-\frac{G_m}{s}\left(\frac{e^{-\xi\sqrt{s^{\alpha}S_c}}}{\frac{s^{\alpha}}{(1-\alpha)s^{\alpha}+\alpha}(S_c-1)-M^2}\right). \quad (30)$$

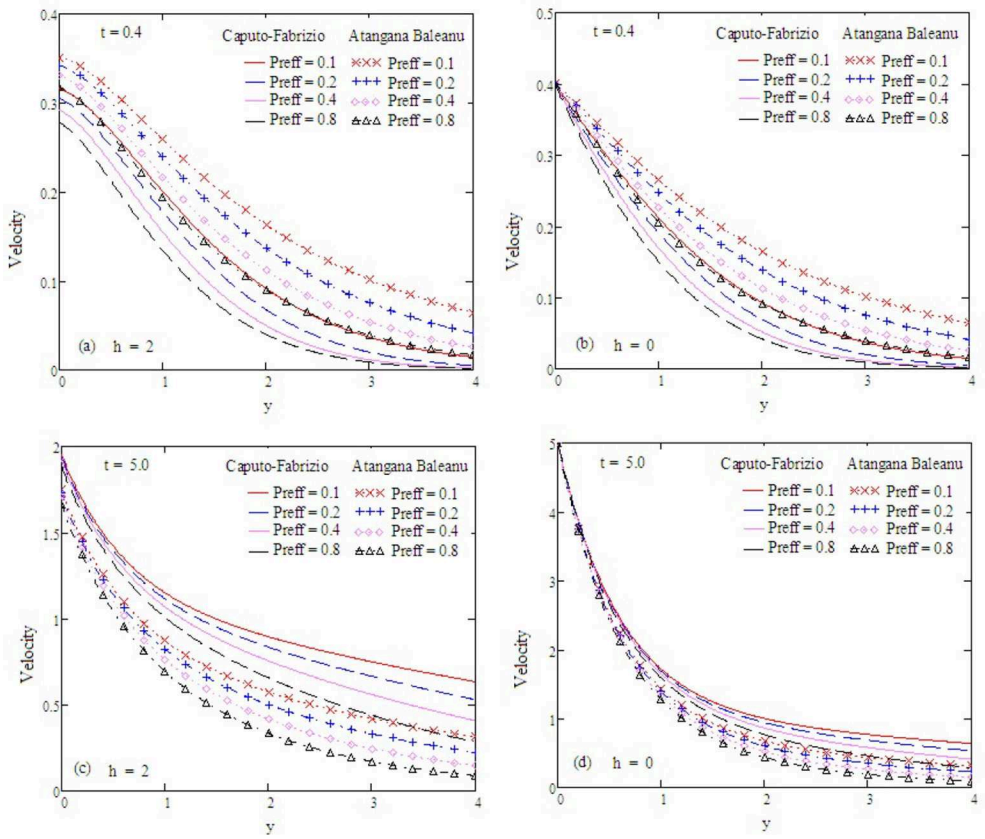

FIGURE 6 | Velocity profiles with altered values of P_{reff} and other parameters are $\alpha = 0.5$, $G_r = 2$, $M = 0.9$, $G_m = 0.75$, $k_p = 1.5$, and $S_c = 0.5$.

4.2. Results Without Thermal Radiation ($N_r \to 0$)

The velocity profile is obtained with the Atangana-Baleanu derivative for the general solution of the given problem at Equation (27) is given as:

$$\bar{v}(\xi,s) = \left[\frac{1}{1+h\sqrt{\frac{s^\alpha}{(1-\alpha)s^\alpha+\alpha}}+k_p+M^2}\right.$$
$$\left\{\frac{G_r(1-e^{-s})}{s^2}\left(\frac{1+h\sqrt{s^\alpha P_r}}{\frac{s^\alpha}{(1-\alpha)s^\alpha+\alpha}(P_r-1)-(k_p+M^2)}\right)\right.$$
$$\left.\left.+\frac{G_m}{s}\left(\frac{1+h\sqrt{s^\alpha S_c}}{\frac{s^\alpha}{(1-\alpha)s^\alpha+\alpha}(S_c-1)-(k_p+M^2)}\right)+Z(s)\right\}\right]$$
$$\left(e^{-\xi\sqrt{\frac{s^\alpha}{(1-\alpha)s^\alpha+\alpha}+k_p+M^2}}\right)$$
$$-\frac{G_r(1-e^{-s})}{s^2}\left(\frac{e^{-\xi\sqrt{s^\alpha P_r}}}{\frac{s^\alpha}{(1-\alpha)s^\alpha+\alpha}(P_r-1)-(k_p+M^2)}\right)$$
$$-\frac{G_m}{s}\left(\frac{e^{-\xi\sqrt{s^\alpha S_c}}}{\frac{s^\alpha}{(1-\alpha)s^\alpha+\alpha}(S_c-1)-(k_p+M^2)}\right). \quad (31)$$

4.3. Result Without Magnetic Parameter ($M \to 0$)

The velocity profile is obtained with the Atangana-Baleanu derivative for the general solution of the given problem at Equation (27) is given as:

$$\bar{v}(\xi,s) = \left[\frac{1}{1+h\sqrt{\frac{s^\alpha}{(1-\alpha)s^\alpha+\alpha}}+k_p}\right.$$
$$\left\{\frac{G_r(1-e^{-s})}{s^2}\left(\frac{1+h\sqrt{s^\alpha P_{reff}}}{\frac{s^\alpha}{(1-\alpha)s^\alpha+\alpha}(P_{reff}-1)-k_p}\right)+\frac{G_m}{s}\right.$$
$$\left.\left.\left(\frac{1+h\sqrt{s^\alpha S_c}}{\frac{s^\alpha}{(1-\alpha)s^\alpha+\alpha}(S_c-1)-k_p}\right)+Z(s)\right\}\right]\left(e^{-\xi\sqrt{\frac{s^\alpha}{(1-\alpha)s^\alpha+\alpha}+k_p}}\right)$$
$$-\frac{G_r(1-e^{-s})}{s^2}\left(\frac{e^{-\xi\sqrt{s^\alpha P_{reff}}}}{\frac{s^\alpha}{(1-\alpha)s^\alpha+\alpha}(P_{reff}-1)-k_p}\right)$$
$$-\frac{G_m}{s}\left(\frac{e^{-\xi\sqrt{s^\alpha S_c}}}{\frac{s^\alpha}{(1-\alpha)s^\alpha+\alpha}(S_c-1)-k_p}\right). \quad (32)$$

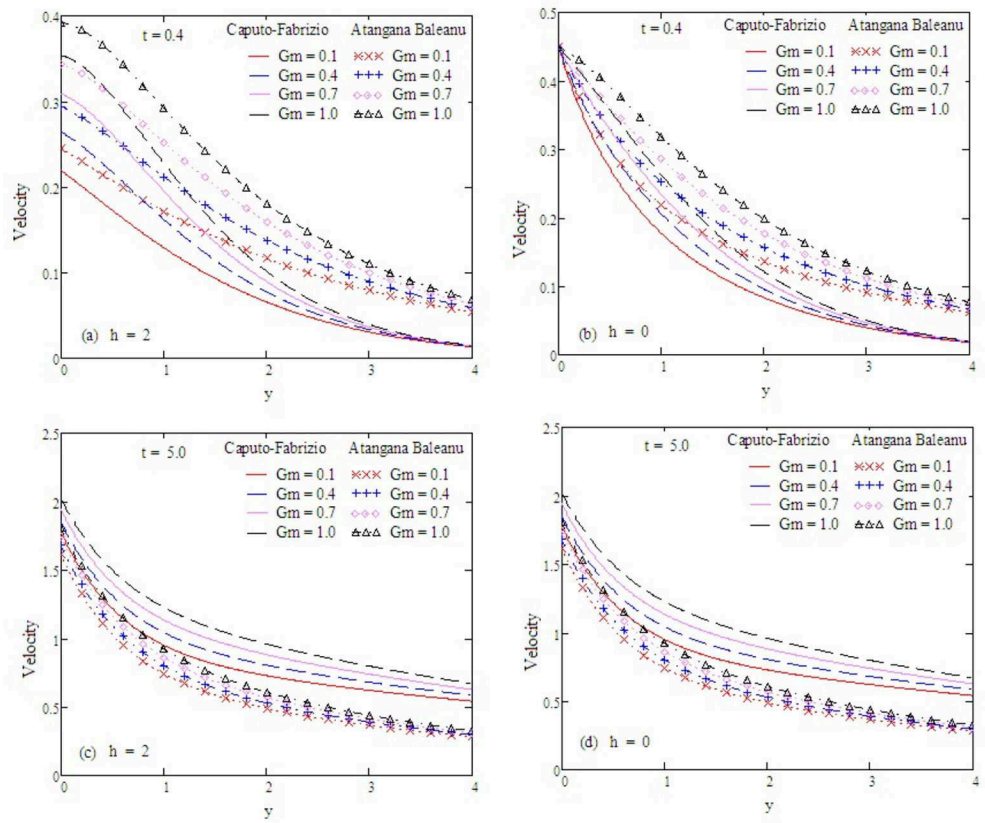

FIGURE 7 | Velocity profiles with altered values of G_m and other parameters are $\alpha = 0.5$, $G_r = 2$, $P_{reff} = 0.1$, $k_p = 1.5$, $M = 0.9$, and $S_c = 0.5$.

5. SPECIAL CASES

For validation and to check our general results in this section, we will discuss some special cases by customizing the value of $f(t)$. Moreover, our aim is to provide a comparison of our results with the Caputo-Fabrizio (*CF*) time fractional derivative.

5.1. Case-I

By putting $z(t) = t$ into Equation (27), we obtain a suitable result for the velocity profile:

$$\bar{v}(\xi,s) = \left[\frac{1}{1+h\sqrt{\frac{s^\alpha}{(1-\alpha)s^\alpha+\alpha}}+k_p+M^2}\right.$$
$$\left\{\frac{G_r(1-e^{-s})}{s^2}\left(\frac{1+h\sqrt{s^\alpha P_{reff}}}{\frac{s^\alpha}{(1-\alpha)s^\alpha+\alpha}(P_{reff}-1)-(k_p+M^2)}\right)\right.$$
$$\left.\left.+\frac{G_m}{s}\left(\frac{1+h\sqrt{s^\alpha S_c}}{\frac{s^\alpha}{(1-\alpha)s^\alpha+\alpha}(S_c-1)-(k_p+M^2)}\right)+\frac{1}{s^2}\right\}\right]$$
$$\left(e^{-\xi\sqrt{\frac{s^\alpha}{(1-\alpha)s^\alpha+\alpha}+k_p+M^2}}\right)$$
$$-\frac{G_r(1-e^{-s})}{s^2}\left(\frac{e^{-\xi\sqrt{s^\alpha P_{reff}}}}{\frac{s^\alpha}{(1-\alpha)s^\alpha+\alpha}(P_{reff}-1)-(k_p+M^2)}\right)$$
$$-\frac{G_m}{s}\left(\frac{e^{-\xi\sqrt{s^\alpha S_c}}}{\frac{s^\alpha}{(1-\alpha)s^\alpha+\alpha}(S_c-1)-(k_p+M^2)}\right). \quad (33)$$

The analogs of the velocity profile are obtained by (Equation 40, [27]) using the *CF* operator:

$$\bar{v}(\xi,s) = \left[\frac{1}{1+h\sqrt{\frac{s}{(1-\alpha)s+\alpha}}+k_p+M^2}\right.$$
$$\left\{\frac{G_r(1-e^{-s})}{s^2}\left(\frac{1+h\sqrt{sP_{reff}}}{sP_{reff}-\frac{s}{(1-\alpha)s+\alpha}-(k_p+M^2)}\right)\right.$$
$$\left.\left.+\frac{G_m}{s}\left(\frac{1+h\sqrt{sS_c}}{sS_c-\frac{s}{(1-\alpha)s+\alpha}-(k_p+M^2)}\right)+\frac{1}{s^2}\right\}\right]$$
$$\left(e^{-\xi\sqrt{\frac{s}{(1-\alpha)s+\alpha}+k_p+M^2}}\right)$$
$$-\frac{G_r(1-e^{-s})}{s^2}\left(\frac{e^{-\xi\sqrt{sP_{reff}}}}{sP_{reff}-\frac{s}{(1-\alpha)s+\alpha}-(k_p+M^2)}\right)$$
$$-\frac{G_m}{s}\left(\frac{e^{-\xi\sqrt{sS_c}}}{sS_c-\frac{s}{(1-\alpha)s+\alpha}-(k_p+M^2)}\right). \quad (34)$$

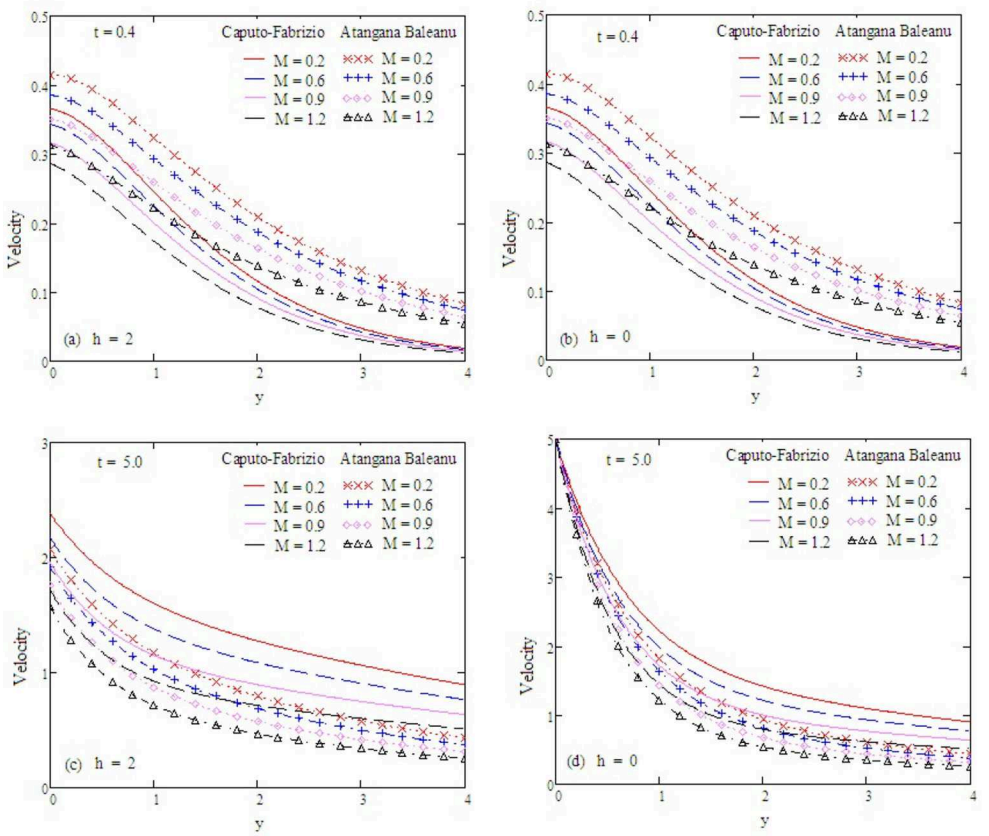

FIGURE 8 | Velocity profiles with altered values of M and other parameters are $\alpha = 0.5$, $G_r = 2$, $P_{reff} = 0.1$, $G_m = 0.75$, $k_p = 1.5$, and $S_c = 0.5$.

Graphs for the profiles of the velocity for both operators for the variation of physical parameters α, P_{reff}, M, G_r, G_m, S_c, and k_p are prepared. Moreover, the slip and no slip effects are significant. It is noted that the memory effects obtained by the Atangana-Baleanu derivative express more significant results than the results recovered by the Caputo-Fabrizio derivative.

5.2. Case-II

By putting $z(t) = te^t$ into Equation (27), we obtain a suitable result for the velocity profile:

$$\bar{v}(\xi,s) = \left[\frac{1}{1+h\sqrt{\frac{s^\alpha}{(1-\alpha)s^\alpha+\alpha}}+k_p+M^2}\right.$$
$$\left\{\frac{G_r(1-e^{-s})}{s^2}\left(\frac{1+h\sqrt{s^\alpha P_{reff}}}{\frac{s^\alpha}{(1-\alpha)s^\alpha+\alpha}(P_{reff}-1)-(k_p+M^2)}\right)\right.$$
$$\left.\left.+\frac{G_m}{s}\left(\frac{1+h\sqrt{s^\alpha S_c}}{\frac{s^\alpha}{(1-\alpha)s^\alpha+\alpha}(S_c-1)-(k_p+M^2)}\right)+\frac{1}{(s-1)^2}\right\}\right]$$
$$\left(e^{-\xi\sqrt{\frac{s^\alpha}{(1-\alpha)s^\alpha+\alpha}+k_p+M^2}}\right)$$
$$-\frac{G_r(1-e^{-s})}{s^2}\left(\frac{e^{-\xi\sqrt{s^\alpha P_{reff}}}}{\frac{s^\alpha}{(1-\alpha)s^\alpha+\alpha}(P_{reff}-1)-(k_p+M^2)}\right)$$
$$-\frac{G_m}{s}\left(\frac{e^{-\xi\sqrt{s^\alpha S_c}}}{\frac{s^\alpha}{(1-\alpha)s^\alpha+\alpha}(S_c-1)-(k_p+M^2)}\right). \quad (35)$$

The analogs of the velocity profile are obtained by (Equation 42, [27]) using *CF* operator:

$$\bar{v}(\xi,s) = \left[\frac{1}{1+h\sqrt{\frac{s}{(1-\alpha)s+\alpha}}+k_p+M^2}\right.$$
$$\left\{\frac{G_r(1-e^{-s})}{s^2}\left(\frac{1+h\sqrt{sP_{reff}}}{sP_{reff}-\frac{s}{(1-\alpha)s+\alpha}-(k_p+M^2)}\right)\right.$$
$$\left.\left.+\frac{G_m}{s}\left(\frac{1+h\sqrt{sS_c}}{sS_c-\frac{s}{(1-\alpha)s+\alpha}-(k_p+M^2)}\right)+\frac{1}{(s-1)^2}\right\}\right]$$
$$\left(e^{-\xi\sqrt{\frac{s}{(1-\alpha)s+\alpha}+k_p+M^2}}\right)$$
$$-\frac{G_r(1-e^{-s})}{s^2}\left(\frac{e^{-\xi\sqrt{sP_{reff}}}}{sP_{reff}-\frac{s}{(1-\alpha)s+\alpha}-(k_p+M^2)}\right)$$
$$-\frac{G_m}{s}\left(\frac{e^{-\xi\sqrt{sS_c}}}{sS_c-\frac{s}{(1-\alpha)s+\alpha}-(k_p+M^2)}\right). \quad (36)$$

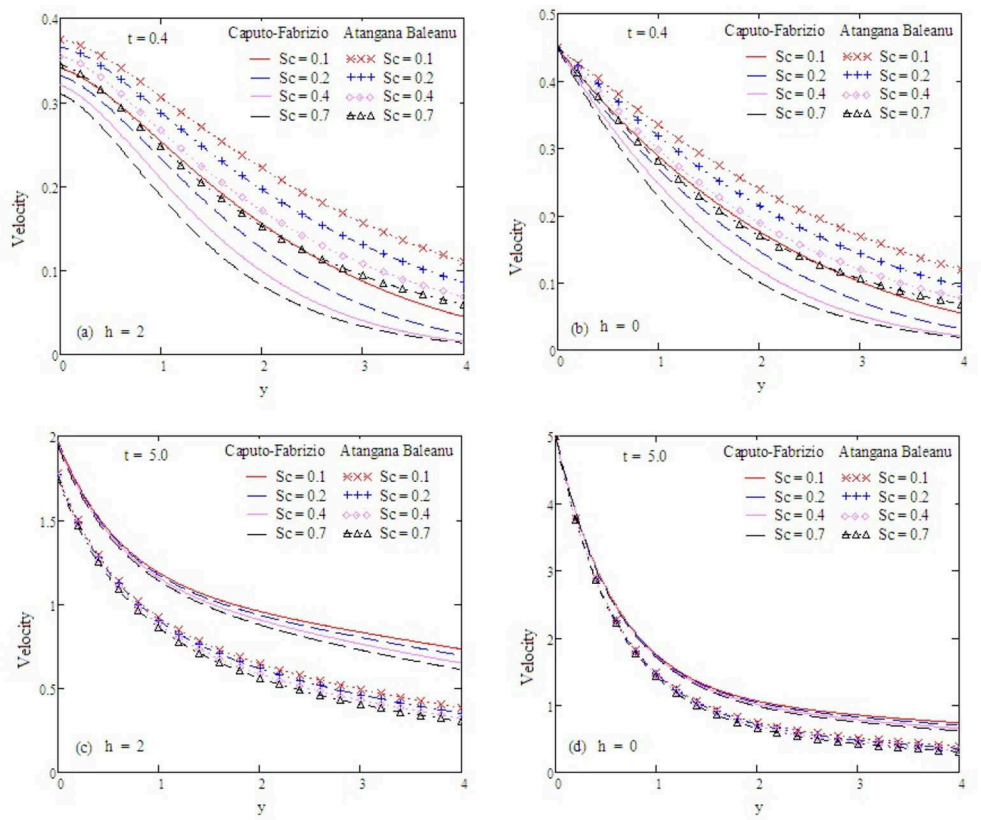

FIGURE 9 | Velocity profiles with altered values of S_c and other parameters are $\alpha = 0.5$, $G_r = 2$, $P_{reff} = 0.1$, $G_m = 0.75$, $k_p = 1.5$, and $M = 0.9$.

5.3. Case-III

By putting $z(t) = \sin(\omega t)$ into Equation (27), we obtain a suitable result for the velocity profile:

$$\bar{v}(\xi,s) = \left[\frac{1}{1+h\sqrt{\frac{s^{\alpha}}{(1-\alpha)s^{\alpha}+\alpha}}+k_p+M^2}\right.$$
$$\left\{\frac{G_r(1-e^{-s})}{s^2}\left(\frac{1+h\sqrt{s^{\alpha}P_{reff}}}{\frac{s^{\alpha}}{(1-\alpha)s^{\alpha}+\alpha}(P_{reff}-1)-(k_p+M^2)}\right)\right.$$
$$\left.\left.+\frac{G_m}{s}\left(\frac{1+h\sqrt{s^{\alpha}S_c}}{\frac{s^{\alpha}}{(1-\alpha)s^{\alpha}+\alpha}(S_c-1)-(k_p+M^2)}\right)+\frac{\omega}{s^2+\omega^2}\right\}\right]$$
$$\left(e^{-\xi\sqrt{\frac{s^{\alpha}}{(1-\alpha)s^{\alpha}+\alpha}+k_p+M^2}}\right)-\frac{G_r(1-e^{-s})}{s^2}$$
$$\left(\frac{e^{-\xi\sqrt{s^{\alpha}P_{reff}}}}{\frac{s^{\alpha}}{(1-\alpha)s^{\alpha}+\alpha}(P_{reff}-1)-(k_p+M^2)}\right)$$
$$-\frac{G_m}{s}\left(\frac{e^{-\xi\sqrt{s^{\alpha}S_c}}}{\frac{s^{\alpha}}{(1-\alpha)s^{\alpha}+\alpha}(S_c-1)-(k_p+M^2)}\right). \quad (37)$$

The analogs of the velocity profile are obtained by (Equation 44, [27]) using *CF* operator:

$$\bar{v}(\xi,s) = \left[\frac{1}{1+h\sqrt{\frac{s}{(1-\alpha)s+\alpha}}+k_p+M^2}\right.$$
$$\left\{\frac{G_r(1-e^{-s})}{s^2}\left(\frac{1+h\sqrt{sP_{reff}}}{sP_{reff}-\frac{s}{(1-\alpha)s+\alpha}-(k_p+M^2)}\right)\right.$$
$$\left.\left.+\frac{G_m}{s}\left(\frac{1+h\sqrt{sS_c}}{sS_c-\frac{s}{(1-\alpha)s+\alpha}-(k_p+M^2)}\right)+\frac{\omega}{s^2+\omega^2}\right\}\right]$$
$$\left(e^{-\xi\sqrt{\frac{s}{(1-\alpha)s+\alpha}+k_p+M^2}}\right)$$
$$-\frac{G_r(1-e^{-s})}{s^2}\left(\frac{e^{-\xi\sqrt{sP_{reff}}}}{sP_{reff}-\frac{s}{(1-\alpha)s+\alpha}-(k_p+M^2)}\right)$$
$$-\frac{G_m}{s}\left(\frac{e^{-\xi\sqrt{sS_c}}}{sS_c-\frac{s}{(1-\alpha)s+\alpha}-(k_p+M^2)}\right). \quad (38)$$

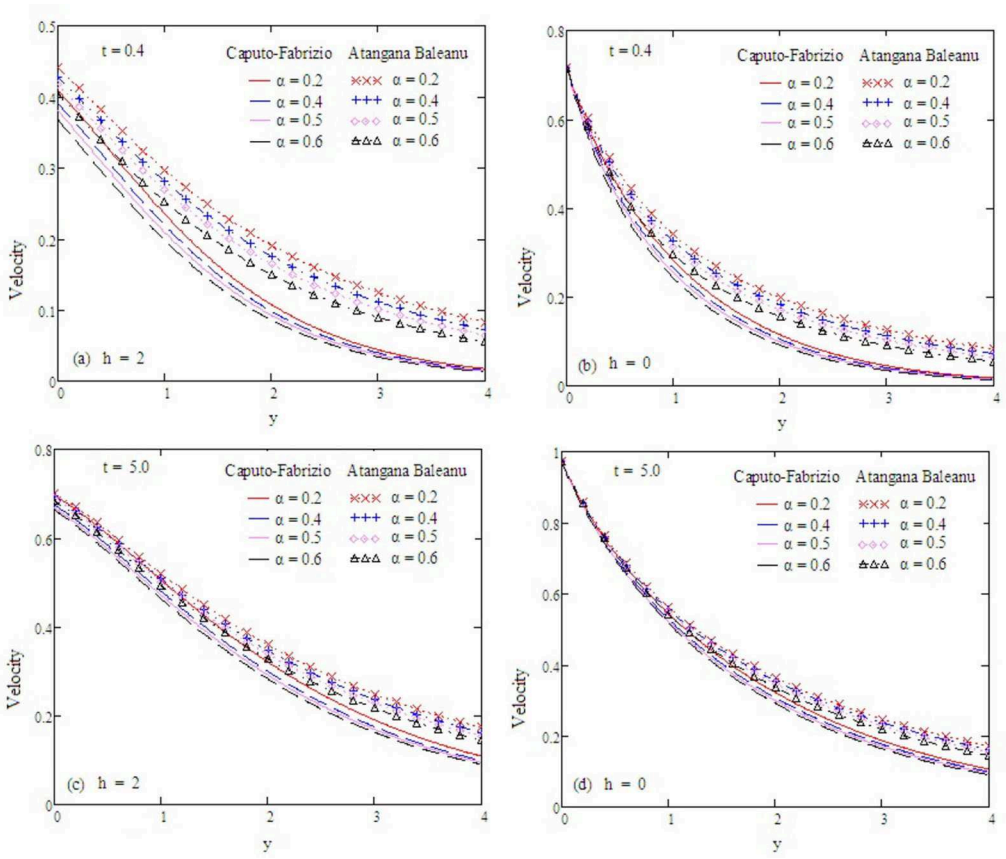

FIGURE 10 | Velocity profiles with altered values of α and other parameters are $\omega = 0.2$, $G_r = 2$, $P_{reff} = 0.1$, $G_m = 0.75$, $k_p = 1.5$, $S_c = 0.5$, and $M = 0.9$.

5.4. Case-IV

By putting $z(t) = t\sin(\omega t)$ into Equation (27), we obtain a suitable result for the velocity profile:

$$\bar{v}(\xi,s) = \left[\frac{1}{1+h\sqrt{\frac{s^{\alpha}}{(1-\alpha)s^{\alpha}+\alpha}}+k_p+M^2}\right.$$
$$\left\{\frac{G_r(1-e^{-s})}{s^2}\left(\frac{1+h\sqrt{s^{\alpha}P_{reff}}}{\frac{s^{\alpha}}{(1-\alpha)s^{\alpha}+\alpha}(P_{reff}-1)-(k_p+M^2)}\right)\right.$$
$$\left.\left.+\frac{G_m}{s}\left(\frac{1+h\sqrt{s^{\alpha}S_c}}{\frac{s^{\alpha}}{(1-\alpha)s^{\alpha}+\alpha}(S_c-1)-(k_p+M^2)}\right)+\frac{2s\omega}{s^2+\omega^2}\right\}\right]$$
$$\left(e^{-\xi\sqrt{\frac{s^{\alpha}}{(1-\alpha)s^{\alpha}+\alpha}+k_p+M^2}}\right)$$
$$-\frac{G_r(1-e^{-s})}{s^2}\left(\frac{e^{-\xi\sqrt{s^{\alpha}P_{reff}}}}{\frac{s^{\alpha}}{(1-\alpha)s^{\alpha}+\alpha}(P_{reff}-1)-(k_p+M^2)}\right)$$
$$-\frac{G_m}{s}\left(\frac{e^{-\xi\sqrt{s^{\alpha}S_c}}}{\frac{s^{\alpha}}{(1-\alpha)s^{\alpha}+\alpha}(S_c-1)-(k_p+M^2)}\right). \quad (39)$$

The analogs of the velocity profile are obtained by (Equation 46, [27]) using *CF* operator:

$$\bar{v}(\xi,s) = \left[\frac{1}{1+h\sqrt{\frac{s}{(1-\alpha)s+\alpha}}+k_p+M^2}\right.$$
$$\left\{\frac{G_r(1-e^{-s})}{s^2}\left(\frac{1+h\sqrt{sP_{reff}}}{sP_{reff}-\frac{s}{(1-\alpha)s+\alpha}-(k_p+M^2)}\right)\right.$$
$$\left.\left.+\frac{G_m}{s}\left(\frac{1+h\sqrt{sS_c}}{sS_c-\frac{s}{(1-\alpha)s+\alpha}-(k_p+M^2)}\right)+\frac{2s\omega}{s^2+\omega^2}\right\}\right]$$
$$\left(e^{-\xi\sqrt{\frac{s}{(1-\alpha)s+\alpha}+k_p+M^2}}\right)$$
$$-\frac{G_r(1-e^{-s})}{s^2}\left(\frac{e^{-\xi\sqrt{sP_{reff}}}}{sP_{reff}-\frac{s}{(1-\alpha)s+\alpha}-(k_p+M^2)}\right)$$
$$-\frac{G_m}{s}\left(\frac{e^{-\xi\sqrt{sS_c}}}{sS_c-\frac{s}{(1-\alpha)s+\alpha}-(k_p+M^2)}\right). \quad (40)$$

By making $\alpha \to 1$ in Equations (20), (23), and (27) we obtain a result for a classical model, the same as that discussed by Ghalib et al. [27]. This validates our obtained results. In our flow models,

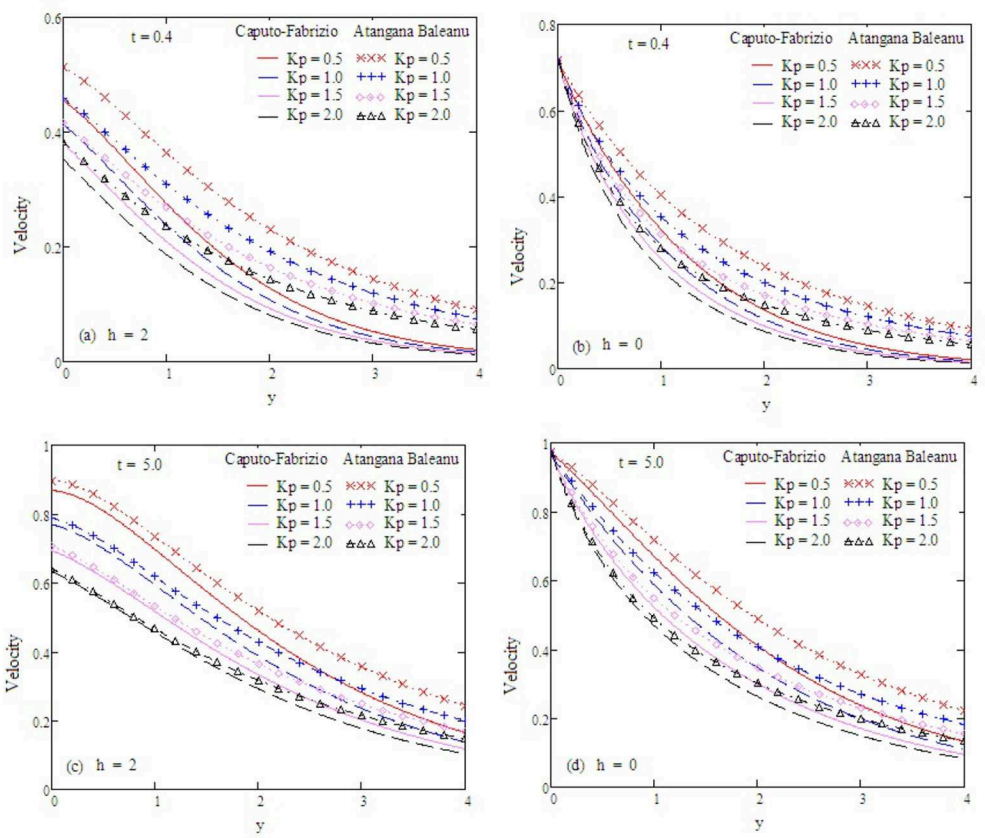

FIGURE 11 | Velocity profiles with altered values of k_p and other parameters are $\omega = 0.2$, $G_r = 2$, $P_{reff} = 0.1$, $G_m = 0.75$, $\alpha = 0.5$, $S_c = 0.5$, and $M = 0.9$.

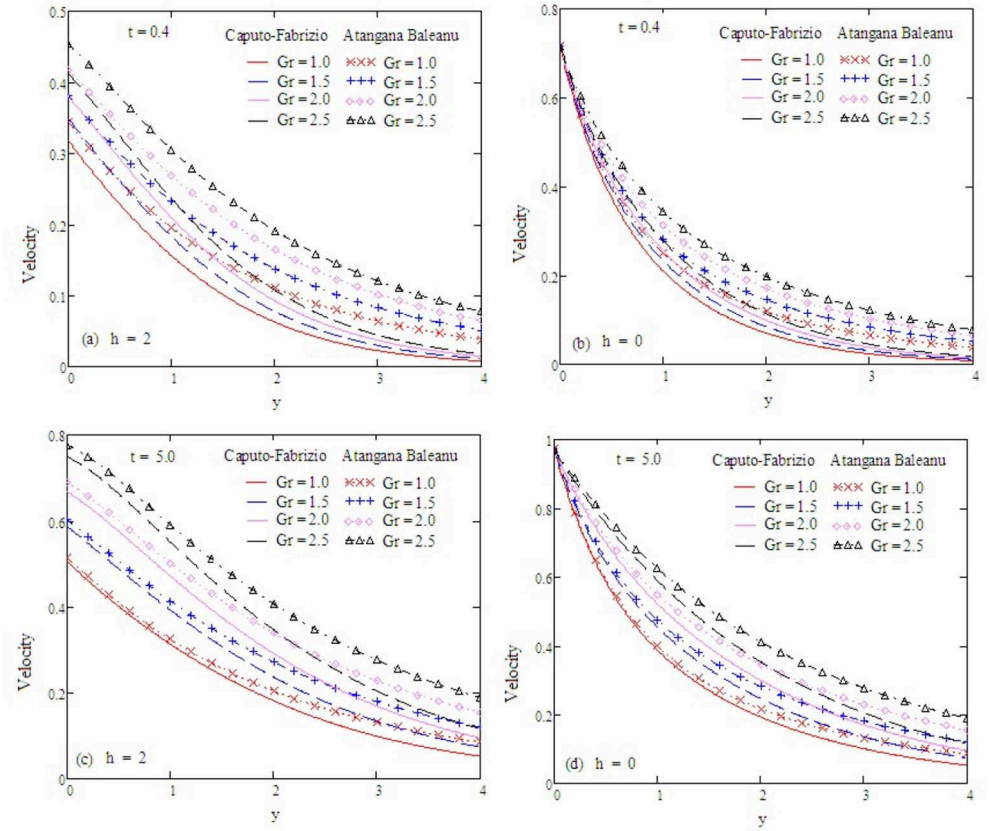

FIGURE 12 | Velocity profiles with altered values of G_r and other parameters are $\omega = 0.2$, $\alpha = 0.5$, $P_{reff} = 0.1$, $G_m = 0.75$, $k_p = 1.5$, $S_c = 0.5$, and $M = 0.9$.

we use the Laplace transform technique to solve this model, using the definition of the *ABC* model. In order to find the inverse, we use Stehfest's algorithms [29] for semi-analytical solutions. Stehfest's algorithms are used for the verification of our inverse Laplace transformation

$$v(y,t) = \frac{ln(2)}{t}\sum_{j=1}^{2m} d_j \bar{v}(y, j\frac{ln(2)}{t}),$$

$$d_j = (-1)^{j+m}\sum_{i=[\frac{j+1}{2}]}^{min(j,m)} \frac{i^m(2i)!}{(m-i)!i!(i-1)!(j-i)!(2i-j)!}.$$

6. RESULTS AND DISCUSSION

The physical aspects of the *CF* and *ABC* time derivative are discussed in the given problem. Numerical results for T, C, and v are plotted using MATHCAD for embedded physical parameters, such as M, k_p, P_{reff}, G_r, G_m, S_c, and slip parameter h. **Figure 1** shows the behavior of α on temperature. It is shown that the value of α increases, while the temperature of the fluid decreases. The memory effect is explained well with the *ABC* derivative in comparison to the *CF* derivative.

Figure 2 examines the behavior of α on concentration. It reduces as the value of α increases. The Antangna-Baleanu derivative shows significant behavior in comparison to the Caputo-Febrizio derivative for different values of α. Graphs for the velocity, with function $f(t) = t$, are shown in **Figures 3–9**, and with function $f(t) = sin(\omega t)$, as shown in **Figures 10–16**. Fluid velocity decreases with the increase of α as well as for slip and non-slip boundary conditions. **Figure 3** shows that the memory effects of the Antangna Baleanu derivatives, with short and long time for the velocity profile, as well as with slip and non-slip conditions, are more significant than the memory effects of the Caputo Febrizio derivatives. For longer times, the graphical representation of the velocity shows inverse behavior, as the velocity increases with the increase of the value of α, for both the velocity profile and slip and non-slip velocity. Variation in fluid velocity with respect to the porosity coefficient is displayed in **Figures 4**, **11**. It represents the increase in the porosity coefficient, resulting in the decrease in the velocity profile, as well as the velocity with slip and non-slip boundary conditions for both a short and long time. The representation of the velocity profile with the Antangna Baleanu derivatives, for a short and long time, as well as fluid velocity with the slip and non-slip effect is more significant than the velocities recovered with the Caputo-Fabrizio derivatives. **Figures 5**, **12** illustrate the influence of the Grashof

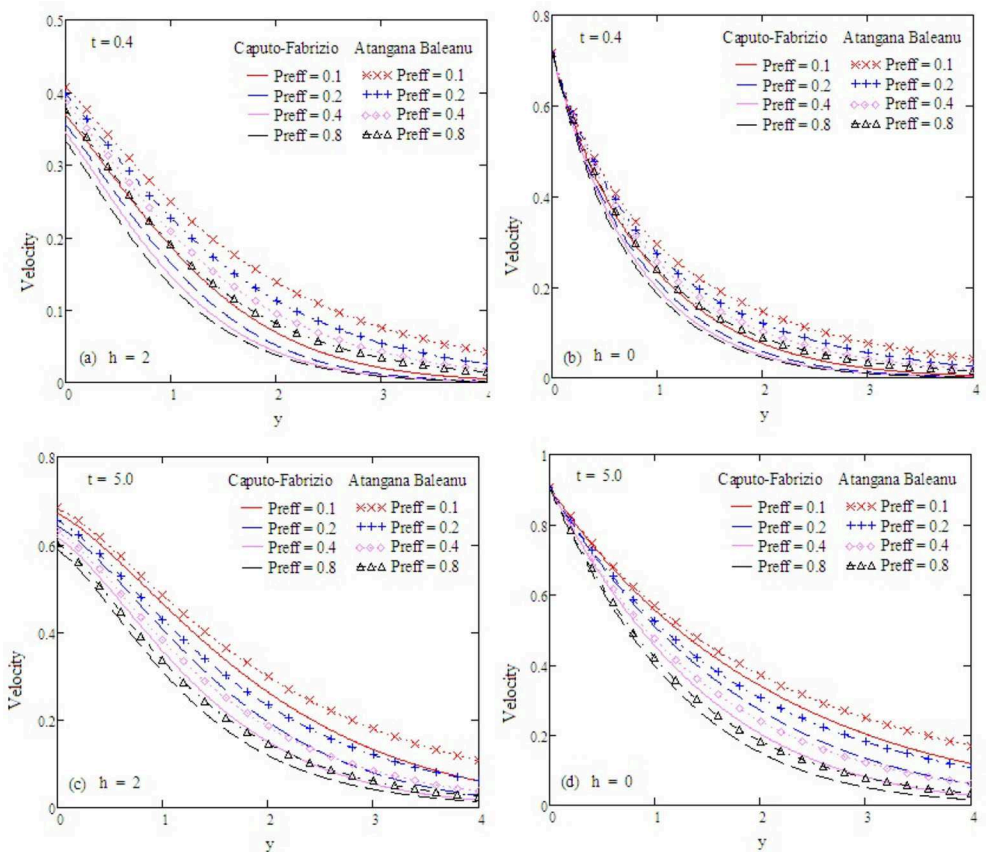

FIGURE 13 | Velocity profiles with altered values of P_{reff} and other parameters are $\omega = 0.2$, $G_r = 2$, $M = 0.9$, $G_m = 0.75$, $\alpha = 0.5$, $S_c = 0.5$, and $k_p = 1.5$.

number G_r on the fluid velocity, which increases with the increase of the Grashof number G_r for a short time as well as for a long time, both in the case of the slip and non-slip effects, because the thermal buoyancy forces tend to accelerate the fluid velocity for different times. The memory effects of the Antangna Baleanu derivatives for the variation of G_r with a short time and long time, oncovers more significant memory effects than the Caputo Febrizio derivatives. The velocity profile for different values of the effective Prandtl number P_{reff} are shown in **Figures 6**, **13**. Fluid velocity decreases with the increase of P_{reff} for different times, also in the case of slip and non-slip boundary conditions. Graphical representation for various values of P_{reff} with the Antangna-Baleanu derivative is more impressive for short and long times as well as for slip and non-slip boundary conditions, than it is for the caputo-Fabrizio derivatives. **Figures 7**, **14** display the influence of the variation of a modified Grashof number G_m, and the fluid velocity increases with the increase of G_m for various times, as well as with the slip and non-slip parameters. Memory effects with the Antangna-Baleanu derivatives are better than with the Caputo-Fabrizio derivatives. The velocity profile for different values of magnetic field M are given in **Figures 8**, **15**. Fluid velocity shrinks on a large value of M with a short time as well as with long time. It also displays the same behavior for both slip and non-slip boundary conditions, particularly, on increasing the value of M causes to enhance the frictional force which tends to resist the flow of fluid and, thus, velocity ultimately decreases. Moreover, we observed that the fluid velocity obtained with the Atangana-Baleanu derivatives for the variation of M, in case of both a short and long time, is more significant than the velocity obtained with the Caputo-Fabrizio derivatives. In **Figures 9**, **16** velocity profiles with variations of S_c are shown. It was found that the velocity decreases when increasing the value of S_c for both short and long times, as well as for slip and non-slip parameters. The velocity profile of different values of S_c with the Atangana-Baleanu derivatives for various times, are more expressive than the velocity that is obtained with the Caputo-Fabrizio derivatives. In **Figure 10** fluid velocity reduces with enlarged values of α. It also shows the same behavior with slip as well as non-slip fluid flow conditions, and it shows the same behavior for short and long times. Memory effects show better results with the Atangana-Baleanu derivative in comparison to the Caputo-Fabrizio derivative.

7. CONCLUSION

Ramped wall velocity and temperature conditions had a significant impact on MHD fractional Oldroyd-B fluid over

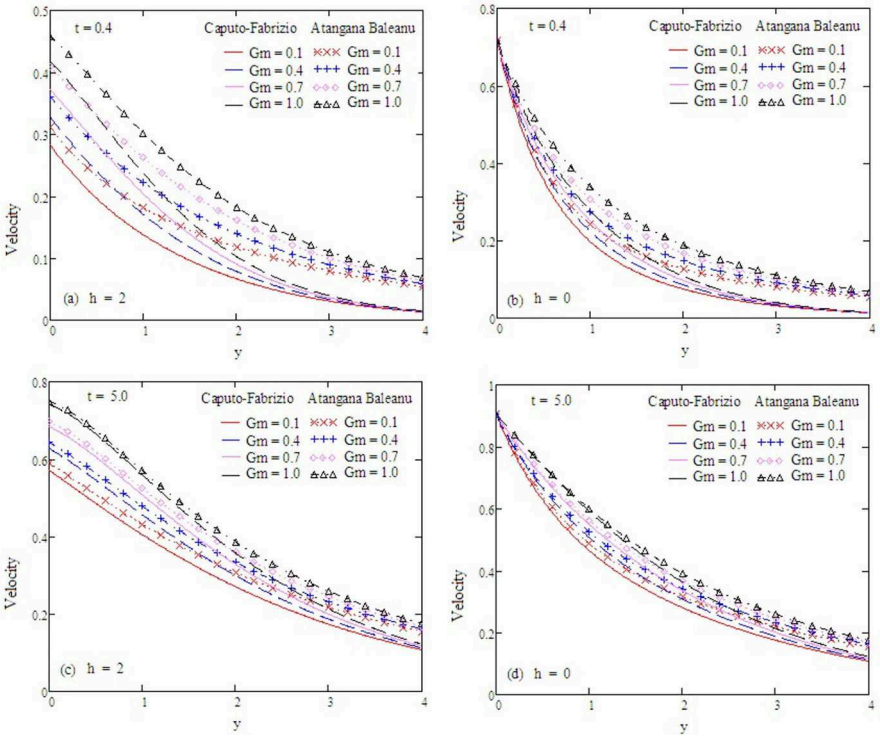

FIGURE 14 | Velocity profiles with altered values of G_m and other parameters are $\omega = 0.2$, $G_r = 2$, $P_{reff} = 0.1$, $\alpha = 0.5$, $k_p = 1.5$, $S_c = 0.5$, and $M = 0.9$.

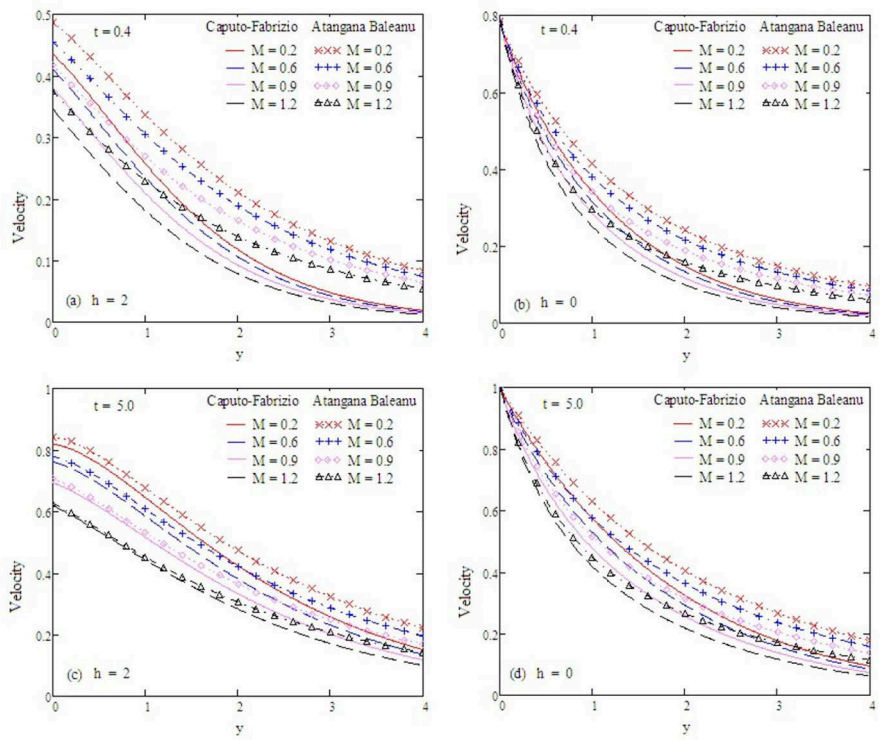

FIGURE 15 | Velocity profiles with altered values of M and other parameters are $\omega = 0.2$, $G_r = 2$, $P_{reff} = 0.1$, $G_m = 0.75$, $\alpha = 0.5$, $S_c = 0.5$, and $k_p = 1.5$.

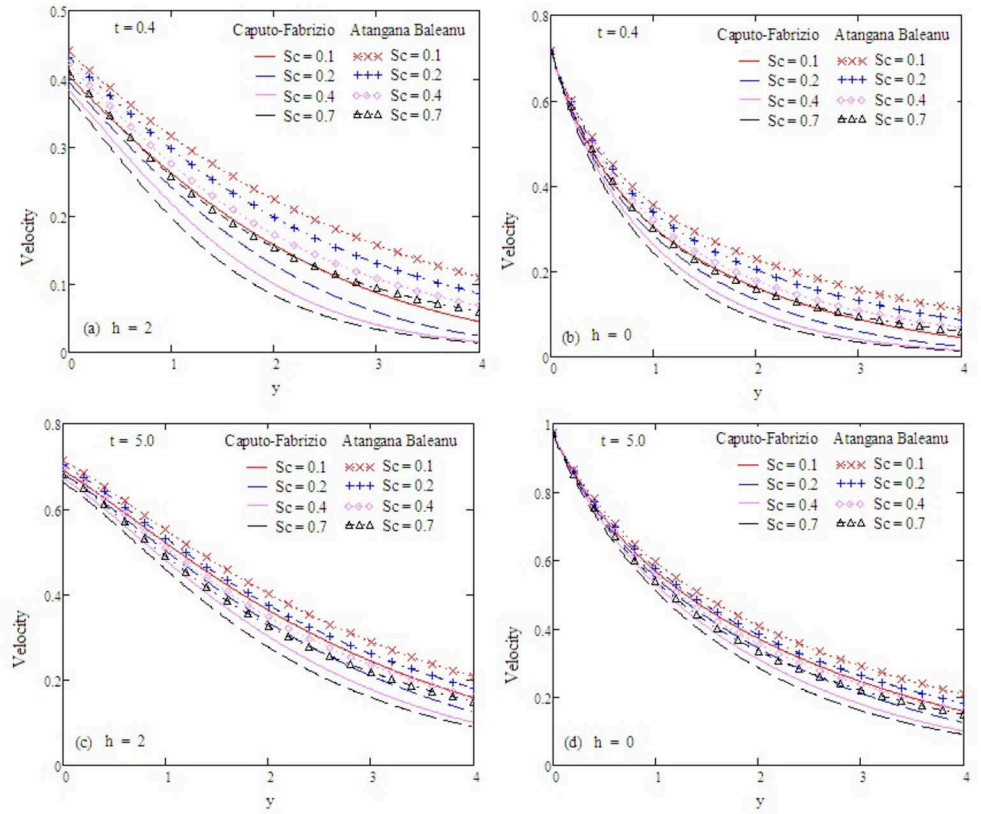

FIGURE 16 | Velocity profiles with altered values of S_c and other parameters are $\omega = 0.2$, $G_r = 2$, $P_{reff} = 0.1$, $G_m = 0.75$, $\alpha = 0.5$, $M = 0.9$, and $k_p = 1.5$.

a infinite vertical plate on a permeable surface. Fractional derivative operators are used to find the analytical solution using the Laplace transformation and inversion algorithm. Fluid velocity was analyzed through graphical results with the effect of different physical parameters. The main points of this problem are:

- The *ABC* fractional derivative is more significant compared to the classical model and other fractional models.
- The magnitude of the velocity increases with an increase in the fractional parameter α.
- The relationship between fractional parameters α and γ are reversed.
- Retardation time and relaxation time have a strong impact on the motion of fluid velocity.
- Velocity enhances with an increase in the value of λ_r.
- The relationship between λ and λ_r is the opposite to each other.
- The fluid velocity decreases with a large value of P_r.
- In the velocity field, the velocity reduces with the expansion of M.

DATA AVAILABILITY STATEMENT

All datasets generated for this study are included in the article/supplementary material.

AUTHOR CONTRIBUTIONS

MR and DB: conceptualization, investigation, and final review and editing. MR, DB, and SS: methodology. MG: software. SS: formal analysis. SS and MG: resources and original draft preparation. All authors contributed to the article and approved the submitted version.

REFERENCES

1. Das K, Jana S. Heat and mass transfer effects on unsteady MHD free convection flow near moving vertical plate in porous medium. *Bull Soc Math Banja Luka.* (2010) **17**:15–32.
2. Hayat T, Khan I, Ellahi R, Fetecau C. Some MHD flows of a second grade fluid through the porous medium. *J Por Media.* (2008) **11**:389–400. doi: 10.1615/JPorMedia.v11.i4.50
3. Chandrakala P. Radiation effects on flow past an impulsively started vertical oscillating plate with uniform heat flux. *Int J Dyn Fluids.* (2011) **7**:1–8.

4. Narahari M, Nayan MY. Free convection flow past an impulsively started infinite vertical plate with Newtonian heating in the presence of thermal radiation and mass diffusion. *Turk J Eng Environ Sci.* (2011) **35**:187–98.
5. Chandran P, Sacheti NC, Singh AK. Natural convection near a vertical plate with ramped wall temperature. *Heat Mass Trans.* (2005) **41**:459–64. doi: 10.1007/s00231-004-0568-7
6. Narahari M, Beg OA, Ghosh SK. Mathematical modelling of mass transfer and free convection current effects on unsteady viscous flow with ramped wall temperature. *World J Mech.* (2011) **1**:176–84. doi: 10.4236/wjm.2011.14023
7. Toki CJ, Tokis JN. Exact solutions for the unsteady free convection flows on a porous plate with time-dependent heating. *ZAMM Z Angew Math Mech.* (2007) **87**:4–13. doi: 10.1002/zamm.200510291
8. Senapati N, Dhal RK, Das TK. Effects of chemical reaction on free convection MHD flow through porous medium bounded by vertical surface with slip flow region. *Am J Comput Appl Math.* (2012) **2**:124–35. doi: 10.5923/j.ajcam.20120203.10
9. Khan I, Fakhar K, Sharidan S. Magnetohydrodynamic free convection flow past an oscillating plate embedded in a porous medium. *J Phys Soc Jpn.* (2011) **80**:1–10. doi: 10.1143/JPSJ.80.104401
10. Das SS, Maity M, Das JK. Unsteady hydromagnetic convective flow past an infinite vertical porous flat plate in a porous medium. *Int J Energy Environ.* (2012) **3**:109–18.
11. Narahari M, Ishaq A. Radiation effects on free convection flow near a moving vertical plate with Newtonian heating. *J Appl Sci.* (2011) **11**:1096–104. doi: 10.3923/jas.2011.1096.1104
12. Kumar D, Singh J, Baleanu D. A fractional model of convective radial fins with temperature-dependent thermal conductivity. *Rom Rep Phys.* (2017) **69**:103–5.
13. Gupta S, Kumar D, Singh J. MHD mixed convective stagnation point flow and heat transfer of an incompressible nanofluid over an inclined stretching sheet with chemical reaction and radiation. *Int J Heat Mass Trans.* (2018) **118**:378–87. doi: 10.1016/j.ijheatmasstransfer.2017.11.007
14. Khan A, Karim F, Khan I, Ali F, Khan D. Irreversibility analysis in unsteady flow over a vertical plate with arbitrary wall shear stress and ramped wall temperature. *Results Phys.* (2018) **8**:1283–90. doi: 10.1016/j.rinp.2017.12.032
15. Imran MA, Riaz MB, Shah NA, Zafar AA. Boundary layer flow of MHD generalized Maxwell fluid over an exponentially accelerated infinite vertical surface with slip and Newtonian heating at the boundary. *Results Phys.* (2018) **8**:1061–7. doi: 10.1016/j.rinp.2018.01.036
16. Fetecau C, Vieru D, Fetecau C, Akhtar S. General solutions for magneto-hydrodynamic natural convection flow with radiative heat transfer and slip condition over a moving plat. *Z Naturforsch.* (2013) **68**:659–67. doi: 10.5560/zna.2013-0041
17. Jha BK, Apere CA. Combined effect of hall and ion-slip currents on unsteady MHD couette flows in a rotating system. *J Phys Soc Jpn.* (2010) **79**:1–9. doi: 10.1143/JPSJ.79.104401
18. Seth GS, Mahato GK, Sakar S. MHD natural convection flow with radiative heat transfer past an impulsively moving vertical plate with ramped temperature in the presence of hall current and thermal diffusion. *Int J Appl Mech Eng.* (2013) **18**:1201–20. doi: 10.2478/ijame-2013-0073
19. Yavuz M, Bonyah E. New approaches to the fractional dynamics of schistosomiasis disease model. *Phys A.* (2019) **525**:373–93. doi: 10.1016/j.physa.2019.03.069
20. Yavuz M. Characterizations of two different fractional operators without singular kernel. *Math Mod Nat Phen.* (2019) **14**:302. doi: 10.1051/mmnp/2018070
21. Atangana A, Baleanu D. New fractional derivatives with nonlocal and non-singular kernel: theory and application to heat transfer model. *Therm Sci.* (2016) **20**:18. doi: 10.2298/TSCI160111018A
22. Abdelijawad T. Different type kernel H-fractional differences and their fractional H-sums. *Chaos Solit Fract.* (2018) **116**:146–56. doi: 10.1016/j.chaos.2018.09.022
23. Siyal A, Abra KA, Solangi MA. Thermodynamics of magnetohydrodynamic Brinkman fluid in porous medium. *J Therm Anal Calori.* (2019) **136**:2295–304. doi: 10.1007/s10973-018-7897-0
24. Riaz MB, Atangana A, Saeed ST. MHD free convection flow over a vertical plate with ramped wall temperature and chemical reaction in view of non-singular kernel. In: Dutta H, Ocak A, Atangana A, editors. *Fractional Order Analysis Theory, Methods and Application*. Wiley-Blackwell (2020), 253–79.
25. Riaz MB, Saeed ST. Comprehensive analysis of integer order, Caputo-fabrizio and Atangana-Baleanu fractional time derivative for MHD Oldroyd-B fluid with slip effect and time dependent boundary condition. *Dis Con Dyn Sys.* (2020).
26. Saeed ST, Riaz MB, Baleanu D, Abro KA. A mathematical study of natural convection flow through a channel with non-singular kernels: an application to transport phenomena. *Alex Engg J.* (2020) **59**:2269–81. doi: 10.1016/j.aej.2020.02.012
27. Ghalib MM, Zafar AA, Riaz MB, Hammouch Z, Shabbir K. Analytical approach for the steady MHD conjugate viscous fluid flow in a porous medium with nonsingular fractional derivative. *Phys A.* (2020) **554**:123941. doi: 10.1016/j.physa.2019.123941
28. Asjad MI, Aleem M, Riaz MB, Ali R, Khan I. A comprehensive report on convective flow of fractional (ABC) and (CF) MHD viscous fluid subject to generalized boundary conditions. *Chaos Solit Fract.* (2019) **118**:274–89. doi: 10.1016/j.chaos.2018.12.001
29. Stehfest H, Goethe JW. Numerical inversion of Laplace transformation. *Commun ACM.* (1970) **13**:47–9. doi: 10.1145/361953.361969

Conflict of Interest: The authors declare that the research was conducted in the absence of any commercial or financial relationships that could be construed as a potential conflict of interest.

The handling editor declared a past co-authorship with the author DB.

Copyright © 2020 Riaz, Saeed, Baleanu and Ghalib. This is an open-access article distributed under the terms of the Creative Commons Attribution License (CC BY). The use, distribution or reproduction in other forums is permitted, provided the original author(s) and the copyright owner(s) are credited and that the original publication in this journal is cited, in accordance with accepted academic practice. No use, distribution or reproduction is permitted which does not comply with these terms.

frontiers in Physics

ORIGINAL RESEARCH
published: 11 September 2020
doi: 10.3389/fphy.2020.00378

Fractional Derivative Modeling on Solute Non-Fickian Transport in a Single Vertical Fracture

Chuantaidou Qiao[1], Yi Xu[2], Weidong Zhao[1], Jiazhong Qian[1]*, Yongting Wu[3] and HongGuang Sun[2]*

[1] School of Resources and Environmental Engineering, Hefei University of Technology, Hefei, China, [2] State Key Laboratory of Hydrology-Water Resources and Hydraulic Engineering, College of Mechanics and Materials, Hohai University, Nanjing, China, [3] Shandong Luqing Safety Assessment Technology Co., Ltd., Jinan, China

Solute transport in a single vertical fracture (SVF) cannot be reliably described by the classical advection-dispersion equation (ADE) model, due to the heterogeneity nature of fracture. This study conducted a group of experiments to investigate chloride ion transport in the SVFs under different rough-walled conditions, and then applied a time fractional advection-dispersion equation (F-ADE) model to offer an accurate description. A comparison between F-ADE model and a classical ADE model in describing experimental data, was also carried out. Results show that the FADE model is better than the ADE model in describing the breakthrough curve and heavy-tail phenomenon of solute transport in the fracture. Especially in the experiments with lower flow rate and higher roughness fracture, the FADE model can offer a better description for non-Fickian transport, indicating that it is a promising tool for characterizing solute transport heterogeneous vertical fracture.

Keywords: solute transport, single vertical fracture, fractional advection-dispersion equation, non-Fickian transport, hydrodynamics, hydraulic condition

OPEN ACCESS

Edited by:
Jagdev Singh, JECRC University, India

Reviewed by:
Antonella Lupica, University of Tuscia, Italy
Yilun Shang, Northumbria University, United Kingdom

***Correspondence:**
Weidong Zhao
zhaowd@hfut.edu.cn
Jiazhong Qian
qianjiazhong@hfut.edu.cn

Specialty section:
This article was submitted to Mathematical and Statistical Physics, a section of the journal Frontiers in Physics

Received: *05 June 2020*
Accepted: *05 August 2020*
Published: *11 September 2020*

Citation:
Qiao C, Xu Y, Zhao W, Qian J, Wu Y and Sun H (2020) Fractional Derivative Modeling on Solute Non-Fickian Transport in a Single Vertical Fracture. Front. Phys. 8:378. doi: 10.3389/fphy.2020.00378

INTRODUCTION

Fracture water as part of underground water, is of great significance in water resources. It is closely related to the production and living activities of human beings and involves complex natural and human factors [1]. In heterogeneous media such as rock fractures, the assessment of solute transport in fractures can avoid overexploitation of groundwater resources and predict the diffusion of fluids and pollutants, which is one of the main tasks of hydrogeology [2, 3]. Therefore, quantifying pollutant transport in fractures has always been regarded as an important research topic [4, 5]. In recent years, how to quantitatively describe and experiment solute transport in fractured media has attracted more and more attention [6].

Until now, researchers have developed several theoretical and empirical models to quantify solute transport in fractured media [7–9]. But solute particles in heterogeneous media will have different retention zones due to the change of flow rate and space, then the classical solute transport model deviates from experimental results [10–13]. In many tests, the breakthrough curves (BTCs) showed anomalous and trailing phenomena, indicating that the classic advection-dispersion equation (ADE) model based on the average transport could not accurately describe these phenomena [14–17].

To overcome the drawbacks of classic ADE model, some researchers developed new models to simulate the non-Fickian transport [18–25]. For example, a continuous time random walk (CTRW)

framework using a set of Langevin equations, has been used to approximate the random process of particle trajectory [18]. Qian et al. used the mobile-immobile (MIM) model to prove that it is better than the ADE model in describing the dispersion phenomenon of BTCs [19]. Fractional-order model has been used to describe the non-Fickian phenomenon of solute transport in recent decade. It describes the solute transport in residence zone by introducing fractional derivative operator in time. But there are only a few studies have been carried out in fractured media. Sun et al. [20] developed the time F-ADE model used to characterize sodium chloride transport in a single fracture and capture non-Fician transport. But the selection of model parameters and mechanism of anomalous transport have not been fully understood.

The objective of this study is to conduct a group of experiments to investigate chloride ion transport in the SVFs under different rough-walled conditions, especially observe the non-Fickian transport phenomena, and to establish a time fractional advection-dispersion equation (F-ADE) model to offer an effective description for the anomalous transport. This study includes the following contents. First, we introduce the experimental device and the experiment of NaCl transport in a single fracture, while the classic ADE model and fractional order model are provided. Then, we provide experimental analysis and discussion of experimental results with a comparison of the ADE model and the time F-ADE model. At last, some conclusions are given.

MATERIALS AND METHODS

Experiment Description

In last century, some researchers have described breakthrough curves and concentration profiles, revealing the important effects of flow velocity, matrix porosity and matrix distribution coefficient on solute transport in fractures [26]. To investigate the solute transport in smooth and rough fractures under

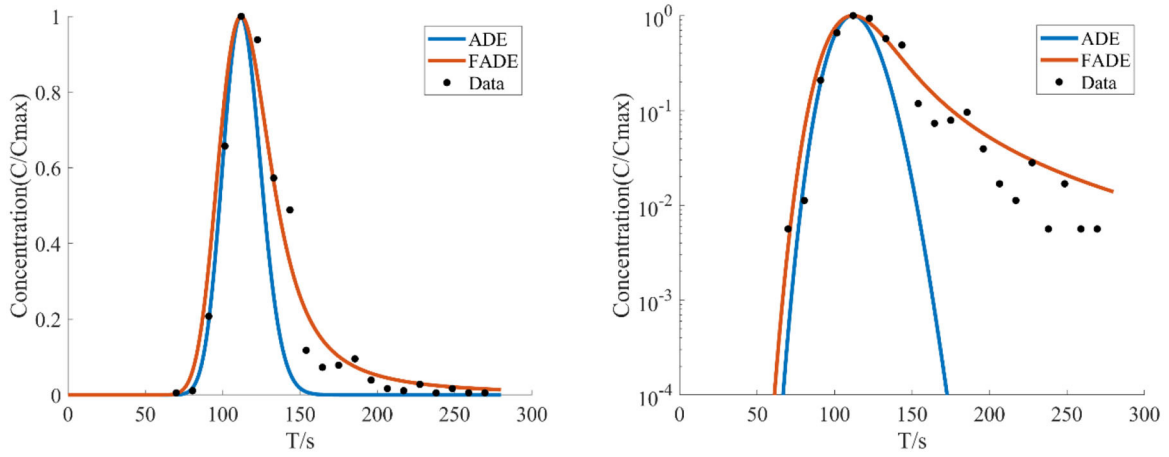

FIGURE 1 | The average flow velocity is $v = 6.785$ mm/s, the crack width is $B = 4$ mm, and the breakthrough curves (BTCs) fitted by ADE model and FADE model is used.

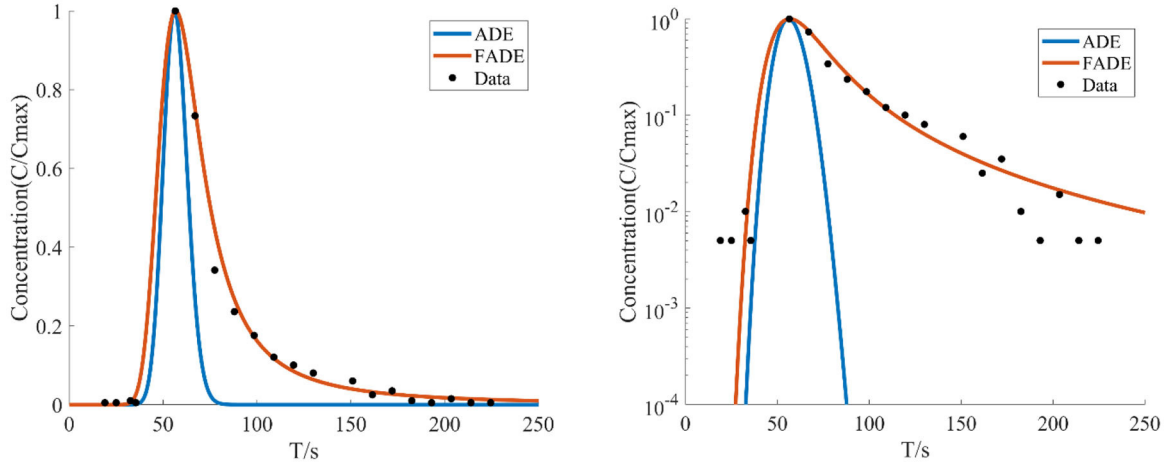

FIGURE 2 | The average flow rate is $v = 13.675$ mm/s, the crack width is $B = 4$ mm, and BTCs fitted by ADE model and FADE model is used.

a single fracture, an experiment was conducted here. This experiment is composed by three parts: upstream water supply and downstream water discharge and single fracture. Some concentration measuring devices are also included.

According to the previous experimental design, the main body of the experimental design is cuboid, which is made of 6 mm plexiglass plate. In order to conduct multiple experiments, the width of cracks can be adjusted [27], and glass plates with different roughness can be attached to the walls of the plexiglass plate. To construct an artificial rough single crack, we select two types of plexiglass plates of coarse degree to stick the inner wall and ensured that the same rough surface of each test is parallel, with dimensions are $40 \times 40 \times 1$ mm and $40 \times 40 \times 2$ mm [28]. So, the thickness of the plywood is the concave-convex height of the crack, denoted by the symbol Δ. The relative roughness is Δ/e. Regarding the average fracture width e, a formula can be given

$$e = \frac{Vol_f}{\frac{1}{2}(h_1 + h_2)\, l} \tag{1}$$

where, Vol_f represents the water volume in the fracture, h_1 is the water level of the inlet of the fracture, h_2 is the water level of theoutlet of the fracture, and l is the distance from the inlet of the fracture to the outlet.

In addition, to maintain the stability of water pressure at the inlet, the high-water tank is used for water supply in the test. The overflow tank is set in the water tank to keep the water level in the tank stable. In this way, the problem of unstable water pressure and flow due to voltage instability can be avoided in the water supply by the inlet pump to reduce the systematic error of the test. The flow meter is installed at both ends of the test device. By adjusting the flow meter valves at the inlet and outlet, the solute transport can be measured at different flow rates.

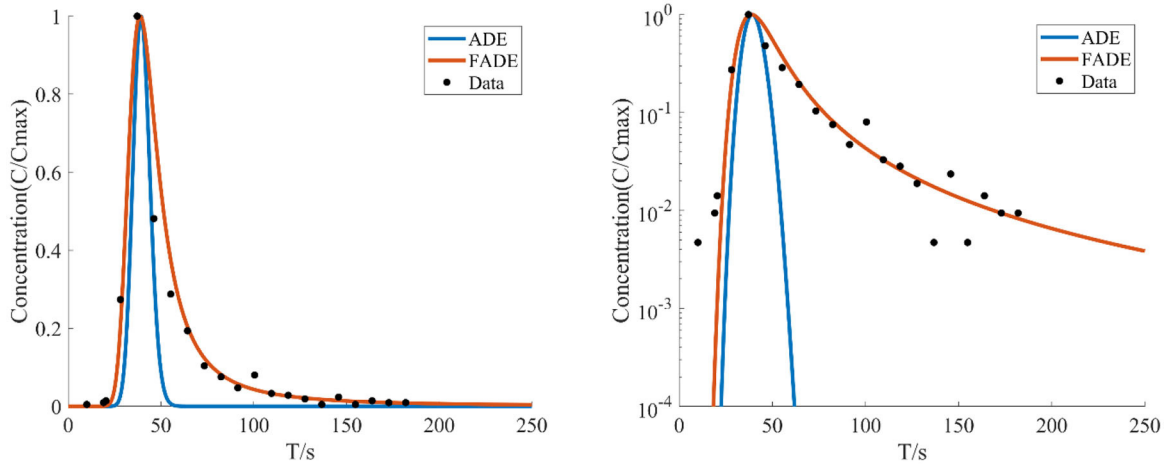

FIGURE 3 | The average flow rate is $v = 20.36$ mm/s, the crack width is $B = 4$ mm, and BTCs fitted by using the ADE model and the FADE model.

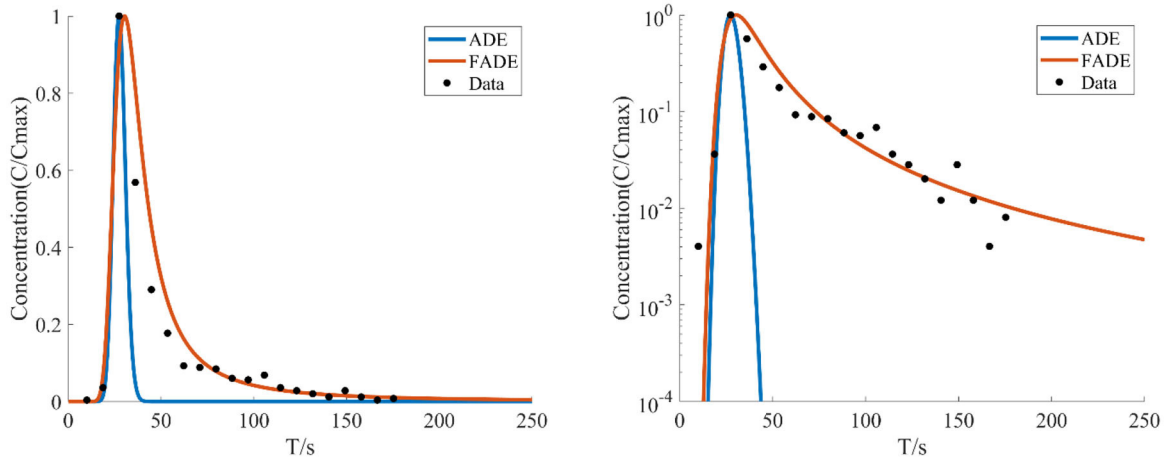

FIGURE 4 | The average flow rate is $v = 26.962$ mm/s, the crack width is $B = 4$ mm, the BTCs are fitted by ADE model and FADE model.

METHODS

Experimental Method

First, we make the model according to the designed size, and then confirm the water tightness of the whole device is intact before further test. Second, adjust the upstream and downstream water tanks and fill them with water to stabilize the water level. The configured NaCl solution is then rapidly injected, and the timing starts. Samples were taken at regular intervals and the concentration was measured. Third, clean the equipment after every experiment. According to the above method, two kinds of experiments were carried out in the crack with different flow rate, different surface roughness and different crack width.

(1) Seven pulse tracer tests are successfully carried out under different hydraulic conditions and different fracture widths.
(2) Five experiments are carried out on the cracks under different occurrence conditions, including multiple gap widths, multiple relative roughness and multiple average flow rates.

TABLE 1 | Parameter fitting of the FADE model with fracture width of 4 mm at different flow rates.

V(mm/s)	α	R^2	RMSE
6.785	0.95	0.9529	0.0663
13.675	0.9	0.9898	0.0268
20.36	0.9	0.9408	0.0612
26.962	0.86	0.9172	0.0743

Test Methods

NaCl solution is used as the tracer solution in this experiment. Since trace determination is needed, the conductivity method is selected for the determination within the permitted range of

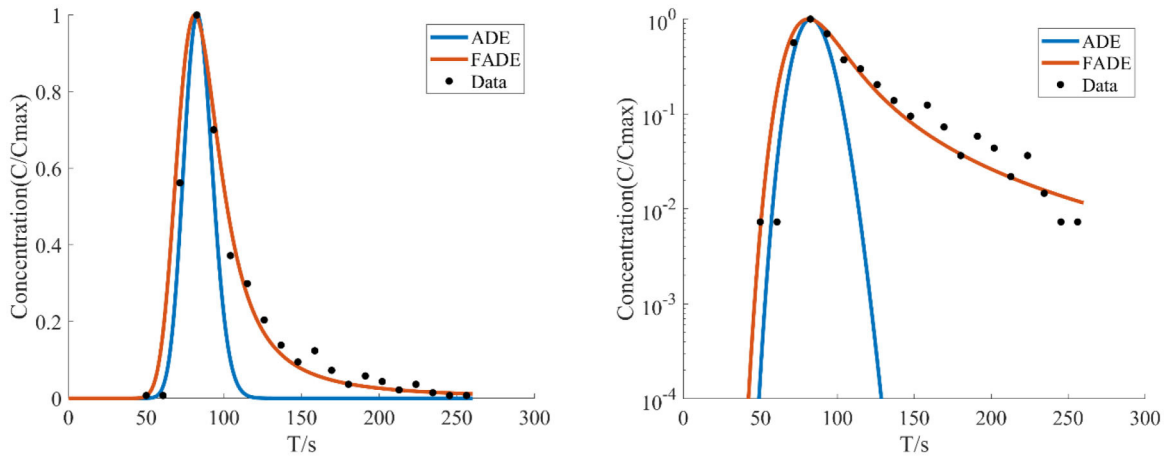

FIGURE 5 | The average flow rate is $v = 9.02$ mm/s, the crack width is $B = 6$ mm, the BTCs are fitted by ADE model and FADE model.

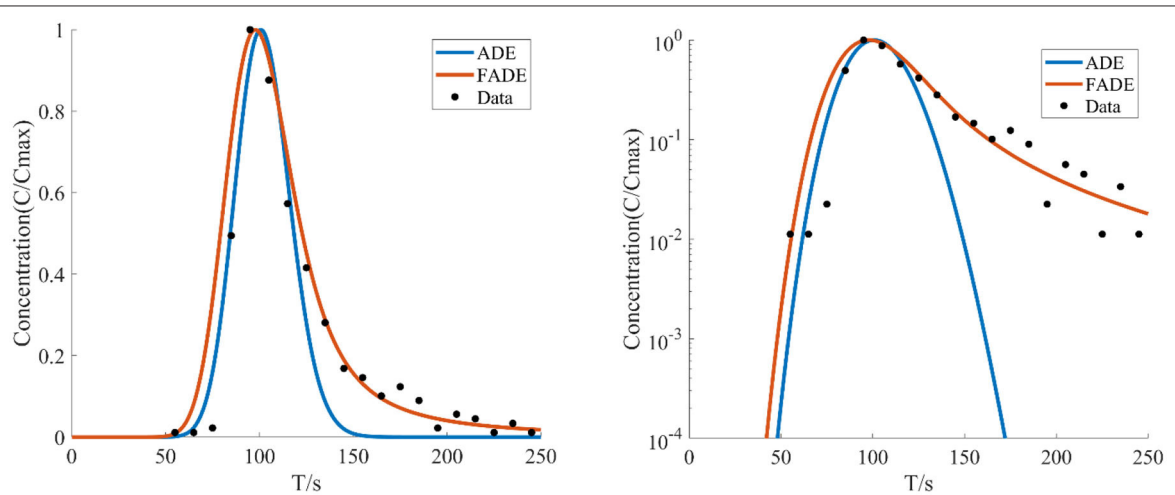

FIGURE 6 | The average flow rate is $v = 7.924$ mm/s, the crack width is $B = 7$ mm, the BTCs are fitted by ADE model and FADE model.

experimental conditions. Its basic principle is the conductivity of water and its inorganic acid, alkali, salt content has a certain relationship. When the concentration is low, the conductivity increases with the concentration, so this index can be used to predict the total concentration or salt content of ions in water. The solution concentration can be converted by measuring the conductivity of the solution and the background value of the conductivity of tap water. The conductivity used in the test has the function of temperature compensation, that is, regardless of the solution temperature, it can be automatically converted to the conductivity value at 25°C.

Before the experiment, a series of NaCl solutions with different concentrations were accurately prepared by using an electronic balance, and their conductivity values were measured [29]. Then, the standard curve equation is solved by using the least square method

$$c = 0.0006771 * EC + 0.00014 \tag{2}$$

Where c is the concentration of NaCl in g/L, EC is the electrical conductivity value in us/cm, and the correlation coefficient of the equation is 0.99977.

Model Methods

For many years, the advection—dispersion equation (ADE) based on Fick's law has been used to simulate the curve (BTCs) of solute transport in uniform media. For one-dimensional flow, the expression of ADE is

$$\frac{\partial C}{\partial t} = D\frac{\partial^2 C}{\partial x^2} - v\frac{\partial C}{\partial x} \tag{3}$$

Where C is the solute concentration, D is the dispersion coefficient, v is the average flow rate, x is the solute transport distance, and t is the transport time. In recent years, fractional differential equations have been used more and more widely, which can better describe some natural physical phenomena and dynamic processes [30–32]. In the aspect of solute transport in groundwater, F-ADE model can be used to describe the non-Fickian phenomena and anomalous diffusion in solute transport [33, 34]. If time dependence is considered, the time FADE is established as

$$\frac{\partial^\alpha C(x,t)}{\partial t^\alpha} = D\frac{\partial^2 C(x,t)}{\partial x^2} - v\frac{\partial C(x,t)}{\partial x} \tag{4}$$

In the formula, α is the fractional derivative order. According to the experimental results of Sun *et al.* [20], because the time fractional derivative term can well-describe the influence of fracture heterogeneity, the time fractional derivative model can accurately describe the overall trend of BTCs, especially the phenomena of tail-dragging [35].

To evaluate the fitting results of the time fractional advection-dispersion equation, the root mean square error (RMSE) and the coefficient of determination (R^2) are selected as the important parameters [36, 37]. RMSE is also known as the effective value [37], which is the square root of the square number of deviations between the predicted value and the true value and the ratio of n times of observation. R^2 shows the extent to which all the explanatory variables included in the model affect the association of dependent variables. In this experiment, the closer the error value is to 0, the value of the coefficient is to 1, indicating that the

TABLE 2 | Parameters of the FADE model with similar low average velocity and different fracture widths.

B(mm)	*V*(mm/s)	α	R^2	RMSE
4	6.785	0.95	0.9529	0.0663
6	9.02	0.93	0.955	0.0607
7	7.924	0.94	0.9062	0.096
9	6.161	0.94	0.9239	0.0858

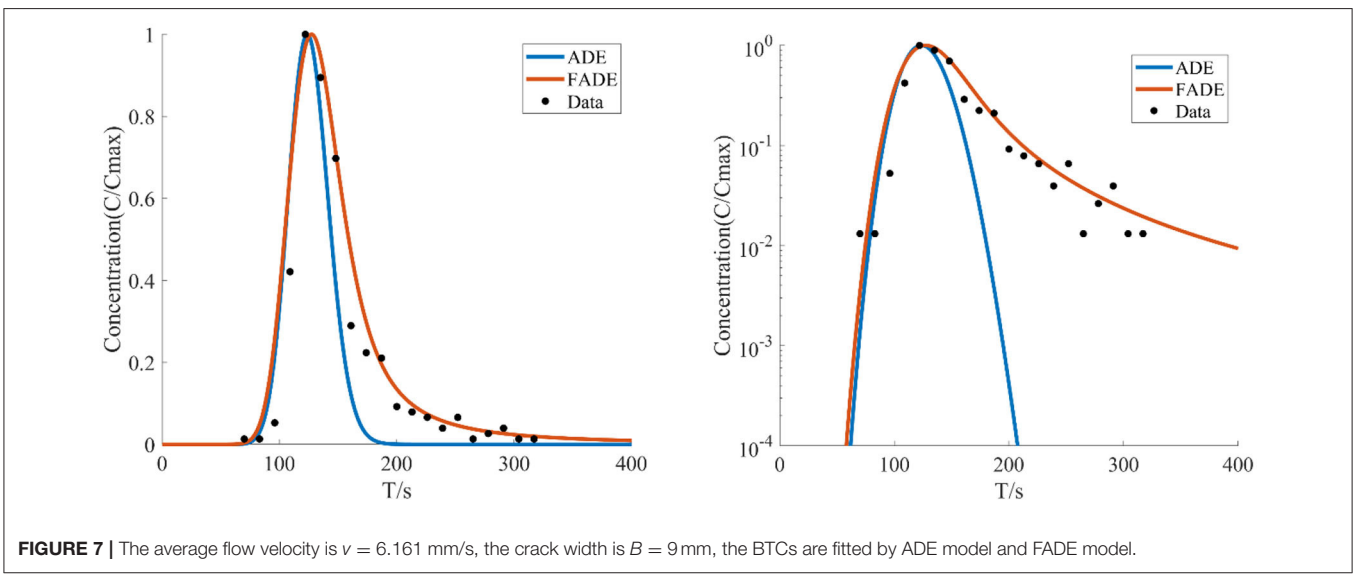

FIGURE 7 | The average flow velocity is $v = 6.161$ mm/s, the crack width is $B = 9$ mm, the BTCs are fitted by ADE model and FADE model.

fitting result is better. The expression is

$$RMSE = \sqrt{\frac{1}{N}\sum_{i=1}^{N}(C_{io} - C_{ie})^2} \quad (5)$$

$$R^2 = 1 - \frac{\sum_{i=1}^{N}(C_{io} - C_{ie})^2}{\sum_{i=1}^{N}(C_{io} - C_{io})^2} \quad (6)$$

where N is the number of individual observation points,C_{io} is the measured value of the concentration,C_{ie} is the simulated value of the concentration, $\bar{C}_{io}$ is the average value of the measured concentration.

RESULTS AND DISCUSSION

Non-Fickian Transport of Solute in Smooth Fractures

In order to better observe the trailing phenomenon of solute transport, **Figure 1**(left) is the graph of test results after taking logarithm, and the right side is the graph of test results under normal coordinate system.

Figures 1–4 show the fitting curves of different average flow rates for the same crack width $B = 4$ mm, and **Table 1** shows the fitting results of the FADE model. The results show that the ADE model approximately presents a normal distribution, while the FADE model can well-describe the tail phenomenon of BTCs. It shows that the time fractional derivative has an obvious advantage in describing the non-Fickian phenomenon of solute transport. In addition, according to the observation,

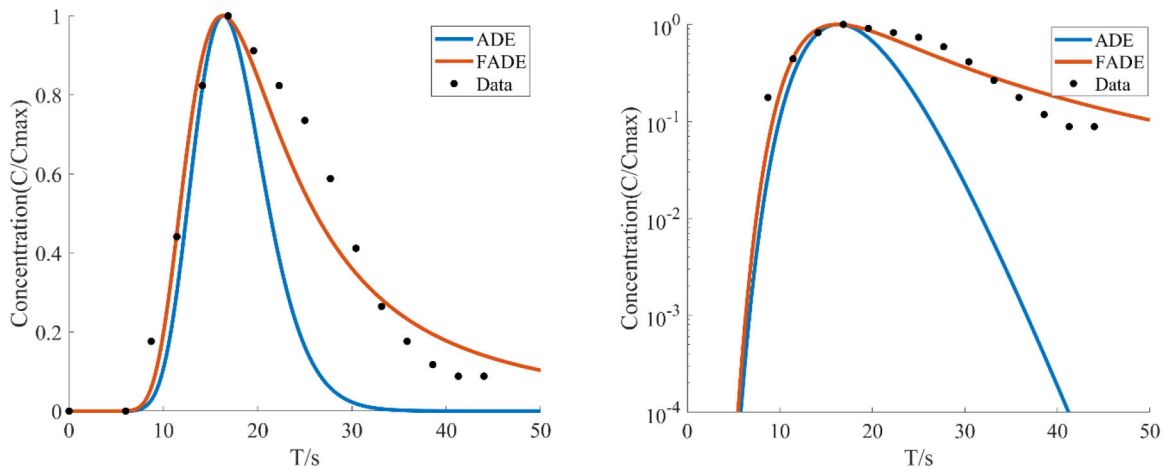

FIGURE 8 | With the average flow velocity $v = 40.5887$ mm/s, the average fracture width is $e = 4.9$ mm, the concentration of the relative roughness Δ/e is 0.2041 test data, the BTCs are fitted by ADE model and FADE model.

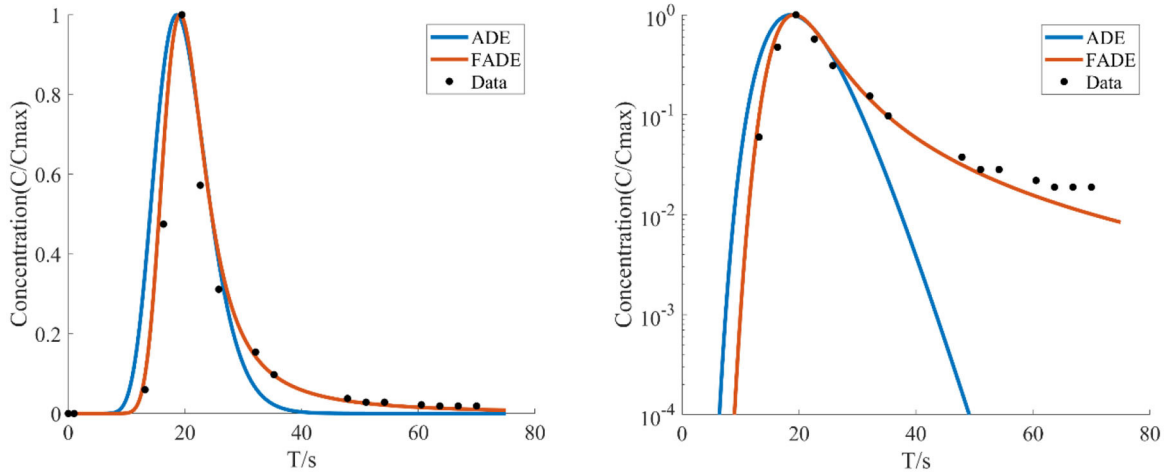

FIGURE 9 | With the average flow velocity $v = 31.2064$ mm/s, the average fracture width is $e = 4.9$ mm, the concentration of the relative roughness Δ/e is 0.2041 test data, the BTCs are fitted by ADE model and FADE model.

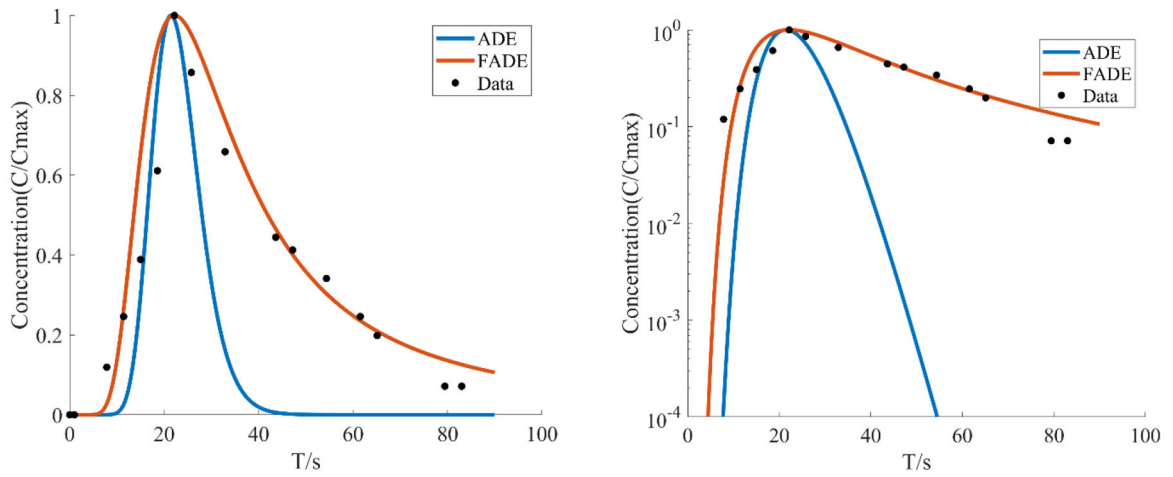

FIGURE 10 | With the average flow velocity $v = 23.3541$ mm/s, the average fracture width is $e = 4.9$ mm, the concentration of the relative roughness Δ/e is 0.2041 test data, the BTCs are fitted by ADE model and FADE model.

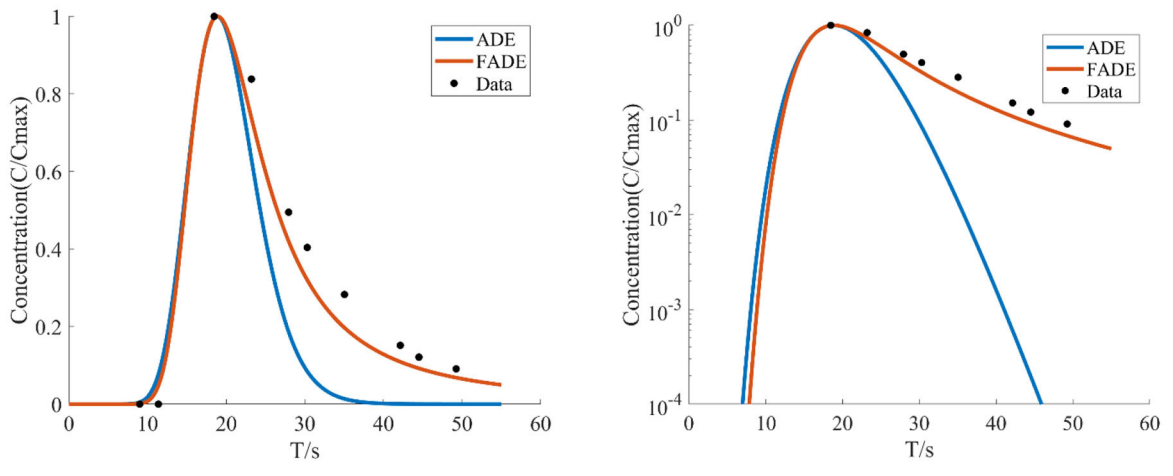

FIGURE 11 | With the average flow velocity $v = 22.5909$ mm/s, the average fracture width is $e = 4.5$ mm, the concentration of the relative roughness Δ/e is 0.4444 test data, the BTCs are fitted by ADE model and FADE model.

the fitting accuracy of the fade-away model is the highest at a lower average flow rate, indicating that the average flow rate plays an important role in characterization of the solute transport in fracture.

Figures 5–7 show the fitting curve of similar low average flow rate with different fracture widths. **Table 2** shows the fitting results of the FADE model with 4 types of fracture widths ranging from 4 to 9 mm. The results show, the peak arrival time of BTCs curve is gradually delayed and the peak duration is gradually prolonged with the increase of fracture width. Although the ADE model also offered an approximate trend, there is still a gap to the fitting results, while the FADE model is accurate. In addition, it is found that the FADE model provides a higher fitting accuracy in the smaller fracture widths, indicating that fracture width is also an important factor affecting the description of non-Fickian phenomena.

Non-Fickian Transport of Solute in Coarse Fractures

The First (Non-anastomosis) Experiment

Three experiments are conducted on the fracture pattern of a parallel plexiglass plate with a spacing of 6 mm and a length, width and height of 40 × 40 × 1 mm in the adhesion of a rough plastic plate (with a protuberance of 1 mm).

The Second (Non-anastomosis) Experiment

Three experiments are conducted on the fracture pattern of a parallel plexiglass plate with a spacing of 6 mm and a length, width and height of 40 × 40 × 2 mm in the adhesion of a rough plastic plate (with a protuberance of 1 mm).

Figures 8–12 show the fitting curves of the experimental results of two kinds of different fracture occurrence, while **Table 3** shows the fitting results of the FADE model of the five groups of

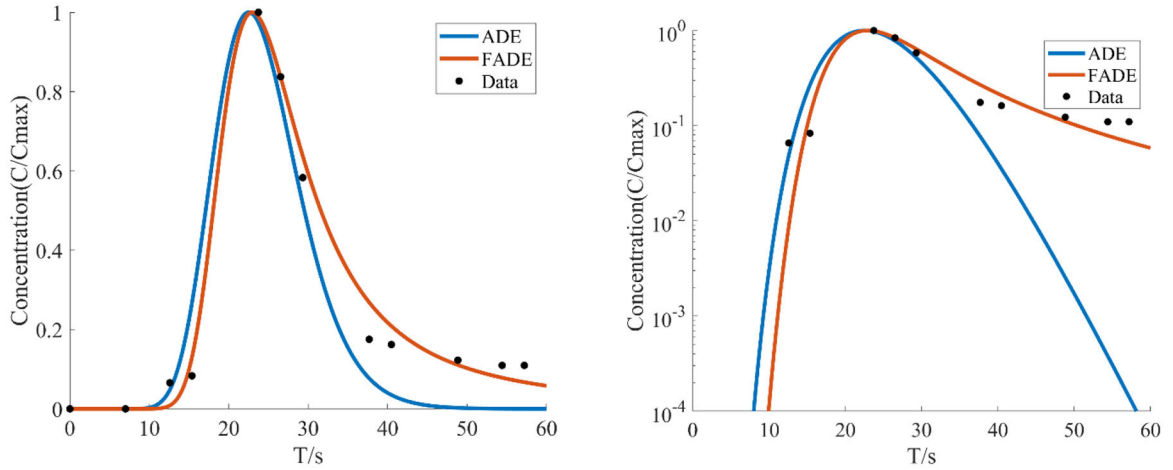

FIGURE 12 | With the average flow velocity $v = 18.0257$ mm/s, the average fracture width is $e = 4.5$ mm, the concentration of the relative roughness Δ/e is 0.4444 test data, the BTCs are fitted by ADE model and FADE model.

TABLE 3 | Parameter fitting of the FADE model with different mean flow rates under two groups of same relative roughness fracture conditions.

e(mm)	Δ/e	v(mm/s)	α	R^2	RMSE
4.9	0.2041	40.5887	0.8	0.9285	0.084
4.9	0.2041	31.2064	0.92	0.9626	0.0585
4.9	0.2041	23.3541	0.75	0.9268	0.0905
4.5	0.4444	18.0257	0.88	0.9774	0.0468
4.5	0.4444	22.5909	0.83	0.9681	0.054

experiments. Under the same relative roughness condition, the peak arrival time of the medium and low average flow rate is gradually delayed, and the accuracy of ADE model description is reduced accordingly. However, it can be observed from **Table 3** that the fitting accuracy of the FADE model is better. Under different roughness conditions, the higher the relative roughness value is, the better the fitting result of the FADE model in the experiment of low average flow rate is. It also indicates that the average flow rate and fracture roughness have significant influence on the non-Fickian phenomenon of solute transport in the fracture.

CONCLUSIONS

Two groups of experiments, a total of 12 times for different flow velocity, roughness of fracture, the width of fracture condition were carried out. Non-Fickian phenomena of solute transport were clearly observed. According to the fitting results of BTCs diagram and numerical analysis, it is clear that the heavy-tail phenomena of BTCs can be well-captured and described by the FADE model, while the ADE model can only roughly describe the peak value of BTCs. In addition, we found that the BTCs peak of rough fracture reaches earlier than that of smooth crack, and the phenomenon of long tail is more obvious. Compared with the traditional ADE model, the FADE model has a great advantage in describing the anomalous transport in a single fracture under the conditions of rough fracture and low average flow rate. However, the main disadvantage of the FADE model is that it takes more computational time, which is caused by the inclusion of convolution integral in the model. In the future, we can also study the law of solute transport in porous media and a more complicated transport process of reactive solutes. Furthermore, there are still many problems for our model to be solved such as how to determine the fractional derivative order, non-linear modeling of the fractional order and so on. More and more theoretical analysis and complex experiments need to be carried out to study in depth.

DATA AVAILABILITY STATEMENT

The original contributions presented in the study are included in the article/supplementary material, further inquiries can be directed to the corresponding author/s.

AUTHOR CONTRIBUTIONS

CQ mainly responsible for model making, conducting experiments, and writing paper. YX was responsible for the analysis and processing of experimental data, and paper writing, etc. WZ was responsible for the overall design of the experiment and the guidance of the paper. JQ assists in the overall design of the experimental plan and the design of the paper. YW assists in the analysis and processing of experimental data, and paper writing, etc. HS directs experiments and paper writing. All authors contributed to the article and approved the submitted version.

FUNDING

This study was supported by National Natural Science Foundation of China (41831289; 41772250; and 41877191). The National Natural Science Foundation of China (41831289) received for open access publication fees.

REFERENCES

1. Lee JY, Lee KK. Use of hydrologic time series data for identification of recharge mechanism in a fractured bedrock aquifer system. *J Hydrol.* (2000) **229**:190–201. doi: 10.1016/s0022-1694(00)00158-x
2. Le Borgne T, Bour O, Paillet FL, Caudal JP. Assessment of preferential flow path connectivity and hydraulic properties at single-borehole and cross-borehole scales in a fractured aquifer. *J Hydrol.* (2006) **328**:347–59. doi: 10.1016/j.jhydrol.2005.12.029
3. Manna F, Walton KM, Cherry JA, Parker BL. Mechanisms of recharge in a fractured porous rock aquifer in a semi-arid region. *J Hydrol.* (2017) **555**:869–80. doi: 10.1016/j.jhydrol.2017.10.060
4. Malard F, Reygrobellet JL, Soulie M. Transport and retention of fecal bacteria at sewage-polluted fractured rock sites. *J Environ Qual.* (1994) **23**:1352–63.doi: 10.2134/jeq1994.00472425002300060032x
5. Kreitler CW, Browning LA. Nitrogen-isotope analysis of groundwater nitrate in carbonate aquifers: natural sources versus human pollution. *J Hydrol.* (1983) **61**:285–301.doi: 10.1016/0022-1694(83)90254-8
6. Wang M, Zhao WD, Garrard R, Zhang Y, Liu Y, Qian JZ. Revisit of advection-dispersion equation model with velocity-dependent dispersion in capturing tracer dynamics in single empty fractures. *J Hydrodyn.* (2018) **30**:1055–63. doi: 10.1007/s42241-018-0134-2
7. Johns RA, Roberts PV. A solute transport model for channelized flow in a fracture. *Water Resour Res.* (1991) **27**:1797–808. doi: 10.1016/0148-9062(92)92286-l
8. Tsang YW, Tsang CF, Hale FV, Dverstorp B. Tracer transport in a stochastic continuum model of fractured media. *Water Resour Res.* (1996) **32**:3077–92. doi: 10.1029/96wr01397
9. Tsang YW, Tsang CF. Channel model of flow through fractured media. *Water Resour Res.* (1987) **23**:467–79. doi: 10.1029/wr023i003p00467
10. Morales T, Uriarte JA, Olazar M, Antigüedad I, Angulo B. Solute transport modelling in karst conduits with slow zones during different hydrologic conditions. *J Hydrol.* (2010) **390**:182–9.doi: 10.1016/j.jhydrol.2010.06.041
11. Marion A, Zaramella M, Bottacin-Busolin A. Solute transport in rivers with multiple storage zones: the STIR model. *Water Resour Res.* (2008) 44:W10406. doi: 10.1029/2008wr007037
12. Zhang Y, Benson DA, Reeves DM. Time and space nonlocalities underlying fractional-derivative models: distinction and literature review of field applications. *Adv Water Resour.* (2009) **32**:561–81. doi: 10.1016/j.advwatres.2009.01.008
13. Roubinet D, De Dreuzy JR, Tartakovsky DM. Particle-tracking simulations of anomalous transport in hierarchically fractured rocks. *Computers Geosci.* (2013) **50**:52–8.doi: 10.1016/j.cageo.2012.07.032
14. Pedretti D, Fernàndez-Garcia D, Bolster D, Sanchez-Vila X. On the formation of breakthrough curves tailing during convergent flow tracer tests in three-dimensional heterogeneous aquifers. *Water Resour Res.* (2013) **49**:4157–73. doi: 10.1002/wrcr.20330
15. Dentz M, Cortis A, Scher H, Berkowitz B. Time behavior of solute transport in heterogeneous media: transition from anomalous to normal transport. *Adv Water Resour.* (2004) **27**:155–73.doi: 10.1016/j.advwatres.2003.11.002
16. Chen Z, Qian JZ, Qin H. Experimental study of the non-darcy flow and solute transport in a channeled single fracture. *J Hydrodyn.* (2011) **23**:745–51.doi: 10.1016/s1001-6058(10)60172-2
17. Tan YF, Zhou ZF. Simulation of solute transport in a parallel single fracture with LBM/MMP mixed method. *J Hydrodyn.* (2008) **20**:365–72. doi: 10.1016/s1001-6058(08)60069-4
18. Srinivasan G, Tartakovsky DM, Dentz M, Viswanathan H, Berkowitz B, Robinson BA. Random walk particle tracking simulations of non-Fickian transport in heterogeneous media. *J Comput Phys.* (2010) **229**:4304–14. doi: 10.1016/j.jcp.2010.02.014
19. Qian J, Zhan H, Chen Z, Ye H. Experimental study of solute transport under non-Darcian flow in a single fracture. *J Hydrol.* (2011) **399**:246–54. doi: 10.1016/j.jhydrol.2011.01.003
20. Sun HG, Wang,Y., Jiazhong Qian J, Zhang Y, Zhou D. An investigation on fractional derivative model in characterizing sodium chloride transport in a single fracture. *Eur Phys J Plus.* (2019) **134**:440. doi: 10.1140/epjp/i2019-12954-9
21. Liu F, Anh VV, Turner I, Zhuang P. Time fractional advection-dispersion equation. *J Appl Math Comput.* (2003) **13**:233–45. doi: 10.1007/bf02936089
22. Huang F, Liu F. The fundamental solution of the space-time fractional advection-dispersion equation. *J Appl Math Comput.* (2005) **18**:339–50. doi: 10.1007/bf02936577
23. Benson DA, Meerschaert MM, Revielle J. Fractional calculus in hydrologic modeling: a numerical perspective. *Adv Water Resour.* (2013) **51**:479–97. doi: 10.1016/j.advwatres.2012.04.005
24. Fomin SA, Chugunov VA, Hashida T. Non-Fickian mass transport in fractured porous media. *Adv Water Resour.* (2011) **34**:205–14. doi: 10.1016/j.advwatres.2010.11.002
25. Suzuki A, Fomin SA, Chugunov VA, Niibori Y, Hashida T. Fractional diffusion modeling of heat transfer in porous and fractured media. *Int J Heat Mass Transfer.* (2016) **103**:611–8.doi: 10.1016/j.ijheatmasstransfer.2016.08.002
26. Grisak GE, Pickens JF. Solute transport through fractured media: 1. The effect of matrix diffusion. *Water Resour Res.* (1980) **16**:719–30. doi: 10.1029/wr016i004p00719
27. Qian JZ, Chen Z, Zhan HB, Luo SH. Solute transport in a filled single fracture under non-Darcian flow. *Int J Rock Mech Mining Sci.* (2011) **48**:132–40. doi: 10.1016/j.ijrmms.2010.09.009
28. Qian J, Chen Z, Zhan H, Guan H. Experimental study of the effect of roughness and Reynolds number on fluid flow in rough-walled single fractures: a check of local cubic law. *Hydrol Proc.* (2011) **25**:614–22. doi: 10.1002/hyp.7849
29. Peyman A, Gabriel C, Grant EH. Complex permittivity of sodium chloride solutions at microwave frequencies. *Bioelectromagnet J Bioelectromagnet Soc.* (2007) **28**:264–74.doi: 10.1002/bem.20271
30. Chen Y, Yi M, Yu C. Error analysis for numerical solution of fractional differential equation by Haar wavelets method. *J Comput Sci.* (2012) **3**:367–73. doi: 10.1016/j.jocs.2012.04.008
31. Xu M, Tan W. Intermediate processes and critical phenomena: theory, method and progress of fractional operators and their applications to modern mechanics. *Sci China Series G.* (2006) **49**:257–72.doi: 10.1007/s11433-006-0257-2
32. Shang YL. Vulnerability of networks: fractional percolation on random graphs. *Phys Rev E Stat Nonlin Soft Matter Phys.* (2014) **89**:012813. doi: 10.1103/PhysRevE.89.012813
33. Atangana A, Kilicman A. Analytical solutions of the space-time fractional derivative of advection dispersion equation. *Math Probl Eng.* (2013) **2013**:1–9. doi: 10.1155/2013/853127
34. Garrard RM, Zhang Y, Wei S, Sun H, Qian J. Can a time fractional-derivative model capture scale-dependent dispersion in saturated soils. *Groundwater.* (2017) **55**:857–70.doi: 10.1111/gwat.12532
35. Sun H, Chen W, Li C, Chen Y. Fractional differential models for anomalous diffusion. *Physica A Statist Mech Appl.* (2010) **389**:2719–24. doi: 10.1016/j.physa.2010.02.030
36. Wang W, Lu Y. Analysis of the mean absolute error (MAE) and the root mean square error (RMSE) in assessing rounding model. In: *IOP Conference Series: Materials Science and Engineering*. Kuala Lumpur: IOP Publishing (2018). doi: 10.1088/1757-899x/324/1/012049
37. Willmott CJ, Matsuura K. Advantages of the mean absolute error (MAE) over the root mean square error (RMSE) in assessing average model performance. *Clim Res.* (2005) **30**:79–82. doi: 10.3354/cr030079

Conflict of Interest: YW was employed by company Shandong Luqing Safety Assessment Technology Co., Ltd.

The remaining authors declare that the research was conducted in the absence of any commercial or financial relationships that could be construed as a potential conflict of interest.

Copyright © 2020 Qiao, Xu, Zhao, Qian, Wu and Sun. This is an open-access article distributed under the terms of the Creative Commons Attribution License (CC BY). The use, distribution or reproduction in other forums is permitted, provided the original author(s) and the copyright owner(s) are credited and that the original publication in this journal is cited, in accordance with accepted academic practice. No use, distribution or reproduction is permitted which does not comply with these terms.

frontiers in Physics

ORIGINAL RESEARCH
published: 23 September 2020
doi: 10.3389/fphy.2020.00352

New Aspects of ZZ Transform to Fractional Operators With Mittag-Leffler Kernel

Rajarama Mohan Jena[1], *Snehashish Chakraverty*[1]*, *Dumitru Baleanu*[2,3] and *Maysaa M. Alqurashi*[4]

[1] Department of Mathematics, National Institute of Technology Rourkela, Rourkela, India, [2] Department of Mathematics, Faculty of Art and Sciences, Cankaya University Balgat, Ankara, Turkey, [3] Institute of Space Sciences, Magurele-Bucharest, Romania, [4] Department of Mathematics, King Saud University, Riyadh, Saudi Arabia

In this paper, we discuss the relationship between the Zain Ul Abadin Zafar (ZZ) transform with Laplace and Aboodh transforms. Further, the ZZ transform is applied to the fractional derivative with the Mittag-Leffler kernel defined in both the Caputo and Riemann-Liouville sense. In order to illustrate the validity and applicability of the transform, we solve some illustrative examples.

Keywords: ZZ transform, fractional calculus, aboodh transform, non-singular kernel, mittag-leffler kernel

OPEN ACCESS

Edited by:
Jordan Yankov Hristov, University of Chemical Technology and Metallurgy, Bulgaria

Reviewed by:
Praveen Agarwal, Anand International College of Engineering, India
Yang Liu, Inner Mongolia University, China
Shilpi Jain, Poornima College of Engineering, India

***Correspondence:**
Snehashish Chakraverty
sne_chak@yahoo.com

Specialty section:
This article was submitted to Mathematical and Statistical Physics, a section of the journal Frontiers in Physics

Received: *25 February 2020*
Accepted: *24 July 2020*
Published: *23 September 2020*

Citation:
Jena RM, Chakraverty S, Baleanu D and Alqurashi MM (2020) New Aspects of ZZ Transform to Fractional Operators With Mittag-Leffler Kernel. Front. Phys. 8:352. doi: 10.3389/fphy.2020.00352

1. OUTLINE AND MOTIVATION

In recent years, fractional calculus (FC) has gained considerable achievements in various fields of science and engineering. Many physical problems [1–7] are modeled by using fractional differential equations (FDE) more accurately than classical differential equations [8–11]. Earlier, various real-life problems were modeled by using the Caputo and Riemann-Liouville (R-L) fractional derivatives. However, Caputo and Fabrizio proposed a new idea that reflects the exponential kernel [12] to address a new way of modeling phenomena with non-local effects. Further, in [13], a new fractional operator (AB) with a Mittag-Leffler kernel was developed. So, in this regard, many researchers [14–16] have given their interest in this definition to solve various problems/models. In fact, in modeling real phenomena, we need a variety of fractional operators to thoroughly describe the complexity of the problem studied. Some other studies regarding fractional calculus and special functions can be found in the literature [17–26].

In the present study, we establish the relationship between the ZZ transform (ZZT) with the Aboodh transform (AT), and the Laplace transform (LT) having their various applications given in [27–31]. Next, the ZZT has been applied to AB fractional operators defined in the Caputo and R-L sense, which are described in terms of theorems. Later, we have solved some test examples defined in the AB sense using this ZZT. The contribution of the present authors to this manuscript are (i) firstly establishing the relationship among ZZT, LT, and AT, (ii) secondly applying ZZT to fractional differential equations defined in the AB derivative to get the solution of the problems. The ZZ transform is the generalization of some famous transforms and we can relate this transformation to other well-known transforms. If we divide the ZZ transform by the transformed variable, then we get the Natural transform. Similarly, relations with other integral transforms in terms of theorems have been included in this paper. The main benefit of this transformation is that it may converge to the Sumudu transform and is advantageous in solving FDEs with variable coefficients.

The organization of the paper is as follows: In section Preliminaries and Basic Definitions, we establish the connection between the Aboodh and ZZ transform; we prove some significant results and create the relationships between AB derivatives with ZZT. In section Applications, some FDEs are solved using ZZT. Finally, a conclusion section is included in section Conclusion.

2. PRELIMINARIES AND BASIC DEFINITIONS

Definition 2.1

The Aboodh transform is obtained on the set of functions

$$B = \left\{ f(t) : \exists\, M, m_1, m_2 > 0, \left| f(t) \right| < Me^{-st} \right\}$$

and is defined as [27, 28]

$$A\left\{ f(t) \right\} = \frac{1}{s} \int_0^\infty f(t)\, e^{-st} dt, t > 0 \text{ and } m_1 \le s \le m_2$$

Theorem 2.1

Let us consider G and Fas the Aboodh and Laplace transforms of $f(t) \in B$ then [32]

$$G(s) = \frac{F(s)}{s}. \tag{2.1}$$

The ZZT was introduced by Zain Ul Abadin Zafar [29, 30]. It generalizes the Aboodh and Laplace integral transforms. In the following definition, we discuss the definition of ZZT.

Definition 2.2 (ZZ Transform)

Suppose $f(t)\ \forall\ t \ge 0$ is a function then the ZZT $Z(v, s)$ of $f(t)$ is defined as [29, 30]

$$ZZ\left(f(t) \right) = Z(v, s) = s \int_0^\infty f(vt)\ e^{-st} dt.$$

Similar to the Aboodh and Laplace transforms, the ZZT is also linear. The MLF is an extension of exponential function which is defined as.

$$E_\alpha(z) = \sum_{n=0}^{\infty} \frac{z^n}{\Gamma(1 + n\alpha)}, \quad \text{Re}(\alpha) > 0.$$

Definition 2.3

Let us consider a function $\xi(x, t) \in H^1(a, b)$, then for $\alpha \in (0, 1)$, the Atangana-Baleanu Caputo (ABC) derivative is written as [13].

$${}^{ABC}{}_a D_t^\alpha \xi(x, t) = \frac{\psi(\alpha)}{1 - \alpha} \int_a^t \xi'(x, \tau)\, E_\alpha \left(\frac{-\alpha (t - \tau)^\alpha}{1 - \alpha} \right) d\tau.$$

Definition 2.4

Let $\xi(x, t) \in H^1(a, b)$, then for $\alpha \in (0, 1)$, the Atangana-Baleanu Riemann-Liouville (ABR) derivative is given as [13]

$${}^{ABR}_{\ a} D_t^\alpha \xi(x, t) = \frac{\psi(\alpha)}{1 - \alpha} \frac{d}{dt} \int_a^t \xi(x, \tau)\, E_\alpha \left(\frac{-\alpha (t - \tau)^\alpha}{1 - \alpha} \right) d\tau,$$

where $\psi(\alpha)$is a function with the conditions $\psi(0) = \psi(1) =$ 1and $b > a$.

Theorem 2.2

The LT of ABC and ABR derivative are, respectively, given as [13]

$$\mathrm{L}\left\{ {}^{ABC}_{a} D_t^\alpha \xi(x, t) \right\}(s) = \frac{\psi(\alpha)}{1 - \alpha} \frac{s^\alpha L\{\xi(x, t)\} - s^{\alpha - 1} \xi(x, 0)}{s^\alpha + \frac{\alpha}{1 - \alpha}} \tag{2.2}$$

and

$$\mathrm{L}\left\{ {}^{ABR}_{\ a} D_t^\alpha \xi(x, t) \right\}(s) = \frac{\psi(\alpha)}{1 - \alpha} \frac{s^\alpha L\{\xi(x, t)\}}{s^\alpha + \frac{\alpha}{1 - \alpha}}. \tag{2.3}$$

The following theorems have been proposed where it is assumed that $f(t) \in H^1(a, b)$, $b > a$and $\alpha \in (0, 1)$.

Theorem 2.3

The AT of ABC derivative is given as.

$$\begin{aligned} G(s) &= A\left\{ {}^{ABC}_{a} D_t^\alpha \xi(x, t) \right\}(s) \\ &= \frac{1}{s} \left[\frac{\psi(\alpha)}{1 - \alpha} \frac{s^\alpha L\{\xi(x, t)\} - s^{\alpha - 1} \xi(x, 0)}{s^\alpha + \frac{\alpha}{1 - \alpha}} \right]. \end{aligned} \tag{2.4}$$

Proof: Using Theorem 2.1 and Equation. (2.2), we may get the desired result.

Theorem 2.4

The Aboodh transform of ABR derivative is written as.

$$G(s) = A\left\{ {}^{ABR}_{\ a} D_t^\alpha \xi(x, t) \right\}(s) = \frac{1}{s} \left[\frac{\psi(\alpha)}{1 - \alpha} \frac{s^\alpha L\{\xi(x, t)\}}{s^\alpha + \frac{\alpha}{1 - \alpha}} \right]. \tag{2.5}$$

Proof

Applying the Theorem 2.1 and Equation (2.3), we obtain the required result.

The connection between the transforms of Aboodh and ZZ is given in the theorem below.

Theorem 2.5

If $G(s)$ and$Z(v, s)$ are the Aboodh and ZZ transforms of $f(t) \in B$. Then, we obtain

$$Z(v, s) = \frac{s^2}{v^2} G\left(\frac{s}{v} \right).$$

Proof. From the definition of ZZ transform we have

$$Z(v, s) = s \int_0^\infty f(vt)\ e^{-st} dt. \tag{2.6}$$

Substituting $vt = \tau$ in Equation (2.6) we get

$$Z(v,s) = \frac{s}{v}\int_0^\infty f(\tau)\, e^{-\frac{s\tau}{v}} d\tau. \tag{2.7}$$

The right-hand side of the above Equation (2.7) may be written as.

$$Z(v,s) = \frac{s}{v}F\left(\frac{s}{v}\right), \tag{2.8}$$

where $F(.)$ denotes the Laplace transform of $f(t)$.

Applying the Theorem 2.1, Equation (2.8) can be expressed as

$$Z(v,s) = \frac{s}{v}\frac{F\left(\frac{s}{v}\right)}{\left(\frac{s}{v}\right)} \times \left(\frac{s}{v}\right) = \left(\frac{s}{v}\right)^2 G\left(\frac{s}{v}\right), \tag{2.9}$$

where $G(.)$ denotes the Aboodh transform of $f(t)$.

Theorem 2.6

ZZ transform of $f(t) = t^{\alpha-1}$ is given as

$$Z(v,s) = \Gamma(\alpha)\left(\frac{v}{s}\right)^{\alpha-1}. \tag{2.10}$$

Proof. The Aboodh transform of $f(t) = t^\alpha, \alpha \geq 0$ is

$$G(s) = \frac{\Gamma(\alpha)}{s^{\alpha+1}},$$

$$\text{Now,} \quad G\left(\frac{s}{v}\right) = \frac{\Gamma(\alpha)\, v^{\alpha+1}}{s^{\alpha+1}}.$$

Using Equation (2.9), we obtain.

$$Z(v,s) = \frac{s^2}{v^2}G\left(\frac{s}{v}\right) = \frac{s^2}{v^2}\frac{\Gamma(\alpha)\, v^{\alpha+1}}{s^{\alpha+1}} = \Gamma(\alpha)\left(\frac{v}{s}\right)^{\alpha-1}.$$

Theorem 2.7

Let $\alpha, \omega \in C$ and $\mathrm{Re}(\alpha) > 0$, then the ZZ transform of $E_\alpha(\omega t^\alpha)$ is given as

$$ZZ\left\{\left(E_\alpha\left(\omega t^\alpha\right)\right)\right\} = Z(v,s) = \left(1 - \omega\left(\frac{v}{s}\right)^\alpha\right)^{-1} \tag{2.11}$$

Proof. We know that Aboodh transform of $E_\alpha(\omega t^\alpha)$ is written as.

$$G(s) = \frac{F(s)}{s} = \frac{s^{\alpha-1}}{s\,(s^\alpha - \omega)}, \tag{2.12}$$

$$\text{So,} \quad G\left(\frac{s}{v}\right) = \frac{\left(\frac{s}{v}\right)^{\alpha-1}}{\left(\frac{s}{v}\right)\left(\left(\frac{s}{v}\right)^\alpha - \omega\right)}, \tag{2.13}$$

Using the Theorem 2.9, we obtain.

$$\begin{aligned} Z(v,s) &= \left(\frac{s}{v}\right)^2 G\left(\frac{s}{v}\right) = \left(\frac{s}{v}\right)^2 \frac{\left(\frac{s}{v}\right)^{\alpha-1}}{\left(\frac{s}{v}\right)\left(\left(\frac{s}{v}\right)^\alpha - \omega\right)} \\ &= \frac{\left(\frac{s}{v}\right)^\alpha}{\left(\frac{s}{v}\right)^\alpha - \omega} = \left(1 - \omega\left(\frac{v}{s}\right)^\alpha\right)^{-1}. \end{aligned}$$

Theorem 2.8

If $G(s)$ and $Z(v,s)$ are the Aboodh and ZZ transforms of $f(t)$. Then the ZZT of ABC derivative is written as.

$$ZZ\left\{{}_0^{ABC}D_t^\alpha f(t)\right\} = \left[\frac{\psi(\alpha)}{1-\alpha}\frac{\frac{s^{\alpha+2}}{v^{\alpha+2}}G\left(\frac{s}{v}\right) - \frac{s^\alpha}{v^\alpha}f(0)}{\frac{s^\alpha}{v^\alpha} + \frac{\alpha}{1-\alpha}}\right]. \tag{2.14}$$

Proof. Using the Equations (2.1) and (2.4), we have

$$G\left(\frac{s}{v}\right) == \frac{v}{s}\left[\frac{\psi(\alpha)}{1-\alpha}\frac{\left(\frac{s}{v}\right)^{\alpha+1}G\left(\frac{s}{v}\right) - \left(\frac{s}{v}\right)^{\alpha-1}f(0)}{\left(\frac{s}{v}\right)^\alpha + \frac{\alpha}{1-\alpha}}\right]. \tag{2.15}$$

So, the ZZ transform of ABC is given as.

$$\begin{aligned} Z(v,s) &= \left(\frac{s}{v}\right)^2 G\left(\frac{s}{v}\right) \\ &= \left(\frac{s}{v}\right)^2 \frac{v}{s}\left[\frac{\psi(\alpha)}{1-\alpha}\frac{\left(\frac{s}{v}\right)^{\alpha+1}G\left(\frac{s}{v}\right) - \left(\frac{s}{v}\right)^{\alpha-1}f(0)}{\left(\frac{s}{v}\right)^\alpha + \frac{\alpha}{1-\alpha}}\right] \\ &= \left[\frac{\psi(\alpha)}{1-\alpha}\frac{\left(\frac{s}{v}\right)^{\alpha+2}G\left(\frac{s}{v}\right) - \left(\frac{s}{v}\right)^\alpha f(0)}{\left(\frac{s}{v}\right)^\alpha + \frac{\alpha}{1-\alpha}}\right] \end{aligned}$$

Theorem 2.9

Let us assume that$G(s)$ and $Z(v,s)$ are the Aboodh and ZZ transform of $f(t)$. Then the ZZ transform of ABR derivative is given as

$$ZZ\left\{{}_0^{ABR}D_t^\alpha f(t)\right\} = \left[\frac{\psi(\alpha)}{1-\alpha}\frac{\frac{s^{\alpha+2}}{v^{\alpha+2}}G\left(\frac{s}{v}\right)}{\frac{s^\alpha}{v^\alpha} + \frac{\alpha}{1-\alpha}}\right]. \tag{2.16}$$

Proof. Using the Equations (2.1) and (2.5), we get

$$G\left(\frac{s}{v}\right) = \frac{v}{s}\left[\frac{\psi(\alpha)}{1-\alpha}\frac{\left(\frac{s}{v}\right)^{\alpha+1}G\left(\frac{s}{v}\right)}{\left(\frac{s}{v}\right)^\alpha + \frac{\alpha}{1-\alpha}}\right]. \tag{2.17}$$

From the Equation (2.9), the ZZ transform of ABR is written as.

$$\begin{aligned} Z(v,s) = \left(\frac{s}{v}\right)^2 G\left(\frac{s}{v}\right) &= \left(\frac{s}{v}\right)^2 \left(\frac{v}{s}\right)\left[\frac{\psi(\alpha)}{1-\alpha}\frac{\left(\frac{s}{v}\right)^{\alpha+1}G\left(\frac{s}{v}\right)}{\left(\frac{s}{v}\right)^\alpha + \frac{\alpha}{1-\alpha}}\right] \\ &= \left[\frac{\psi(\alpha)}{1-\alpha}\frac{\left(\frac{s}{v}\right)^{\alpha+2}G\left(\frac{s}{v}\right)}{\left(\frac{s}{v}\right)^\alpha + \frac{\alpha}{1-\alpha}}\right]. \end{aligned}$$

3. APPLICATIONS

Let us consider the following initial value problem (IVP) defined in ABC sense [15]

$$\begin{cases} {}_0^{ABC}D_t^{\alpha} y(t) = f\left(t, y(t)\right), \ t > 0, \\ y(0) = k, \quad k \in \Re. \end{cases} \tag{3.1}$$

Suppose $Z(v,s)$ and $T(v,s)$ are the ZZ transforms of $y(t)$and f, respectively. Then by taking the ZZT on both sides of Equation (3.1) and using Equations (2.9) and (2.14), we may get

$$\left[\frac{\psi(\alpha)}{1-\alpha}\frac{\left(\frac{s}{v}\right)^{\alpha} Z(v,s) - \left(\frac{s}{v}\right)^{\alpha} y(0)}{\left(\frac{s}{v}\right)^{\alpha} + \frac{\alpha}{1-\alpha}}\right] = T(v,s).$$

$$\left[\psi(\alpha)\frac{Z(v,s)-k}{\left(1-\alpha+\alpha\left(\frac{v}{s}\right)^{\alpha}\right)}\right] = T(v,s)$$

$$\text{Thus, } Z(v,s) = \frac{1-\alpha+\alpha\left(\frac{v}{s}\right)^{\alpha}}{\psi(\alpha)} T(v,s) + k. \tag{3.2}$$

Then, by applying the inverse ZZT on both sides of Equation (3.2), we obtain the exact solution.

Similarly, we may solve Equation (3.1) defined in ABR derivative.

Example 3.1

Let us take the following fractional IVP [15]

$$\begin{cases} {}_0^{ABC}D_t^{\alpha} y(t) = y(t), \ t > 0, \\ y(0) = 1. \end{cases} \tag{3.3}$$

Firstly, we apply the ZZT on both sides of Equation (3.3) which gives

$$\left[\frac{\psi(\alpha)}{1-\alpha}\frac{\left(\frac{s}{v}\right)^{\alpha} Z(v,s) - \left(\frac{s}{v}\right)^{\alpha} y(0)}{\left(\frac{s}{v}\right)^{\alpha} + \frac{\alpha}{1-\alpha}}\right] = Z(v,s). \tag{3.4}$$

Simplifying Equation (3.4) and using the initial condition, we have

$$\left[\psi(\alpha)\frac{Z(v,s)-1}{\left(1-\alpha+\alpha\left(\frac{v}{s}\right)^{\alpha}\right)}\right] = Z(v,s). \tag{3.5}$$

The simplification of Equation (3.5) gives us the following:

$$Z(v,s) = \frac{1}{1-\frac{1-\alpha+\alpha\left(\frac{v}{s}\right)^{\alpha}}{\psi(\alpha)}} = \frac{\psi(\alpha)}{\psi(\alpha)-1+\alpha-\alpha\left(\frac{v}{s}\right)^{\alpha}}. \tag{3.6}$$

Equation (3.6) may be rewritten as.

$$Z(v,s) = \frac{\psi(\alpha)}{(\psi(\alpha)-1+\alpha)}\left(1 - \frac{\alpha}{\psi(\alpha)-1+\alpha}\left(\frac{v}{s}\right)^{\alpha}\right)^{-1} \tag{3.7}$$

Applying the inverse of the ZZT on Equation (3.7) and using Equation (2.11), Equation (3.7) is reduced to

$$y(t) = \frac{\psi(\alpha)}{(\psi(\alpha)-1+\alpha)} E_{\alpha}\left(\frac{\alpha}{\psi(\alpha)-1+\alpha} t^{\alpha}\right), \tag{3.8}$$

where $E_{\alpha}(t)$ is the MLF.

Substituting $\alpha = 1$ in Equation (3.8), we obtain

$$y(t) = E_1(t) = e^t, \tag{3.9}$$

which is the exact solution of Equation (3.3) when $\alpha = 1$.

Example 3.2

Considering the following fractional IVP [15]

$$\begin{cases} {}_0^{ABC}D_t^{\alpha} y(t) = \eta t, \ t > 0, \\ y(0) = 0. \end{cases} \tag{3.10}$$

Taking the ZZT on both sides of Equation (3.10) and plugging the initial condition, we get

$$\left[\frac{\psi(\alpha)}{1-\alpha}\frac{\left(\frac{s}{v}\right)^{\alpha} Z(v,s) - \left(\frac{s}{v}\right)^{\alpha} y(0)}{\left(\frac{s}{v}\right)^{\alpha} + \frac{\alpha}{1-\alpha}}\right] = \eta\left(\frac{v}{s}\right),$$

$$\left[\psi(\alpha)\frac{Z(v,s)}{\left(1-\alpha+\alpha\left(\frac{v}{s}\right)^{\alpha}\right)}\right] = \eta\left(\frac{v}{s}\right),$$

$$\begin{aligned} Z(v,s) &= \eta\left(\frac{v}{s}\right)\frac{\left(1-\alpha+\alpha\left(\frac{v}{s}\right)^{\alpha}\right)}{\psi(\alpha)} \\ &= \frac{\eta}{\psi(\alpha)}\left[(1-\alpha)\left(\frac{v}{s}\right) + \alpha\left(\frac{v}{s}\right)^{\alpha+1}\right]. \end{aligned} \tag{3.11}$$

Applying inverse ZZT on both sides of Equation (3.11), we obtain

$$y(t) = \frac{\eta}{\psi(\alpha)}\left[(1-\alpha)t + \frac{\alpha}{\Gamma(\alpha+2)} t^{\alpha+1}\right]. \tag{3.12}$$

It is noticed that if we put $\alpha = 0$, then Equation (3.12) reduces to $y(t) = \eta t$ and substituting $\alpha = 1$ in Equation (3.12), we obtain $y(t) = \eta\frac{t^2}{2}$. Plugging $\alpha = 0.5$, we get $y(t) = \frac{\eta}{\psi(0.5)}\left[\frac{t}{2} + \frac{2}{3\sqrt{\pi}} t^{\frac{3}{2}}\right]$.

4. CONCLUSION

In this manuscript, the ZZT is debated and the associated properties of ZZT are established. Some theorems related to the connection between the ZZ, Aboodh, and Laplace transforms are successfully proven. ZZT was applied to FDEs within the AB derivatives. Besides, some fractional initial value problems are solved in order to illustrate the validity and performance of this transformation.

DATA AVAILABILITY STATEMENT

The original contributions presented in the study are included in the article/supplementary materials, further inquiries can be directed to the corresponding author/s.

AUTHOR CONTRIBUTIONS

RJ: conceptualization, writing–original draft, methodology, software, and validation. SC and DB: project administration and supervision. MA and DB: funding acquisition. SC, DB, and MA: contributed to the analysis, discussion of the results, and help in revision. All authors listed have made a substantial, direct and intellectual contribution to the work, and approved it for publication.

ACKNOWLEDGMENTS

The first author would like to acknowledge the Department of Science and Technology of the Government of India for providing financial support under the scheme of the INSPIRE Fellowship (IF170207) to carry out the present research.

REFERENCES

1. Jena RM, Chakraverty S. Residual power series method for solving time-fractional model of vibration equation of large membranes. *J Appl Comput Mech.* (2019) **5**:603–15. doi: 10.22055/jacm.2018.26668.1347
2. Jena RM, Chakraverty S. A new iterative method based solution for fractional black-scholes option pricing equations (BSOPE). *SN Appl Sci.* (2019) **1**:95. doi: 10.1007/s42452-018-0106-8
3. Jena RM, Chakraverty S, Jena SK. Dynamic response analysis of fractionally damped beams subjected to external loads using homotopy analysis method (HAM). *J Appl Comput Mech.* (2019) **5**:355–66. doi: 10.22055/JACM.2019.27592.1419
4. Edeki SO, Akinlabi GO, Jena RM, Ogundile OP. Conformable decomposition method for time-space fractional intermediate scalar transportation model. *J Theor Appl Inform Technol.* (2019) **97**:4251–8.
5. Jena RM, Chakraverty S, Baleanu D. On the solution of imprecisely defined nonlinear time-fractional dynamical model of marriage. *Mathematics.* (2019) **7**:689. doi: 10.3390/math7080689
6. Jena RM, Chakraverty S, Baleanu D. On new solutions of time-fractional wave equations arising in shallow water wave propagation. *Mathematics.* (2019) **7**:722. doi: 10.3390/math7080722
7. Jena RM, Chakraverty S. Boundary characteristic orthogonal polynomials-based galerkin and least square methods for solving bagley–torvik equations. *Recent Trends Wave Mech Vibrations.* (2019) **13**:327–42. doi: 10.1007/978-981-15-0287-3_24
8. Baleanu D, Machado JAT, Luo ACJ. *Fractional Dynamics, and Control*. New York, NY: Springer (2012). doi: 10.1007/978-1-4614-0457-6
9. Baleanu D, Diethelm K, Scalas E, Trujillo JJ. *Fractional Calculus: Models and Numerical Methods*. Singapore: World Scientific Publishing Company (2012). doi: 10.1142/8180
10. Kilbas AA, Srivastava HM, Trujillo JJ. *Theory and Application of Fractional Differential Equations*. Amsterdam: Elsevier Science B.V (2006).
11. Yang XJ, Baleanu D, Srivastava HM. *Local Fractional Integral Transform and their Applications*. New York, NY: Academic Press (2015). doi: 10.1016/B978-0-12-804002-7.00004-8
12. Caputo M, Fabrizio M. A new definition of fractional derivative without singular kernel. *Progr Fract Differ Appl.* (2015) **1**:1–13. doi: 10.18576/pfda/020101
13. Atangana A, Baleanu D. New fractional derivatives with nonlocal and non-singular kernel: theory and application to heat transfer model. *Therm Sci.* (2016) **20**:763–9. doi: 10.2298/TSCI160111018A
14. Saad KM, Atangana A, Baleanu D. New fractional derivatives with non-singular kernel applied to the burgers equation. *Chaos Interdiscip J Nonlinear Sci.* (2018) **28**:063109. doi: 10.1063/1.5026284
15. Bokhari A, Baleanu D, Belgacem R. Application of shehu transform to atangana-Baleanu derivatives. *J Math Computer Sci.* (2020) **20**:101–7. doi: 10.22436/jmcs.020.02.03
16. Kumar S, Kumar A, Nieto JJ, Sharma B. *Atangana–Baleanu Derivative With Fractional Order Applied to the Gas Dynamics Equations, Fractional Derivatives With Mittag-Leffler Kernel, Studies in Systems, Decision, and Control*. Cham: Springer (2019). p. 194. doi: 10.1007/978-3-030-11662-0_14
17. Liu Y, Fan E, Yin B, Li H. Fast algorithm based on the novel approximation formula for the Caputo-Fabrizio fractional derivative. *AIMS Mathe.* (2020) **5**:1729–44. doi: 10.3934/math.2020117
18. Jena RM, Chakraverty S, Rezazadeh H, Ganji DD. On the solution of time-fractional dynamical model of Brusselator reaction-diffusion system arising in chemical reactions. *Mathe Methods Appl Sci.* (2020) **43**:1–11. doi: 10.1002/mma.6141
19. Agarwal P, Baleanu D, Chen Y, Momani S, Machado JAT. *Fractional Calculus: ICFDA, Springer Proceedings in Mathematics & Statistics Book*. Jordan: Springer (2018). p. 16–18. doi: 10.1007/978-981-15-0430-3
20. Jena RM, Chakraverty S, Baleanu D. A novel analytical technique for the solution of time-fractional Ivancevic option pricing model. *Phys A: Statist Mech Appl.* (2020) **550**:124380. doi: 10.1016/j.physa.2020.124380
21. Agarwal P. *A Study of New Trends and Analysis of Special Function*. Germany: LAP LAMBERT Academic Publishing (2013).
22. Jena RM, Chakraverty S, Yavuz M. Two-hybrid techniques coupled with an integral transformation for caputo time-fractional navier- stokes equations. *Prog Fract Different App.* (2020) **6**:201–13. doi: 10.18576/pfda/060304
23. Chakraverty S, Jena RM, Jena SK. Time-fractional order biological systems with uncertain parameters. *Morgan Claypool Publ.* (2020) **12**:1–60. doi: 10.2200/S00976ED1V01Y201912MAS031
24. Srivastava HM, Jena RM, Chakraverty S, Jena SK. Dynamic response analysis of fractionally-damped generalized bagley-torvik equation subject to external loads. *Rus J Mathe Phys.* (2020) **27**:254–68. doi: 10.1134/S1061920820020120
25. Agarwal P, Jain S, Mansour T. Further extended caputo fractional derivative operator and its applications. *Rus J Mathe Phys.* (2017) **24**:415–25. doi: 10.1134/S106192081704001X
26. Jena RM, Chakraverty S, Baleanu D. Solitary wave solution for a generalized hirota-Satsuma coupled KdV and MKdV equations: A semi-analytical approach. *Alex Eng J*. (2020). doi: 10.1016/j.aej.2020.01.002
27. Aboodh KS. Application of new transform aboodh transform to partial differential equations. *Glob J Pure Appl Mathe.* (2014) **10**:249–54.
28. Aboodh KS. Solving fourth order parabolic PDE with variable coefficients using Aboodh transform homotopy perturbation method. *Pure Appl Mathe J.* (2015) **4**:219–24. doi: 10.11648/j.pamj.20150405.13

29. Zafar ZUA. Application of ZZ transform method on some fractional differential equations. *Int J Adv Eng Global Technol.* (2016) **4**:1355–63.
30. Zafar ZUA. ZZ transform method. *Int J Adv Eng Glob Technol.* (2016) **4**:1605–11.
31. Riabi L, Belghaba K, Cherif MH, Ziane D. Homotopy perturbation method combined with ZZ transform to solve some nonlinear fractional differential equations. *Int J Anal App.* (2019) **17**:406–19. doi: 10.28924/2291-8639-17-2019-406
32. Aboodh KS, Idris A, Nuruddeen RI. On the aboodh transform connections with some famous integral transforms. *Int J Eng Inform Syst.* (2017) **1**:143–51.

Conflict of Interest: The authors declare that the research was conducted in the absence of any commercial or financial relationships that could be construed as a potential conflict of interest.

Copyright © 2020 Jena, Chakraverty, Baleanu and Alqurashi. This is an open-access article distributed under the terms of the Creative Commons Attribution License (CC BY). The use, distribution or reproduction in other forums is permitted, provided the original author(s) and the copyright owner(s) are credited and that the original publication in this journal is cited, in accordance with accepted academic practice. No use, distribution or reproduction is permitted which does not comply with these terms.

frontiers in Physics

ORIGINAL RESEARCH
published: 23 September 2020
doi: 10.3389/fphy.2020.00288

Numerical Treatment of Time-Fractional Klein–Gordon Equation Using Redefined Extended Cubic B-Spline Functions

Muhammad Amin[1,2], *Muhammad Abbas*[3,4]*, *Muhammad Kashif Iqbal*[5] and *Dumitru Baleanu*[6,7,8]

[1] Department of Mathematics, National College of Business Administration & Economics, Lahore, Pakistan, [2] Department of Mathematics, University of Sargodha, Sargodha, Pakistan, [3] Informetrics Research Group, Ton Duc Thang University, Ho Chi Minh City, Vietnam, [4] Faculty of Mathematics and Statistics, Ton Duc Thang University, Ho Chi Minh City, Vietnam, [5] Department of Mathematics, Government College University, Faisalabad, Pakistan, [6] Department of Mathematics, Faculty of Arts and Sciences, Cankaya University, Ankara, Turkey, [7] Department of Medical Research, China Medical University, Taichung, Taiwan, [8] Institute of Space Sciences, Bucharest, Romania

In this article we develop a numerical algorithm based on redefined extended cubic B-spline functions to explore the approximate solution of the time-fractional Klein–Gordon equation. The proposed technique employs the finite difference formulation to discretize the Caputo fractional time derivative of order $\alpha \in (1, 2]$ and uses redefined extended cubic B-spline functions to interpolate the solution curve over a spatial grid. A stability analysis of the scheme is conducted, which confirms that the errors do not amplify during execution of the numerical procedure. The derivation of a uniform convergence result reveals that the scheme is $O(h^2 + \Delta t^{2-\alpha})$ accurate. Some computational experiments are carried out to verify the theoretical results. Numerical simulations comparing the proposed method with existing techniques demonstrate that our scheme yields superior outcomes.

Keywords: redefined extended cubic B-spline, time fractional Klein-Gorden equation, Caputo fractional derivative, finite difference method, convergence analysis

OPEN ACCESS

Edited by:
Jordan Yankov Hristov, University of Chemical Technology and Metallurgy, Bulgaria

Reviewed by:
Praveen Agarwal, Anand International College of Engineering, India
Hossein Jaferi, University of South Africa, South Africa

***Correspondence:**
Muhammad Abbas
muhammadabbas@tdtu.edu.vn

Specialty section:
This article was submitted to Mathematical and Statistical Physics, a section of the journal Frontiers in Physics

Received: *02 March 2020*
Accepted: *25 August 2020*
Published: *23 September 2020*

Citation:
Amin M, Abbas M, Iqbal MK and Baleanu D (2020) Numerical Treatment of Time-Fractional Klein–Gordon Equation Using Redefined Extended Cubic B-Spline Functions. Front. Phys. 8:288. doi: 10.3389/fphy.2020.00288

1. INTRODUCTION

The subject of fractional-order differential equations has attracted considerable interest due to its applications in a wide range of fields, such as traffic flow, earthquakes and other physical phenomena, signal processing, finance, control theory, fractional dynamics, and mathematical modeling [1–10]. In recent years, the analytical and numerical study of fractional-order differential equations has become a dynamic area of research. Several numerical and analytical techniques have been developed to handle these types of equations [11–22]. There are a number of different definitions of fractional-order derivatives, with different applications. An excellent overview can be found in the works [23–31]. This article is concerned with the following time-fractional non-linear Klein–Gordon equation (KGE):

$$\frac{\partial^\alpha}{\partial t^\alpha} v(x,t) + \rho \frac{\partial^2}{\partial x^2} v(x,t) + \rho_1 v(x,t) + \rho_2 v^\sigma(x,t) = f(x,t), \quad 0 < x \le L,\ t_0 < t \le T, \quad (1)$$

$$v(x,t_0)=\varphi_1(x),\quad v_t(x,t_0)=\varphi_2(x), \tag{2}$$

$$v(0,t)=\varphi_3(t),\quad v(L,t)=\varphi_4(t), \tag{3}$$

where $\frac{\partial^\alpha}{\partial t^\alpha}$ represents the Caputo fractional time derivative, $v = v(x,t)$ denotes the displacement of the wave at (x,t), $\alpha \in (1,2]$ is the fractional order of the time derivative, $f(x,t)$ is the source term, ρ, ρ_1 and ρ_2 are real numbers, and $\sigma = 2$ or 3.

The fractional KGE plays a significant role in quantum mechanics, the study of solitons, and condensed matter physics. Many approaches have been adopted to solve equations of Klein/sine–Gordon type efficiently, including the Adomian decomposition method, the variational iteration method [32–34], and the homotopy analysis method [35]; see also the references cited in these works. Jafari et al. proposed using fractional B-splines for approximate solution of fractional differential equations [36]. In Vong and Wang [37, 38] space compact difference schemes were applied to one- and two-dimensional time-fractional Klein–Gordon-type equations, and stability and convergence of the proposed numerical approaches were established with the aid of an energy method. In Dehghan et al. [39] the authors used a meshless method based on radial basis functions to develop an unconditionally stable numerical scheme for fractional Klein/sine–Gordon equations. The Adomian decomposition method and an iterative method were applied in Jafari [40] to solve Klein–Gordon-type equations involving fractional time derivatives. A fully spectral approach was employed in Chen et al. [41] that uses finite differences for time discretization and Legendre spectral approximation in the spatial direction to construct numerical solutions of non-linear partial differential equations involving fractional derivatives. A sinc–Chebyshev collocation method (SCCM) was developed in Nagy [42] for numerical treatment of the time-fractional non-linear KGE. Recently, in Kanwal et al. [43], Genocchi polynomials were employed together with the Ritz–Galerkin scheme to solve fractional KGEs and diffusion wave equations. A linearized second-order scheme was introduced in Lyu and Vong [44] to solve non-linear time-fractional Klein–Gordon-type equations. Later on, in Doha et al. [45], a space–time spectral approximation was proposed for solving non-linear variable-order fractional Klein/sine–Gordon differential equations.

In this article we propose using redefined extended cubic B-spline (RECBS) functions for numerical solution of the time-fractional KGE. RECBS functions are basically a generalization of typical cubic B-spline functions that involve a free parameter which provides the flexibility to fine-tune the solution curve. We employ the usual finite central difference approach to discretize the Caputo fractional time derivative and use RECBS functions for spatial integration.

This article is organized as follows. The Caputo definition of fractional time derivative and the finite difference formulation for temporal discretization are reviewed in section 2; this section also includes a brief introduction to extended cubic B-spline and RECBS functions and their applications to space discretization. The stability analysis of the proposed algorithm is presented in section 3, and the description of theoretical convergence is given in section 4. The approximate results are reported and discussed in section 5. Finally, concluding remarks are given in section 6.

2. DESCRIPTION OF NUMERICAL TECHNIQUE

2.1. Time Discretization

Let the time domain $[0,T]$ be divided into R subintervals of equal length $\Delta t = \frac{T}{R}$ with endpoints $0 = t_0 < t_1 < \cdots < t_R = T$, where $t_r = r\Delta t$ and $r = 0:1:R$. We first discretize the Caputo fractional derivative at $t = t_{r+1}$ as [46]

$$\begin{aligned}
&\frac{\partial^\alpha v(x,t_{r+1})}{\partial t^\alpha} = \frac{1}{\Gamma(2-\alpha)}\int_0^{t_k}\frac{\partial^2 v(x,w)}{\partial w^2}(t_{r+1}-w)^{-\alpha+1}\,dw\\
&(1<\alpha\le 2)\\
&=\frac{1}{\Gamma(2-\alpha)}\sum_{k=0}^{r}\int_{t_k}^{t_{k+1}}\frac{\partial^2 v(x,w)}{\partial w^2}(t_{r+1}-w)^{-\alpha+1}\,dw.\\
&=\frac{1}{\Gamma(2-\alpha)}\sum_{k=0}^{r}\frac{v(x,t_{k+1})-2v(x,t_k)+v(x,t_{k-1})}{\Delta t^2}\\
&\int_{t_k}^{t_{k+1}}(t_{r+1}-w)^{-\alpha+1}\,dw + l_{\Delta t}^{r+1}\\
&=\frac{1}{\Gamma(2-\alpha)}\sum_{k=0}^{r}\frac{v(x,t_{k+1})-2v(x,t_k)+v(x,t_{k-1})}{\Delta t^2}\\
&\int_{t_{r-k}}^{t_{r-k+1}}(\epsilon)^{-\alpha+1}\,d\epsilon + l_{\Delta t}^{r+1}\\
&=\frac{1}{\Gamma(2-\alpha)}\sum_{k=0}^{r}\frac{v(x,t_{r-k+1})-2v(x,t_{r-k})+v(x,t_{r-k-1})}{\Delta t^2}\\
&\int_{t_k}^{t_{k+1}}(\epsilon)^{-\alpha+1}\,d\epsilon + l_{\Delta t}^{r+1}\\
&=\frac{1}{\Gamma(3-\alpha)}\sum_{k=0}^{r}\frac{v(x,t_{r-k+1})-2v(x,t_{r-k})+v(x,t_{r-k-1})}{\Delta t^\alpha}\\
&((k+1)^{2-\alpha}-k^{2-\alpha}) + l_{\Delta t}^{r+1}\\
&=\frac{1}{\Gamma(3-\alpha)}\sum_{k=0}^{r}p_k\frac{\begin{array}{c}v(x,t_{r-k+1})-2v(x,t_{r-k})+\\ v(x,t_{r-k-1})\end{array}}{\Delta t^\alpha} + l_{\Delta t}^{r+1},
\end{aligned} \tag{4}$$

where $p_k = (k+1)^{2-\alpha} - k^{2-\alpha}$, $\epsilon = (t_{r+1} - w)$, and $l_{\Delta t}^{r+1}$ is the truncation error. The truncation error is bounded, i.e.,

$$|l_{\Delta t}^{r+1}| \le \psi(\Delta t)^{2-\alpha}, \tag{5}$$

where ψ is a constant. The coefficients p_k in (4) possess the following attributes:

- the p_k's are non-negative for $k = 0, 1, 2, \ldots, r$;
- $1 = p_0 > p_1 > p_2 > p_3 > \cdots > p_n$, and $p_n \to 0$ as $n \to \infty$;
- $(2p_0 - p_1) + \sum_{k=1}^{r-1}(-p_{k+1} + 2p_k - p_{k-1}) + (2p_r - p_{r-1}) - p_r = 1$.

Substituting Equation (4) into Equation (1), we get

$$\frac{1}{\Gamma(3-\alpha)(\Delta t)^{\alpha}}\sum_{k=0}^{r} p_k\left[v(x,t_{r-k+1}) - 2v(x,t_{r-k}) + v(x,t_{r-k-1})\right] + \rho v_{xx}(x,t) + \rho_1 v(x,t) + \rho_2 v^{\sigma}(x,t) = f(x,t) \quad (r = 0, 1, 2, \ldots, R-1). \tag{6}$$

Suppose $\beta = \frac{1}{\Gamma(3-\alpha)(\Delta t)^{\alpha}}$ and $v(x, t_{r+1}) = v^{r+1}$. Applying a θ-weighted scheme, Equation (6) takes the form

$$\beta p_0(v^{r+1} - 2v^r + v^{r-1}) + \beta\sum_{k=1}^{r} p_k(v^{r-k+1} - 2v^{r-k} + v^{r-k-1}) + \theta(\rho v_{xx}^{r+1} + \rho_1 v^{r+1}) = f^{r+1} - (1-\theta)(\rho v_{xx}^{r} + \rho_1 v^{r}) - \rho_2(v^{\sigma})^r \quad (r = 0, 1, 2, \ldots, R-1). \tag{7}$$

For $\theta = 1$, we obtain the following semi-discretized numerical scheme:

$$(\beta p_0 + \rho_1)v^{r+1} + \rho v_{xx}^{r+1} = 2\beta p_0 v^r + \beta\sum_{k=1}^{r} p_k(v^{r-k+1} - 2v^{r-k} + v^{r-k-1}) - \rho_2(v^{\sigma})^r - \beta p_0 v^{r-1} + f^{r+1} (r = 0, 1, 2, \ldots, R-1). \tag{8}$$

2.2. Extended Cubic B-Spline Functions

Let the spatial domain $[a, b]$ be partitioned into M parts of equal length $h = \frac{b-a}{M}$ with boundary points $a = x_0 < x_1 < \cdots < x_M = b$, where $x_m = x_0 + mh$ for $m = 0 : 1 : M$. For a sufficiently continuous function $v(x, t)$, there always exists a unique extended cubic B-spline (ECBS) approximation $V^*(x, t)$:

$$V^*(x,t) = \sum_{m=-1}^{M+1} \xi_m(t) S_m(x,\lambda), \tag{9}$$

where the $\xi_m(t)$ are to be calculated and the fourth-degree ECBS blending functions $S_m(x, \lambda)$ are defined as [47]

$$S_m(x,\lambda) = \frac{1}{24h^4}\begin{cases} 4h(x-x_{m-2})^3(1-\lambda) + 3(x-x_{m-2})^4\lambda & \text{if } x \in [x_{m-2}, x_{m-1}), \\ h^4(4-\lambda) + 12h^3(x-x_{m-1}) + 6h^2(x-x_{m-1})^2(2+\lambda) & \\ \quad -12h(x-x_{m-1})^3 - 3(x-x_{m-1})^4\lambda & \text{if } x \in [x_{m-1}, x_m), \\ h^4(4-\lambda) - 12h^3(x-x_{m+1}) - 6h^2(x-x_{m+1})^2(2+\lambda) & \\ \quad +12h(x-x_{m+1})^3 + 3(x-x_{m-1})^4\lambda & \text{if } x \in [x_m, x_{m+1}), \\ -4h(x-x_{m+2})^3(1-\lambda) - 3(x-x_{m+2})^4\lambda & \text{if } x \in [x_{m+1}, x_{m+2}), \\ 0 & \text{otherwise.} \end{cases} \tag{10}$$

Here λ, with $-n(n-2) \le \lambda \le 1$, is a real number responsible for fine-tuning the curve, and n gives the degree of the ECBS used to generate different forms of ECBS functions. The approximate solution $(V^*)_m^r = V^*(x_m, t^r)$ and its first two derivatives with respect to the spatial variable x at the rth time step can be expressed in terms of ξ_m as [48]

$$\begin{cases} (V^*)_m^r = b_1\xi_{m-1}^r + b_2\xi_m^r + b_1\xi_{m+1}^r, \\ (V_x^*)_m^r = b_3\xi_{m-1}^r - b_3\xi_{m+1}^r, \\ (V_{xx}^*)_m^r = b_4\xi_{m-1}^r + b_5\xi_m^r + b_4\xi_{m+1}^r, \end{cases} \tag{11}$$

where $b_1 = \frac{4-\lambda}{24}$, $b_2 = \frac{16+2\lambda}{24}$, $b_3 = \frac{-1}{2h}$, $b_4 = \frac{2+\lambda}{2h^2}$, and $b_5 = \frac{-4-2\lambda}{2h^2}$.

2.3. Redefined Extended Cubic B-Spline Functions

In the typical ECBS collocation method, the basis functions $S_{-1}, S_0, \ldots, S_{M+1}$ do not vanish at the boundaries of the spatial domain when Dirichlet-type end conditions are imposed. Therefore, we need to redefine them so that the resulting set of basis functions will vanish at the boundaries. For this, a weight function $\Phi(x, t)$ is introduced to eliminate ξ_{-1} and ξ_{M+1} from Equation (9) in the following manner [49]:

$$V(x,t) = \Phi(x,t) + \sum_{m=0}^{M} \xi_m(t)\tilde{S}_m(x,\lambda), \tag{12}$$

where the weight function $\Phi(x, t)$ and the redefined ECBS (RECBS) functions are given by

$$\Phi(x,t) = \frac{S_{-1}(x,\lambda)}{S_{-1}(x_0,\lambda)}\varphi_3(t) + \frac{S_{M+1}(x,\lambda)}{S_{M+1}(x_M,\lambda)}\varphi_4(t) \tag{13}$$

and.

$$\begin{cases} \tilde{S}_m(x,\lambda) = S_m(x,\lambda) - \frac{S_m(x_0,\lambda)}{S_{-1}(x_0,\lambda)}S_{-1}(x,\lambda) & \text{for } m = 0, 1, \\ \tilde{S}_m(x,\lambda) = S_m(x,\lambda) & \text{for } m = 2:1:M-2, \\ \tilde{S}_m(x,\lambda) = S_m(x,\lambda) - \frac{S_m(x_M,\lambda)}{S_{M+1}(x_M,\lambda)}S_{M+1}(x,\lambda) & \text{for } m = M-1, M. \end{cases} \tag{14}$$

2.4. Space Discretization

Using Equation (12) in Equation (8) at $t = t_{r+1}$, we obtain

$$(\beta p_0 + \rho_1)V^{r+1} + \rho V_{xx}^{r+1} = 2\beta p_0 V^r + \beta\sum_{k=1}^{r} p_k(V^{r-k+1} - 2V^{r-k} + V^{r-k-1}) - \rho_2(V^{\sigma})^r - \beta p_0 V^{r-1} + f^{r+1}. \tag{15}$$

Discretizing at $x = x_j$, we get

$$(\beta + \rho_1)V_j^{r+1} + \rho(V_{xx})_j^{r+1} = 2\beta V_j^r + \beta\sum_{k=1}^{r} p_k(V_j^{r-k+1} - 2V_j^{r-k}$$

$$+ V_j^{r-k-1}) - \rho_2 (V^{\sigma})_j^r - \beta V_j^{r-1} + f_j^{r+1} (j = 0, 1, 2, \ldots, M). \tag{16}$$

Using (12), the last expression takes the form

$$\begin{aligned}(\beta + \rho_1)\left[\Phi_j^{r+1} + \sum_{m=0}^{M} \xi_m^{r+1} \tilde{S}_m(x_j, \lambda)\right] + \rho\left[(\Phi_{xx})_j^{r+1}\right. \\ \left. + \sum_{m=0}^{M} \xi_m^{r+1} \tilde{S}_m(x_j, \lambda)\right] \\ = 2\beta V_j^r + \beta \sum_{k=1}^{r} p_k (V_j^{r-k+1} - 2V_j^{r-k} + V_j^{r-k-1}) \\ - \rho_2 (V^{\sigma})_j^r - \beta V_j^{r-1} + f_j^{r+1} \\ (j = 0, 1, 2, \ldots, M). \end{aligned} \tag{17}$$

Consequently, we get the following system of $M + 1$ equations in $M + 1$ unknowns:

$$\begin{pmatrix} a_1^* & & & & & & \\ a_1 & a_2 & a_1 & & & & \\ & a_1 & a_2 & a_1 & & & \\ & & \ddots & \ddots & \ddots & & \\ & & & a_1 & a_2 & a_1 & \\ & & & & a_1 & a_2 & a_1 \\ & & & & & & a_1^* \end{pmatrix} \begin{pmatrix} \xi_0^{r+1} \\ \xi_1^{r+1} \\ \vdots \\ \vdots \\ \xi_{M-1}^{r+1} \\ \xi_M^{r+1} \end{pmatrix} = \begin{pmatrix} y_0 \\ y_1 \\ \vdots \\ \vdots \\ y_{M-1} \\ y_M \end{pmatrix}, \tag{18}$$

where

$$\begin{aligned} a_1^* &= \frac{12\rho(\lambda + 2)}{h^2(\lambda - 4)}, \quad a_1 = \frac{h^2(\beta + \rho_1)(\lambda - 4) + 12\rho(\lambda + 2)}{24h^2}, \\ a_2 &= \frac{h^2(\beta + \rho_1)(\lambda + 8) - 12\rho(\lambda + 2)}{12h^2}, \\ y_j &= 2\beta V_j^r + \beta \sum_{k=1}^{r} p_k (V_j^{r-k+1} - 2V_j^{r-k} + V_j^{r-k-1}) \\ &\quad - \rho_2 (V^{\sigma})_j^r - \beta V_j^{r-1} + \Psi_j^{r+1}, \\ \Psi_j^r &= f_j^r - (\beta + \rho_1)\Phi_j^r - \rho(\Phi_{xx})_j^r. \end{aligned}$$

To start the numerical procedure, we use the given initial conditions to obtain the set of equations

$$\begin{cases} (V')_m^0 = \varphi_1'(x_m) & \text{for } m = 0, \\ (V)_m^0 = \varphi_1(x_m) & \text{for } m = 1:1:M-1, \\ (V')_m^0 = \varphi_1'(x_m) & \text{for } m = M. \end{cases} \tag{19}$$

The matrix representation of (19) is

$$\begin{pmatrix} b_1^* & b_2^* & & & & & \\ b_1 & b_2 & b_1 & & & & \\ & b_1 & b_2 & b_1 & & & \\ & & \ddots & \ddots & \ddots & & \\ & & & b_1 & b_2 & b_1 & \\ & & & & b_1 & b_2 & b_1 \\ & & & & & -b_2^* & -b_1^* \end{pmatrix} \begin{pmatrix} \xi_0^0 \\ \xi_1^0 \\ \vdots \\ \vdots \\ \xi_{M-1}^0 \\ \xi_M^0 \end{pmatrix} = \begin{pmatrix} (\varphi_1')_0 - (\Phi')_0^0 \\ (\varphi_1)_1 - \Phi_1^0 \\ \vdots \\ \vdots \\ (\varphi_1)_{M-1} - \Phi_{M-1}^0 \\ (\varphi_1')_M - (\Phi')_M^0 \end{pmatrix}, \tag{20}$$

where $b_1^* = \frac{8+\lambda}{h(4-\lambda)}$ and $b_2^* = \frac{1}{h}$. We solve (20) to obtain $[\xi_0^0, \xi_1^0, \ldots, \xi_M^0]^T$. The ξ_j values are then substituted into (12) to get V^0. Now we can use (18) for $r = 0, 1, 2, \ldots, R-1$. However, for $r = 0$ the term involving V^{-1} appears in Equation (18). This issue is resolved by using the following substitution derived from the velocity condition given in (2):

$$V^{-1} = V^0 - \Delta t \phi_2(x).$$

3. STABILITY ANALYSIS

We use the Fourier method to study the stability of the proposed numerical method. Let ε_m^r and $\tilde{\varepsilon}_m^r$ denote, respectively, the exact and approximate growth factors of the Fourier modes. The error, ϱ_m^r, is given by

$$\varrho_m^r = \varepsilon_m^r - \tilde{\varepsilon}_m^r, \qquad m = 1:1:M-1, \quad r = 0:1:R, \tag{21}$$

where $\varrho^r = [\varepsilon_1^r, \varepsilon_2^r, \ldots, \varepsilon_{M-1}^r]^T$.

For the sake of simplicity, we shall investigate the stability of the proposed scheme with $f = 0$. The equation for the round-off error is derived from Equations (8) and (21) as

$$\begin{aligned} &(\beta b_1 + \rho_1 b_1 + \rho b_4)\varrho_{m-1}^{r+1} + (\beta b_2 + \rho_1 b_2 + \rho b_5)\varrho_m^{r+1} \\ &+ (\beta b_1 + \rho_1 b_1 + \rho b_4)\varrho_{m+1}^{r+1} \\ &= 2\beta\left(b_1 \varrho_{m-1}^r + b_2 \varrho_m^r + b_1 \varrho_{m+1}^r\right) - \beta\left(b_1 \varrho_{m-1}^{r-1} + b_2 \varrho_m^{r-1}\right. \\ &\left. + b_1 \varrho_{m+1}^{r-1}\right) \\ &\quad - \beta \sum_{k=1}^{r} p_k \Big[b_1\left(\varrho_{m-1}^{r-k+1} - 2\varrho_{m-1}^{r-k} + \varrho_{m-1}^{r-k-1}\right) \\ &+ b_2\left(\varrho_m^{r-k+1} - 2\varrho_m^{r-k} + \varrho_m^{r-k-1}\right) \\ &\qquad + b_1\left(\varrho_{m+1}^{r-k+1} - 2\varrho_{m+1}^{r-k} + \varrho_{m+1}^{r-k-1}\right)\Big]. \end{aligned} \tag{22}$$

The error equation satisfies the end conditions

$$\varrho_m^0 = \varphi_1(x_m), \quad m = 1:1:M, \tag{23}$$

and

$$\varrho_0^r = \varphi_3(t_r), \quad \varrho_M^r = \varphi_4(t_r), \quad r = 0:1:R. \tag{24}$$

We define the grid function as

$$\varrho^r = \begin{cases} \varrho_m^r & \text{if } x_m - \frac{h}{2} < x \le x_m + \frac{h}{2}, \text{ for } m = 1:1:M-1, \\ 0 & \text{if } a \le x \le \frac{2a+h}{2} \text{ or } \frac{2b-h}{2} \le x \le b. \end{cases} \tag{25}$$

Now, $\varrho^r(x)$ can be written in the form of a Fourier series as follows:

$$\varrho^r(x) = \sum_{r=-\infty}^{\infty} \varepsilon_r(n) e^{\frac{2\pi\iota nx}{b-a}}, \quad r = 1:1:R, \tag{26}$$

where

$$\varepsilon_r(n) = \frac{1}{b-a}\int_a^b \varrho^r(x) e^{\frac{-2\pi\iota nx}{b-a}}\, dx. \tag{27}$$

Taking the $\|\cdot\|_2$ norm, we get

$$\begin{aligned}\|\varrho^r\|_2 &= \left(\sum_{n=1}^{R-1} h|\varrho_n^r|^2\right)^{\frac{1}{2}} \\ &= \left(\int_a^{a+\frac{h}{2}} |\varrho^r|^2\, dx + \sum_{n=1}^{R-1}\int_{x_n-\frac{h}{2}}^{x_n+\frac{h}{2}} |\varrho^r|^2\, dx + \int_{b-\frac{h}{2}}^{b} |\varrho^r|^2\, dx\right)^{\frac{1}{2}} \\ &= \left(\int_a^b |\varrho^r|^2\, dx\right)^{\frac{1}{2}}.\end{aligned}$$

From Parseval's equality we have $\int_a^b |\varrho^r(n)|^2\, dx = \sum_{-\infty}^{\infty} |\varepsilon_n(m)|^2$, so the above expression can be written as

$$\|\varrho^r\|_2^2 = \sum_{r=-\infty}^{\infty} |\varepsilon_r(n)|^2. \tag{28}$$

Next, we consider the solution in terms of Fourier series,

$$\varrho_k^r = \varepsilon_r e^{\iota\nu kh}, \tag{29}$$

where $\iota = \sqrt{-1}$ and $\nu = \frac{2\pi n}{b-a}$. Using Equation (29) in Equation (22) and then dividing by $e^{i\nu kh}$ gives

$$\begin{aligned}&(\beta b_1 + \rho_1 b_1 + \rho b_4)\varepsilon_{r+1} e^{-\iota\nu h} + (\beta b_2 + \rho_1 b_2 + \rho b_5)\varepsilon_{r+1} \\ &+ (\beta b_1 + \rho_1 b_1 + \rho b_4)\varepsilon_{r+1} e^{\iota\nu h} \\ &= 2\beta\left(b_1\varepsilon_r e^{-\iota\nu h} + b_2\varepsilon_r + b_1\varepsilon_r e^{i\nu h}\right) - \beta\left(b_1\varepsilon_{r-1}e^{-\iota\nu h}\right. \\ &\left. + b_2\varepsilon_{r-1} + b_1\varepsilon_{r-1}e^{i\nu h}\right) \\ &- \beta\sum_{k=1}^{r} p_k\Big[b_1\left(\varepsilon_{r-k+1}e^{-\iota\nu h} - 2\varepsilon_{r-k} + \varepsilon_{r-k-1}e^{\iota\nu h}\right) \\ &+ b_2\left(\varepsilon_{r-k+1} - 2\varepsilon_{r-k} + \varepsilon_{r-k-1}\right) \\ &+ b_1\left(\varepsilon_{r-k+1}e^{-\iota\nu h} - 2\varepsilon_{r-k}e^{\iota\nu h} + \varepsilon_{r-k-1}e^{\iota\nu h}\right)\Big].\end{aligned} \tag{30}$$

We know that $e^{i\nu h} + e^{-i\nu h} = 2\cos(\nu h)$, so after collecting like terms, the following useful relation is obtained:

$$\varepsilon_{r+1} = \frac{1}{\eta}\left[2\varepsilon_r - \varepsilon_{r-1} - \sum_{k=1}^{r} p_k\left(\varepsilon_{r-k+1} - 2(b_1+b_2)\varepsilon_{r-k} + \varepsilon_{r-k-1}\right)\right], \tag{31}$$

where $\eta = 1 + \frac{\rho 1}{\beta} + \frac{12\rho(2+\nu)\sin^2(\nu h/2)}{\beta h^2\{-6+(4-\nu)\sin^2(\nu h/2)\}}$. Now it is obvious that $\eta \geq 1$ for $\nu > -2$.

TABLE 2 | Absolute and relative errors for Example 5.1 with $M = 100$, $\Delta t = 0.001$, and $\alpha = 1.6$.

		SCCM [42]		Proposed method	
t	***x***	L_∞	L_2	L_∞	L_2
0.4	0.4	9.3726×10^{-4}	1.3282×10^{-2}	1.6174×10^{-5}	1.2207×10^{-5}
	0.6	9.4592×10^{-4}	1.6950×10^{-2}	6.3939×10^{-6}	1.1035×10^{-6}
	0.8	6.5448×10^{-4}	1.4462×10^{-1}	5.1612×10^{-6}	3.2573×10^{-6}
0.8	0.4	1.7359×10^{-4}	8.6999×10^{-4}	2.4030×10^{-5}	9.1532×10^{-6}
	0.6	1.2080×10^{-4}	1.6683×10^{-3}	6.7766×10^{-6}	2.8126×10^{-6}
	0.8	2.4657×10^{-4}	1.9263×10^{-2}	3.5003×10^{-6}	9.0128×10^{-7}

TABLE 1 | Absolute errors for Example 5.1 with $M = 100$, $\Delta t = 0.001$, and different values of α.

	SCCM [42]			Proposed method		
x	$\alpha = 1.5$	$\alpha = 1.7$	$\alpha = 1.9$	$\alpha = 1.5$	$\alpha = 1.7$	$\alpha = 1.9$
0.1	8.7105×10^{-4}	4.3675×10^{-4}	5.0452×10^{-4}	1.0827×10^{-6}	4.6777×10^{-6}	9.5482×10^{-6}
0.2	8.7781×10^{-4}	9.8359×10^{-4}	7.5328×10^{-5}	9.2126×10^{-6}	1.1035×10^{-6}	3.6308×10^{-5}
0.3	6.2089×10^{-4}	4.8897×10^{-5}	1.1241×10^{-4}	2.9024×10^{-6}	1.2573×10^{-5}	9.1646×10^{-6}
0.4	5.7015×10^{-4}	7.6534×10^{-4}	1.6772×10^{-4}	3.6966×10^{-6}	8.1441×10^{-6}	7.0990×10^{-6}
0.5	5.1476×10^{-4}	9.3043×10^{-4}	2.5022×10^{-4}	8.3386×10^{-6}	2.5203×10^{-7}	2.3918×10^{-5}
0.6	4.8948×10^{-4}	9.4248×10^{-4}	2.5022×10^{-4}	1.0128×10^{-5}	7.3829×10^{-6}	9.8467×10^{-5}
0.7	5.1671×10^{-4}	7.5585×10^{-5}	2.5022×10^{-4}	8.9851×10^{-6}	7.1672×10^{-6}	7.1855×10^{-6}
0.8	5.3919×10^{-4}	5.2006×10^{-4}	2.5022×10^{-4}	5.3467×10^{-6}	7.2518×10^{-6}	3.2774×10^{-5}
0.9	6.0660×10^{-4}	5.4848×10^{-4}	2.5022×10^{-5}	1.7505×10^{-7}	9.7572×10^{-6}	2.8528×10^{-6}

Lemma 3.1. *Let ε_r be the solution of Equation (31). Then $|\varepsilon_r| \leq |\varepsilon_0|$ for $r = 0:1:R$.*

Proof: For $r = 0$ in (31), we have

$$|\varepsilon_1| = \frac{1}{\eta}|\varepsilon_0| \leq |\varepsilon_0| \quad \text{for } \eta \geq 1.$$

Suppose that the result is true for $r = 1:1:R$. Then, from Equation (31) we get

$$\begin{aligned}|\varepsilon_{r+1}| &\leq \frac{1}{\eta}|\varepsilon_r| - \frac{1}{\eta}\sum_{k=1}^{r} p_k\big(|\varepsilon_{r-k+1}| - 2|\varepsilon_{r-k}| + |\varepsilon_{r-k-1}|\big)\\ &\leq \frac{1}{\eta}|\varepsilon_0| - \frac{1}{\eta}|\varepsilon_0| - \sum_{k=1}^{r} p_k\big(|\varepsilon_0| - |\varepsilon_0|\big)\\ &\leq |\varepsilon_0|.\end{aligned}$$

Theorem 1. *The implic it collocation technique presented in Equation (13) is unconditionally stable.*

Proof: Using Lemma (3.1) and Equation (28), we obtain

$$\|\varrho^r\|_2 \leq |\varrho^0|_2, \quad r = 0:1:R.$$

4. CONVERGENCE OF THE SCHEME

To investigate the convergence of the proposed scheme, we follow the approach in Khalid et al. [50]. Before proceeding, we state the following useful theorems [51, 52].

Theorem 2. *Let $\Pi = \{a = x_0, x_1, \ldots, x_M = b\}$ be a partition of $[a, b]$ with $x_m = mh$ for $m = 0, \ldots, M$, and let $v \in C^4[a, b]$ and $f \in C^2[a, b]$. Suppose $\tilde{V}(x, t)$ is the spline that interpolates the solution curve of this problem at the knots $x_m \in \Pi$. Then there exist constants F_m, not depending on h, such that*

$$\|\xi^j\big(v(x,t) - \tilde{V}(x,t)\big)\|_\infty \leq F_j h^{4-j} \quad \forall\, t \geq 0,\ \ j = 0, 1, 2. \quad (32)$$

Lemma 4.1. *The extended B-splines in (10) satisfy the inequality*

$$\sum_{m=0}^{M} |S_m(x,\lambda)| \leq 1.75 \quad \text{for } 0 \leq x \leq 1. \quad (33)$$

Proof: By the triangle inequality we have

$$\left|\sum_{m=0}^{M} S_m(x,\lambda)\right| \leq \sum_{m=0}^{M} |S_m(x,\lambda)|.$$

For any knot x_m, we have

$$\begin{aligned}\sum_{m=0}^{M} |S_m(x,\lambda)| &= |S_{m-1}(x_m,\lambda)| + |S_m(x_m,\lambda)|\\ &+ |S_{m+1}(x_m,\lambda)| = 1 < \frac{7}{4}.\end{aligned}$$

From (11) we obtain

$$\begin{aligned}S_m(x_m,\lambda) &= \frac{1}{12}(8+\lambda), \quad S_{m-1}(x_{m-1},\lambda) = \frac{1}{12}(8+\lambda),\\ S_{m+1}(x_m,\lambda) &= \frac{1}{24}(4-\lambda), \quad S_{m-2}(x_{m-1},\lambda) = \frac{1}{24}(4-\lambda).\end{aligned}$$

Then, for $x \in [x_{m-1}, x_m]$, $S_m(x,\lambda)$ and $S_{m-1}(x,\lambda)$ are bounded above by $\frac{1}{12}(8+\lambda)$.

Similarly, $S_{m+1}(x,\lambda)$ and $S_{m-2}(x,\lambda)$ are bounded above by $\frac{1}{24}(4-\lambda)$

TABLE 3 | Comparison of absolute errors for Example 5.1 using three different methods with $M = 100$, $\Delta t = 0.001$, and $\alpha = 1.4$ or 1.6.

α	(x, t)	VIM [34]	SCCM [42]	Proposed method
	(0.1, 0.1)	9.2852×10^{-3}	8.4385×10^{-4}	3.6460×10^{-7}
	(0.2, 0.2)	2.2201×10^{-3}	1.1433×10^{-4}	3.0191×10^{-7}
	(0.3, 0.3)	3.5651×10^{-2}	5.3780×10^{-3}	1.1558×10^{-6}
	(0.4, 0.4)	4.9628×10^{-2}	1.5545×10^{-4}	1.6174×10^{-5}
1.4	(0.5, 0.5)	6.4449×10^{-2}	5.3227×10^{-4}	8.4214×10^{-6}
	(0.6, 0.6)	7.9514×10^{-2}	1.3268×10^{-3}	6.5725×10^{-6}
	(0.7, 0.7)	9.1443×10^{-2}	1.9159×10^{-3}	3.6215×10^{-6}
	(0.8, 0.8)	8.7942×10^{-2}	2.0414×10^{-3}	3.5112×10^{-6}
	(0.9, 0.9)	9.2321×10^{-4}	1.8996×10^{-3}	5.7354×10^{-8}
	(0.1, 0.1)	4.1518×10^{-4}	1.1685×10^{-4}	7.3256×10^{-6}
	(0.2, 0.2)	1.0319×10^{-3}	2.5887×10^{-4}	2.3576×10^{-5}
	(0.3, 0.3)	1.7757×10^{-2}	2.8863×10^{-5}	2.1107×10^{-5}
	(0.4, 0.4)	2.6987×10^{-2}	2.3912×10^{-4}	1.6174×10^{-5}
1.6	(0.5, 0.5)	3.8327×10^{-2}	1.7692×10^{-5}	8.3440×10^{-6}
	(0.6, 0.6)	5.0993×10^{-2}	1.4174×10^{-4}	6.9744×10^{-7}
	(0.7, 0.7)	6.1379×10^{-2}	1.4334×10^{-5}	3.5898×10^{-6}
	(0.8, 0.8)	5.6577×10^{-2}	1.6653×10^{-4}	3.5003×10^{-6}
	(0.9, 0.9)	3.8618×10^{-2}	1.7449×10^{-5}	5.5205×10^{-8}

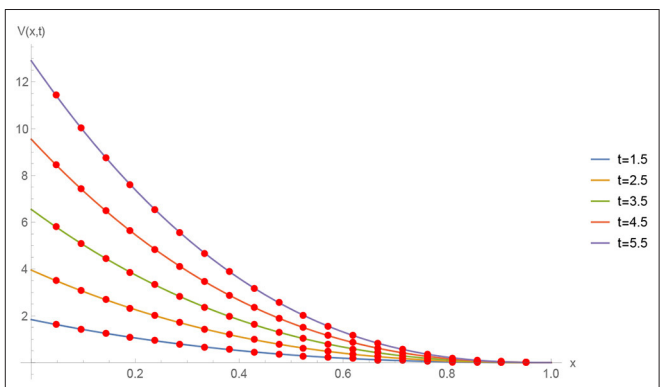

FIGURE 1 | Numerical solution of Example 5.1 with $\Delta t = 0.001$, $M = 100$, and $\alpha = 1.5$ at different time stages.

For any point $x_{m-1} \le x \le x_m$, we obtain

$$\sum_{m=0}^{M} |S_m(x,\lambda)| = |S_{m-1}(x,\lambda)| + |S_m(x,\lambda)| + |S_{m+1}(x,\lambda)| + |S_{m-2}(x,\lambda)| = \frac{1}{12}(\lambda + 20).$$

Since $\lambda \in [-8, 1]$, we have $1 \le \frac{5}{3} + \lambda \le 1.75$. Hence,

$$\sum_{m=0}^{M} |S_m(x,\lambda)| \le 1.75.$$

Theorem 3. *The extended cubic B-spline approximation $V(x,t)$ for the analytical exact solution $v(x,t)$ of problem (1)–(3) exists, and if $f \in C^2[0,1]$ then*

$$\|v(x,t) - V(x,t)\|_\infty \le \widetilde{F} h^2 \quad \forall\, t \ge 0, \tag{34}$$

where h is reasonably small and $\widetilde{F} > 0$ is a constant not depending on h.

Proof: Let $\tilde{V}(x,t) = \sum_{m=0}^{M} d_m(t)\eta_m(x)$ be the calculated spline for the approximate solution $V(x,t)$ and the exact solution $v(x,t)$.

Let $Lv(x_m,t) = LV(x_m,t) = \tilde{y}(x_m,t)$, with $m = 0:1:M$, be the collocation conditions. Then

$$L\tilde{V}(x,t) = \tilde{y}(x_m,t), \quad m = 0:1:M.$$

Now, at any time step, the problem can be expressed in the form of a difference equation $L(\tilde{V}(x_m,t) - V(x_m,t))$ as

$$\begin{aligned}
&(\beta b_1 + \rho_1 b_1 + \rho b_4)\zeta_{m-1}^{r+1} + (\beta b_2 + \rho_1 b_2 + \rho b_5)\zeta_m^{r+1} \\
&+ (\beta b_1 + \rho_1 b_1 + \rho b_4)\zeta_{m+1}^{r+1} \\
&= 2\beta\left(b_1\zeta_{m-1}^{r} + b_2\zeta_m^{r} + b_1\zeta_{m+1}^{r}\right) - \beta\left(b_1\zeta_{m-1}^{r-1} + b_2\zeta_m^{r-1}\right. \\
&\quad \left. + b_1\zeta_{m+1}^{r-1}\right) - \beta\sum_{k=1}^{r} p_k\Big[b_1\left(\zeta_{m-1}^{r-k+1} - 2\zeta_{m-1}^{r-k} + \zeta_{m-1}^{r-k-1}\right) \\
&+ b_2\left(\zeta_m^{r-k+1} - 2\zeta_m^{r-k} + \zeta_m^{r-k-1}\right) \\
&\quad + b_1\left(\zeta_{m+1}^{r-k+1} - 2\zeta_{m+1}^{r-k} + \zeta_{m+1}^{r-k-1}\right)\Big] + \frac{1}{h^2}\eta_m^{r+1}.
\end{aligned} \tag{35}$$

The boundary conditions can be rewritten as

$$b_1\zeta_{m-1}^{r+1} + b_2\zeta_m^{r+1} + b_1\zeta_{m+1}^{r+1} = 0, \quad m = 0, M,$$

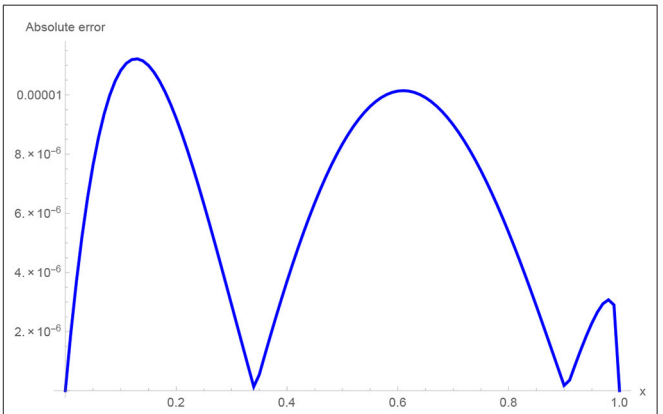

FIGURE 3 | Absolute error for Example 5.1 when $M = 100$, $\alpha = 1.50$, and $\Delta t = 0.001$.

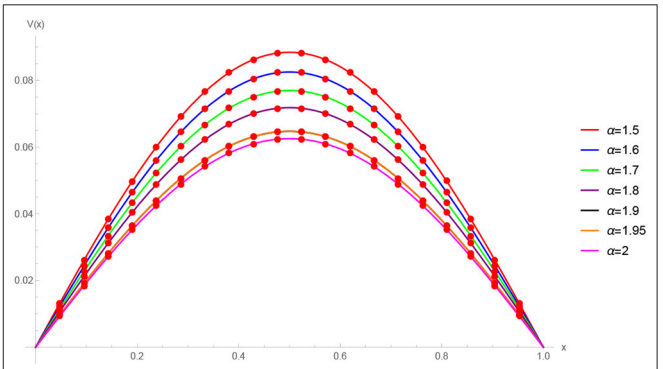

FIGURE 4 | Approximate solution of Example 5.1 with $M = 100$, $t = 0.5$, and different values of α.

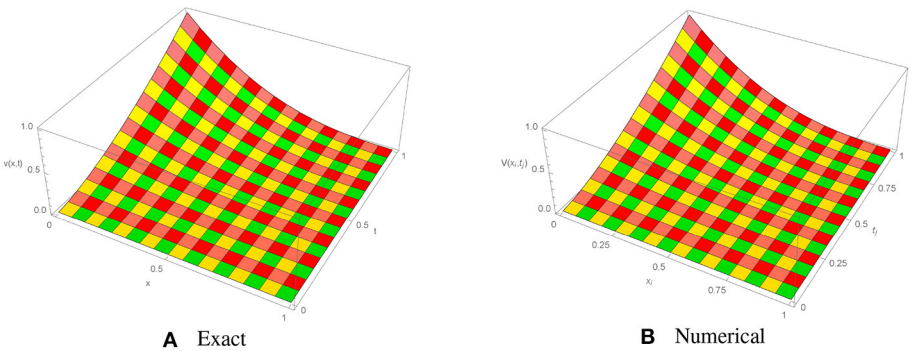

FIGURE 2 | Exact and approximate solutions of Example 5.1 with $M = 100$, $\Delta t = 0.001$, and $\alpha = 1.50$. **(A)** Exact. **(B)** Numerical.

where

$$\zeta_m^r = \xi_m^r - d_m^r, \quad m = 0:1:M,$$

and

$$\eta_m^r = h^2[y_m^r - \tilde{y}_m^r], \quad m = 0:1:M.$$

From (32) we have

$$|\eta_m^r| = h^2|y_m^r - \tilde{y}_m^r| \leq \digamma h^4.$$

We define $\eta^r = \max\{|\eta_m^r| : 0 \leq m \leq M\}$, $\tilde{e}_m^r = |\zeta_m^r|$ and $\tilde{e}^r = \max\{|e_m^r| : 0 \leq m \leq M\}$.

For $r = 0$, Equation (35) transforms into the following relation:

$$\begin{aligned}&(\beta b_1 + \rho_1 b_1 + \rho b_4)\zeta_{m-1}^1 + (\beta b_2 + \rho_1 b_2 + \rho b_5)\zeta_m^1\\ &+ (\beta b_1 + \rho_1 b_1 + \rho b_4)\zeta_{m+1}^1\\ &= (\beta + \rho_1)\big(b_1\zeta_{m-1}^0 + b_2\zeta_m^0 + b_1\zeta_{m+1}^0\big) + \frac{1}{h^2}\eta_m^1.\end{aligned}$$

Using the initial condition $e^0 = 0$, we obtain

$$\begin{aligned}&(\beta b_2 + \rho_1 b_2 + \rho b_5)\zeta_m^1 = (\beta b_1 + \rho b_4)(\zeta_{m+1}^1 - \zeta_{m-1}^1)\\ &+\rho_1 b_1(\zeta_{m+1}^1 - \zeta_{m-1}^1) + \frac{1}{h^2}\eta_m^1.\end{aligned}$$

Taking absolute values of η_m^r and ζ_m^r and with adequately small h, we have

$$\tilde{e}_m^1 \leq \frac{6\digamma h^4}{\beta h^2(\lambda + 2) + 12(-2 - \lambda)\rho + \rho_1 h^2(2 + \lambda)}$$

using the boundary conditions, from which we conclude that

$$\tilde{e}^1 \leq \digamma_1 h^2, \tag{36}$$

where $\digamma_1$ is independent of the spatial grid spacing.

Using the induction technique, we assume that $\tilde{e}_m^k \leq \digamma_k h^2$ is true for $k = 1:1:r$.

Let $\digamma = \max\{\digamma_k : 0 \leq k \leq r\}$; then Equation (35) becomes

$$\begin{aligned}&(\beta b_1 + \rho_1 b_1 + \rho b_4)\zeta_{m-1}^{r+1} + (\beta b_2 + \rho_1 b_2 + \rho b_5)\zeta_m^{r+1}\\ &+ (\beta b_1 + \rho_1 b_1 + \rho b_4)\zeta_{m+1}^{r+1}\\ &= 2\beta\big(b_1\zeta_{m-1}^r + b_2\zeta_m^r + b_1\zeta_{m+1}^r\big) - \beta\big(b_1\zeta_{m-1}^{r-1} + b_2\zeta_m^{r-1} + b_1\zeta_{m+1}^{r-1}\big)\\ &+ \beta\Big[(p_0 - 2p_1 + p_2)(b_1\zeta_{m-1}^r + b_2\zeta_m^r + b_1\zeta_{m+1}^r)\\ &+ (p_1 - 2p_2 + p_3)(b_1\zeta_{m-1}^{r-1} + b_2\zeta_m^{r-1} + b_1\zeta_{m+1}^{r-1})\\ &+ \cdots + (p_{r-4} - 2p_{r-3} + p_{r-2})(b_1\zeta_{m-1}^1 + b_2\zeta_m^1\\ &+ b_1\zeta_{m+1}^1) + p_{r-1}(b_1\zeta_{m-1}^0 + b_2\zeta_m^0 + b_1\zeta_{m+1}^0)\Big] + \frac{1}{h^2}\eta_m^{r+1}.\end{aligned}$$

Again, taking absolute values of η_m^r and ζ_m^r, we have

$$\begin{aligned}\tilde{e}_m^{r+1} \leq \frac{6\digamma h^2}{\beta h^2(2 + \lambda) + 12(-2 - \lambda)\rho + \rho_1 h^2(2 + \lambda)}\\ \Big[2\beta(b_1\zeta_{m-1}^r + b_2\zeta_m^r + b_1\zeta_m^r)\\ - \beta\sum_{k=0}^{r-1}(p_{k+1} - 2p_k - p_{k-1})\digamma h^2 + \digamma h^2\Big].\end{aligned}$$

TABLE 4 | Experimental order of convergence (EOC) for Example 5.1 with $\alpha = 1.3$ and $\Delta t = 0.001$.

M	L_∞	EOC	L_2	EOC
10	3.1950×10^{-2}	—	2.9355×10^{-2}	—
20	9.0451×10^{-3}	1.8206	8.7109×10^{-3}	1.7527
40	2.4778×10^{-3}	1.8680	2.2128×10^{-3}	1.9769
80	6.3842×10^{-4}	1.9564	5.9376×10^{-4}	1.8979

TABLE 6 | Absolute and relative errors for Example 5.2 when $M = 100$, $\Delta t = 0.001$ and $\alpha = 1.6$.

		SCCM [42]		Proposed method	
t	x	L_∞	L_2	L_∞	L_2
	0.4	3.1780×10^{-6}	9.0475×10^{-5}	1.1769×10^{-7}	9.1321×10^{-8}
0.4	0.6	3.1780×10^{-6}	9.0475×10^{-5}	1.0126×10^{-6}	8.0341×10^{-7}
	0.8	2.1040×10^{-5}	9.6921×10^{-4}	7.2740×10^{-6}	1.2573×10^{-6}
	0.4	5.8118×10^{-4}	7.6534×10^{-4}	1.8278×10^{-5}	8.9616×10^{-6}
0.8	0.6	2.4754×10^{-4}	5.8118×10^{-4}	1.2788×10^{-6}	7.8014×10^{-7}
	0.8	4.7365×10^{-4}	1.7994×10^{-3}	1.0951×10^{-5}	9.5597×10^{-6}

TABLE 5 | Absolute errors for Example 5.2 when $M = 100$, $\Delta t = 0.001$ using different values of α.

	SCCM [42]			Proposed method		
x	$\alpha = 1.5$	$\alpha = 1.7$	$\alpha = 1.9$	$\alpha = 1.5$	$\alpha = 1.7$	$\alpha = 1.9$
0.1	1.6396×10^{-3}	1.5471×10^{-3}	1.4380×10^{-3}	2.6129×10^{-6}	8.4422×10^{-6}	9.8439×10^{-6}
0.2	1.2808×10^{-3}	1.1272×10^{-3}	9.4914×10^{-4}	3.0564×10^{-5}	1.4959×10^{-7}	6.7965×10^{-6}
0.3	1.0869×10^{-3}	8.9663×10^{-4}	6.7913×10^{-4}	9.7609×10^{-6}	$2,7610 \times 10^{-6}$	1.0853×10^{-5}
0.4	8.4196×10^{-4}	6.3348×10^{-4}	3.9687×10^{-4}	1.9015×10^{-6}	5.8360×10^{-6}	7.0990×10^{-6}
0.5	7.8252×10^{-4}	5.6868×10^{-4}	3.2651×10^{-4}	3.2181×10^{-6}	7.1727×10^{-6}	3.1898×10^{-5}
0.6	8.4196×10^{-4}	6.3348×10^{-4}	3.9687×10^{-4}	1.9015×10^{-5}	5.8360×10^{-6}	4.1207×10^{-6}
0.7	1.0869×10^{-3}	8.9663×10^{-4}	6.7913×10^{-4}	9.7609×10^{-6}	2.7610×10^{-6}	8.6781×10^{-6}
0.8	1.2808×10^{-3}	1.1272×10^{-3}	9.4914×10^{-4}	3.0564×10^{-5}	1.4959×10^{-7}	6.7965×10^{-6}
0.9	1.6396×10^{-3}	1.5471×10^{-3}	1.4380×10^{-3}	2.6129×10^{-6}	8.4422×10^{-6}	9.8439×10^{-6}

Using the boundary conditions, we have

$$\tilde{e}_m^{r+1} \leq F h^2.$$

Hence, for all values of n,

$$\tilde{e}_m^{r+1} \leq F h^2. \tag{37}$$

Now,

$$\tilde{V}(x,t) - V(x,t) = \sum_{m=0}^{M} \big(d_m(t) - \xi_m(t)\big) S_m(x).$$

Taking the infinity norm and applying Lemma (3.1), we obtain

$$\|\tilde{V}(x,t) - V(x,t)\|_\infty \leq 1.75 F h^2. \tag{38}$$

Making use of the triangle inequality, we get

$$\|v(x,t) - V(x,t)\|_\infty \leq \|v(x,t) - \tilde{V}(x,t)\|_\infty + \|\tilde{V}(x,t) - V(x,t)\|_\infty. \tag{39}$$

Using the inequalities (32) and (38) in (39), we obtain

$$\|v(x,t) - V(x,t)\|_\infty \leq F_0 h^4 + 1.75 F h^2 = \widetilde{F} h^2,$$

where $\widetilde{F} = F_0 h^2 + 1.75F$.

Using the above theorem with expression (5), it is easy to conclude that the numerical approach converges unconditionally. Therefore,

$$\|v(x,t) - V(x,t)\|_\infty \leq \widetilde{F} h^2 + \psi(\Delta t)^{2-\alpha},$$

where $\widetilde{F}$ is a constant and $\alpha \in (1,2]$. Hence, theoretically, the proposed scheme is $O(h^2 + \Delta t^{2-\alpha})$ accurate.

5. NUMERICAL RESULTS AND DISCUSSION

To examine the accuracy of the proposed method, we conduct a numerical study of some test problems. The L_∞ and L_2 error norms are calculated as [53]

$$L_\infty = \max_{0 \leq m \leq M} |V(x_m,t) - v(x_m,t)|,$$

$$L_2 = \sqrt{h \sum_{m=0}^{M} |V(x_m,t) - v(x_m,t)|^2}.$$

Also, the experimental order of convergence (EOC) is computed by the following important formula [54]:

$$\text{EOC} = \frac{1}{\log 2} \log\left[\frac{L_\infty(2m)}{L_\infty(m)}\right].$$

All numerical computations were performed using `Mathematica` 9.0.

Example 5.1. Consider the non-linear time-fractional KGE [42]

$$\frac{\partial^\alpha v}{\partial t^\alpha} - \frac{\partial^2 v}{\partial x^2} + v^2(x,t) = f(x,t), \qquad 0 < t \leq 1,\ 0 < x \leq 1, \tag{40}$$

TABLE 7 | Absolute errors for Example 5.2 when $M = 100$ and $\Delta t = 0.001$.

α	(x,t)	VIM [34]	SCCM [42]	Proposed method
	(0.1, 0.1)	3.9211×10^{-5}	2.3809×10^{-5}	1.9749×10^{-6}
	(0.2, 0.2)	6.1713×10^{-4}	5.2644×10^{-5}	1.7326×10^{-5}
	(0.3, 0.3)	2.1989×10^{-3}	6.0187×10^{-6}	5.2839×10^{-6}
	(0.4, 0.4)	2.5545×10^{-3}	6.6640×10^{-5}	9.9062×10^{-6}
1.4	(0.5, 0.5)	5.3405×10^{-3}	4.0011×10^{-5}	1.3396×10^{-6}
	(0.6, 0.6)	3.1409×10^{-2}	1.5837×10^{-4}	1.3557×10^{-5}
	(0.7, 0.7)	8.0092×10^{-2}	9.1922×10^{-4}	9.6832×10^{-6}
	(0.8, 0.8)	1.3528×10^{-1}	2.9084×10^{-3}	3.5290×10^{-5}
	(0.9, 0.9)	1.4272×10^{-1}	3.8732×10^{-3}	9.0059×10^{-6}
	(0.1, 0.1)	1.0402×10^{-5}	2.3809×10^{-5}	1.4963×10^{-6}
	(0.2, 0.2)	1.4424×10^{-4}	5.2644×10^{-5}	1.5765×10^{-6}
	(0.3, 0.3)	6.7115×10^{-5}	6.0187×10^{-6}	2.1699×10^{-7}
	(0.4, 0.4)	3.0493×10^{-3}	6.4440×10^{-5}	1.1769×10^{-6}
1.6	(0.5, 0.5)	1.6350×10^{-2}	4.0011×10^{-5}	1.2375×10^{-6}
	(0.6, 0.6)	4.9599×10^{-2}	1.5837×10^{-4}	2.1232×10^{-6}
	(0.7, 0.7)	1.0675×10^{-1}	9.1922×10^{-4}	1.8721×10^{-6}
	(0.8, 0.8)	1.6942×10^{-1}	2.9084×10^{-3}	1.0951×10^{-5}
	(0.9, 0.9)	1.7521×10^{-1}	3.8732×10^{-3}	2.2989×10^{-5}

TABLE 8 | Experimental order of convergence (EOC) for Example 5.2 with $\alpha = 1.5$ and $\Delta t = 0.001$.

M	L_∞	EOC	L_2	EOC
10	2.0835×10^{-2}	–	1.8459×10^{-2}	–
20	5.2813×10^{-3}	1.9760	4.7833×10^{-3}	1.9482
40	1.3057×10^{-3}	2.0161	1.1406×10^{-3}	2.0688
80	3.2509×10^{-4}	2.0059	2.8172×10^{-4}	2.0174

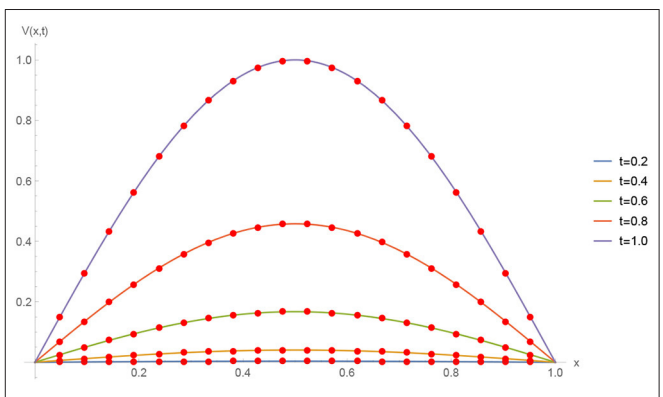

FIGURE 5 | Numerical solution for Example 5.2 with $\Delta t = 0.001$, $M = 100$, and $\alpha = 1.5$ at different time stages.

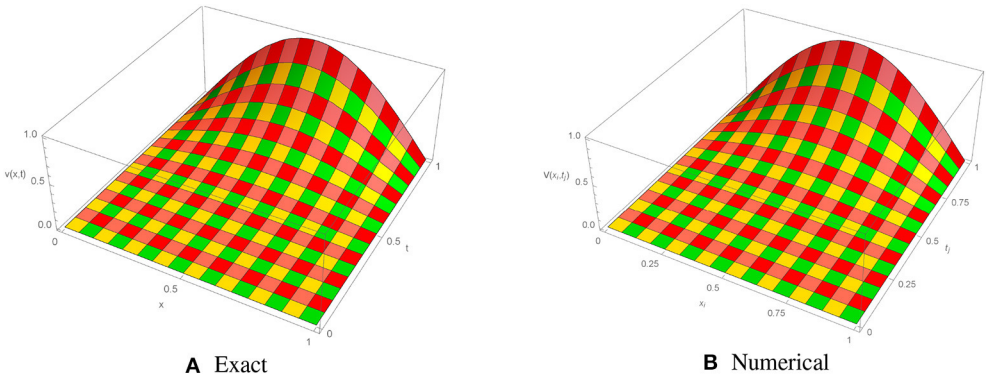

FIGURE 6 | Exact and numerical solutions of Example 5.2 with $M = 100$, $\Delta t = 0.001$, and $\alpha = 1.5$. **(A)** Exact. **(B)** Numerical.

where $f(x,t) = \frac{\Gamma(\frac{5}{2})}{\Gamma(\frac{5}{2}-\alpha)}(1-x)^{\frac{5}{2}}t^{\frac{3}{2}-\alpha} - \frac{15}{4}(1-x)^{\frac{1}{2}}t^{\frac{3}{2}} + (1-x)^5t^3$. The initial/end conditions can be extracted from the analytical exact solution $(1-x)^{\frac{5}{2}}t^{\frac{3}{2}-\alpha}$.

For Example 5.1, the piecewise-defined approximate solution obtained using the proposed method with $\alpha = 1.25$, $0 \le x \le 1$, $n = 100$, and $\Delta t = 0.01$ is given by

$$V(x) = \begin{cases} 0. + x(297.276 + x(-29930.4 + x(993222. + 225927.x))) & \text{if } x \in [0.00, 0.01], \\ 0.999999 + x(-2.49738 + x(1.82587 + (1.38305 - 27.8749x)x)) & \text{if } x \in [0.01, 0.02], \\ 0.99999 + x(-2.49605 + x(1.75961 + (2.48215 - 27.7432x)x)) & \text{if } x \in [0.02, 0.03], \\ 0.99996 + x(-2.49308 + x(1.66094 + (3.57055 - 27.6103x)x)) & \text{if } x \in [0.03, 0.04], \\ \vdots & \vdots \\ -0.118298 + x(6.72761 + x(-26.6775 + (38.9565 - 20.3042x)x)) & \text{if } x \in [0.49, 0.50], \\ -0.201484 + x(7.21369 + x(-27.5747 + (39.3734 - 20.1068x)x)) & \text{if } x \in [0.50, 0.51], \\ \vdots & \vdots \\ -2.7339 + x(13.6165 + x(-24.3154 + (18.715 - 5.28228x)x)) & \text{if } x \in [0.96, 0.97], \\ -1.89304 + x(10.2593 + x(-19.2941 + (15.3811 - 4.45319x)x)) & \text{if } x \in [0.97, 0.98], \\ -0.518579 + x(5.07656 + x(-12.0155 + (10.8746 - 3.41708x)x)) & \text{if } x \in [0.98, 0.99], \\ 4.86293 + x(-13.1733 + x(10.3424 + (-0.616646 - 1.41541x)x)) & \text{if } x \in [0.99, 1.00]. \end{cases}$$

The absolute numerical errors at different grid points of the RECBS solution for Example 5.1 using $\Delta t = 0.001$ and $M = 100$ are reported in **Table 1**. It can easily be seen that our scheme is more accurate than the SCCM [42]. In **Table 2** the absolute and relative numerical errors are listed for our method with $M = 100$, $\Delta t = 0.001$, and $\alpha = 1.6$ at $x = 0.4, 0.6, 0.8$ when $t = 0.4, 0.8$. We can see that the computational results are superior to those obtained from the SCCM [42]. **Table 3** compares the absolute errors of the proposed method, the variational iteration method (VIM) [34], and the SCCM [42] under different values of α. **Figure 1** shows the behavior at different time stages of numerical solutions obtained using $\alpha = 1.5$, $M = 100$, and $\Delta t = 0.001$. The 3D visuals of exact and numerical solutions with $\alpha = 1.5$ and $M = 100$ are shown in **Figure 2**. The comparison between the exact and approximate solutions using $M = 100$ is plotted in **Figure 3**. **Figure 4** depicts the absolute error between the exact and numerical solutions when $\alpha = 1.3$, $M = 100$, and $\Delta t = 0.001$. The values of the EOC along the spatial grid, using $\Delta t = 0.001$ and $\alpha = 1.5$, are given in **Table 4**. The experimental rate of convergence of the proposed method is found to be in line with the theoretical results.

Example 5.2. Consider the fractional KGE [34, 42]

$$\frac{\partial^\alpha}{\partial t^\alpha}v(x,t) - \frac{\partial^2}{\partial x^2}v(x,t) + v(x,t) + \frac{3}{2}v^3(x,t) = f(x,t), \quad 0 < x \le 1, \ 0 < t \le 1, \quad (41)$$

where the forcing term $f(x,t)$ on right-hand side is given by

$$f(x,t) = \frac{1}{2}\Gamma(3+\alpha)\sin(\pi x)t^2 + (1+\pi^2)t^{2+\alpha}\sin(\pi x) + \frac{3}{2}\left[\sin(\pi x)t^{2+\alpha}\right]^3,$$

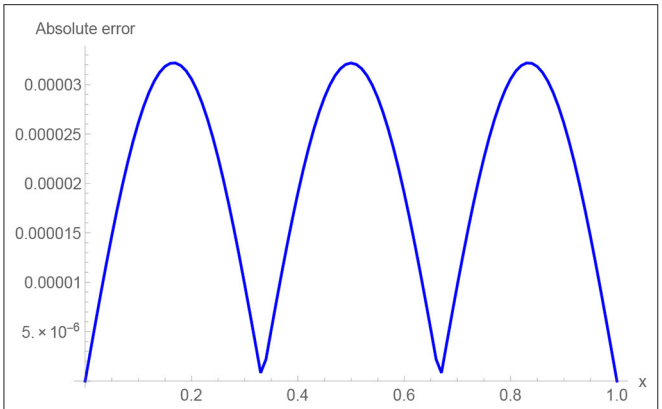

FIGURE 7 | Absolute error for Example 5.2 when $M = 100$, $\alpha = 1.5$, and $\Delta t = 0.001$.

For Example 5.2, the piecewise-defined numerical solution obtained using the proposed method with $\alpha = 1.5$, $0 \leq x \leq 1$, $n = 100$, and $\Delta t = 0.01$ is given by

$$V(x) = \begin{cases} 8.71156 \times 10^{-19} + x(3.13867 + x(2.8549 \times 10^{-}14 + (-4.97167 - 11.4015x)x)) & \text{if } x \in [0.00, 0.01], \\ -1.14461 \times 10^{-6} + x(3.13904 + x(-0.041176 + (-3.14329 - 34.194x)x)) & \text{if } x \in [0.01, 0.02], \\ -0.0000194466 + x(3.14196 + x(-0.205754 + (0.51013 - 56.9551x)x)) & \text{if } x \in [0.02, 0.03], \\ -0.000112001 + x(3.15183 + x(-0.575584 + (5.98188 - 79.6639x)x)) & \text{if } x \in [0.03, 0.04], \\ \vdots & \vdots \\ -40.7681 + x(339.328 + x(-1039.38 + (1422.21 - 733.23x)x)) & \text{if } x \in [0.49, 0.50], \\ -44.2829 + x(360.934 + x(-1083.83 + (1453.18 - 733.97x)x)) & \text{if } x \in [0.50, 0.51], \\ \vdots & \vdots \\ -71.1059 + x(298.709 + x(-460.613 + (312.674 - 79.6639x)x)) & \text{if } x \in [0.96, 0.97], \\ -53.5088 + x(223.56 + x(-340.406 + (227.31 - 56.9551x)x)) & \text{if } x \in [0.97, 0.98], \\ -34.2394 + x(143.149 + x(-214.635 + (139.919 - 34.194x)x)) & \text{if } x \in [0.98, 0.99], \\ -13.2345 + x(57.3823 + x(-83.3239 + (50.5776 - 11.4015x)x)) & \text{if } x \in [0.99, 1.00]. \end{cases}$$

The initial/boundary conditions can be extracted from the analytical exact solution $v(x,t) = \sin(\pi x)t^{2+\alpha}$. The absolute numerical errors at different grid points of the RECBS solution for Example 5.2 using $\Delta t = 0.001$ and $M = 100$ are listed in **Table 5**. Again it can be observed that our scheme is more accurate than the SCCM [42]. **Table 6** reports the absolute and relative errors in our numerical computation with $M = 100$, $\Delta t = 0.001$, and $\alpha = 1.6$ at $x = 0.4, 0.6, 0.8$ when $t = 0.4, 0.8$. It is clear that the results are better than those obtained by the SCCM [42]. **Table 7** compares the absolute errors of the proposed method, VIM [34], and SCCM [42] under different values of α.

The EOC in the spatial direction, using $\Delta t = 0.001$ and $\alpha = 1.50$, is tabulated in **Table 8**. The experimental rate of convergence of the proposed scheme is found to be in line with the theoretical prediction. **Figure 5** shows the behavior at different time stages of numerical solutions obtained using $\alpha = 1.5$, $M = 100$, and $\Delta t = 0.001$. The 3D plots of exact and numerical solutions with $\alpha = 1.5$ and $M = 100$ are displayed in **Figure 6**. The absolute error between the exact and approximate solutions using $\alpha = 1.3$, $M = 100$, and $\Delta t = 0.001$ is plotted in **Figure 7**.

6. CONCLUSION

In this work we have conducted a numerical investigation of the time-fractional Klein–Gordon equation by applying the redefined extended cubic B-spline collocation method. A finite central difference formulation is employed for temporal discretization, while a set of redefined extended cubic B-spline functions is used to interpolate the solution curve in the spatial direction. The unconditional stability of the proposed scheme is established, and the orders of convergence along the space and time grids are shown to be $O(h^2)$ and $O(\Delta t)^{2-\alpha}$, respectively. The computational outcomes of the proposed algorithm show that the order of convergence agrees with the theoretical results. The numerical scheme has been tested on different problems, and comparison of the results reveals our method's advantage over VIM [34] and SCCM [42].

AUTHOR CONTRIBUTIONS

All authors listed have made a substantial, direct and intellectual contribution to the work, and approved it for publication.

REFERENCES

1. Rossikhin YA, Shitikova M. Application of fractional derivatives to the analysis of damped vibrations of viscoelastic single mass systems. *Acta Mech.* (1997) **120**:109–25. doi: 10.1007/BF01174319
2. Rudolf H. *Applications of FractionalCalculus in Physics*. Singapore; River Edge, NJ: World Scientific (2000).
3. Metzler R, Klafter J. The restaurant at the end of the random walk: recent developments in the description of anomalous transport by fractional dynamics. *J Phys A Math Gen.* (2004) **37**:R161. doi: 10.1088/0305-4470/37/31/R01

4. Luo MJ, Milovanovic GV, Agarwal P. Some results on the extended beta and extended hypergeometric functions. *Appl Math Comput*. (2014) **248**:631–51. doi: 10.1016/j.amc.2014.09.110
5. Zhang Y. Time-fractional Klein-Gordon equation: formulation and solution using variational methods. *WSEAS Trans Math*. (2016) **15**:206–14.
6. Ruzhansky M, Cho YJ, Agarwal P, Area I. *Advances in Real and Complex Analysis With Applications*. Singapore: Springer (2017).
7. Owolabi KM, Hammouch Z. Mathematical modeling and analysis of two-variable system with noninteger-order derivative. *Chaos*. (2019) **29**:013145. doi: 10.1063/1.5086909
8. Agarwal P, Baleanu D, Chen Y, Momani S, Machado JAT. Fractional calculus. In: *ICFDA: International Workshop on Advanced Theory and Applications of Fractional Calculus*. Amman (2019). doi: 10.1007/978-981-15-0430-3
9. Babaei A, Jafari H, Ahmadi M. A fractional order HIV/AIDS model based on the effect of screening of unaware infectives. *Math Methods Appl Sci*. (2019) **42**:2334–43. doi: 10.1002/mma.5511
10. Babaei A, Jafari H, Liya A. Mathematical models of HIV/AIDS and drug addiction in prisons. *Eur Phys J Plus*. (2020) **135**:395. doi: 10.1140/epjp/s13360-020-00400-0
11. Yuste SB, Acedo L. An explicit finite difference method and a new von Neumann-type stability analysis for fractional diffusion equations. *SIAM J Numer Anal*. (2005) **42**:1862–74. doi: 10.1137/030602666
12. Sweilam N, Nagy A. Numerical solution of fractional wave equation using Crank-Nicholson method. *World Appl Sci J*. (2011) **13**:71–5.
13. Ur-Rehman M, Khan RA. The Legendre wavelet method for solving fractional differential equations. *Commun Nonlin Sci Numer Simul*. (2011) **16**:4163–73. doi: 10.1016/j.cnsns.2011.01.014
14. Bhrawy A, Tharwat M, Yildirim A. A new formula for fractional integrals of Chebyshev polynomials: application for solving multi-term fractional differential equations. *Appl Math Modell*. (2013) **37**:4245–52. doi: 10.1016/j.apm.2012.08.022
15. Rad J, Kazem S, Shaban M, Parand K, Yildirim A. Numerical solution of fractional differential equations with a Tau method based on Legendre and Bernstein polynomials. *Math Methods Appl Sci*. (2014) **37**:329–42. doi: 10.1002/mma.2794
16. Mohebbi A, Abbaszadeh M, Dehghan M. High-order difference scheme for the solution of linear time fractional Klein-Gordon equations. *Numer Methods Partial Differ Equat*. (2014) **30**:1234–53. doi: 10.1002/num.21867
17. Heydari M, Hooshmandasl M, Mohammadi F, Cattani C. Wavelets method for solving systems of nonlinear singular fractional Volterra integro-differential equations. *Commun Nonlin Sci Numer Simul*. (2014) **19**:37–48. doi: 10.1016/j.cnsns.2013.04.026
18. Salahshour S, Ahmadian A, Senu N, Baleanu D, Agarwal P. On analytical solutions of the fractional differential equation with uncertainty: application to the basset problem. *Entropy*. (2015) **17**:885–902. doi: 10.3390/e17020885
19. Sweilam N, Nagy A, El-Sayed AA. Second kind shifted Chebyshev polynomials for solving space fractional order diffusion equation. *Chaos Solit Fract*. (2015) **73**:141–7. doi: 10.1016/j.chaos.2015.01.010
20. Ramezani M, Jafari H, Johnston SJ, Baleanu D. Complex b-spline collocation method for solving weakly singular Volterra integral equations of the second kind. *Miskolc Math Notes*. (2015) **16**:1091–103. doi: 10.18514/MMN.2015.1469
21. Badr M, Yazdani A, Jafari H. Stability of a finite volume element method for the time-fractional advection-diffusion equation. *Numer Methods Partial Differ Equat*. Wiley online Library. (2018) **34**:1459–71. doi: 10.1002/num.22243
22. Agarwal P, Agarwal RP, Ruzhansky M. *Special Functions and Analysis of Differential Equations*. (2020).
23. Atangana A, Secer A. A note on fractional order derivatives and table of fractional derivatives of some special functions. *Abstr Appl Anal*. (2013) **2013**:279681. doi: 10.1155/2013/279681
24. Srivastava H, Agarwal P. Certain fractional integral operators and the generalized incomplete hypergeometric functions. *Appl Appl Math*. (2013) **8**:333–45.
25. Goufo EFD. Solvability of chaotic fractional systems with 3D four-scroll attractors. *Chaos Solit Fract*. (2017) **104**:443–51. doi: 10.1016/j.chaos.2017.08.038
26. Asif N, Hammouch Z, Riaz M, Bulut H. Analytical solution of a Maxwell fluid with slip effects in view of the Caputo-Fabrizio derivative. *Eur Phys J Plus*. (2018) **133**:272. doi: 10.1140/epjp/i2018-12098-6
27. Singh J, Kumar D, Hammouch Z, Atangana A. A fractional epidemiological model for computer viruses pertaining to a new fractional derivative. *Appl Math Comput*. (2018) **316**:504–15. doi: 10.1016/j.amc.2017.08.048
28. Atangana A, Goufo EFD. Conservatory of Kaup-Kupershmidt equation to the concept of fractional derivative with and without singular kernel. *Acta Math Appl Sin*. (2018) **34**:351–61. doi: 10.1007/s10255-018-0757-7
29. Owolabi KM, Atangana A. Computational study of multi-species fractional reaction-diffusion system with ABC operator. *Chaos Solit Fract*. (2019) **128**:280–9. doi: 10.1016/j.chaos.2019.07.050
30. Uçar S, Uçar E, Özdemir N, Hammouch Z. Mathematical analysis and numerical simulation for a smoking model with Atangana-Baleanu derivative. *Chaos Solit Fract*. (2019) **118**:300–6. doi: 10.1016/j.chaos.2018.12.003
31. Goufo EFD, Toudjeu IT. Analysis of recent fractional evolution equations and applications. *Chaos Solit Fract*. (2019) **126**:337–50. doi: 10.1016/j.chaos.2019.07.016
32. Batiha B, Noorani MSM, Hashim I. Numerical solution of sine-Gordon equation by variational iteration method. *Phys Lett A*. (2007) **370**:437–40. doi: 10.1016/j.physleta.2007.05.087
33. Yusufoğlu E. The variational iteration method for studying the Klein-Gordon equation. *Appl Math Lett*. (2008) **21**:669–74. doi: 10.1016/j.aml.2007.07.023
34. Odibat Z, Momani S. The variational iteration method: an efficient scheme for handling fractional partial differential equations in fluid mechanics. *Comput Math Appl*. (2009) **58**:2199–208. doi: 10.1016/j.camwa.2009.03.009
35. Jafari H, Saeidy M, Arab Firoozjaee M. Solving nonlinear Klein-Gordon equation with a quadratic nonlinear term using homotopy analysis method. *Iran J Optimiz*. (2010) **2**:130–38.
36. Jafari H, Khalique CM, Ramezani M, Tajadodi H. Numerical solution of fractional differential equations by using fractional B-spline. *Central Eur J Phys*. (2013) **11**:1372–6. doi: 10.2478/s11534-013-0222-4
37. Vong S, Wang Z. A compact difference scheme for a two dimensional fractional Klein-Gordon equation with Neumann boundary conditions. *J Comput Phys*. (2014) **274**:268–82. doi: 10.1016/j.jcp.2014.06.022
38. Vong S, Wang Z. A high-order compact scheme for the nonlinear fractional Klein-Gordon equation. *Numer Methods Partial Differ Equat*. (2015) **31**:706–22. doi: 10.1002/num.21912
39. Dehghan M, Abbaszadeh M, Mohebbi A. An implicit RBF meshless approach for solving the time fractional nonlinear sine-Gordon and Klein-Gordon equations. *Eng Anal Bound Elements*. (2015) **50**:412–34. doi: 10.1016/j.enganabound.2014.09.008
40. Jafari H. Numerical solution of time-fractional Klein-Gordon equation by using the decomposition methods. *J Comput Nonlin Dyn*. (2016) **11**:041015. doi: 10.1115/1.4032767
41. Chen H, Lü S, Chen W, et al. A fully discrete spectral method for the nonlinear time fractional Klein-Gordon equation. *Taiwan J Math*. (2017) **21**:231–51. doi: 10.11650/tjm.21.2017.7357
42. Nagy A. Numerical solution of time fractional nonlinear Klein-Gordon equation using Sinc-Chebyshev collocation method. *Appl Math Comput*. (2017) **310**:139–48. doi: 10.1016/j.amc.2017.04.021
43. Kanwal A, Phang C, Iqbal U. Numerical solution of fractional diffusion wave equation and fractional Klein-Gordon equation via two-dimensional Genocchi polynomials with a Ritz-Galerkin method. *Computation*. (2018) **6**:40. doi: 10.3390/computation6030040
44. Lyu P, Vong S. A linearized second-order scheme for nonlinear time fractional Klein-Gordon type equations. *Numer Algorithms*. (2018) **78**:485–511. doi: 10.1007/s11075-017-0385-y
45. Doha E, Abdelkawy M, Amin A, Lopes AM. A space-time spectral approximation for solving nonlinear variable-order fractional sine and Klein-Gordon differential equations. *Comput Appl Math*. (2018) **37**:6212–29. doi: 10.1007/s40314-018-0695-2
46. Amin M, Abbas M, Iqbal MK, Ismail AIM, Baleanu D. A fourth order non-polynomial quintic spline collocation technique for solving time fractional superdiffusion equations. *Adv Differ Equat*. (2019) **2019**:1–21. doi: 10.1186/s13662-019-2442-4
47. Khalid N, Abbas M, Iqbal MK, Baleanu D. A numerical algorithm based on modified extended B-spline functions for solving time-fractional diffusion

wave equation involving reaction and damping terms. *Adv Differ Equat*. (2019) **2019**:378. doi: 10.1186/s13662-019-2318-7

48. Wasim I, Abbas M, Iqbal M. A new extended B-spline approximation technique for second order singular boundary value problems arising in physiology. *J Math Comput Sci*. (2019) **19**:258–67. doi: 10.22436/jmcs.019.04.06
49. Sharifi S, Rashidinia J. Numerical solution of hyperbolic telegraph equation by cubic B-spline collocation method. *Appl Math Comput*. (2016) **281**:28–38. doi: 10.1016/j.amc.2016.01.049
50. Khalid N, Abbas M, Iqbal MK, Baleanu D. A numerical investigation of Caputo time fractional Allen-Cahn equation using redefined cubic B-spline functions. *Adv Differ Equat*. (2020) **2020**:1–22. doi: 10.1186/s13662-020-02616-x
51. De Boor C. On the convergence of odd-degree spline interpolation. *J Approx Theory*. (1968) **1**:452–63. doi: 10.1016/0021-9045(68)90033-6
52. Hall CA. On error bounds for spline interpolation. *J Approx Theory*. (1968) **1**:209–18. doi: 10.1016/0021-9045(68)90025-7
53. Iqbal MK, Abbas M, Zafar B. New quartic B-spline approximations for numerical solution of fourth order singular boundary value problems. *Punjab Univ J Math*. (2020) **52**:47–63.
54. Wasim I, Abbas M, Amin M. Hybrid B-spline collocation method for solving the generalized Burgers-Fisher and Burgers-Huxley equations. *Math Probl Eng*. (2018) **2018**:6143934. doi: 10.1155/2018/6143934

Conflict of Interest: The authors declare that the research was conducted in the absence of any commercial or financial relationships that could be construed as a potential conflict of interest.

Copyright © 2020 Amin, Abbas, Iqbal and Baleanu. This is an open-access article distributed under the terms of the Creative Commons Attribution License (CC BY). The use, distribution or reproduction in other forums is permitted, provided the original author(s) and the copyright owner(s) are credited and that the original publication in this journal is cited, in accordance with accepted academic practice. No use, distribution or reproduction is permitted which does not comply with these terms.

frontiers in Physics

ORIGINAL RESEARCH
published: 23 September 2020
doi: 10.3389/fphy.2020.00281

An Efficient Computational Method for the Time-Space Fractional Klein-Gordon Equation

Harendra Singh[1], *Devendra Kumar*[2*] *and Ram K. Pandey*[3]

[1] Department of Mathematics, Post Graduate College Ghazipur, Ghazipur, India, [2] Department of Mathematics, University of Rajasthan, Jaipur, India, [3] Department of Mathematics and Statistics, Dr. H.S. Gour Vishwavidyalaya, Sagar, India

In this paper, we present a computational method to solve the fractional Klein-Gordon equation (FKGE). The proposed technique is the grouping of orthogonal polynomial matrices and collocation method. The benefit of the computational method is that it reduces the FKGE into a system of algebraic equations which makes the problem straightforward and easy to solve. The main reason for using this technique is its high accuracy and low computational cost compared to other methods. The main solution behaviors of these equations are due to fractional orders, which are explained graphically. Numerical results obtained by the proposed computational method are also compared with the exact solution. The results obtained by the suggested technique reveals that the method is very useful for solving FKGE.

Keywords: fractional Klein-Gordon equation, fractional derivative, numerical solution, Chebyshev polynomials, operational matrices

OPEN ACCESS

Edited by:
Jordan Yankov Hristov,
University of Chemical Technology and Metallurgy, Bulgaria

Reviewed by:
Babak Shiri,
Neijiang Normal University, China
Ndolane Sene,
Cheikh Anta Diop University, Senegal

***Correspondence:**
Devendra Kumar
devendra.maths@gmail.com

Specialty section:
This article was submitted to Mathematical and Statistical Physics, a section of the journal Frontiers in Physics

Received: *25 February 2020*
Accepted: *22 June 2020*
Published: *23 September 2020*

Citation:
Singh H, Kumar D and Pandey RK (2020) An Efficient Computational Method for the Time-Space Fractional Klein-Gordon Equation. Front. Phys. 8:281. doi: 10.3389/fphy.2020.00281

INTRODUCTION

The standard Klein-Gordon equation (KGE) is written as

$$\frac{\partial^2 v}{\partial t^2} - \frac{\partial^2 v}{\partial x^2} + v = h(x,t), \quad x \geq 0,\ t \geq 0 \tag{1}$$

where v indicates an unknown function in variables x and t, and $h(x,t)$ stands for the source term. Due to the non-local nature and real-life applications of fractional derivatives, the fractional extension of this equation is very useful [1–12]. The fractional extension of this model handles the initial and boundary conditions of the model very accurately. The non-integer derivative helps in understanding the complete memory effect of the system. A broad literature of models with fractional derivatives can be found in [13–17]. Therefore, motivated by our ongoing research work into this special branch of mathematics (namely, fractional calculus), we study non-integer KGE by changing integer order derivative in both time and space using the Liouville-Caputo derivative of fractional order in the following manner:

$$\frac{\partial^{\beta} v(x,t)}{\partial t^{\beta}} - \frac{\partial^{\gamma} v(x,t)}{\partial x^{\gamma}} + v(x,t) = h(x,t), \quad 1 < \beta \leq 2, \ 1 < \gamma \leq 2 \tag{2}$$

having the initial conditions:

$$v(x,0) = h_1(x), \frac{\partial v(x,0)}{\partial t} = h_2(x), \text{for } 0 \leq x, \ t \leq 1 \tag{3}$$

and boundary conditions:

$$v(0,t) = g_1(t), v(1,t) = g_2(t) \tag{4}$$

The KGE is used in science, plasma (especially in quantum field theory), optical fibers, and dispersive wave-phenomena. Due to the great importance of KGE, many authors have studied it using various numerical and analytical schemes [18–27], each with their own limitations and shortcomings. The operational matrix method [28–38] is also applied to solve problems in fractional calculus. There are several other numerical and analytical methods which have been used to solve non-linear problems pertaining to fractional calculus, which can be found in [39, 40]. Some other applications of orthogonal polynomials-based solutions can be found in [41, 42].

In this paper, we present a computational technique which is a combination of the operational matrix and collocation method. We have used Chebyshev polynomials as a basis function for the construction of operational matrices of differentiations and integrations. In our proposed method, first the unknown function and their derivatives are approximated by taking finite dimensional approximations. Then, by using these approximations along with operational matrices of differentiations and integrations in the FKGE, we obtain a system of equations. Finally, by collocating this system, we get an approximate solution for the FKGE. The efficiency and accuracy of the used technique is shown by making a comparison amongst the results derived by our technique, exact solutions, and numerical results by some existing methods.

SOME BASIC DEFINITIONS

In this paper, we use non-integer order integrals and derivatives in the Riemann-Liouville and Caputo sense, respectively, which are given as:

Definition 2.1: The Riemann-Liouville non-integer integral operator of order α is presented as

$$I^{\alpha} f(x) = \frac{1}{\Gamma(\alpha)} \int_0^x (x-t)^{\alpha-1} f(t) dt, \alpha > 0, \ x > 0,$$

$I^0 f(x) = f(x)$.

Definition 2.2: The Liouville-Caputo non-integer derivative of order β are defined as [1–3]

$D^{\beta} f(x) = I^{l-\beta} D^l f(x) = \frac{1}{\Gamma(l-\beta)} \int_0^x (x-t)^{l-\beta-1} \frac{d^l}{dt^l} f(t) dt$, $l-1 < \beta < l, x > 0$ and l is a natural number.

Chebyshev polynomial of the third kind of degree i on [0, 1] is given as,

$$H_i(t) = \sum_{k=0}^{i} (-1)^{i-k} \frac{\Gamma(i+\frac{3}{2})\Gamma(i+k+1)}{\Gamma\left(k+\frac{3}{2}\right)\Gamma(i+1)(i-k)!k!} t^k \tag{5}$$

The orthogonal property of these polynomials is given as:

$$\int_0^1 H_n(t) H_m(t) w(t) dt = \begin{cases} \frac{\pi}{2}, & n = m \\ 0, & n \neq m \end{cases} \tag{6}$$

where, $w(t) = \sqrt{\frac{t}{1-t}}$, is a weight function and n *and* m are the degrees of polynomials.

A function $g(x,t) \in L^2_{w(t)}([0,1] \times [0,1])$ can be approximated as

$$g(x,t) \cong \sum_{i_1=0}^{n_1} \sum_{i_2=0}^{n_2} c_{i_1,i_2} H_{i_1,i_2}(x,t) = C^T \theta_{n_1,n_2}(x,t) \tag{7}$$

where, $C = [c_{0,0}, \ldots, c_{0,n_2}, \ldots, c_{n_1,1}, \ldots, c_{n_1,n_2}]^T$ and

$$\theta_{n_1,n_2}(x,t) = [H_{0,0}(x,t), \ldots, H_{0,n_2}(x,t), \ldots . H_{n_1,0}(x,t), \ldots H_{n_1,n_2}(x,t)]^T.$$

For any approximation taking $n_1 = n_2 = n$ then Equation (6), can be written as,

$$g(x,t) \cong \theta_n^T(x) C \theta_n(t) \tag{8}$$

The matrix C in Equation (8), is given as:

$$C = P^{-1} \left(\int_0^1 \int_0^1 \theta_n(x) C \theta_n^T(t) w(x) w(t) dx dt \right) P^{-1} \tag{9}$$

where, $P = \int_0^1 \theta_n(x) \theta_n^T(x) w(x) dx$, is called the matrix of dual.

Theorem 1. If $\theta_n(t) = [H_0, H_1, \ldots, H_n]^T$, is Chebyshev vector and we consider $\nu > 0$, then

$$I^{\nu} H_i(t) = I^{(\nu)} \theta_n(t) \tag{10}$$

where, $I^{(\nu)} = \left(e(i,j)\right)$, is $(n+1) \times (n+1)$ matrix of integral of non-integer order ν and its entries are given by

$$e(i,j) = \sum_{k=0}^{i}\sum_{l=0}^{j}(-1)^{i+j-k-l} \times \frac{\Gamma(\frac{1}{2})\Gamma(i+\frac{3}{2})\Gamma(i+k+1)\Gamma(j+l+1)\Gamma(\nu+k+l+\frac{3}{2})(2j+1)\,j!}{(i-k)!\,(j-l)!(l)!\,\Gamma(k+\frac{3}{2})\Gamma(i+1)\Gamma(\nu+k+1)\Gamma(j+\frac{1}{2})\Gamma(l+\frac{3}{2})\Gamma(k+l+\nu+2)}.$$

Proof. Please see [30, 32, 38].

Theorem 2. If $\theta_n(t) = [H_0, H_1, \ldots., H_n]^T$, is Chebyshev vector and we consider $\beta > 0$, then

$$D^{\beta}H_i(t) = D^{(\beta)}\theta_n(t) \tag{11}$$

where, $D^{(\beta)} = \left(s(i,j)\right)$, is $(n+1) \times (n+1)$ matrix of differentiation of non-integer order β and its entries are given by

$$s(i,j) = \sum_{k=\lceil\beta\rceil}^{i}\sum_{l=0}^{j}(-1)^{i+j-k-l} \times \frac{\Gamma(\frac{1}{2})\Gamma(i+\frac{3}{2})\Gamma(i+k+1)\Gamma(j+l+1)\Gamma(k+l-\beta+\frac{3}{2})(2j+1)\,j!}{(i-k)!\,(j-l)!(l)!\,\Gamma(k+\frac{3}{2})\Gamma(i+1)\Gamma(k-\beta+1)\Gamma(j+\frac{1}{2})\Gamma(l+\frac{3}{2})\Gamma(k+l-\beta+2)}.$$

Proof. Please see [38].

METHOD OF SOLUTION

In this section, we apply our proposed algorithm to solve a fractional model of KGE. We use equal number basis elements i.e. $n_1 = n_2 = n$, for any approximations of space and time variables. We initially approximate the time derivative of the unknown function as follows:

$$\frac{\partial^{\beta}\nu(x,t)}{\partial t^{\beta}} = \theta_n^T(x)C\theta_n(t) \tag{12}$$

Taking integral of order β with respect to t on both sides of Equation (12), we have

$$\nu(x,t) = \theta_n^T(x)\,CI^{(\beta)}\theta_n(t) + \theta_n^T(x)\,AI^{(1)}\theta_n(t) + \theta_n^T(x)\,B\theta_n(t) \tag{13}$$

where $I^{(\beta)}$and $I^{(1)}$ are operational matrices of integration of order β and 1, respectively, and are given by Equation (10) and

$$\frac{\partial\nu(x,0)}{\partial t} = h_2(x) = \theta_n^T(x)A\theta_n(t) \tag{14}$$

$$\nu(x,0) = h_1(x) = \theta_n^T(x)B\theta_n(t) \tag{15}$$

where A and B are known square matrices and can be calculated using Equation (9).

Taking the differentiation of order γ on both sides of Equation (13), we get

$$\frac{\partial^{\gamma}\nu(x,t)}{\partial x^{\gamma}} = \theta_n^T(x)\,D^{(\gamma),\,T}CI^{(\beta)}\theta_n(t) + \theta_n^T(x)\,D^{(\gamma),\,T}AI^{(1)}\theta_n(t) + \theta_n^T(x)\,D^{(\gamma),\,T}B\theta_n(t) \tag{16}$$

where, $D^{(\gamma)}$is the operational matrix of differentiation of order γ and is given by Equation (11). Further, the inhomogeneous term can be approximated as

$$h(x,t) = \theta_n^T(x)E\theta_n(t) \tag{17}$$

where E is the known square matrix and can be calculated using Equation (9).

Grouping Equations (12), (13), (16), (17), and (2), we get

$$\begin{aligned}&\theta_n^T(x)\,C\theta_n(t) - \Big(\theta_n^T(x)\,D^{(\gamma),\,T}CI^{(\beta)}\theta_n(t)\\&+\theta_n^T(x)\,D^{(\gamma),\,T}AI^{(1)}\theta_n(t) + \theta_n^T(x)\,D^{(\gamma),\,T}B\theta_n(t)\Big)\\&+\theta_n^T(x)\,CI^{(\beta)}\theta_n(t) + \theta_n^T(x)\,AI^{(1)}\theta_n(t)\\&+\theta_n^T(x)\,B\theta_n(t) = \theta_n^T(x)E\theta_n(t)\end{aligned} \tag{18}$$

Equation (18), can be written as

$$C - D^{(\gamma),\,T}CI^{(\beta)} - D^{(\gamma),\,T}AI^{(1)} - D^{(\gamma),\,T}B + CI^{(\beta)} + AI^{(1)} + B = E \tag{19}$$

Equation (19) is a system of equations which is easy to handle using the collocation method to determine the unknown matrix. By making use of the value of C in Equation (13), we can obtain an approximate solution for FLGE.

NUMERICAL EXPERIMENTS AND DISCUSSION

Example 1. Firstly, we take the time fractional KGE [26] given as $\frac{\partial^{\beta}\nu(x,t)}{\partial t^{\beta}} - \frac{\partial^2\nu(x,t)}{\partial x^2} - \nu(x,t) = 0, \quad 1 < \beta \leq 2$, having the ICs: $\nu(x,0) = 1 + \sin(x)$, $\frac{\partial\nu(x,0)}{\partial t} = 0$, for $0 \leq x, t \leq 1$, and boundary conditions:

$\nu(0,t) = \cosh(t)$, $\nu(1,t) = \sin(1) + \cosh(t)$.

The exact solution is $\nu(x,t) = \sin(x) + \cosh(t)$.

In **Figure 1**, we have shown the three-dimensional trajectory of the approximate solution obtained by our used technique for

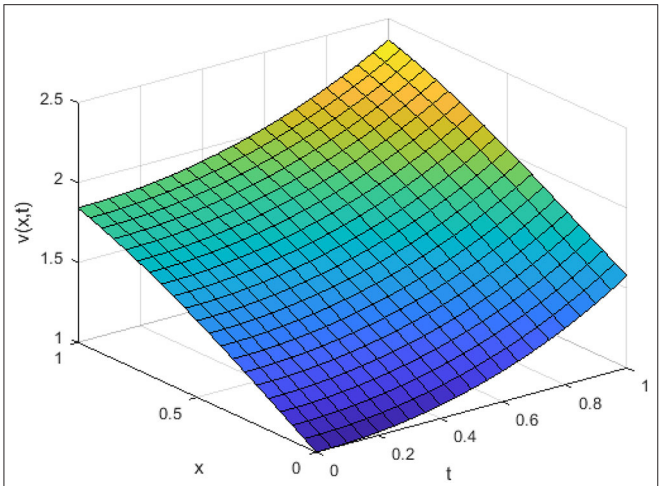

FIGURE 1 | Approximate solution at $\beta = 2$.

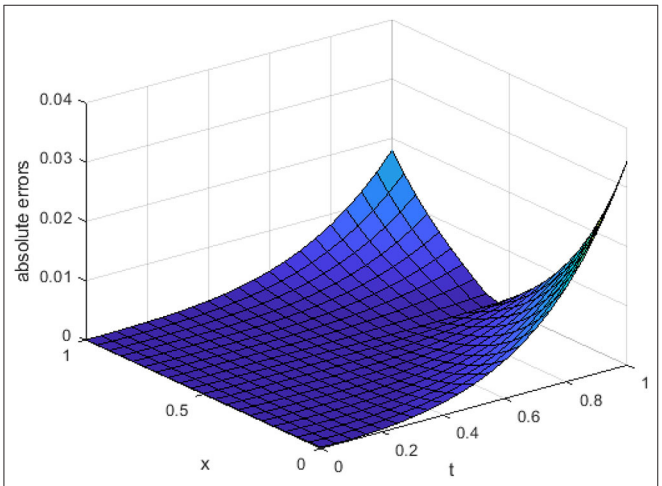

FIGURE 2 | Absolute errors at $\beta = 2$.

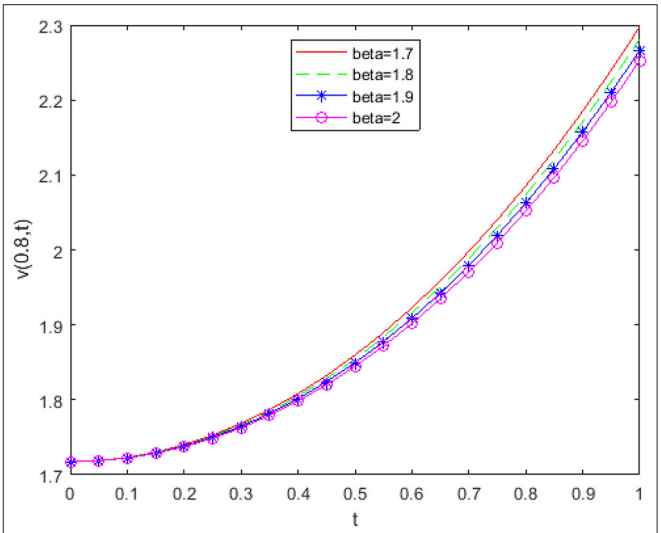

FIGURE 3 | Approximate solution at different values of t and β at $x = 0.8$.

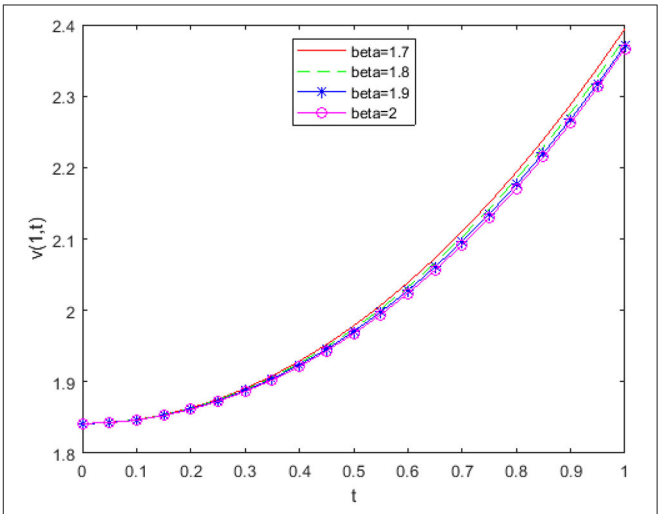

FIGURE 4 | Approximate solution at different values of t and β at $x = 1$.

integer KGE. In **Figure 2**, we have shown absolute errors by our proposed method for integer order KGE at $n = 4$.

From **Figure 2** it is detected that absolute errors are very low, showing good agreement between the exact and approximate solution. In **Figure 3**, we have plotted fractional order KGE by changing the values of β and t at $x = 0.8$. In **Figure 4**, we have plotted fractional order KGE by changing the values of β and t at $x = 1$.

From **Figures 3**, **4**, it can be seen that the solution changes consistently from fractional order to integer solution, showing the consistency of the proposed algorithm for time fractional order models.

Example 2. Secondly, taking the space fractional KGE [26] given as

$\frac{\partial^2 v(x,t)}{\partial t^2} - \frac{\partial^\gamma v(x,t)}{\partial x^\gamma} = h(x,t)$, $1 < \gamma \leq 2$, having the ICs:

$v(x,0) = x^\gamma(1-x)$, $\frac{\partial v(x,0)}{\partial t} = x^\gamma(x-1)$, for $0 \leq x, t \leq 1$, and boundary conditions:

$v(0,t) = 0$, $v(1,t) = 0$, with source function $h(x,t) = x^\gamma(1-x)\exp(-t) - [\lceil(\gamma+1) - \lceil(\gamma+2)\ x]\exp(-t)$and the exact solution $v(x,t) = x^\gamma(1-x)\exp(-t)$.

In **Figure 5**, we have shown the three-dimensional trajectory of the approximate solution obtained by our proposed method for integer KGE. In **Figures 6–8**, we have shown absolute errors by our proposed method for integer order KGE at different values of $n = 3$, 5, and 7, respectively.

From **Figures 6–8**, it is detected that absolute errors are very low and show good agreement between the exact and approximate solution. It is also observed that absolute errors decrease when increasing the basis elements. In **Figure 9**, we have plotted fractional order KGE by changing the values of γ and x at

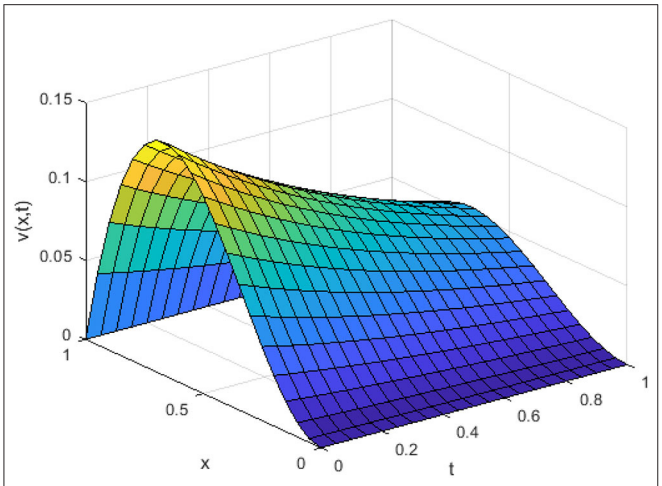

FIGURE 5 | Approximate solution at $\gamma = 2$.

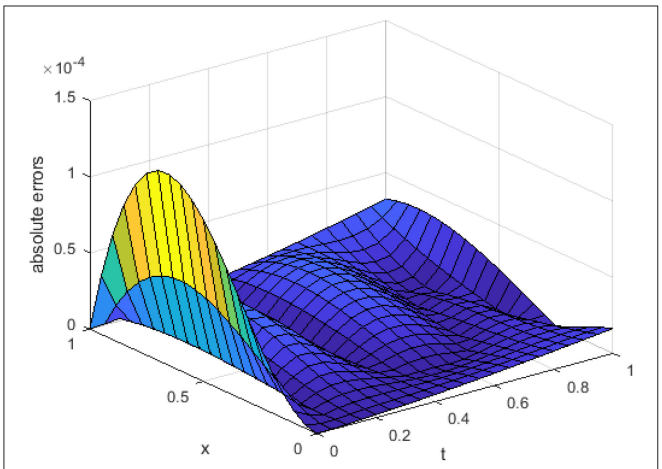

FIGURE 6 | Absolute errors at $n = 3$ and $\gamma = 2$.

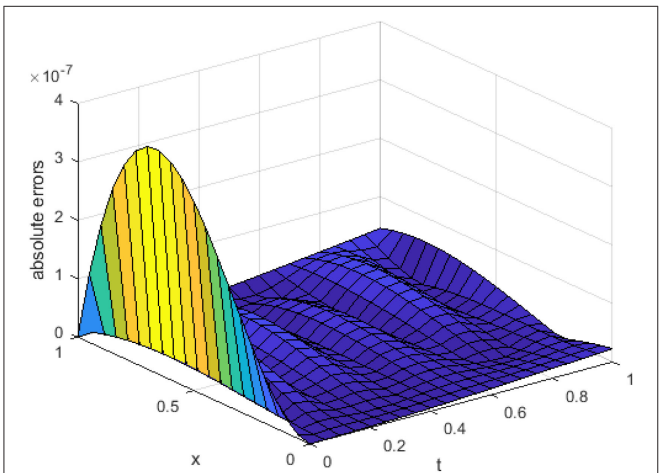

FIGURE 7 | Absolute errors at $n = 5$ and $\gamma = 2$.

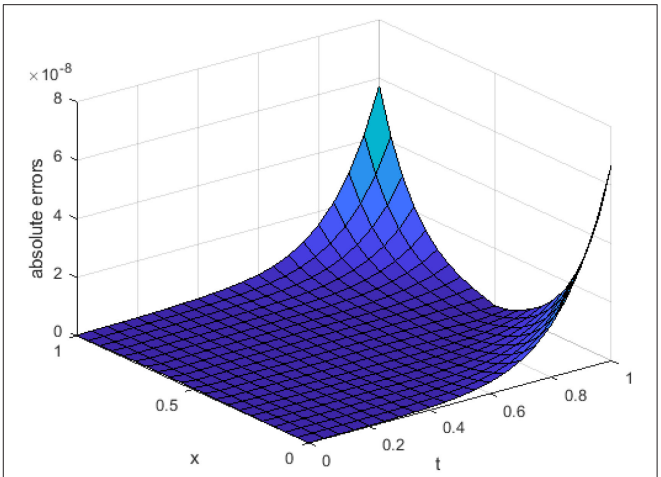

FIGURE 8 | Absolute errors at $n = 7$ and $\gamma = 2$.

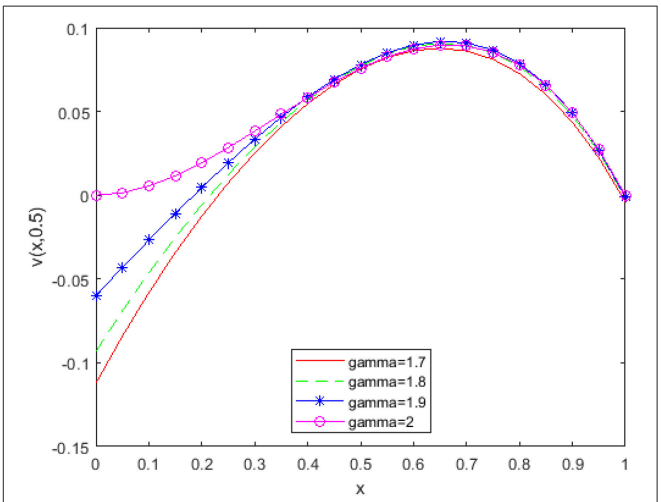

FIGURE 9 | Approximate solution at different values of x and γ at $t = 0.5$.

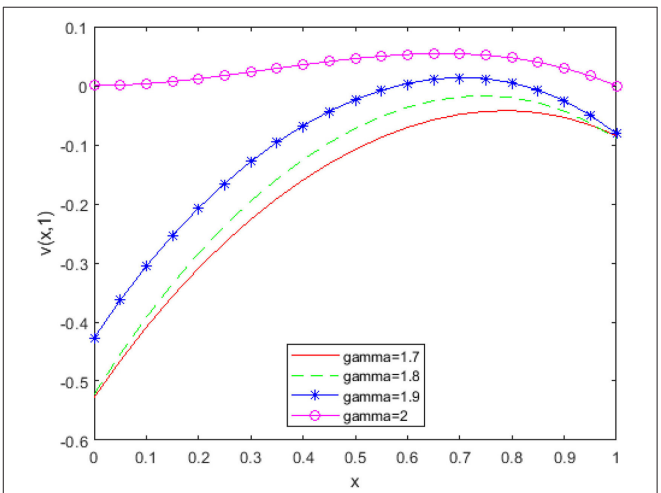

FIGURE 10 | Approximate solution at different values of x and γ at $t = 1$.

TABLE 1 | Comparison of absolute errors by our method and the method in [26] at $t = 1$, Example 2.

x	n = 3		n = 5	
	Present method	Method in [26]	Present method	Method in [26]
0.0	1.6402e-05	1.1234e-03	2.2794e-08	8.1245e-04
0.1	1.0593e-05	2.7894e-03	1.4125e-08	6.8754e-04
0.2	3.4033e-06	4.4561e-03	2.6052e-09	4.9541e-04
0.3	4.5760e-06	1.7418e-03	1.0543e-08	2.4875e-04
0.4	1.2753e-05	7.8527e-03	2.4098e-08	8.5154e-04
0.5	2.0535e-05	5.9634e-03	3.6840e-08	4.0092e-04
0.6	2.7330e-05	6.8527e-03	4.7547e-08	6.1457e-04
0.7	3.2547e-05	3.1237e-03	5.4998e-08	6.9541e-04
0.8	3.5593e-05	1.7595e-03	5.7972e-08	7.1478e-04
0.9	3.5876e-05	3.0030e-03	5.5247e-08	2.0854e-04
1.0	3.2804e-05	0.0129e-03	4.5603e-08	0.0034e-04

TABLE 2 | Comparison approximate and exact solution at $\gamma = 2$ and $n = 5$, Example 2.

(x, t)	Exact solution	Present method	Absolute errors
(0.1, 0.1)	0.00814353	0.00814354	5.9041e-09
(0.2, 0.2)	0.02619938	0.02619938	4.3087e-09
(0.3, 0.3)	0.04667154	0.04667152	2.0611e-08
(0.4, 0.4)	0.06435072	0.06435071	1.2501e-08
(0.5, 0.5)	0.07581633	0.07581635	2.4796e-08
(0.6, 0.6)	0.07902887	0.07902889	2.3619e-08
(0.7, 0.7)	0.07299803	0.07299801	2.7123e-08
(0.8, 0.8)	0.05751410	0.05751405	4.9922e-08
(0.9, 0.9)	0.03293214	0.03293211	2.3894e-08

$t = 0.5$. In **Figure 10**, we have plotted fractional order KGE by changing the values of γ and x at $t = 1$.

From **Figures 9**, **10**, it can be seen that the solution changes consistently from fractional order to integer solution, showing the consistency of the proposed algorithm for space fractional order models. In **Table 1**, we have compared absolute errors by our method and the method used in [26] and observed that our used technique is more accurate in comparison to the technique used in [26].

In **Table 2**, we have compared our solution with the exact solution for different values of x and t at $\gamma = 2$.

CONCLUDING REMARKS

The key benefit of the used algorithm is that it works for both time and space FKGE. Using the proposed algorithm, we can derive an approximate solution for FKGE when the analytical solutions are not possible. It is also easy for computational purposes because FKGE is reduced into algebraic equations. We can apply this method together for time and space fractional, which reduces the time period of computation. Integer and fractional order behavior of KGE is shown. The outcomes of the present study are very helpful for scientists and engineers working in the mathematical modeling of natural phenomena. In a nutshell, we can say that with the aid of this scheme we can examine FKGE for use in quantum field theory, plasma, optical fibers, and dispersive wave-phenomena.

DATA AVAILABILITY STATEMENT

All datasets generated for this study are included in the article/supplementary material.

AUTHOR CONTRIBUTIONS

All authors have worked equally on this manuscript and have read and approved the final manuscript.

REFERENCES

1. Podlubny I. *Fractional Differential Equations*. San Diego, CA: Academic Press. (1999). p. 340.
2. Caputo M. *Elasticita e Dissipazione*. Bologna: Zani-Chelli (1969).
3. Kilbas AA, Srivastava HM, Trujillo JJ. *Theory and Applications of Fractional Differential Equations*. Amsterdam: Elsevier (2006). p. 540.
4. Hristov J. Transient heat diffusion with a non-singular fading memory: from the cattaneo constitutive equation with Jeffrey's kernel to the Caputo-Fabrizio time-fractional derivative. *Thermal Sci.* (2016) **20**:765–70. doi: 10.2298/TSCI160112019H
5. Baskonus HM, Mekkaoui T, Hammouch Z, Bulut H. Active control of a Chaotic fractional order economic system. *Entropy.* (2015) **17**:5771–83. doi: 10.3390/e17085771
6. Singh H. A new stable algorithm for fractional Navier-Stokes equation in polar coordinate. *Int J Appl Comput Math.* (2017) **3**:3705–22. doi: 10.1007/s40819-017-0323-7
7. Yang XJ, Machado JAT, Cattani C, Gao F. On a fractal LC-electric circuit modeled by local fractional calculus. *Commun Nonlin Sci Numeric Simul.* (2017) **47**:200–6. doi: 10.1016/j.cnsns.2016.11.017
8. Yang XJ. A new integral transform operator for solving the heat-diffusion problem. *Appl Math Lett.* (2017) **64**:193–7. doi: 10.1016/j.aml.2016.09.011
9. Srivastava HM, Kumar D, Singh J. An efficient analytical technique for fractional model of vibration equation. *Appl Math Model.* (2017) **45**:192–204. doi: 10.1016/j.apm.2016.12.008
10. Kumar D, Singh J, Baleanu D. A new analysis for fractional model of regularized long-wave equation arising in ion acoustic plasma waves. *Math Methods Appl Sci.* (2017) **40**:5642–53. doi: 10.1002/mma.4414
11. Kumar D, Agarwal RP, Singh J. A modified numerical scheme and convergence analysis for fractional model of Lienard's equation. *J Comput Appl Math.* (2018) **339**:405–13. doi: 10.1016/j.cam.2017.03.011
12. Singh H, Srivastava HM. Numerical simulation for fractional-order Bloch equation arising in nuclear magnetic resonance by using the Jacobi polynomials. *Appl Sci.* (2020) **10**:2850. doi: 10.3390/app10082850
13. Singh H. A new numerical algorithm for fractional model of Bloch equation in nuclear magnetic resonance. *Alex Engl J.* (2016) **55**:2863–9. doi: 10.1016/j.aej.2016.06.032
14. Sumelka W. Non-local Kirchhoff–Love plates in terms of fractional calculus. *Arch Civil Mech Eng.* (2015) **15**:231–42. doi: 10.1016/j.acme.2014.03.006
15. Singh H. Solution of fractional Lienard equation using Chebyshev operational matrix method. *Nonlin Sci Lett A.* (2017) **8**:397–404.

16. Lazopoulos AK. On fractional peridynamic deformations. *Arch Appl Mech.* (2016) **86**:1987–94. doi: 10.1007/s00419-016-1163-3
17. Ying YP, Lian YP, Tang SQ, Liu WK. High-order central difference scheme for Caputo fractional derivative. *Comput Methods Appl Mech Eng.* (2017) **317**:42–54. doi: 10.1016/j.cma.2016.12.008
18. Abbasbandy S. Numerical solutions of nonlinear Klein-Gordon equation by variational iteration method. *Int J Num Meth Engg.* (2007) **70**:876–81. doi: 10.1002/nme.1924
19. Mohyud-Din ST, Noor MA, Noor KI. Some relatively new techniques for nonlinear problems. *Math Porb Engg.* (2009) **2009**:234849. doi: 10.1155/2009/234849
20. Wazwaz AM. The modified decomposition method for analytic treatment of differential equations. *Appl Math Comput.* (2006) **173**:165–76. doi: 10.1016/j.amc.2005.02.048
21. Kumar D, Singh J, Kumar S, Sushila. Numerical computation of Klein-Gordon equations arising in quantum field theory by using homotopy analysis transform method. *Alexandria Eng J.* (2014) **53**:469–74. doi: 10.1016/j.aej.2014.02.001
22. Golmankhaneh AK, Baleanu D. On nonlinear fractional Klein-Gordon equation. *Signal Proc.* (2011) **91**:446–51. doi: 10.1016/j.sigpro.2010.04.016
23. Kurulay M. Solving the fractional nonlinear Klein-Gordon equation by means of the homotopy analysis method. *Adv Diff Eqs.* (2012) **13**:529–39. doi: 10.1186/1687-1847-2012-187
24. Gepreel KA, Mohamed MS. Analytical approximate solution for nonlinear space-time fractional Klein-Gordon equation. *Chin Phys B.* (2013) **22**:010201. doi: 10.1088/1674-1056/22/1/010201
25. Kumar D, Singh J, Baleanu D. A hybrid computational approach for Klein- Gordon equations on Cantor sets. *Nonlin Dyn.* (2017) **87**:511–7. doi: 10.1007/s11071-016-3057-x
26. Khader MM, Kumar S. An accurate numerical method for solving the linear fractional Klein–Gordon equation. *Math Meth Appl Sci.* (2013) **37**:2972–9. doi: 10.1002/mma.3035
27. Yousif MA, Mahmood BA. Approximate solutions for solving the Klein-Gordon sine-Gordon equations. *J Assoc Arab Univ Bas Appl Sci.* (2017) **22**:83–90. doi: 10.1016/j.jaubas.2015.10.003
28. Singh H, Srivastava HM, Kumar D. A reliable numerical algorithm for the fractional vibration equation. *Chaos Solitons Fractals.* (2017) **103**:131–8. doi: 10.1016/j.chaos.2017.05.042
29. Singh CS, Singh H, Singh VK, Om Singh P. Fractional order operational matrix methods for fractional singular integro-differential equation. *Appl Math Model.* (2016) **40**:10705–18. doi: 10.1016/j.apm.2016.08.011
30. Singh H, Srivastava HM. Jacobi collocation method for the approximate solution of some fractional-order Riccati differential equations with variable coefficients. *Phys A.* (2019) **523**:1130–49. doi: 10.1016/j.physa.2019.04.120
31. Singh CS, Singh H, Singh S, Kumar D. An efficient computational method for solving system of nonlinear generalized Abel integral equations arising in astrophysics. *Phys A.* (2019) **525**:1440–8. doi: 10.1016/j.physa.2019.03.085
32. Singh H, Pandey RK, Baleanu D. Stable numerical approach for fractional delay differential equations. *Few Body Syst.* (2017) **58**:156. doi: 10.1007/s00601-017-1319-x
33. Singh H, Singh CS. Stable numerical solutions of fractional partial differential equations using Legendre scaling functions operational matrix. *Ain Shams Eng J.* (2018) **9**:717–25. doi: 10.1016/j.asej.2016.03.013
34. Singh H. Operational matrix approach for approximate solution of fractional model of Bloch equation. *J King Saud Univ Sci.* (2017) **29**:235–40. doi: 10.1016/j.jksus.2016.11.001
35. Wu JL. A wavelet operational method for solving fractional partial differential equations numerically. *Appl Math Comput.* (2009) **214**:31–40. doi: 10.1016/j.amc.2009.03.066
36. Singh H. An efficient computational method for the approximate solution of nonlinear Lane-Emden type equations arising in astrophysics. *Astrophys Space Sci.* (2018) **363**:71. doi: 10.1007/s10509-018-3286-1
37. Singh H, Sahoo MR, Singh OP. Numerical method based on Galerkin approximation for the fractional advection-dispersion equation. *Int J Appl Comput Math.* (2016) **3**:2171–87. doi: 10.1007/s40819-016-0233-0
38. Singh H. Approximate solution of fractional vibration equation using Jacobi polynomials. *Appl Math Comput.* (2018) **317**:85–100. doi: 10.1016/j.amc.2017.08.057
39. Bhatter S, Mathur A, Kumar D, Singh J. A new analysis of fractional Drinfeld–Sokolov–Wilson model with exponential memory. *Physi A.* (2020) **537**:122578. doi: 10.1016/j.physa.2019.122578
40. Dubey VP, Kumar R, Kumar D, Khan I, Singh J. An efficient computational scheme for nonlinear time fractional systems of partial differential equations arising in physical sciences. *Adv Diff Equat.* (2020) **2020**:46. doi: 10.1186/s13662-020-2505-6
41. Shiri B, Perfilieva I, Alijani Z. Classical approximation for fuzzy Fredholm integral equation, fuzzy sets and systems. (2020). doi: 10.1016/j.fss.2020.03.023
42. Alijani Z, Shiri B, Baleanu D. A Chebyshev based numerical methods for solving fractional fuzzy differential equations (2019).

Conflict of Interest: The authors declare that the research was conducted in the absence of any commercial or financial relationships that could be construed as a potential conflict of interest.

Copyright © 2020 Singh, Kumar and Pandey. This is an open-access article distributed under the terms of the Creative Commons Attribution License (CC BY). The use, distribution or reproduction in other forums is permitted, provided the original author(s) and the copyright owner(s) are credited and that the original publication in this journal is cited, in accordance with accepted academic practice. No use, distribution or reproduction is permitted which does not comply with these terms.

frontiers in Physics

ORIGINAL RESEARCH
published: 24 September 2020
doi: 10.3389/fphy.2020.00377

Basic Control Theory for Linear Fractional Differential Equations With Constant Coefficients

Sebastián Buedo-Fernández[1,2†] *and Juan J. Nieto*[1,2*†]

[1] *Departamento de Estadística, Análisis Matemático y Optimización, Universidade de Santiago de Compostela, Santiago de Compostela, Spain,* [2] *Instituto de Matemáticas, Universidade de Santiago de Compostela, Santiago de Compostela, Spain*

In this paper we present an analogous result of the famous Kalman controllability criterion for first order linear ordinary differential equations with constant coefficients that applies to the case of linear differential equations of fractional order with constant coefficients. We use the fractional Gramian matrix, the range space and the Kalman matrix as main tools to derive a sufficient and necessary condition for the controllability of the fractional system. Moreover, we provide some simple examples, including a linear fractional harmonic oscillator, to illustrate our results. Finally, several open problems arising from this topic are suggested, including another simple linear system of incommensurate fractional orders.

Keywords: linear differential equations, controllability, fractional Gramian, fractional differential equations, Kalman matrix

OPEN ACCESS

Edited by:
Jagdev Singh,
JECRC University, India

Reviewed by:
Devendra Kumar,
University of Rajasthan, India
Ndolane Sene,
Cheikh Anta Diop University, Senegal

****Correspondence:***
Juan J. Nieto
juanjose.nieto.roig@usc.es

†ORCID:
Sebastián Buedo-Fernández
orcid.org/0000-0002-5485-5667
Juan J. Nieto
orcid.org/0000-0001-8202-6578

Specialty section:
This article was submitted to Mathematical and Statistical Physics, a section of the journal Frontiers in Physics

Received: *05 May 2020*
Accepted: *04 August 2020*
Published: *24 September 2020*

Citation:
Buedo-Fernández S and Nieto JJ (2020) Basic Control Theory for Linear Fractional Differential Equations With Constant Coefficients. Front. Phys. 8:377. doi: 10.3389/fphy.2020.00377

1. INTRODUCTION

Controllability is a mathematical problem consisting in determining the targets to which one can drive the state of a dynamical system by means of a control input appearing in the equation. We have a dynamical system on which we can exert a certain influence. Is it possible to use this to make the system reach a desirable state? In other words, given a future time, an initial state and a target state, is it possible to find a control function such that the solution of the system starting from the initial state reaches the desirable state at the prescribed future time? For some classical and modern references on control theory we refer to references [1–3].

On the other hand, fractional calculus and fractional differential equations have recently been applied in various areas of engineering, mathematics, physics and bio-engineering, and other applied sciences. We refer the reader to the monographs [4–7] and the articles [8, 9]. In particular, there are a growing number of research areas in physics which employ fractional calculus [10] and it has many applications among its different branches, ranging from imaging processing to fractional quantum harmonic oscillator [11]. Recently, in Yıldız [12] the dynamics of a waterborne pathogen fractional model under the influence of environmental pollution has been studied and the solutions of a generalized fractional kinetic equations are obtained [13] using the generalized fractional integrations of the generalized Mittag-Leffler type function. Finally, we highlight that different fractional systems have also been considered in the framework of control theory [14–18].

In the context of the latter application of fractional calculus, we present the current work, which deals with the controllability of a linear fractional differential equation with constant coefficients. The paper is organized as follows: In section 2, we recall the Kalman criterion for controllability of a linear system of first order. In section 3 we consider a linear system of fractional order, whose general solution is presented in terms of the Mittag-Leffler function. By using that representation we finally give in section 4 a new criterion for controllability.

Although this criterion is known since 1996 [19] we give another approach and use some elements of fractional calculus and a different proof to obtain the results. Also we reveal some interesting connections between linear differential equations of fractional order, control problems, linear algebra, Mittag-Leffler functions, geometry and physics.

For the relation between controllability of standard and fractional systems, see Klamka [20]. The calculation of the Gramian is useful to find a control to steer a given initial state to another prescribed final state.

2. CLASSICAL LINEAR CONTROL

Let $A \in \mathcal{M}_{n\times n}(\mathbb{R})$ and $f:[0,\infty) \to \mathbb{R}$ be continuous. Consider the linear system

$$x'(t) = Ax(t) + f(t), \tag{1}$$

with the initial condition

$$x(0) = x_0 \in \mathbb{R}^n. \tag{2}$$

The solution of problem (1) and (2) is given by

$$x(t) = e^{At}x_0 + \int_0^t e^{A(t-s)}f(s)ds.$$

Now consider the same system with a control function, so (1) is written like

$$x'(t) = Ax(t) + Bu(t), \tag{3}$$

where $B \in \mathcal{M}_{n\times m}(\mathbb{R})$ and $u:[0,\infty) \to \mathbb{R}^m$ is a possible control. For a given continuous control input u, the solution of (3) with initial condition $x(0) = x_0$ is

$$x(t) = e^{At}x_0 + \int_0^t e^{A(t-s)}Bu(s)ds.$$

For a given time $t > 0$ and an initial state $x(0) = x_0$, the reachable set of (1) at time $t > 0$ related to x_0 is the set $\mathcal{R}_t(x_0)$ of all states $x(t)$ that can be reached from x_0 by any control input. The linear system (3) is controllable if for any $x_0, x_1 \in \mathbb{R}^n$, there exists a control u such that the corresponding solution satisfies $x(0) = x_0$ and $x(t) = x_1$.

There is a simple criterion, the celebrated Kalman criterion for controllability.

Theorem 1. *The linear system (3) is controllable if and only if the Kalman matrix*

$$K = (B|AB|A^2B|\dots|A^{n-1}B)$$

has full rank.

To prove this (see [21]), one of the main ingredients is the controllability Gramian of matrices A and B:

$$W(t) := \int_0^t e^{As}BB^*e^{A^*s}ds \in \mathcal{M}_{n\times n}(\mathbb{R}), \tag{4}$$

where A^* and B^* are, respectively, the adjoint matrices of A and B. The matrix $W(t)$ is positive semi-definite and its range coincides with the range of the Kalman matrix.

Also a relevant ingredient is the following property for a matrix A. Let $\varphi(z) = \sum_{k=0}^{\infty} a_k z^k$ be an analytic complex function. An application of the Cayley-Hamilton Theorem implies that there exists a polynomial p of degree less than n such that $\varphi(A) = p(A)$, i.e.,

$$\varphi(A) = p(A) = \sum_{k=0}^{n-1} c_k A^k,$$

for certain $c_0, \dots, c_{n-1} \in \mathbb{C}$.

We recall a relevant geometric interpretation. The subspace

$$\mathcal{R} := \mathcal{R}(B|AB|\dots|A^{n-1}B)$$

is the smallest A-invariant subspace containing $\mathcal{R}(B)$. The linear system (3) is controllable if and only if $W(t)$ is non-singular for $t > 0$. A physical interpretation of the controllability Gramian is that the input of the system is white Gaussian noise. Then, $W(t)$ is the covariance of the state (see p. 854 in [22]).

3. LINEAR CONTROL OF FRACTIONAL ORDER

Consider now the linear differential equation of fractional order $\alpha \in (0, 1]$

$$D^\alpha x(t) = Ax(t) + f(t), \tag{5}$$

with initial condition

$$x(0) = x_0 \in \mathbb{R}^n, \tag{6}$$

where, as before, $A \in \mathcal{M}_{n\times n}(\mathbb{R})$, $f \in \mathcal{C}([0,\infty), \mathbb{R}^n)$ and $D^\alpha x$ is the fractional derivative of x. We use here the Caputo fractional derivative, which can be defined for any $x:[0,\infty) \to \mathbb{R}^n$ absolutely continuous and has the following form:

$$D^\alpha x(t) = \frac{1}{\Gamma(1-\alpha)} \int_0^t (t-s)^{-\alpha} x'(s)ds,$$

where Γ is the classical gamma function. For some applications of fractional differential equations we refer, for example, to references [5, 23, 24].

Note that $D^\alpha x(t) = I^{1-\alpha}x'(t)$, where $I^{1-\alpha}$ is the fractional integral of Riemann-Liouville. In fact, for $\beta > 0$ and $x \in L^1_{loc}(0,\infty)$,

$$I^\beta x(t) = \frac{1}{\Gamma(\beta)} \int_0^t (t-s)^{\beta-1} x(s)ds.$$

Now, let $B \in \mathcal{M}_{n\times m}(\mathbb{R})$ and $u \in \mathcal{C}([0,\infty), \mathbb{R}^m)$. Letting $f(t) = Bu(t)$, we rewrite the Equation (5) as

$$D^\alpha x(t) = Ax(t) + Bu(t). \tag{7}$$

Analogously to the ordinary case, for any $t > 0$, $\mathcal{R}_t^\alpha$ will be defined as the reachable set of (7) related to the origin, which is the set of all states $x(t)$ that can be reached from the initial state zero for some continuous control input. We say that the system (7) is controllable if for any $x_0, x_1 \in \mathbb{R}^n$ there exists a control u such that the solution of (7) with $x(0) = x_0$ satisfies $x(t) = x_1$.

The solution of the first order equation (1) is given in terms of f and the exponential of A:

$$e^{At} = \sum_{k=0}^{\infty} \frac{A^k t^k}{k!}.$$

For the fractional order equation (5) the role of this exponential is played by the Mittag-Leffler functions: for $\alpha > 0$ and for $z \in \mathbb{C}$,

$$E_\alpha(z) = \sum_{k=0}^{\infty} \frac{z^k}{\Gamma(\alpha k + 1)}.$$

Note that for $\alpha = 1$, $E_\alpha(z) = e^z$.

In general, for $\alpha, \beta > 0$, the function

$$E_{\alpha,\beta}(z) = \sum_{k=0}^{\infty} \frac{z^k}{\Gamma(\alpha k + \beta)}. \tag{8}$$

is well-defined in $\mathbb{C}$, since the series in (8) is convergent for every $z \in \mathbb{C}$ [25]. For instance, if $\beta = 1$, we recover the previous case: $E_{\alpha,1}(z) = E_\alpha(z)$.

We can substitute z by a matrix A in (8) and the corresponding series converges. Hence, we can define the Mittag-Leffler function of a matrix A as

$$E_{\alpha,\beta}(A) = \sum_{k=0}^{\infty} \frac{A^k}{\Gamma(\alpha k + \beta)}.$$

The solution of (5) is given by the variation of constants formula for fractional differential equations (see Theorem 5.15, p. 323 in [5] or Theorem 7.2, p. 135 in [23]):

$$x(t) = E_\alpha(t^\alpha A)c + \int_0^t (t-s)^{\alpha-1} E_{\alpha,\alpha}((t-s)^\alpha A) f(s) ds,$$

where c is any constant. Imposing the initial condition $x(0) = x_0$, then $c = x_0$.

In the case of (7) with the initial condition (6), the solution is [5, 17]

$$x(t) = E_\alpha(t^\alpha A)x_0 + \int_0^t (t-s)^{\alpha-1} E_{\alpha,\alpha}((t-s)^\alpha A) B u(s) ds.$$

At this point, we raise the following questions: In the fractional case, is there an analogous rule to the Kalman criterion? What is the Gramian matrix in such case?

4. PROOF OF THE FRACTIONAL CONTROL

We are ready to provide the reasoning that will lead us toward a controllability criterion for system (5).

Let $\alpha \in (0, 1)$. By applying the definition of the Mittag-Leffler function, the expression

$$\int_0^t (t-s)^{\alpha-1} E_{\alpha,\alpha}((t-s)^\alpha A) B u(s) ds$$

is equal to

$$\int_0^t (t-s)^{\alpha-1} \sum_{k=0}^{\infty} \frac{[(t-s)^\alpha A]^k}{\Gamma(\alpha k + \alpha)} B u(s) ds.$$

Then, by using the uniform convergence, we arrive to the following expression

$$\sum_{k=0}^{\infty} \int_0^t (t-s)^{\alpha-1} \frac{(t-s)^{\alpha k} A^k}{\Gamma(\alpha k + \alpha)} B u(s) ds,$$

which is obviously equal to

$$\lim_{N\to\infty} \sum_{k=0}^{N} A^k B \int_0^t (t-s)^{\alpha-1} \frac{(t-s)^{\alpha k}}{\Gamma(\alpha k + \alpha)} u(s) ds.$$

In the previous series, each term is a linear combination of the columns of $B, AB, A^2B, \ldots, A^NB$. Any of these matrices is a linear combination of $B, AB, A^2B, \ldots, A^{n-1}B$. Hence, the vector

$$\sum_{k=0}^{N} A^k B \int_0^t (t-s)^{\alpha-1} \frac{(t-s)^{\alpha k}}{\Gamma(\alpha k + \alpha)} u(s) ds \tag{9}$$

is a linear combination of the columns of $B, AB, A^2B, \ldots, A^{n-1}B$, i.e., it belongs to the range space of the Kalman matrix K. Therefore, as in the ordinary case, we get $\mathcal{R}_t^\alpha \subset \mathcal{R}(K)$. This is a necessary condition for controllability of the linear fractional system (7): The Kalman matrix has full rank. We cannot reach any state outside the range of the Kalman matrix.

The question is how can we get a control u so that

$$\int_0^t (t-s)^{\alpha-1} E_{\alpha,\alpha}((t-s)^\alpha A) B u(s) ds = x_1.$$

In order to do that, we define the α-Gramian as

$$\begin{aligned} W_t^\alpha &= \int_0^t (t-s)^{\alpha-1} E_{\alpha,\alpha}((t-s)^\alpha A) B B^* E_{\alpha,\alpha}((t-s)^\alpha A^*)(t-s)^{\alpha-1} ds \\ &= \int_0^t (t-s)^{2\alpha-2} E_{\alpha,\alpha}((t-s)^\alpha A) B B^* E_{\alpha,\alpha}((t-s)^\alpha A^*) ds. \end{aligned}$$

Note that for $\alpha = 1$ we recover the Gramian in (4).

If we prove that $\mathcal{R}(K) \subset \mathcal{R}(W_t^\alpha)$, then, for $x_1 \in \mathcal{R}(K)$, we get $x_1 \in \mathcal{R}(W_t^\alpha)$ and there exists y such that $W_t^\alpha y = x_1$. By taking the control

$$u(s) = B^* E_{\alpha,\alpha}((t-s)^\alpha A^*)(t-s)^{\alpha-1} y,$$

we see that

$$\begin{aligned} x_1 &= W_t^\alpha y \\ &= \int_0^t (t-s)^{2\alpha-2} E_{\alpha,\alpha}((t-s)^\alpha A) BB^* E_{\alpha,\alpha}((t-s)^\alpha A^*) y ds \\ &= \int_0^t (t-s)^{\alpha-1} E_{\alpha,\alpha}((t-s)^\alpha A) Bu(s) ds. \end{aligned}$$

Thus, we steers the initial condition 0 to the state x_1 at time $t > 0$. This proves that $\mathcal{R}(K) \subset \mathcal{R}_t^\alpha$. It only remains proving that $\mathcal{R}(K) \subset \mathcal{R}(W_t^\alpha)$.

Let $z \in \mathbb{R}^n$ and suppose that $(W_t^\alpha)^* z \equiv z^* W_t^\alpha = 0$. For every $z \in \mathbb{R}^n$, this leads to

$$\begin{aligned} 0 &= z^* W_t^\alpha z = \langle z, W_t^\alpha z \rangle \\ &= \int_0^t (t-s)^{2\alpha-2} z^* E_{\alpha,\alpha}((t-s)^\alpha A) BB^* E_{\alpha,\alpha}((t-s)^\alpha A^*) z ds \\ &= \int_0^t (t-s)^{2\alpha-2} ||z^* E_{\alpha,\alpha}((t-s)^\alpha A) B||^2 ds \geq 0. \end{aligned}$$

For $s \in [0,t]$, $(t-s)^\alpha \in [0, t^\alpha]$. Therefore,

$$z^* \sum_{k=0}^{\infty} \frac{x^k A^k}{\Gamma(\alpha k + \alpha)} B = 0, \quad x \in [0, t^\alpha].$$

Differentiating k times ($k = 0, 1, 2, \dots$) with respect to x and taking the limit when $x \to 0^+$ implies that $z^* A^k B = 0$, for $k = 0, \dots, n-1$; i.e.,

$$z^* B = 0, \dots, z^* A^{n-1} B = 0.$$

This gives us that

$$z^* \in \mathcal{N}(W_t^\alpha) = \mathcal{N}((W_t^\alpha)^*) \Rightarrow z^* \in \mathcal{N}(K^*).$$

We have that $\mathcal{N}((W_t^\alpha)^*) \subset \mathcal{N}(K^*)$ and we can write $\mathcal{N}(K^*)^\perp \subset \mathcal{N}((W_t^\alpha)^*)^\perp$. Therefore, we arrive to $\mathcal{R}(K) \subset \mathcal{R}(W_t^\alpha)$.

By gathering all the previous reasonings, we can finally state the following result.

Theorem 2. *The fractional system (7) is controllable if and only if the Kalman matrix K has full rank.*

As a direct implication, given $\alpha', \alpha'' \in (0,1]$, there exists a link between the controllability of the system (7) for order α' and the one for order α":

Corollary 3. *If the fractional system (7) is controllable for a certain order $\hat{\alpha} \in (0,1]$, then the system is controllable for every order $\alpha \in (0,1]$.*

To conclude, we give several examples showing how Theorem 2 can be applied.

Example 1. Let $\alpha \in (0,1)$. Consider the case $n = 2$, $m = 1$, with

$$x(t) = \begin{pmatrix} x_1(t) \\ x_2(t) \end{pmatrix}, \quad A = \begin{pmatrix} 1 & 0 \\ 0 & 1 \end{pmatrix}, \quad B = \begin{pmatrix} 1 \\ 0 \end{pmatrix}.$$

The system can be written as

$$\begin{cases} D^\alpha x_1(t) = x_1(t) + u(t), \\ D^\alpha x_2(t) = x_2(t). \end{cases} \tag{10}$$

The system is not controllable since the second equation is independent of the control as in the first order case ($\alpha = 1$). Nevertheless, it is possible to control x_1 and in that sense one may say that (10) is partially controllable. In this example,

$$K = \left(\begin{array}{c|c} 1 & 1 \\ 0 & 0 \end{array}\right)$$

and $rank(K) = 1 < 2$.

Example 2. Let $n = 2$, $m = 1$, $\alpha \in (0,1]$ and consider the system

$$D^\alpha x(t) = Ax(t) + Bu(t),$$

where

$$A = \begin{pmatrix} -2 & 2 \\ 2 & 1 \end{pmatrix}, \quad B = \begin{pmatrix} B_1 \\ B_2 \end{pmatrix} \in \mathcal{M}_{2\times 1}(\mathbb{R}).$$

The Kalman matrix would be a 2×2 real matrix, whose columns are identified with B and AB. Moreover, if B is identified with an eigenvector of A, the system will not be controllable. For example, if

$$B = \begin{pmatrix} 1 \\ 2 \end{pmatrix},$$

the Kalman matrix takes the form of

$$K = \left(\begin{array}{c|c} 1 & 2 \\ 2 & 4 \end{array}\right),$$

which has not full rank [$rank(K) = 1 < 2$]. The system would not be therefore controllable.

Something similar happens with the choice

$$B = \begin{pmatrix} -2 \\ 1 \end{pmatrix}.$$

Nonetheless, any other choice of B which is not a multiple of one of the previous cases, leads to a controllable system regardless the value of $\alpha \in (0,1]$.

Example 3. The classical linear harmonic oscillator $\xi" + \xi = u$ is equivalent to the system (3) taking the position $x_1 = \xi$ and the velocity $x_2 = \xi'$ with

$$A = \begin{pmatrix} 0 & 1 \\ -1 & 0 \end{pmatrix}, \quad B = \begin{pmatrix} 0 \\ 1 \end{pmatrix}.$$

A fractional control harmonic oscillator would be (7), which takes the form

$$\begin{cases} D^\alpha x_1 = x_2, \\ D^\alpha x_2 = u - x_1. \end{cases} \tag{11}$$

The first equation is independent of the control, but it appears in the second equation, involving both components and the fractional control system (11) is controllable. Indeed, the Kalman matrix

$$K = \left(\begin{array}{c|c} 0 & 1 \\ 1 & 0 \end{array}\right)$$

has full rank.

Example 4. Another possibility is to consider a coupled system of linear incommesurate fractional differential control system $\alpha_1, \alpha_2 \in (0, 1)$:

$$\begin{cases} D^{\alpha_1} x_1 = a_{11} x_1 + a_{12} x_2 + u_1, \\ D^{\alpha_2} x_2 = a_{21} x_1 + a_{22} x_2 + u_2, \end{cases} \tag{12}$$

but, to the best of our knowledge, no analytical solution is known.

5. CONCLUSIONS

In this work, we have studied the controllability of the linear fractional differential equation

$$D^{\alpha} x(t) = Ax(t) + Bu(t),$$

where the Caputo fractional derivative is considered, $A \in \mathcal{M}_{n\times n}(\mathbb{R})$, $B \in \mathcal{M}_{n\times m}(\mathbb{R})$ and u is a m-dimensional control function. In particular, we have shown that such a system is controllable if and only if the Kalman matrix has full rank, which constitutes the main result, namely Theorem 2.

Although the criterion given in Theorem 2 does not depend on α and thus it becomes an analogous result to the classic one (ordinary case), the tools that we have used actually involve some adaptated reasonings. There are still several relations between the controllability of the system, the corresponding Gramian matrix W_t^{α}, the kernel of the associated operator, the range space $\mathcal{R}_t^{\alpha}$ and the Kalman matrix, but some arguments depend on the fractional order α. For instance, we recall that the Gramian matrix W_t^{α} has a singularity if $\alpha \in (0, 1)$ and the control steering the initial data x_0 to a final state x_1 depends on α, so as the coefficients of the linear combination of the matrices $B, \ldots, A^{n-1}B$ (which form the Kalman matrix) do in Equation (9).

In the future, some research deserves to be done with respect to further questions related to this work. For example, a couple of crucial problems are the cases where the matrices A and B are not constant, that is, the control system

$$D^{\alpha} x(t) = A(t)x(t) + B(t)u(t),$$

and the non-linear case

$$D^{\alpha} x(t) = f(x(t), u(t)),$$

which is also very relevant in applications and will be considered in detail. In general, in many situations, delay may also appear and functional fractional differential equations of the type

$$D^{\alpha} x(t) = f(x(t), x(t-\tau), u(t))$$

have to be considered.

In addition to the former comments, systems with impulses due to impacts are of interest too. Indeed, in Spong [26] and Nieto and Tisdell [27], the problem of controlling a physical object through impacts, called impulsive manipulation, is studied and it arises in a number of robotic applications [28, 29].

Another interesting line is to address the controllability of fractional order systems in the light of other fractional derivatives, such as Riemann-Liouville, Hadamard, Caputo-Fabrizio, etc.

Furthermore, some physical models will be considered under those fractional calculus approaches and the relations among them will be scrutinized.

Moreover, the incommesurate fractional system of Example 4 will also be a relevant problem to consider.

Finally, partial differential equations of fractional order could be treated both from the mathematical point of view and from the physical point of view too.

DATA AVAILABILITY STATEMENT

The original contributions presented in the study are included in the article/supplementary material, further inquiries can be directed to the corresponding author/s.

AUTHOR CONTRIBUTIONS

SB-F and JN have contributed equally and significantly to the contents of this paper. All authors contributed to the article and approved the submitted version.

FUNDING

This research has been partially supported by the AEI of Spain under Grant MTM2016-75140-P, co-financed by European Community fund FEDER and XUNTA de Galicia under grant ED431C 2019/02.

SB-F also acknowledges current funding from Ministerio de Educación, Cultura y Deporte of Spain (FPU16/04416) and previous funding from Xunta de Galicia (ED481A-2017/030).

REFERENCES

1. Bellman R. *Introduction to the Mathematical Theory of Control Processes. Vol. II: Nonlinear Processes*. New York, NY; London: Academic Press (1971).
2. Isidori A. *Nonlinear Control Systems: An Introduction*. 2nd ed. Berlin; Heidelberg: Springer-Verlag (1989).
3. Ivancevic VG, Reid DJ. *Complexity and Control. Towards a Rigorous Behavioral Theory of Complex Dynamical Systems*. Hackensack, NJ: World Scientific Publishing Co. Pte. Ltd. (2015).
4. Hilfer R. *Applications of Fractional Calculus in Physics*. Singapore: World Scientific (2000).
5. Kilbas AA, Srivastava HM, Trujillo JJ. *Theory and Applications of Fractional Differential Equations*. Amsterdam: Elsevier Science (2006).
6. Samko SG, Kilbas AA, Marichev OI. *Fractional Integrals and Derivatives. Theory and Applications*. Amsterdam: Gordon and Breach (1993).
7. Tarasov VE. *Fractional Dynamics: Application of Fractional Calculus to Dynamics of Particles, Fields and Media*. Berlin; Heidelberg: Springer-Verlag Berlin Heidelberg; Higher Education Press (2010).
8. Agarwal RP, Baleanu D, Nieto JJ, Torres DFM, Zhou Y. A survey on fuzzy fractional differential and optimal control nonlocal evolution equations. *J Comput Appl Math.* (2018) **339**:3–29. doi: 10.1016/j.cam.2017.09.039
9. Alshabanat A, Jleli M, Kumar S, Samet B. Generalization of Caputo-Fabrizio fractional derivative and applications to electrical circuits. *Front Phys.* (2020) **8**:64. doi: 10.3389/fphy.2020.00064
10. Hilfer R, editor. *Applications of Fractional Calculus in Physics*. Singapore: World Scientific (2000).
11. Herrmann R. *Fractional Calculus: An Introduction For Physicists*. 2nd ed. Singapore: World Scientific (2014).
12. Yıldız TA. Optimal control problem of a non-integer order waterborne pathogen model in case of environmental stressors. *Front Phys.* (2019) **7**:95. doi: 10.3389/fphy.2019.00095
13. Nisar KS. Generalized Mittag-Leffler type function: fractional integrations and application to fractional kinetic equations. *Front Phys.* (2020) **8**:33. doi: 10.3389/fphy.2020.00033
14. Zhang JE. Multisynchronization for coupled multistable fractional-order neural networks via impulsive control. *Complexity.* (2017) **2017**:9323172. doi: 10.1155/2017/9323172
15. Rajagopal K, Guessas L, Karthikeyan A, Srinivasan A, Adam G. Fractional order memristor no equilibrium chaotic system with its adaptive sliding mode synchronization and genetically optimized fractional order PID synchronization. *Complexity.* (2017) **2017**:1892618. doi: 10.1155/2017/1892618
16. Sheng D, Wei Y, Cheng S, Shuai J. Adaptive backstepping control for fractional order systems with input saturation. *J Franklin Inst.* (2017) **354**:2245–68. doi: 10.1016/j.jfranklin.2016.12.030
17. Sene N, Srivastava G. Generalized Mittag-Leffler input stability of the fractional differential equations. *Symmetry.* (2019) **11**:608. doi: 10.3390/sym11050608
18. Sene N. Fractional input stability and its application to neural network. *Discrete Contin Dyn-S.* (2020) **13**:853–65. doi: 10.3934/dcdss.2020049
19. Matignon D, d'Andréa-Novel B. Some results on controllability and observability of finite-dimensional fractional differential systems. *Comput Eng Syst Appl.* (1996) **2**:952–6.
20. Klamka J. Relationship between controllability of standard and fractional linear systems. In: Mitkowski W, Kacprzyk J, Oprzedkiewicz K, Skruch P, editors. *Trends in Advanced Intelligent Control, Optimization and Automation. KKA 2017. Advances in Intelligent Systems and Computing*. Kraków: Springer International Publishing (2017). p. 455–9. doi: 10.1007/978-3-319-60699-6_44
21. Kalman RE, Falb PL, Arbib MA. *Topics in Mathematical System Theory*. New York, NY: McGraw-Hill (1969).
22. Franklin GF. *Feedback Control of Dynamical Systems*. 4th ed. Upper Saddle River, NJ: Prentice Hall (2002).
23. Diethelm K. *The Analysis of Fractional Differential Equations*. Berlin; Heidelberg: Springer-Verlag Berlin Heidelberg (2004).
24. Kaminski JY, Shorten R, Zeheb E. Exact stability test and stabilization for fractional systems. *Syst Control Lett.* (2015) **85**:95–9. doi: 10.1016/j.sysconle.2015.08.005
25. Gorenflo R, Kilbas AA, Mainardi F, Rogosin SV. *Mittag-Leffler Functions, Related Topics and Applications*. Berlin; Heidelberg: Springer-Verlag Berlin Heidelberg (2014).
26. Spong MW. Impact controllability of an air hockey puck. *Syst Control Lett.* (2001) **42**:333–45. doi: 10.1016/S0167-6911(00)00105-5
27. Nieto JJ, Tisdell CC. On exact controllability of first-order impulsive differential equations. *Adv Differ Equat.* (2010) **2010**:136504. doi: 10.1155/2010/136504
28. Tang Y, Xing X, Karimi HR, Kocarev L, Kurths J. Tracking control of networked multi-agent systems under new characterizations of impulses and its applications in robotic systems. *IEEE Trans Ind Electron.* (2016) **63**:1299–307. doi: 10.1109/TIE.2015.2453412
29. Zeng B, Liu Z. Existence results for impulsive feedback control systems. *Nonlin Anal Hybrid Syst.* (2019) **33**:1–16. doi: 10.1016/j.nahs.2019.01.008

Conflict of Interest: The authors declare that the research was conducted in the absence of any commercial or financial relationships that could be construed as a potential conflict of interest.

Copyright © 2020 Buedo-Fernández and Nieto. This is an open-access article distributed under the terms of the Creative Commons Attribution License (CC BY). The use, distribution or reproduction in other forums is permitted, provided the original author(s) and the copyright owner(s) are credited and that the original publication in this journal is cited, in accordance with accepted academic practice. No use, distribution or reproduction is permitted which does not comply with these terms.

frontiers in Physics

ORIGINAL RESEARCH
published: 23 October 2020
doi: 10.3389/fphy.2020.00309

On the *(k,s)*-Hilfer-Prabhakar Fractional Derivative With Applications to Mathematical Physics

Muhammad Samraiz[1], *Zahida Perveen*[1], *Gauhar Rahman*[2], *Kottakkaran Sooppy Nisar*[3] *and Devendra Kumar*[4]*

[1] Department of Mathematics, University of Sargodha, Sargodha, Pakistan, [2] Department of Mathematics, Shaheed Benazir Bhutto University, Upper Dir, Pakistan, [3] Department of Mathematics, College of Arts and Sciences, Prince Sattam Bin Abdulaziz University, Wadi Aldawaser, Saudi Arabia, [4] Department of Mathematics, University of Rajasthan, Jaipur, India

In this paper we introduce the (k, s)-Hilfer-Prabhakar fractional derivative and discuss its properties. We find the generalized Laplace transform of this newly proposed operator. As an application, we develop the generalized fractional model of the free-electron laser equation, the generalized time-fractional heat equation, and the generalized fractional kinetic equation using the (k, s)-Hilfer-Prabhakar derivative.

Keywords: modified (k, s) fractional integral operator, (k, s)-Prabhakar fractional derivative, (k, s)-Hilfer-Prabhakar fractional derivative, fractional heat equation, fractional kinetic equation

OPEN ACCESS

Edited by:
Jordan Yankov Hristov, University of Chemical Technology and Metallurgy, Bulgaria

Reviewed by:
Mehmet Yavuz, Necmettin Erbakan University, Turkey
Necati Özdemir, Balıkesir University, Turkey

***Correspondence:**
Devendra Kumar
devendra.maths@gmail.com

Specialty section:
This article was submitted to Mathematical and Statistical Physics, a section of the journal Frontiers in Physics

Received: *03 May 2020*
Accepted: *06 July 2020*
Published: *23 October 2020*

Citation:
Samraiz M, Perveen Z, Rahman G, Nisar KS and Kumar D (2020) On the (k,s)-Hilfer-Prabhakar Fractional Derivative With Applications to Mathematical Physics. Front. Phys. 8:309. doi: 10.3389/fphy.2020.00309

1. INTRODUCTION

Fractional calculus is the area of mathematical analysis that deals with the study and application of integrals and derivatives of arbitrary order. In recent decades, fractional calculus has become of increasing significance due to its applications in many fields of science and engineering [1–5]. The first application of fractional calculus was given by Abel [6] and includes the solution to the tautocrone problem. Fractional calculus also has applications in biophysics, wave theory, polymers, quantum mechanics, continuum mechanics, field theory, Lie theory, group theory, spectroscopy, and other scientific areas [7–9]. Although this calculus has a long history, over the past few decades it has attracted greater attention because of the fascinating results obtained when it is used to model certain real-world problems [10–13]. What makes fractional calculus special is that there are numerous types of fractional operators, so any scientist modeling real-world phenomena can choose the operator that fits their purposes the best. Each classical fractional derivative is usually defined in terms of a specific integral. Among the most well-known concepts of fractional derivatives are the Riemann-Liouville, Caputo, Grünwald-Letnikov, and Hadamard derivatives [10, 14, 15], whose formulations involve single-kernel integrals and which are used to investigate, for example, memory effect problems [16].

The Riemann-Liouville fractional derivative is remarkable, but it has some drawbacks when used to model physical phenomena because of its improper physical conditions. Caputo's great contribution was to develop a concept of fractional derivative appropriate for physical conditions [17]. A number of other families of fractional operators have been established, such as the Liouville, Erdlyi-Kober, Hadamard, Grünwald-Letnikov, Hilfer, Hilfer-Prabhakar, and k-Hilfer-Prabhakar operators, to mention just a few [10, 18–20]. Because there are so many concepts of fractional operator, it has become necessary to define generic fractional operators, of which the classical ones are particular cases. One class of extensions of Riemann-Liouville fractional operators comprises the so-called k-Prabhakar integral operators, which can be found in [21]. Inspired by the definitions

of k-Prabhakar integral operators and k-Hilfer-Prabhakar derivatives [20], the authors introduced the (k,s)-Hilfer fractional derivative, which unifies a large class of fractional operators [19, 20]; [Samraiz et al., accepted].

In recent years, the generalization of integral and differential operators has become an important subject of research in fractional calculus [9, 20, 22–28]. Different special functions, including the Gauss hypergeometric function, Mittag-Leffler-style functions, the Wright function, Meijer's G function, and Fox's H function, appear in the kernels of several generalizations of the integral operators. R. Hilfer introduced the Hilfer fractional derivative in [9], which is a generalization of the Riemann-Liouville and Caputo fractional derivatives.The Prabhakar integral and derivative operators are obtained from the Riemann-Liouville integral operator by extending its kernel to involve the three-parameter Mittag-Leffler function [19].

This paper is motivated by the rich applications of fractional differential equations (FDEs) in physics, economics, engineering, and many other branches of science [8, 10, 13, 17]. Since no general method exists that can be used to analytically solve every FDE, one of the most pressing and challenging tasks is to develop suitable methods for finding analytical solutions to certain classes of FDEs [29–31]. Researchers have become interested in fractional interpretations of the classical integral transforms, i.e., Laplace and Fourier transforms [32–34], in the past few years. It can be shown that integral transformations such as the Laplace, Fourier, generalized Laplace, and ρ-Laplace transforms are useful methods for obtaining analytical solutions to some classes of FDEs. In this framework, we use a generalized Laplace transform to obtain analytical solutions to certain classes of FDEs that contain (k,s)-Hilfer-Prabhakar fractional derivatives. Given the wide range of fractional operators available in the literature, it can be difficult to choose the most suitable approach for a given problem. It is therefore essential to consider generalizations of classical fractional operators to aid in choosing an appropriate operator.

Diaz et al. [35] defined k-gamma and k-beta functions as follows.

Definition 1.1. *The k-gamma function is a generalization of the classical* Γ *function given by*

$$\Gamma_k(\theta) = \lim_{n\to\infty} \frac{n!k^n(nk)^{\frac{\theta}{k}-1}}{(\theta)_{n,k}}, \quad k>0,\ \mathrm{Re}(\theta)>0,$$

where $(\theta)_{n,k} = \theta(\theta+k)(\theta+2k)\cdots(\theta+(n-1)k)$ *for* $n\geq 1$ *is called the Pochhammer k symbol. The integral representation is*

$$\Gamma_k(\theta) = \int_0^\infty x^{\theta-1}e^{\frac{-x^k}{k}}\,dx, \quad \mathrm{Re}(\theta)>0.$$

Clearly, $\Gamma(\theta) = \lim_{k\to 1}\Gamma_k(\theta)$ *and* $\Gamma_k(\theta) = k^{\frac{\theta}{k}-1}\Gamma(\frac{\theta}{k})$.

Definition 1.2. *For* $\mathrm{Re}(\theta)>0$, $k>0$, *and* $\mathrm{Re}(\zeta)>0$, *the k-beta function is given by*

$$B_k(\theta,\zeta) = \frac{1}{k}\int_0^1 \tau^{\frac{\theta}{k}-1}(1-\tau)^{\frac{\zeta}{k}-1}\,d\tau.$$

The functions Γ_k *and* B_k *are related by an identity*

$$B_k(\theta,\zeta) = \frac{\Gamma_k(\theta)\Gamma_k(\zeta)}{\Gamma_k(\theta+\zeta)}.$$

The k-Mittag-Leffler function given in [36] is defined as follows.

Definition 1.3. *Let* $n\in N$, $k\in\mathbb{R}^+$, $\mu,\rho,\gamma\in\mathbb{C}$, $\mathrm{Re}(\rho)>0$, *and* $\mathrm{Re}(\mu)>0$. *Then the k-Mittag-Leffler function is defined by*

$$E^{\gamma}_{k,\rho,\mu}(\theta) = \sum_{n=0}^{\infty}\frac{(\gamma)_{n,k}\theta^n}{\Gamma_k(\rho n+\mu)n!}.$$

The modified (k,s)-fractional integral operator involving the k-Mittag-Leffler function given in [Samraiz et al., accepted] is defined as follows.

Definition 1.4. *Let* $s\in\mathbb{R}\backslash\{-1\}$, $k\in\mathbb{R}^+$, $\mu,\rho,\omega,\gamma\in\mathbb{C}$, $\mathrm{Re}(\rho)>0$, $\mathrm{Re}(\gamma)>0$, $\mathrm{Re}(\mu)>0$, *and* $\Phi\in L^1[0,\beta]$. *Then the modified* (k,s)*-fractional integral operator involving the k-Mittag-Leffler function is given by*

$$({}^{s}_{k}\mathfrak{J}^{\omega,\gamma}_{0^+;\rho,\mu}\Phi)(\theta) = \frac{(s+1)^{1-\frac{\mu}{k}}}{k}\int_0^\theta (\theta^{s+1}-\zeta^{s+1})^{\frac{\mu}{k}-1}\zeta^s E^{\gamma}_{k,\rho,\mu}(\omega(\theta^{s+1}-\zeta^{s+1})^{\frac{\rho}{k}})\Phi(\zeta)\,d\zeta. \tag{1.1}$$

Definition 1.5 ([Samraiz et al., accepted])**.** *Let* $s\in\mathbb{R}\backslash\{-1\}$, $k\in\mathbb{R}^+$, $\mu,\rho,\omega,\gamma\in\mathbb{C}$, $\mathrm{Re}(\rho)>0$, $\mathrm{Re}(\mu)>0$, $n=\lceil\frac{\mu}{k}\rceil+1$, *and* $\Phi\in L^1[0,\beta]$. *Then the* (k,s)*-Prabhakar fractional derivative operator with the k-Mittag-Leffler function as its kernel is given by*

$$({}^{s}_{k}\mathfrak{D}^{\omega,\gamma}_{0^+;\rho,\mu}\Phi)(\theta) = \left(\frac{1}{\theta^s}\frac{d}{d\theta}\right)^n k^n({}^{s}_{k}\mathfrak{J}^{\omega,-\gamma}_{0^+;\rho,nk-\mu}\Phi)(\theta). \tag{1.2}$$

Definition 1.6 ([Samraiz et al., accepted])**.** *Let* $s\in\mathbb{R}\backslash\{-1\}$, $k\in\mathbb{R}^+$, $\mu,\rho,\omega,\gamma\in\mathbb{C}$, $\mathrm{Re}(\rho)>0$, $\mathrm{Re}(\mu)>0$, $n=\lceil\frac{\mu}{k}\rceil+1$, *and* $\Phi\in C^n[0,\beta]$ *with* $0<\theta<\beta<\infty$. *Then the regularized version of the* (k,s)*-Prabhakar derivative is*

$${}^{C}_{s,k}\mathfrak{D}^{\omega,\gamma}_{0^+;\rho,\mu}\Phi(\theta) = k^{ns}{}_{k}\mathfrak{J}^{\omega,-\gamma}_{0^+;\rho,nk-\mu}\left(\frac{1}{\theta^s}\frac{d}{d\theta}\right)^n\Phi(\theta). \tag{1.3}$$

Definition 1.7. *Let* $g\in C^n[\alpha,\beta]$ *such that* $g'(\zeta)>0$ *on* $[\alpha,\beta]$. *Then*

$$\mathrm{AC}^n_g[\alpha,\beta] = \left\{\Phi:[\alpha,\beta]\to\mathbb{C}\ \textit{with}\ \Phi^{[n-1]}\in\mathrm{AC}[\alpha,\beta]\right\},$$

where $\Phi^{[n-1]} = \left(\frac{1}{g'(\zeta)}\frac{d}{d\zeta}\right)^{n-1}\Phi$.

The generalized Laplace transform introduced by Jarad et al. [34] is presented in the following definition.

Definition 1.8. *Let Φ and g be real-valued functions on $[\alpha,\infty)$ such that $g(\zeta)$ is continuous and $g'(\zeta) > 0$ on $[\alpha,\infty)$. The generalized Laplace transform of Φ is*

$$L_g\{\Phi(\theta)\}(u) = \int_\alpha^\infty e^{-u(g(\theta)-g(\alpha))}\Phi(\theta)g'(\theta)\,d\theta$$

for all values of u.

Definition 1.9 ([34]). *Let Φ and Ψ be two piecewise-continuous functions on each interval $[0,T]$ that are of exponential order. The generalized convolution of Φ and Ψ is given by*

$$(\Phi *_g \Psi)(\theta) = \int_\alpha^\theta \Phi(\zeta)\Psi\big(g^{-1}(g(\theta)+g(\alpha)-g(\zeta))\big)g'(\zeta)\,d\zeta.$$

Theorem 1.10 ([34]). *Let $\Phi \in C_g^{n-1}[\alpha,T]$ be such that $\Phi^{[1]}$ is of g-exponential order. Let $\Phi^{[1]}$ be a piecewise-continuous function on the interval $[\alpha,T]$. Then the generalized Laplace transform of $\Phi^{[1]}(\zeta)$ exists and*

$$L_g\{\Phi^{[1]}(\theta)\}(u) = sL_g\{\Phi(\theta)\}(u) - \Phi(\alpha).$$

Proposition 1.11. *Let $s \in \mathbb{R}\backslash\{-1\}$, $k \in \mathbb{R}^+$, $\mu,\rho,\omega,\gamma \in \mathbb{C}$, $\mathrm{Re}(\rho) > 0$, $\mathrm{Re}(\mu) > 0$, and $\beta > 0$. Then the integral operator ${}_k^s\mathfrak{J}_{0^+;\rho,\mu}^{\omega,\gamma}$ is bounded on $C[0,\beta]$, i.e.,*

$$|({}_k^s\mathfrak{J}_{0^+;\rho,\mu}^{\omega,\gamma}\Phi)(\theta)| \le G\|\Phi\|_{C[0,\beta]},$$

where

$$\|\Phi\|_{C[0,\beta]} = \max\{|\Phi| : 0 < x < \beta\}$$

and

$$G = \frac{(s+1)^{-\frac{\mu}{k}}(\beta^{s+1})^{\mathrm{Re}(\frac{\mu}{k})}}{k} \sum_{n=0}^{\infty}\frac{|(\gamma)_{n,k}\omega^n|}{|\Gamma_k(\rho n+\mu)|n!}\frac{(\beta^{s+1})^{\mathrm{Re}(\frac{\rho}{k})n}}{\big[n\mathrm{Re}(\frac{\rho}{k})+\mathrm{Re}(\frac{\mu}{k})\big]}. \tag{1.4}$$

Theorem 1.12. *Let $s \in \mathbb{R}\backslash\{-1\}$, $k \in \mathbb{R}^+$, $\mu,\rho,\omega,\gamma \in \mathbb{C}$, $\mathrm{Re}(\rho) > 0$, $\mathrm{Re}(\gamma) > 0$, and $\mathrm{Re}(\mu) > 0$. Let $\Phi \in L^1[0,\beta]$ be a piecewise-continuous function on each interval $[0,\theta]$ that is of $g(\theta)$-exponential order. Then*

$$L_g\{({}_k^s\mathfrak{J}_{0^+;\rho,\mu}^{\omega,\gamma}\Phi)(\theta)\}(u) = \big((s+1)(ku)\big)^{-\frac{\mu}{k}}\big(1-k\omega(ku)^{-\frac{\rho}{k}}\big)^{-\frac{\gamma}{k}}L_g\{\Phi(\theta)\}(u).$$

Theorem 1.13 ([Samraiz et al., accepted]). *Let $k \in \mathbb{R}^+$, $s \in [0,\infty)$, $\mu,\rho,\omega,\gamma \in \mathbb{C}$, $\mathrm{Re}(\rho) > 0$, $\mathrm{Re}(\gamma) > 0$, $\mathrm{Re}(\mu) > 0$, and $g(\theta) = \theta^{s+1}$. Let $\Phi \in \mathrm{AC}_g^n[0,\beta]$ and ${}_k^s\mathfrak{J}_{0^+;\rho,nk-m-\mu}^{\omega,\gamma}\Phi$ for $m = 0,1,2,\ldots,n-1$ be of $g(\theta)$-exponential order. Then*

$$L_g\{({}_k^s\mathfrak{D}_{0^+;\rho,\mu}^{\omega,\gamma}\Phi)(\theta)\}(u) = (s+1)^{-\frac{nk-\mu}{k}}(ku)^{\frac{\mu}{k}}\big(1-k\omega(ku)^{-\frac{\rho}{k}}\big)^{\frac{\gamma}{k}}L_g\{\Phi(t)\}(u) - \sum_{m=0}^{n-1}k^{n-m}u^{n-m-1}\Big({}_k^s\mathfrak{D}_{0^+;\rho,\mu-(n-m)k}^{\omega,-\gamma}\Phi\Big)(0^+),$$

with $|k\omega(ku)^{-\frac{\rho}{k}}| < 1$.

Theorem 1.14 ([Samraiz et al., accepted]). *The generalized Laplace transform of the regularized version of the (k,s)-Prabhakar fractional derivative is*

$$L_g\{{}_{s,k}^C\mathfrak{D}_{0^+;\rho,\mu}^{\omega,\gamma}\Phi(\theta)\}(u) = (s+1)^{-\frac{nk-\mu}{k}}\Big[(ku)^{\frac{\mu}{k}}\big(1-k\omega(ku)^{-\frac{\rho}{k}}\big)^{\frac{\gamma}{k}}L_g\{\Phi(\theta)\}(u) - \sum_{m=0}^{n-1}k^{m+1}(ku)^{\frac{\mu-(m+1)k}{k}}\big(1-k\omega(ku)^{-\frac{\rho}{k}}\big)^{\frac{\gamma}{k}}\big(\Phi^{[m]}\big)(0^+)\Big],$$

with $|k\omega(ku)^{-\frac{\rho}{k}}| < 1$.

2. THE (k,s)-HILFER-PRABHAKAR FRACTIONAL DERIVATIVE AND GENERALIZED LAPLACE TRANSFORMS

In this section we introduce a new family of operators called the (k,s)-Hilfer-Prabhakar fractional derivative. The generalized Laplace transforms of these operators are also studied in this section.

Definition 2.1. *Let $\Phi \in C^1[0,\beta]$, $0 < \theta < \beta < \infty$, $s \in \mathbb{R}\backslash\{-1\}$, $k,\rho > 0$, $\omega,\gamma \in \mathbb{R}$, $\mu \in (0,1)$, $\nu \in [0,1]$, and $\big(\Phi * {}_k^s\mathfrak{J}_{0^+;\rho,(1-\nu)(k-\mu)}^{\omega,-\gamma(1-\nu)}\big)(\theta) \in \mathrm{AC}^1[0,\beta]$. The (k,s)-Hilfer-Prabhakar derivative is defined as*

$${}_k^s\mathfrak{D}_{0^+;\rho,\omega}^{\gamma,\mu,\nu}\Phi(\theta) = k\Big({}_k^s\mathfrak{J}_{0^+;\rho,\nu(k-\mu)}^{\omega,-\gamma\nu}\Big(\frac{1}{\theta^s}\frac{d}{d\theta}\Big){}_k^s\mathfrak{J}_{0^+;\rho,(1-\nu)(k-\mu)}^{\omega,-\gamma(1-\nu)}\Phi\Big)(\theta).$$

Note that if we choose $\nu = 0$ in the above definition, we get (1.2) corresponding to $m = 1$; and if we take $\nu = 1$, we obtain (1.3) corresponding to $m = 1$.

Theorem 2.2. *For $s \in \mathbb{R}\backslash\{-1\}$, $k,\rho > 0$, $\omega,\gamma \in \mathbb{R}$, $\mu \in (0,1)$, $\nu \in [0,1]$, and $\Phi \in L^1[0,\beta]$, the operator ${}_k^s\mathfrak{D}_{0^+;\rho,\omega}^{\gamma,\mu,\nu}$ is bounded on $C[0,\beta]$, i.e.,*

$$\|{}_k^s\mathfrak{D}_{0^+;\rho,\omega}^{\gamma,\mu,\nu}\Phi(\theta)\| \le C_1C_2\|\Phi\|_{[0,\beta]},$$

where

$$C_1 = \frac{(s+1)^{-\frac{\nu(k-\mu)}{k}}(\beta^{s+1})^{\mathrm{Re}(\frac{\nu(k-\mu)}{k})}}{k} \sum_{n=0}^{\infty}\frac{|(-\gamma\nu)_{n,k}\omega^n|}{|\Gamma_k(\rho n+\nu(k-\mu))|n!}\frac{(\beta^{s+1})^{\mathrm{Re}(\frac{\rho}{k})n}}{\big[n\mathrm{Re}(\frac{\rho}{k})+\mathrm{Re}(\frac{\nu(k-\mu)}{k})\big]} \tag{2.1}$$

and

$$C_2 = \frac{(s+1)^{-\frac{(1-\nu)(k-\mu)-k}{k}}(\beta^{s+1})^{\mathrm{Re}(\frac{(1-\nu)(k-\mu)-k}{k})}}{k} \sum_{m=0}^{\infty}\frac{|(\gamma(\nu-1))_{m,k}\omega^m|}{|\Gamma_k(\rho m+(1-\nu)(k-\mu))|m!} \times\frac{(\beta^{s+1})^{\mathrm{Re}(\frac{\rho}{k})m}}{\big[m\mathrm{Re}(\frac{\rho}{k})+\mathrm{Re}(\frac{(1-\nu)(k-\mu)}{k})\big]}. \tag{2.2}$$

Proof Using the estimates in Proposition 1.11, we get

$$\begin{aligned}
&\|{}_k^s\mathfrak{D}_{0^+;\rho,\omega}^{\gamma,\mu,\nu}\Phi(\theta)\| \\
&= \left\|k\left({}_k^s\mathfrak{J}_{0^+;\rho,\nu(k-\mu)}^{\omega,-\gamma\nu}\left(\frac{1}{\theta^s}\frac{d}{d\theta}\right)\left({}_k^s\mathfrak{J}_{0^+;\rho,(1-\nu)(k-\mu)}^{\omega,-\gamma(1-\nu)}\Phi\right)(\theta)\right)\right\| \\
&\leq C_1\left\|\left(\frac{1}{\theta^s}\frac{d}{d\theta}\right)\left({}_k^s\mathfrak{J}_{0^+;\rho,(1-\nu)(k-\mu)}^{\omega,-\gamma(1-\nu)}\Phi\right)(\theta)\right\| \\
&= C_1\left\|\left({}_k^s\mathfrak{J}_{0^+;\rho,(1-\nu)(k-\mu)-k}^{\omega,-\gamma(1-\nu)}\Phi\right)(\theta)\right\| \\
&\leq C_1C_2\|\Phi\|_{[0,\beta]},
\end{aligned}$$

where C_1 and C_2 are the constants defined by (2.1) and (2.2).

Proposition 2.3. *Let $s \in \mathbb{R}\backslash\{-1\}$, $k, \rho, \lambda > 0$, $\omega, \gamma, \sigma \in \mathbb{R}$, $\mu \in (0,1)$, $\nu \in [0,1]$, $\lambda > \mu + \nu k - \mu\nu$, and $\Phi \in L^1[0,\beta]$. Then*

$$\left({}_k^s\mathfrak{D}_{0^+;\rho,\omega}^{\gamma,\mu,\nu}\left({}_k^s\mathfrak{J}_{0^+;\rho,\lambda}^{\omega,\sigma}\Phi\right)\right)(\theta) = \left({}_k^s\mathfrak{J}_{0^+;\rho,\lambda-\mu}^{\omega,\sigma-\gamma}\Phi\right)(\theta).$$

In particular,

$$\left({}_k^s\mathfrak{D}_{0^+;\rho,\omega}^{\gamma,\mu,\nu}\left({}_k^s\mathfrak{J}_{0^+;\rho,\mu}^{\omega,\gamma}\Phi\right)\right)(\theta) = \Phi(\theta).$$

Proof. By using Definition 2.1 and the semigroup property of the modified (k,s)-fractional integral operator with the k-Mittag-Leffler function, we obtain

$$\begin{aligned}
&\left({}_k^s\mathfrak{D}_{0^+;\rho,\omega}^{\gamma,\mu,\nu}\left({}_k^s\mathfrak{J}_{0^+;\rho,\lambda}^{\omega,\sigma}\Phi\right)\right)(\theta) \\
&= k\left({}_k^s\mathfrak{J}_{0^+;\rho,\nu(k-\mu)}^{\omega,-\gamma\nu}\left(\frac{1}{\theta^s}\frac{d}{d\theta}\right){}_k^s\mathfrak{J}_{0^+;\rho,(1-\nu)(k-\mu)}^{\omega,-\gamma(1-\nu)}\left({}_k^s\mathfrak{J}_{0^+;\rho,\lambda}^{\omega,\sigma}\Phi\right)\right)(\theta) \\
&= k\left({}_k^s\mathfrak{J}_{0^+;\rho,\nu(k-\mu)}^{\omega,-\gamma\nu}\left(\frac{1}{\theta^s}\frac{d}{d\theta}\right)\left({}_k^s\mathfrak{J}_{0^+;\rho,(1-\nu)(k-\mu)+\lambda}^{\omega,-\gamma(1-\nu)+\sigma}\Phi\right)\right)(\theta) \\
&= \left({}_k^s\mathfrak{J}_{0^+;\rho,\nu(k-\mu)}^{\omega,-\gamma\nu}\left({}_k^s\mathfrak{J}_{0^+;\rho,(1-\nu)(k-\mu)+\lambda-k}^{\omega,-\gamma(1-\nu)+\sigma}\Phi\right)\right)(\theta) \\
&= \left({}_k^s\mathfrak{J}_{0^+;\rho,\lambda-\mu}^{\omega,\sigma-\gamma}\Phi\right)(\theta).
\end{aligned}$$

This completes the proof.

Theorem 2.4. *Let $s \in \mathbb{R}\backslash\{-1\}$, $k, \rho, \lambda > 0$, $\omega, \gamma \in \mathbb{R}$, $\mu \in (0,1)$, $\nu \in [0,1]$, $\lambda > \mu + \nu k - \mu\nu$, and $\Phi \in L^1[0,\beta]$. Then*

$$\left({}_k^sJ_{0^+}^{\lambda}\left({}_k^s\mathfrak{D}_{0^+;\rho,\omega}^{\gamma,\mu,\nu}\Phi\right)\right)(\theta) = \left({}_k^s\mathfrak{J}_{0^+;\rho,\lambda-\mu}^{\omega,-\gamma}\Phi\right)(\theta).$$

Proof. By using Definition 2.1 and Theorem 2 in [Samraiz et al., accepted], we get

$$\begin{aligned}
&\left({}_k^sJ_{0^+}^{\lambda}\left({}_k^s\mathfrak{D}_{0^+;\rho,\omega}^{\gamma,\mu,\nu}\Phi\right)\right)(\theta) \\
&= k\left({}_k^sJ_{0^+}^{\lambda}{}_k^s\mathfrak{J}_{0^+;\rho,\nu(k-\mu)}^{\omega,-\gamma\nu}\left(\frac{1}{\theta^s}\frac{d}{d\theta}\right){}_k^s\mathfrak{J}_{0^+;\rho,(1-\nu)(k-\mu)}^{\omega,-\gamma(1-\nu)}\Phi\right)(\theta) \\
&= k\left({}_k^s\mathfrak{J}_{0^+;\rho,\nu(k-\mu)+\lambda}^{\omega,-\gamma\nu}\left(\frac{1}{\theta^s}\frac{d}{d\theta}\right){}_k^s\mathfrak{J}_{0^+;\rho,(1-\nu)(k-\mu)}^{\omega,-\gamma(1-\nu)}\Phi\right)(\theta) \\
&= \left({}_k^s\mathfrak{J}_{0^+;\rho,\nu(k-\mu)+\lambda}^{\omega,-\gamma\nu}\left({}_k^s\mathfrak{J}_{0^+;\rho,(1-\nu)(k-\mu)-k}^{\omega,-\gamma(1-\nu)}\Phi\right)\right)(\theta) \\
&= \left({}_k^s\mathfrak{J}_{0^+;\rho,\lambda-\mu}^{\omega,-\gamma}\Phi\right)(\theta),
\end{aligned}$$

and thus the result is proved.

Theorem 2.5. *The Laplace transform of the (k,s)-Hilfer-Prabhakar fractional derivative is*

$$\begin{aligned}
&L_g\{{}_k^s\mathfrak{D}_{0^+;\rho,\omega}^{\gamma,\mu,\nu}\Phi(\theta)\}(u) \\
&= (s+1)^{\frac{\mu-k}{k}}(ku)^{\frac{\mu}{k}}\left(1-k\omega(ku)^{-\frac{\rho}{k}}\right)^{\frac{\gamma}{k}} \\
&\quad\times L_g\{\Phi(\theta)\}(u) - k(s+1)^{-\frac{\nu(k-\mu)}{k}}(ku)^{\frac{-\nu(k-\mu)}{k}} \\
&\quad\times\left(1-k\omega(ku)^{-\frac{\rho}{k}}\right)^{\frac{\gamma\nu}{k}}{}_k^s\mathfrak{J}_{0^+;\rho,(1-\nu)(k-\mu)}^{\omega,-\gamma(1-\nu)}\Phi(0^+).
\end{aligned}$$

Proof. By using Definition 2.1, Theorem 1.12, and Theorem 1.10, we obtain

$$\begin{aligned}
&L_g\{{}_k^s\mathfrak{D}_{0^+;\rho,\omega}^{\gamma,\mu,\nu}\Phi(\theta)\}(u) \\
&= k(s+1)^{-\frac{\nu(k-\mu)}{k}}(ku)^{\frac{-\nu(k-\mu)}{k}}\left(1-k\omega(ku)^{-\frac{\rho}{k}}\right)^{\frac{\gamma\nu}{k}} \\
&\quad L_g\left\{{}_k^s\mathfrak{J}_{0^+;\rho,(1-\nu)(k-\mu)}^{\omega,-\gamma(1-\nu)\ [1]}\Phi(\theta)\right\}(u) \\
&= k(s+1)^{-\frac{\nu(k-\mu)}{k}}(ku)^{\frac{-\nu(k-\mu)}{k}}\left(1-k\omega(ku)^{-\frac{\rho}{k}}\right)^{\frac{\gamma\nu}{k}} \\
&\quad\times\left[uL_g\left\{{}_k^s\mathfrak{J}_{0^+;\rho,(1-\nu)(k-\mu)}^{\omega,-\gamma(1-\nu)}\Phi(\theta)\right\}(u) - {}_k^s\mathfrak{J}_{0^+;\rho,(1-\nu)(k-\mu)}^{\omega,-\gamma(1-\nu)}\Phi(0^+)\right] \\
&= (ku)(s+1)^{-\frac{\nu(k-\mu)}{k}}(ku)^{\frac{-\nu(k-\mu)}{k}}\left(1-k\omega(ku)^{-\frac{\rho}{k}}\right)^{\frac{\gamma\nu}{k}} \\
&\quad L_g\{{}_k^s\mathfrak{J}_{0^+;\rho,(1-\nu)(k-\mu)}^{\omega,-\gamma(1-\nu)}\Phi(\theta)\}(u) \\
&\quad - k(s+1)^{-\frac{\nu(k-\mu)}{k}}(ku)^{\frac{-\nu(k-\mu)}{k}}\left(1-k\omega(ku)^{-\frac{\rho}{k}}\right)^{\frac{\gamma\nu}{k}}{}_k^s\mathfrak{J}_{0^+;\rho,(1-\nu)(k-\mu)}^{\omega,-\gamma(1-\nu)}\Phi(0^+) \\
&= (ku)(s+1)^{-\frac{\nu(k-\mu)}{k}}(ku)^{\frac{-\nu(k-\mu)}{k}}\left(1-k\omega(ku)^{-\frac{\rho}{k}}\right)^{\frac{\gamma\nu}{k}} \\
&\quad\times\left[(s+1)^{-\frac{(1-\nu)(k-\mu)}{k}}(ku)^{\frac{-(1-\nu)(k-\mu)}{k}}\left(1-k\omega(ku)^{-\frac{\rho}{k}}\right)^{\frac{\gamma(1-\nu)}{k}}\right. \\
&\quad\left. L_g\{\Phi(\theta)\}(u)\right] \\
&\quad - k(s+1)^{-\frac{\nu(k-\mu)}{k}}(ku)^{\frac{-\nu(k-\mu)}{k}}\left(1-k\omega(ku)^{-\frac{\rho}{k}}\right)^{\frac{\gamma\nu}{k}}{}_k^s\mathfrak{J}_{0^+;\rho,(1-\nu)(k-\mu)}^{\omega,-\gamma(1-\nu)}\Phi(0^+) \\
&= (s+1)^{\frac{\mu-k}{k}}(ku)^{\frac{\mu}{k}}\left(1-k\omega(ku)^{-\frac{\rho}{k}}\right)^{\frac{\gamma}{k}}L_g\{\Phi(\theta)\}(u) \\
&\quad - k(s+1)^{-\frac{\nu(k-\mu)}{k}} \\
&\quad\times(ku)^{\frac{-\nu(k-\mu)}{k}}\left(1-k\omega(ku)^{-\frac{\rho}{k}}\right)^{\frac{\gamma\nu}{k}}{}_k^s\mathfrak{J}_{0^+;\rho,(1-\nu)(k-\mu)}^{\omega,-\gamma(1-\nu)}\Phi(0^+),
\end{aligned}$$

which proves the result.

3. GENERALIZATION OF THE FREE-ELECTRON LASER EQUATION

The integrodifferential free-electron laser equation describes the unsaturated behavior of the free-electron laser. Several attempts have been made to solve the generalized fractional integrodifferential free-electron laser equation in recent years. In this section, we develop a generalized fractional model of the free-electron laser equation that involves the novel (k,s)-Hilfer-Prabhakar derivative.

Theorem 3.1. *The solution of the Cauchy problem*

$${}_k^s\mathfrak{D}_{0^+;\rho,\omega}^{\gamma,\mu,\nu}\Phi(\theta) = \lambda{}_k^s\mathfrak{J}_{0^+;\rho,\mu}^{\sigma,\omega}\Phi(\theta) + f(\theta), \tag{3.1}$$

$${}_k^s\mathfrak{J}_{0^+;\rho,(1-\nu)(k-\mu)}^{\omega,-\gamma(1-\nu)}\Phi(0^+) = C, \quad C \geq 0, \tag{3.2}$$

where $\theta \in (0,\infty)$, $f \in L^1[0,\infty)$, $\mu \in (0,1)$, $\nu \in [0,1]$, $\omega, \lambda \in \mathbb{R}$, $\rho > 0$, *and* $\gamma, \sigma \geq 0$, *is given by*

$$\Phi(\theta) = C\sum_{m=0}^{\infty} \lambda^m (s+1)^{-\frac{\nu(k-\mu)+\mu-k}{k}} (\theta^{s+1})^{\frac{\nu(k-\mu)+\mu(1+2m)}{k}-1} \times E^{(\gamma+\sigma)m-\gamma(\nu-1)}_{k,\rho,\nu(k-\mu)+\mu(1+2m)}\left(\omega(\theta^{s+1})^{\frac{\rho}{k}}\right) + \sum_{m=0}^{\infty} \lambda^m (s+1)^{2m} \left({}^{s}_{k}\mathfrak{J}^{\omega,(\gamma+\sigma)m+\gamma}_{k,\rho,\mu(1+2m)} f\right)(\theta).$$

Proof. By applying the generalized Laplace transform to both sides of (3.1) and using Theorems 2.5 and 1.12, we get

$$L_g\{{}^{s}_{k}\mathfrak{D}^{\gamma,\mu,\nu}_{0^+;\rho,\omega}\Phi(\theta)\}(u) = \lambda L_g\{{}^{s}_{k}\mathfrak{J}^{\sigma,\omega}_{0^+;\rho,\mu}\Phi(\theta)\}(u) + L_g\{f(\theta)\}(u),$$

which can also be written as

$$L_g\{\Phi(\theta)\}(u) = \frac{Ck(s+1)^{-\frac{\nu(k-\mu)}{k}}(ku)^{\frac{-\nu(k-\mu)}{k}}\left(1-k\omega(ku)^{\frac{\rho}{k}}\right)^{\frac{\gamma\nu}{k}}}{(s+1)^{\frac{\mu-k}{k}}(ku)^{\frac{\mu}{k}}\left(1-k\omega(ku)^{\frac{-\rho}{k}}\right)^{\frac{\gamma}{k}}} + \frac{L_g\{f(\theta)\}(u)}{(s+1)^{\frac{\mu-k}{k}}(ku)^{\frac{\mu}{k}}\left(1-k\omega(ku)^{\frac{-\rho}{k}}\right)^{\frac{\gamma}{k}}} \left(1-\lambda(ku)^{-\frac{2\mu}{k}}\left(1-k\omega(ku)^{\frac{-\rho}{k}}\right)^{-\frac{\gamma+\sigma}{k}}\right)^{-1}.$$

Using the binomial expansion gives

$$\begin{aligned} L_g\{\Phi(\theta)\}(u) &= \frac{Ck(s+1)^{-\frac{\nu(k-\mu)}{k}}(ku)^{\frac{-\nu(k-\mu)}{k}}\left(1-k\omega(ku)^{\frac{\rho}{k}}\right)^{\frac{\gamma\nu}{k}}}{(s+1)^{\frac{\mu-k}{k}}(ku)^{\frac{\mu}{k}}\left(1-k\omega(ku)^{\frac{-\rho}{k}}\right)^{\frac{\gamma}{k}}} \\ &+ \frac{L_g\{f(\theta)\}(u)}{(s+1)^{\frac{\mu-k}{k}}(ku)^{\frac{\mu}{k}}\left(1-k\omega(ku)^{\frac{-\rho}{k}}\right)^{\frac{\gamma}{k}}} \\ &\sum_{m=0}^{\infty}\lambda^m(ku)^{-2\frac{\mu m}{k}}\left(1-k\omega(ku)^{\frac{-\rho}{k}}\right)^{-\frac{(\gamma+\sigma)}{k}m} \\ &= Ck\sum_{m=0}^{\infty}\lambda^m(s+1)^{-\frac{\nu(k-\mu)+\mu-k}{k}}(ku)^{-\frac{\nu(k-\mu)+\mu(1+2m)}{k}} \\ &\left(1-k\omega(ku)^{\frac{-\rho}{k}}\right)^{-\frac{(\gamma+\sigma)m-\gamma(\nu-1)}{k}} \\ &+ \sum_{m=0}^{\infty}\lambda^m(s+1)^{-\frac{\mu-k}{k}}(ku)^{-\frac{\mu(1+2m)}{k}} \\ &\left(1-k\omega(ku)^{\frac{-\rho}{k}}\right)^{-\frac{\gamma+m(\gamma+\sigma)}{k}} L_g\{f(\theta)\}(u). \end{aligned}$$

Applying the inverse Laplace transform, we obtain

$$\Phi(\theta) = C\sum_{m=0}^{\infty}\lambda^m(s+1)^{-\frac{\nu(k-\mu)+\mu-k}{k}}(\theta^{s+1})^{\frac{\nu(k-\mu)+\mu(1+2m)}{k}-1} E^{(\gamma+\sigma)m-\gamma(\nu-1)}_{k,\rho,\nu(k-\mu)+\mu(1+2m)}(\omega(\theta^{s+1})^{\frac{\rho}{k}}) + \sum_{m=0}^{\infty}\lambda^m(s+1)^{2m}\left({}^{s}_{k}\mathfrak{J}^{\omega,(\gamma+\sigma)m+\gamma}_{k,\rho,\mu(1+2m)}f\right)(\theta),$$

hence the result.

Remark 3.2. *If* $s = 0$, $k = 1$, $\gamma = \nu = 0$, $\rho = \sigma = 1$, $\mu \to 1$, $f(\theta) = 0$, $\omega = ir$, *and* $\lambda = -i\Pi p$ *(with* $r, p \in \mathbb{R}$*), then above Cauchy problem reduces to the following free-electron laser equation:*

$$\frac{d}{d\theta}\Phi(\theta) = -ip\Pi\int_0^{\theta}(\theta-t)e^{ir(\theta-t)}\Phi(t)\,dt, \quad \Phi(0) = 1.$$

Corollary 3.3. *If we take* $s = 0$ *and* $k = 1$, *then we get the Cauchy problem given in [19]:*

$$\mathfrak{D}^{\gamma,\mu,\nu}_{0^+;\rho,\omega}\Phi(\theta) = \lambda\mathfrak{J}^{\sigma,\omega}_{0^+;\rho,\mu}\Phi(\theta) + f(\theta), \tag{3.3}$$

$$\mathfrak{J}^{\omega,-\gamma(1-\nu)}_{0^+;\rho,(1-\nu)(k-\mu)}\Phi(0^+) = C, \quad C \geq 0, \tag{3.4}$$

where $\theta \in (0,\infty)$, $f \in L^1[0,\infty)$, $\mu \in (0,1)$, $\nu \in [0,1]$, $\omega, \lambda \in \mathbb{R}$, $\rho > 0$, *and* $\gamma, \sigma \geq 0$, *and its solution is given by*

$$\Phi(\theta) = C\sum_{m=0}^{\infty}\lambda^m(\theta)^{\nu(1-\mu)+\mu(1+2m)-1}E^{(\gamma+\sigma)m-\gamma(\nu-1)}_{\rho,\nu(1-\mu)+\mu(1+2m)}(\omega(\theta)^{\rho}) + \sum_{m=0}^{\infty}\lambda^m\left(\mathfrak{J}^{\omega,(\gamma+\sigma)m+\gamma}_{0^+,\rho,\mu(1+2m)}f\right)(\theta).$$

4. THE TIME-FRACTIONAL HEAT EQUATION

Lately, numerous papers have been devoted to mathematical analysis of variations of the time-fractional heat equation and its applications in mathematical physics and probability theory [see, for example, [37, 38] and the references therein]. This section focuses on the generalized time-fractional heat equation involving the (k,s)-Hilfer-Prabhakar derivative.

Theorem 4.1. *The solution of the Cauchy problem*

$${}^{s}_{k}\mathfrak{D}^{\gamma,\mu,\nu}_{0^+;\rho,\omega}V(\theta,\zeta) = G\frac{\partial^2}{\partial\zeta^2}V(\theta,\zeta), \quad \zeta > 0,\ \theta \in \mathbb{R}, \tag{4.1}$$

$$\left[{}^{s}_{k}\mathfrak{J}^{-\gamma(1-\nu),\omega}_{0^+;\rho,(1-\nu)(k-\mu)}V(\theta,\zeta)\right]_{\zeta=0^+} = h(\theta), \tag{4.2}$$

$$\lim_{\theta\to\infty}V(\theta,\zeta) = 0, \tag{4.3}$$

where $s \in [0,\infty)$, $\mu \in (0,1)$, $\nu \in [0,1]$, $\omega \in \mathbb{R}$, $G, k, \rho > 0$, *and* $\gamma \geq 0$, *is given by*

$$V(\theta,\zeta) = \int_{-\infty}^{+\infty}dp\,e^{-ip\theta}\hat{h}(p) \frac{1}{2\Pi}\sum_{m=0}^{\infty}(-G)^m(s+1)^{-\frac{(1-\nu)(k-\mu)-(\mu-k)m}{k}}(\zeta^{s+1})^{\frac{\mu(m+1)-\nu(\mu-k)}{k}-1} \times E^{\gamma(m+1-\nu)}_{k,\rho,\mu(m+1)-\nu(k-\mu)}(\omega(\zeta^{s+1})^{\frac{\rho}{k}})p^{2m}\hat{h}(p).$$

Proof. Let $\hat{V}(p,t) = F(V)(p,\zeta)$ denote the Fourier transform with respect to the space variable θ. Taking the Fourier transform of (4.1) and using (4.3), we obtain

$$ {}_k^s\mathfrak{D}^{\gamma,\mu,\nu}_{0^+;\rho,\omega}\hat{V}(p,\zeta) = -Gp^2\hat{V}(p,\zeta). $$

Now, applying the generalized Laplace transform to both sides of above equation, we get

$$\begin{aligned}
&L_g\{{}_k^s\mathfrak{D}^{\gamma,\mu,\nu}_{0^+;\rho,\omega}\hat{V}(p,\zeta)\}\\
&= -Gp^2L_g\{\hat{V}(p,\zeta)\}(u)(s+1)^{\frac{\mu-k}{k}}(ku)^{\frac{\mu}{k}}\left(1-k\omega(ku)^{-\frac{\rho}{k}}\right)^{\frac{\gamma}{k}}\\
&L_g\{\hat{V}(p,\zeta)\}(u)\\
&\quad - k(s+1)^{-\frac{\nu(k-\mu)}{k}}(ku)^{\frac{-\nu(k-\mu)}{k}}\left(1-k\omega(ku)^{-\frac{\rho}{k}}\right)^{\frac{\gamma\nu}{k}}\\
&\left[{}_k^s\mathfrak{J}^{\omega,-\gamma(1-\nu)}_{0^+;\rho,(1-\nu)(k-\mu)}\hat{V}(p,\zeta)\right]_{\zeta=0^+}\\
&= -Gp^2L_g\{\hat{V}(p,\zeta)\}(u),
\end{aligned}$$

which can be written as

$$\begin{aligned}
&L_g\{\hat{V}(p,\zeta)\}(u)\\
&= \frac{k(s+1)^{-\frac{\nu(k-\mu)}{k}}(ku)^{\frac{-\nu(k-\mu)}{k}}\left(1-k\omega(ku)^{-\frac{\rho}{k}}\right)^{\frac{\gamma\nu}{k}}\hat{h}(p)}{(s+1)^{\frac{\mu-k}{k}}(ku)^{\frac{\mu}{k}}\left(1-k\omega(ku)^{-\frac{\rho}{k}}\right)^{\frac{\gamma}{k}}+Gp^2}L_g\{\hat{V}(p,\zeta)\}(u)\\
&= k(s+1)^{\frac{\nu(\mu-k)-(\mu-k)}{k}}(ku)^{\frac{\nu(\mu-k)-\mu}{k}}\left(1-k\omega(ku)^{-\frac{\rho}{k}}\right)^{\frac{\gamma(\nu-1)}{k}}\hat{h}(p)\\
&\quad\times\left(1+\frac{Gp^2}{(s+1)^{\frac{\mu-k}{k}}(ku)^{-\frac{\mu}{k}}\left(1-k\omega(ku)^{-\frac{\rho}{k}}\right)^{\frac{\gamma}{k}}}\right)^{-1}\\
&= k(s+1)^{\frac{\nu(\mu-k)-(\mu-k)}{k}}(ku)^{\frac{\nu(\mu-k)-\mu}{k}}\left(1-k\omega(ku)^{-\frac{\rho}{k}}\right)^{\frac{\gamma(\nu-1)}{k}}\hat{h}(p)\\
&\quad\times\sum_{m=0}^{\infty}(-G)^m(s+1)^{\frac{(\mu-k)m}{k}}(ku)^{\frac{\mu}{k}m}\left(1-k\omega(ku)^{-\frac{\rho}{k}}\right)^{\frac{\gamma}{k}m}\\
&= k\sum_{m=0}^{\infty}(-G)^m(s+1)^{\frac{(1-\nu)(k-\mu)+(k-\mu)m}{k}}(ku)^{\frac{\nu(\mu-k)-\mu(m+1)}{k}}\\
&\qquad\times\left(1-k\omega(ku)^{-\frac{\rho}{k}}\right)^{-\frac{\gamma(m+1-\nu)}{k}}\hat{h}(p).
\end{aligned}$$

Applying the inverse Laplace transform, we get

$$\begin{aligned}
\hat{V}(p,\zeta) = \sum_{m=0}^{\infty}(-G)^m(s+1)^{\frac{(1-\nu)(k-\mu)+(k-\mu)m}{k}}(\zeta^{s+1})^{\frac{\mu(m+1)-\nu(\mu-k)}{k}-1}\\
\times E^{\gamma(m+1-\nu)}_{k,\rho,\mu(m+1)-\nu(k-\mu)}(\omega(\zeta^{s+1})^{\frac{\rho}{k}})p^{2m}\hat{h}(p).
\end{aligned}$$

Now, applying the inverse Fourier transform yields

$$\begin{aligned}
&V(\theta,\zeta) = \int_{-\infty}^{+\infty}dp\,e^{-ip\theta}\hat{h}(p)\\
&\frac{1}{2\Pi}\sum_{m=0}^{\infty}(-G)^m(s+1)^{-\frac{(1-\nu)(k-\mu)-(\mu-k)m}{k}}(\zeta^{s+1})^{\frac{\mu(m+1)-\nu(\mu-k)}{k}-1}\\
&\times E^{\gamma(m+1-\nu)}_{k,\rho,\mu(m+1)-\nu(k-\mu)}(\omega(\zeta^{s+1})^{\frac{\rho}{k}})p^{2m}\hat{h}(p).
\end{aligned}$$

Remark 4.2. *If $s=0$, $k=1$, $\gamma=0$, and $\mu\to 1$, then the above Cauchy problem reduces to*

$$ \frac{\partial}{\partial\theta}V(\theta,\zeta) = G\frac{\partial^2}{\partial\theta^2}V(\theta,\zeta) $$

$$ \left[V(\theta,\zeta)\right]_{\zeta=0^+} = h(\theta), \quad \lim_{\theta\to\infty}V(\theta,\zeta) = 0, $$

which is the heat equation.

Corollary 4.3. *If we take $s=0$ and $k=1$, we get the following Cauchy problem given in [19]:*

$$ \mathfrak{D}^{\gamma,\mu,\nu}_{0^+;\rho,\omega}V(\theta,\zeta) = G\frac{\partial^2}{\partial\theta^2}V(\theta,\zeta), \quad \zeta>0,\ \theta\in\mathbb{R}, $$

$$ \left[\mathfrak{J}^{-\gamma(1-\nu),\omega}_{0^+;\rho,(1-\nu)(1-\mu)}V(\theta,\zeta)\right]_{\zeta=0^+} = h(\theta), $$

$$ \lim_{\theta\to\infty}V(\theta,\zeta) = 0, $$

where $\mu\in(0,1)$, $\nu\in[0,1]$, $\omega\in\mathbb{R}$, $R,\rho>0$, and $\gamma\geq 0$, with solution given by

$$\begin{aligned}
V(\theta,\zeta) = \int_{-\infty}^{+\infty}dp\,e^{-ip\theta}\hat{h}(p)\,\frac{1}{2\Pi}\sum_{m=0}^{\infty}(-G)^m\zeta^{\mu(m+1)-\nu(\mu-1)-1}\\
\times E^{\gamma(m+1-\nu)}_{\rho,\mu(m+1)-\nu(\mu-1)}(\omega\zeta^{\rho})p^{2m}h(p).
\end{aligned}$$

5. GENERALIZATION OF THE FRACTIONAL KINETIC DIFFERINTEGRAL EQUATION

Fractional differential equations are important tools for developing mathematical models of numerous phenomena in fields such as physics, dynamic systems, control systems, and engineering. In mathematical modeling, kinetic equations describe the continuity of the motion of a substance and are basic equations of mathematical physics and the natural sciences. In this section, we consider an equation that generalizes kinetic equations. For related literature, we refer the reader to [39–42].

Theorem 5.1. *Consider the Cauchy problem*

$$ a{}_k^s\mathfrak{D}^{\gamma,\mu,\nu}_{0^+;\rho,\omega}N(t) - N_0f(t) = b{}_k^s\mathfrak{J}^{\omega,\sigma}_{0^+;\rho,q}N(t), \quad f\in L^1[0,\infty), \tag{5.1} $$

$$ {}_k^s\mathfrak{J}^{\omega,-\gamma(1-\nu)}_{0^+;\rho,(1-\nu)(k-\mu)}N(0) = d, \quad d\geq 0, \tag{5.2} $$

where $s\in[0,\infty)$, $\nu\in[0,1]$, $\omega\in\mathbb{C}$, $a,b\in\mathbb{R}$ $(a\neq 0)$, $\mu,\rho,q,k>0$, and $\gamma,\sigma\geq 0$. The solution to the problem is

$$\begin{aligned}
N(t) = d\sum_{n=0}^{\infty}\left(\frac{b}{a}\right)^n(s+1)^{-\frac{\nu(k-\mu)+(\mu-k)(n+1)+qn}{k}}(t^{s+1})^{\frac{\nu(k-\mu)+\mu+(q+\mu)n}{k}-1}\\
E^{(\gamma+\sigma)n+\gamma(1-\nu)}_{k,\rho,\nu(k-\mu)+\mu+(q+\mu)n}(\omega(t^{s+1})^{\frac{\rho}{k}})\\
+\frac{N_0}{a}\sum_{n=0}^{\infty}\left(\frac{b}{a}\right)^n(s+1)^{n+1}{}_k^s\mathfrak{J}^{\omega,(\gamma+\sigma)n+\gamma}_{0^+;\rho,(q+\mu)n+\mu}f(t).
\end{aligned}$$

Proof. Applying the generalized Laplace transform to both sides of (5.1), we get

$$ aL_g\{{}_k^s\mathfrak{D}^{\gamma,\mu,\nu}_{0^+;\rho,\omega}N(t)\}(u) - N_0L_g\{f(t)\}(u) = bL_g\{{}_k^s\mathfrak{J}^{\omega,\sigma}_{0^+;\rho,q}N(t)\}(u). $$

Using Theorems 2.5 and 1.12, we get

$$\begin{aligned}
&a\Big[(s+1)^{\frac{\mu-k}{k}}(ku)^{\frac{\mu}{k}}\big(1-k\omega(ku)^{-\frac{\rho}{k}}\big)^{\frac{\gamma}{k}}L_g\{N(t)\}(u)\\
&-k(s+1)^{-\frac{\nu(k-\mu)}{k}}(ku)^{\frac{-\nu(k-\mu)}{k}}\\
&\quad\times\big(1-k\omega(ku)^{-\frac{\rho}{k}}\big)^{\frac{\gamma\nu}{k}}{}_k\mathfrak{J}^{\omega,-\gamma(1-\nu)}_{0^+;\rho,(1-\nu)(k-\mu)}N(0^+)\Big]\\
&-N_0L_g\{f(t)\}(u)\\
&=b(s+1)^{-\frac{\mu}{k}}(ku)^{-\frac{\mu}{k}}\big(1-k\omega(ku)^{-\frac{\rho}{k}}\big)^{-\frac{\sigma}{k}}L_g\{N(t)\},
\end{aligned}$$

which can be written as

$$\begin{aligned}
&\left[\frac{a-b(s+1)^{-\frac{\mu-k+q}{k}}(ku)^{-\frac{\mu+q}{k}}\big(1-k\omega(ku)^{-\frac{\rho}{k}}\big)^{-\frac{\gamma+\sigma}{k}}}{(s+1)^{-\frac{\mu-k}{k}}(ku)^{-\frac{\mu}{k}}\big(1-k\omega(ku)^{-\frac{\rho}{k}}\big)^{-\frac{\gamma}{k}}}\right]\\
&L_g\{N(t)\}(u)\\
&=akd(s+1)^{-\frac{\nu(k-\mu)}{k}}(ku)^{-\frac{\nu(k-\mu)}{k}}\big(1-k\omega(ku)^{-\frac{\rho}{k}}\big)^{\frac{\gamma\nu}{k}}\\
&+N_0L_g\{f(t)\}(u),
\end{aligned}$$

$$\begin{aligned}
&L_g\{N(t)\}(u)\\
&=akd\left[\frac{(s+1)^{-\frac{\nu(k-\mu)+(\mu-k)}{k}}(ku)^{-\frac{\nu(k-\mu)+\mu}{k}}\big(1-k\omega(ku)^{-\frac{\rho}{k}}\big)^{\frac{\gamma(\nu-1)}{k}}}{a-b(s+1)^{-\frac{\mu-k+q}{k}}(ku)^{-\frac{\mu+q}{k}}\big(1-k\omega(ku)^{-\frac{\rho}{k}}\big)^{-\frac{\gamma+\sigma}{k}}}\right]\\
&+\left[\frac{(s+1)^{-\frac{\mu-k}{k}}(ku)^{-\frac{\mu}{k}}\big(1-k\omega(ku)^{-\frac{\rho}{k}}\big)^{-\frac{\gamma}{k}}}{a-b(s+1)^{-\frac{\mu-k+q}{k}}(ku)^{-\frac{\mu+q}{k}}\big(1-k\omega(ku)^{-\frac{\rho}{k}}\big)^{-\frac{\gamma+\sigma}{k}}}\right]\\
&N_0L_g\{f(t)\}(u).
\end{aligned}$$

Taking $\left|\frac{b}{a}(s+1)^{-\frac{\mu-k+q}{k}}(ku)^{-\frac{\mu+q}{k}}\big(1-k\omega(ku)^{-\frac{\rho}{k}}\big)^{-\frac{\gamma+\sigma}{k}}\right|<1$ gives

$$\begin{aligned}
&L_g\{N(t)\}(u)\\
&=\Big[kd(s+1)^{-\frac{\nu(k-\mu)+(\mu-k)}{k}}(ku)^{-\frac{\nu(k-\mu)+\mu}{k}}\big(1-k\omega(ku)^{-\frac{\rho}{k}}\big)^{\frac{\gamma(\nu-1)}{k}}\\
&\quad+(s+1)^{-\frac{\mu-k}{k}}(ku)^{-\frac{\mu}{k}}\big(1-k\omega(ku)^{-\frac{\rho}{k}}\big)^{-\frac{\gamma}{k}}a^{-1}N_0L_g\{f(t)\}(u)\Big]\\
&\quad\times\sum_{n=0}^{\infty}\Big(\frac{b}{a}\Big)^n(s+1)^{-\frac{(\mu-k+q)n}{k}}(ku)^{-\frac{(\mu+q)n}{k}}\\
&\quad\big(1-k\omega(ku)^{-\frac{\rho}{k}}\big)^{-\frac{(\gamma+\sigma)n}{k}}\\
&=dk\sum_{n=0}^{\infty}\Big(\frac{b}{a}\Big)^n(s+1)^{-\frac{\nu(k-\mu)+(\mu-k)(n+1)+q n}{k}}(ku)^{-\frac{\nu(k-\mu)+\mu+(\mu+q)n}{k}}\\
&\quad\big(1-k\omega(ku)^{-\frac{\rho}{k}}\big)^{-\frac{(\gamma+\sigma)n+\gamma(1-\nu)}{k}}\\
&\quad+\frac{N_0}{a}\sum_{n=0}^{\infty}\Big(\frac{b}{a}\Big)^n(s+1)^{-\frac{(\mu-k)(n+1)+qn}{k}}(ku)^{-\frac{\mu+(\mu+q)n}{k}}\\
&\quad\big(1-k\omega(ku)^{-\frac{\rho}{k}}\big)^{-\frac{(\gamma+\sigma)n+\gamma}{k}}.
\end{aligned}$$

Applying the inverse Laplace transform, we get

$$\begin{aligned}
N(t)&=d\sum_{n=0}^{\infty}\Big(\frac{b}{a}\Big)^n(s+1)^{-\frac{\nu(k-\mu)+(\mu-k)(n+1)+qn}{k}}\\
&\quad(t^{s+1})^{\frac{\nu(k-\mu)+\mu+(q+\mu)n}{k}-1}E^{(\gamma+\sigma)n+\gamma(1-\nu)}_{k,\rho,\nu(k-\mu)+\mu+(q+\mu)n}(\omega(t^{s+1})^{\frac{\rho}{k}})\\
&\quad+\frac{N_0}{a}\sum_{n=0}^{\infty}\Big(\frac{b}{a}\Big)^n(s+1)^{n+1}{}_k\mathfrak{J}^{\omega,(\gamma+\sigma)n+\gamma}_{0^+;\rho,(q+\mu)n+\mu}f(t),
\end{aligned}$$

which is the required result.

Remark 5.2. *If we take $s=0$, $k=1$, $\nu=\gamma=\sigma=0$, $\mu\to 0$, $a=1$, and $b=-c^p$, then we get the following fractional kinetic equation given in [39]:*

$$N(t)-N_0f(t)=-c^pD^p_{0^+}N(t),\quad N(0)=d,\quad d\geq 0,$$

where $D^p_{0^+}$ is the Riemann-Liouville fractional integral operator, defined as

$$D^p_{0^+}N(t)=\frac{1}{\Gamma(p)}\int_0^t(t-\tau)^{p-1}N(\tau)\,d\tau.$$

Here $N(t)$ denotes the number density of a given species at time t, with $N_0=N(0)$ being the number density of that species at time $t=0$, c is a constant, and $f\in L^1[0;\infty)$.

Corollary 5.3. *If we take $s=0$ and $\nu=0$, then we get the following Cauchy problem given in [42]:*

$$\begin{aligned}
a_k\mathfrak{D}^{\gamma,\mu}_{0^+;\rho,\omega}N(t)-N_0f(t)&=b_k\mathfrak{J}^{\omega,\sigma}_{0^+;\rho,q}N(t),\quad f\in L^1[0,\infty),\\
{}_k\mathfrak{J}^{\omega,-\gamma}_{0^+;\rho,k-\mu}N(0)&=d,\quad d\geq 0,
\end{aligned}$$

where $\omega\in\mathbb{C}$, $a,b\in\mathbb{R}(a\neq 0)$, $\mu,\rho,q,k>0$, and $\gamma,\sigma\geq 0$. The solution to the problem is

$$\begin{aligned}
N(t)&=d\sum_{n=0}^{\infty}\Big(\frac{b}{a}\Big)^n t^{\frac{\mu+(q+\mu)n}{k}-1}E^{(\gamma+\sigma)n+\gamma}_{k,\rho,\mu+(q+\mu)n}(\omega(t)^{\frac{\rho}{k}})\\
&\quad+\frac{N_0}{a}\sum_{n=0}^{\infty}\Big(\frac{b}{a}\Big)^n{}_k\mathfrak{J}^{\omega,(\gamma+\sigma)n+\gamma}_{0^+;\rho,(q+\mu)n+\mu}f(t).
\end{aligned}$$

6. CONCLUSION

A new generalized fractional derivative operator, referred to as the (k,s)-Hilfer-Prabhakar fractional derivative, is developed in this article. The generalized Laplace transform of the proposed operator is also studied. Potential applications of the proposed operator are discussed, which concern fractional models of the free-electron laser equation, heat equation, and kinetic equation that involve the new operator. The results in this article suggest that this novel operator can be used to solve various types of problems arising in mathematical physics and other fields.

DATA AVAILABILITY STATEMENT

All datasets generated for this study are included in the article/supplementary material.

AUTHOR CONTRIBUTIONS

MS, KN, and DK: Conceptualization. MS, ZP, GR, and KN: Writing original draft. KN and DK: Methodology.

ZP, GR, and DK: Formal analysis. MS and GR: Validation. KN and DK: Revision and final check. All authors contributed to the article and approved the submitted version.

REFERENCES

1. Kumar D, Singh J, Tanwar K, Baleanu D. A new fractional exothermic reactions model having constant heat source in porous media with power, exponential and Mittag-Leffler Laws. *Int J Heat Mass Transfer*. (2019) **138**:1222–7. doi: 10.1016/j.ijheatmasstransfer.2019.04.094
2. Kumar D, Singh J, Qurashi MA, Baleanu D. A new fractional SIRS-SI malaria disease model with application of vaccines, anti-malarial drugs, and spraying. *Adv Differ Equat*. (2019) **2019**:278. doi: 10.1186/s13662-019-2199-9
3. Kumar, D, Singh J, Baleanu, D. A new numerical algorithm for fractional Fitzhugh-Nagumo Equation arising in transmission of nerve impulses. *Nonlinear Dyn*. (2018) **91**:307–17. doi: 10.1007/s11071-017-3870-x
4. Kumar D, Singh J, Baleanu D. Analysis of regularized long-wave equation associated with a new fractional operator with Mittag-Leffler type kernel. *Physica A*. (2018) **492**:155–67. doi: 10.1016/j.physa.2017.10.002
5. Singh J, Kumar D, Baleanu D. New aspects of fractional Biswas-Milovic model with Mittag-Leffler law. *Math Model Nat Phenomena*. (2019) **14**:303. doi: 10.1051/mmnp/2018068
6. Abel, N. Solution de quelques problemes l'aide d'integrales definies. *Mag Nat*. (1823) **1**:1–27.
7. Herrmann R. *Fractional Calculus: An Introduction for Physicists*. 3rd revised ed. Singapore: World Scientific Publishing (2018).
8. Hilfer R. *Applications of Fractional Calculus in Physics*. Singapore: World Scientific Publishing (2000).
9. Hilfer R. *Threefold Introduction to Fractional Derivatives*. Anomalous Transport: Foundations and Applications. Weinheim: Germany Publishing (2008).
10. Kilbas A, Srivastava HM, Trujillo JJ. *Theory and Application of Fractional Differential Equations*. Amsterdam: North Holland Mathematics Studies (2006). p. 204.
11. Lorenzoand CF, Hartley TT. Variable order and distributed order fractional operators. *Nonlinear Dynam*. (2002) **29**:57–98. doi: 10.1023/A:1016586905654
12. Magin RL. *Fractional Calculus in Bioengineering*. Redding, CA: House Publishers (2006).
13. Podlubny I. *Fractional Differential Equations*. San Diego CA: Academic Press (1999).
14. Oldham KB, Spanier J. *The Fractional Calculus*. New York, NY: Academic Press (1974).
15. Baleanu D, Diethelm K, Scalas E, Trujillo JJ. *Fractional Calculus: Models and Numerical Methods*. Series on Complexity, Nonlinearity and Chaos. New Jersey, NJ: World Scientific Publishing (2012).
16. Mainardi F. *Fractional Calculus and Waves in Linear Viscoelasticity: An Introduction to Mathematical Models*. Singapore; London; Hong Kong: World Scientific (2010).
17. Diethelm K. *The Analysis of Fractional Differential Equations: An Application-Oriented Exposition Using Differential Operators of Caputo Type*. Berlin; Heidelberg: Springer (2010).
18. Hilfer R, Luchko Y, Tomovski Z. Operational method for solution of the fractional differential equations with the generalized Riemann-Liouville fractional derivatives. *Fract Calc Appl Anal*. (2009) **12**:299–318. Available online at: https://www.researchgate.net/publication/228746820_Operational_method_for_the_solution_of_fractional_differential_equations_with_generalized_Riemann-Liouville_fractional_derivatives
19. Garra R, Goreno R, Polito F, Tomovski Z. Hilfer-Prabhakar derivative and some applications. *Appl Math Comput*. (2014) **242**:576–89. doi: 10.1016/j.amc.2014.05.129
20. Panchal SK, Pravinkumar VD, Khandagale AD. *k*-Hilfer-Prabhakar fractional derivatives and its applications. *Indian J Math*. (2017) **59**:367–83. Available online at: http://www.amsallahabad.org/pdf/ijm593.pdf
21. Dorrego GA. Generalized Riemann-Liouville fractional operators associated with a generalization of the Prabhakar integral operator. *Prog Fract Differ Appl*. (2016) **2**:131–40. doi: 10.18576/pfda/020206
22. Nisar KS, Rahman G, Baleanu D, Mubeen S, Arshad M. The (k, s)-fractional calculus of *k*-Mittag-Leffler function. *Adv Differ Equat*. (2017) 118:1–2. doi: 10.1186/s13662-017-1239-6
23. Gaboury S, Tremblay R, Fugere B. Some relations involving a generalized fractional derivative operator. *J Inequal Appl*. (2013) 167:1–9. doi: 10.1186/1029-242X-2013-167
24. Rahman G, Nisar KS, Mubeen S. A new extension of extended Caputo fractional derivative operator. *Math Eng Sci Aerospace*. (2020) **11**:265–79.
25. Bohner M, Rahman G, Mubeen S, Nisar KS. A further extension of the extended Riemann-Liouville fractional derivative operator. *Turk J Math*. (2018) **42:**2631–42. doi: 10.3906/mat-1805-139
26. Nisar KS, Rahman G, Tomovski Z. On a certain extension of the Riemann-Liouville fractional derivative operator. *Commun Korean Math Soc*. (2019) **34:**507–22. doi: 10.4134/CKMS.c180140
27. Rahman G, Mubeen S, Nisar KS, Choi J. Certain extended special functions and fractional integral and derivative operators via an extended beta functions. *Nonlinear Funct Anal Appl*. (2019) **24**:1–13. Available online at: http://nfaa.kyungnam.ac.kr/journal-nfaa/index.php/NFAA/article/view/1148/990
28. Rahman G, Mubeen S, Nisar KS. On generalized *k*-fractional derivative operator. *AIMS Math*. (2020) **5**:1936–45. doi: 10.3934/math.2020129
29. Modanl M. On the numerical solution for third order fractional partial differential equation by difference scheme method. *Int J Optim Control Theor Appl*. (2019) **9**:1–5. doi: 10.11121/ijocta.01.2019.00678
30. Vivek D, Kanagarajan K, Sivasundaram S. Dynamics and stability results for Hilfer fractional type thermistor problem. *Fractal Fract*. (2017) 1:5. doi: 10.3390/fractalfract1010005
31. Ozdemir N, Avci D, Iskender B. The numerical solutions of a two-dimensional space-time Riesz-Caputo fractional diffusion equation. *Int J Optim Control Theor Appl*. (2011) **1**:17–26. doi: 10.11121/ijocta.01.2011.0028
32. Jarad F, Abdeljawad T. A modified Laplace transform for certain generalized fractional operators. *Results Nonlinear Anal*. (2018) **2**:88–98. doi: 10.3934/dcdss.2020039
33. Kerr FH. Namias fractional Fourier-Transforms on L2 and applications to differential equations. *J Math Anal Appl*. (1988) **136**:404–18.
34. Jarad F, Abdeljawad T. Generalized fractional derivatives and laplace transform. *Discrete Contin Dyn Syst Ser S*. (2020) **13**:709–22.
35. Diaz R, Pariguan E. On hypergeometric functions and pochhammer *k*-symbol. *Divulg Math*. (2007) **15**:179–92. Available online at: https://citeseerx.ist.psu.edu/viewdoc/download?doi=10.1.1.930.1846&rep=rep1&type=pdf
36. Dorrego GA, Cerutti RA. The *k*-Mittag-Leffler function. *Int J Contemp Math Sci*. (2012) **7**:705–16. Available online at: http://www.m-hikari.com/ijcms/ijcms-2012/13-16-2012/ceruttiIJCMS13-16-2012-2.pdf
37. Luchko Y. Some uniqueness and existence results for the initial-boundary-value problems for the generalized time-fractional diffusion equation. *Comput Math Appl*. (2010) **59**:1766–72. doi: 10.1016/j.camwa.2009.08.015
38. Luchko Y. Initial-boundary-value problems for the generalized multi-term time-fractional diffusion equation. *J Math Anal Appl*. (2011) **374**:538–48. doi: 10.1016/j.jmaa.2010.08.048
39. Saxena RK, Kalla SL. On the solutions of certain fractional kinetic equations. *Appl Math Comput*. (2008) **199**:504–11. doi: 10.1016/j.amc.2007.10.005
40. Choi J, Kumar D. Solutions of generalized fractional kinetic equations involving Aleph functions. *Math. Commun*. (2015) **20**:113–23. Available online at: https://www.mathos.unios.hr/mc/index.php/mc/article/view/1125
41. Kumar D, Choi J. Generalized fractional kinetic equations associated with aleph function. *Proc Jangjeon Math Soc*. (2016) **19**:145–55. Available online at: http://www.jangjeon.or.kr/etc/view.html?id=1684

42. Dorrego GA, Kumar D. A generalization of the kinetic equation using the Prabhakar-type operators. *Honam Math J.* (2017) **39**:401–16.

Conflict of Interest: The authors declare that the research was conducted in the absence of any commercial or financial relationships that could be construed as a potential conflict of interest.

Copyright © 2020 Samraiz, Perveen, Rahman, Nisar and Kumar. This is an open-access article distributed under the terms of the Creative Commons Attribution License (CC BY). The use, distribution or reproduction in other forums is permitted, provided the original author(s) and the copyright owner(s) are credited and that the original publication in this journal is cited, in accordance with accepted academic practice. No use, distribution or reproduction is permitted which does not comply with these terms.

frontiers in Physics

ORIGINAL RESEARCH
published: 23 November 2020
doi: 10.3389/fphy.2020.00280

A Correlation Between Solutions of Uncertain Fractional Forward Difference Equations and Their Paths

Hari Mohan Srivastava[1] *and Pshtiwan Othman Mohammed*[2]*

[1] Department of Mathematics and Statistics, University of Victoria, Victoria, BC, Canada, [2] Department of Mathematics, College of Education, University of Sulaimani, Sulaymaniyah, Iraq

We consider the comparison theorems for the fractional forward *h*-difference equations in the context of discrete fractional calculus. Moreover, we consider the existence and uniqueness theorem for the uncertain fractional forward *h*-difference equations. After that the relations between the solutions for the uncertain fractional forward *h*-difference equations with symmetrical uncertain variables and their α-paths are established and verified using the comparison theorems and existence and uniqueness theorem. Finally, two examples are provided to illustrate the relationship between the solutions.

Keywords: uncertain fractional *h*-difference equations, the comparison theorems, α-paths, existence and uniqueness theorem, discrete fractional calculus

OPEN ACCESS

Edited by:
Jordan Yankov Hristov, University of Chemical Technology and Metallurgy, Bulgaria

Reviewed by:
Praveen Agarwal, Anand International College of Engineering, India
Amar Debbouche, 8 May 1945 University of Guelma, Algeria

***Correspondence:**
Pshtiwan Othman Mohammed
pshtiwansangawi@gmail.com

Specialty section:
This article was submitted to Mathematical and Statistical Physic, a section of the journal Frontiers in Physics

Received: *09 March 2020*
Accepted: *22 June 2020*
Published: *23 November 2020*

Citation:
Srivastava HM and Mohammed PO (2020) A Correlation Between Solutions of Uncertain Fractional Forward Difference Equations and Their Paths. Front. Phys. 8:280. doi: 10.3389/fphy.2020.00280

1. INTRODUCTION

The study of fractional calculus and fractional differential equations has received recent attention from both applied and theoretical disciplines. Indeed, it was observed that the use of them are very useful for modeling many problems in mathematical analysis, medical labs, engineering sciences, and integral inequalities (see for e.g., [1–14]). There is much interesting research on what is usually called integer-order difference equations (see for e.g., [15, 16]). Discrete fractional calculus and fractional difference equations represent a new branch of fractional calculus and fractional differential equations, respectively. Also, for scientists, they represent new areas that have, in their early stages, developed slowly. Some works are dedicated to boundary value problems, initial value problems, chaos, and stability for the fractional difference equations (see for e.g., [17–23]).

Besides the discrete fractional calculus, the uncertain fractional differential and difference equations have been introduced and investigated in order to model the continuous or discrete systems with memory effects and human uncertainty (see for e.g., [24–28]). In Lu and Zhu [27], the relations between uncertain fractional differential equations and the associated fractional differential equations have been created via comparison theorems for fractional differential equations of Caputo type in Lu and Zhu [26]. Lu et al. [28] presented analytic solutions to a type of special linear uncertain fractional difference equation (UFDE) by the Picard iteration method. Moreover, they provided an existence and uniqueness theorem for the solutions by applying the Banach contraction mapping theorem. After that, Mohammed [29] generalized the above work.

Nowadays, discrete fractional calculus shows incredible performance in the fields of physical and mathematical modeling. The motivation behind solving the fractional difference equations relies on fast investigation of the properties within models of fractional sum and difference operators (see for e.g., [20, 30–36]).

Motivated by the aforementioned results, we will try to create a link between uncertain fractional forward *h*-difference equations (UFFhDEs) and associated fractional forward

h-difference equations (FFhDEs) in the sense of Riemann–Liouville fractional operators via the comparison theorems and existence and uniqueness theorem.

The rest of our article is designed as follows. In section 2, we presented the preliminary definitions and important features that are useful in the accomplishment of this study. In section 3, the comparison theorems of the fractional differences are pointed out. Inverse uncertainty distribution, the existence and uniqueness theorem, the relation between UFFhDEs and associated FFhDEs, and some related examples are pointed out in section 4. Finally, the future scope and concluding remarks are summarized in section 5.

2. PRELIMINARIES

In what follows, we recall some results in discrete fractional calculus that has been developed in the last few years; for more details, we refer to references [24–28, 29, 37, 38] and the related references therein.

Definition 2.1 ([39]). The forward difference operator on $h\mathbb{Z}$ is defined by

$$\Delta_h f(\eta) = \frac{f(\eta + h) - f(\eta)}{h},$$

and the backward difference operator on $h\mathbb{Z}$ is defined by

$$\nabla_h f(\eta) = \frac{f(\eta) - f(\eta - h)}{h}.$$

For $h = 1$, we get the classical forward and backward difference operators $\Delta\psi(\eta) = \psi(\eta + 1) - \psi(\eta)$ and $\nabla\psi(\eta) = \psi(\eta) - \psi(\eta - h)$, respectively. The forward jumping operator on $h\mathbb{Z}$ is $\sigma(r) = r + h$ and the backward jumping operator is $\rho(r) = r - h$.

For $a, b \in \mathbb{R}$ with $a < b$, $\frac{b-a}{h} \in \mathbb{N}$ and $0 < h \leq 1$, we use the notations $\mathbb{N}_{a,h} = \{a, a+h, a+2h, ...\}$, ${}_{b,h}\mathbb{N} = \{b, b-h, b-2h, ...\}$.

Definition 2.2 ([39]). Let $\eta, \theta \in \mathbb{R}$ and $0 < h \leq 1$, the delta h-factorial of η is defined by

$$\eta_h^{(\theta)} = \frac{\Gamma\left(\frac{\eta}{h} + 1\right)}{\Gamma\left(\frac{\eta}{h} + 1 - \theta\right)}, \tag{2.1}$$

where we use the convention that division at a pole yields zero and θ is the falling delta h-factorial order of η. It is worth mentioning that $\eta_h^{(\theta)}$ is a function of η for given θ and h.

Definition 2.3 ([37, 38, 40]). Let f be defined on $\mathbb{N}_{a,h}$ for the left case and ${}_{b,h}\mathbb{N}$ for the right case. Then, the left delta h-fractional sum of order $\theta > 0$ is defined by

$$\begin{aligned}\left({}_a\Delta_h^{-\theta}\psi\right)(\eta) &= \int_a^{\sigma(\eta-\theta h)} (\eta - \sigma(\tau))_h^{(\theta-1)}\psi(\tau)\Delta_h\tau \\ &= \frac{1}{\Gamma(\theta)} \sum_{r=\frac{a}{h}}^{\frac{\eta}{h}-\theta} (\eta - \sigma(rh))_h^{(\theta-1)}\psi(rh)h, \quad \eta \in \mathbb{N}_{a+\theta h,h},\end{aligned}$$

and the right delta h-fractional sum is defined by

$$\begin{aligned}\left({}_h\Delta_b^{-\theta}\psi\right)(\eta) &= \int_{\rho(\eta+\theta h)}^{b} (\rho(\tau) - \eta)_h^{(\theta-1)}\psi(\tau)\nabla_h\tau \\ &= \frac{1}{\Gamma(\theta)} \sum_{r=\frac{\eta}{h}+\theta}^{\frac{b}{h}} (rh - \sigma(\eta))_h^{(\theta-1)}\psi(rh)h, \\ \eta &\in {}_{b-\theta h,h}\mathbb{N}.\end{aligned}$$

Lemma 2.1 ([40]). *Let $\theta, \mu > 0, h > 0$, and p be defined on $\in \mathbb{N}_{a,h}$. We then have*

$$\begin{aligned}\left({}_{a+\mu h}\Delta_h^{-\theta}\,{}_a\Delta_h^{-\mu}p\right)(\eta) &= \left({}_a\Delta_h^{-(\mu+\theta)}p\right)(\eta) \\ &= \left({}_{a+\theta h}\Delta_h^{-\mu}\,{}_a\Delta_h^{-\theta}p\right)(\eta),\end{aligned} \tag{2.2}$$

for all $\eta \in \mathbb{N}_{a+(\theta+\mu)h,h}$.

Lemma 2.2 ([40]). *Let $\theta > 0$ and ψ be defined on $\mathbb{N}_{a,h}$ and ${}_{b,h}\mathbb{N}$, respectively. Then the left and right delta h-fractional differences of order θ are defined by*

$$\left({}_a\Delta_h^{\mu}\psi\right)(\eta) = \left(\Delta_h^m\,{}_a\Delta_h^{-(m-\mu)}\psi\right)(\eta), \tag{2.3}$$

$$\left({}_h\Delta_b^{\mu}\psi\right)(\eta) = (-1)^m\left(\nabla_h^m\,{}_h\Delta_b^{-(m-\mu)}\psi\right)(\eta), \tag{2.4}$$

where $m = [\theta] + 1$.

Lemma 2.3 ([40]). *Let ψ be defined on $\mathbb{N}_{a,h}$, then, for any $\theta > 0$, we have*

$$\left({}_a\Delta_h^{-\theta}\,\Delta_h\psi\right)(\eta) = \Delta_h\,{}_a\Delta_h^{-\theta}\psi(\eta) - \frac{(\eta - a)_h^{(\theta-1)}}{\Gamma(\theta)}\psi(a). \tag{2.5}$$

Lemma 2.4 ([40]). *Let $\theta > 0, \mu > 0$, and $h > 0$, and we then have*

$${}_{a+\mu h}\Delta_h^{\theta}(\eta - a)_h^{(\mu)} = \frac{\Gamma(\mu + 1)}{\Gamma(\mu + \theta + 1)}(\eta - a)_h^{(\theta+\mu)},$$

$${}_h\Delta_{b-\mu h}^{\theta}(b - \eta)_h^{(\theta)} = \frac{\Gamma(\mu + 1)}{\Gamma(\mu + \theta + 1)}(b - \eta)_h^{(\theta+\mu)}.$$

Lemma 2.5 ([40]). *Let $\theta \in \mathbb{R}$ and q be any positive integer, then*

$$\begin{aligned}\left({}_a\Delta_h^{-\theta}\,\Delta_h^q\psi\right)(\eta) &= \left(\Delta_h^q\,{}_a\Delta_h^{-\theta}\psi\right)(\eta) \\ &\quad - \sum_{k=0}^{q-1} \frac{(\eta - a)_h^{(\nu-q+k)}}{\Gamma(\nu - q + k + 1)}\Delta_h^k\psi(a),\end{aligned} \tag{2.6}$$

for $\eta \in \mathbb{N}_{a+\theta h,h}$.

Lemma 2.6 ([38]). *Suppose that $\frac{\mu}{h}, \frac{\mu}{h} + \theta \in \mathbb{R} \setminus \{..., -2, -1\}$, then we have*

$${}_a\Delta_h^{-\theta}(\eta - a + \mu)_h^{(\frac{\mu}{h})} = \frac{\Gamma\left(\frac{\mu}{h} + 1\right)}{\Gamma\left(\frac{\mu}{h} + \theta + 1\right)}(\eta - a + \mu)_h^{(\frac{\mu}{h}+\theta)},$$

for each $\eta \in \mathbb{N}_{a+\theta h,h}$.

Lemma 2.7. *Let ψ be defined on $\mathbb{N}_{a,h}$ and m be a positive integer with $0 < m-1 < \mu \leq m$. The definition of the fractional h-difference (2.3) is then equivalent to*

$$\left({}_a\Delta_h^{-\mu}\psi\right)(\eta) = \begin{cases} \frac{1}{\Gamma(-\mu)} \sum\limits_{r=\frac{a}{h}}^{\frac{\eta}{h}+\mu} (\eta-\sigma(rh))_h^{(-\mu-1)}\psi(rh)h, & m-1<\mu<m, \\ {}_a\Delta_h^m p(\eta), & \mu = m, \end{cases}$$

for $\eta \in \mathbb{N}_{a,h}$.

Motivated by the definition of nth order forward sum for uncertain sequence ξ_η, we define the θth order forward sum for uncertain sequence ξ_η as follows:

Definition 2.4. Let θ be a positive real number, $a \in \mathbb{R}$, and ξ_η be an uncertain sequence indexed by $\eta \in \mathbb{N}_{a,h}$. Then,

$${}_a\Delta_h^{-\theta}\xi_\eta = \frac{1}{\Gamma(\theta)} \sum_{r=\frac{a}{h}}^{\frac{\eta}{h}-\theta} (\eta-\sigma(rh))_h^{(\theta-1)}\xi_{rh}\,h$$

is called the θth order forward fractional sum of uncertain sequence ξ_η, where $\sigma(r) = r+h$.

Definition 2.5. The fractional Riemann–Liouville-like forward difference for uncertain sequence ξ_η is defined by

$${}_a\Delta_h^{\mu}\xi_\eta = \Delta_h^n\left({}_a\Delta_h^{-(n-\mu)}\xi_\eta\right),$$

where $\theta > 0$ and $0 \leq n-1 < \mu \leq n$, n represents a positive integer.

3. THE COMPARISON THEOREMS

Consider the following FFhDEs:

$${}_{(\theta-n)h}\Delta_h^{\theta}\psi(\eta) = g(\eta+(\theta-n)h, \psi(\eta+(\theta-n)h)), \tag{3.1}$$

subject to the initial conditions

$${}_{(\theta-n)h}\Delta_h^{\theta-n+i}\psi(\eta)\Big|_{t=0} = \psi_i, \quad i = 0,1,...,n-1, \tag{3.2}$$

where ${}_{(\theta-n)h}\Delta_h^{\theta}$ denotes a fractional Riemann–Liouville forward h-difference with $0 \leq n-1 < \theta \leq n$, g is a real-valued function defined on $[0,\infty)\times\mathbb{R}$, $\eta \in \mathbb{N}_{0,h}$, and $\psi_i \in \mathbb{R}$ for $i = 0,1,...,n-1$.

Now, by applying the operator ${}_0\Delta_h^{-\theta}$ to Equation (3.1), then the initial value problem (3.1) and (3.2) is equivalent to the following fractional sum equation:

$$\psi(\eta) = \sum_{i=0}^{n-1} \frac{(\eta)_h^{(\theta-n+i)}}{\Gamma(\theta-n+i+1)}\psi_i + \frac{1}{\Gamma(\theta)} \sum_{r=0}^{\frac{\eta}{h}-\theta} \left(\eta-\sigma(rh)\right)_h^{(\theta-1)} g(r+(\theta-n)h, \psi(r+(\theta-n)h))h, \tag{3.3}$$

where we have used Lemma 2.1, Lemma 2.5, and the fact that $\Delta_h^n\Delta_h^{-n}\psi(\eta) = \psi(\eta)$.

First, a comparison theorem for Riemann–Liouville fractional h-difference equations with $\theta \in (0,1]$ will be presented.

Theorem 3.1. *Suppose $g(\eta,\psi)$ and $k(\eta,\psi)$ are two real-value functions defined on $[0,\infty]\times\mathbb{R}$. Function k is Lipschitz continuous in y with Lipschitz constant L_k that has $0 < L_k \leq h^{-\theta}\theta$. If $\psi_1(\eta)$ and $\psi_2(\eta)$ are, respectively, unique solutions of the following IVPs*

$$\begin{cases} {}_{(\theta-1)h}\Delta_h^{\theta}\psi(\eta) = g(\eta+(\theta-1)h, \psi(\eta+(\theta-1)h)), & \eta \in \mathbb{N}_0, \\ {}_{(\theta-1)h}\Delta_h^{\theta-1}\psi(\eta)\Big|_{t=0} = \mathbf{X}_0, \end{cases} \tag{3.4}$$

and

$$\begin{cases} {}_{(\theta-1)h}\Delta_h^{\theta}\psi(\eta) = k(\eta+(\theta-1)h, \psi(\eta+(\theta-1)h)), & \eta \in \mathbb{N}_0, \\ {}_{(\theta-1)h}\Delta_h^{\theta-1}\psi(\eta)\Big|_{t=0} = \psi_0. \end{cases} \tag{3.5}$$

1. *if $g(\eta,\psi) \leq k(\eta,\psi)$, then $\psi_1(\eta) \leq \psi_2(\eta)$ for each $\eta \in \mathbb{N}_{(\theta-1)h,h}$,*
2. *if $g(\eta,\psi) > k(\eta,\psi)$, then $\psi_1(\eta) > \psi_2(\eta)$ for each $\eta \in \mathbb{N}_{\theta\,h,h}$.*

Proof: **(1)** Assume that the condition $\psi_1(\eta) \leq \psi_2(\eta)$ is not valid; there thus exists $\eta_0 \in \mathbb{N}_{(\theta-1)h,h}$ such that $\psi_1(\eta_0) > \psi_2(\eta_0)$. Let $\eta_1 = \min\left\{\eta \in \mathbb{N}_{(\theta-1)h,h};\ \psi_1(\eta) > \psi_2(\eta)\right\}$ and $\mathbf{X}(\eta) = \psi_1(\eta) - \psi_2(\eta)$. Then, we have

$$\mathbf{X}(\eta_1) > 0, \tag{3.6}$$

$$\mathbf{X}(\eta) \leq 0, \quad \eta \in \mathbb{N}_{(\theta-1)h,h} \cap [0, \eta_1 - h]. \tag{3.7}$$

Considering the fractional sum equations equivalent to IVPs (3.4) and (3.5), we have

$$\psi_1(\theta\,h) = \theta\,h^{\nu-1}\psi_0 + h^{\theta}g((\theta-1)h, \mathbf{X}_0),$$
$$\psi_2(\theta\,h) = \theta\,h^{\nu-1}\psi_0 + h^{\theta}k((\theta-1)h, \mathbf{X}_0).$$

Subtracting these and then making use of $h^{\theta} > 0$ for $h > 0, \theta \in (0,1]$, and $g(\eta,\psi) \leq k(\eta,\psi)$, we get

$$\psi_1(\theta h) - \psi_2(\theta h) = h^{\nu}\left(g((\theta-1)h, \mathbf{X}_0) - k((\theta-1)h, \mathbf{X}_0)\right) \leq 0.$$

This verifies that $\eta_1 > \theta\, h$. From this and since $\eta_1 \in \mathbb{N}_{(\theta-1)h,h}$, we can write $\eta_1 = (\theta+\ell)h, l = 1, 2, ...$ By Lemma 2.6, we then get

$$\begin{aligned}
&{}_{(\theta-1)h}\Delta_h^{\theta}\mathbf{X}(\eta_1 - \theta\, h)\\
&\quad= \frac{1}{\Gamma(-\theta)}\sum_{r=\theta-1}^{\frac{\eta_1}{h}}\left(\eta_1 - \theta\, h - \sigma(rh)\right)_h^{(-\theta-1)}\mathbf{X}(rh)h\\
&\quad= \frac{1}{\Gamma(-\theta)}\sum_{r=\theta-1}^{\theta+\ell}\left(\ell\, h - \sigma(rh)\right)_h^{(-\theta-1)}\mathbf{X}(rh)h\\
&\quad= h^{-\theta}\mathbf{X}((\theta+\ell)h) - \theta h^{-\theta}\mathbf{X}((\theta+\ell-1)h)\\
&\quad+ \frac{1}{\Gamma(-\theta)}\sum_{r=\theta-1}^{\theta+\ell-2}\left(\ell\, h - \sigma(rh)\right)_h^{(-\theta-1)}\mathbf{X}(rh)h.
\end{aligned}$$

That is,

$$\begin{aligned}
h^{-\theta}\mathbf{X}((\theta+\ell)h) = {}&{}_{(\theta-1)h}\Delta_h^{\theta}\mathbf{X}(\eta_1 - \theta\, h) + \theta h^{-\theta}\mathbf{X}((\theta+\ell-1)h)\\
&- \frac{1}{\Gamma(-\theta)}\sum_{r=\theta-1}^{\theta+\ell-2}\left(\ell\, h - \sigma(rh)\right)_h^{(-\theta-1)}\mathbf{X}(rh)h.
\end{aligned} \tag{3.8}$$

Now, by using the Lipschitz continuity of k in y, $g(\eta, x) \le k(\eta, x)$, and (3.7), we get

$$\begin{aligned}
{}_{(\theta-1)h}\Delta_h^{\theta}\mathbf{X}(\eta_1 - \theta\, h) &= {}_{(\theta-1)h}\Delta_h^{\theta}\psi_1(\eta_1 - \theta\, h)\\
&\quad- {}_{(\theta-1)h}\Delta_h^{\theta}\psi_2(\eta_1 - \theta\, h)\\
&= g(\eta_1 - h, \psi_1(\eta_1 - h))\\
&\quad- k(\eta_1 - h, \psi_2(\eta_1 - h))\\
&\le k(\eta_1 - h, \psi_1(\eta_1 - h))\\
&\quad- k(\eta_1 - h, \psi_2(\eta_1 - h))\\
&\le -L_k\left(\psi_1(\eta_1 - h) - \psi_2(\eta_1 - h)\right)\\
&\le -L_k\mathbf{X}(\eta_1 - h).
\end{aligned}$$

Denoting $\omega(\eta_1 - h) := {}_{(\theta-1)h}\Delta_h^{\theta}\mathbf{X}(\eta_1 - \theta\, h) + L_k\mathbf{X}(\eta_1 - h)$, it follows that

$$\omega((\theta+\ell-1)h) \le 0. \tag{3.9}$$

This gives

$${}_{(\theta-1)h}\Delta_h^{\theta}\mathbf{X}(\eta_1 - \theta\, h) = -L_k\mathbf{X}((\theta+\ell-1)h) + \omega((\theta+\ell-1)h).$$

Thus, Equation (3.8) becomes

$$\begin{aligned}
h^{-\theta}\mathbf{X}((\theta+\ell)h) = {}&\left(\theta h^{-\theta} - L_k\right)\mathbf{X}((\theta+\ell-1)h) + \omega((\theta+\ell-1)h)\\
&- \frac{1}{\Gamma(-\theta)}\sum_{r=\theta-1}^{\theta+\ell-2}\left(\ell\, h - \sigma(rh)\right)_h^{(-\theta-1)}\mathbf{X}(rh)h.
\end{aligned} \tag{3.10}$$

We write $r = \nu - 1 + i,\ i = 0, 1, ..., \ell - 1$ to obtain

$$\begin{aligned}
\frac{\left(\ell\, h - \sigma(rh)\right)_h^{(-\theta-1)}}{\Gamma(-\theta)} &= \frac{\left(\ell\, h - (\theta+i)h\right)_h^{(-\theta-1)}}{\Gamma(-\theta)}\\
&= h^{-\theta-1}\frac{\Gamma(\ell - i + 1 - \theta)}{\Gamma(-\theta)\Gamma(\ell - i + 2)}\\
&= h^{-\theta-1}\frac{(\ell - i - \theta)(\ell - i - 1 - \theta)\cdots(-\theta)\Gamma(-\theta)}{\Gamma(-\theta)\Gamma(\ell - i + 2)}\\
&= h^{-\theta-1}\frac{(-\theta)(-\theta+1)\cdots(\ell - i - 1 - \theta)(\ell - i - \theta)}{\Gamma(\ell - i + 2)}\\
&= h^{-\theta-1}\frac{(-\theta)(-\theta+1)\cdots(-\theta - 1 + c)(-\theta + c)}{\Gamma(c+1)},
\end{aligned}$$

where $c = \ell - i$.

Since $\theta \in (0, 1]$ and $h^{-\theta-1} > 0$, so

$$\frac{\left(\ell\, h - \sigma(rh)\right)_h^{(-\theta-1)}}{\Gamma(-\theta)} \le 0. \tag{3.11}$$

Considering $L_k < \theta\, h^{-\theta}$, $h^{-\theta} > 0$ and Equations (3.9)–(3.11), it follows that

$$h^{-\theta}\mathbf{X}((\theta+\ell)h) \le 0.$$

This implies that $\mathbf{X}(\eta_1) \le 0$, which contradicts with (3.6).

(2) By the same technique of (1), we assume that the condition $\psi_1(\eta) > \psi_2(\eta)$ is not valid. There thus exists $\eta_2 \in \mathbb{N}_{\theta\, h,h}$, such that $\psi_1(\eta_2) \le \psi_2(\eta_2)$. Let $\eta_3 = \min\left\{\eta \in \mathbb{N}_{\theta\, h,h};\ \psi_1(\eta) \le \psi_2(\eta)\right\}$ and $z(\eta) = \psi_2(\eta) - \psi_1(\eta)$. We then have

$$z(\eta_3) \ge 0, \tag{3.12}$$

$$z(\eta) < 0, \quad \eta \in \mathbb{N}_{\theta\, h,h} \cap [0, \eta_3 - h]. \tag{3.13}$$

Considering the fractional sum equations equivalent to IVPs (3.4) and (3.5), $h^{\theta} > 0$ and $g(\eta, \psi) > k(\eta, \psi)$, we find $\psi_1(\theta\, h) > \psi_2(\theta\, h)$. That is; $\eta_3 > \theta\, h$. If we write $\eta_3 = (\theta+\ell)h, l = 1, 2, ...,$ then, by Lemma 2.6, we get

$$\begin{aligned}
&{}_{(\theta-1)h}\Delta_h^{\theta}z(\eta_3 - \theta\, h)\\
&\quad= \frac{1}{\Gamma(-\theta)}\sum_{r=\theta-1}^{\frac{\eta_3}{h}}\left(\eta_3 - \theta\, h - \sigma(rh)\right)_h^{(-\theta-1)}z(rh)h\\
&\quad= h^{-\theta}z((\theta+\ell)h) - \theta h^{-\theta}z((\theta+\ell-1)h)\\
&\quad+ \frac{1}{\Gamma(-\theta)}\sum_{r=\theta-1}^{\theta+\ell-2}\left(\ell\, h - \sigma(rh)\right)_h^{(-\theta-1)}z(rh)h,
\end{aligned}$$

or equivalently,

$$\begin{aligned}
h^{-\theta}z((\theta+\ell)h) = {}&{}_{(\theta-1)h}\Delta_h^{\theta}z(\eta_3 - \theta\, h) + \theta h^{-\theta}z((\theta+\ell-1)h)\\
&- \frac{1}{\Gamma(-\theta)}\sum_{r=\theta-1}^{\theta+\ell-2}\left(\ell\, h - \sigma(rh)\right)_h^{(-\theta-1)}z(rh)h.
\end{aligned} \tag{3.14}$$

Now, by using the Lipschitz continuity of k in y, $g(\eta, z) > k(\eta, z)$, and (3.13), we get

$$\begin{aligned}
{}_{(\theta-1)h}\Delta_h^{\theta} z(\eta_3 - \theta\, h) &= {}_{(\theta-1)h}\Delta_h^{\theta} \psi_1(\eta_3 - \theta\, h) \\
&\quad - {}_{(\theta-1)h}\Delta_h^{\theta} \psi_2(\eta_3 - \theta\, h) \\
&= w(\eta_3 - h, \psi_2(\eta_3 - h)) \\
&\quad - k(\eta_3 - h, \psi_1(\eta_3 - h)) \\
&\le k(\eta_3 - h, \psi_2(\eta_3 - h)) \\
&\quad - k(\eta_3 - h, \psi_1(\eta_3 - h)) \\
&\le -L_k \left(\psi_2(\eta_3 - h) - \psi_1(\eta_3 - h)\right) \\
&\le -L_k z(\eta_3 - h).
\end{aligned}$$

Denoting $w(\eta_3 - h) := {}_{(\theta-1)h}\Delta_h^{\theta} z(\eta_3 - \theta\, h) + L_k z(\eta_3 - h)$, it follows that

$$w((\theta + \ell - 1)h) \le 0. \tag{3.15}$$

This gives

$${}_{(\theta-1)h}\Delta_h^{\theta} z(\eta_3 - \theta\, h) = -L_k z((\theta + \ell - 1)h) + w((\theta + \ell - 1)h).$$

Equation (3.14) thus becomes

$$\begin{aligned}
h^{-\theta} z((\theta + \ell)h) &= \left(\theta h^{-\theta} - L_k\right) z((\theta + \ell - 1)h) + w((\theta + \ell - 1)h) \\
&\quad - \frac{1}{\Gamma(-\theta)} \sum_{r=\theta-1}^{\theta+\ell-2} \left(\ell\, h - \sigma(rh)\right)_h^{(-\theta-1)} z(rh)h.
\end{aligned} \tag{3.16}$$

Similarly for $\theta \in (0, 1]$ and $h^{-\theta-1} > 0$, we can show that

$$\frac{\left(\ell\, h - \sigma(rh)\right)_h^{(-\theta-1)}}{\Gamma(-\theta)} \le 0. \tag{3.17}$$

Considering $L_k < \theta\, h^{-\theta}$, $h^{-\theta} > 0$ and Equations (3.15)–(3.17), it follows that

$$h^{-\theta} z((\theta + \ell)h) \le 0.$$

This implies that $z(\eta_3) \le 0$, which contradicts with (3.12). The proof of Theorem 3.1 is thus completed. □

In the sequel, we will extend a comparison theorem for Riemann-Liouville fractional h-difference equations of the order θ with $0 \le n - 1 < \theta \le n$.

Theorem 3.2. *Suppose $g(\eta, \psi)$, and $k(\eta, \psi)$ are two real-value functions defined on $[0, \infty] \times \mathbb{R}$. Function k is Lipschitz continuous in y with a Lipschitz constant L_k that has $0 < L_k \le h^{-\theta}\theta$. If $\psi_1(\eta)$ and $\psi_2(\eta)$ are, respectively, unique solutions of the following IVPs*

$$\begin{cases}
{}_{(\theta-n)h}\Delta_h^{\theta} \psi(\eta) = g(\eta + (\theta - n)h, \psi(\eta + (\theta - n)h)), \quad \eta \in \mathbb{N}_0, \\
{}_{(\theta-n)h}\Delta_h^{\theta-n+i} \psi(\eta)\Big|_{t=0} = \psi_i, i = 0, 1, ..., n - 1
\end{cases} \tag{3.18}$$

and

$$\begin{cases}
{}_{(\theta-n)h}\Delta_h^{\theta} \psi(\eta) = k(\eta + (\theta - n)h, \psi(\eta + (\theta - n)h)), \quad \eta \in \mathbb{N}_0, \\
{}_{(\theta-n)h}\Delta_h^{\theta-n+i} \psi(\eta)\Big|_{t=0} = \psi_i, i = 0, 1, ..., n - 1.
\end{cases} \tag{3.19}$$

1. *if $g(\eta, \psi) \le k(\eta, \psi)$, then $\psi_1(\eta) \le \psi_2(\eta)$ for each $\eta \in \mathbb{N}_{(\theta-n)h,h}$,*
2. *if $g(\eta, \psi) > k(\eta, \psi)$, then $\psi_1(\eta) > \psi_2(\eta)$ for each $\eta \in \mathbb{N}^h_{(\theta-n+1)h}$.*

Proof: **(1)** For $\mu = \theta - n + 1 \in (0, 1]$ and $\eta \in \mathbb{N}_{0,h}$, we have ${}_{(\theta-n)h}\Delta_h^{\theta} \psi(\eta) = \Delta_h^{n-1}\, {}_{(\mu-1)h}\Delta_h^{\mu} \psi(\eta)$. By using Lemma 2.5, the IVPs (3.18) and (3.19) can be easily converted to the following IVPs, respectively,

$$\begin{cases}
{}_{(\mu-1)h}\Delta_h^{\mu} \psi(\eta) = \frac{1}{\Gamma(n-1)} \sum_{r=0}^{\frac{\eta}{h}-(n-1)} \left(\eta - \sigma(rh)\right)_h^{(\mu-2)} g(r + (\mu - 1)h, \\
\qquad\qquad \psi(r + (\mu - 1)h))h + \sum_{i=0}^{n-2} \frac{(\eta)_h^{(i)}}{\Gamma(i+1)} \psi_{i+1}, \\
{}_{(\mu-1)h}\Delta_h^{\mu-1} \psi(\eta)\Big|_{t=0} = \psi_0,
\end{cases} \tag{3.20}$$

and

$$\begin{cases}
{}_{(\mu-1)h}\Delta_h^{\mu} \psi(\eta) = \frac{1}{\Gamma(n-1)} \sum_{r=0}^{\frac{\eta}{h}-(n-1)} \left(\eta - \sigma(rh)\right)_h^{(\mu-2)} k(r + (\mu - 1)h, \\
\qquad\qquad \psi(r + (\mu - 1)h))h + \sum_{i=0}^{n-2} \frac{(\eta)_h^{(i)}}{\Gamma(i+1)} \psi_{i+1}, \\
{}_{(\mu-1)h}\Delta_h^{\mu-1} \psi(\eta)\Big|_{t=0} = \psi_0.
\end{cases} \tag{3.21}$$

Denote

$$\begin{aligned}
\bar{g}(\eta, x) = \frac{1}{\Gamma(n-1)} &\sum_{r=0}^{\frac{\eta}{h}-(n-1)} \left(\eta - \sigma(rh)\right)_h^{(n-2)} g(r + (\mu - 1)h, \\
&\psi(r + (\mu - 1)h))h + \sum_{i=0}^{n-2} \frac{(\eta)_h^{(i)}}{\Gamma(i+1)} \psi_{i+1},
\end{aligned}$$

and

$$\begin{aligned}
\bar{k}(\eta, x) = \frac{1}{\Gamma(n-1)} &\sum_{r=0}^{\frac{\eta}{h}-(n-1)} \left(\eta - \sigma(rh)\right)_h^{(n-2)} k(r + (\mu - 1)h, \\
&\psi(r + (\mu - 1)h))h + \sum_{i=0}^{n-2} \frac{(\eta)_h^{(i)}}{\Gamma(i+1)} \psi_{i+1},
\end{aligned}$$

for $\eta \in \mathbb{N}_{(\theta-1)h,h}$. These give

$$\bar{g}(\eta,x)-\bar{k}(\eta,x)=\frac{1}{\Gamma(n-1)}\sum_{r=0}^{\frac{\eta}{h}-(n-1)}\left(\eta-\sigma(rh)\right)_h^{(n-2)} \times\Big[g(r+(\mu-1)h,\psi(r+(\mu-1)h))-k(r+(\mu-1)h, \psi(r+(\mu-1)h))\Big]h. \tag{3.22}$$

Since $g(\eta,\psi)\le k(\eta,\psi)$ and

$$\frac{\left(\eta-\sigma(rh)\right)_h^{(n-2)}}{\Gamma(n-1)}=\frac{\left(\eta-(r+1)h\right)_h^{(n-2)}}{\Gamma(n-1)} =h^{-n-2}\frac{\Gamma\left(\frac{\eta}{h}-r\right)}{\Gamma(n-1)\Gamma\left(\frac{\eta}{h}-r-n+2\right)} =h^{-n-2}\frac{\Gamma(c)}{\Gamma(n-1)\Gamma(c-n+2)}, \text{ where } c=\frac{\eta}{h}-r, r=0,1,...,\frac{\eta}{h}-n+1>0,$$

it follows from (3.22) that $\bar{g}(\eta,\psi)\le\bar{k}(\eta,\psi)$ for $\eta\in\mathbb{N}_{(\theta-1)h,h}$. Then, by applying Theorem 3.1 for the above findings, we get $\psi_1(\eta)\le\psi_2(\eta)$ for $\eta\in\mathbb{N}_{(\theta-n)h,h}$. Hence, the proof of the first item is completed.

(2) Analogously, we can obtain the proof of this item, and thus our proof is completely done. □

4. INVERSE UNCERTAINTY DISTRIBUTION

In this section, we make a link between the solution for an UFFhDE and the solution for the associated FFhDE; we firstly define a symmetrical uncertain variable and α-path for an UFFhDE in view of Lu and Zhu [27]. After that, we state and verify a theorem that demonstrates a link between solution for the UFFhDE with symmetrical uncertain variables and its α-path via the comparison theorems in section 3. To understand the theory of inverse uncertainty distribution, we advise the readers to read [41] carefully.

First, we recall the inverse uncertainty distribution theory:

Definition 4.1 ([41])**.** An uncertainty distribution Ψ is called regular if it is a continues and strictly increasing function and satisfies

$$\lim_{x\to-\infty}\Psi(x)=0,\quad \lim_{x\to+\infty}\Psi(x)=1. \tag{4.1}$$

Definition 4.2 ([41])**.** Let ξ be an uncertain variable with a regular uncertainty distribution Ψ. Then, the inverse function Ψ^{-1} is called the inverse uncertainty distribution of ξ.

Example 4.1. From definition 4.2, we deduce that

(i) the inverse uncertainty distribution of a linear uncertain variable $\mathcal{L}(a,b)$ is given by

$$\Psi^{-1}(\theta)=(1-\theta)a+\theta\, b; \tag{4.2}$$

(ii) the inverse uncertainty distribution of a normal uncertain variable $\mathcal{N}(e,\sigma)$ is given by

$$\Psi^{-1}(\theta)=e+\frac{\sqrt{3}\sigma}{\pi}\ln\left(\frac{\theta}{1-\theta}\right); \tag{4.3}$$

(iii) and the inverse uncertainty distribution of a normal uncertain variable $\mathcal{LOGN}(e,\sigma)$ is given by

$$\Psi^{-1}(\theta)=\exp(e)+\left(\frac{\theta}{1-\theta}\right)^{\frac{\sqrt{3}\sigma}{\pi}}. \tag{4.4}$$

Definition 4.3 ([41])**.** We say that an uncertain variable ξ is symmetrical if

$$\Psi(x)+\Psi(-x)=1, \tag{4.5}$$

where $\Psi(x)$ is a regular uncertainty distribution of ξ.

Remark 4.1. *From definition 4.3, we can deduce that the symmetrical uncertain variable has the inverse uncertainty distribution $\Psi^{-1}(\theta)$, which satiates*

$$\Psi^{-1}(\theta)+\Psi^{-1}(1-\theta)=0. \tag{4.6}$$

Example 4.2. From definition 4.3, we deduce the following:

1. the linear uncertain variable $\mathcal{L}(-a,a)$ is symmetrical for any positive real number a.
2. The normal uncertain variable $\mathcal{N}(0,1)$ is symmetrical.

Consider the following UFFhDE with Riemann-Liouville-like forward difference:

$${}_{(\theta-n)h}\Delta_h^{\theta}\mathbf{X}(\eta)=\mathbf{F}(\eta+(\theta-n)h,\mathbf{X}(\eta+(\theta-n)h)) +\mathbf{G}(\eta+(\theta-n)h,\mathbf{X}(\eta+(\theta-n)h))\xi_{\eta+(\theta-n)h}, \tag{4.7}$$

subject to the crisp initial conditions

$${}_{(\theta-n)h}\Delta_h^{\theta-n-k}\mathbf{X}(\eta)\Big|_{t=0}=\mathbf{X}_k,\quad k=0,1,...,n-1, \tag{4.8}$$

where ${}_{(\theta-n)h}\Delta_h^{\theta}$ denotes a fractional Riemann–Liouville forward h-difference with $0\le n-1<\theta\le n$, M,N are two real-valued functions defined on $[0,\infty)\times\mathbb{R}$, $\eta\in\mathbb{N}_{0,h}\cap[0,Th]$, $\mathbf{X}_k\in\mathbb{R}$ for $k=0,1,...,n-1$, and $\xi_{(\theta-n)h},\xi_{(\theta-n+1)h},\cdots,\xi_{\eta+(\theta-n)h}$ are i.i.d. uncertain variables with symmetrical uncertainty distribution $\mathcal{L}(a,b)$.

Definition 4.4 ([41])**.** An UFFhDE (4.7) with crisp initial conditions (4.8) is said to have an α-path if it is the solution of the corresponding FFhDE

$${}_{(\theta-n)h}\Delta_h^{\theta}\mathbf{X}(\eta)=\mathbf{F}(\eta+(\theta-n)h,\mathbf{X}(\eta+(\theta-n)h)) +|\mathbf{G}(\eta+(\theta-n)h,\mathbf{X}(\eta+(\theta-n)h))|\Psi^{-1}(\theta) \tag{4.9}$$

with the same initial conditions (4.8), where $\Psi^{-1}(\theta)$ is the inverse uncertainty distribution of uncertain variables ξ_η for $\eta\in\mathbb{N}_{(\theta-n)h,h}\cap[0,Th]$.

Theorem 4.1. *Let* $\eta \in \mathbb{N}_{0,h} \cap [0, Th], n \in \mathbb{N}, \lambda \in (0,1)$ *and* $\theta \in (0,1]$. *The linear UFFhDE:*

$$_{(\theta-n)h}\Delta_h^{\theta}\mathbf{X}(\eta) = \lambda\,\mathbf{X}(\eta+(\theta-n)h) + \lambda\,\xi_{\eta+(\theta-n)h},$$

with the initial conditions

$$_{(\theta-n)h}\Delta_h^{\theta-n-i}\mathbf{X}(\eta)\Big|_{t=0} = \mathbf{X}_i, \quad i = 0,1,...,n-1,$$

has a solution

$$\mathbf{X}(\eta) = \mathbf{X}_i F_{\mu,\lambda;h}(\eta) + \xi_\eta, \quad , \ i = 0,1,...,n-1,$$

where ξ_η *is an uncertain sequence with the uncertainty distribution* $\mathcal{L}\left(a\cdot e_{\theta,\lambda;h}(\eta), b\cdot e_{\theta,\lambda;h}(\eta)\right)$, *and*

$$F_{\theta,\lambda;h}(\eta) = \sum_{k=0}^{\infty}\lambda^k \sum_{i=0}^{n-1}\frac{(\eta+k(\theta-n)h)_h^{((k+1)\theta\, h-nh+i)}}{\Gamma((k+1)\theta-n+i+1)},$$

and

$$e_{\theta,\lambda;h}(\eta) = \sum_{k=1}^{\infty}\lambda^k\frac{(\eta+(k-1)(\theta-n)h)_h^{(k\theta)}}{\Gamma(k\theta+1)}.$$

Proof: By making the use of Lemma 2.5, we can easily prove this theorem by the similar technique of [29, Theorem 3.1], so it is omitted. □

Example 4.3. Consider the following UFFhDE:

$$_{(\theta-1)h}\Delta_h^{\theta}\mathbf{X}(\eta) = \lambda\,\mathbf{X}(\eta+(\theta-1)h) + \lambda\,\xi_{\eta+(\theta-1)h}, \quad \eta \in \mathbb{N}_{0,h}\cap[0,Th], \lambda\in(0,1), \theta\in(0,1], \quad (4.10)$$

where $\xi_{(\theta-1)h}, \xi_{\theta\, h}, \ldots, \xi_{\eta+(\theta-1)h}$ are i.i.d linear uncertain variable $\mathcal{L}(-2,2)$, which has the inverse uncertainty distribution $\Psi^{-1}(\theta) = 4\theta - 2$ by (4.2).

By Theorem 4.1, the associated FFhDE of (4.10) with its initial condition

$$_{(\theta-1)h}\Delta_h^{\theta}\mathbf{X}(\eta) = \lambda\,\mathbf{X}(\eta+(\theta-1)h) + \lambda\,\Psi^{-1}(\theta),$$
$$_{(\theta-1)h}\Delta_h^{\theta-1}\mathbf{X}(\eta)\Big|_{t=0} = \mathbf{X}_0$$

has a solution

$$\mathbf{X}(\eta) = \mathbf{X}_0\sum_{k=0}^{\infty}\lambda^k\frac{(\eta+k(\theta-1)h)_h^{((k+1)\theta-1)}}{\Gamma((k+1)\theta)} + \sum_{k=1}^{\infty}\lambda^k\frac{(\eta+(k-1)(\theta-1)h)_h^{(k\theta)}}{\Gamma(k\theta+1)}(4\theta-2).$$

The UFFhDE (4.10) has an α-path

$$\mathbf{X}_\eta^{\theta} = \mathbf{X}_0\sum_{k=0}^{\infty}\lambda^k\frac{(\eta+k(\theta-1)h)_h^{((k+1)\theta-1)}}{\Gamma((k+1)\theta)} + \sum_{k=1}^{\infty}\lambda^k\frac{(\eta+(k-1)(\theta-1)h)_h^{(k\theta)}}{\Gamma(k\theta+1)}(4\theta-2).$$

with the initial condition $_{(\theta-1)h}\Delta_h^{\theta-1}\mathbf{X}(\eta)\Big|_{t=0} = \mathbf{X}_0$.

Example 4.4. Consider the following UFFhDE:

$$_{(\theta-2)h}\Delta_h^{\theta}\mathbf{X}(\eta) = q\,\mathbf{X}(\eta+(\theta-2)h) + q\,\xi_{\eta+(\theta-1)h}, \quad \eta\in\mathbb{N}_{0,h}\cap[0,Th], q\in(0,1), \theta\in(0,1], \quad (4.11)$$

where $\xi_{(\theta-2)h}, \xi_{(\theta-1)\,h}, \ldots, and \xi_{\eta+(\theta-2)h}$ are the i.i.d normal uncertain variable $\mathcal{N}(0,1)$, which has the inverse uncertainty distribution $\Psi^{-1}(\theta) = \frac{\sqrt{3}}{\pi}\ln\left(\frac{\theta}{1-\theta}\right)$ by (4.2).

By Theorem 4.1, the associated FFhDE of (4.11) with its initial condition

$$_{(\theta-2)h}\Delta_h^{\theta}\mathbf{X}(\eta) = q\mathbf{X}(\eta+(\theta-2)h) + q\Psi^{-1}(\theta),$$
$$_{(\theta-2)h}\Delta_h^{\theta-2+i}\mathbf{X}_i(\eta)\Big|_{t=0} = \mathbf{X}_i, \quad i = 0,1$$

has a solution

$$\mathbf{X}(\eta) = \sum_{k=0}^{\infty}q^k\sum_{i=0}^{1}\mathbf{X}_i\frac{(\eta+k(\theta-2)h)_h^{((k+1)\theta\, h-2h+i)}}{\Gamma((k+1)\theta-1+i)} + \frac{\sqrt{3}}{\pi}\ln\left(\frac{\theta}{1-\theta}\right)\sum_{k=1}^{\infty}q^k\frac{(\eta+(k-1)(\theta-2)h)_h^{(k\theta)}}{\Gamma(k\theta+1)}.$$

The UFFhDE (4.11) has an α-path

$$\mathbf{X}_\eta^{\theta} = \sum_{k=0}^{\infty}q^k\sum_{i=0}^{1}\mathbf{X}_i\frac{(\eta+k(\theta-2)h)_h^{((k+1)\theta\, h-2h+i)}}{\Gamma((k+1)\theta-1+i)} + \frac{\sqrt{3}}{\pi}\ln\left(\frac{\theta}{1-\theta}\right)\sum_{k=1}^{\infty}q^k\frac{(\eta+(k-1)(\theta-2)h)_h^{(k\theta)}}{\Gamma(k\theta+1)}.$$

with the initial condition $_{(\theta-2)h}\Delta_h^{\theta-2+i}\mathbf{X}_i(\eta)\Big|_{t=0} = \mathbf{X}_i$, i=0,1.

In the following theorem, we make a relationship between uncertain fractional forward h-difference equations (UFFhDEs) and fractional h-difference equations (FFhDEs) based on the comparison theorems in section 3.

Theorem 4.2. *If* $\mathbf{X}_\eta$ *and* $\mathbf{X}_\eta^{\theta}$ *are the unique solution and* α*-path of UFFhDE (4.7) with the initial conditions (4.8), respectively. Assume that* $\mathbf{F} + |\mathbf{G}|\Psi^{-1}(\theta)$ *is a Lipschitz continues function in x with a Lipschitz constant* L_k *that has* $0 < L_k < \theta\, h^{-\theta}$. *Assume that* ξ_η *is the i.i.d. symmetrical uncertain variable for* $\eta \in \mathbb{N}^h_{(\theta-(n-1))h,h}\cap[0,Th]$, *then*

(i) $\mathbf{X}_\eta \le \mathbf{X}_\eta^{\theta}$ *if* $\xi_\eta(\gamma) \le \Psi^{-1}(\theta)$ *for* $\eta\in\mathcal{D}^+$ *and* $\xi_\eta(\gamma) \ge \Psi^{-1}(1-\theta)$ *for* $\eta\in\mathcal{D}^-$, *where*

$$\mathcal{D}^+ = \left\{\eta\in\mathbb{N}_{(\theta-(n-1))h,h}\cap[0,Th];\ \mathbf{G}(\eta,x)\ge 0\right\},$$

and

$$\mathcal{D}^- = \left\{\eta\in\mathbb{N}_{(\theta-(n-1))h,h}\cap[0,Th];\ \mathbf{G}(\eta,x)< 0\right\},$$

(ii) $\mathbf{X}_\eta > \mathbf{X}^\theta_\eta$ *if* $\xi_\eta(\gamma) > \Psi^{-1}(\theta)$ *for* $\eta \in \mathcal{D}^+$ *and* $\xi_\eta(\gamma) < \Psi^{-1}(1-\theta)$ *for* $\eta \in \mathcal{D}^-$.

Proof: First, we let $\xi_\eta(\gamma) \leq \Psi^{-1}(\theta)$ for $\eta \in \mathcal{D}^+$. Then $\eta \in \mathbb{N}_{(\theta-(n-1))h,h} \cap [0, Th]$ and $\mathbf{G}(\eta, x) \geq 0$. Therefore,

$$\mathbf{G}(\eta, x)\xi_\eta(\gamma) \leq |\mathbf{G}(\eta, x)|\Psi^{-1}(\theta). \tag{4.12}$$

Moreover, if $\xi_\eta(\gamma) \geq \Psi^{-1}(1-\theta)$ for $\eta \in \mathcal{D}^-$, we have $\eta \in \mathbb{N}_{(\theta-(n-1))h,h} \cap [0, Th]$ and $\mathbf{G}(\eta, x) < 0$. Since ξ_η is symmetrical, we have $\Psi^{-1}(\theta) + \Psi^{-1}(1-\theta) = 0$. Thus,

$$\begin{aligned}\mathbf{G}(\eta, x)\xi_\eta(\gamma) &\leq \mathbf{G}(\eta, x)\Psi^{-1}(1-\theta) = -\mathbf{G}(\eta, x)\Psi^{-1}(\theta)\\ &= |\mathbf{G}(\eta, x)|\Psi^{-1}(\theta).\end{aligned} \tag{4.13}$$

Since $\mathbf{X}_\eta(\gamma)$ and $\mathbf{X}^\theta_\eta$ are the unique solution and α-path of UFFhDE (4.7) with the initial conditions (4.8), respectively, we have

$$\begin{aligned}{}_{(\theta-n)h}\Delta^\theta_h\mathbf{X}(\eta) &= \mathbf{F}(\eta + (\theta-n)h, \mathbf{X}(\eta + (\theta-n)h))\\ &\quad + \mathbf{G}(\eta + (\theta-n)h, \mathbf{X}(\eta + (\theta-n)h))\xi_{\eta+(\theta-n)h}(\gamma),\end{aligned} \tag{4.14}$$

$$\begin{aligned}{}_{(\theta-n)h}\Delta^\theta_h\mathbf{X}(\eta) &= \mathbf{F}(\eta + (\theta-n)h, \mathbf{X}(\eta + (\theta-n)h))\\ &\quad + |\mathbf{G}(\eta + (\theta-n)h, \mathbf{X}(\eta + (\theta-n)h))|\Psi^{-1}(\theta).\end{aligned} \tag{4.15}$$

Hence, by use of Theorem 3.2 with (4.12)–(4.15), we get the proof of item (i). The proof of the second item (ii) is similar to (i). Thus, the proof of Theorem 4.2 is completed. □

Theorem 4.3 (Existence and Uniqueness)**.** *Assume that* $\mathbf{F}(\eta, x)$ *and* $\mathbf{G}(\eta, x)$ *satisfy the Lipschitz condition*

$$|\mathbf{F}(\eta, x) - \mathbf{F}(\eta, \psi)| + |\mathbf{G}(\eta, x) - \mathbf{G}(\eta, \psi)| \leq L|x - y|, \tag{4.16}$$

and there is a positive number L *that satisfies the following inequality:*

$$L < h^{-\theta-1}\frac{\Gamma(\theta+1)\Gamma(T+1-\theta)}{\Gamma(T+1)(Q+1)}, \tag{4.17}$$

where $Q = |a| \vee |b|$. *Then UFFhDE (4.7) with the initial conditions (4.8) has a unique solution* $\mathbf{X}(\eta)$ *for* $\eta \in \mathbb{N}_{\theta\, h,h} \cap [0, Th]$.

Proof: Proof of this theorem is similar to the existence and uniqueness theorem [29, Theorem 3.2], and it is therefore omitted. □

Example 4.5. Consider the following UFFhDE:

$${}_{-1}\Delta^{0.5}_2\mathbf{X}(\eta) = \frac{\sin \mathbf{X}(\eta-1)}{50 + (\eta-1)^2} + \xi_{\eta-1}, \quad \eta \in \mathbb{N}^2_0 \cap [0, 8], \tag{4.18}$$

where $\xi_{-1}, \xi_1, \xi_3, \xi_5, \xi_7$ are 5 i.i.d. linear uncertain variables with linear uncertainty distribution $\mathcal{L}(-2, 2)$.

In this example $h = 2, \theta = 0.5, T = 4$,

$$|\mathbf{F}(\eta, x) - \mathbf{F}(\eta, \psi)| + |\mathbf{G}(\eta, x) - \mathbf{G}(\eta, \psi)| \leq \frac{1}{50}|x - y| = 0.02|x - y|,$$

and

$$\begin{aligned}h^{-\theta-1}\frac{\Gamma(\theta+1)\Gamma(T+1-\theta)}{\Gamma(T+1)(Q+1)} &= 2^{-1.5}\frac{\Gamma(0.5+1)\Gamma(4+1-0.5)}{3\Gamma(4+1)}\\ &\approx 0.05 > 0.02.\end{aligned}$$

Thus, the existence and uniqueness Theorem 4.3 confirms that UFFhDE (4.18) has a unique solution.

Now, since

$$\mathbf{F}(\eta, x) + |\mathbf{G}(\eta, x)|\Psi^{-1}(\theta) = \frac{\sin x}{50 + (\eta-1)^2} + 4\theta - 2,$$

we deduce that $\mathbf{F}(\eta, x) + |\mathbf{G}(\eta, x)|\Psi^{-1}(\theta)$ is Lipschitz continues in x with Lipschitz constant $L = 0.02 < 0.35 = \theta\, h^{-\theta}$.

We see that $\mathbf{G}(\eta, x) = 1 > 0$, and, from example 4.2, we see $\mathcal{L}(-2, 2)$ is symmetrical. Hence, by Theorem 4.2, we deduce the following link between unique solution and α-path of UFFhDE (4.18):

(i) $\mathbf{X}_\eta \leq \mathbf{X}^\theta_\eta$ if $\xi_\eta \leq 4\theta - 2$,
(ii) $\mathbf{X}_\eta > \mathbf{X}^\theta_\eta$ if $\xi_\eta > 4\theta - 2$.

Example 4.6. Consider the following UFFhDE:

$${}_{-\frac{3}{8}}\Delta^{\frac{1}{4}}_{\frac{1}{2}}\mathbf{X}(\eta) = 0.025\,\mathbf{X}^2\left(\eta - \frac{3}{8}\right) + \xi_{\eta-\frac{3}{8}}, \quad \eta \in \mathbb{N}^{\frac{1}{2}}_0 \cap \left[0, \frac{3}{2}\right], \tag{4.19}$$

where $\xi_{-\frac{3}{8}}, \xi_{\frac{1}{8}}, \xi_{\frac{5}{8}}, \xi_{\frac{9}{8}}$ are 4 i.i.d. linear uncertain variables with linear uncertainty distribution $\mathcal{L}(-3, 3)$.

In this example $h = 0.5, \theta = 0.25, T = 3$,

$$\begin{aligned}|\mathbf{F}(\eta, x) - \mathbf{F}(\eta, \psi)| + |\mathbf{G}(\eta, x) - \mathbf{G}(\eta, \psi)| &\leq 0.025|x + y||x - y|\\ &= 0.1|x - y|, \quad \text{for } x \in [-2, 2],\end{aligned}$$

and

$$\begin{aligned}h^{-\theta-1}\frac{\Gamma(\theta+1)\Gamma(T+1-\theta)}{\Gamma(T+1)(Q+1)} &= \left(\frac{1}{2}\right)^{-\frac{5}{4}}\frac{\Gamma(0.25+1)\Gamma(3+1-0.25)}{4\Gamma(3+1)}\\ &\approx 0.4 > 0.1.\end{aligned}$$

Thus, the existence and uniqueness Theorem 4.3 confirms that UFFhDE (4.19) has a unique solution.

Now, since

$$\mathbf{F}(\eta, x) + |\mathbf{G}(\eta, x)|\Psi^{-1}(\theta) = 0.025x^2 + 6\theta - 3,$$

we deduce that $\mathbf{F}(\eta, x) + |\mathbf{G}(\eta, x)|\Psi^{-1}(\theta)$ is Lipschitz, continued in x with Lipschitz constant $L = 0.1 < 0.3 = \theta\, h^{-\theta}$.

We see that $\mathbf{G}(\eta, x) = 1 > 0$, and, from example 4.2, we see $\mathcal{L}(-3, 3)$ is symmetrical. Hence, by use of Theorem 4.2, we deduce that $\mathbf{X}_\eta \leq \mathbf{X}_\eta^\theta$ if $\xi_\eta \leq 6\theta - 3$ and $\mathbf{X}_\eta > \mathbf{X}_\eta^\theta$ if $\xi_\eta > 6\theta - 3$. This is a link between unique solution and α-path of UFFhDE (4.19).

5. CONCLUSIONS

We have considered the fractional forward h-difference equations and uncertain fractional forward h-difference equations in the context of discrete fractional calculus. The comparison theorems and existence and uniqueness theorem for the FFhDEs and UFFhDEs have been found. From a theoretical point of view, we have created a strong relationship between the solutions for UFFhDEs with the symmetrical uncertain variables and the solutions for associated UFFhDEs (namely the α-path of UFFhDEs).

Our presented results are in the sense of Riemann-Liouville fractional operator. It is important to point out the future scope of our results. There is an important task here that the researchers will be able to consider in the future. What is the task? The interested readers can extend the ideas that were presented in this article to the two well-known models of fractional calculus that were defined by operators similar to the Riemann-Liouville fractional operator but with Mittag-Leffler functions in the kernel, namely the Atangana–Baleanu (or briefly AB) [42, 43] and Prabhakar [44] models.

DATA AVAILABILITY STATEMENT

The original contributions presented in the study are included in the article/supplementary materials, further inquiries can be directed to the corresponding author/s.

AUTHOR CONTRIBUTIONS

All authors listed have made a substantial, direct and intellectual contribution to the work, and approved it for publication.

REFERENCES

1. Miller KS, Ross B. *An Introduction to the Fractional Calculus and Fractional Differential Equations*. New York, NY: John Wiley & Sons (1993).
2. Podlubny I. *Fractional Differential Equations*. San Diego, CA: Academic Press (1999).
3. Kilbas AA, Srivastava HM, Trujillo JJ. *Theory and Applications of Fractional Differential Equations*. Amsterdam: Elsevier B.V. (2006).
4. Diethelm K. *The Analysis of Fractional Differential Equations*. Berlin: Springer (2010).
5. Hamasalh FK, Mohammed PO. Generalized quartic fractional spline approximation function with applications. *Math Sci Lett.* (2016) 5:131–36.
6. Martinez F, Mohammed PO, Valdes JEN. Non-conformable fractional Laplace transform. *Kragujevac J Math.* (2022) 46:341–54.
7. Mohammed PO. Some integral inequalities of fractional quantum type. *Malaya J Mat.* (2016) 4:93–9.
8. Mohammed PO. Hermite-Hadamard inequalities for Riemann-Liouville fractional integrals of a convex function with respect to a monotone function. *Math Meth Appl Sci.* (2019) 1–11. doi: 10.1002/mma.5784
9. Mohammed PO, Abdeljawad T. Modification of certain fractional integral inequalities for convex functions. *Adv Differ Equ.* (2020) 2020:69. doi: 10.1186/s13662-020-2541-2
10. Mohammed PO, Brevik I. A new version of the Hermite-Hadamard inequality for Riemann-Liouville fractional integrals. *Symmetry.* (2020) 12:610. doi: 10.3390/sym12040610
11. Mohammed PO, Sarikaya MZ. Hermite-Hadamard type inequalities for F-convex function involving fractional integrals. *J Inequal Appl.* (2018) 2018:359. doi: 10.1186/s13660-018-1950-1
12. Mohammed PO, Sarikaya MZ. On generalized fractional integral inequalities for twice differentiable convex functions. *J Comput Appl Math.* (2020) 372:112740. doi: 10.1016/j.cam.2020.112740
13. Mohammed PO, Sarikaya MZ, Baleanu D. On the generalized Hermite-Hadamard inequalities via the tempered fractional integrals. *Symmetry.* (2020) 12:595. doi: 10.3390/sym12040595
14. Qi F, Mohammed PO, Yao JC, Yao YH. Generalized fractional integral inequalities of Hermite–Hadamard type for (α, m)-convex functions. *J Inequal Appl.* (2019) 2019:135. doi: 10.1186/s13660-019-2079-6
15. Agarwal RP. *Difference Equations and Inequalities: Theory, Methods, and Application*. New York, NY: Marcel Dekker (2000).
16. Bohner M, Peterson AC. *Advances in Dynamic Equations on Time Scales*. Boston, MA: Birkhauser (2003).
17. Atici F, Eloe P. A transform method in discrete fractional calculus. *IJDE.* (2007) 2:165–76.
18. Atici F, Eloe P. Initial value problems in discrete fractional calculus. *P Am Math Soc.* (2009) 137:981–89. doi: 10.1090/S0002-9939-08-09626-3
19. Goodrich C. Existence of a positive solution to a system of discrete fractional boundary value problems. *Appl Math Comput.* (2011) 217:4740–53. doi: 10.1016/j.amc.2010.11.029
20. Goodrich C, Peterson A. *Discrete Fractional Calculus*. Berlin: Springer (2015).
21. Wu G, Baleanu D. Discrete chaos in fractional delayed logistic maps. *Nonlin Dyn.* (2015) 80:1697–703. doi: 10.1007/s11071-014-1250-3
22. Wu G, Baleanu D, Luo W. Lyapunov functions for Riemann–Liouville-like fractional difference equations. *Appl Math Comput.* (2017) 314:228–36. doi: 10.1016/j.amc.2017.06.019
23. Wu G, Baleanu D, Zeng S. Finite-time stability of discrete fractional delay systems: Gronwall inequality and stability criterion. *Commun Nonlin Sci.* (2018) 57:299–308. doi: 10.1016/j.cnsns.2017.09.001
24. Zhu Y. Uncertain fractional differential equations and an interest rate model. *Math Meth Appl Sci.* (2015) 38:3359–68. doi: 10.1002/mma.3335
25. Zhu Y. Existence and uniqueness of the solution to uncertain fractional differential equation. *J Uncertain Anal Appl.* (2015) 3:1–11. doi: 10.1186/s40467-015-0028-6
26. Lu Z, Zhu Y. Comparison principles for fractional differential equations with the Caputo derivatives. *Adv Differ Equat.* (2018) 237:1–11. doi: 10.1186/s13662-018-1691-y
27. Lu Z, Zhu Y. Numerical approach for solution to an uncertain fractional differential equation. *Appl Math Comput.* (2019) 343:137–48. doi: 10.1016/j.amc.2018.09.044
28. Lu Q, Zhu Y, Lu Z. Uncertain fractional forward difference equations for Riemann–Liouville type. *Adv Differ Equ.* (2019) 2019:147. doi: 10.1186/s13662-019-2093-5
29. Mohammed PO. A generalized uncertain fractional forward difference equations of Riemann-Liouville Type. *J Math Res.* (2019) 11:43–50. doi: 10.5539/jmr.v11n4p43
30. Atici F, Sengul S. Modeling with fractional difference equations. *J Math Anal Appl.* (2010) 369:1–9. doi: 10.1016/j.jmaa.2010.02.009
31. Abdeljawad T, Baleanu D. Discrete fractional differences with nonsingular discrete Mittag-Leffler kernels. *Adv Differ. Equat.* (2016) 2016:232. doi: 10.1186/s13662-016-0949-5

32. Abdeljawad T. Fractional difference operators with discrete generalized Mittag-Leffler kernels. *Chaos Soliton Fract.* (2019) 126:315–24. doi: 10.1016/j.chaos.2019.06.012
33. Shah K, Jarad F, Abdeljawad T. On a nonlinear fractional order model of dengue fever disease under Caputo-Fabrizio derivative. *Alex Eng J.* (2020) 59:2305–13. doi: 10.1016/j.aej.2020.02.022
34. Abdeljawad T, Baleanu D. Monotonicity results for fractional difference operators with discrete exponential kernels. *Adv Differ Equat.* (2017) 2017:78. doi: 10.1186/s13662-017-1126-1
35. Abdeljawad T. On delta and Nabla Caputo fractional differences and dual identities. *Discrete Dyn Nat Soc.* (2013) 2013:12. doi: 10.1155/2013/406910
36. Abdeljawad T. Dual identities in fractional difference calculus within Riemann. *Adv Differ Equat.* (2017) 2017:36. doi: 10.1186/1687-1847-2013-36
37. NRO Bastos, Ferreira RAC, Torres DFM. Discrete-time fractional variational problems. *Signal Process* (2011) 91:513–24. doi: 10.1016/j.sigpro.2010.05.001
38. Ferreira RAC, Torres DFM. Fractional *h*-difference equations arising from the calculus of variations. *Appl Anal Discrete Math.* (2011) 5:110–2. doi: 10.2298/AADM110131002F
39. Suwan I, Abdeljawad T, Jarad F. Monotonicity analysis for nabla *h*-discrete fractional Atangana-Baleanu differences. *Chaos Solit Fract.* (2018) 117:50–9. doi: 10.1016/j.chaos.2018.10.010
40. Abdeljawad T. Different type kernel *h*–fractional differences and their fractional *h*–sums. *Chaos Solit Fract.* (2018) 116:146–56. doi: 10.1016/j.chaos.2018.09.022
41. Liu B. *Uncertainty Theory: A Branch of Mathematics for Modeling Human Uncertainty*. Berlin: Springer (2010).
42. Atangana A, Baleanu D. New fractional derivatives with nonlocal and non-singular kernel: theory and application to heat transfer model. *Thermal Sci.* (2016) 20:763–9. doi: 10.2298/TSCI16011 1018A
43. Baleanu D, Fernandez A. On some new properties of fractional derivatives with Mittag-Leffler kernel. *Commun Nonlin Sci.* (2018) 59:444–62. doi: 10.1016/j.cnsns.2017.12.003
44. Prabhakar TR. A singular integral equation with a generalized Mittag Leffler function in the kernel. *Yokohama Math J.* (1971) 19:7–15.

Conflict of Interest: The authors declare that the research was conducted in the absence of any commercial or financial relationships that could be construed as a potential conflict of interest.

Copyright © 2020 Srivastava and Mohammed. This is an open-access article distributed under the terms of the Creative Commons Attribution License (CC BY). The use, distribution or reproduction in other forums is permitted, provided the original author(s) and the copyright owner(s) are credited and that the original publication in this journal is cited, in accordance with accepted academic practice. No use, distribution or reproduction is permitted which does not comply with these terms.

Advantages of publishing in Frontiers

OPEN ACCESS
Articles are free to read for greatest visibility and readership

FAST PUBLICATION
Around 90 days from submission to decision

HIGH QUALITY PEER-REVIEW
Rigorous, collaborative, and constructive peer-review

TRANSPARENT PEER-REVIEW
Editors and reviewers acknowledged by name on published articles

Frontiers
Avenue du Tribunal-Fédéral 34
1005 Lausanne | Switzerland

Visit us: www.frontiersin.org
Contact us: info@frontiersin.org | +41 21 510 17 00

REPRODUCIBILITY OF RESEARCH
Support open data and methods to enhance research reproducibility

DIGITAL PUBLISHING
Articles designed for optimal readership across devices

FOLLOW US
@frontiersin

IMPACT METRICS
Advanced article metrics track visibility across digital media

EXTENSIVE PROMOTION
Marketing and promotion of impactful research

LOOP RESEARCH NETWORK
Our network increases your article's readership